Light-Driven Molecular Complexity: Cascade Functionalization of Alkynes via Selenium and/or Sulfonyl Radicals

A Dissertation

Submitted in partial fulfilment of the

Requirements for the Degree of

Doctor of Philosophy

by

Mithu Roy

Roll no.-196122108

Department of Chemistry

Indian Institute of Technology Guwahati

Guwahati, 781039

Assam, India

Dedicated
to
My Family and Teachers

INDIAN INSTITUTE OF TECHNOLOGY GUWAHATI
ASSAM, INDIA, 781039
Department of Chemistry

Statement

I, hereby declare that the work comprised in this thesis entitled "***Light-Driven Molecular Complexity: Cascade Functionalization of Alkynes via Selenium and/or Sulfonyl Radicals***" is the outcome of the research work carried out by me under the supervision of **Prof. Dipankar Srimani, Department of Chemistry, Indian Institute of Technology Guwahati, India**, for the award of the degree of Doctor of Philosophy.

In harmony with the general practice of reporting scientific observations, due acknowledgments have been made if the work is established on the findings of other investigators.

Mithu Roy

Guwahati
November, 2025

Mithu Roy
Roll no: **196122108**
Department of Chemistry
IIT Guwahati, Assam
India, 781039

INDIAN INSTITUTE OF TECHNOLOGY GUWAHATI
ASSAM, INDIA, 781039
Department of Chemistry

Prof. Dipankar Srimani **Email: dsrimani@iitg.ac.in**
Professor, Department of Chemistry

Certificate

This is to certify that the work incorporated in the thesis entitled ***"Light-Driven Molecular Complexity: Cascade Functionalization of Alkynes via Selenium and/or Sulfonyl Radicals"*** which is being submitted to the Indian Institute of Technology Guwahati for the award of Doctor of Philosophy in Chemistry by **Mr. Mithu Roy** (Roll No: **196122108**) was carried out by him under my supervision at this institute. The work presented in his thesis is original and has not been submitted elsewhere for a degree.

Guwahati
November, 2025

Prof. Dipankar Srimani
(Thesis Supervisor)
Professor
Department of Chemistry
IIT Guwahati
Assam-781039
India

~Acknowledgements~

This work would not have reached fruition without the exceptional contributions, unwavering support, and invaluable mentorship of numerous individuals and institutions. I offer my profound gratitude to all who have illuminated this path.

My deepest gratitude goes to my thesis supervisor, ***Prof. Dipankar Srimani,*** *for his constant guidance, support, and insightful advice throughout my research work. He inspired me to pursue scientific research, and I am grateful for the opportunity to work under his supervision.*

Besides my advisor, I would like to acknowledge my doctoral committee members, ***Prof. Anil Kumar Saikia*** *(Chairman) (IIT Guwahati),* ***Prof. Subhas Chandra Pan*** *(IIT Guwahati), and* ***Prof. Sunanda Chatterjee*** *(IIT Guwahati) for their valuable suggestions and encouragement, which helped a lot to improve my thesis.*

I sincerely appreciate the whole-hearted cooperation and valuable help rendered by the teaching and non-teaching staff of the Department of Chemistry, Indian Institute of Technology Guwahati. I am also grateful to IIT Guwahati, the Department of Chemistry, and the Central Instrumental Facilities (CIF) for providing research and instrumental facilities. I wish to extend my thanks to MoE for the PMRF.

My deepest gratitude to my lab mates for their support during my PhD period. I am very much thankful to my seniors, Dr. Ramen Jamatia, Dr. T. S. Manikandan, Dr. Kalicharan Das, Dr. Nandita Biswas, Dr. Sundarraman Balaji, Dr. Avijit Mondal, Dr. Bitan Sardar, Dr. Debjyoti Pal, Dr. Rahul Sharma, and my labmates, Arup, Kailash, Hirak, Rajashri, Itu, Krishna, Rohit, Rinku, and Sanatjit. M.Sc. project students Manami, Anirban, Sudipta, Ujjwal, Amit, Chandrika, Soumen, Saurabh, Bikram, Kaushik, Bishal, and Sonu.

I greatly appreciate and acknowledge the support received from other laboratories within the Department of Chemistry at IIT Guwahati.

I am also thankful to all of my teachers for their contributions to my education at various stages. Sri Amit Kumar Deb, Sri Biswajit Bhaumik, Dr. Bablee Mandal, and my master's thesis supervisor, Prof. Apurba K. Das, are deeply acknowledged in this regard. I want to thank my previous institutions, Belakoba High School, Surya Sen Mahavidyalaya, and IIT Indore.

On a personal note, I would like to express my deepest appreciation to my family for their endless patience, sacrifices, and unconditional love. Your support was my constant source of strength, and you provided the indispensable motivation to complete this journey.

I want to thank all my batchmates, seniors, and school and college friends for their priceless friendship and moral support.

It's tough to fit all of the names into a single paper; any absence in this brief acknowledgement does not imply a lack of appreciation.

Thank You

-Mithu

Contents

	Subjects	Page No.
Chapter-I	***A brief introduction to the visible light-induced photocatalytic selenium/sulfonyl radical-mediated cascade reaction of alkynes***	*1-22*
	1.1. Introduction	*2-4*
	1.2. General photocatalytic single electron transfer (SET) mechanism	*5*
	1.3. Importance of organoselenium compounds	*6-7*
	1.4. Selected examples for the selenylation reaction of alkynes	*7-8*
	1.5. Importance of sulfone compounds	*8-9*
	1.6. Selected examples for the sulfonylation reaction of alkynes	*9-11*
	1.7. Photocatalytic radical cascade cyclization of 1,6-enynes to generate molecular complexity	*11-14*
	1.8. Concluding remarks	*14*
	1.9. Aim of the thesis	*14*
	1.10. References	*15-22*
Chapter II	***Photocatalytic selective synthesis of 1,1-diselenide alkene derivatives and selenium-containing α, β-unsaturated carboxylic acids***	*23-57*
	2.1. Introduction	*24*
	2.2. Previous reports	*24-25*
	2.3. Present work	*25-26*
	2.4. Results and discussion	*26-30*
	2.5. Post-functionalization	*30*
	2.6. Control experiments	*30-32*
	2.7. Plausible mechanism	*32-33*
	2.8. Conclusion	*33*
	2.9. Experimental section	*34-38*
	2.10. Analytical data	*38-48*
	2.11. References	*48-50*
	2.12. Selected NMR spectra	*51-57*
Chapter III	***Substituent-dependent, switchable synthesis of nonaromatic and aromatic heterocyclic sulfones using visible light***	*58-116*
	3.1. Introduction	*59*

	3.2. Previous reports	*59-60*
	3.3. Present work	*60-61*
	3.4. Results and discussion	*61-65*
	3.5. Post-functionalization	*66-67*
	3.6. Control experiments	*67-71*
	3.7. Plausible mechanism	*71-72*
	3.8. Conclusion	*73*
	3.9. Experimental section	*73-77*
	3.10. Analytical data	*78-90*
	3.11. Crystal data	*91-101*
	3.12. References	*102-106*
	3.12. Selected NMR spectra	*107-116*
Chapter IV	***Visible-light mediated divergent synthesis of sulfonylated dihydropyrrole-3 carboxaldehydes and tricyclic sulfones via sulfonyl radical source modulation***	*117-177*
	4.1. Introduction	*118*
	4.2. Previous reports	*118-119*
	4.3. Present work	*120*
	4.4. Results and discussion	*120-124*
	4.5. Post-functionalization	*125-126*
	4.6. Control experiments	*126-131*
	4.7. Plausible mechanism	*131-133*
	4.8. Conclusion	*133*
	4.9. Experimental section	*134-137*
	4.10. Analytical data	*138-154*
	4.11. Crystal data	*155-161*
	4.12. References	*162-165*
	4.13. Selected NMR spectra	*166-177*
Chapter V	***Visible-light-enabled sulfonyl radical-triggered radical cyclization strategy for the efficient synthesis of benzosultams***	*178-221*
	5.1. Introduction	*179*
	5.2. Previous reports	*179-181*
	5.3. Present work	*181*

	5.4. Results and discussion	*181-185*
	5.5. Post-functionalization	*185-186*
	5.6. Control experiments	*186-188*
	5.7. Plausible mechanism	*188-189*
	5.8. Conclusion	*190*
	5.9. Experimental section	*190-192*
	5.10. Analytical data	*193-205*
	5.11. Crystal data	*206-212*
	5.12. References	*213-215*
	5.13. Selected NMR spectra	*216-221*
	Thesis overview	*222*
	List of publications	*223*
	Conferences and workshops	*224*
	Copyright Permission	*225-231*

Abbreviation

Ac	Acetyl
α	Alpha
Å	Angstrom
Ar	Argon
ACN	Acetonitrile
β	Beta
Bn	Benzyl
Bu	Butyl
Cat	Catalyst
D	doublet
Dd	Doublet of doublet
δ	Chemical shift
DA	Donor-acceptor
DCE	1,2-dichloroethane
DCM	Dichloromethane
DMSO	Dimethylsulfoxide
DMF	Dimethylformamide
DMA	Dimethyacetamide
EtOAc	Ethyl acetate
Equiv.	Equivalent
ESI	Electrospray ionization
Et	Ethyl
EWG	Electron-withdrawing group
EDG	Electron-donating group
g	Grams
γ	Gamma
HRMS	High-resolution mass spectrometry
Hz	Hertz
MHz	Mega Hertz
i	Iso
FT-IR	Fourier transform infrared spectroscopy
J	Coupling constant
m	multiplet
mg	Milligram

mmol	Millimole
MS	Molecular sieves
Mp	Melting point
NMR	Nuclear magnetic resonance
Ts	Tosylate
o	*Ortho*
m	*Meta*
p	*Para*
ppm	Parts per million
THF	Tetrahydrofuran
TEMPO	2,2,6,6-tetramethyl-1-piperidinyloxy
t	Tert
TMS	Tetramethylsilane
TS	Transition state
XRD	X-ray diffraction
rt	Room temperature
ORTEP	Oak ridge thermal ellipsoid plot program

Abstract

The contents of the present thesis, entitled "**Light-Driven Molecular Complexity: Cascade Functionalization of Alkynes via Selenium and/or Sulfonyl Radicals**" have been divided into five chapters. The first chapter contains a brief overview of photo-redox catalysis, the importance of organoselenium and heterocyclic sulfone compounds, and some relevant literature reports on organo-photocatalytic selenium or sulfonyl radical addition to alkyne systems, and the last four chapters were based on the results achieved from the experimental works performed during the entire course of the PhD research programme.

Chapter I: A brief introduction to the visible light-induced photocatalytic selenium/sulfonyl radical mediated cascade reaction of alkynes

Visible light-induced photo-redox catalysis has become a valuable tool for facilitating a wide range of organic transformations. Easy access to visible light, combined with its gentle and harmless nature, makes the entire process environmentally benign. The majority of organic compounds require an additional catalyst or photosensitizer, as they are unable to absorb visible light in their ground state. Examples of photocatalysts include organic dyes, semiconductors, and catalysts based on precious metals, such as ruthenium and iridium-polypyridyl complexes. These metal-based compounds exhibit high redox potentials, advantageous photophysical characteristics, and significant absorption. Despite being important in terms of efficiency and photophysical characteristics, their low abundance, toxicity, and expense limit them. In **Chapter I,** we present a brief overview of photo-redox catalysis, the importance of organoselenium and heterocyclic sulfone compounds, and some relevant literature reports on organo-photocatalytic selenium or sulfonyl radical addition to alkyne systems.

Aim of the Thesis:

Over the last few decades, the increasing demand for photo-redox catalysis and the biological significance of organoselenium and heterocyclic sulfone compounds have inspired us to develop a sustainable photocatalytic approach for the construction of organoselenium and heterocyclic sulfone compounds. The primary goal of this thesis is the eosin Y photocatalytic selenium/sulfonyl radical-mediated cascade functionalization of alkynes. Here, we have developed a photocatalytic selenium radical-mediated 1,4-aryl migration process for the synthesis of selenium-containing α, β-unsaturated carboxylic acid and 1,1-diselenide compounds, sulfonyl radical-mediated 5-exo-dig cyclisation of 1,6-diyne and 1,6-enyne to construct the heterocyclic sulfones, and the synthesis of benzosultams from N-alkyl N-propargyl arylsulfonamide with sulfonyl radical addition.

Chapter II: Photocatalytic Selective Synthesis of 1,1-Diselenide Alkene Derivatives and Selenium-Containing α, β-Unsaturated Carboxylic Acids

Chemists are interested in organoselenides because they have several uses in synthetic organic chemistry, functional materials, probe imaging, catalysis, and fluorescence. In mice, bis-selenide alkene derivatives are effective antinociceptive and antioxidant agents. It is also known that certain polyselenide alkene derivatives may inhibit human erythrocyte aminolevulinate dehydratase (d-ALA-D). Derivatives of polyselenides have also been used in a molecular magnetic superconductor device. In **Chapter II,** we discussed how aryl alkynoates can undergo a domino reaction with selenium radicals produced by visible light, resulting in the selective production of 1,1-diselenide alkene derivatives and selenium-containing α, β-unsaturated carboxylic acids, depending on the photocatalytic conditions. The procedure is scalable, gentle, and metal-free. The selectivity was controlled by using a catalytic amount of Eosin Y dye and cesium carbonate as a base, which obstacle the room temperature decarboxylation step, helping to manage the product selectivity. The method produces respectable product yields and exhibits good functional group tolerance. Additionally, by creating the vinylic halides, allylic alcohol, and α, β-unsaturated ester, the synthetic usefulness of this approach was further increased.

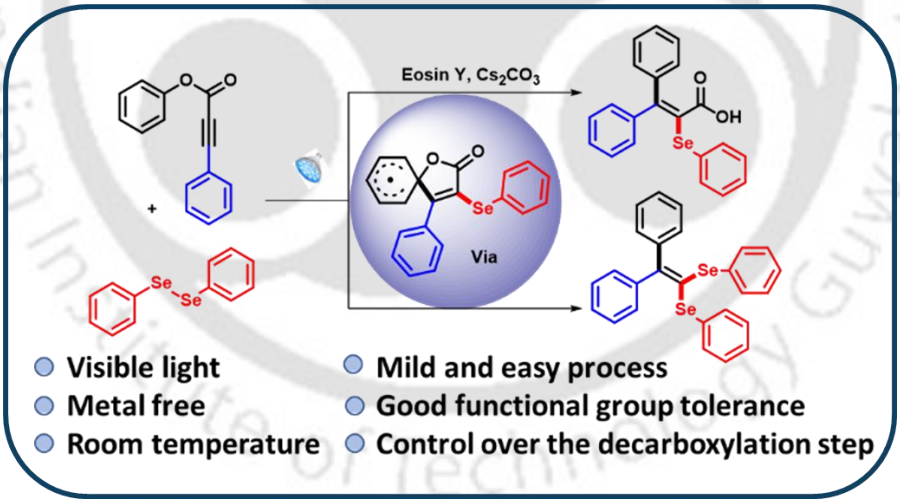

Scheme 1: Schematic representation of Chapter **II**.

Publication: *Org. Lett.* **2022**, *24,* 8180−8185.

Chapter III: Substituent-Dependent, Switchable Synthesis of Nonaromatic and Aromatic Heterocyclic Sulfones Using Visible Light

In synthetic organic chemistry, heterocyclic molecules have long been desirable targets due to their diverse range of biological functions. Likewise, sulfone derivatives are a significant

family of bioactive substances with a wide range of biological characteristics. Natural products, agrochemicals, medicinal, and organic functional materials frequently contain both heterocyclic and carbocyclic sulfones. In **Chapter III**, the switchable synthesis of aromatic and nonaromatic sulfonyl heterocycles was described by using visible light. Here, we reported an intriguing transition between pyrrole and 2,5-dihydropyrrole, which was influenced by the substitution on the N atom of the 1,6-diyne. First, disulfonylated 2,5-dihydropyrrole was produced by the sulfonyl radical-mediated 5-exodig cyclization, which can then be converted to sulfonylated pyrrole through photocatalytic dehydrogenative aromatization (PDA). Our analysis shows that the PDA process is impacted by the type of substituents on the N-atom. The product selectivity depending on the substituent of the N-atom of 1,6-diyne was supported with a strong mechanistic study. This advanced and gentle methodology shows high functional group tolerance and highlights its potential as a strong substitute for conventional synthetic methods.

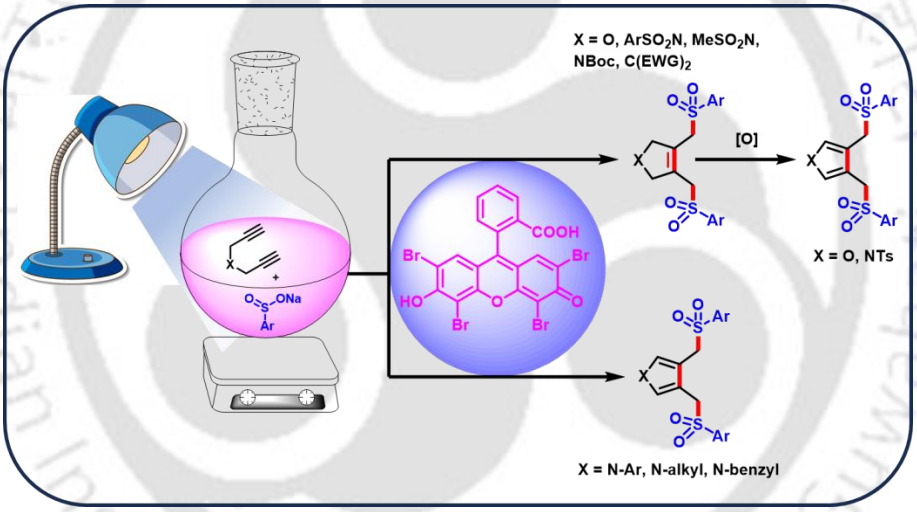

Scheme 2: Schematic representation of Chapter **III**.

Publication: *Org. Lett.* **2024**, *26*, 9357−9362.

Chapter IV: Visible-Light Mediated Divergent Synthesis of Sulfonylated Dihydropyrrole-3-Carboxaldehydes and Tricyclic Sulfones via Sulfonyl Radical Source Modulation

Sulfones are important organosulfur compounds, have a wide range of uses as solvents, polymer constituents, and biopharmaceutical agents. Their usefulness in both industrial and medicinal contexts has been demonstrated by their use as synthetic intermediates in the manufacture of several chemical and physiologically active compounds, including protease and β-lactamase inhibitors. Therefore, developing novel pathways for visible light catalysis-based

functionalized sulfone synthesis would be crucial. In **Chapter IV,** we documented a green and effective photocatalytic approach that selectively forms tricyclic benzofused seven-membered sulfones and sulfonylated dihydropyrrole-3-carboxaldehydes by the cyclization of 1,6-enynes induced by sulfonyl radicals. The switchable nature of the method depends on the selection of a sulfonyl radical source, which determines the selective control between radical cyclization and radical cascade cyclization. Under photocatalytic conditions, sodium aryl sulfinates produced tricyclic benzo-fused seven-membered sulfoness, whereas selenosulfonates produced sulfonylated heterocyclic carboxaldehydes. Selenosulfonates on the exposers of blue LEDs get cleaved to produce sulfonyl and phenylselenyl radicals. Then chemoselective addition of sulfonyl radical to the alkene part, followed by 5-exo-dig cyclization, produces a vinyl radical, which is trapped by phenylselenyl radical. Further, selenosulfonylated intermediates undergo photocatalytic aerobic oxidation to produce sulfonylated 4,5-dihydropyrrole-3-carboxaldehydes. Tricyclic benzo-fused seven-membered sulfones are produced when sodium arylsulfinates react with 1,6-enynes in the presence of photocatalyst EY-Na_2 under blue LEDs in HFIP solvent. Furthermore, the tricyclic sulfone is easily converted into a special exocyclic double-bonded bicyclic seven-membered sulfone. The ring opening may be via quaternary ammonium salts (QAs) formation, followed by Hoffmann-type elimination.

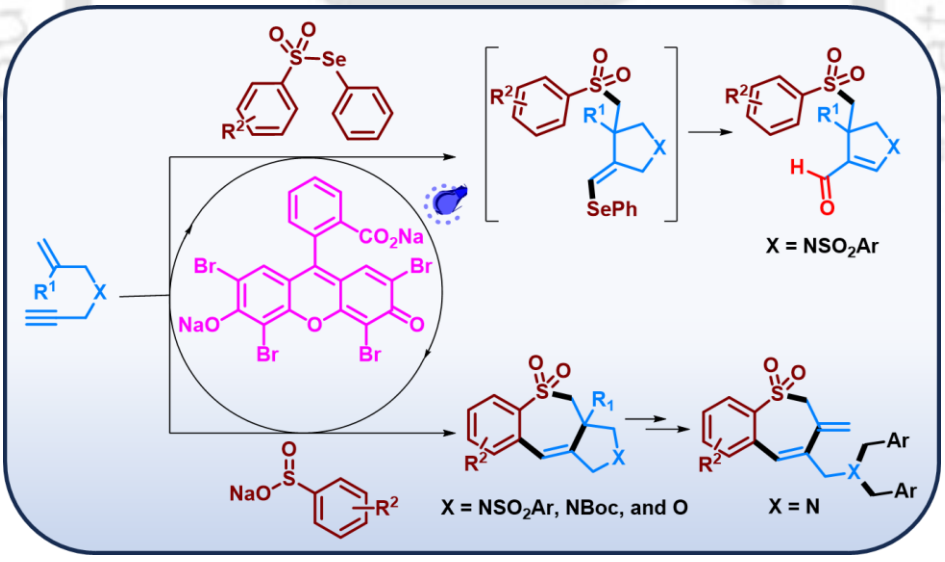

Scheme 3: Schematic representation of Chapter **IV**.

Publication: *Chem. Eur. J.* **2025**, *31*, e02052.

Chapter V: Visible Light-Induced Access of Benzosultams via Sulfonyl Radical-Triggered 6-Exo-Dig Cyclization of N-Alkyl N-Propargyl Arylsulfonamide

Benzosultams are a subclass of bicyclic sulfonamides that are present in many medicines, agricultural agents, physiologically active substances, and OLEDs. They are essential in the synthesis of many drugs because they exhibit a variety of interesting pharmacological actions, including inhibitory, antibacterial, anticancer, anti-inflammatory, and anti-HIV properties. A variety of oxicams, including piroxicam, ampiroxicam, and meloxicam, are used as non-steroidal anti-inflammatory medicines (NSAIDs) to treat arthritis. In **Chapter V**, we show how to use Eosin Y as an active photocatalyst to perform a visible light-induced sulfonyl radical-triggered synthesis of the benzosultam derivatives at room temperature, from N-alkyl-N-propargyl arylsulfonamide and sodium aryl sulfinate salts. The reaction proceeds through a radical pathway via 6-exo-dig cyclization. The technique also exhibits good yields and a broad variety of substrate scope. As a direct alternative to the traditional synthetic methods for the synthesis of benzosultam derivatives, the procedure is gentle, metal-free, less sensitive, and environmentally benign. Further, the synthetic usefulness was extended by isomerizing benzosultams with an exocyclic double bond to the corresponding benzosultams with an endocyclic double bond via simple treatment of KOH at room temperature.

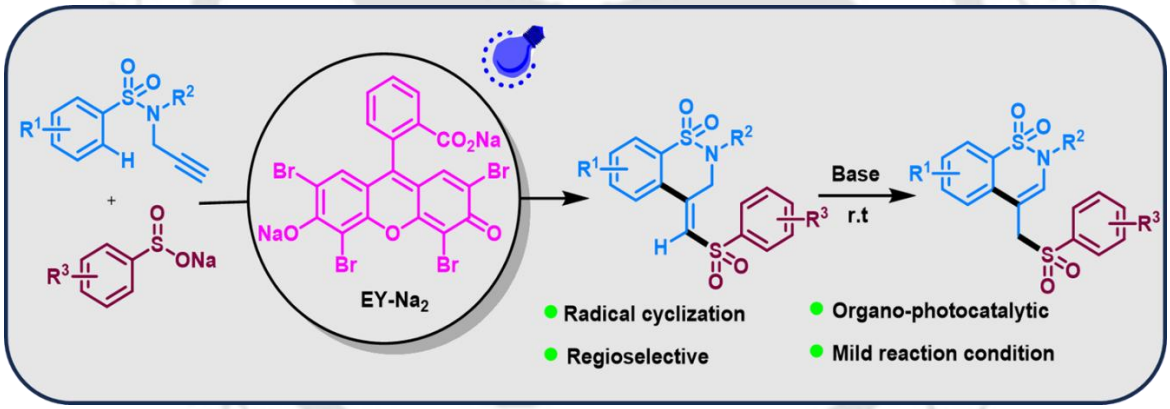

Scheme 4: Schematic representation of Chapter **V**.

Publication: *Org. Lett.* (accepted).

Chapter I:

A brief introduction to the visible light-induced photocatalytic selenium/sulfonyl radical-mediated cascade reaction of alkynes

Chapter I: A brief introduction to the photocatalytic selenium/sulfonyl radical mediated cascade reactions

1.1 Introduction:

In the last few decades, the utilization of visible light as an energy source for organic transformations has increased significantly. Visible light is considered an ideal energy source for organic transformations due to its energy efficiency in reactions at the laboratory scale.[1] Affordable and energy-efficient light sources for photocatalysis are now readily available due to technological advancements and the widespread commercial availability of light-emitting diodes (LEDs), which can produce high-intensity visible light across a limited wavelength range for all colors. In the meantime, difficulties with upscaling and reproducibility of photochemical reactions, two important aspects for any larger-scale industrial application, have been addressed through developments in flow chemistry and the use of transparent flow reactors in photocatalysis.[2]

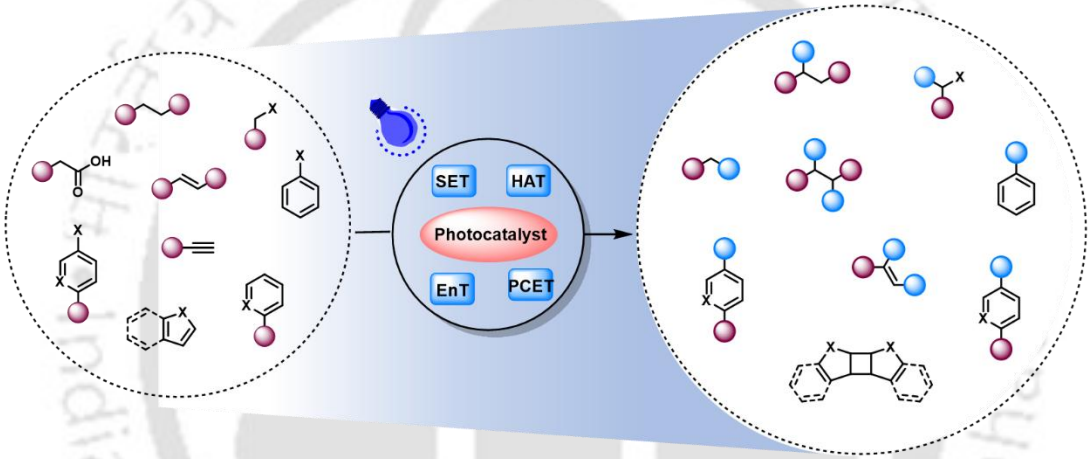

Figure 1.1: Graphical representation of the importance of photoredox catalysis in organic synthesis

Classical photochemistry is a well-established and well-developed branch of chemistry that utilizes ultraviolet light to directly excite organic molecules.[3] Unfortunately, many organic chemists thought that this technique is not easy to apply for practical purposes due to the use of harmful ultraviolet light. The combined use of visible light and photocatalysts or sensitizers has altered this perception. The light source is the only significant difference between the reaction setup in the photochemistry and that of conventional thermal chemistry. Compared to ultraviolet irradiation, which is typically used in classical photochemistry, visible light has lower energy, making the reactions more selective, predictable, and controllable. The process of many photoredox reactions mediated by visible light involves radical or radical ion intermediates. Radical reactions for organic synthesis have regained attention due to the ease

and effectiveness of producing these reactive intermediates through visible light photoredox-catalysis.

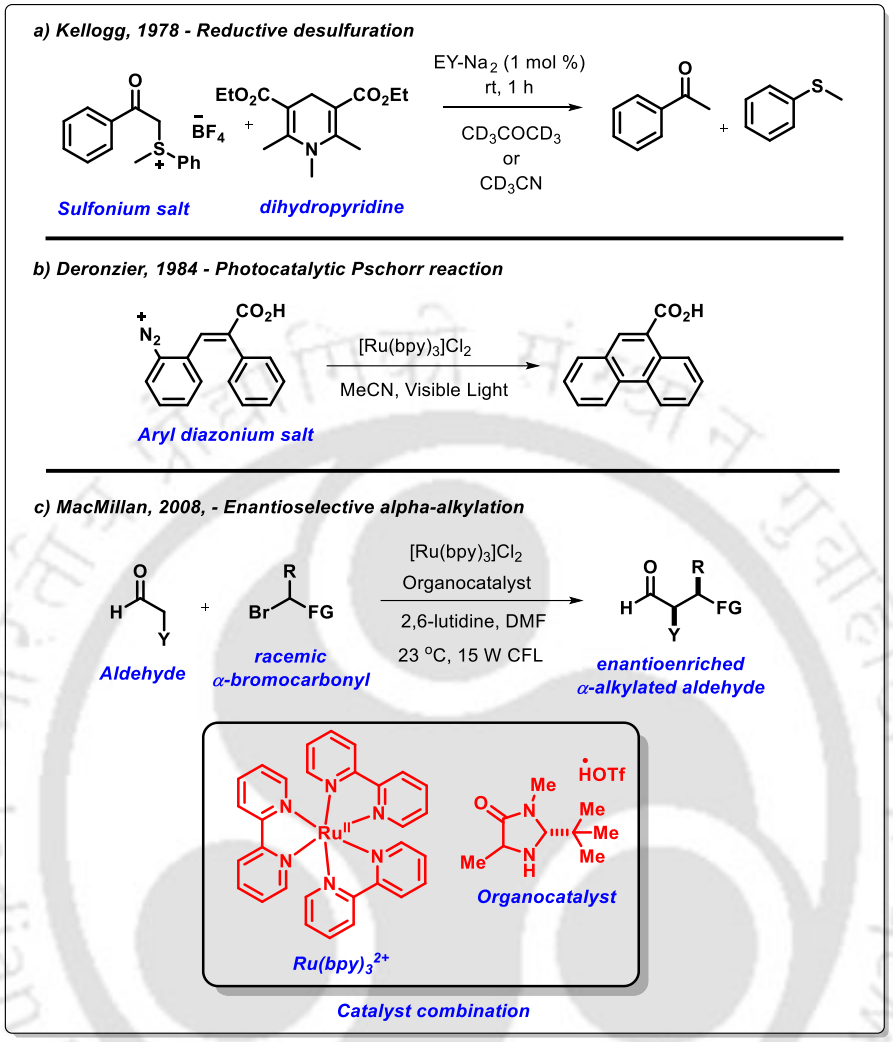

Figure 1.2: Early contribution to organic photoredox catalysis

A significant step in the adoption of photocatalytic techniques by chemists involved in organic synthesis and catalysis was the 2008 report by the MacMillan group on visible-light singly occupied molecular orbital (SOMO) photoredox catalysis, which allowed for enantioselective alpha-alkylations through a combination of photoredox catalysis and organocatalysis (Figure 1.2c).[4] Although significant progress has been made in recent decades, the idea of using visible light to promote organic reactions is not new. To discover where it came from, we must travel back more than a century in time. Photochemical reactions utilizing visible light were developed by Italian chemist Giacomo Ciamician and his colleague Paul Silber at the University of Bologna at the start of the 19th century.[5] In 1978, Kellogg and his coworkers demonstrated the visible light-induced reduction of sulfonium salts to the corresponding

thioethers and alkanes by using an organic dye as the photocatalyst and 1,4-dihydropyridines as the terminal reductant (Figure 1.2a). The first visible-light photocatalytic Pschorr reaction was published by Alain Deronzier using the aryl diazonium salts and $[Ru(bpy)_3]Cl_2$ as the photocatalyst to provide the phenanthrene product (Figure 1.2b).[6] Using nearly visible light (395 nm), Ganesh Pandey, an Indian organic chemist, discovered photocatalytic cycloadditions.[7] Among many others, Frederick Lewis (Northwestern University, Illinois) in the United States, Vincenzo Balzani (Bologna) and Angelo Albini (Pavia) in Italy, and Janine Cossy (Paris) in France studied the application of photoinduced electron-transfer processes in organic synthesis.[8,9]

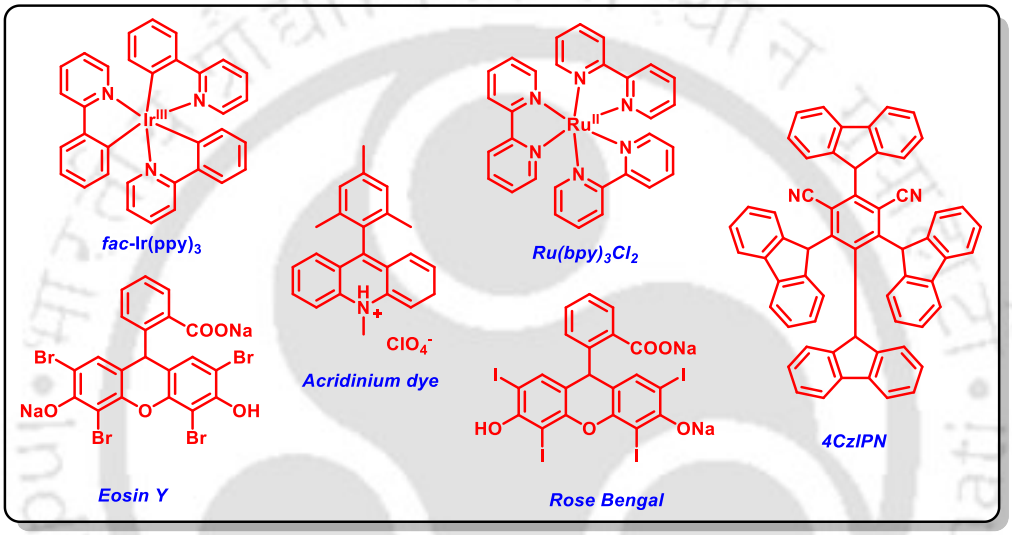

Figure 1.3: Most commonly used photo redox catalysts

The commonly used photoredox catalysts for these transformations are redox-active metal complexes like ruthenium or iridium polypridyl complexes,[10] organic dyes such as eosin Y or rose bengal,[11] and to a lesser extent, heterogeneous photocatalysts like carbon nitrides or inorganic semiconductors (Figure 1.3).[12] Although ruthenium and iridium polypyridyl complexes exhibit good photophysical characteristics in visible light photocatalysis, their high cost and potential toxicity result in significant drawbacks for larger-scale applications.[13] In photoredox catalysis, organic dyes have proven to be a promising alternative to transition metal complexes.[14] They are usually cheaper, less hazardous, easier to handle, and in certain situations, even more effective than inorganic and organometallic catalysts.[15]

1.2 General photocatalytic single electron transfer (SET) mechanism:

In the presence of light photocatalyst gets excited to a higher energy state. After getting excited, it can follow either the oxidative quenching cycle or the reductive quenching cycle. In the case of the oxidative quenching cycle, the excited catalyst first donates one electron to the acceptor reactant (A) and itself becomes the oxidized cation radical. Further, this oxidized form of the catalyst takes one electron from the donor reactant (D) and goes back to its ground state. Similarly, in the case of reductive quenching cycle excited catalyst first takes one electron from the donor reactant (D) and itself goes to a reduced anion radical form. Then this anion radical form of the catalyst gives one electron to the acceptor reactant (A) and comes back to the ground state. In both these quenching cycles, it will generate some reactive key intermediates in the form of radical, radical cation, radical anion, and ion, which are responsible for carrying forward a photocatalytic reaction (Figure 1.4).

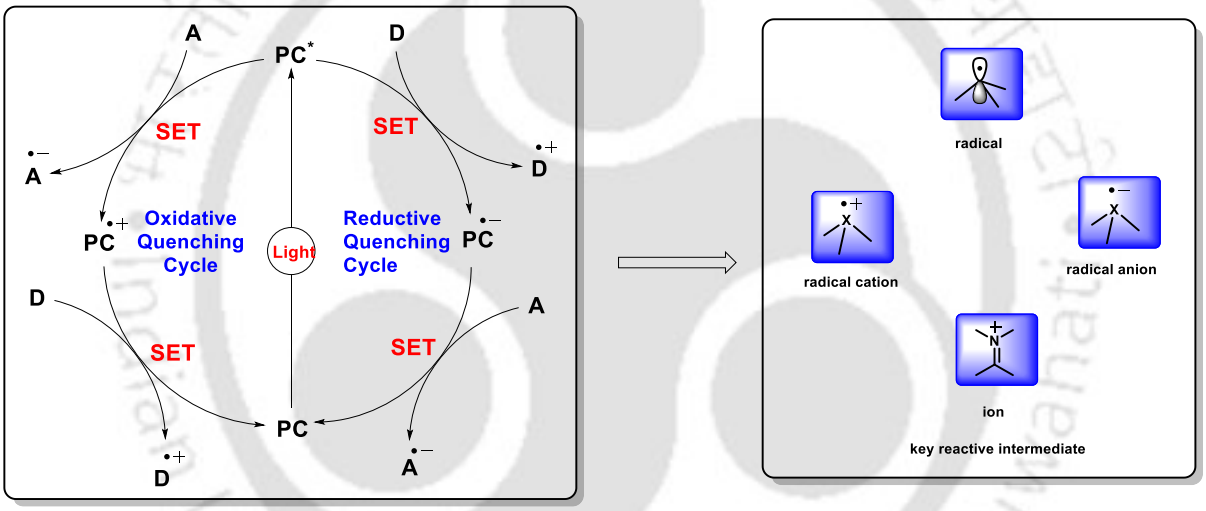

Figure 1.4: General single electron transfer (SET) mechanism and key reactive intermediates

As of right now, a wide range of significant organic transformations have been accomplished through photoredox catalysis using visible light. These include simple oxidations[16] and reductions,[17] C–C bond formation,[18-20] and numerous carbon–heteroatom bond-forming reactions, such as C–S, C–N, C–O, and C–P bonds,[21-24] as well as cycloaddition reactions.[25] Due to the mild and efficient nature of the photocatalytic radical addition reaction, the present thesis primarily focused on the visible light-induced photocatalytic selenium and sulfonyl radical addition to the alkyne system for the synthesis of organoselenium and sulfonyl compounds (Figure 1.1).

1.3 Importances of organoselenium compounds:

Jons Jacob Berzelius, a Swedish chemist, discovered selenium in 1817.[26] The synthesis of diethyl selenide by Lowig in 1836 marked the beginning of the study of organoselenium, and Rathke isolated the pure form of the compound in 1869, several years later.[27] Simple aliphatic compounds, including selenides (RSeR), diselenides (RSeSeR), and selenols (RSeH), were synthesized in the early stages of organoselenium chemistry. However, the development of selenium chemistry was hindered by the unpleasant odour of these molecules, their instability, and the challenges of handling and purifying them.

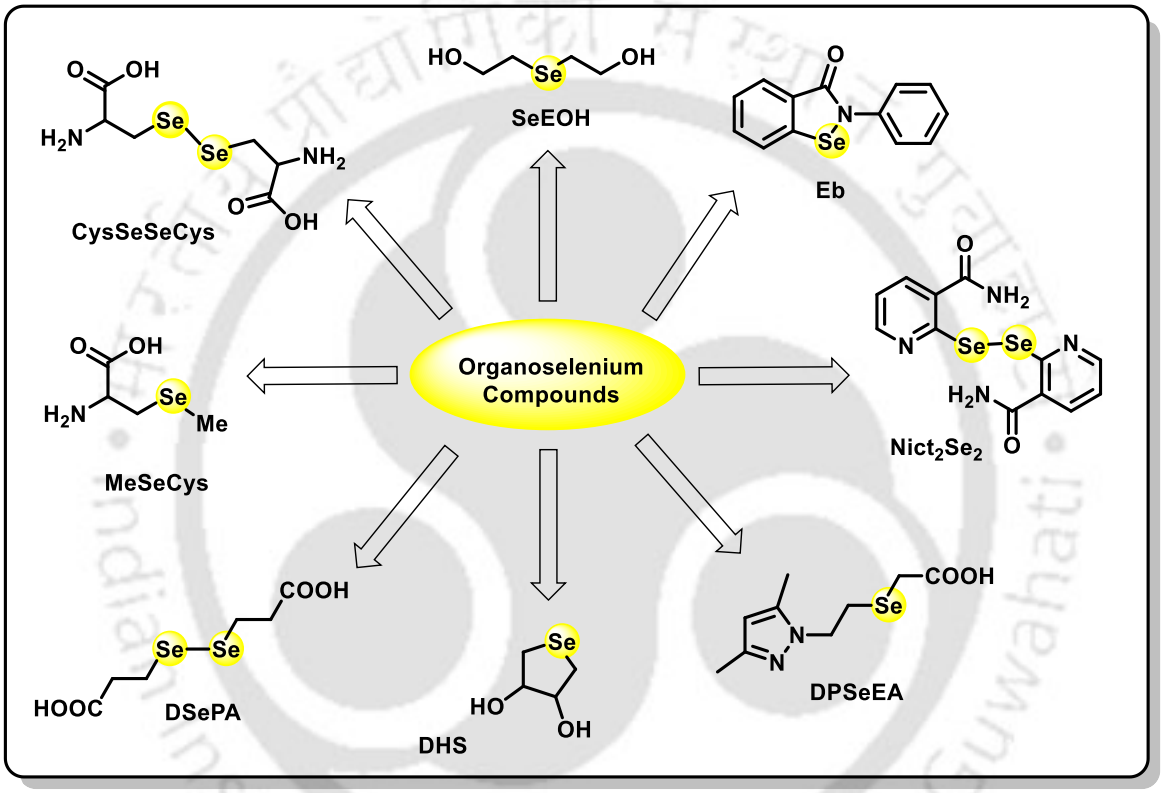

Figure 1.5: Some biologically important organoselenium compounds

As an essential trace element, selenium is mostly found in the human body as selenocysteine.[28] The discovery of selenocysteine in the active site of glutathione peroxidase, a crucial enzyme functioning as an antioxidant in biological systems, has increased attention in selenium chemistry.[29] The chemistry of organoselenium has garnered a lot of interest in recent years because of its unique chemical reactivity and even its increasing significance in catalysis.[30] Aside from a few intriguing uses in material science, compounds containing selenium are being studied extensively in the pharmaceutical sector due to their wide spectrum of bioactivities (e.g., as antioxidants, anticancers, antimicrobials, antivirals, or antitumoral drugs). Figure 1.5 lists a few instances of bioactive compounds that contain selenium.[31] Therefore, developing

efficient methods for synthesizing a range of organic compounds containing selenium is highly desired. The selenylating agent is often a diselenide RSeSeR, where R is typically an aryl group. Diselenides exhibit an absorption tail in the visible region (λ < 500 nm) as a result of the n → σ* transition.[32] These compounds can be excited by direct exposure to visible light or with the aid of a photocatalyst (PC), which results in the homolytic breaking of the Se-Se bond to generate aryl/alkyl selenium radical.[33]

1.4 Selected examples for selenylation reactions of alkynes:

Alkynes are important reagents in radical addition reactions because of their numerous applications in organic synthesis. It is very useful from a synthetic standpoint to initiate a cascade reaction through the radical addition of alkynes, as this provides a way to create complex molecular structures with only a few steps and typically mild conditions. Alkynes can be seleno-functionalized via the selenium radical addition, which offers an effective method of producing organoselenium compounds.

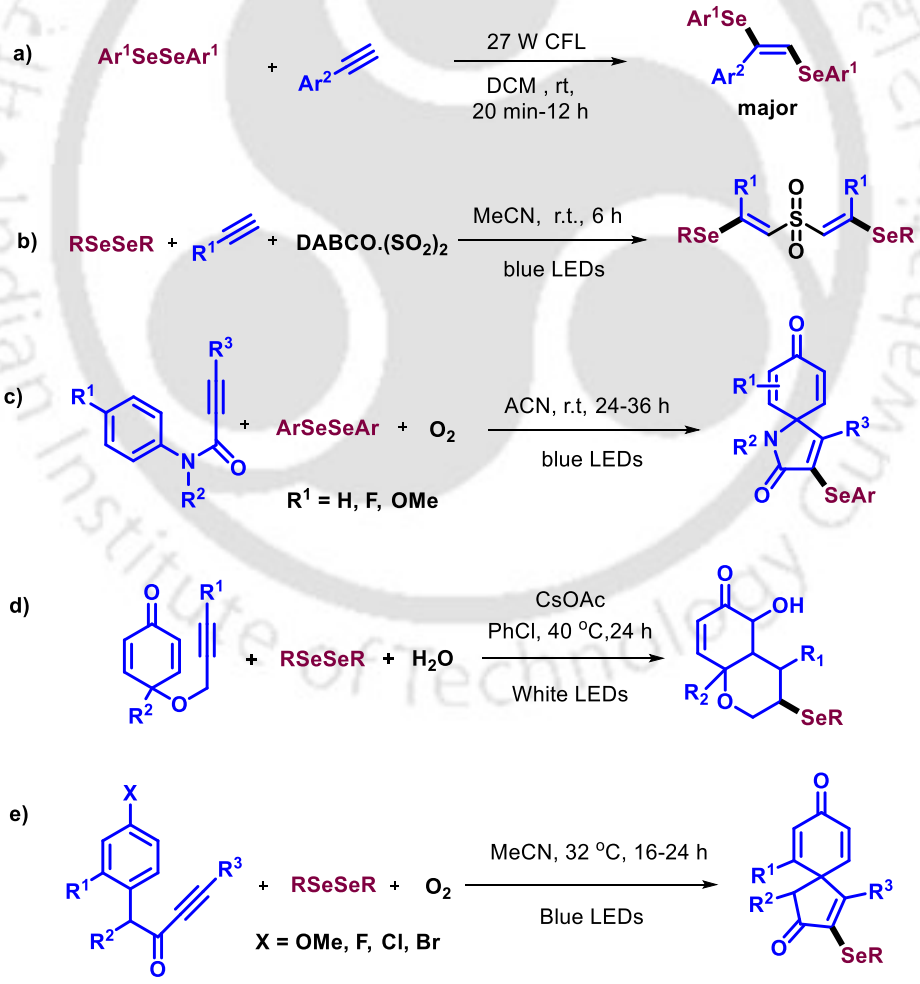

Figure 1.6: Selected examples for selenylation of alkynes

Recently, various methods such as photocatalytic, electrochemical, and organocatalyzed selenylation have been utilized in the synthesis of organoselenium compounds. In 2018, Schneider and co-workers reported the photoinduced selenylation of alkynes to synthesize 1,2-bis-arylylselanyl alkenes. Thermal synthesis of such derivatives typically requires severe reaction conditions as well as transition-metal catalysts and reductants.[34] The photochemical methods for the synthesis of 1,2-bis-arylylselanyl alkenes take place at room temperature and without the need for additives. The mixture of arylacetylene and diaryl diselenide in DCM was irradiated with white light at room temperature to generate the aryl selenium radical, which, upon addition of the C-C triple bond, produces the mixture of E/Z 1,2-bis-arylylselanyl alkenes. Then, photoisomerization of the Z isomer to E isomer exclusively generates the E-stereoisomer (Figure 1.6a).[35] The Xu group described the visible light-induced selenation of the terminal alkynes and the incorporation of sulfur dioxide to synthesize β-sulfonylvinylselanes with high selectivity for the E-configuration. This multicomponent cascade reaction requires two molecules of terminal alkynes, two fragments of selenyl radicals, and DABCO.$(SO_2)_2$. The plausible mechanism follows a cascade sequence consisting of selenyl radical formation from the diaryldiselenide under the exposure of visible light, then selenium radical addition to the alkyne, followed by sulfur dioxide insertion (Figure 1.6b).[36]

Baidya and his group demonstrated that N-aryl alkynamides can undergo a selenylative spirocyclization reaction at room temperature, resulting in the production of 3-selenospiro [4,5] trienones by using O_2 (in a balloon) as the primary oxidant under visible light irradiation (Figure 1.6c).[37] A metal-catalyst-free cyclization method for alkyne-tethered cyclohexadienones under visible light irradiation conditions was reported by the Xin group.[38] Diselenides produce selenyl radicals when exposed to light, and these radicals then combine with alkynes to form vinyl radicals, which undergo intramolecular cyclization and are trapped by another selenyl radical, followed by nucleophilic substitution with water in the presence of CsOAc, providing the final product (Figure 1.6d). The Sahoo group studied the synthesis of selenylative spiro-cyclohexadienones through a visible light-mediated dearomative selenylative carbo-spirocyclization of aromatic homologated ynones using molecular oxygen as the oxidant (Figure 1.6e).[39]

1.5 Importances of sulfone compounds:

Sulfones are significant organosulfur compounds that have a wide range of uses as biopharmaceutical agents, solvents, and polymer constituents.[40] Their significance in medicine and industry has been demonstrated by their use as synthetic intermediates in the synthesis of several chemical and physiologically active compounds, including protease and β-lactamase

inhibitors.[41] Naturally occurring chemicals, manufactured medicines, biologically active compounds, and organic functional materials are all rich in sulfonyl groups (Figure 1.7).[42] They can also act as reagents in a range of synthetic transformations or as multifunctional building blocks for additional modification.[43]

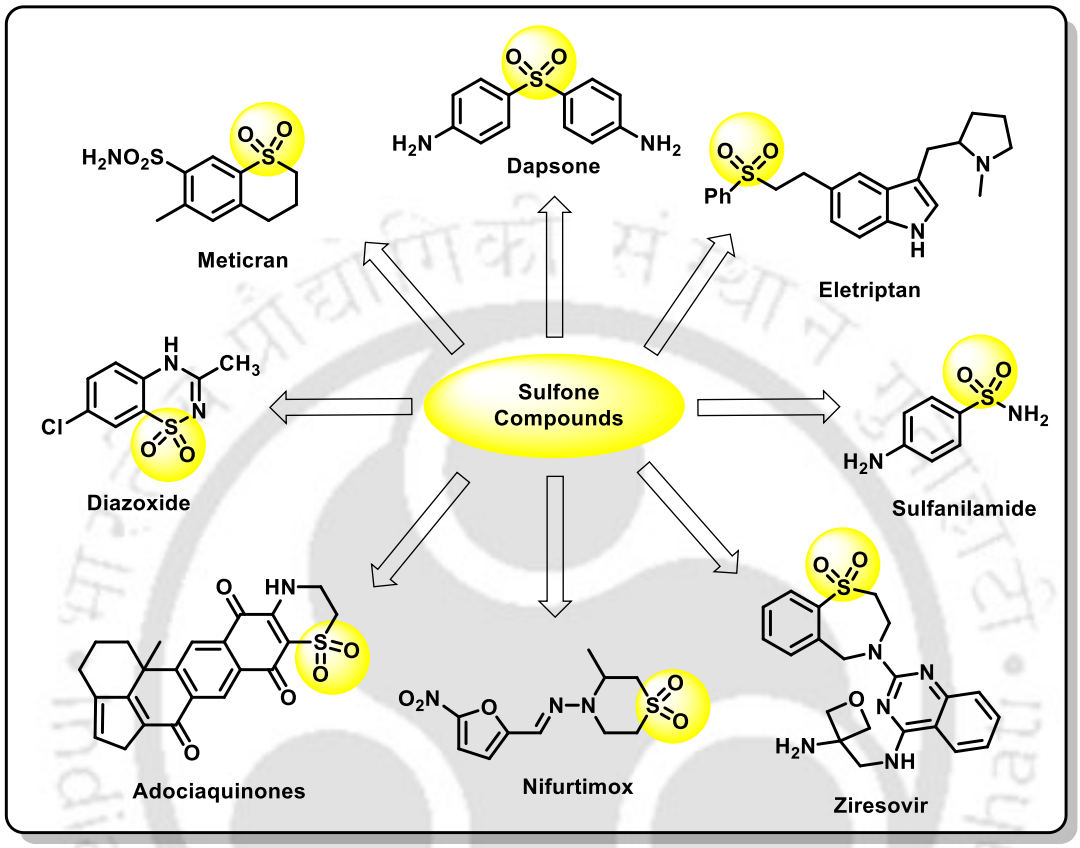

Figure 1.7: Representative examples of biologically active sulfone compounds

Throughout the past few decades, the synthesis of sulfonated derivatives has drawn considerable interest from the materials, agrochemical, and pharmaceutical industries due to the distinct structure and electronic characteristics of sulfonyl groups.[44] Conventional approaches to the synthesis of sulfonated compounds mostly depended on oxidation of sulfides,[45] nucleophilic aromatic substitutions,[46] and Friedel-Crafts-type sulfonylation of arenes.[47] These techniques, however, typically suffer from severe reaction conditions, including high temperatures, harmful chemicals, and the addition of potent oxidants and stoichiometric acids.[48] Thus, there remains a significant need for efficient and sustainable synthetic pathways to produce these sulfonyl molecules.

1.6 Selected examples for sulfonylation reactions of alkynes:

Alkynes can easily produce different carbon-centered radicals via radical addition, which can participate in numerous reactions like vicinal difunctionalization to produce stereoselective

olefins, oxidative functionalization for the synthesis of β-ketosulfoxides, annulation and cycloaddition reactions, etc. In 2018, Kim and Han's research group collaboratively reported a visible-light-mediated, *fac*-Ir(ppy)$_3$-catalyzed regio- and stereoselective chlorosulfonylation of internal aryl–alkyl alkynes with various aliphatic, aromatic, and heteroaromatic sulfonyl chlorides.[49]

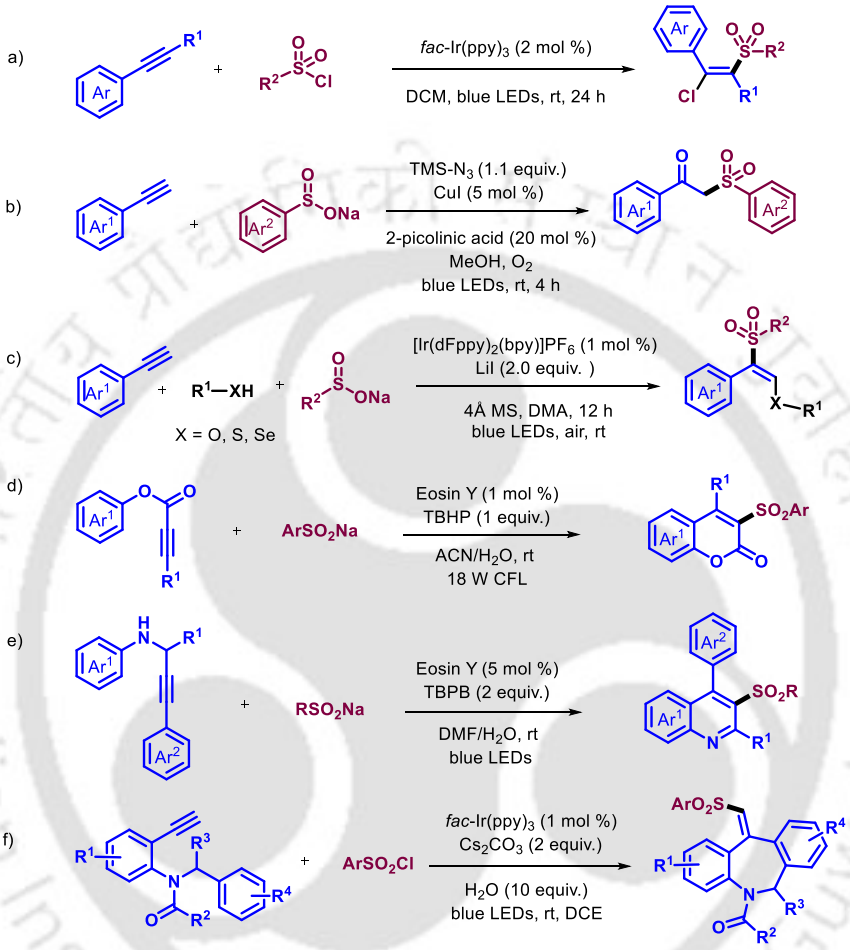

Figure 1.8: Selected examples for the sulfonylation of alkynes

The synthesis of (E)-β-chlorovinyl sulfone derivatives at room temperature under additive-free conditions was demonstrated using this synthetic transformation effectively and appealingly. Notably, the reaction demonstrated a high degree of regioselectivity, with the Cl atom attached to the carbon atom next to the aryl group and the sulfonyl group primarily positioned on the carbon atom next to the alkyl group. The high regioselectivity for the sulfonyl radical addition may arise due to the generation of vinyl radicals, which are stabilized by the nearby aryl ring (Figure 1.8a). Hwang and his group reported an oxy-sulfonylation of terminal alkynes using visible-light-induced trimethylsilyl azide (TMS-N$_3$) assisted copper-catalysis to synthesize β-keto sulfone.[50] TMS-N$_3$ facilitates the production of sulfonyl radicals, which, upon exposure

to light, decompose into N_2 gas, thereby accelerating the process. This oxidative coupling reaction follows *in situ* generation of a copper complex, which gets photoexcited to catalyze the C-S bond formation reaction via single electron transfer (SET) with molecular oxygen as a sustainable oxidant (Figure 1.8b). Photoinduced multicomponent radical cross-coupling of terminal alkynes with sulfinates and a variety of alcohols, thiophenols, or selenophenols has been investigated for α-sulfonylation of alkynes by Wu and coworkers.[51] They have developed an aerobic photoinduced and LiI-accelerated multicomponent α-sulfonylation of terminal alkynes with a range of sulfinates and easily accessible alcohols, thiophenols, and selenophenols to produce 1,2-hetero sulfonylation products in high α-selectivity and stereoselectivity. The mechanism of the reaction follows a sulfonyl radical pathway (Figure 1.8c). The Wang group developed a novel, straightforward method for the synthesis of 3-sulfonated coumarins by performing an efficient arylsulfonylation of alkynes with arylsulfinic acids, triggered by visible light (Figure 1.8d).[52] Huang and coworkers demonstrated a metal-free visible-light-promoted radical cascade reaction of N-propargylanilines with sodium sulfinates as precursors of sulfonyl radicals.[53] This gentle procedure is a quick and effective way to create 3-sulfonylquinolines by forming C–S and C–C bonds simultaneously (Figure 1.8e). Chen and his group describe a novel visible-light photoredox-catalysis technique for the synthesis of sulfonated dibenz[b,e]azepines.[54] Sulfonated dibenzazepine is produced by an alkyne addition reaction followed by a 7-membered radical cyclization step, which is made possible by using cheap and readily accessible sulfonyl chlorides as the sulfonyl radical source (Figure 1.8f).

1.7 Photocatalytic radical cascade cyclization of 1,6-enynes to generate molecular complexity:

Cyclic compounds have more conformational rigidity than acyclic structures because of their stable molecular scaffold. Due to these behaviors, carbo- and heterocycles are frequently found in natural compounds that show promising bioactive properties that are very relevant for medicinal chemistry applications.[55] In the synthesis of carbo and heterocyclic compounds through cyclization, the bond-forming step that transforms the acyclic precursor into the intended cyclic compound is crucial. Domino reactions were already recognized as a practical and effective method in this field.[56] In the last few decades, for the construction of new chemical bonds radical addition strategy has become an effective synthetic technique and attracted a lot of attention.[57] In comparison with transition metal-catalyzed coupling cyclization reactions, radical chemistry is typically characterized by mild reaction conditions and found to be a good alternative for the coupling cyclization process. Moreover, the wide availability of

potential radical precursors and initiation strategies further supports the adaptability of these transformations. Specifically, following intramolecular radical addition, a new cycle is often created, with the cyclization process according to the basic principles known as the Baldwin rules.[58] Particularly useful in the creation of monocyclic and fused cyclic compounds are cascade radical reactions, which involve two or more radical additions in a single transformation, because the core motifs are created in a single step.[59]

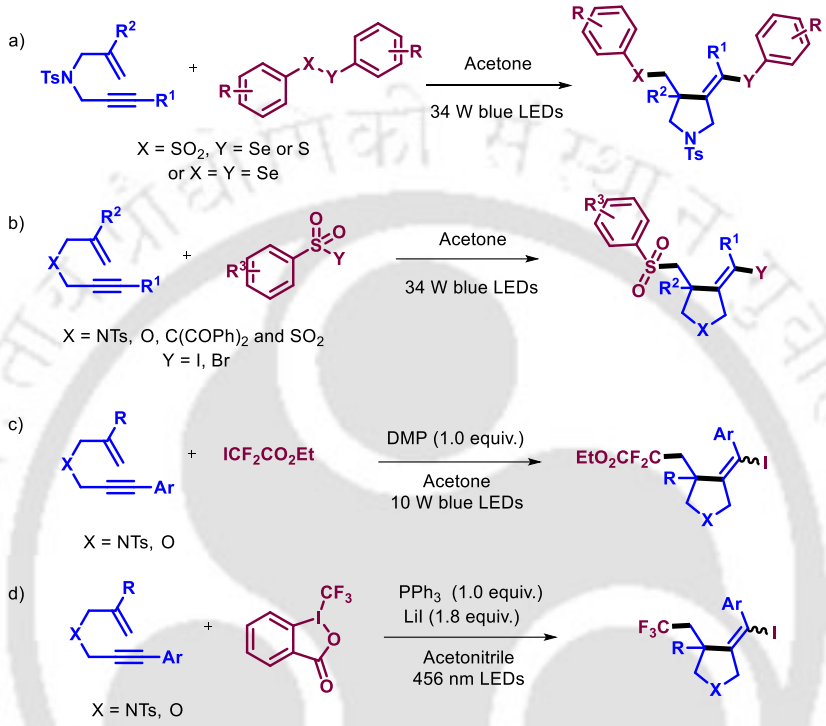

Figure 1.9: Formation of five-membered monocycles from 1,6-enynes

For a long time, 1,6-enynes have been known as classic radical acceptors in organic synthesis, enabling the construction of a wide range of mono- and polycyclic ring structures through cascade radical cyclizations.[60] Wang and colleagues demonstrated a metal and oxidant-free radical cascade cyclization of unactivated 1,6-enynes with selenosulfonates under visible light irradiation to synthesize substituted pyrrolidines bearing chalcogens.[61] Under the exposure of light, selenosufonates get homolytically cleaved to generate aryl selenium and aryl sulfonyl radical. Then, sulfonyl radical-triggered cyclization of 1,6-enynes, followed by selenium radical trapping, produces the substituted pyrrolidine product with selenium and sulfonyl functionality (Figure 1.9a). Later, the same group described a three-component radical iodosulfonylative cyclization of 1,6-enynes using an analogous photo-induced method.[62] Under visible light irradiation, catalyst, and oxidant-free conditions, 1,6-enyne reacted with sulfonyl halides as sulfonyl radical precursors, generating sulfonyl radicals which trigger the

radical addition, cyclization, and iodination cascade reaction to produce the cyclized product (Figure 1.9b).

In 2022, Li and coworkers documented the difluoroalkylation/cyclization/iodination of 1,6-enynes with ethyl difluoroiodoacetate (ICF_2CO_2Et) through a visible light-driven base-promoted radical cascade reaction.[63] Under exposure to visible light, the authors reported that ICF_2CO_2Et and N, N′-dimethylpiperazine (DMP) may combine to create a complex that could subsequently liberate the CF_2-containing radical, which attacks the double bond of enyne and followed by a 5-exo-dig cyclization. Then an iodine atom from ICF_2CO_2Et is captured by an intermediate vinyl radical, and the (Z)-isomer is preferentially produced as a desired product with strong configurational selectivity (Figure 1.9c). At the same time, they have also described another visible light-mediated PPh_3/LiI-promoted intermolecular tandem trifluoromethyl radical addition, 5-exo-dig cyclization, and iodination of 1,6-enynes with Togni's reagent.[64] Where Togni's reagent is used for the trifluoromethyl radical source and lithium iodide as the iodine source. It was assumed that the reaction proceeded via the formation of an electron donor-acceptor (EDA) complex by the combination of PPh_3, LiI, and Togni's reagent (Figure 1.9d).

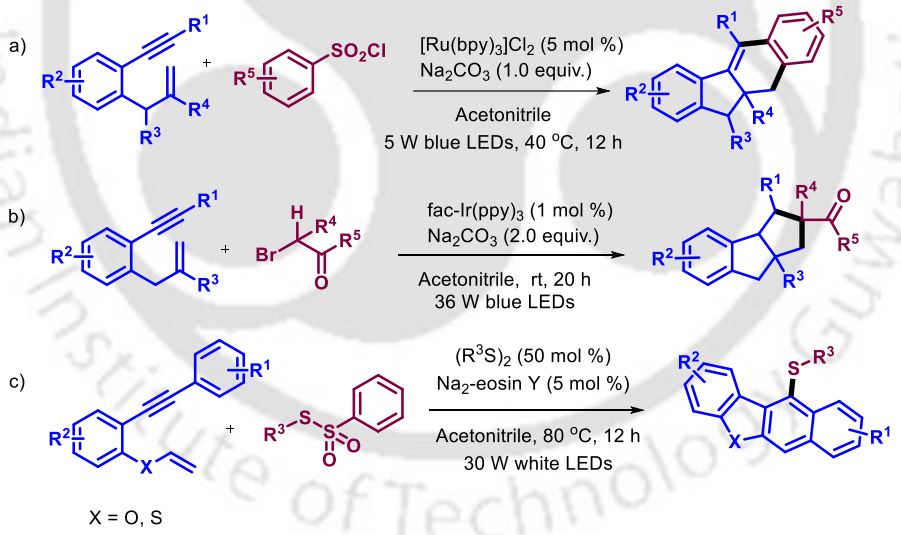

Figure 1.10: Formation of fused cyclic compounds from 1,6-enynes.

The synthesis of polycyclic compounds by a radical bicyclization strategy seemed more difficult than the formation of monocycles, and as a result, it was the subject of continuous investigation. In 2013, Li and his group showed a visible light-induced photocatalytic tandem cyclizations of 1,6-enynes with aryl sulfonyl chloride.[65] Two modes of operation for aryl sulfonyl chlorides were discovered. Firstly, they act as a precursor for aryl radicals that add to

the C-C triple bond of 1,6-enynes and followed by a cascade cyclization. Furthermore, the accessible *ortho*-C(aryl)–H bond takes part in the cascade cyclization as well to deliver the final product (Figure 1.10a). Soon after, the same group demonstrated a technique for the construction of useful fused polycyclic compounds through a one-step functionalization of C(sp^3)–Br and C(sp^3)–H bonds, which intriguingly proceeds via a new light-induced 1,5-hydride radical shift (Figure 1.10b).[66] Chen and his group illustrated a visible light-mediated cascade cyclization/aromatization of 2-vinyloxy arylalkynes with thiosulfonates to produce the thio-substituted dibenzofuran derivatives.[67] According to mechanistic investigations, the essential intermediate was the thiosulfonylation product of 2-vinyloxy arylalkyne. Additionally, it was observed that the disulfide additive plays a crucial role in the aromatization process that takes place by hydrogen abstraction (Figure 1.10c).

1.8 Concluding remarks:

The aforementioned discussion illustrated how the application of photoredox catalysis garnered a great deal of attention and became a vital tool in the field of synthetic organic chemistry for the development of environmentally friendly, sustainable, and atom-economic methods for the preparation of key building blocks. But the photoredox catalysis basically relies on the use of noble iridium or ruthenium metal-based complexes, which are high in cost and expose potential toxicity to the environment. Since the world is moving towards sustainability, scientists are looking for alternatives, and they have found that organic dye molecules can serve a similar purpose. They are less expensive, safer, simpler to work with, and in some cases, even more efficient than inorganic and organometallic catalysts. Apart from that, the biological significance of the organoselenium and the sulfonyl compounds was also discussed in this section. So, the development of an efficient method for the synthesis of organoselenium and sulfonyl compounds using visible-light photoredox catalysis is in high demand.

1.9 Aim of the thesis:

This thesis aims to introduce new, efficient photocatalytic approaches for the synthesis of organoselenium and organosulfonyl molecules. To achieve this, inexpensive and readily available organic dyes have been selected as photocatalysts, offering a cost-effective and sustainable alternative to traditional metal-based systems. The strategy relies on visible-light activation to produce sulfonyl and selenyl radicals, which then participate in cascade radical reactions with alkynes. This approach is designed to provide a useful and practical route for synthesizing valuable selenium- and sulfur-containing molecular frameworks under mild, environmentally benign conditions.

1.10 References:

1. Anastas, P. T.; Warner, J. C. *Green Chemistry: Theory and Practice*; Oxford University Press: New York, 1998.

2. Cambié, D.; Bottecchia, C.; Straathof, N. J. W.; Hessel, V.; Noël, T. Applications of Continuous-Flow Photochemistry in Organic Synthesis, Material Science, and Water Treatment. *Chem. Rev*. **2016**, *116*, 10276−10341.

3. Klán, P.; Wirz, J. *Photochemistry of Organic Compounds: From Concepts to Practice*; Wiley-VCH: Weinheim, 2009.

4. Nicewicz, D. A.; MacMillan, D. W. C. Merging Photoredox Catalysis with Organocatalysis: The Direct Asymmetric Alkylation of Aldehydes. *Science* **2008**, *322*, 77−80.

5. Ciamician, G. The Photochemistry of the Future. *Science* **1912**, *36*, 385−394.

6. Cano-Yelo, H.; Deronzier, A. Photocatalysis of the Pschorr Reaction by Tris-(2,2′-bipyridyl)ruthenium(II) in the Phenanthrene Series. *J. Chem. Soc., Perkin Trans. 2* **1984**, *6*, 1093−1098.

7. Pandey, G.; Hajra, S.; Ghorai, M. K.; Kumar, K. R. Designing Photosystems for Harvesting Photons into Electrons by Sequential Electron-Transfer Processes: Reversing the Reactivity Profiles of α, β-Unsaturated Ketones as Carbon Radical Precursor by One-Electron Reductive β-Activation. *J. Am. Chem. Soc.* **1997**, *119*, 8777-8787.

8. Mariano P. S. *Advances in Electron Transfer Chemistry*, 1996, JAI Press, London.

9. Mattay, J. Photoinduced Electron Transfer V. *Top. Curr. Chem*. **1993**, volume *168*.

10. Prier, C. K.; Rankic, D. A.; MacMillan, D. W. C. Visible Light Photoredox Catalysis with Transition Metal Complexes: Applications in Organic Synthesis. *Chem. Rev.* **2013**, *113*, 5322−5363.

11. Romero, N. A.; Nicewicz, D. A. Organic Photoredox Catalysis. *Chem. Rev.* **2016**, *116*, 10075−10166.

12. Kisch, H. Semiconductor Photocatalysis-Mechanistic and Synthetic Aspects. *Angew. Chemie Int. Ed.* **2013**, *52*, 812−847.

13. Ravelli, D.; Fagnoni, M.; Albini, A. Photoorganocatalysis. What For? *Chem. Soc. Rev.* **2013**, *42*, 97−113.

14. (a) Huang, L.; Zhao, J. Iodo-Bodipys as Visible-Light-Absorbing Dual-Functional Photoredox Catalysts for Preparation of Highly Functionalized Organic Compounds by Formation of C−C Bonds via Reductive and Oxidative Quenching Catalytic Mechanisms. *RSC Adv.* **2013**, *3*, 23377−23388. (b) Huang, L.; Zhao, J. C60-Bodipy Dyad Triplet Photosensitizers as Organic Photocatalysts for Photocatalytic Tandem Oxidation/[3 + 2] Cycloaddition

Reactions to Prepare Pyrrolo[2,1-a]isoquinoline. *Chem. Commun.* **2013**, *49*, 3751−3753. (c) Guo, S.; Zhang, H.; Huang, L.; Guo, Z.; Xiong, G.; Zhao, J. Porous Material-Immobilized Iodo-Bodipy as an Efficient Photocatalyst for Photoredox Catalytic Organic Reaction to Prepare Pyrrolo[2,1a]Isoquinoline. *Chem. Commun.* **2013**, *49*, 8689-8691. (d) Zhao, J.; Wu, W.; Sun, J.; Guo, S. Triplet photosensitizers: from molecular design to applications. *Chem. Soc. Rev.* **2013**, *42*, 5323−5351.

15. (a) Nicewicz, D. A.; Nguyen, T. M. Recent Applications of Organic Dyes as Photoredox Catalysts in Organic Synthesis. *ACS Catal.* **2014**, *4*, 355−360. (b) Teo, Y. C.; Pan, Y.; Tan, C. H. Organic Dye-Photocatalyzed Acylnitroso Ene Reaction. *ChemCatChem* **2013**, *5*, 235−240. (c) Cantillo, D.; de Frutos, O.; Rincon, J. A.; Mateos, C.; Kappe, C. O. Continuous Flow α-Trifluoromethylation of Ketones by Metal-Free Visible Light Photoredox Catalysis. *Org. Lett.* **2014**, *16*, 896−899.

16. Lechner, R.; König, B. Oxidation and Deprotection of Primary Benzylamines by Visible Light Flavin Photocatalysis. *Synthesis* **2010**, *2010*, 1712−1718.

17. Ghosh, T.; Slanina, T.; König, B. Visible Light Photocatalytic Reduction of Aldehydes by Rh(III)−H: A Detailed Mechanistic Study. *Chem. Sci.* **2015**, *6*, 2027−2034.

18. Ghosh, I.; Marzo, L.; Das, A.; Shaikh, R.; König, B. Visible Light Mediated Photoredox Catalytic Arylation Reactions. *Acc. Chem. Res.* **2016**, *49*, 1566−1577.

19. (a) Tellis, J. C.; Primer, D. N.; Molander, G. A. Single-Electron Transmetalation in Organoboron Cross-Coupling by Photoredox/Nickel Dual Catalysis. *Science* **2014**, *345*, 433−436. (b) Jouffroy, M.; Primer, D. N.; Molander, G. A. Base-Free Photoredox/Nickel Dual-Catalytic Cross-Coupling of Ammonium Alkylsilicates. *J. Am. Chem. Soc.* **2016**, *138*, 475−478. (c) Zhang, P.; Le, C. C.; MacMillan, D. W. C. Silyl Radical Activation of Alkyl Halides in Metallaphotoredox Catalysis: A Unique Pathway for Cross-Electrophile Coupling. *J. Am. Chem. Soc.* **2016**, *138*, 8084−8087.

20. Johnston, C. P.; Smith, R. T.; Allmendinger, S.; MacMillan, D. W. C. Metallaphotoredox-catalysed sp3-sp3 cross-coupling of carboxylic acids with alkyl halides. *Nature* **2016**, *536*, 322−325.

21. Majek, M.; von Wangelin, A. J. Organocatalytic Visible Light Mediated Synthesis of Aryl Sulfides. *Chem. Commun.* **2013**, *49*, 5507−5509.

22. Corcoran, E. B.; Pirnot, M. T.; Lin, S.; Dreher, S. D.; Dirocco, D. A.; Davies, I. W.; Buchwald, S. L.; MacMillan, D. W. C. Aryl Amination Using Ligand-Free Ni(II) Salts and Photoredox Catalysis. *Science* **2016**, *353*, 279−283.

23. Terrett, J. A.; Cuthbertson, J. D.; Shurtleff, V. W.; MacMillan, D. W. C. Switching on Elusive Organometallic Mechanisms with Photoredox Catalysis. *Nature* **2015**, *524*, 330−334.

24. Shaikh, R. S.; Düsel, S. J. S.; König, B. Visible-Light Photo-Arbuzov Reaction of Aryl Bromides and Trialkyl Phosphites Yielding Aryl Phosphonates. *ACS Catal.* **2016**, *6*, 8410−8414.

25. Yoon, T. P. Photochemical Stereocontrol Using Tandem Photoredox−Chiral Lewis Acid Catalysis. *Acc. Chem. Res.* **2016**, *49*, 2307−2315.

26. (a) Berzelius J. Bemerkungen zu den beiden vorstehenden Aufsätzen über das färbende Princip im Blute der Thiere. *Ann. Phys.* **1817**, *57*, 24–34. (b) J. J. Berzelius, *in A Hist. Chem.,* Macmillan Education UK, London, 1964, pp. 142–177.

27. (a) Löwig, C. J. Ueber Schwefelwasserstoff- und Selenwasserstoffather. *Ann. Phys.* **1836**, *113*, 550−553. (b) Mugesh, G.; Singh, H. B. Synthetic organoselenium compounds as antioxidants: glutathione peroxidase activity. *Chem. Soc. Rev.* **2000**, *29*, 347−357. (c) Rathke, B. Beiträge zur Kenntniss des Selens. *Ann. Chem. Pharm.* **1869**, *152*, 181–220. (d) Foster, D. G.; Brown, S. F. Organic selenium compounds. Some derivatives of aromatic seleno-ethers. *J. Am. Chem. Soc.* **1928**, *50*, 1182–1188.

28. Wu, D.; Qiu, J. S.; Li, C. Q.; Yuan, L. X.; Yin, H. Q.; Chen, F. X. Lewis Acid-Catalyzed Asymmetric Selenocyanation of β-Ketoesters with N-Selenocyanatosaccharin. *J. Org. Chem.* **2020**, *85*, 934−941.

29. Mills, G. C. Hemoglobin catabolism: I. Glutathione peroxidase, an erythrocyte enzyme which protects hemoglobin from oxidative breakdown. *J. Biol. Chem.* **1957**, *229*, 189-197.

30. (a) Wei, W.; Liao, L.; Qin, T.; Zhao, X. Access to Saturated Thiocyano-Containing Azaheterocycles via Selenide-Catalyzed Regioand Stereoselective Thiocyanoaminocyclization of Alkenes. *Org. Lett.* **2019**, *21*, 7846−7850. (b) Liao, L.; Zhao, X. Indane-Based Chiral Aryl Chalcogenide Catalysts: Development and Applications in Asymmetric Electrophilic Reactions. *Acc. Chem. Res*. **2022**, *55*, 2439−2453.

31. (a) Brutchey, R. L. Diorganyl dichalcogenides as useful synthons for colloidal semiconductor nanocrystals. *Acc. Chem. Res*. **2015**, *48*, 2918−2926. (b) Gu, J.; Zhao, Z. Q.; Ding, Y.; Chen, H. L.; Zhang, Y. W.; Yan, C. H. Liquid-Phase Syntheses and Material Properties of Two-Dimensional Nanocrystals of Rare Earth-Selenium Compound Containing Planar Se Layers: RESe2 Nanosheets and RE4O4Se3 Nanoplates. *J. Am. Chem. Soc.* **2013**, *135*, 8363−8371. (c) Narajji, C.; Karvekar, M.; Das, A. Biological Importance of Organoselenium Compounds. *Indian J. Pharm. Sci.* **2007**, *69*, 344−351. (d) Gallo-Rodriguez, C.; Rodrigues, J. B. Organoselenium Compounds in Medicinal Chemistry. *ChemMedChem*

2024, *19*, No. e202400063. (e) Mugesh, G.; du Mont, W. W.; Sies, H. Chemistry of biologically important synthetic organoselenium compounds. *Chem. Rev.* **2001**, *101*, 2125−2180.

32. Tsuchii, K.; Tsuboi, Y.; Kawaguchi, S.-i.; Takahashi, J.; Sonoda, N.; Nomoto, A.; Ogawa, A. Highly Selective Double Chalcogenation of Isocyanides with Disulfide-Diselenide Mixed Systems. *J. Org. Chem.* **2007**, *72*, 415−423.

33. Protti, S.; Ravelli, D.; Fagnoni, M. Designing Radical Chemistry by Visible-Light Promoted Homolysis. *Trends Chem.* **2022**, *4*, 305−317.

34. Sartori, G.; Neto, J. S. S.; Pesarico, A. P.; Back, D. F.; Nogueira, C. W.; Zeni, G. Bis-vinyl selenides obtained via iron(III) catalyzed addition of PhSeSePh to alkynes: synthesis and antinociceptive activity. *Org. Biomol. Chem.* **2013**, *11*, 1199−1208.

35. Weber, A. C. H.; Coelho, F. L.; Affeldt, R. F.; Schneider, P. H. Visible-Light Promoted Stereoselective Arylselanyl Functionalization of Alkynes. *Eur. J. Org. Chem.* **2018**, *2018*, 6738−6742.

36. Chen, H.; Ding, R.; Tang, H.; Pan, Y.; Xu, Y.; Chen, Y. Simultaneous Construction of C-Se and C-S Bonds via the Visible Light-Mediated Multicomponent Cascade Reaction of Diselenides, Alkynes, and SO_2. *Chem. Asian J.* **2019**, *14*, 3264−3268.

37. Sahoo, H.; Mandal, A.; Dana, S.; Baidya, M. Visible Light-Induced Synthetic Approach for Selenylative Spirocyclization of N-Aryl Alkynamides with Molecular Oxygen as Oxidant. *Adv. Synth. Catal.* **2018**, *360*, 1099−1103.

38. Ma, X.-L.; Wang, Q.; Feng, X.-Y.; Mo, Z.-Y.; Pan, Y.-M.; Chen, Y.-Y.; Xin, M.; Xu, Y.-L. Metal-free visible-light induced cyclization/substitution cascade reaction of alkyne-tethered cyclohexadienones and diselenides: access to 5-hydroxy-3-selenyl-4a, 8a-dihydro-2H-chromen-6(5H)-ones. *Green Chem.* **2019**, *21*, 3547−3551.

39. Sahoo, S. R.; Das, B.; Sarkar, D.; Henkel, F.; Reuter, H. Visible Light Assisted Selenylative Intramolecular Dearomative Carbo Spirocyclisation (IDCS) of Homologated-Ynones. *Eur. J. Org. Chem.* **2020**, *2020*, 891−896.

40. Ahmad, I.; Shagufta. Shagufta, Sulfones: An Important Class of Organic Compounds with Diverse Biological Activities. *Int. J. Pharm. Pharm. Sci.* **2015**, *3*, 19−27.

41. (a) Ghosh, A. K.; Thompson, W. J.; Munson, P. M.; Liu, W.; Huff, J. R. Cyclic sulfone-3-carboxamides as novel P2-ligands for Ro 31-8959 based HIV-1 protease inhibitors. *Bioorg. Med. Chem. Lett.* **1995**, *5*, 83–88. (b) Richter, H. G. F.; Angehrn, P.; Hubschwerlen, C.; Kania, M.; Page, M. G. P.; Specklin, J.-L.; Winkler, F. K. Design, Synthesis, and Evaluation of 2β-Alkenyl Penam Sulfone Acids as Inhibitors of β-Lactamases. *J. Med. Chem.* **1996**, *39*, 3712-3722.

42. (a) Lin, S.-Y.; Yeh, T.-K.; Kuo, C.-C.; Song, J.-S.; Cheng, M.-F.; Liao, F.-Y.; Chao, M.-W.; Huang, H.-L.; Chen, Y.-L.; Yang, C.-Y.; Wu, M.-H.; Hsieh, C.-L.; Hsiao, W. C.; Peng, Y.-H.; Wu, J.-S.; Lin, L.-M.; Sun, M. W.; Chao, Y.-S.; Shih, C.; Wu, S.-Y.; Pan, S.-L.; Hung, M.-S.; Ueng, S.-H. Phenyl Benzenesulfonylhydrazides Exhibit Selective Indoleamine 2,3-Dioxygenase Inhibition with Potent in Vivo Pharmacodynamic Activity and Antitumor Efficacy. *J. Med. Chem*. **2016**, *59*, 419−430. (b) Patel, J. J.; Morja, M. I.; Chauhan, P. M.; Chikhalia, K. H. Potent biological investigation into a new class of sulfone derivatives endowed with quinolinyl–cyclopropane analogue. *J. Iran. Chem. Soc.* **2022**, *19*, 1613–1629. (c) Wang, M.; Jiang, X.-F. Prospects and Challenges in Organosulfur Chemistry. *ACS Sustainable Chem. Eng.* **2022**, *10*, 671−677.

43. (a) Kaga, A.; Nogi, K.; Yorimitsu, H. Synthesis of N-Alkyl and N-H Carbazoles via SNAr-based Aminations of Dibenzothiophene Dioxides. *Chem. Eur. J.* **2019**, *25*, 14780−14784. (b) Kong, X.; Chen, Y.; Liu, Q.; Wang, W.; Zhang, S.; Zhang, Q.; Chen, X.; Xu, Y.-Q.; Cao, Z.-Y. Selective Fluorosulfonylation of Thianthrenium Salts enabled by Electrochemistry. *Org. Lett.* **2023**, *25*, 581−586.

44. (a) Ilardi, E. A.; Vitaku, E.; Njardarson, J. T. Data Mining for Sulfur and Fluorine: An Evaluation of Pharmaceuticals to Reveal Opportunities for Drug Design and Discovery. *J. Med. Chem.* **2014**, *57*, 2832−2842. (b) Wang, X.; Meng, J.; Zhao, D.; Tang, S.; Sun, K. Synthesis and Applications of Thiosulfonates and Selenosulfonates as Free-Radical Reagents. *Chin. Chem. Lett.* **2023**, *34*, 107736-107750. (c) Chen, P.; Tian, L.; Ji, X.; Deng, G.-J.; Huang, H. Copper Catalyzed 1,2-Sulfonyletherification of 1,3-Dienes. *Org. Lett.* **2024**, *26*, 2939−2944. (d) Lu, M.; Liang, R. B.; Zhu, C. M.; Tong, Q. X.; Zhong, J. J. Photoredox Synthesis of Thio-Functionalized Cyclic Ethers Using N-Sulfenyl Phthalimides as a Thiyl-Radical Precurso. *Chin. J. Chem.* **2023**, *41*, 1823–1828. (e) Xiao, Q.; Lu, M.; Deng, Y.; Jian, J.; Tong, Q.-X.; Zhong, J.-J. Photoinduced Radical Cascade Cyclization: A Metal-Free Approach to Access Difluoroalky lated Dioxodibenzothiazepines. *Org. Lett.* **2021**, *23*, 9303−9308.

45. Jereb, M. Highly Atom-Economic, Catalyst- and Solvent-Free Oxidation of Sulfides into Sulfones Using 30 % Aqueous H_2O_2. *Green Chem.* **2012**, *14*, 3047−3052.

46. Maloney, K. M.; Kuethe, J. T.; Linn, K. A Practical, One-Pot Synthesis of Sulfonylated Pyridines. *Org. Lett.* **2011**, *13*, 102−105.

47. Graybill, B. M. Synthesis of aryl sulfones. *J. Org. Chem.* **1967**, *32*, 2931−2933.

48. (a) Zhu, X. Y.; Li, M.; Han, Y. P.; Chen, S.; Li, X. S.; Liang, Y. M. Copper-Catalyzed Oxidative Cyclization of Alkynes with Sulfonylhydrazides Leading to 2-Sulfonated 9H-pyrrolo[1,2-a]indol-9-ones. *J. Org. Chem.* **2017**, *82*, 8761−8768. (b) Wu, J.; Zong, Y.; Zhao,

C.; Yan, Q.; Sun, L.; Li, Y.; Zhao, J.; Ge, Y.; Li, Z. Silver or Cerium-promoted Free Radical Cascade Difunctionalization of o-Vinylanilides with Sodium Aryl- or Alkylsulfinates. *Org. Biomol. Chem.* **2019**, *17*, 794−797.

49. Chakrasali, P.; Kim, K.; Jung, Y.-S.; Kim, H.; Han, S. B. Visible-Light-Mediated Photoredox-Catalyzed Regio- and Stereoselective Chlorosulfonylation of Alkynes. *Org. Lett.* **2018**, *20*, 7509−7513.

50. Pampana, V. K. K.; Charpe, V. P.; Sagadevan, A.; Das, D. K.; Lin, C.-C.; Hwu, J. R.; Hwang, K. C. Oxy-Sulfonylation of Terminal Alkynes via C−S Coupling Enabled by Copper Photoredox Catalysis. *Green Chem.* **2021**, *23*, 3569−3574.

51. Zheng, M.; Zhuang, X.; Jia, Q.; Ren, Q.; Wu, J. Photoredox-Catalyzed Multicomponent α-Sulfonylation of Terminal Alkynes. *Org. Lett.* **2024**, *26*, 9978−9983.

52. Yang, W.; Yang, S.; Li, P.; Wang, L. Visible-Light Initiated Oxidative Cyclization of Phenyl Propiolates with Sulfinic Acids to Coumarin Derivatives under Metal-Free Conditions. *Chem. Commun.* **2015**, *51*, 7520−7523.

53. Yuan, J.-M.; Li, J.; Zhou, H.; Xu, J.; Zhu, F.; Liang, Q.; Liu, Z.; Huang, G.; Huang, J. Synthesis of 3-sulfonylquinolines by visible-light promoted metal-free cascade cycloaddition involving N-propargylanilines and sodium sulfinates. *New J. Chem.* **2020**, *44*, 3189−3193.

54. Qu, C.; Song, G.; Ou, J.; Tang, D.; Xu, Z.; Chen, Z. Visible Light-Mediated Construction of Sulfonated Dibenzazepines. *Chin. J. Chem.* **2021**, *39*, 2220-2226.

55. (a) Bon, R. S.; Waldmann, H. Bioactivity-Guided Navigation of Chemical Space. *Acc. Chem. Res.* **2010**, *43*, 1103-1114. (b) Suzen, S. Antioxidant activities of synthetic indole derivatives and possible activity mechanisms. Top. Heterocycl. Chem. 2007, 11, 145−178. (c) Katritzky, A. R. Introduction: Heterocycles. *Chem. Rev.* **2004**, *104*, 2125-2126. (d) Parsons, P. J.; Penkett, C. S.; Shell, A. J. Tandem Reactions in Organic Synthesis: Novel Strategies for Natural Product Elaboration and the Development of New Synthetic Methodology. *Chem. Rev.* **1996**, *96*, 195−206.

56. Tietze, L. F. Domino Reactions in Organic Synthesis. *Chem. Rev.* **1996**, *96*, 115−136.

57. (a) Wille, U. Radical Cascades Initiated by Intermolecular Radical Addition to Alkynes and Related Triple Bond Systems. *Chem. Rev*. **2013**, *113*, 813−853. (b) Latrache, M.; Hoffmann, N. Photochemical Radical Cyclization Reactions with Imines, Hydrazones, Oximes and Related Compounds. *Chem. Soc. Rev*. **2021**, *50*, 7418−7435. (c) Studer, A.; Curran, D. P. Catalysis of Radical Reactions: A Radical Chemistry Perspective. *Angew. Chem. Int. Ed.* **2016**, *55*, 58−102.

58. Gilmore, K.; Alabugin, I. V. Cyclizations of alkynes: revisiting baldwin's rules for ring closure. *Chem. Rev*. **2011**, *111*, 6513-6556.

59. (a) Liao, J.; Yang, X.; Ouyang, L.; Lai, Y.; Huang, J.; Luo, R. Recent advances in cascade radical cyclization of radical acceptors for the synthesis of carbo- and heterocycles. Org. Chem. Front. 2021, 8, 1345−1363. (b) Tan, T.-D.; Chen, Y.-B.; Fan, X.-Y.; Ye, L.-W. Recent Progress in the Copper-Catalyzed Cascade Cyclization Involving Intramolecular Hydroamination of Terminal Alkynes. Synlett 2019, 30, 2035−2040.

60. (a) Patel, R. I.; Singh, J.; Sharma, A. Visible Light-Mediated Manipulation of 1, n-Enynes in Organic Synthesis. *ChemCatChem* **2022**, *14*, No. e202200260. (b) Wei, W.-T.; Li, Q.; Zhang, M.-Z.; He, W.-M. N-Radical enabled cyclization of 1, n-enynes. *Chin. J. Catal.* **2021**, *42*, 731-742. (c) Jiang, L.-L.; Hu, S.-J.; Xu, Q.; Zheng, H.; Wei, W.-T. Radical Cyclization of 1, n-Enynes and 1, n-Dienes for the Synthesis of 2-Pyrrolidone. *Chem. Asian J.* **2021**, *16*, 3068−3081. (d) Hu, M.; Song, R.-J.; Li, J.-H. Metal-Free Radical 5-exo-dig Cyclizations of Phenol-Linked 1,6-Enynes for the Synthesis of Carbonylated Benzofurans. Angew. Chem., Int. Ed. 2015, 54, 608−612.

61. Mutra, M. R.; Kudale, V. S.; Li, J.; Tsai, W.-H.; Wang, J.-J. Alkene Versus Alkyne Reactivity in Unactivated 1,6 Enynes: Regioand Chemoselective Radical Cyclization with Chalcogens under Metal- and Oxidant-Free Conditions. *Green Chem.* **2020**, *22*, 2288−2300.

62. Mutra, M. R.; Li, J.; Chen, Y.-T.; Wang, J.-J. Time and Atom Economical Regio- and Chemoselective Radical Cyclization of Unactivated 1,6-Enynes Under Metal- and Oxidant-Free Conditions. *Chem. Eur. J.* **2022**, *28*, No. e202200742.

63. Wang, Y.; Liu, R.; Zhou, P.; Wu, J.; Li, W.; Wang, C.; Li, H.; Li, D.; Yang, J. Visible-Light-Driven Base-Promoted Radical Cascade Difluoroalkylation-Cyclization-Iodination of 1,6-Enynes with Ethyl Difluoroiodoacetate. *Eur. J. Org. Chem.* **2022**, *2022*, No. e202101395.

64. Liu, H.; Fan, X.; Hu, J.; Ma, T.; Wang, F.; Yang, J.; Li, D. Visible-Light-Enabled Ph3P/LiI-Promoted Tandem Radical Trifluoromethylation/Cyclization/Iodination of 1,6-Enynes with Togni's Reagent. *J. Org. Chem.* **2022**, *87*, 12877−12889.

65. Deng, G. B.; Wang, Z. Q.; Xia, J. D.; Qian, P. C.; Song, R. J.; Hu, M.; Gong, L. B.; Li, J. H. Tandem cyclizations of 1,6-enynes with arylsulfonyl chlorides by using visible-light photoredox catalysis. *Angew. Chem., Int. Ed.* **2013**, *52*, 1535−1538.

66. Li, Y.; Liu, B.; Song, R.-J.; Wang, Q.-A.; Li, J.-H. Visible Light-Initiated C(sp3)-Br/C(sp3)-H Functionalization of α-Carbonyl Alkyl Bromides through Hydride Radical Shift. *Adv. Synth. Catal.* **2016**, *358*, 1219−1228.

67. Chen, H.; Yan, Y.; Zhang, N.; Mo, Z.; Xu, Y.; Chen, Y. Visible-Light-Induced Cyclization/Aromatization of 2-VinyloxyArylalkynes: Synthesis of Thio-Substituted Dibenzofuran Derivatives. *Org. Lett.* **2021**, *23*, 376−381.

Chapter II:

Photocatalytic Selective Synthesis of 1,1-Diselenide Alkene Derivatives and Selenium-Containing α, β-Unsaturated Carboxylic Acids

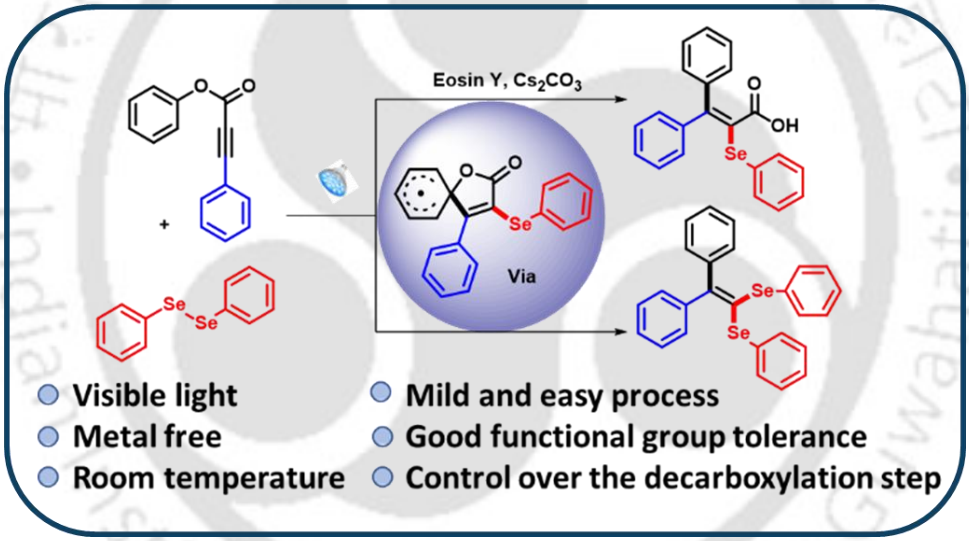

Roy, M.; Jamatia, R.; Samanta, A.; Mohar, K.; Srimani, D. *Org. Lett.* **2022**, *24,* 8180−8185

2.1 Introduction:

Organoselenides, or compounds having C-Se bonds, are a common structural motif in a wide variety of natural products, agrochemicals, and medicinal chemistry.[1] Organoselenides offer a wide range of applications in synthetic organic chemistry, functional materials[2] catalysis[3] and fluorescence probe imaging[4] which has piqued the interest of chemists. Bis-selenide alkene derivatives are found to be good antioxidant and antinociceptive agents in mice.[5] Some polyselenide alkene derivatives are also known as potential inhibitors of erythrocyte aminolevulinate dehydratase (δ-ALA-D) in humans.[6] Polyselenide derivatives have also been utilized in a device as a molecular magnetic superconductor (Figure 2.1).[7] As a result, the efficient construction of selenide-containing alkene frameworks is particularly important. Synthetic approaches that readily introduce selenium activity into organic compounds are therefore highly desirable. Unsymmetrical tetrasubstituted acyclic alkene containing carboxylate functionality can be easily transformed into a wide range of functional groups, indicating that it has a wide range of applications in chemical manufacturing.[8] Thus, installation of selenium in such a type of scaffold is worthy. However, due to problems in regulating stereoselectivity, the synthesis of unsymmetrical tetrasubstituted, *α, β*-unsaturated acids are extremely difficult.[9]

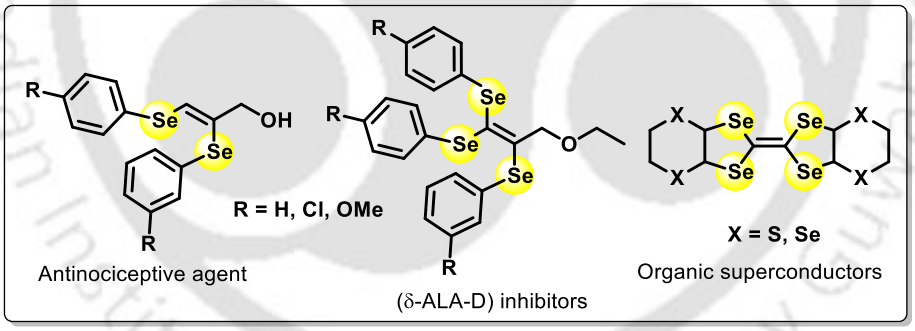

Figure 2.1: Important alkenes bearing selenium functionality

2.2 Previous reports:

In 2018, Baidya and his group reported the synthesis of tetrasubstituted *α, β*-unsaturated carboxylic acid with selenium functionality.[8a] However, the method typically relied on the use of excess oxidizing reagent (TBHP, 2 equiv.) and diphenyldiselenide (2 equiv.) (Figure 2.2a). Later, the same group reported the synthesis of 1,1-dichalcogenide tetrasubstituted alkenes via the chalcogenide radical-triggered intramolecular 1,4-aryl migration/decarboxylation cascade reaction (Figure 2.2b).[8b] Here, the decarboxylation steps for the oxidative trifunctionalization

of aryl alkynoates require high temperature and a strong oxidizing agent, di-*tert*-butyl peroxide (DTBP). Thus, the synthesis of such scaffolds using mild oxidant-free and room temperature conditions is attractive. The UV–visible spectrum of the diaryl diselenide clearly shows that it absorbs visible light to a significant extent. In addition, the Se-Se bond energy is also quite low (172 kJ mol-1).[10] As a result, irradiating diaryl diselenide with direct visible light could facilitate the formation of selenide radical, which can be employed in the C-Se bond formation reaction.[11]

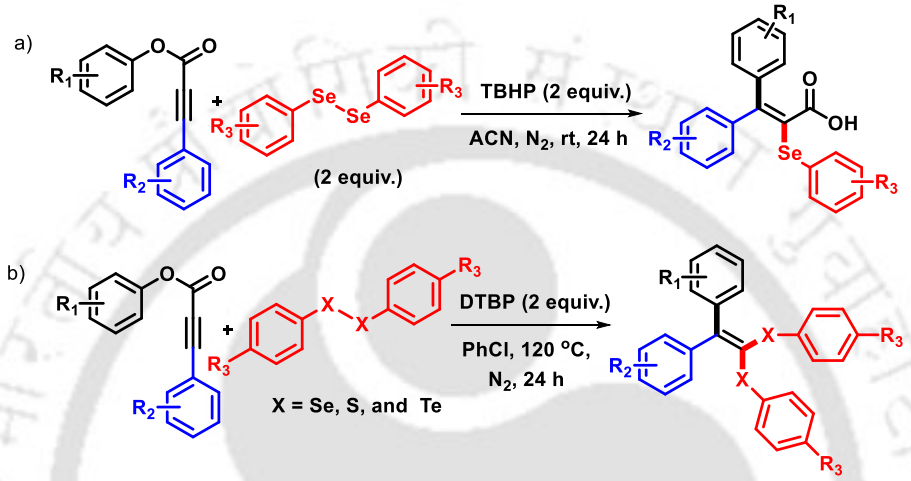

Figure 2.2: Previous literature reports for selenylation of aryl alkynoates

Thus, it was envisioned that an unsymmetrical tetrasubstituted α, β-unsaturated carboxylic acid could be synthesized using a catalytic amount of an organic dye under visible light irradiation. This would avoid the use of excessive amounts of oxidizing agents, which would eventually improve the reaction's e-factor. So, the development of mild and efficient methods for the selective synthesis of 1,1-diselenide alkene derivatives and selenium-containing α, β-unsaturated carboxylic acids is highly desirable.

2.3 Present Work:

In this chapter, a visible light-induced photocatalytic selective synthesis of 1,1-diselenide alkene derivatives and selenium-containing α, β-unsaturated carboxylic acids was done. Aryl alkynoates were reacted with diaryldiselenide under the blue LEDs irradiation in acetonitrile solvents at room temperature to provide the desired product. Eosin Y and Cs_2CO_3 are used to tune the product selectivity by inhibiting the decarboxylation step (Figure 2.3).

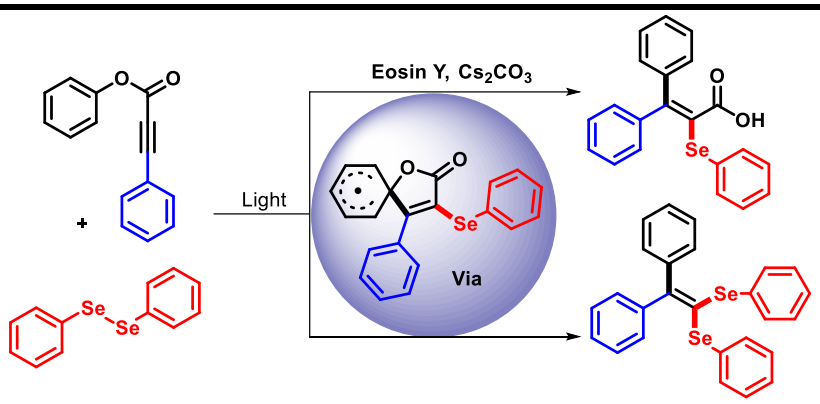

Figure 2.3: Present work for the selenylation of aryl alkynoates

2.4 Results and discussions:

Table 2.1. Catalyst and base optimization table[a]

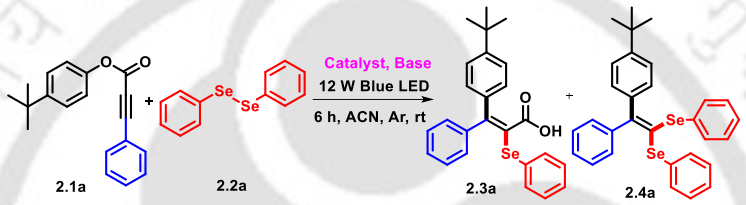

Sl. No.	2.2a (equiv.)	Catalyst (mol %)	Base (equiv.)	[b]Yield of 2.3a (%)	[b]Yield of 2.4a (%)
1.	1	EY	Na_2CO_3(1)	40	58
2.	1	EY	Li_2CO_3(1)	37	55
3.	1	EY	K_2CO_3(1)	72	trace
4.	1	EY	K_2CO_3(2)	74	trace
5.	1	EY	K_2CO_3(0.5)	74	trace
6.	1	EY	K_2CO_3(0.25)	35	43
7.	1	EY	Cs_2CO_3(0.5)	81	-
8.	1	EY	-	-	93
9.	1	-	Cs_2CO_3(0.5)	-	96
10.	**1**	**-**	**-**	**-**	**96**
11.	**0.5**	**EY**	**Cs_2CO_3(0.5)**	**81**	**-**
12.[c]	0.5	EY	Cs_2CO_3(0.5)	69	-
13.	0.5	EY	CsOH(0.5)	51	29
14.	0.5	EY	CsF(0.5)	34	33
15.	0.5	RB	Cs_2CO_3(0.5)	59	trace
16.	0.5	Ru PC	Cs_2CO_3(0.5)	43	trace
17.[d]	0.5	EY	Cs_2CO_3(0.5)	-	-

[a]**Conditions**: **2.1a** (0.2 mmol), **2.2a** (0.1-0.2 mmol), Catalyst (5 mol %), base (0.1-0.2 mmol), under argon, blue LED (2×12 Watt), ACN solvent, 6 h. EY = Eosin Y, RB = Rose Bengal, Ru PC = $Ru(bpy)_3(PF_6)_2$. b = isolated yield, c = in open air, d = in dark.

With this in mind, the investigation was started by taking aryl alkynoate (**2.1a**, 1 equiv.) and diphenyldiselenide (**2.2a**, 1 equiv.) as the model substrate in the presence of visible light. When the mixture of **2.1a** and **2.2a** was stirred at room temperature in the presence of catalyst Eosin

Y (5 mol% and base Na_2CO_3 (1 equiv.), in acetonitrile under blue LED irradiation, the formation of a mixture of **2.3a** (40 %) and **2.4a** (58 %) was obtained (Table 2.1, entry 1). The yield of **2.3a** was further improved to 72 % by employing a K_2CO_3 base (Table 2.1, entry 3). The optimal base loading was found to be 0.5 eq (Table 2.1, entries 3-6). The yield of **2.3a** was further improved (81 %) by employing Cs_2CO_3 (0.5 equiv.) as base (Table 2.1, entry 11). The higher efficacy of K_2CO_3 and Cs_2CO_3 with respect to other carbonate bases may be due to the stabilization of the carboxylate anion by the cesium and potassium metal cations.

Table 2.2. Solvent and light optimisation table[a]

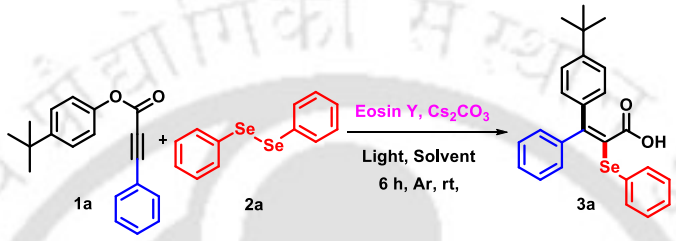

Sl. No.	Catalyst (5 mol %)	Base (0.5 equiv.)	Light (watt)	Solvent (2 mL)	Yield of 3a (%)
1.	**EY**	**Cs_2CO_3**	**Blue LED (24)**	**ACN**	**81**
2.	EY	Cs_2CO_3	Blue LED (24)	DMF	37
3.	EY	Cs_2CO_3	Blue LED (24)	MeOH	15
4.	EY	Cs_2CO_3	Blue LED (24)	DCM	trace
5.	EY	Cs_2CO_3	Blue LED (24)	DMSO	29
6.	EY	Cs_2CO_3	Blue LED (24)	THF	trace
7.	EY	Cs_2CO_3	-	ACN	-
8.	EY	Cs_2CO_3	Blue LED (12)	ACN	65
9.	EY	Cs_2CO_3	Blue LED (6)	ACN	57
10.	EY	Cs_2CO_3	Green LED (14)	ACN	39

Conditions: 1a (0.2 mmol), **2a** (0.1 mmol), Eosin Y (5 mol %), Cs_2CO_3 (0.1 mmol), under argon, light, solvent, 6 h, EY = Eosin Y.

When the reaction was performed in the absence of both base and Eosin Y, selectively **2.4a** was formed in 96% yield (Table 2.1, entry 10). Other bases such as CsOH and CsF showed a detrimental effect (Table 2.1, entries 13 and 14). Among the various solvents screened, CH_3CN was found to be the best solvent of choice (Table 2.2 entry 1-6). Also, when the reaction was performed with Rose Bengal or a traditional metal-based photocatalyst such as $Ru(bpy)_3(PF_6)_2$, the reaction provided inferior yield, showcasing the superiority of Eosin Y in the present reaction (Table 2.1, entries 15 and 16).

Scheme 2.1. Substrate scope for *α, β*-unsaturated carboxylic acid products[a]

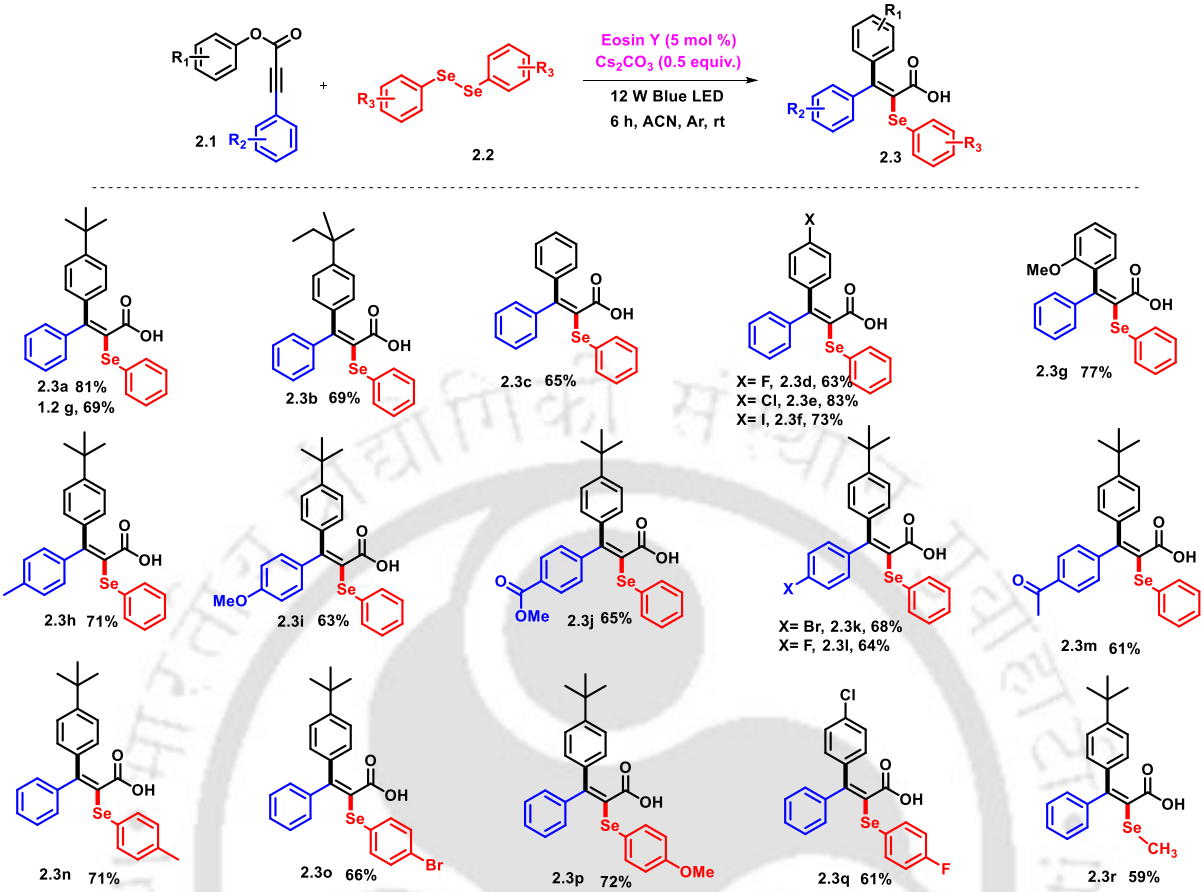

[a]**Conditions**: **2.1a** (0.2 mmol), **2.2a** (0.1 mmol), Eosin Y (EY) (5 mol %), Cs_2CO_3 (0.1 mmol), under argon, blue LED (2×12 Watt), ACN solvent, 6 h.

After achieving the optimized reaction parameters, the substrate scope study for the unsymmetrical tetrasubstituted *α, β*-unsaturated carboxylic acid was done. It was observed that the reactions progressed very smoothly for electron-donating (*tert*-C_4H_9, -*iso*-C_5H_{11}, -OCH_3) and electron-withdrawing (-F, -Cl, -I) groups in the *para*- or *ortho*-position of the *O*-aryl ring, establishing very good yields of the corresponding products (**2.3a-2.3g**, 63-83 %). Electron-donating (-CH_3, -OCH_3) and electron-withdrawing (-Br, -F) substituents in the *para* position of the alkyne aryl ring were also competent to bring about the following transformation in good yields (63-71 %). The inherent mild nature of the present visible-light strategy enabled the formation of products **2.3j** containing both ester- and carboxylic acid functionality in good isolated yield (65%). Similarly, the product **2.3m**, containing keto- and carboxylic acid substituents, was isolated in 61% yield. Diaryldiselenides containing electron-donating (-CH_3, -OCH_3) and electron-withdrawing (-F, -Br) substituents in the *para*-position also furnished the desired products in good isolated yields (59-72%). A gram-scale synthesis of **2.3a** was also

performed to check the scalability of the reaction and resulted in 69 % isolated yield of the desired product (Scheme 2.1, entry **2.3a**).

Scheme 2.2. Substrate scope for 1,1-diselenide products[a]

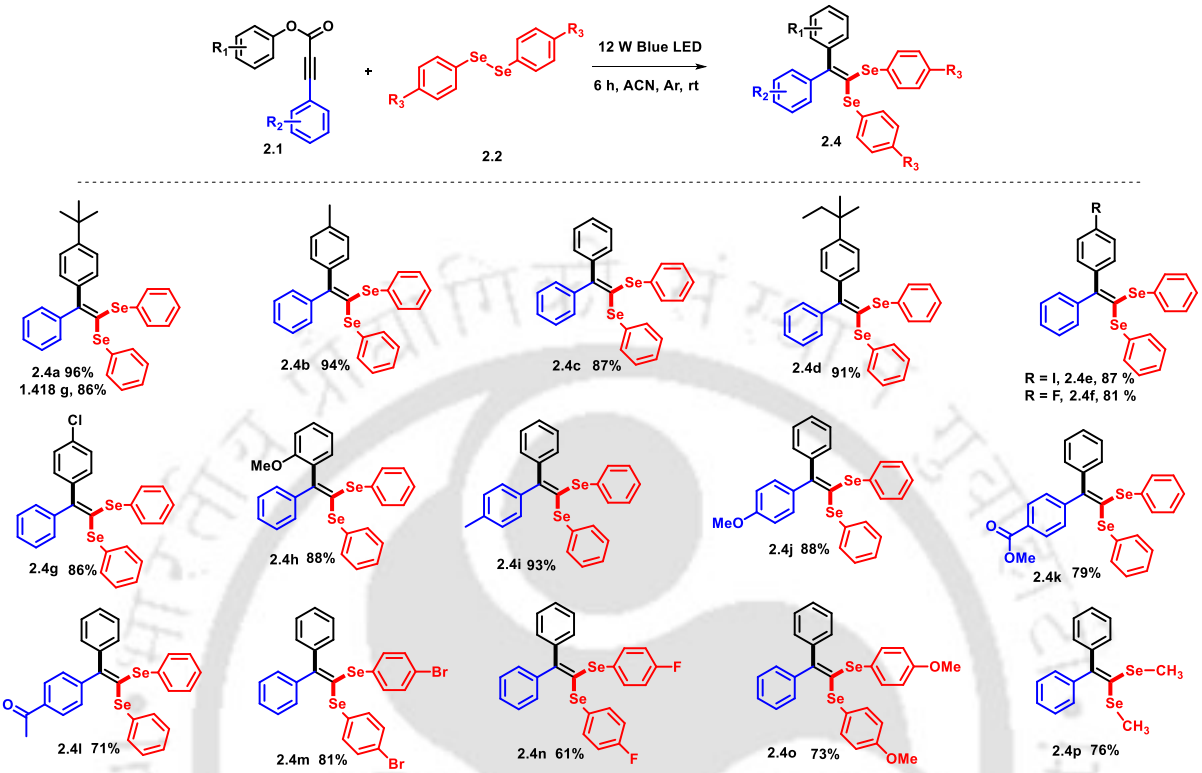

[a]**Conditions**: **2.1a** (0.2 mmol), **2.2a** (0.2 mmol), under argon, blue LED (2×12 Watt), ACN solvent, 6 h.

During the investigation of optimization parameters, it was observed that the tetrasubstituted 1,1-diselenide product could be easily achieved on simple irradiation with a blue LED. This can be a useful means to achieve tetrasubstituted 1,1-diselenide employing such mild conditions. Therefore, an investigation of the substrate scope to synthesize various tetrasubstituted 1,1-diselenides was also done (Scheme 2.2). In the case of electron-donating and withdrawing substituents in the *para*-position of the *O*-aryl ring, the reaction progressed competently, delivering the corresponding products (**2.4a-2.4g**) in excellent yield (87-94 %). The sterically hindered *ortho*-substitution in the *O*-aryl ring also produced the corresponding product (**2.4h**) in equal efficacy (88 %). Further, electron-donating substituents (-CH_3 and -OCH_3) in the *para*-position on the alkyne aryl ring provided the desired products (**2.4i-2.4j**) in excellent yields (88-93 %). It is also worth mentioning that the keto-group and sensitive ester (-COOMe) group in the *para* position of the alkyne aryl ring were tolerated to yield the corresponding products (**2.4k,** and **2.4l**) in 71 and 79 % isolated yield, respectively. To check the practicability of this procedure, a gram-scale synthesis of compound **2.4a** was performed and resulted in 86 % isolated yield of the desired product (Scheme 2.2, entry **2.4a**). Further

absence of an aryl ring in any of the sides of alkynoates was not able to furnish the desired products.

2.5 Post-functionalization:

Further, the synthetic applicability of this method was exposed by transforming **2.3a** into other valuable molecules like allylic alcohol, α, β-unsaturated ester, and vinylic halides (Figure 2.4). The compound **2.3a** was treated with aq. Conc. H_2SO_4 in EtOH at 82 °C to produce compound **2.6** in 76 % yield, and also compound **2.3a** can be reduced by applying BH_3-THF to produce allylic alcohol product **2.7** in 67 % yield. Further, a halogen functionality was also introduced by treating with DTBP, NIS, or NBS, in chlorobenzene at 120 °C. The introduction of halogen functionality further opens the window for several coupling reactions. The iodide compound **2.8** and bromide compound **2.9** were isolated in 73 % and 65 % yield, respectively.

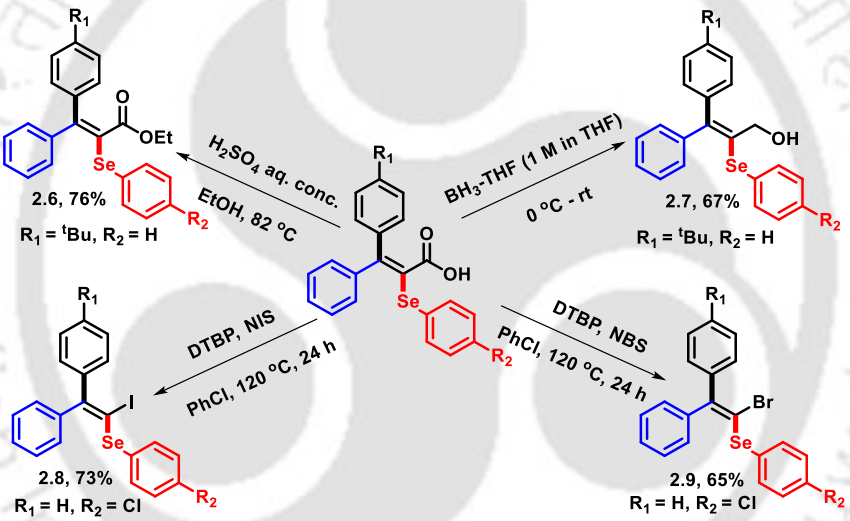

Figure 2.4. Post functionalization.

2.6 Control experiments:

Control experiments were performed to understand the mechanism (Figure 2.5). Under the standard conditions, 2.0 equiv. of 2,2,6,6-tetramethylpiperidine N-oxide (TEMPO) and 2,6-di-tert-butyl-4-methylphenol (BHT) were introduced to the model reactions as radical scavengers. The desired products **2.3a** and **2.4a** were not obtained. I have observed the TEMPO-adduct in the HRMS analysis of the crude reaction mixture. This finding suggested the involvement of a radical route. To confirm the 1,4-aryl migration, a control experiment employing methyl alkynoate **2.1r** was explored under the optimized reaction conditions. The reaction did not furnish the corresponding targeted product. Instead, a 1,2-addition product involving the addition of diphenyldiselenide to the alkyne of aryl alkynoate was observed **2.5**, isolated in 31

% yield. These results indicated that the aryl group linked to the oxygen atom plays an important role in this 1,4-migration.

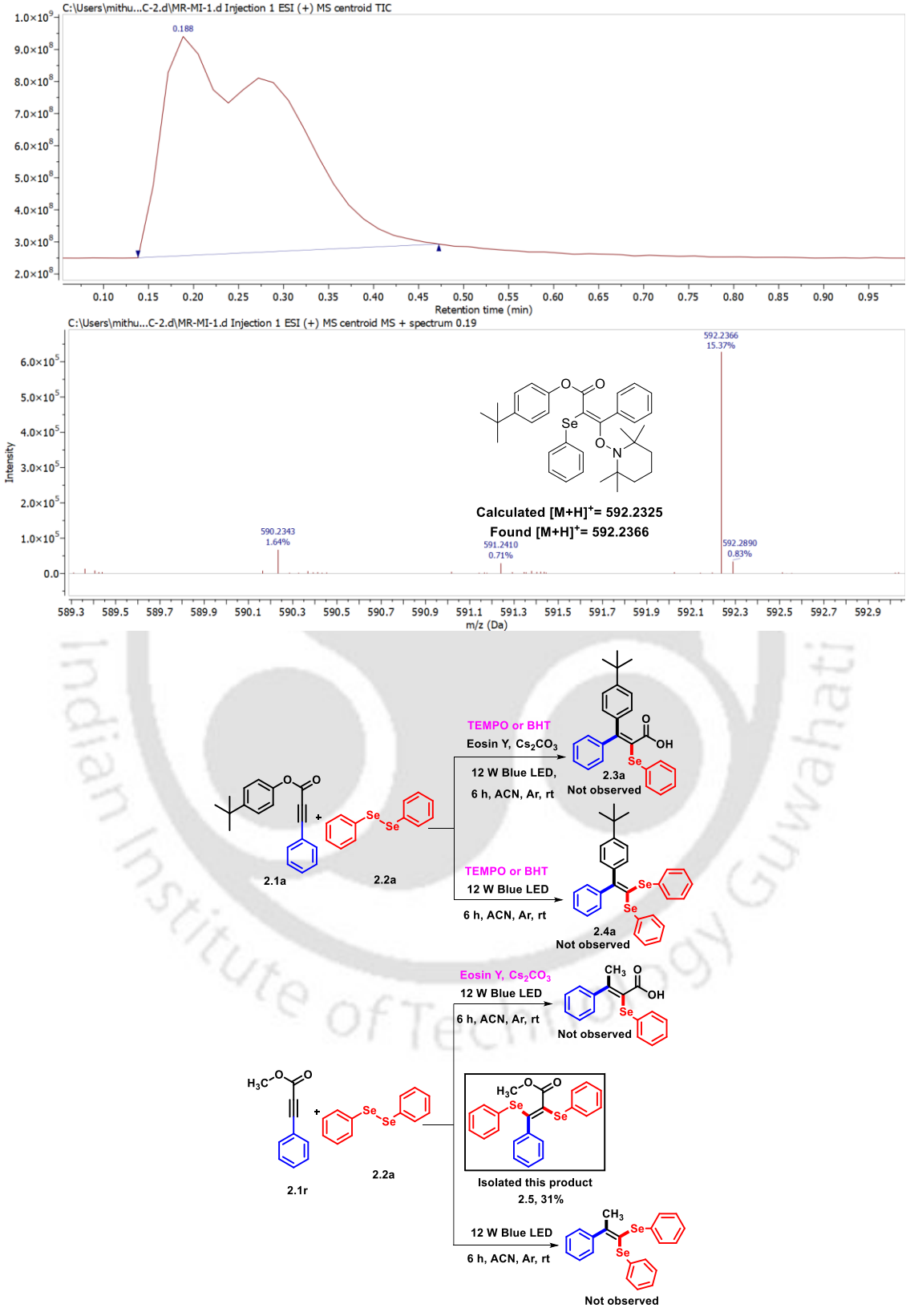

Figure 2.5. HRMS spectrum of TEMPO-adduct and Control experiments.

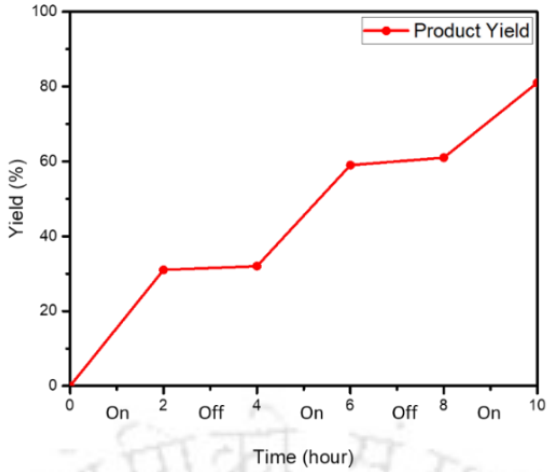

Figure 2.6. Light on/off experiment.

Further, an on/off experiment was carried out to examine the importance of light in the reaction. This led to a complete halt of the reaction in the absence of light, followed by reactivation upon further irradiation, which allows us to control the whole reaction duration. These findings show that light is an essential component of this reaction (Figure 2.6).

2.7 Plausible Mechanism:

Based on the control experiments and literature reports, a probable mechanism for the reaction was hypothesized as illustrated in Figure 2.7. Firstly, diphenyl diselenide **2.2a** generates the aryl selenium radical in the presence of blue LED,[10] then this aryl selenium radical adds to the alkyne bond of **2.1a** and generates the vinyl radical **2.A**. The intermediate **2.A** undergoes intramolecular radical ipsocyclization[12] to provide spirocyclic intermediate **2.B**, which is then converted to the carboxyl radical **2.C** via 1,4-aryl migration from the oxygen center to the carbon center. In the absence of a photocatalyst (i.e., in the case of product **2.4a** formation), the intermediate **2.C** undergoes simple decarboxylation and produces the vinyl radical **2.D**.[13] This further reacts with another molecule of aryl selenium radical to give the desired product **2.4a**. Interestingly, here formation of any six-membered cyclic lactone product was not observed.[14] When eosin Y (EY) was used as a photocatalyst, the reaction mechanism is a little different; upon irradiation with blue LED, eosin Y gets excited to its higher energy state. Then this excited eosin Y (EY^*) gives one electron to the carboxyl radical **2.C** to generate the carboxylate anion and itself goes to its cation radical ($EY^{\cdot+}$) form. After that cation radical ($EY^{\cdot+}$) of eosin Y takes one electron from the carbonate anion (CO_3^{2-})[15] and goes back to its ground state (EY). In the presence of base, the photo-redox catalytic cycle obstructs the decarboxylation step and stops the reaction at *α, β*-unsaturated carboxylic acid salt. After that, workup with 1(N) HCl provided the desired product, i.e., *α, β*-unsaturated carboxylic acids. This result indicates that a base is

necessary to achieve the unsymmetrically tetrasubstituted *α, β*-unsaturated carboxylic acid (**2.3a**).

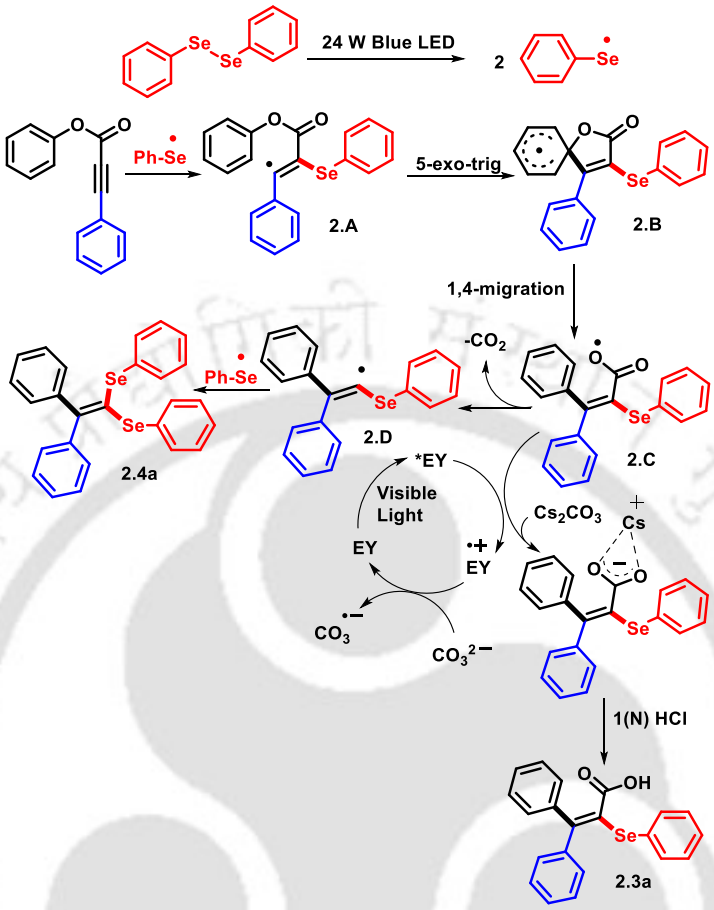

Figure 2.7. Plausible reaction mechanism.

2.8 Conclusions:

In this chapter, a visible light-induced selenium radical-based cascade reaction of aryl alkynoates was developed for the selective synthesis of 1,1-diselenide alkene derivatives and fully substituted α, β-unsaturated carboxylic acid with selenium functionality. Eosin Y and Cs_2CO_3 are used to tune the product selectivity by inhibiting the decarboxylation step. This metal-free visible light strategy provides a wide range of functional group tolerance for both products in good to excellent yield.

2.9 Experimental section:

a) General procedure for the synthesis of aryl alkynoates

Arylalkynoate derivatives were prepared by following the reported procedures.[16]

The phenylpropiolic acid was purchased and used directly from a commercial source. The derivatives of phenylpropiolic acid were prepared in the following procedure.

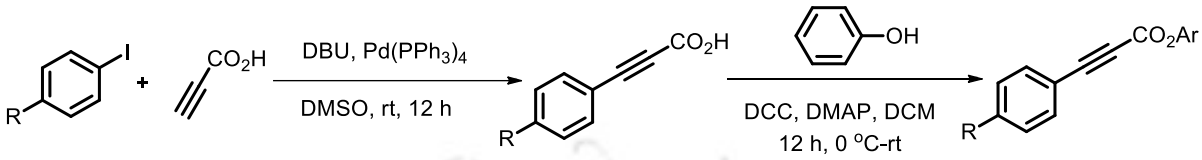

Step 1: Preparation of aryl alkynyl carboxylic acids derivatives

The aryl iodides (2.5 mmol, 1.0 equiv), DBU (6.0 mmol, 2.4 equiv), and $Pd(PPh_3)_4$ (0.0625 mmol, 2.5 mol %) were taken in an oven-dried schlenk tube with a magnetic stir. The reaction tube was purged with nitrogen and then, dry DMSO (5 mL) was added via a syringe. A solution of propiolic acid (3.0 mmol, 1.2 equiv) in DMSO (2 mL) was added into the flask. The mixture was stirred at room temperature for 12 h. After completion of the reaction, ethyl acetate (10 mL) was added into the reaction mixture. The reaction mixture was extracted with saturated aqueous $NaHCO_3$. The aqueous layer was separated, acidified to pH = 1 by addition of cold 1 (N) HCl, and extracted with DCM. The combined organic layers were dried with anhydrous Na_2SO_4 and filtered, and the solvent was removed under reduced pressure. The resulting crude product was purified by column chromatography on silica gel to provide the desired product.

Step 2: Preparation of aryl alkynoates

To a solution of phenol (5.0 mmol, 1.0 equiv) in DCM (20 mL) was added aryl alkynyl carboxylic acids (5 mmol, 1.0 equiv) at 0 °C. Then, a mixture of DCC (6.6 mmol, 1.1 equiv) and DMAP (0.6 mmol, 0.1 equiv) in DCM (5 mL) was added dropwise. The resulting mixture was stirred at room temperature for 12 hours. Then the crude mixture was filtered and washed with DCM (15 mL). The combined organic phase was concentrated under reduced pressure to give a residue which was purified by silica gel column chromatography to give the desired product.

b) General procedure for the preparation of diselenides

Diselenide derivatives were synthesized by following the reported procedure.[17]

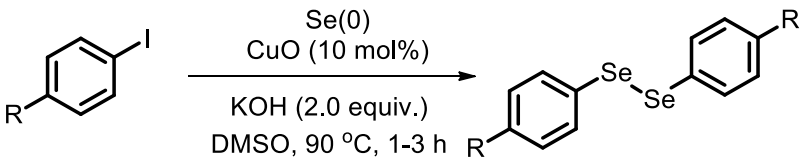

To a stirred solution of aryl iodides (2.0 mmol) and Se powder metal (4.0 mmol) in dry DMSO (3.0 mL) was added CuO (10 mol %) followed by KOH (2.0 equiv) under nitrogen atmosphere

at 90 °C. After the reaction was completed, Et2O (10 mL) and water (2 × 20 mL) were added, and the mixture was washed successively three times. The organic layer was dried by adding anhydrous Na_2SO_4 and evaporated under reduced pressure. The resulting residue was purified by column chromatography on silica gel with a gradient eluent of petroleum ether and ethyl acetate (98:2) to get pure diselenides.

c) General Procedure for the synthesis of compound 2.3:

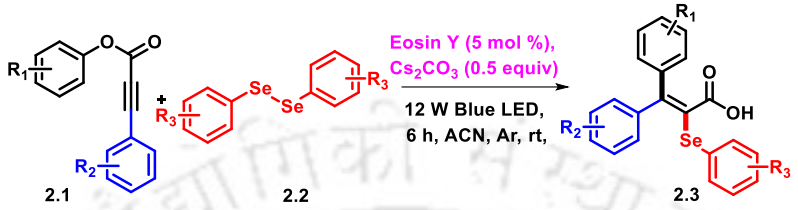

The aryl alkynoates **2.1** (0.20 mmol), diaryl diselenides **2.2** (0.10 mmol) Eosin Y (5 mol%) and Cs_2CO_3 (0.10 mmol) were taken in an oven dried 5 mL round bottom flask with a magnetic bead. The round bottom flask was evacuated and filled with argon for three times, after that CH_3CN (2 mL) was added via a syringe. The reaction mixture was allowed to stir under the blue light irradiation (2×12W blue LED) at room temperature for 6 h. After completion of the reaction solvent was evaporated and the residue was dissolved in water and acidified with 1 N HCl. After that the product was extracted with ethyl acetate for three times followed by a brine wash. Then the organic layer was separated out and dried over Na_2SO_4. Solvent was evaporated under reduced pressure to get the crude product, further the purification of crude product was done by column chromatography on silica gel by using petroleum ether and ethyl acetate as the eluent.

d) General Procedure for the synthesis of compound 2.4:

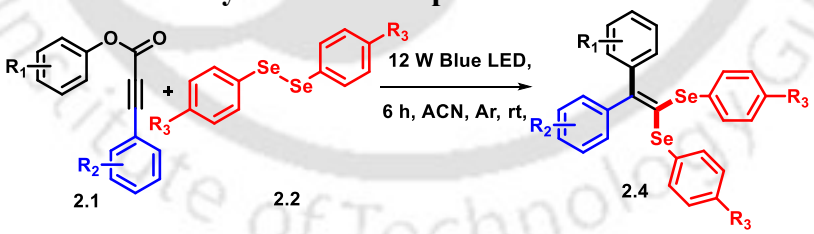

The aryl alkynoates **2.1** (0.20 mmol), diaryl diselenides **2.2** (0.10 mmol) were taken in an oven dried 5 mL round bottom flask with a magnetic bead. The round bottom flask was evacuated and filled with argon for the three times, after that CH_3CN (2 mL) was added via a syringe. The reaction mixture was allowed to stir under the blue light irradiation (2×12W blue LED) at room temperature for 6 h. After completion of the reaction solvent was evaporated to get the crude product, further the purification was done by column chromatography on silica gel by using petroleum ether and ethyl acetate as the eluent.

e) Gram Scale synthesis of product 2.3a:

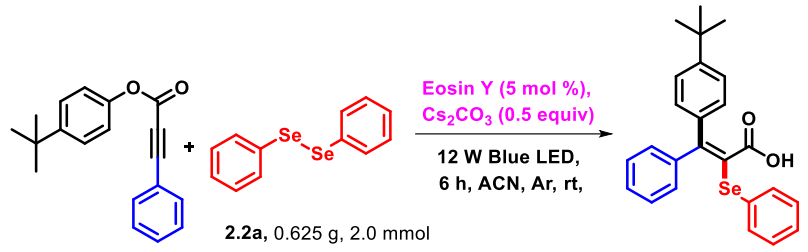

2.1a, 1.113 g, 4.0 mmol

2.2a, 0.625 g, 2.0 mmol

2.3a, 1.2 g, 69 %

4-(tert-butyl)phenyl 3-phenylpropiolate **2.1a** (4.00 mmol), diphenyl diselenides **2.2a** (2.00 mmol) Eosin Y (5 mol%) and Cs_2CO_3 (2.00 mmol) were taken in an oven dried 50 mL round bottom flask with a magnetic bead. The round bottom flask was evacuated and filled with argon for three times, after that CH_3CN (25 mL) was added via a syringe. The reaction mixture was allowed to stir under the blue light irradiation at room temperature for 9 h. After completion of the reaction solvent was evaporated and the residue was dissolved in water and acidified with 1 N HCl. After that the product was extracted with ethyl acetate for three times followed by a brine wash. Then the organic layer was separated out and dried over Na_2SO_4. Solvent was evaporated under reduced pressure to get the crude product, further the purification was done by column chromatography on silica gel by 70:30 hexane and ethyl acetate as the eluent to provide the pure product **2.3a** in 69 % yield (1.2 g).

f) Gram Scale synthesis of product 2.4a:

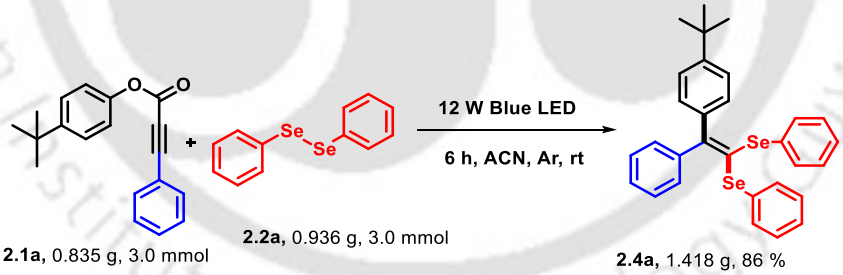

2.1a, 0.835 g, 3.0 mmol

2.2a, 0.936 g, 3.0 mmol

2.4a, 1.418 g, 86 %

4-(tert-butyl)phenyl 3-phenylpropiolate **2.1a** (0.835 g, 3.00 mmol), diphenyl diselenides **2.2a** (0.936 g, 3.00 mmol) were taken in an oven dried 50 mL round bottom flask with a magnetic bead. The round bottom flask was evacuated and filled with argon for the three times, after that CH_3CN (25 mL) was added via a syringe. The reaction mixture was allowed to stir under the blue light irradiation (2×12W blue LED) at room temperature for 9 h. After completion of the reaction solvent was evaporated to get the crude product, further the purification was done by column chromatography on silica gel by using 99:1 petroleum ether and ethyl acetate as the eluent to provide the pure product **2.4a** in 86 % yield (1.418 g).

g) Synthesis of compound 2.6[18]:

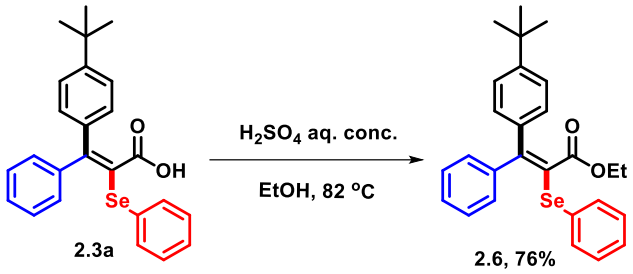

A suspension of the compound **2.3a** (0.25 mmol) in ethanol (2.0 mL) was dissolved by the addition of a 98 % aqueous solution of sulphuric acid (1.0 mL). The solution was magnetically stirred at 82 °C, and monitored by TLC analysis. After the disappearance of the starting carboxylic acid, the reaction was cooled to room temperature, and water (10 mL) was added. The resulting ethyl ester was extracted with ethyl acetate (3 × 10 mL), combining the organic phases, that were dried over Na_2SO_4. Compound **2.6** was purified by column chromatography by using 95:5 petroleum ether and ethyl acetate with 76% yield.

h) Synthesis of compound 2.7[19]:

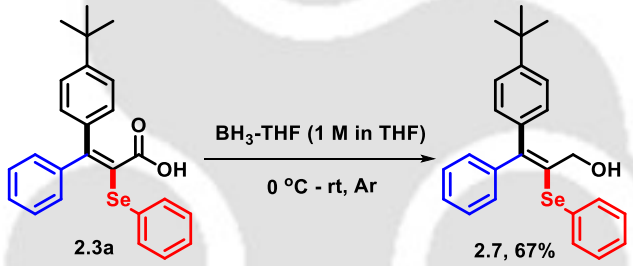

To a solution of compound **2.3a** (0.25 mmol) in anhydrous THF (2 mL) under argon at 0 °C was added a solution of BH_3-THF (1.0 M in THF, 3 mL) drop wise. The resulting solution was stirred at room temperature until no starting material was detected by TLC. The reaction was quenched with H_2O (25 mL) and extracted with ethyl acetate (30 × 3). The combined organic layer was washed with brine, dried over anhydrous Na_2SO_4, and concentrated in vacuum to give the crude product, which was purified by silica gel column chromatography (PE : EA = 95 : 5) to obtain the product **2.7** as a white solid in 67 % yield.

i) Synthesis of compound 2.8[8]:

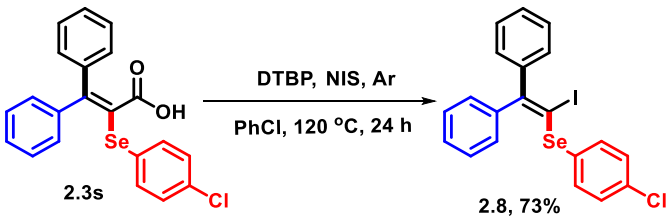

The product **2.3s** (0.2 mmol), N-iodosuccinimide (0.4 mmol), and DTBP (0.4 mmol) were taken in an oven-dried round-bottom flask equipped with a magnetic bead. Then,

chlorobenzene (2 mL) was added, and the mixture was allowed to stir at 120 °C for 24 h. After completion of the reaction, it was diluted with CH_2Cl_2. The volatiles were evaporated to dryness under reduced pressure, and the resulting residue was purified by column chromatography on silica gel with 98:2 petroleum ether and ethyl acetate as the eluent to get pure product **2.8** in 73% yield.

j) Synthesis of compound 2.9[8]:

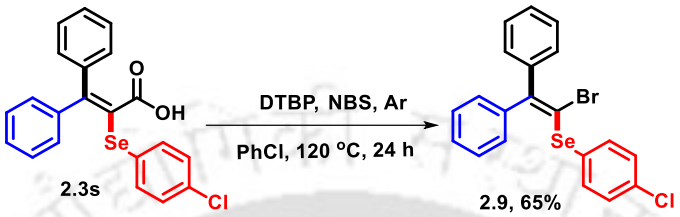

The product **2.3s** (0.2 mmol), N-bromosuccinimide (0.4 mmol) and DTBP (0.4 mmol) were taken in an oven-dried round-bottom flask equipped with a magnetic bead. Then, chlorobenzene (2 mL) was added, and the mixture was allowed to stir at 120 °C for 24 h. After completion of the reaction, it was diluted with CH_2Cl_2. The volatiles were evaporated to dryness under reduced pressure, and the resulting residue was purified by column chromatography on silica gel with 98:2 petroleum ether and ethyl acetate as the eluent to get pure product **2.9** in 65% yield.

2.10 Analytical data:

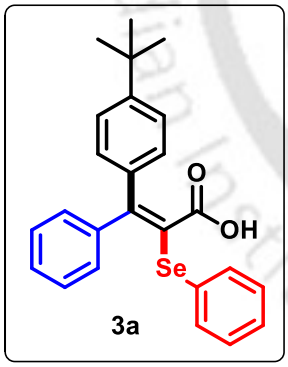

(*E*)-3-(4-(tert-butyl)phenyl)-3-phenyl-2-(phenylselanyl)acrylic acid (**2.3a**) : Yellow solid (30 % ethyl acetate in petroleum ether) Yield: (71 mg) 81 %; **^{1}H NMR** (500 MHz, $CDCl_3$) δ 7.50 – 7.47 (m, 2H), 7.33 – 7.31 (m, 3H), 7.29 – 7.25 (m, 4H), 7.22 – 7.20 (m, 3H), 7.16 – 7.13 (m, 2H), 1.29 (s, 9H). **^{13}C NMR** (125 MHz, $CDCl_3$) δ 171.6, 151.8, 151.7, 141.8, 137.9, 133.4, 129.9, 129.34, 129.30, 128.6, 128.4, 128.3, 127.9, 125.3, 121.9, 34.8, 31.4. **HRMS** (ESI-TOF): m/z calcd. for $C_{25}H_{24}O_2Se$: 435.0868 $[M-H]^-$, Found: 435.0875.

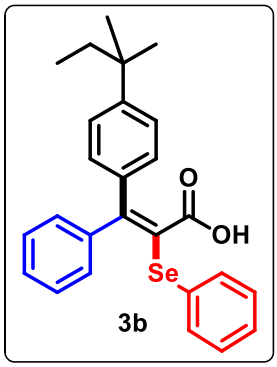

(*E*)-3-(4-(tert-pentyl)phenyl)-3-phenyl-2-(phenylselanyl)acrylic acid (**2.3b**): Yellow solid (30 % ethyl acetate in petroleum ether) Yield: (62 mg) 69 %; **^{1}H NMR** (500 MHz, DMSO-d_6) δ 7.51 – 7.49 (m, 2H), 7.41 – 7.38 (m, 2H), 7.35 – 7.31 (m, 4H), 7.29 – 7.24 (m, 4H), 7.17 (d, J = 8.2 Hz, 2H), 1.58 (q, J = 7.4 Hz, 2H), 1.21 (s, 6H), 0.60 (t, J = 7.4 Hz, 3H). **^{13}C NMR** (126 MHz, DMSO-d_6) δ 168.0, 148.9, 146.6, 141.4, 137.7, 132.9, 129.3, 129.2, 128.6, 128.3, 128.0, 127.9, 127.7, 125.6, 123.9, 37.5, 36.0, 28.0, 9.0. **HRMS** (ESI-TOF): m/z calcd. for $C_{26}H_{26}O_2Se$: 449.1024 $[M-H]^-$, Found: 449.1021.

3,3-diphenyl-2-(phenylselanyl)acrylic acid (**2.3c**)[5]: Yellow solid (30 % ethyl acetate in petroleum ether) Yield: (49 mg) 65 %; **^{1}H NMR** (500 MHz, $CDCl_3$) δ 7.49 (d, *J* = 7.0 Hz, 2H), 7.35 – 7.31 (m, 3H), 7.29 (d, *J* = 7.7 Hz, 2H), 7.26 – 7.21 (m, 8H). **^{13}C NMR** (125 MHz, $CDCl_3$) δ 171.3, 151.1, 141.5, 141.1, 133.6, 129.6, 129.33, 129.31, 128.8, 128.6, 128.5, 128.37, 128.35, 128.0, 122.9.

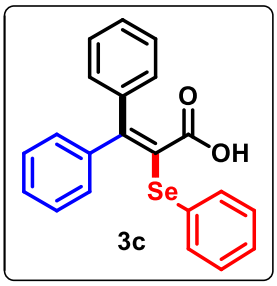

(*E*)-3-(4-fluorophenyl)-3-phenyl-2-(phenylselanyl)acrylic acid (**2.3d**)[5]: Yellow solid (30 % ethyl acetate in petroleum ether) Yield: (51 mg) 65 %; **^{1}H NMR** (500 MHz, $CDCl_3$) δ 7.49 – 7.47 (m, 2H), 7.34 – 7.32 (m, 3H), 7.28 – 7.21 (m, 5H), 7.19 – 7.16 (m, 2H), 6.92 (t, *J* = 8.5 Hz, 2H). **^{13}C NMR** (125 MHz, $CDCl_3$) δ 171.4, 162.9 (d, *J* = 247.3 Hz), 149.8, 141.3, 137.14, 137.12, 133.7, 130.7 (d, *J* = 8.2 Hz), 129.4, 129.3, 128.7, 128.5, 128.2, 123.2, 115.4 (d, *J* = 21.5 Hz).

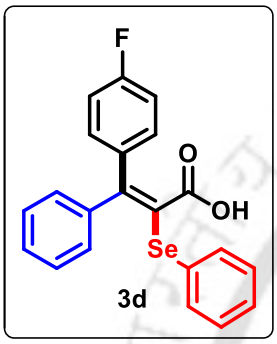

(*E*)-3-(4-chlorophenyl)-3-phenyl-2-(phenylselanyl)acrylic acid (**2.3e**)[5]: Yellow solid (30 % ethyl acetate in petroleum ether) Yield: (68 mg) 83 %; **^{1}H NMR** (500 MHz, DMSO-*d*$_6$) δ 12.76 (s, 1H), 7.52 – 7.50 (m, 2H), 7.42 – 7.38 (m, 4H), 7.33 – 7.27 (m, 6H), 7.25 – 7.22 (m, 2H). **^{13}C NMR** (125 MHz, $CDCl_3$) δ 170.4, 149.1, 141.0, 139.5, 134.7, 134.0, 130.2, 129.4, 129.3, 129.2, 128.74, 128.65, 128.5, 128.3, 123.8.

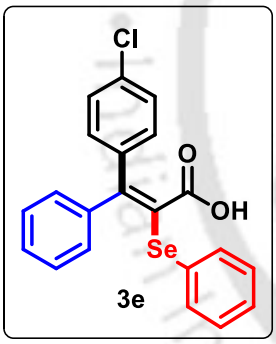

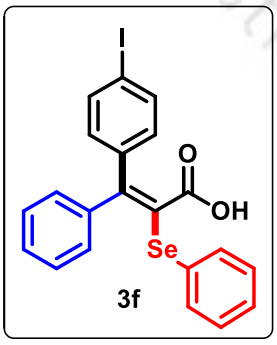

(*E*)-3-(4-iodophenyl)-3-phenyl-2-(phenylselanyl)acrylic acid (**2.3f**): Yellow solid (30 % ethyl acetate in petroleum ether) Yield: (73 mg) 73 %; **^{1}H NMR** (500 MHz, DMSO-*d*$_6$) δ 12.74 (s, 1H), 7.69 (d, *J* = 8.0 Hz, 2H), 7.52 – 7.47 (m, 2H), 7.41 – 7.38 (m, 2H), 7.36 – 7.31 (m, 4H), 7.28 – 7.26 (m, 2H), 7.02 – 6.99 (m, 2H). **^{13}C NMR** (125 MHz, DMSO-*d*$_6$) δ 167.5, 144.8, 140.7, 140.3, 137.0, 133.4, 130.4, 129.2, 128.8, 128.7, 128.5, 128.1, 127.9, 125.8, 94.5. **HRMS** (ESI-TOF): m/z calcd. for $C_{21}H_{15}IO_2Se$: 460.9305 $[M-CO_2]^-$, Found: 460.9307.

(*E*)-3-(2-methoxyphenyl)-3-phenyl-2-(phenylselanyl)acrylic acid (**2.3g**)[5]: Yellow solid (30 % ethyl acetate in petroleum ether) Yield: (63 mg) 77 %; **^{1}H NMR** (500 MHz, $CDCl_3$) δ 7.49 – 7.47 (m, 2H), 7.29 – 7.25 (m, 6H), 7.24 – 7.21 (m, 4H), 7.09 – 7.08 (m, 1H), 6.85 (t, *J* = 7.5 Hz, 1H), 6.78 (d, *J* = 8.3 Hz, 1H), 3.58 (s, 1H). **^{13}C NMR** (125 MHz, $CDCl_3$) δ 170.6, 156.4, 150.2, 141.9, 132.7, 130.5, 130.4, 130.3, 129.9, 129.3, 128.9, 128.1, 128.0, 127.6, 123.8, 120.7, 111.5, 55.5.

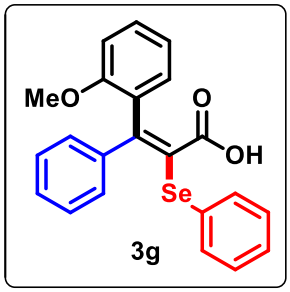

(*E*)-3-(4-(tert-butyl)phenyl)-2-(phenylselanyl)-3-(p-tolyl)acrylic acid (**2.3h**): Yellow solid (30 % ethyl acetate in petroleum ether) Yield: (63 mg) 71 %; **^{1}H NMR** (500 MHz, $CDCl_3$) δ 7.52 – 7.50 (m, 2H), 7.27 – 7.23 (m, 6H), 7.20 – 7.14 (m, 6H), 2.36 (s, 3H), 1.28 (s, 9H). **^{13}C NMR** (125 MHz, $CDCl_3$) δ 170.8, 152.0, 151.7, 139.0, 138.4, 138.2, 133.3, 130.1, 129.34, 129.30, 129.0, 128.6, 127.8, 125.3, 121.3, 34.8, 31.4, 21.5. **HRMS** (ESI-TOF): m/z calcd. for $C_{26}H_{26}O_2Se$: 449.1024 $[M-H]^-$, Found: 449.1025.

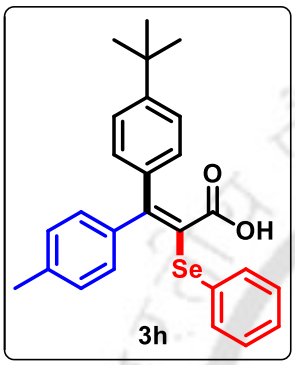

(*Z*)-3-(4-(tert-butyl)phenyl)-3-(4-methoxyphenyl)-2-(phenylselanyl)acrylic acid (**2.3i**): Yellow solid (30 % ethyl acetate in petroleum ether) Yield: (58 mg) 63 %; **^{1}H NMR** (500 MHz, $CDCl_3$) δ 7.51 – 7.49 (m, 2H), 7.27 – 7.22 (m, 8H), 7.16 – 7.14 (m, 2H), 6.85 (d, *J* = 8.7 Hz, 2H), 3.81 (s, 3H), 1.29 (s, 9H). **^{13}C NMR** (125 MHz, $CDCl_3$) δ 171.0, 159.8, 152.2, 151.8, 138.4, 134.2, 132.9, 131.1, 130.3, 129.3, 128.8, 127.7, 125.2, 120.6, 113.6, 55.4, 34.8, 31.4. **HRMS** (ESI-TOF): m/z calcd. for $C_{26}H_{26}O_3Se$: 421.1071 $[M-CO_2]^-$, Found: 421.1078.

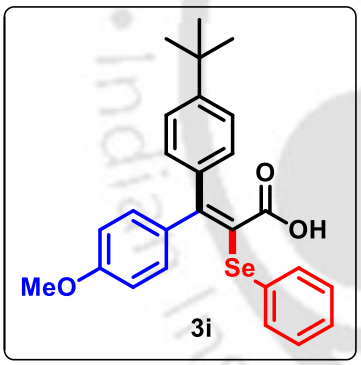

(*Z*)-3-(4-(tert-butyl)phenyl)-3-(4-(methoxycarbonyl)phenyl)-2-(phenylselanyl)acrylic acid (**2.3j**): Yellow solid (30 % ethyl acetate in petroleum ether) Yield: (64 mg) 65 %; **^{1}H NMR** (500 MHz, $CDCl_3$) δ 8.01 (d, *J* = 8.0 Hz, 2H), 7.50 – 7.47 (m, 2H), 7.37 (d, *J* = 8.0 Hz, 2H), 7.28 – 7.21 (m, 6H), 7.14 (d, *J* = 8.0 Hz, 2H), 3.91 (s, 3H), 1.28 (s, 9H). **^{13}C NMR** (125 MHz, $CDCl_3$) δ 170.0, 166.9, 152.1, 150.0, 146.3, 137.3, 133.6, 129.9, 129.7, 129.50, 129.46, 129.4, 128.5, 128.1, 125.5, 123.2, 52.3, 34.8, 31.4. **HRMS** (ESI-TOF): m/z calcd. for $C_{27}H_{26}O_4Se$: 495.1070 $[M-H]^-$, Found: 495.1055.

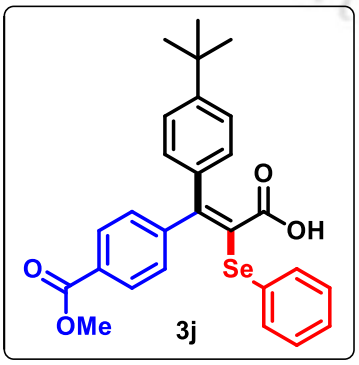

(*Z*)-3-(4-bromophenyl)-3-(4-(tert-butyl)phenyl)-2-(phenylselanyl)acrylic acid (**2.3k**): Yellow solid (30 % ethyl acetate in petroleum ether) Yield: (70 mg) 68 %; **^{1}H NMR** (500 MHz, $CDCl_3$) δ 7.49 – 7.45 (m, 4H), 7.28 – 7.23 (m, 6H), 7.17 – 7.12 (m, 4H), 1.28 (s, 9H). **^{13}C NMR** (125 MHz, $CDCl_3$) δ 170.4, 152.1, 150.3, 140.6, 137.5, 133.5, 131.6, 131.2, 129.7, 129.4, 128.6, 128.1, 125.4, 122.7, 122.4, 34.8, 31.4. **HRMS** (ESI-TOF): m/z calcd. for $C_{25}H_{23}BrO_2Se$: 512.9973 $[M-H]^-$, Found: 512.9989.

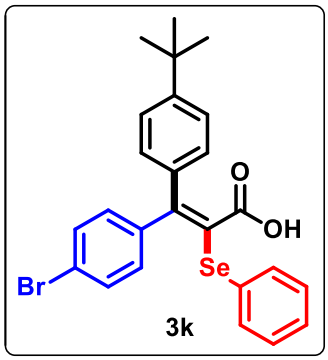

(*Z*)-3-(4-(tert-butyl)phenyl)-3-(4-fluorophenyl)-2-(phenylselanyl)acrylic acid (**2.3l**): Yellow solid (30 % ethyl acetate in petroleum ether) Yield: (58 mg) 64 %; **^{1}H NMR** (500 MHz, $CDCl_3$) δ 7.49 – 7.47 (m, 2H), 7.28 – 7.22 (m, 8H), 7.13 (d, J = 8.1 Hz, 2H), 7.01 (t, J = 8.6 Hz, 2H), 1.29 (s, 9H). **^{13}C NMR** (125 MHz, $CDCl_3$) δ 170.8, 162.7 (d, J = 246.8 Hz), 152.0, 150.6, 137.9, 137.7, 133.3, 131.4 (d, J = 8.2 Hz), 129.8, 129.4, 128.6, 128.0, 125.4, 122.2, 115.3 (d, J = 21.5 Hz), 34.8, 31.4. **HRMS** (ESI-TOF): m/z calcd. for $C_{25}H_{23}FO_2Se$: 453.0773 $[M-H]^-$, Found: 453.0787.

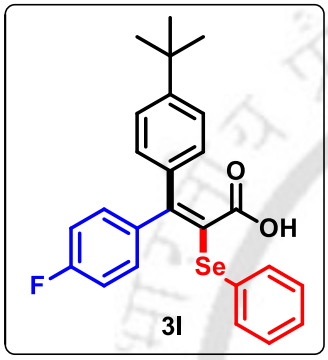

(*Z*)-3-(4-acetylphenyl)-3-(4-(tert-butyl)phenyl)-2-(phenylselanyl)acrylic acid (**2.3m**): Yellow solid (30 % ethyl acetate in petroleum ether) Yield: (58 mg) 61 %; **^{1}H NMR** (500 MHz, $CDCl_3$) δ 7.93 (d, J = 8.3 Hz, 2H), 7.51 – 7.49 (m, 2H), 7.39 (d, J = 8.1 Hz, 2H), 7.28 – 7.22 (m, 6H), 7.14 (d, J = 8.4 Hz, 2H), 2.60 (s, 3H), 1.28 (s, 9H). **^{13}C NMR** (125 MHz, $CDCl_3$) δ 197.8, 170.2, 152.1, 149.7, 146.5, 137.3, 136.7, 133.5, 129.7, 129.5, 129.4, 128.53, 128.45, 128.1, 125.5, 123.4, 34.8, 31.4, 26.8. **HRMS** (ESI-TOF): m/z calcd. for $C_{27}H_{26}O_3Se$: 477.0973 $[M-H]^-$, Found: 477.0992.

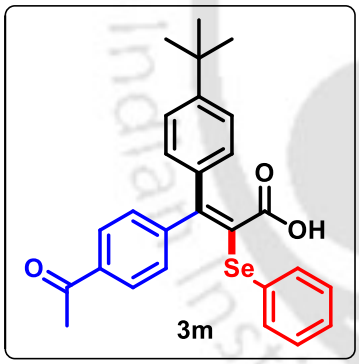

(*E*)-3-(4-(tert-butyl)phenyl)-3-phenyl-2-(p-tolylselanyl)acrylic acid (**2.3n**): Yellow solid (30 % ethyl acetate in petroleum ether) Yield: (63 mg) 71 %; **^{1}H NMR** (500 MHz, $CDCl_3$) δ 7.39 (d, J = 7.8 Hz, 2H), 7.34 – 7.31 (m, 3H), 7.30 – 7.28 (m, 2H), 7.26 – 7.24 (m, 2H), 7.15 – 7.14 (m, 2H), 7.04 (d, J = 7.9 Hz, 2H), 2.30 (s, 3H), 1.28 (s, 9H). **^{13}C NMR** (125 MHz, $CDCl_3$) δ 170.9, 151.7, 150.5, 141.8, 138.1, 138.0, 133.9, 130.1, 129.4, 128.6, 128.31, 128.29, 125.9, 125.3, 122.6, 34.8, 31.4, 21.3. **HRMS** (ESI-TOF): m/z calcd. for $C_{26}H_{26}O_2Se$: 451.1172 $[M+H]^+$, Found: 451.1191.

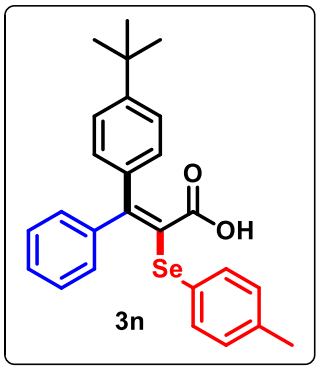

(*E*)-2-((4-bromophenyl)selanyl)-3-(4-(tert-butyl)phenyl)-3-phenylacrylic acid (**2.3o**): Yellow solid (30 % ethyl acetate in petroleum ether) Yield: (67 mg) 66 %; **^{1}H NMR** (500 MHz, $CDCl_3$) δ 7.34 – 7.32 (m, 7H), 7.28 – 7.24 (m, 4H), 7.15 – 7.14 (m, 2H), 1.29 (s, 9H). **^{13}C NMR** (125 MHz, $CDCl_3$) δ 170.9, 152.7, 152.0, 141.7, 137.8, 134.8, 132.4, 129.3, 129.1, 128.6, 128.5, 128.3, 125.4, 122.3, 121.2, 34.8, 31.4. **HRMS** (ESI-TOF): m/z calcd. for $C_{25}H_{23}BrO_2Se$: 512.9973 $[M-H]^-$, Found: 512.9974.

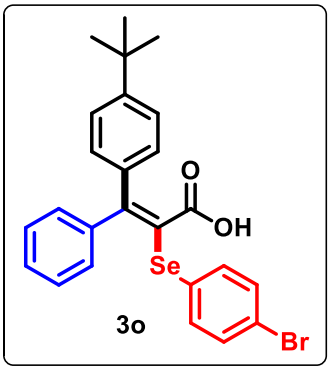

(*E*)-3-(4-(tert-butyl)phenyl)-2-((4-methoxyphenyl)selanyl)-3-phenylacrylic acid (**2.3p**): Yellow solid (30 % ethyl acetate in petroleum ether) Yield: (67 mg) 72 %; **^{1}H NMR** (500 MHz, $CDCl_3$) δ 7.44 (d, J = 8.3 Hz, 2H), 7.38 – 7.29 (m, 5H), 7.24 (d, J = 8.4 Hz, 2H), 7.13 (d, J = 8.2 Hz, 2H), 6.77 (d, J = 8.3 Hz, 2H), 3.77 (s, 3H), 1.27 (s, 9H). **^{13}C NMR** (125 MHz, $CDCl_3$) δ 171.0, 160.1, 151.5, 148.5, 141.7, 137.9, 136.6, 129.4, 128.5, 128.34, 128.26, 125.3, 123.6, 119.2, 115.0, 55.4, 34.8, 31.4. **HRMS** (ESI-TOF): m/z calcd. for $C_{26}H_{26}O_3Se$: 421.1071 $[M-CO_2]^-$, Found: 421.1035.

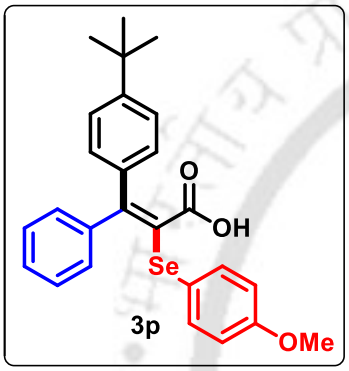

(*E*)-3-(4-chlorophenyl)-2-((4-fluorophenyl)selanyl)-3-phenylacrylic acid (**2.3q**)[5]: Yellow solid (30 % ethyl acetate in petroleum ether) Yield: (52 mg) 61 %; **^{1}H NMR** (500 MHz, $CDCl_3$) δ 7.49 – 7.46 (m, 2H), 7.38 – 7.34 (m, 3H), 7.27 – 7.26 (m, 2H), 7.23 (d, J = 8.3 Hz, 2H), 7.13 (d, J = 8.5 Hz, 2H), 6.93 (t, J = 8.7 Hz, 2H). **^{13}C NMR** (125 MHz, $CDCl_3$) δ 171.1, 163.2 (d, J = 247.3 Hz), 148.4, 140.8, 139.4, 136.8 (d, J = 8.0 Hz), 134.7, 130.1, 129.3, 128.8, 128.6 (d, J = 8.8 Hz), 124.1, 123.43, 123.40, 116.5 (d, J = 21.5 Hz).

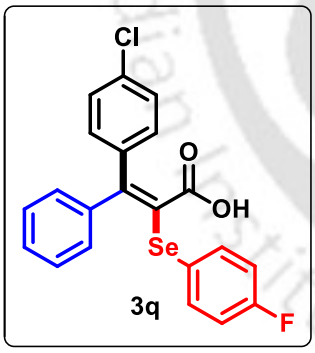

(*E*)-3-(4-(tert-butyl)phenyl)-2-(methylselanyl)-3-phenylacrylic acid (**2.3r**): Yellow solid (30 % ethyl acetate in petroleum ether) Yield: (44 mg) 59 %; **^{1}H NMR** (500 MHz, $CDCl_3$) δ 7.38 – 7.31 (m, 3H), 7.29 – 7.25 (m, 4H), 7.17 – 7.15 (m, 2H), 2.15 (s, 3H), 1.28 (s, 9H). **^{13}C NMR** (125 MHz, $CDCl_3$) δ 172.4, 151.3, 147.4, 141.5, 137.9, 129.4, 128.4, 128.33, 128.27, 125.3, 121.4, 34.7, 31.4, 7.8. **HRMS** (ESI-TOF): m/z calcd. for $C_{20}H_{22}O_2Se$: 373.0707 $[M-H]^-$, Found: 373.0682.

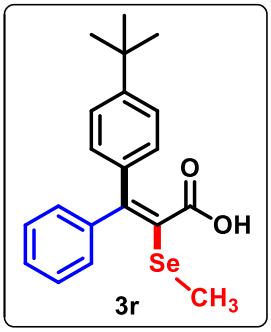

(2-(4-(tert-butyl)phenyl)-2-phenylethene-1,1-diyl)bis(phenylselane) (**2.4a**): Pale yellow solid (2 % ethyl acetate in petroleum ether) Yield: (105 mg) 96 %; **^{1}H NMR** (600 MHz, $CDCl_3$) δ 7.29 – 7.25 (m, 5H), 7.24 – 7.17 (m, 8H), 7.15 – 7.10 (m, 6H), 1.29 (s, 9H). **^{13}C NMR** (125 MHz, $CDCl_3$) δ 153.5, 150.7, 143.6, 140.1, 133.7, 133.5, 132.68, 132.67, 129.5, 129.1, 128.60, 128.57, 128.1, 127.7, 127.3, 127.2, 124.9, 121.7, 34.7, 31.4. **HRMS** (ESI-TOF): m/z calcd. for $C_{30}H_{28}Se_2$: 549.0595 $[M+H]^+$, Found: 549.0605.

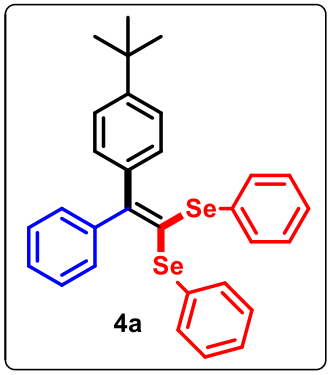

(2-phenyl-2-(p-tolyl)ethene-1,1-diyl)bis(phenylselane) (**2.4b**)[6]: Pale yellow solid (2 % ethyl acetate in petroleum ether) Yield: (94 mg) 94 %; **^{1}H NMR** (500 MHz, $CDCl_3$) δ 7.21 – 7.10 (m, 11H), 7.07 – 7.01 (m, 8H), 2.24 (s, 3H). **^{13}C NMR** (125 MHz, $CDCl_3$) δ 153.7, 143.4, 140.4, 137.7, 133.7, 133.5, 132.64, 132.57, 129.5, 129.4, 128.8, 128.6, 128.1, 127.7, 127.31, 127.25, 121.9, 21.4.

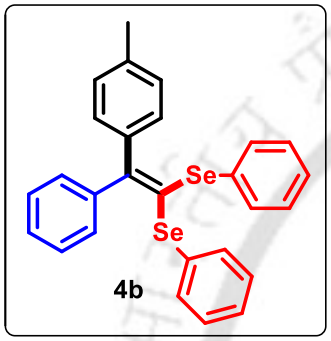

(2,2-diphenylethene-1,1-diyl) bis(phenylselane) (**2.4c**)[6]: White solid (2 % ethyl acetate in petroleum ether) Yield: (85 mg) 87 %; **^{1}H NMR** (500 MHz, $CDCl_3$) δ 7.22 – 7. 10 (m, 16H), 7.05 (t, J = 7.4 Hz, 4H). **^{13}C NMR** (125 MHz, $CDCl_3$) δ 153.5, 143.3, 133.6, 132.5, 129.4, 128.6, 128.1, 127.8, 127.3, 122.5.

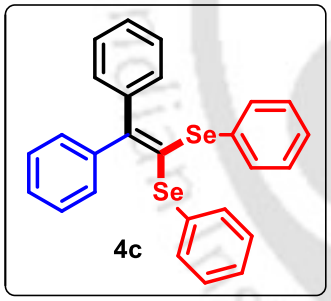

(2-(4-(tert-pentyl)phenyl)-2-phenylethene-1,1-diyl)bisn (phenylselane) (**2.4d**): Pale yellow solid (2 % ethyl acetate in petroleum ether) Yield: (102 mg) 91 %; **^{1}H NMR** (500 MHz, $CDCl_3$) δ 7.28 – 7.10 (m, 19H), 1.60 (q, J = 7.5 Hz, 2H), 1.25 (s, 6H), 0.67 (t, J = 7.4 Hz, 3H). **^{13}C NMR** (125 MHz, $CDCl_3$) δ 153.6, 149.2, 143.7, 140.0, 133.7, 133.5, 132.8, 132.7, 129.5, 129.1, 128.61, 128.57, 128.1, 127.7, 127.3, 127.2, 125.6, 121.7, 38.0, 37.0, 28.4, 9.3. **HRMS** (ESI-TOF): m/z calcd. for $C_{31}H_{30}Se_2$: 562.0672 $[M]^+$, Found: 562.0672.

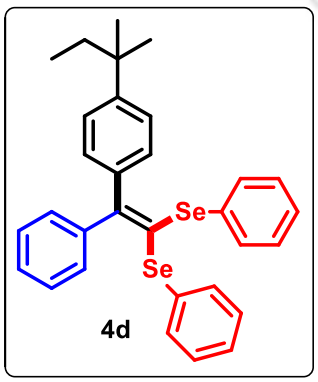

(2-(4-iodophenyl)-2-phenylethene-1,1-diyl)bis(phenylselane) (**2.4e**)[6]: Pale yellow solid (2 % ethyl acetate in petroleum ether) Yield: (107 mg) 87 %; **^{1}H NMR** (500 MHz, $CDCl_3$) δ 7.57 (d, *J* = 8.2 Hz, 2H), 7.30 – 7.25 (m, 4H), 7.23 – 7.18 (m, 7H), 7.14 (t, *J* = 7.5 Hz, 4H), 6.94 (d, *J* = 8.2 Hz, 2H). **^{13}C NMR** (125 MHz, $CDCl_3$) δ 151.6, 142.8, 142.7, 137.2, 134.0, 133.4, 132.4, 132.2, 131.3, 129.4, 128.73, 128.69, 128.3, 128.0, 127.6, 127.4, 123.6, 93.6.

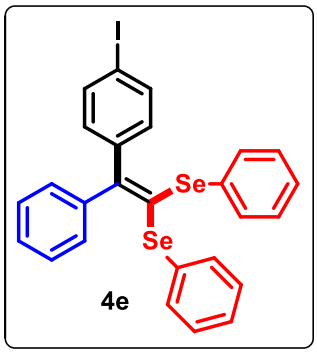

(2-(4-fluorophenyl)-2-phenylethene-1,1-diyl)bis(phenylselane) (**2.4f**)[6]: Pale yellow solid (2 % ethyl acetate in petroleum ether) Yield: (82 mg) 81 %; **^{1}H NMR** (500 MHz, $CDCl_3$) δ 7.31 – 7.25 (m, 4H), 7.23 – 7.18 (m, 9H), 7.17 – 7.12 (m, 4H), 6.94 (t, *J* = 8.5 Hz, 2H). **^{13}C NMR** (125 MHz, $CDCl_3$) δ 162.3 (d, *J* = 246.2 Hz), 151.9, 143.2, 139.24, 139.21, 133.8, 133.5, 132.43, 132.35, 131.2 (d, *J* = 8.1 Hz) 129.4, 128.70, 128.68, 128.2, 127.9, 127.5, 127.4, 123.0, 115.1 (d, *J* = 21.5 Hz).

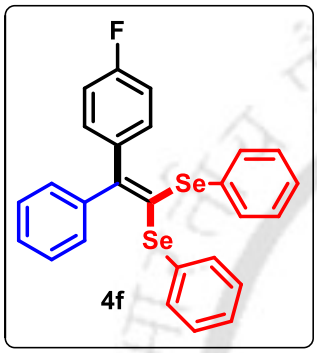

(2-(4-chlorophenyl)-2-phenylethene-1,1-diyl)bis(phenylselane) (**2.4g**)[6]: Pale yellow solid (2 % ethyl acetate in petroleum ether) Yield: (90 mg) 86 %; **^{1}H NMR** (500 MHz, $CDCl_3$) δ 7.28 – 7.19 (m, 13H), 7.15 – 7.12 (m, 6H). **^{13}C NMR** (125 MHz, $CDCl_3$) δ 151.6, 143.0, 141.7, 133.9, 133.6, 133.5, 132.4, 132.3, 130.9, 129.4, 128.73, 128.70, 128.31, 128.28, 128.0, 127.6, 127.4, 123.6.

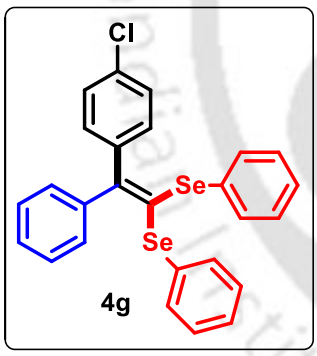

(2-(2-methoxyphenyl)-2-phenylethene-1,1-diyl)bis(phenylselane) (**2.4h**)[6]: Pale yellow solid (2 % ethyl acetate in petroleum ether) Yield: (91 mg) 88 %;**^{1}H NMR** (500 MHz, $CDCl_3$) δ 7.32 – 7.30 (m, 2H), 7.28 – 7.24 (m, 7H), 7.22 – 7.12 (m, 8H), 6.92 (t, *J* = 7.4 Hz, 1H), 6.86 (d, *J* = 8.2 Hz, 1H), 3.80 (s, 3H). **^{13}C NMR** (125 MHz, $CDCl_3$) δ 156.3, 151.0, 142.9, 133.9, 133.1, 132.9, 132.8, 132.6, 130.2, 129.3, 129.1, 128.6, 128.5, 127.8, 127.5, 127.2, 127.0, 123.2, 120.6, 111.3, 55.6.

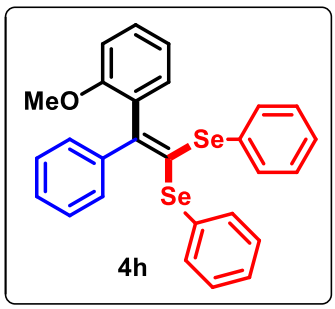

(2-phenyl-2-(p-tolyl)ethene-1,1-diyl)bis(phenylselane) (**2.4i**)[6]: Pale yellow solid (2 % ethyl acetate in petroleum ether) Yield: (83 mg) 83 %; **^{1}H NMR** (500 MHz, $CDCl_3$) δ 7.21 – 7.09 (m, 11H), 7.07 – 7.01 (m, 8H), 2.24 (s, 3H). **^{13}C NMR** (125 MHz, $CDCl_3$) δ 153.7, 143.4, 140.4, 137.7, 133.7, 133.5, 132.63, 132.56, 129.44, 129.35, 128.8, 128.6, 128.1, 127.7, 127.3, 127.2, 121.8, 21.4.

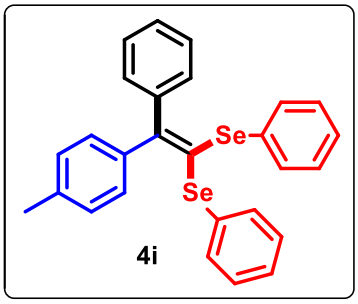

(2-(4-methoxyphenyl)-2-phenylethene-1,1-diyl)bis(phenylselane) (**2.4j**)[6]: Pale yellow solid (2 % ethyl acetate in petroleum ether) Yield: (91 mg) 88 %; **^{1}H NMR** (500 MHz, $CDCl_3$) δ 7.29 – 7.24 (m, 4H), 7.23 – 7.19 (m, 7H), 7.18 – 7.12 (m, 6H), 6.81 (d, J = 8.3 Hz, 2H), 3.78 (s, 3H). **^{13}C NMR** (125 MHz, $CDCl_3$) δ 159.3, 153.4, 143.6, 135.7, 133.7, 133.5, 132.8, 132.7, 130.9, 129.5, 128.6, 128.1, 127.8, 127.3, 127.2, 121.8, 113.5, 55.4.

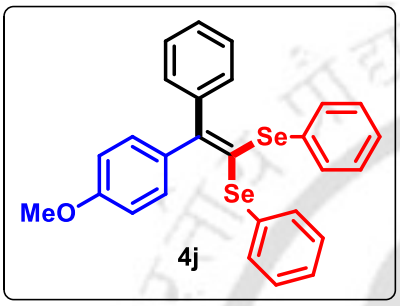

methyl 4-(1-phenyl-2,2-bis(phenylselanyl)vinyl)benzoate (**2.4k**)[6]: Pale yellow solid (2 % ethyl acetate in petroleum ether) Yield: (86 mg) 79 %; **^{1}H NMR** (500 MHz, $CDCl_3$) δ 7.85 (d, J = 7.9 Hz, 2H), 7.23 – 7.20 (m, 4H), 7.18 – 7.17 (m, 2H), 7.16 – 7.11 (m, 7H), 7.09 – 7.04 (m, 4H), 3.82 (s, 3H). **^{13}C NMR** (125 MHz, $CDCl_3$) δ 166.9, 151.7, 147.9, 142.8, 134.1, 133.4, 132.3, 132.1, 129.51, 129.46, 129.4, 129.2, 128.8, 128.7, 128.3, 128.0, 127.7, 127.5, 124.5, 52.2.

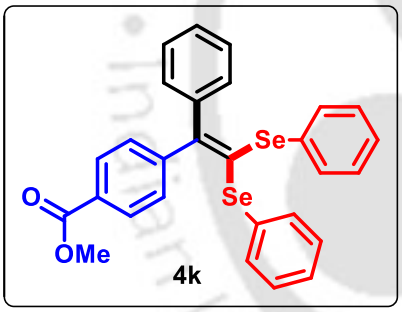

1-(4-(1-phenyl-2,2-bis(phenylselanyl)vinyl)phenyl)ethenone (**2.4l**)[6]: Pale yellow solid (2 % ethyl acetate in petroleum ether) Yield: (76 mg) 71 %; **^{1}H NMR** (500 MHz, $CDCl_3$) δ 7.87 (d, J = 8.2 Hz, 2H), 7.35 – 7.30 (m, 4H), 7.39 – 7.28 (m, 2H), 7.26 – 7.21 (m, 7H), 7.19 – 7.14 (m, 4H), 2.59 (s, 3H). **^{13}C NMR** (125 MHz, $CDCl_3$) δ 197.7, 151.5, 148.1, 142.7, 136.0, 134.1, 133.3, 132.3, 132.1, 129.7, 129.4, 128.8, 128.7, 128.4, 128.2, 128.1, 127.7, 127.5, 124.6, 26.7.

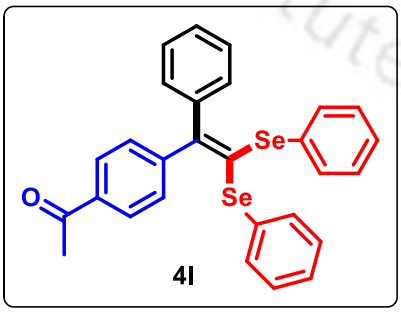

(2,2-diphenylethene-1,1-diyl)bis((4-bromophenyl)selane) (**2.4m**)[6]: White solid (2 % ethyl acetate in petroleum ether) Yield: (105 mg) 81 %; **^{1}H NMR** (500 MHz, $CDCl_3$) δ 7.23 – 7.19 (m, 10H), 7.14 – 7.13 (m, 4H), 6.99 (d, *J* = 8.1 Hz, 4H). **^{13}C NMR** (125 MHz, $CDCl_3$) δ 154.2, 142.9, 135.2, 131.8, 131.1, 129.3, 128.3, 128.1, 122.0, 121.4.

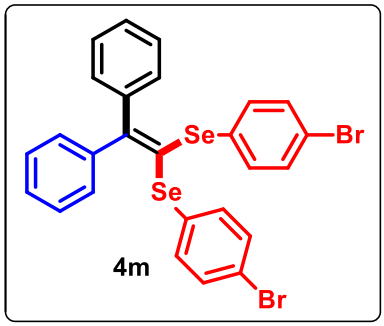

(2,2-diphenylethene-1,1-diyl)bis((4-fluorophenyl)selane) (**2.4n**)[6]: Pale yellow solid (2 % ethyl acetate in petroleum ether) Yield: (64 mg) 61 %; **^{1}H NMR** (500 MHz, $CDCl_3$) δ 7.31 – 7.25 (m, 6H), 7.21 – 7.19 (m, 4H), 7.17 – 7.14 (m, 4H), 6.84 (t, *J* = 8.5 Hz, 4H). **^{13}C NMR** (125 MHz, $CDCl_3$) δ 162.6 (d, *J* = 246.1 Hz), 152.9, 143.1, 135.8 (d, *J* = 8.1 Hz), 129.4, 128.2, 128.0, 126.9 (d, *J* = 3.3 Hz), 122.8, 115.8 (d, *J* = 21.5 Hz).

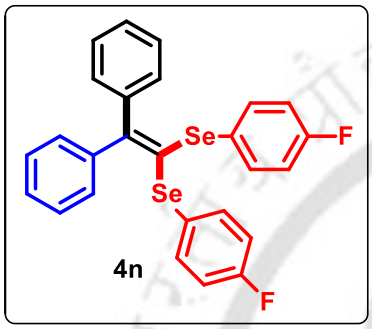

(2,2-diphenylethene-1,1-diyl)bis((4-methoxyphenyl)selane) (**2.4o**)[6]: Pale yellow solid (2 % ethyl acetate in petroleum ether) Yield: (80 mg) 73 %; **^{1}H NMR** (500 MHz, $CDCl_3$) δ 7.29 – 7.24 (m, 6H), 7.21 – 7.19 (m, 4H), 7.12 (d, *J* = 8.2 Hz, 4H), 6.69 (d, *J* = 8.6 Hz, 4H), 3.77 (s, 6H). **^{13}C NMR** (125 MHz, $CDCl_3$) δ 159.5, 151.8, 143.4, 135.7, 129.5, 128.1, 127.7, 124.7, 123.0, 114.3, 55.4.

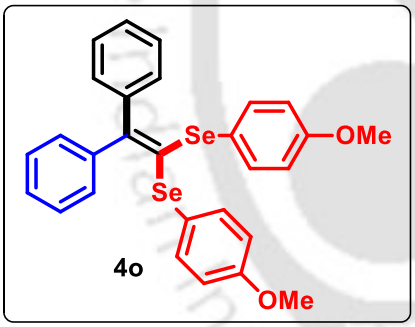

(2,2-diphenylethene-1,1-diyl)bis(methylselane) (**2.4p**)[6]: Pale yellow solid (2 % ethyl acetate in petroleum ether) Yield: (55 mg) 76 %; **^{1}H NMR** (500 MHz, $CDCl_3$) δ 7.25 – 7.22 (m, 4H), 7.20 – 7.17 (m, 2H), 7.15 – 7.12 (m, 4H), 2.04 (s, 6H). **^{13}C NMR** (125 MHz, $CDCl_3$) δ 150.2, 143.7, 129.6, 128.1, 127.5, 122.8, 11.1.

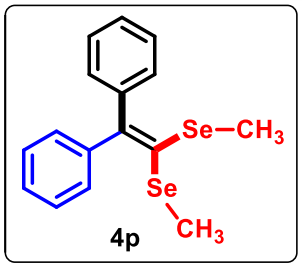

(*E*)-methyl 3-phenyl-2,3-bis(phenylselanyl)acrylate (**2.5**)[5]: Pale yellow solid (3 % ethyl acetate in petroleum ether) Yield: (29 mg) 31 %; **^{1}H NMR** (500 MHz, $CDCl_3$) δ 7.26 – 7.24 (m, 2H), 7.17 – 7.15 (m, 2H), 7.13 – 7.11 (m, 3H), 7.01 – 6.89 (m, 6H), 6.86 – 6.84 (m, 2H), 3.53 (s, 3H). **^{13}C NMR** (125 MHz, $CDCl_3$) δ 167.0, 155.6, 139.6, 136.2, 132.4, 131.6, 130.1, 129.4, 129.0, 128.4, 128.2, 127.8, 127.6, 127.3, 118.7, 52.6.

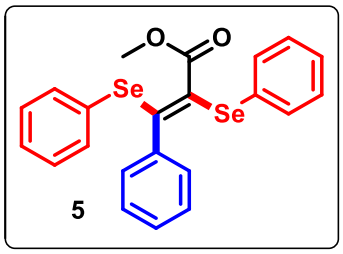

(*E*)-ethyl 3-(4-(tert-butyl)phenyl)-3-phenyl-2-(phenylselanyl)acrylate (**2.6**): Pale yellow solid (5 % ethyl acetate in petroleum ether) Yield: (88 mg) 76 %; **^{1}H NMR** (500 MHz, $CDCl_3$) δ 7.56 – 7.54 (m, 2H), 7.37 – 7.34 (m, 4H), 7.26 – 7.25 (m, 6H), 7.15 – 7.14 (m, 2H), 3.69 (q, *J* = 7.1 Hz, 2H), 1.27 (s, 9H), 0.78 (t, *J* = 7.2 Hz, 3H). **^{13}C NMR** (125 MHz, $CDCl_3$) δ 167.8, 151.3, 148.3, 141.6, 138.4, 134.4, 129.5, 129.4, 129.1, 128.5, 128.4, 128.2, 128.0, 125.1, 124.3, 61.1, 34.7, 31.4, 13.6. **HRMS** (ESI-TOF): m/z calcd. for $C_{27}H_{28}O_2Se$: 391.0965 $[M\text{-}CO_2Et]^+$, Found: 391.0941

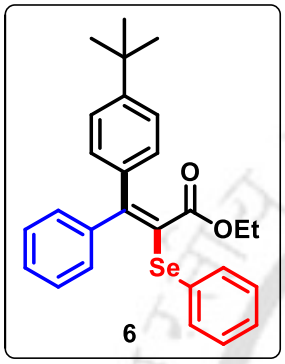

(*E*)-3-(4-(tert-butyl)phenyl)-3-phenyl-2-(phenylselanyl)prop-2-en-1-ol (**2.7**): White solid (10 % ethyl acetate in petroleum ether) Yield: (70 mg) 67 %; **^{1}H NMR** (500 MHz, $CDCl_3$) δ 7.52 – 7.50 (m, 2H), 7.32 – 7.26 (m, 8H), 7.23 – 7.21 (m, 2H), 7.15 (d, *J* = 8.3 Hz, 2H), 4.21 (d, *J* = 6.5 Hz, 2H), 1.98 (t, *J* = 6.5 Hz, 1H), 1.30 (s, 9H). **^{13}C NMR** (125 MHz, $CDCl_3$) δ 150.9, 149.0, 143.3, 137.9, 133.7, 132.7, 129.9, 129.43, 129.36, 129.1, 128.2, 127.74, 127.69, 125.3, 63.0, 34.7, 31.4. **HRMS** (ESI-TOF): m/z calcd. for $C_{25}H_{26}OSe$: 405.1121 $[M\text{-}OH]^+$, Found: 405.1152

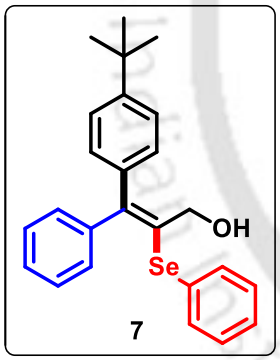

(4-chlorophenyl)(1-iodo-2,2-diphenylvinyl)selane (**2.8**)[5]: Pale yellow solid (2 % ethyl acetate in petroleum ether) Yield: (72 mg) 73 %; **^{1}H NMR** (500 MHz, $CDCl_3$) δ 7.43 (d, *J* = 8.4 Hz, 2H), 7.35 – 7.28 (m, 8H), 7.27 – 7.25 (m, 4H). **^{13}C NMR** (125 MHz, $CDCl_3$) δ 156.8, 146.2, 141.6, 135.5, 134.8, 132.3, 129.5, 128.8, 128.7, 128.5, 128.4, 128.3, 128.0, 81.9.

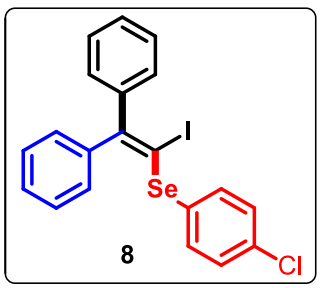

(1-bromo-2,2-diphenylvinyl)(4-chlorophenyl)selane (**2.9**)[5]: Pale yellow solid (2 % ethyl acetate in petroleum ether) Yield: (58 mg) 65 %; **^{1}H NMR** (500 MHz, $CDCl_3$) δ 7.48 – 7.45 (m, 2H), 7.34 – 7.27 (m, 10H), 7.26 – 7.24 (m, 2H). **^{13}C NMR** (125 MHz, $CDCl_3$) δ 151.1, 142.5, 142.0, 135.4, 134.7, 129.7, 129.5, 129.2, 129.1, 128.5, 128.31, 128.29, 128.0, 108.1.

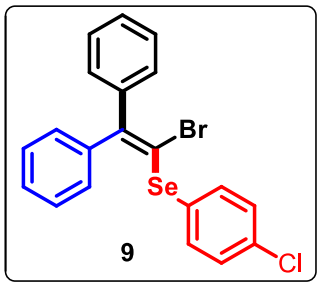

2.11 References:

1. Mugesh, G.; du Mont, W.-W.; Sies, H. Chemistry of Bio-logically Important Synthetic Organoselenium Compounds. *Chem. Rev.* **2001**, *101*, 2125–2180.

2. Frizon, T. E.; Rampon, D. S.; Gallardo, H.; Merlo, A. A.; Schneider, P. H.; Rodrigues, O. E. D.; Braga, A. L. Selenides and Diselenides Containing Oxadiazoles: A New Class of Functionalised Materials. *Liq. Cryst.* **2012**, *39*, 769–777.

3. Manna, D.; Mugesh, G. Regioselective Deiodination of Thyroxine by Iodothyronine Deiodinase Mimics: An Unusual Mechanistic Pathway Involving Cooperative Chalcogen and Halo-gen Bonding. *J. Am. Chem. Soc.* **2012**, *134*, 4269–4279.

4. Tang, B.; Xing, Y.; Li, P.; Zhang, N.; Yu, F.; Yang, G. A Rhodamine-Based Fluorescent Probe Containing a Se−N Bond for Detecting Thiols and Its Application in Living Cells. *J. Am. Chem. Soc.* **2007**, *129*, 11666–11667.

5. Savegnago, L.; Jesse, C. R.; Moro, A. V; Borges, V. C.; Santos, F. W.; Rocha, J. B. T.; Nogueira, C. W. Bis Selenide Alkene Derivatives: A Class of Potential Antioxidant and Antinociceptive Agents. *Pharmacol. Biochem. Behav.* **2006**, *83*, 221–229.

6. Borges, V. C.; Dadalt, G.; Savegnago, L.; Moro, A. V; Ro-cha, J. B. T.; Nogueira, C. W. 1,1,2-Tris-Organoselenide Alkene Derivatives, but Not 1,2-Bis-Organoselenide Alkene Derivatives, Inhibited δ-Aminolevulinate Dehydratase Activity from Human Erythrocytic Cells in Vitro. *Toxicol. Vitr.* **2007**, *21*, 387–391.

7. Takimiya, K.; Jigami, T.; Kawashima, M.; Kodani, M.; Aso, Y.; Otsubo, T. Synthetic Procedure for Various Selenium-Containing Electron Donors of the Bis(Ethylenedithio)Tetrathiafulvalene (BEDT-TTF) Type. *J. Org. Chem.* **2002**, *67*, 4218–4227.

8. (a) Sahoo, H.; Singh, S.; Baidya, M. Radical Cascade Reaction of Aryl Alkynoates at Room Temperature: Synthesis of Fully Substituted α, β-Unsaturated Acids with Chalcogen Functionality. *Org. Lett.* **2018**, *20*, 3678–3681. (b) Sahoo, H.; Ramakrishna, I.; Mandal, A.;

Baidya, M. At-om Transfer Oxidative Radical Cascade of Aryl Alkynoates towards 1,1-Dichalcogenide Olefins. *Chem. – An Asian J.* **2019**, *14*, 4549–4552.

9. Perin, G.; Lenardão, E. J.; Jacob, R. G.; Panatieri, R. B. Synthesis of Vinyl Selenides. *Chem. Rev.* **2009**, *109*, 1277–1301

10. Sahoo, H.; Mandal, A.; Dana, S.; Baidya, M. Visible Light-Induced Synthetic Approach for Selenylative Spirocyclization of N-Aryl Alkynamides with Molecular Oxygen as Oxidant. *Adv. Synth. Catal.* **2018**, *360*, 1099–1103.

11. (a) Lapcinska, S.; Arsenyan, P. Selenocysteinyl Electro-philes Efficiently Promote the Formation of Coumarin and Quinolinone Cores by 6-Endo-Dig Cyclization. *New J. Chem.* **2021**, *45*, 16625–16634. (b) Lapcinska, S.; Dimitrijevs, P.; Lapcinskis, L.; Arsenyan, P. Visible Light-Mediated Functionalization of Seleno-cystine-Containing Peptides. *Adv. Synth. Catal*. **2021**, *363*, 3318–3328. (c) Aganda, K. C. C.; Lee, A. Synthesis of Selenaheterocycles via Visible-Light-Mediated Radical Cyclization. *Adv. Synth. Catal.* **2021**, *363*, 5149–5154.

12. (a) Kong, D.-L.; Cheng, L.; Wu, H.-R.; Li, Y.-X.; Wang, D.; Liu, L. A Metal-Free Yne-Addition/1,4-Aryl Migration/Decarboxylation Cascade Reaction of Alkynoates with Csp3–H Centers. *Org. Biomol. Chem.* **2016**, *14*, 2210–2217. (b) Ni, S.; Zhang, Y.; Xie, C.; Mei, H.; Han, J.; Pan, Y. Oxidative Difunctionalization of Alkynoates through Alkylation and Migration Decarboxylative Arylation. *Org. Lett.* **2015**, *17*, 5524–5527. (c) Ni, S.; Sha, W.; Zhang, L.; Xie, C.; Mei, H.; Han, J.; Pan, Y. N-Iodosuccinimide-Promoted Cascade Trifunctionalization of Alkynoates: Access to 1,1-Diiodoalkenes. *Org. Lett*. **2016**, *18*, 712–715. (d) Ni, S.; Zhang, L.; Zhang, W.; Mei, H.; Han, J.; Pan, Y. Synthesis of Trisubstituted Vinyl Sulfides via Oxidative Thiolation Initiated Cascade Reaction of Alkynoates with Thiols. *J. Org. Chem.* **2016**, *81*, 9470–9475. (e) Wei, W.; Wang, L.; Yue, H.; Jiang, Y.-Y.; Yang, D. Catalyst-Free Synthesis of α-Thioacrylic Acids via Cascade Thiolation and 1,4-Aryl Migration of Aryl Alkynoates at Room Temperature. *Org. Biomol. Chem.* **2018**, *16*, 8379–8383.

13. Lapcinska, S.; Arsenyan, P. Selenocysteinyl Electrophiles Efficiently Promote the Formation of Coumarin and Quinolinone Cores by 6-Endo-Dig Cyclization. *New J. Chem*. **2021**, *45*, 16625–16634.

14. (a) Hua, J.; Fang, Z.; Xu, J.; Bian, M.; Liu, C.; He, W.; Zhu, N.; Yang, Z.; Guo, K. Electrochemical Oxidative Cyclization of Activated Alkynes with Diselenides or Disulfides: Access to Functionalized Coumarins or Quinolinones. *Green Chem.* **2019**, *21*, 4706–4711. b) Mi, X.; Wang, C.; Huang, M.; Zhang, J.; Wu, Y.; Wu, Y. Silver-Catalyzed Synthesis of 3-Phosphorated Coumarins via Radical Cyclization of Alkynoates and Dialkyl H-Phosphonates. *Org. Lett.* **2014**, *16*, 3356–3359. (c) Kanyiva, K. S.; Hamada, D.; Makino, S.; Takano, H.;

Shibata, T. α-Amino Acid Sulfonamides as Versatile Sulfonylation Reagents: Silver-Catalyzed Synthesis of Coumarins and Oxindoles by Radical Cyclization. *European J. Org. Chem.* **2018**, *43*, 5905–5909.

15. Fleming, A. M.; Burrows, C. J. Iron Fenton Oxidation of 2′-Deoxyguanosine in Physiological Bicarbonate Buffer Yields Products Consistent with the Reactive Oxygen Species Carbonate Radical Anion, Not the Hydroxyl Radical. *Chem. Commun.* **2020**, *56*, 9779–9782.

16. Li, H.; Liu, S.; Huang, Y.; Xu, X.-H.; Qing, F.-L. Tandem trifluoromethylthiolation/aryl migration of aryl alkynoates to trifluoromethylthiolated alkenes *Chem. Commun.* **2017**, *53*, 10136–10139.

17. Yan, G.; Borah, A. J.; Wang, L. Efficient silver-catalyzed direct sulfenylation and selenylation of rich arenes. *Org. Biomol. Chem.* **2014**, *12*, 9557–9561.

18. Suárez-Escobedo, L.; Gotor-Fernández, V. Solvent role in the lipase-catalysed esterification of cinnamic acid and derivatives. Optimisation of the biotransformation conditions. *Tetrahedron* **2021**, *81*, 131873.

19. Ma, J.; Chen, L.; Fan, J.; Cao, W.; Zeng, G.; Wang, Y.; Li, Y.; Zhou, Y.; Deng, X. Dual-targeting Rutaecarpine-NO donor hybrids as novel antihypertensive agents by promoting release of CGRP. *Eur. J. Med. Chem*. **2019**, *168*, 146–153.

2.12 Selected NMR spectra:

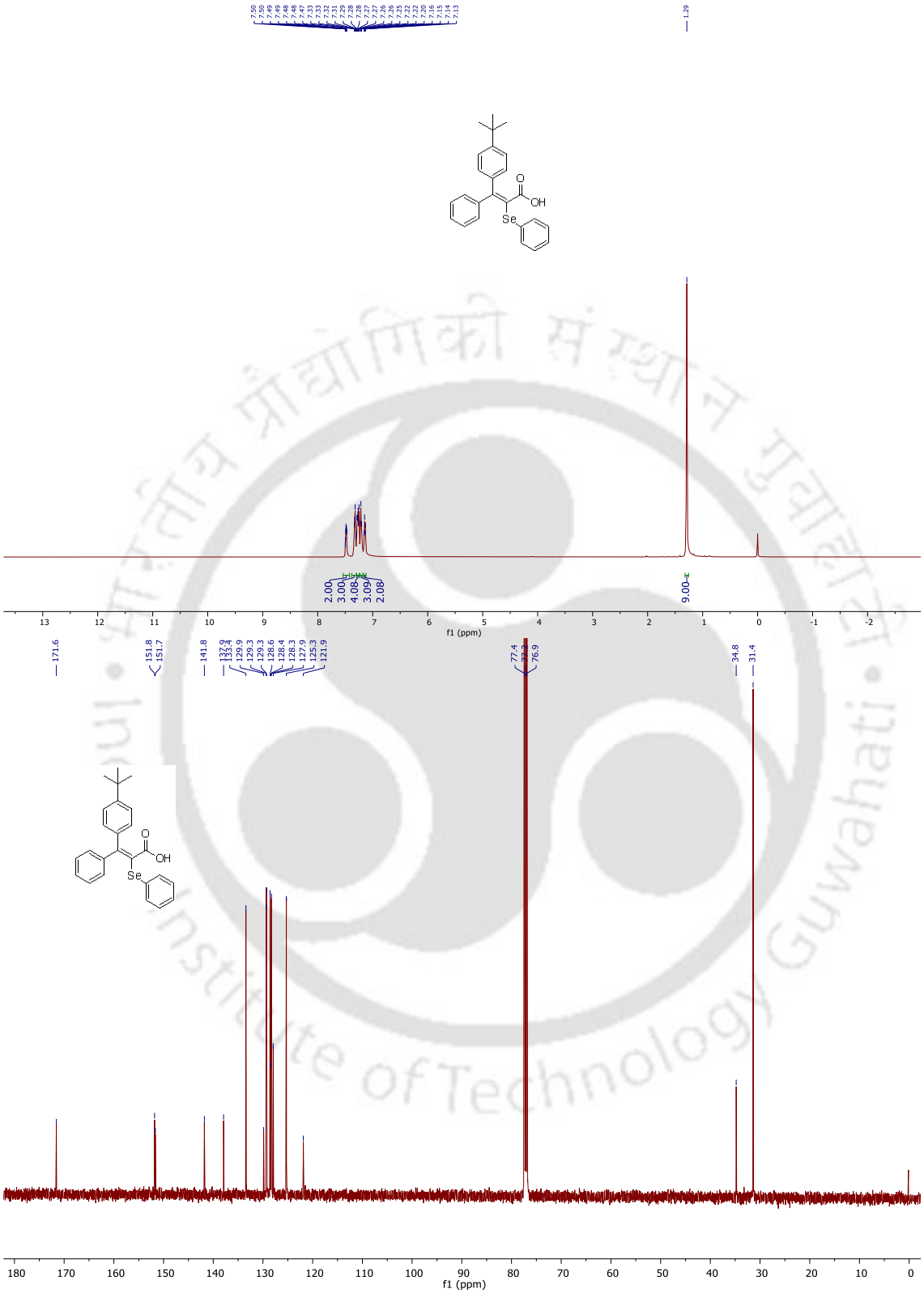

Figure 2.8: ^{1}H NMR (500 MHz) and $^{13}C\{^{1}H\}$ NMR (125 MHz) spectrum of Compound **2.3a** in $CDCl_3$.

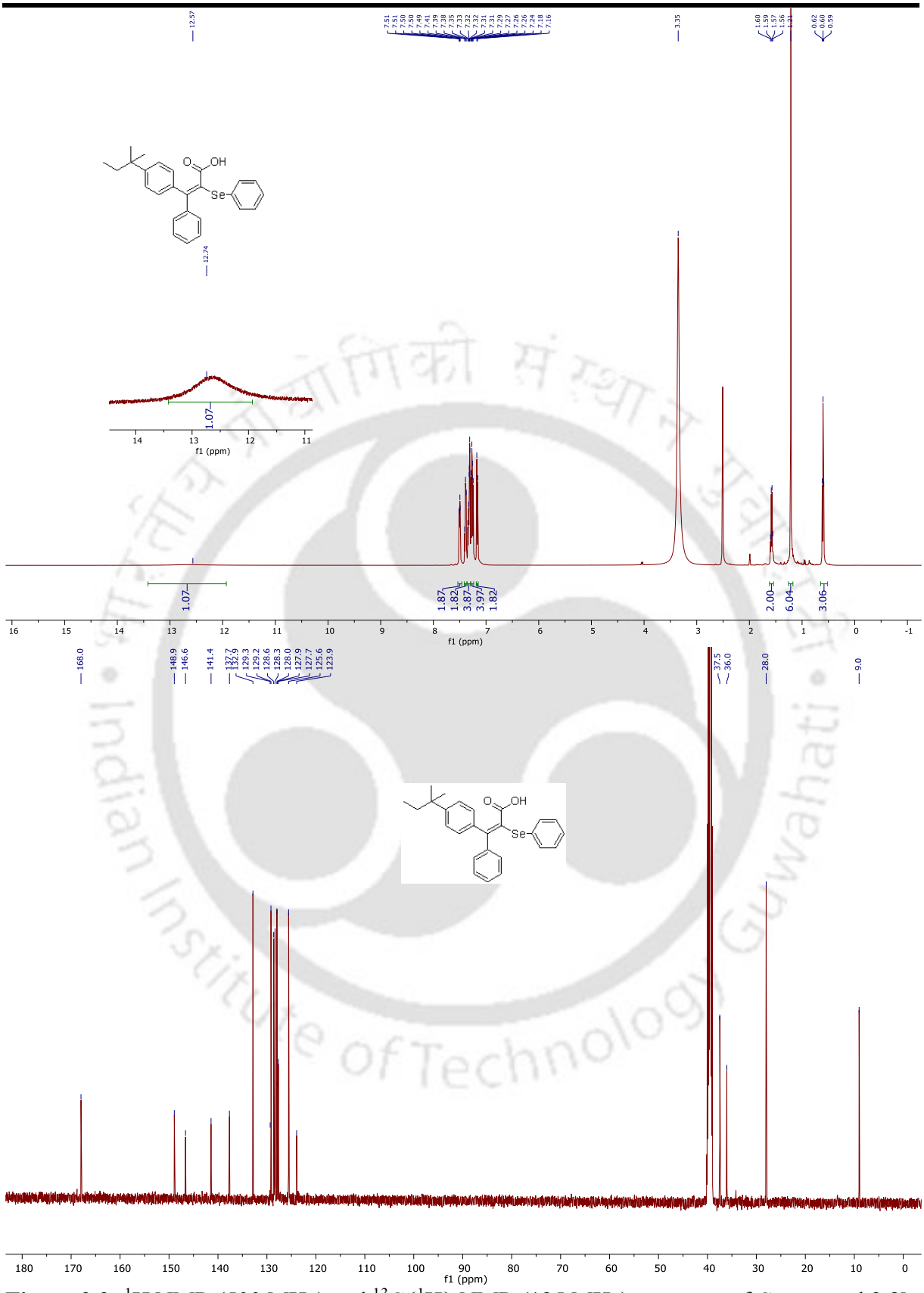

Figure 2.9: ^{1}H NMR (500 MHz) and $^{13}C\{^{1}H\}$ NMR (125 MHz) spectrum of Compound **2.3b** in DMSO-d6.

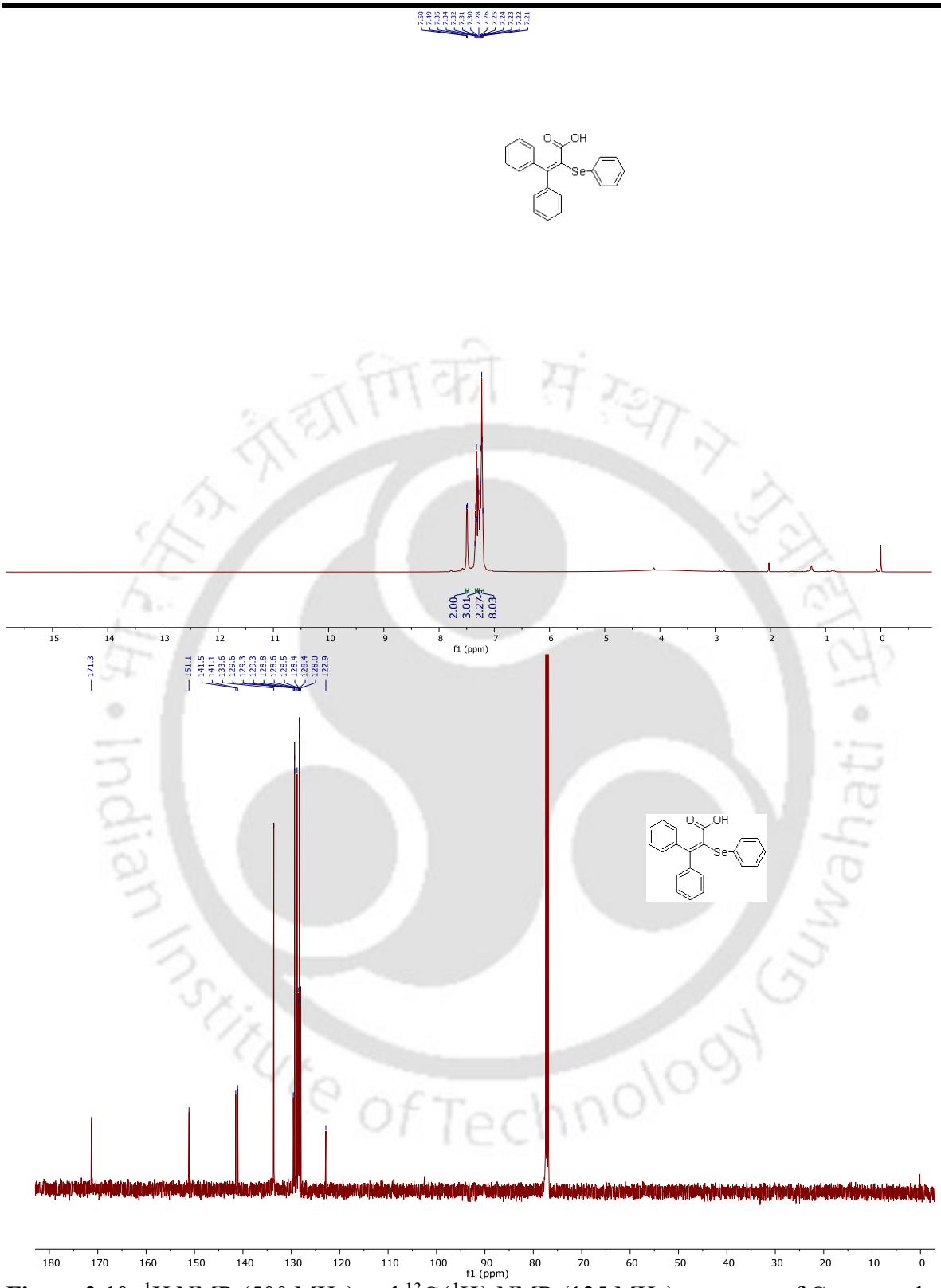

Figure 2.10: ^{1}H NMR (500 MHz) and $^{13}C\{^{1}H\}$ NMR (125 MHz) spectrum of Compound **2.3c** in $CDCl_3$.

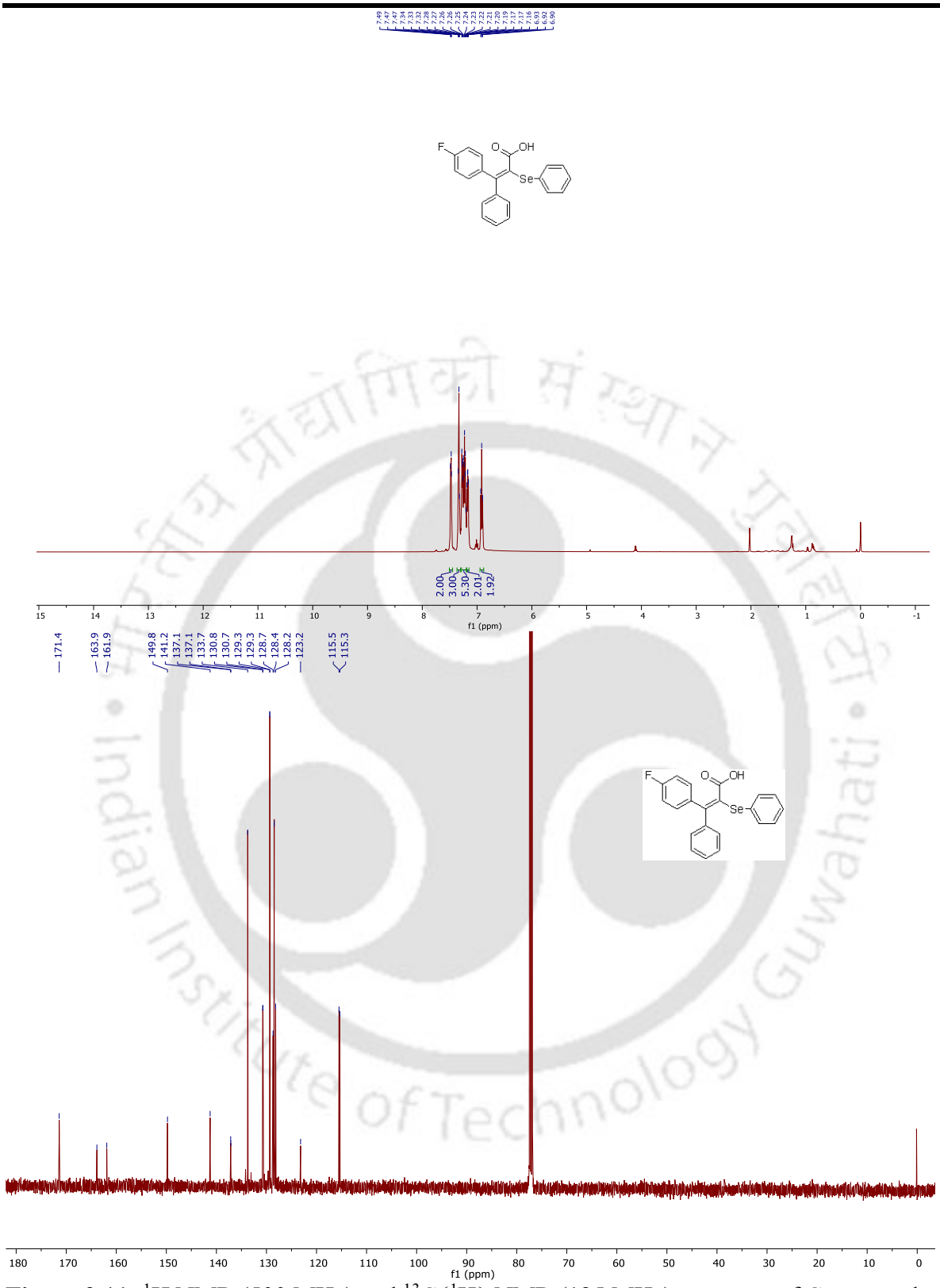

Figure 2.11: ^{1}H NMR (500 MHz) and $^{13}C\{^{1}H\}$ NMR (125 MHz) spectrum of Compound **2.3d** in $CDCl_3$.

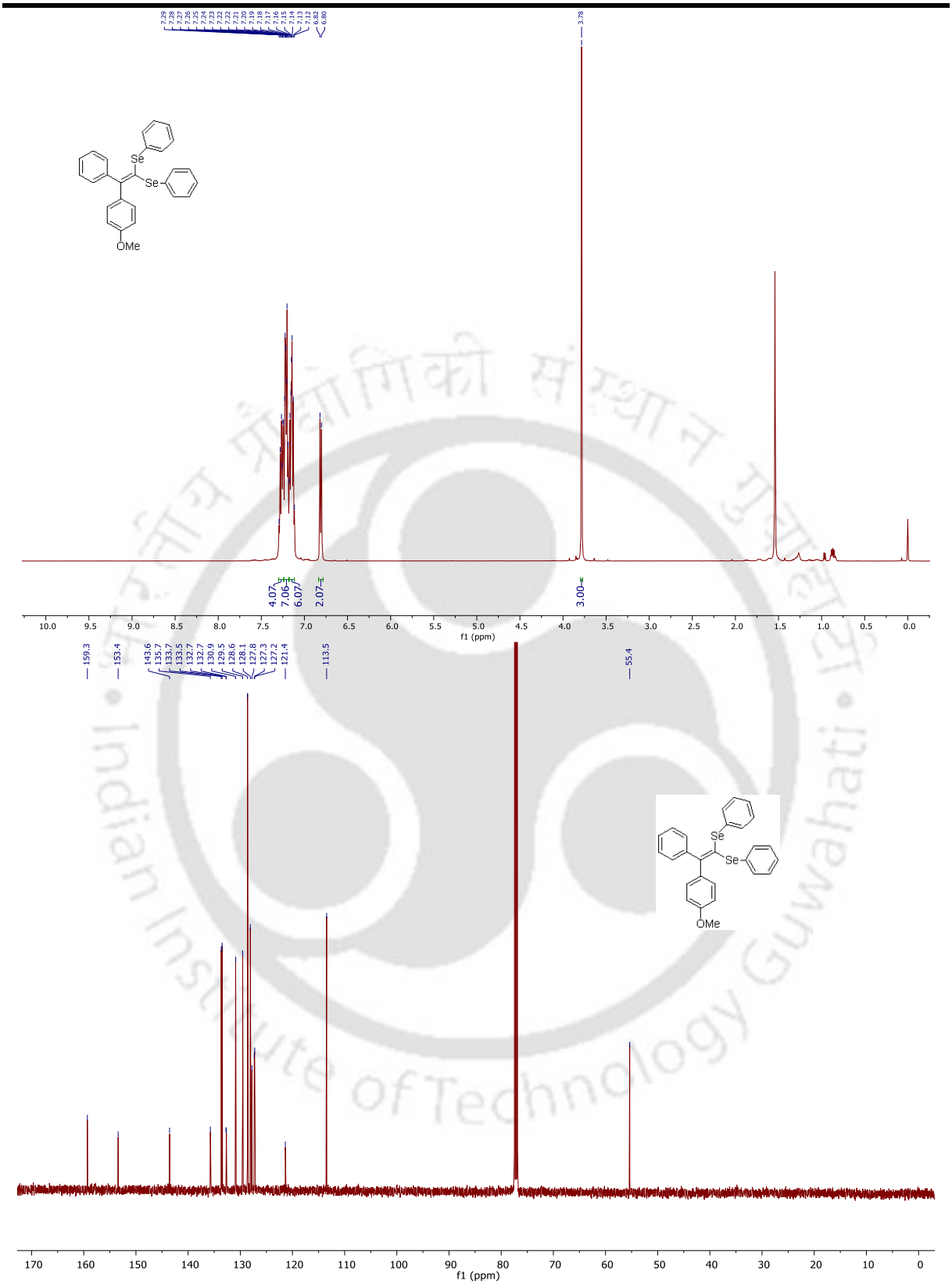

Figure 2.12: ^{1}H NMR (500 MHz) and $^{13}C\{^{1}H\}$ NMR (125 MHz) spectrum of Compound **2.4j** in $CDCl_3$.

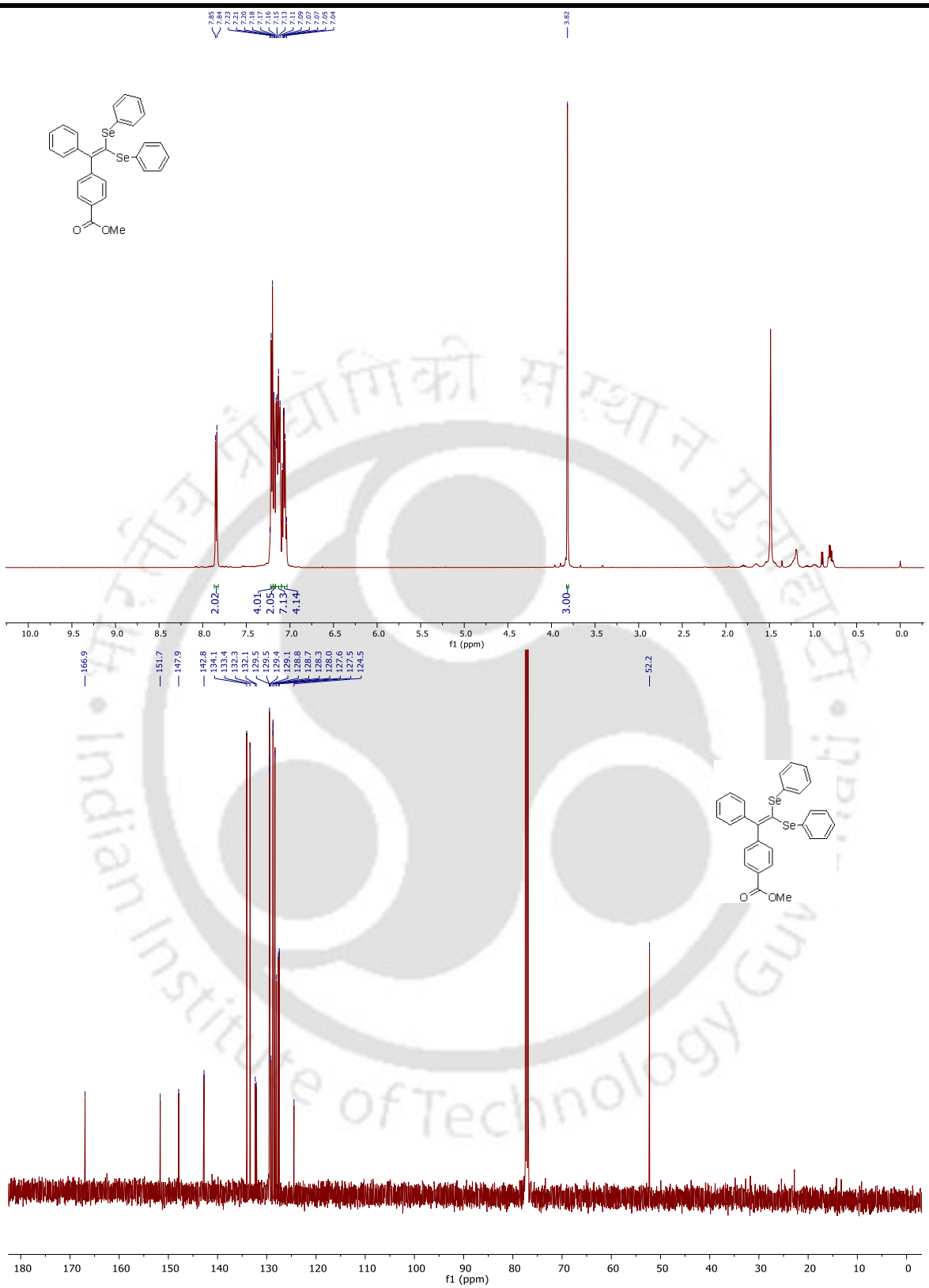

Figure 2.13: ^{1}H NMR (500 MHz) and $^{13}C\{^{1}H\}$ NMR (125 MHz) spectrum of Compound **2.4k** in $CDCl_3$.

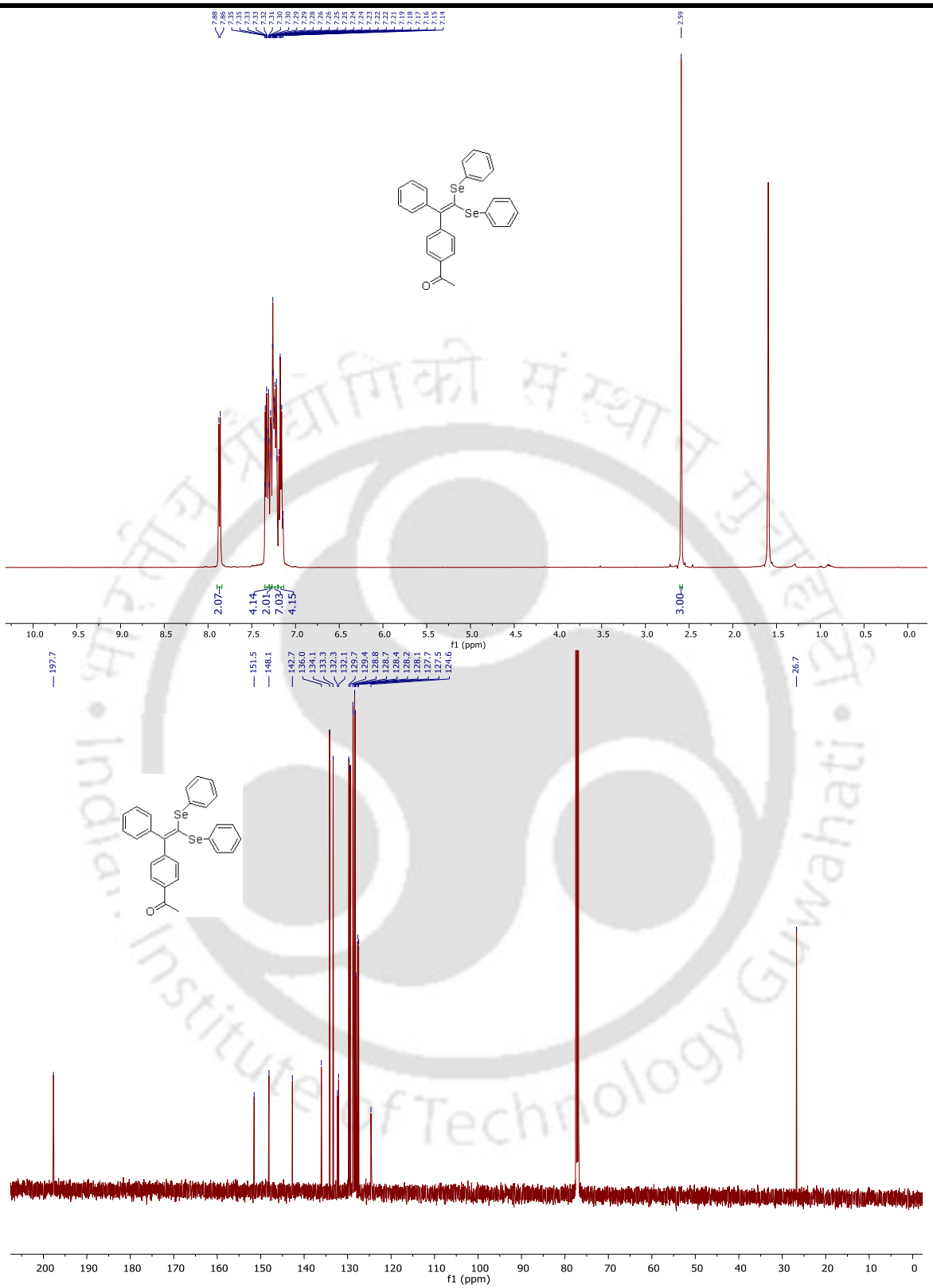

Figure 2.14: ^{1}H NMR (500 MHz) and $^{13}C\{^{1}H\}$ NMR (125 MHz) spectrum of Compound **2.4l** in $CDCl_3$.

Chapter III:

Substituent-Dependent, Switchable Synthesis of Nonaromatic and Aromatic Heterocyclic Sulfones Using Visible Light

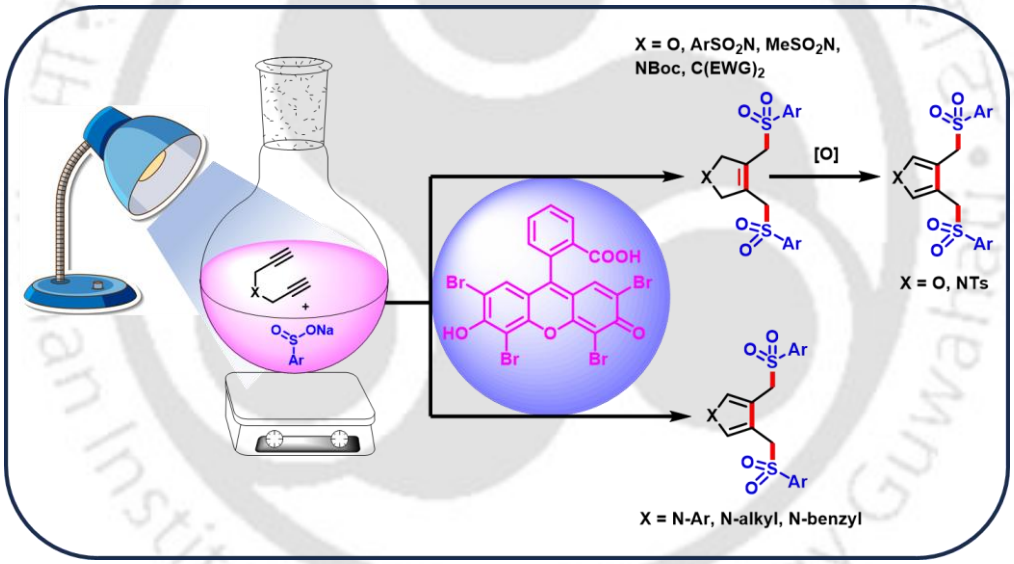

Roy, M.; Mallick, I; Mahapatra, M.; Srimani, D. *Org. Lett.* **2024**, *26*, 9357−9362.

Chapter III: Substituent-dependent, switchable synthesis of nonaromatic and aromatic heterocyclic sulfones using visible light

3.1 Introduction:

Heterocyclic compounds have consistently been appealing targets in synthetic organic chemistry due to their diverse biological activities. Five-membered heterocycles, such as pyrroles, 2,5-dihydropyrroles, 2,5-dihydrofurans, and furans, are present in a wide range of pharmaceuticals, agrochemicals, and bioactive natural compounds.[1] Similarly, sulfone derivatives represent an important class of bioactive compounds with diverse biological properties (Figure 3.1).[2] Both heterocyclic and carbocyclic sulfones are commonly found in natural products, agrochemicals, pharmaceuticals, and organic functional materials.[3] Traditionally, aryl sulfones are synthesized by either oxidizing sulfides[4] or carrying out a sulfonylation reaction with strong acids.[5] Consequently, various transition metal-catalyzed annulation,[6] C-H activation,[7] and radical-mediated cyclization[8] are used for the synthesis of five-membered heterocyclic sulfones. However, many of these methods suffer from drawbacks such as harsh reaction conditions, the formation of stoichiometric amounts of waste, or the reliance on precious transition metals.

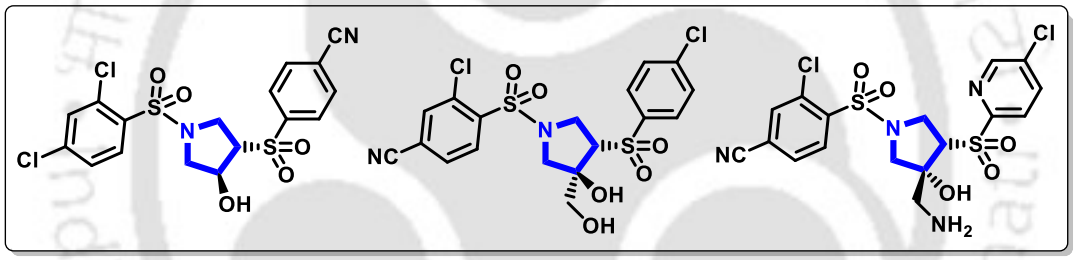

Figure 3.1: Important heterocyclic sulfone

Recently, visible light-mediated, environmentally benign, and mild procedures have been developed to construct sulfonated heterocycles through sulfonyl radical-initiated cyclization of enyne[9] and diyne[10] systems. However, these protocols are limited to the synthesis of non-aromatic sulfonyl heterocycles with exocyclic double bonds. Therefore, the synthesis of sulfone-containing aromatic heterocycles and (dihydro) heteroaromatic compounds under visible light-mediated conditions would be valuable.

3.2 Previous reports:

Petrini and his coworkers in 2011 reported a conventional method for the synthesis of sulfonyl pyrrole by reacting N-triisopropylsilyl pyrrole, aldehydes, and p-toluenesulfinic acid (p-TolSO$_2$H) by using strong p-toluenesulfonic acid (p-TolSO$_3$H) (Figure 3.2a).[11] In 2018, Rueping and his group reported the synthesis of C3-sulfonylated pyrrole via dehydrogenative

aromatization and sulfonylation of pyrrolidines under visible light using an iridium photocatalyst (Figure 3.2b).[12] They also demonstrated visible light-induced synthesis of sulfonated dihydropyrrole and other non-aromatic heterocycles in the presence of palladium catalyst (Figure 3.2c).[13]

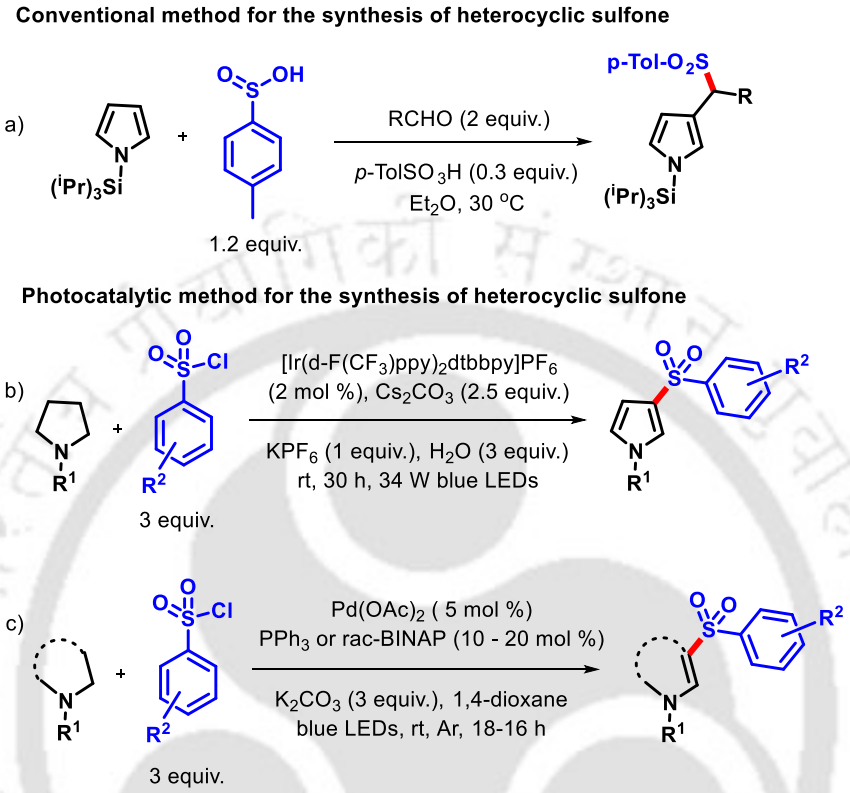

Figure 3.2: Previous reports for the synthesis of heterocyclic sulfone.

All these reported methodologies rely on the use of expensive precious metal catalysts or strong acids. So, there is a growing demand to develop an energy-efficient, sustainable, atom-economical, and environmentally benign method to construct the heterocyclic sulfone molecule. Thus, we anticipated that selectively synthesizing both sulfonyl pyrrole and sulfonylated dihydro-pyrrole under visible light with an inexpensive organophotocatalyst like eosin Y[14] would have a significant impact.

3.3 Present work:

In this chapter, an effective method for synthesizing disulfonylated pyrrole, disulfonylated dihydropyrrole, dihydropyran, and cyclopentene derivatives using visible light catalysis was developed (Figure 3.1d). Initially, the sulfonyl radical-mediated 5-exodig cyclization resulted in the synthesis of disulfonylated 2,5-dihydropyrrole, which can be further transformed to disulfonylated pyrrole via photocatalytic dehydrogenative aromatization (PDA). Our study

reveals that the nature of substituents present on the N-atom influences the PDA process (Figure 3.3).

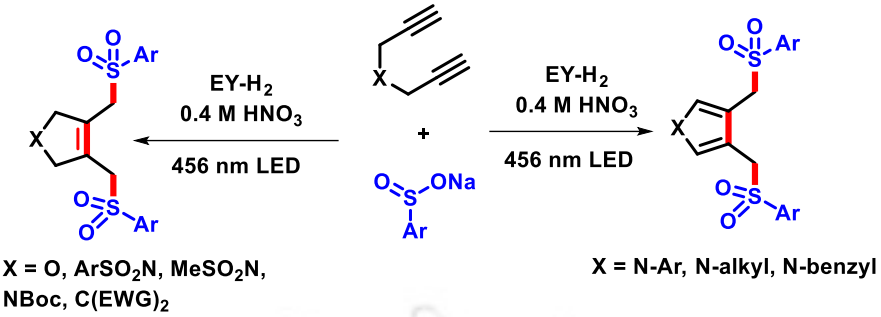

Figure 3.3: Present work for the synthesis of heterocyclic and carbocyclic sulfone.

3.4 Results and Discussions:

Initially, to find out suitable reaction conditions for the synthesis of disulfonated 2,5-dihydropyrrole, the investigation was started by taking N-tosyl-1,6-diyne (**3.1a**) and sodium p-toluenesufinate (**3.2a**) as the model substrates. When a mixture of **3.1a** (1 equiv.) and **3.2a** (4 equiv.) was stirred at room temperature in the presence of organophotocatalyst Eosin Y (10 mol %) and $K_2S_2O_8$ (4 equiv.) as an additive, in DMF solvent under 456 nm LED irradiation, the formation of disulfonated 2,5-dihydropyrrole, **3.3a** was observed with 23 % yield (Table 3.1, entry 1). Similar outcomes were obtained with other additives such as $(NH_4)_2S_2O_8$, and TBHP (Table 3.1, entry 1). The yield of **3.3a** increased from 23% to 47% with the addition of 0.4 M HNO_3 (4 equivalents). To our delight, the yield of **3.3a** was further improved to 85 % just by increasing the amount of 0.4 M HNO_3 (Table 3.1, entry 2). Other acids like H_2SO_4, HCl, and CH_3COOH resulted in a slightly lower yield compared to HNO_3 (Table 3.1, entry 3). Other organic photocatalysts, such as Na_2-EY, Rose Bengal, Fluorescein, and 4CzIPN, delivered inferior results compared to Eosin Y (Table 3.1, entry 4). Solvent screening reveals that DMSO, ACN, Dioxane, THF, and DCM are less effective compared to DMF (Table 3.1, entry 5). Performing the reaction under different lighting conditions, such as CFL, green LED, and ABI True LED, failed to produce satisfactory results (Table 3.1, entry 6). Subsequently, the reaction was conducted in the absence of light, catalyst, and additive, respectively, and in each instance, the desired product **3.3a** was not obtained (Table 3.1, entries 7-9). This highlights the critical role of light, catalysts, and additives in our present protocol.

Table 3.1: Optimization of reaction parameteres[a]

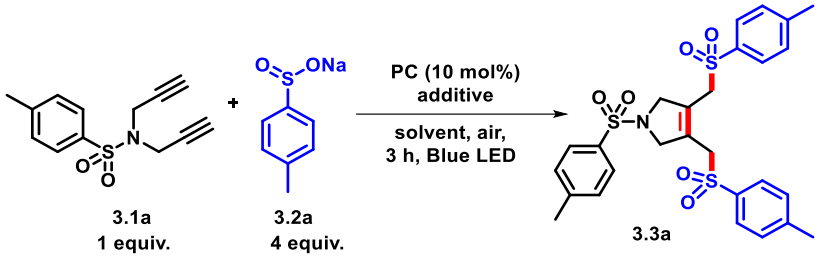

Sl. No.	Catalyst (mol %)	Additive (equiv.)	Solvent (2 mL)	Light	Yield[b] (%)
1.	EY-H_2 (10)	$K_2S_2O_8$ (4 equiv.)	DMF	456 nm LED	23
2.	EY-H_2 (10)	$(NH_4)_2S_2O_8$ (4 equiv.)	DMF	456 nm LED	19
3.	EY-H_2 (10)	TBHP (4 equiv.)	DMF	456 nm LED	27
4.	EY-H_2 (10)	DTBP (4 equiv.)	DMF	456 nm LED	21
5.	EY-H_2 (10)	0.4 M HNO_3 (4 equiv.)	DMF	456 nm LED	47
6.	EY-H_2 (10)	0.4 M HNO_3 (6 equiv.)	DMF	456 nm LED	69
7.	**EY-H_2 (10)**	**0.4 M HNO_3 (8 equiv.)**	**DMF**	**456 nm LED**	**85**
8.	EY-H_2 (10)	0.4 M HNO_3 (10 equiv.)	DMF	456 nm LED	85
9.	EY-H_2 (10)	0.4 M H_2SO_4 (8 equiv.)	DMF	456 nm LED	73
10.	EY-H_2 (10)	0.4 M HCl (8 equiv.)	DMF	456 nm LED	79
11.	EY-H_2 (10)	0.4 M CH_3CO_2H (8 equiv.)	DMF	456 nm LED	79
12.	EY-Na_2 (10)	0.4 M HNO_3 (8 equiv.)	DMF	456 nm LED	75
13.	RB (10)	0.4 M HNO_3 (8 equiv.)	DMF	456 nm LED	64
14.	Fluorescein (10)	0.4 M HNO_3 (8 equiv.)	DMF	456 nm LED	71
15.	4CzIPN (10)	0.4 M HNO_3 (8 equiv.)	DMF	456 nm LED	69
16.	EY-H_2 (10)	0.4 M HNO_3 (8 equiv.)	DMSO	456 nm LED	71
17.	EY-H_2 (10)	0.4 M HNO_3 (8 equiv.)	ACN	456 nm LED	49
18.	EY-H_2 (10)	0.4 M HNO_3 (8 equiv.)	Dioxane	456 nm LED	57
19.	EY-H_2 (10)	0.4 M HNO_3 (8 equiv.)	THF	456 nm LED	43
20.	EY-H_2 (10)	0.4 M HNO_3 (8 equiv.)	DCM	456 nm LED	39
21.	EY-H_2 (10)	0.4 M HNO_3 (8 equiv.)	DMF	CFL Light	54
22.	EY-H_2 (10)	0.4 M HNO_3 (8 equiv.)	DMF	Green LED	47
23.	EY-H_2 (10)	0.4 M HNO_3 (8 equiv.)	DMF	ABI True Blue LED	68
24.	EY-H_2 (10)	0.4 M HNO_3 (8 equiv.)	DMF	-	-
25.	-	0.4 M HNO_3 (8 equiv.)	DMF	Blue LED	-
26.	EY-H_2 (10)	-	DMF	Blue LED	trace

[a]**Conditions**: **3.1a** (0.25 mmol), **3.2a** (1.0 mmol), Catalyst (10 mol %), additive (4-10 equiv.), under air, 456 nm LED, solvent (2 mL), 3 h. EY = Eosin Y, RB = Rose Bengal, b = isolated yield.

After finalizing the optimized reaction conditions, the substrate scope for bi-sulfonated 2,5-dihydropyrrole with respect to N-substituted 1,6-diyne and sodium aryl sulfinates was

examined (Scheme 3.1). The reactions went successfully with a wide variety of N-arylsulfonyl-1,6-diynes. Electron-donating (-H, -Me, -OMe, and -Cl) and electron-withdrawing (-F and -CF_3) groups present at the *para*-position of the aryl ring of N-arylsulfonyl-1,6-diynes, furnishing a good yield of bi-sulfonated 2,5-dihydropyrrole derivatives (**3.3a**-**3.3f**, 67-85 %). Likewise, 1,6-diynes bearing N-methyl sulfone, N-naphthyl sulfone, and -NBoc groups were amenable to form desired bi-sulfonated 2,5-dihydropyrrole derivatives with decent yield (**3.3g**-**3.3i**, 61-85 %). Next, the scope of different sulfonyl radicals by using various sodium aryl sulfinates was investigated, which also delivered the desired products in good isolated yields (**3.3k**-**3.3n**, 59-85%). Even sodium methyl sulfinates were well-compatible with this protocol, yielding the desired product in good amounts (**3.3p**, 64 %). Compounds **3.3a** and **3.3i** were synthesized on a gram scale to demonstrate the scalability of the current process, which resulted in good product yields (74 % and 58 %). The structure of the compounds was also confirmed from the single-crystal X-ray data of molecule **3.3a** (CCDC:2384281).

Scheme 3.1: Substrate scope for bi-sulfonated 2,5-dihydro pyrrole derivatives[a]

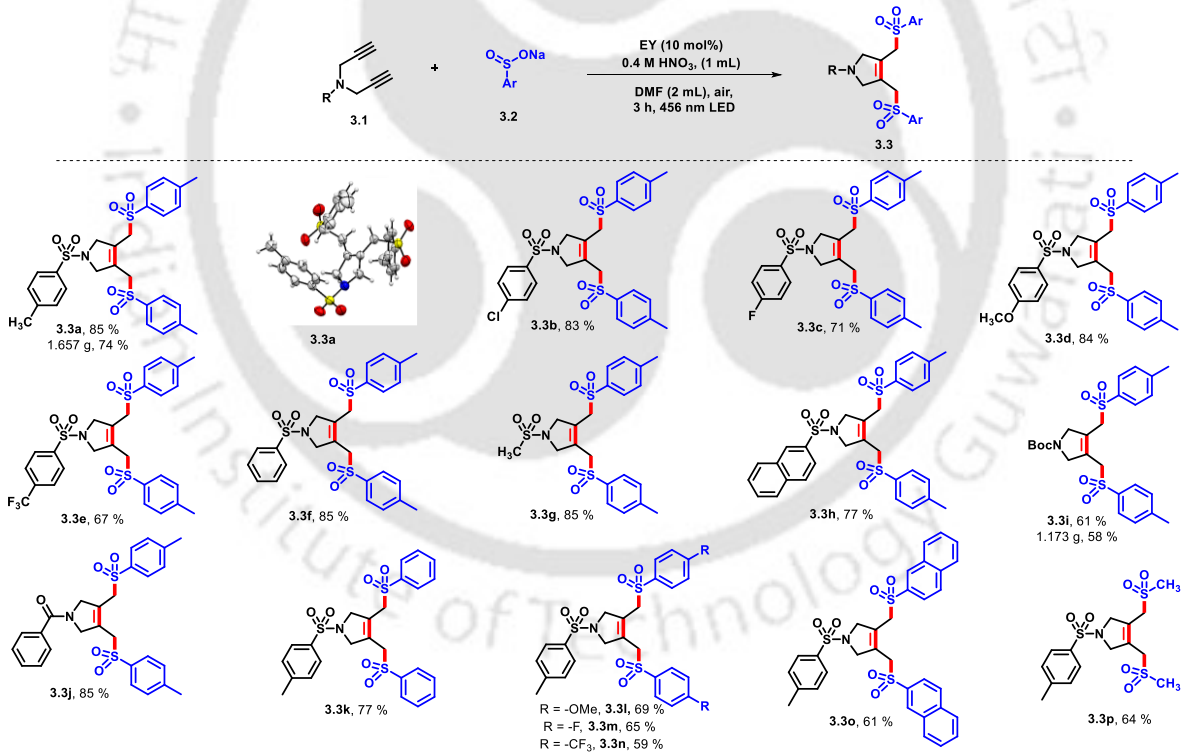

[a]Conditions: **3.1** (0.25 mmol), **3.2** (1.00 mmol) EY-H_2 (10 mol%), 0.4 M HNO_3 (1 mL), DMF (2 mL) in open air, was irradiated with 456 nm Blue LEDs for 3 h.

Recently, oxidative dehydrogenation of N-heterocycles has garnered significant attention.[15] This type of process is initiated with the formation of an amine radical cation. Therefore, it was envisioned that changing the substituent on the N-atom might lead to the formation of

disulfonylated pyrrole via the PDA process. Interestingly, when the reaction was carried out with N-aryl 1,6-diyne, 20 mol % catalyst loading, 0.5 mL 0.4 M HNO_3, in DMF solvent in open air conditions under 456 nm blue LEDs irradiation, and observed the formation of N-aryl di-sulfonated pyrroles (scheme 3.2). Later on, the substrate tolerance for these N-aryl disulfonated pyrrole products was also explored. Screening of various N-aryl 1,6-diyne systems revealed that electron-neutral and electron-donating groups at the *para*-position of the N-aryl ring resulted in the formation of the desired product with good yield (**3.4a-3.4e**, 61 % - 73 %).

Scheme 3.2: Substrate scope for bi-sulfonated pyrrole derivatives[a]

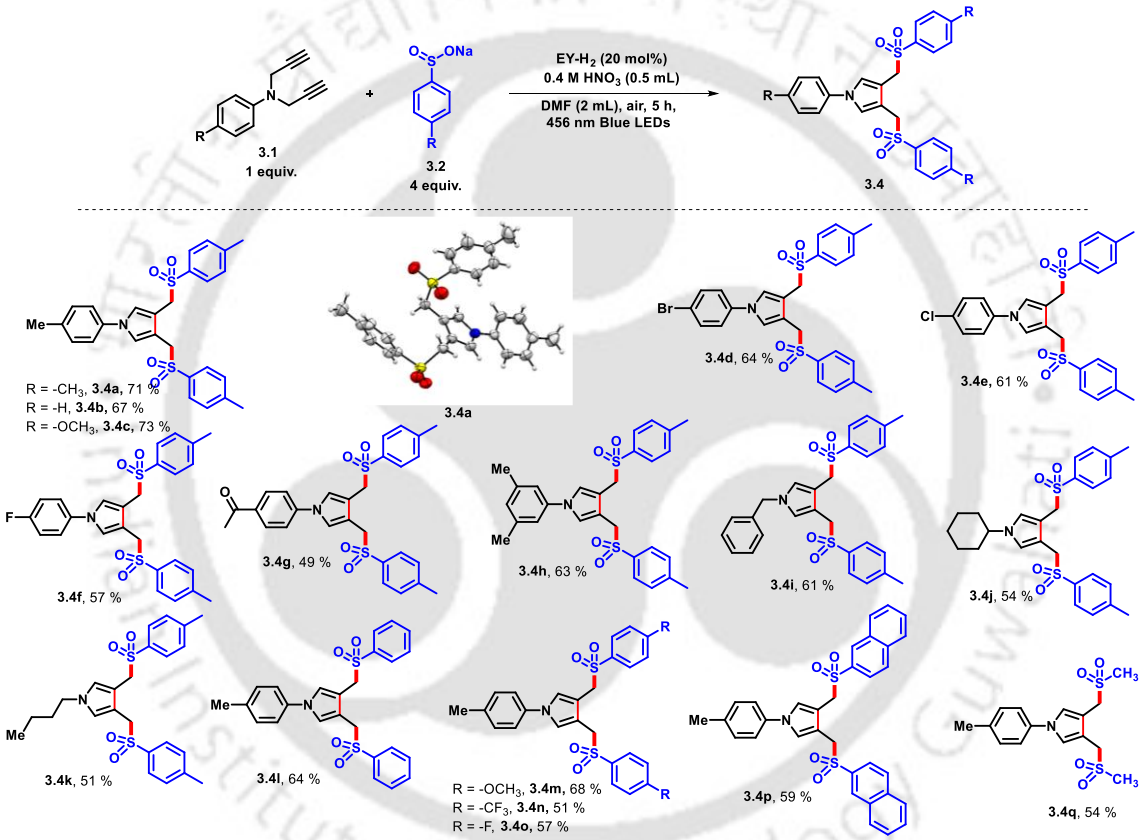

[a]Conditions: **3.1** (0.25 mmol), **3.2** (1.00 mmol) EY-H_2 (20 mol%), 0.4 M HNO_3 (0.5 mL), DMF (2 mL) in open air, was irradiated with 456 nm Blue LEDs for 5 h.

The electron-withdrawing group at the *para*-position of the N-aryl ring led to the formation of the corresponding product with a comparatively lower yield (**3.4f** and **3.4g**, 57 % and 49 %). N-benzyl, N-cyclohexyl, and nBu-N-1,6-diyne are also compatible with this protocol and furnish the pyrrole derivative product with 61 %, 54 %, and 51 % yield, respectively (**3.4i-3.4k**). Differently, substituted sodium aryl sulfonates also furnished the pyrroles in good isolated yields (**3.4l-3.4o**, 51-68 %). Sodium naphthyl sulfinates and sodium methyl sulfinates

also produced the corresponding product in acceptable yields (**3.4p** and **3.4q**, 59 % and 54 % respectively). Single crystal X-ray analysis of molecule **3.4a** (CCDC:2384280) confirmed the compound's structure. Further, the scope of different 1,6-diyne was also checked (Scheme 3.3). Dipropargyl ether was employed to explore the possibility of synthesizing di-sulfonated 2,5-dihydrofuran products, which were obtained in good to excellent yields (**3.5a-3.5d**, 65 % - 81 %). Next, different C-tethered 1,6-diynes were examined to synthesize carbocyclic compounds. Various diyne linker such as $C(CO_2Me)_2$, $C(CO_2Et)_2$, $C(CO_2Me)(COMe)$, $C(COMe)_2$) responded well to deliver good yield (**3.5e-3.5h**, 61-77 %).

Scheme 3.3: Substrate scope for bi-sulfonated 2,5-dihydrofuran and carbocycles[a]

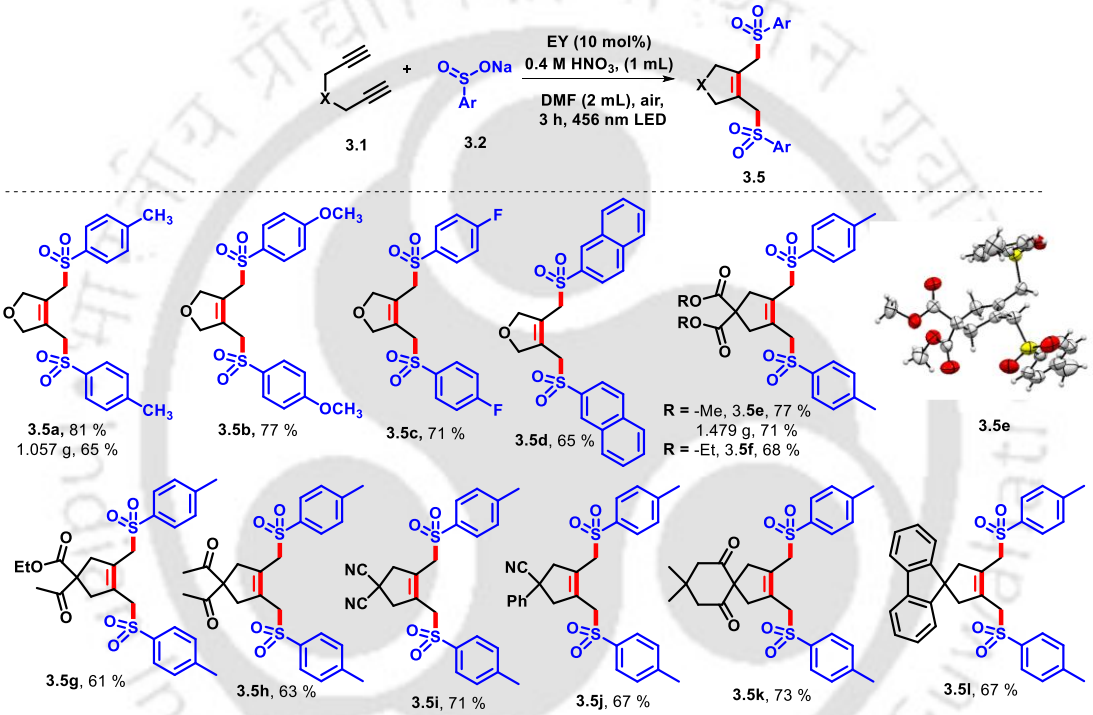

[a]Conditions: **3.1** (0.25 mmol), **3.2** (1.00 mmol) EY-H_2 (10 mol%), 0.4 M HNO_3 (1 mL), DMF (2 mL) in open air, was irradiated with 456 nm Blue LEDs for 3 h.

The inherent mild nature of our current protocol enabled the formation of products **3.5i** and **3.5j** bearing sensitive cyanide groups, with 71% and 67% yield, respectively. Similarly, the methodology worked well for cyclic 1,6-diynes and furnished the corresponding bisulfonated spirocyclic products (**3.5k** and **3.5l**) with decent isolated yields (73% and 67%, respectively). The Gram scale synthesis of **3.5a** demonstrates that the reaction may be easily scaled up without significantly influencing the yield of the product.

3.5 Post-functionalization:

Sulfone-containing compounds are used in a wide range of industries, including polymers, medicines, and agrochemicals.[16] The synthetic utility was further demonstrated by transforming molecule 3 into useful compounds (Figure 3.4). 2,5-dihydropyrrole (**3.3a**) (0.1 mmol) and 2,5-dihydrofuran (**3.5a**) (0.1 mmol) are easily transformed into their corresponding aromatic derivatives (**3.4r** and **3.4s,** respectively) by treating with DDQ (0.4 mmol) in toluene (2 mL) at 120 °C for 5 hours.

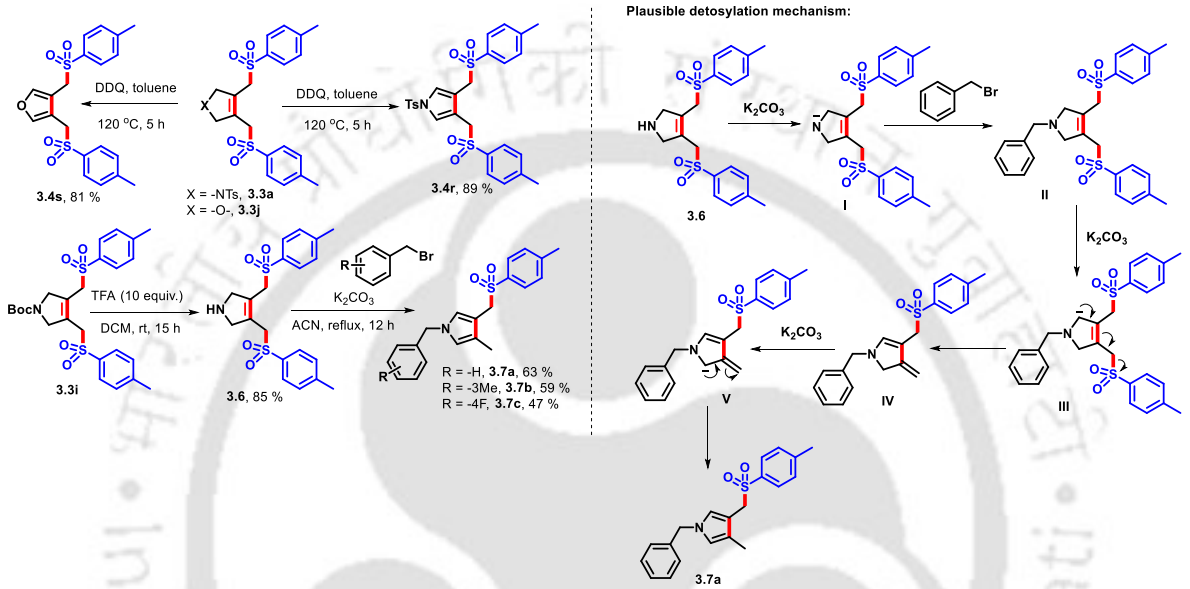

Figure 3.4: Post-functionalization.

Further, the synthetic applicability of this method was exposed by deprotecting the -Boc group of **3.3i** compound and generating the corresponding free -NH product (**3.6**, Figure 3.2). The compound **3.3i** (1.0 equiv., 1.0 mmol, 505.64 mg) was dissolved in DCM (2.0 mL), and TFA (10.0 equiv., 10.0 mmol, 0.77 mL) was added. After 1 h, the reaction was quenched with a saturated aqueous solution of K_2CO_3 (5 mL), and the product was extracted into DCM (3 x 15 mL), dried over Na_2SO_4, filtered, and the solvent was removed under reduced pressure to give **3.6** as a white solid (0.345 mg, 85 %). Additionally, the treatment of compound **3.6** (0.5 mmol) with K_2CO_3 (1.1 mmol) and benzyl bromide (BzBr, 0.55 mmol) in acetonitrile solvent (5 mL) under refluxed conditions generated the aromatic heterocyclic compound N-benzyl sulfonated pyrrole (**3.7a**) with 63 % yield. In the first step, N-benzylation occurs on compound **3.6** in the presence of base K_2CO_3. After the N-benzylation, the base abstracted the adjacent hydrogen atom of intermediate **II**, generating the carbanion intermediate **III**. Which further undergoes

detosylation to produce intermediate compound **IV**. Finally, the intermediate compound **IV** gets aromatized in the presence of base K_2CO_3 to provide the desired product **3.7a**.

3.6 Control experiments:

Various control experiments were performed to understand the mechanism of the reaction. Under the standard conditions, 5.0 equiv. of 2,2,6,6-tetramethylpiperidine N-oxide (TEMPO), 2,6-di-tert-butyl-4-methylphenol (BHT), and 1,1-diphenylethylene were introduced to the model reactions as radical scavengers. The desired product **3.3a** was not observed at all. This finding suggested the involvement of a radical route.

3.6.1 Procedure for radical trapping experiment with TEMPO/BHT/1,1-diphenylethylene:

The 1,6-diynes **3.1a** (0.25 mmol), sodium aryl sulfinates **3.2a** (1.00 mmol) Eosin Y (10 mol%), and TEMPO (1.25 mmol) were taken in an oven-dried reaction tube with a magnetic bead. After that, DMF (2 mL) was added, followed by 0.4 M HNO_3 (1 mL). The reaction mixture was allowed to stir under the 456 nm LED irradiation at room temperature in an open-air atmosphere for 3 h. TLC monitored the reaction, and it was noticed that after the reaction time, there was no spot of our desired product. Similarly, the reaction with another radical scavenger, such as BHT (5 equiv.) and 1,1-diphenylethylene (5 equiv.) was also performed. In the case of BHT, a lower yield of the product (**3.3a**, 43 %) was observed, and in the case of 1,1-diphenylethylene, no desired product formation was noticed (**3.3a**) (Figure 3.5).

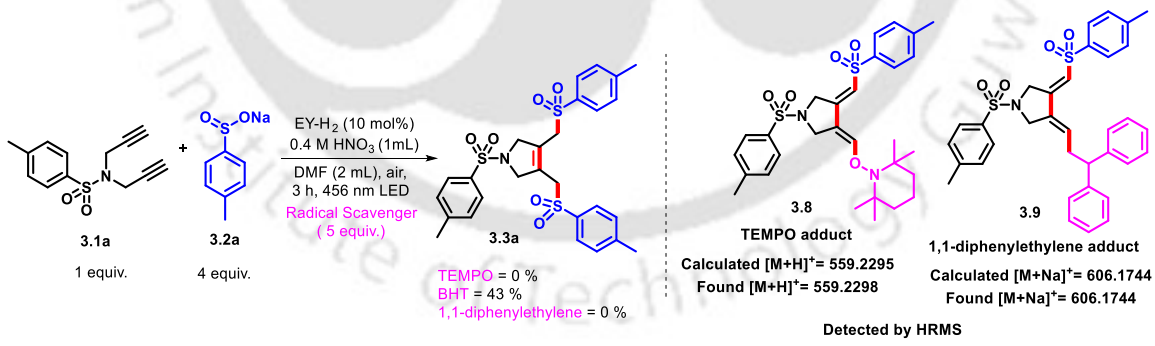

Figure 3.5: Radical trapping experiment

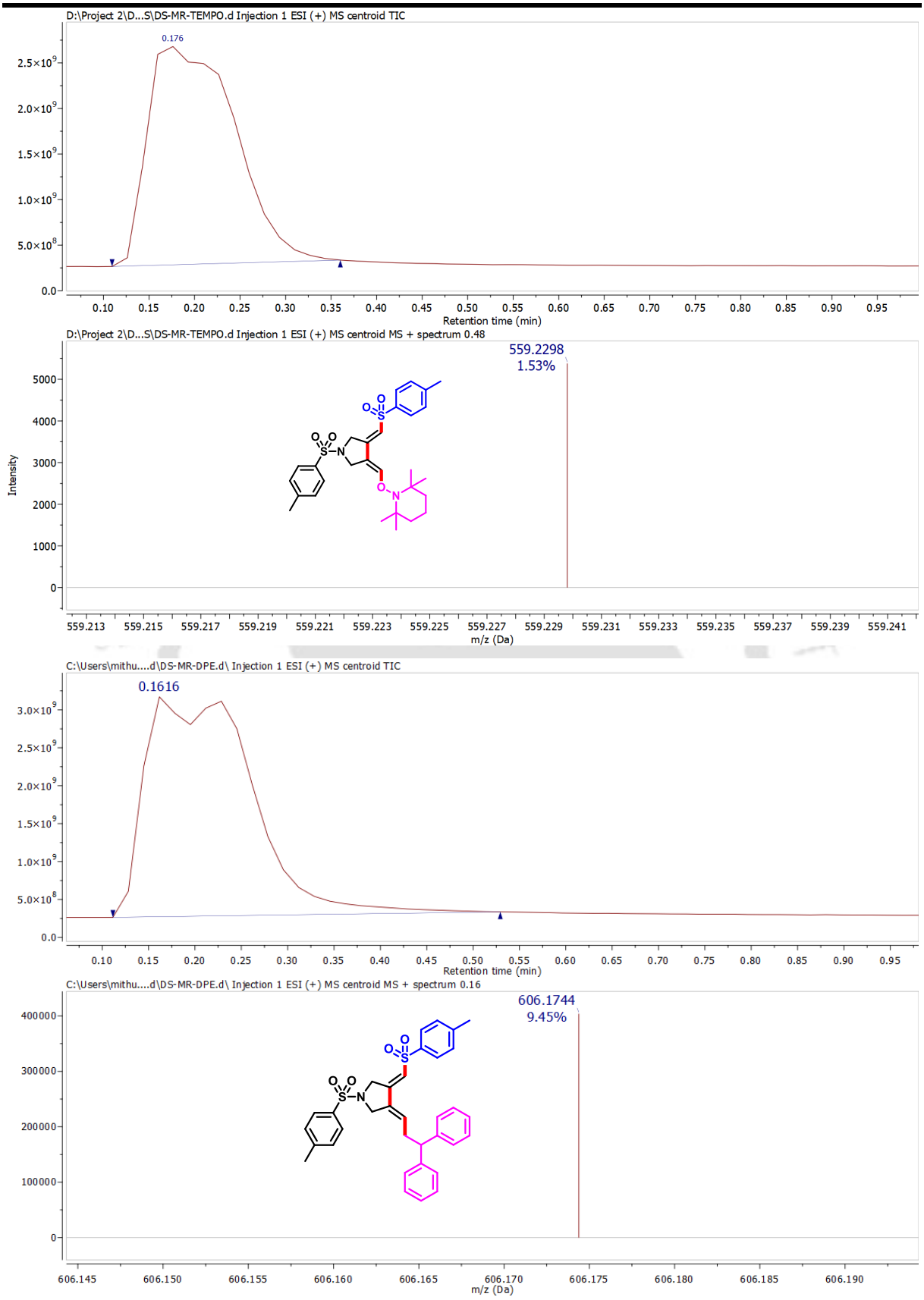

Figure 3.6: HRMS spectra of TEMPO adduct and 1,1-diphenylethylene adduct

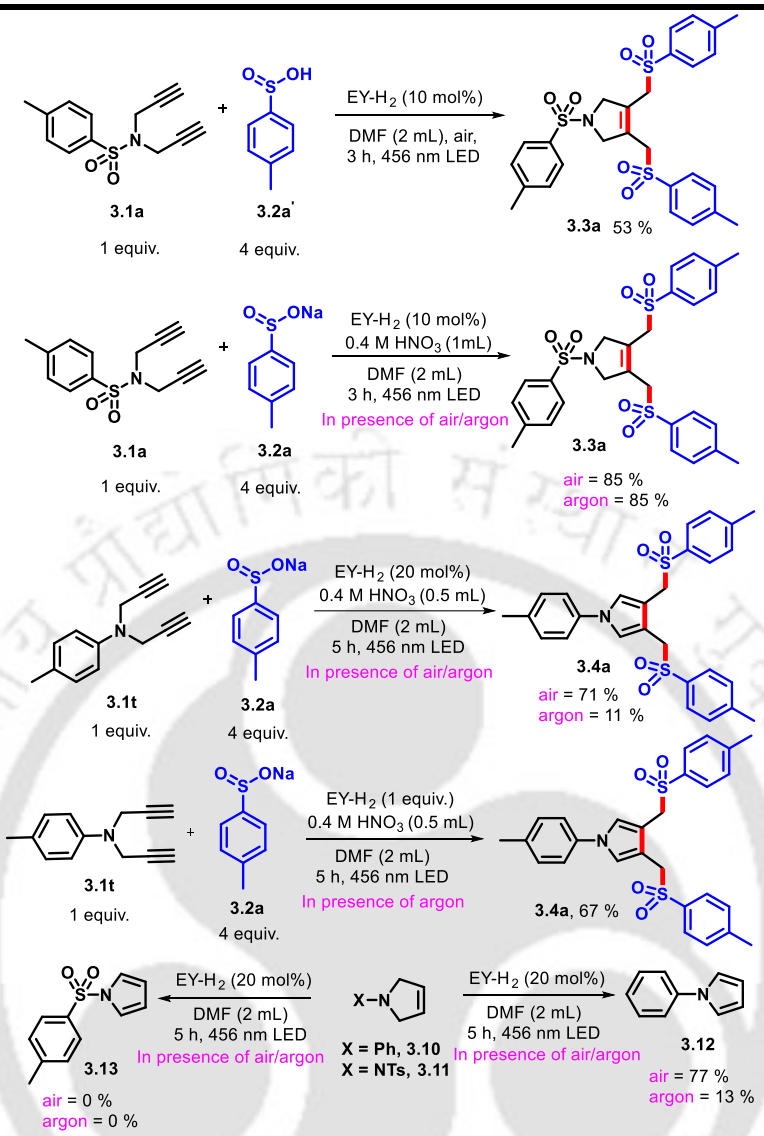

Figure 3.7: Control experiments

When the reaction is conducted without HNO_3, using p-toluene sulfinic acid instead of sodium p-toluene sulfinate, a significant amount of **3.3a** is formed (Figured 3.7). This suggests that p-toluene sulfinic acid, generated from its sodium salt under acidic conditions, is involved in the reaction. Next, the reaction was performed in the presence of both air and argon. For N-tosyl-1,6-diyne (**3.1a**), both conditions resulted in the same yield of product **3.3a** (85%), indicating that atmospheric oxygen does not play a role in the formation of **3.3a**. In contrast, for N-aryl 1,6-diyne (**3.1t**), the reaction under argon produced a minimal amount of N-aryl pyrrole product **3.4a** (11%), while under air, the yield of **3.4a** increased significantly to 71%. These results showcase the importance of atmospheric oxygen for the formation of N-aryl pyrrole products. To verify the role of oxygen, another control experiment was performed by taking one equivalent of EY-H_2 in inert conditions. This provided the desired product **3.4a** with a 67

% yield. This also suggests that atmospheric oxygen plays a role in regenerating the catalyst. Later, N-phenyl-2,5-dihydropyrrole (**3.10**) and N-tosyl-2,5-dihydropyrrole (**3.11**) were taken and performed the reaction separately using 20 mol % eosin Y catalyst in DMF solvent under blue light irradiation, both in open air as well as inert conditions. For N-phenyl-2,5-dihydropyrrole (**3.10**), 77% of N-phenyl pyrrole (**3.12**) was produced under open-air conditions, while only 13% was formed under inert conditions. This strongly indicates that under our reaction conditions, the presence of air facilitates the photocatalytic dehydrogenative aromatization (PDA) of disulfonated-2,5-dihydropyrrole. In the case of N-tosyl-2,5-dihydropyrrole (**3.11**), even under air, no PDA process was observed to furnish N-tosyl pyrrole (**3.13**). This supports the idea that the electron pair on the nitrogen atom, being engaged in conjugation with the electron-withdrawing group, hinders the PDA process.

3.6.2 Fluorescence quenching experiments

Firstly, the fluorescence quenching of the excited photocatalyst eosin Y (3 mL, 20 μM) was tried by exciting at a wavelength of 525 nm and recording the emission spectrum at 553 nm with reactant **3.1a** (1,6-diynes, 30 mM). However, no changes in the fluorescence spectrum of the photocatalyst were observed. Then quenching was tried with reactant **3.2a** (sodium p-toluene-sulfinate, 30 mM), here, also quenching of the fluorescence spectrum of the photocatalyst was not observed. Neither the 1,6-diyne **3.1a** nor the sodium aryl sulfinate **3.2a** was able to quench the excited state of eosin Y (Figure 3.8). These results suggest that there is no direct energy or electron transfer between reactants **3.1a** or **3.2a** and the excited photocatalyst. Next, the fluorescence quenching experiments were done with p-toluene sulfinic acid (**3.2a′**) and observed that the fluorescence spectrum of the excited photocatalyst was quenched and exhibited a linear quenching in the Stern-Volmer plot (Figure 3.8c and 3.8d). These findings suggested the direct interaction of p-toluene sulfinic acid (**3.2a′**) with the photocatalyst.

3.6.3 Light On/Off Experiment:

An On/Off experiment was performed to check the impact of light on this reaction. The experiment was carried out by following the general procedure **3** with alternating exposure (1 hour) of light and darkness. These showed that the reaction process was completely stopped in the absence of light and resumed with further illumination. These results demonstrate that light is an essential component for this reaction (Figure 3.9).

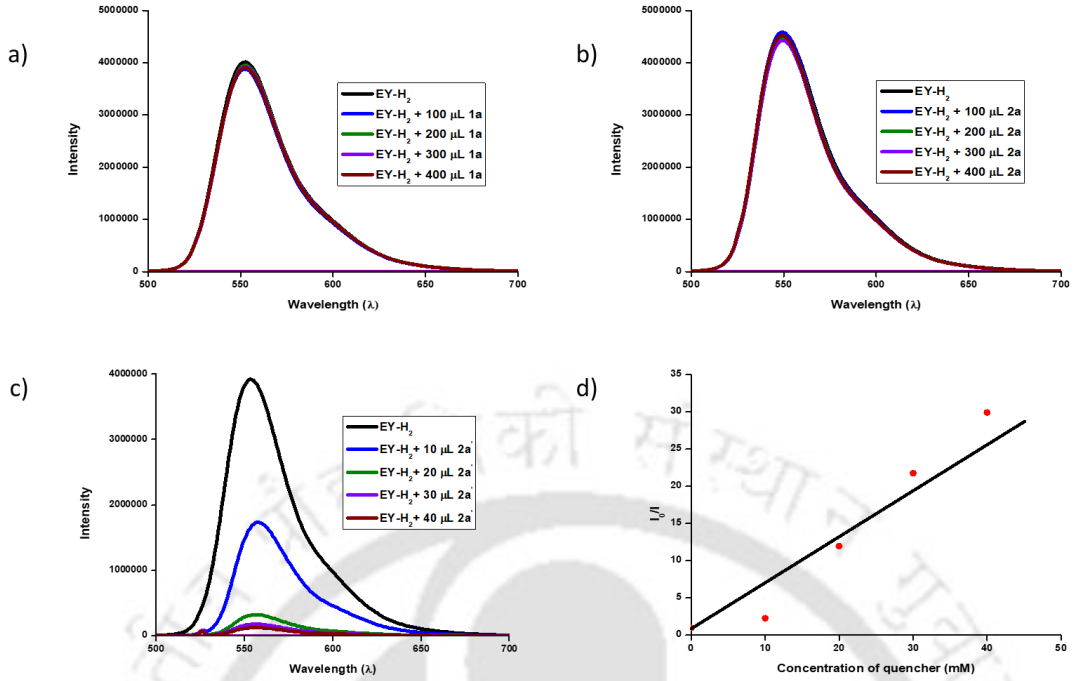

Figure 3.8: a) Fluorescence quenching with reactant **3.1a**, b) Fluorescence quenching with reactant **3.2a**, c) Fluorescence quenching with reactant **3.2a′**, d) Stern-Volmer plot

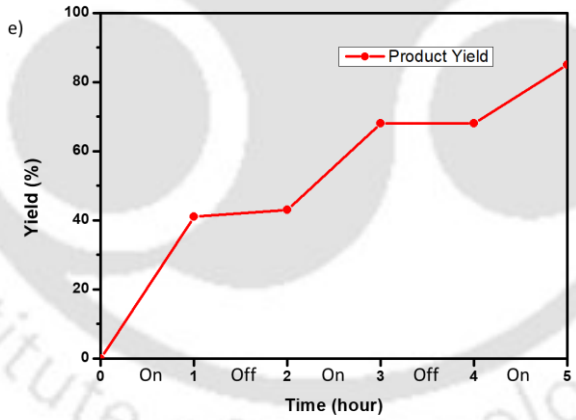

Figure 3.9: Light On/Off Experiment

3.7 Plausible Mechanism:

Based on literature reports[17] and control experiments, a probable reaction pathway for the reaction, as illustrated in Figure 3.8 was proposed. Initially, aryl sulfinic acid **3.2a′** was formed from the corresponding sulfinates **3.2a** under acidic conditions. The *in situ* generated aryl sulfinic acid undergoes single electron transfer (SET) with the excited-state eosin Y catalyst, producing the aryl sulfonyl radical (**3.A**) and the eosin Y radical anion ($EY^{\bullet -}$).[18] This aryl sulfonyl radical (**3.A**) attacks the terminal position of 1,6-diyne to generate vinyl radical

intermediate **3.B**, which undergoes 5-exo-dig cyclization to produce intermediate **3.C**. Next, another SET between $EY^{\bullet-}$ and **3.C** produces the anionic intermediate **3.D**, while simultaneously regenerating eosin Y. Further proton abstraction by the anionic intermediate **3.D** leads to the formation of **3.E**. The intermediate **3.E**, having a terminal exocyclic double bond, was further attacked by another aryl sulfonyl radical to generate the allylic radical intermediate **3.F**. Further, SET between $EY^{\bullet-}$ and **3.F** followed by the proton abstraction furnishes the desired product **3.3** or **3.5**. But the use of N-aryl/Nalkyl-1,6-diyne provided the pyrrole derivatives. In this case, after forming di-sulfonated-2,5-dihydropyrrole it undergoes photocatalytic dehydrogenative aromatization (PDA)[11,12,14], the formation of an amine radical cation (**3.H**), resulting in N-aryl di-sulfonated pyrrole derivatives **3.4** with a good yield.

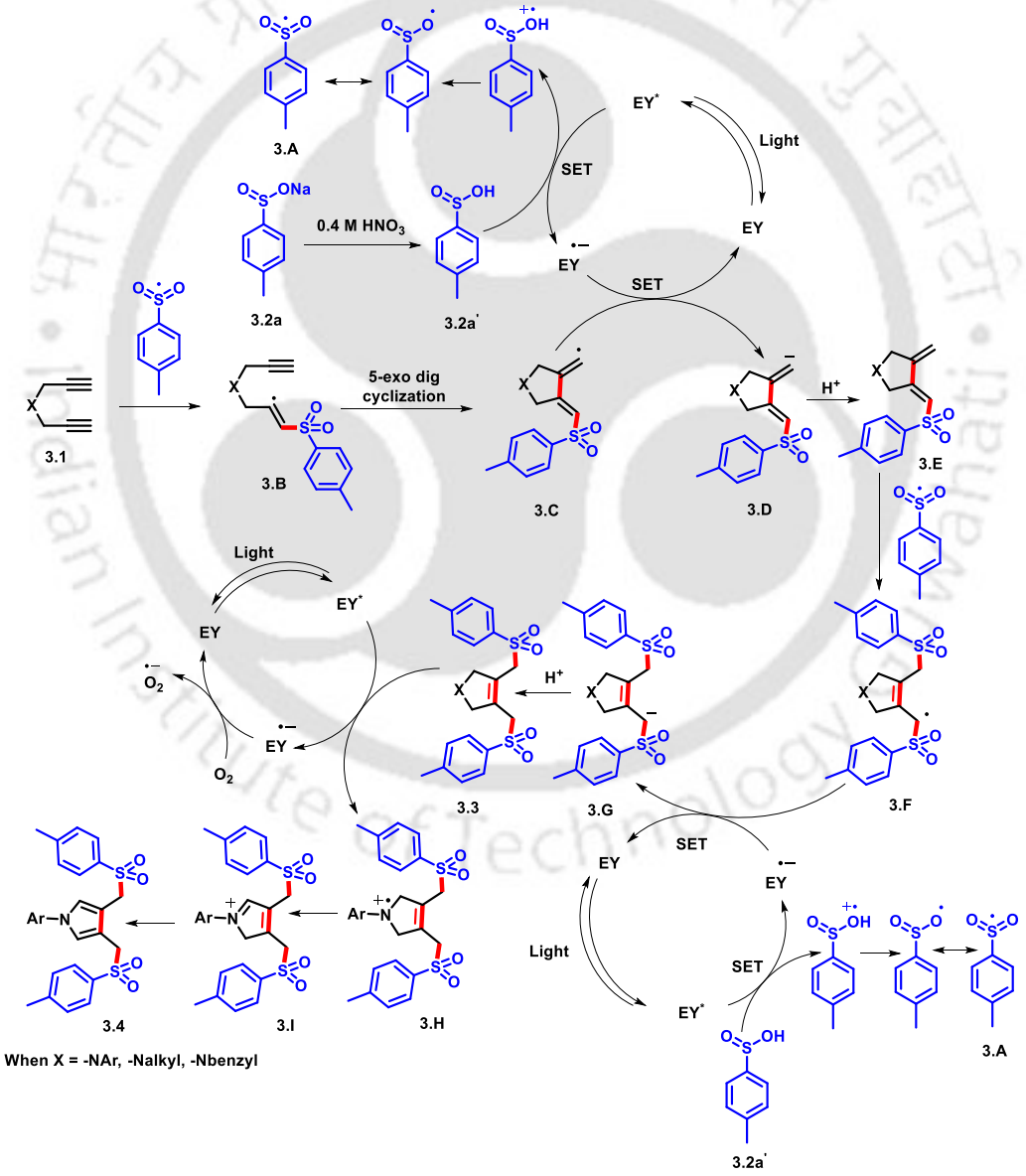

Figure 3.10. Plausible reaction mechanism.

3.8 Conclusions:

In conclusion, a switchable synthesis of both non-aromatic and aromatic sulfonyl heterocycles was developed under visible light, by changing the substitution on the nitrogen atom of 1,6-diyne, the photocatalytic dehydrogenation process can be regulated, which is key to directing the selectivity between 2,5-dihydropyrrole and pyrrole. A diverse range of disulfonated pyrroles, disulfonated dihydropyrroles, dihydrofurans, and cyclopentene derivatives have been synthesized, highlighting the method's versatility under mild conditions and its high tolerance for different functional groups.

3.9 Experimental sections:

a) General procedure for the synthesis of 1,6-diynes:

1,6-diyne derivatives were prepared by following the reported procedures.

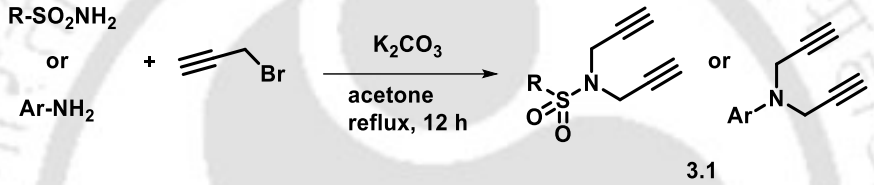

Aryl sulphonamide/aryl amine (5.0 mmol, 1 equiv.), potassium carbonate (25.0 mmol, 5 equiv.), propargyl bromide (80 wt% in toluene, 15.0 mmol, 3 equiv.) was taken in a 50 mL round bottom flask then 30 mL acetone was added. Then the reaction was refluxed for 16 hours at 80 ^{o}C. After completion the reaction was quenched with water and the acetone was removed under reduced pressure. Afterwards, the aqueous phase was extracted three times with ethyl acetate, and the combined organic phases were washed with brine and dried over sodium sulphate. The product was used for the next step without further purification. The compounds **3.1a-3.1h**, **3.1s,** and **3.1t-3.1ad** were prepared by following this procedure.[19]

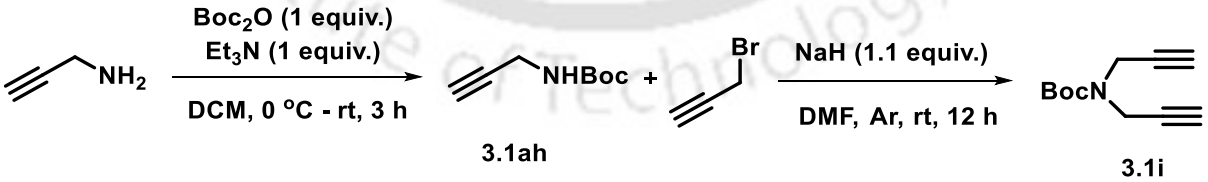

A solution of di-tert-butyl dicarbonate (5.0 mmol, 1.091 g, 1 equiv.) in dry DCM (4.0 mL) was added under argon at 0 °C to a solution of propargylamine (5.0 mmol, 0.32 mL, 1 equiv.) and triethylamine (5.0 mmol, 0.70 mL, 1 equiv.) in dry DCM (11.0 mL). After stirring for 3 h, water was added, the organic layer separated, and the aqueous phase was extracted with DCM (2 x 20 mL). The combined organic layer was washed with brine solution, dried over sodium sulphate, filtered, and concentrated under reduced pressure. The pure tert-butyl

propargylcarbamate (**3.1ah**, 95 %) was isolated from the crude by column chromatography on silica gel using petroleum ether/EtOAc (85:15) as an off-white needle-like crystalline solid.

To a solution of **3.1ah** (2.26 mmol, 0.350 g, 1.0 equiv.) in dry DMF (2.0 mL) under inert atmosphere was added NaH (60% on oil, 1.11 equiv., 2.51 mmol, 0.104 g). The mixture was left under stirring for 30 minutes at room temperature and then a solution of propargyl bromide (80% in toluene, 2.486 mmol, 0.27 mL, 1.1 equiv.) was added dropwise. The reaction mixture was stirred overnight to ensure complete consumption of the starting materials. The solution was poured in water (20 mL) and extracted with diethyl ether (2 x 40 mL). The organic layer was collected and dried over sodium sulphate. The solvent was removed under a vacuum to afford a dark brown oil. Purified this crude by column chromatography on silica gel using a gradient eluent of Petroleum ether/EtOAc (99:1) provided as a pale-yellow oil (**3.1i**, 65 %).[20]

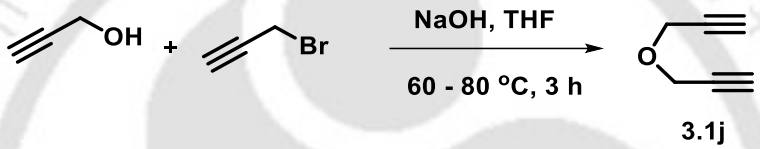

Propargylic alcohol (28 mmol, 1.6 mL, 1.4 equiv.) and propargyl bromide (20.0 mmol, 1.8 mL, 1.0 equiv.) were placed in a flask. Freshly powdered NaOH (30 mmol, 1.2 g, 1.5 equiv.) was added in small portions with vigorous stirring. The temperature was kept between 60 to 70 °C. 5 mL of THF was added to facilitate stirring. When the reaction subsided, the mixture was heated for an additional 1 h in an oil bath at 70-80 °C. Again 15 mL of THF were added. After cooling to room temperature, 30 mL of ice water was added with vigorous stirring. The product is isolated by extraction with Et_2O. After drying the organic solution over sodium sulphate, most of the ether is distilled off at normal pressure to get the almost pure dipropargyl ether **3.1j** as coloreless liquid, which was used in the next step without further purification.[21]

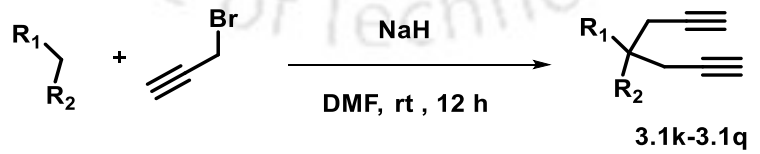

In a 100 mL round-bottom flask equipped with a magnetic stirrer, NaH 60 % in mineral oil (3 equiv.) was washed with hexane under an inert atmosphere and dry THF was then added. The suspension was cooled down to 0 °C and the corresponding active methylene compound (R_1-CH_2-R_2, 1 equiv.) was added. Stirring was continued for 30 minutes, after that propargyl bromide (80% in toluene, 3 equiv.) was added dropwise. The reaction mixture was stirred

overnight while warming up to room temperature. The reaction mixture was quenched with a saturated solution of NH_4Cl and concentrated under reduced pressure. The resulting crude was mixed with water and extracted with DCM. The combined organic layer was dried over anhydrous sodium sulphate, filtered and the solvent was removed in vacuo. The resulting crude was purified by column chromatography to afford the corresponding diyne. The compound **3.1k-3.1q** was prepared by following this procedure.[19]

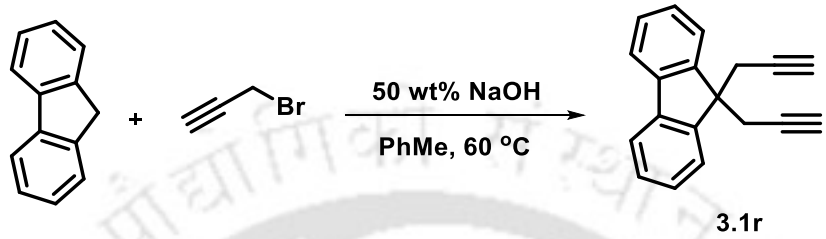

3.1r

To a solution of fluorene (5 mmol) in toluene (10 mL) were added propargyl bromide (3.0 equiv., 80% in toluene), 50 wt% aqueous NaOH solution (5 mL), and tetrabutylammonium bromide (0.5 mmol). The mixture was stirred at 60 °C until complete conversion. The resulting mixture was poured into water until all the salt dissolved. The aqueous layer was extracted with ether. The combined organic layer was dried over sodium sulphate. The solvent was removed in vacuo to obtain crude product **3.1r** in 71% yield, which was used in the next step without further purification.[22]

b) General procedure for the preparation of sodium aryl sulfinates

sodium aryl sulfinates **3.2a**, **3.2b**, and **3.2g** are commercially available. **3.2c-3.2f** were synthesized by following the reported procedure.[23]

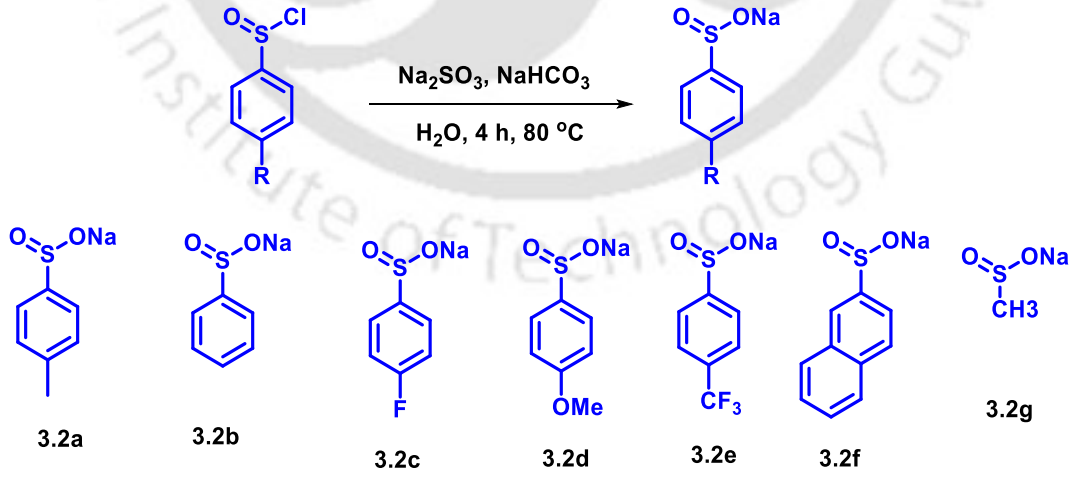

3.2a 3.2b 3.2c 3.2d 3.2e 3.2f 3.2g

Sodium sulphite (20.0 mmol, 2.0 equiv.), sodium bicarbonate (20.0 mmol, 2.0 equiv.), and the corresponding aryl sulfonyl chloride (10.0 mmol, 1.0 equiv.) were dissolved in distilled water (10 mL). The reaction mixture was stirred for 4 h at 80 °C. After cooling to room temperature, water was removed by lyophilization overnight. The white residue was extracted with ethanol

(25 mL) to obtain the desired aryl sulfinate as a white crystalline powder. The product was used for the next step without further purification.

c) General Procedure for the synthesis of bi-sulfonated 2,5-dihydropyrrole, 2,5-dihydrofuran and carbocycles:

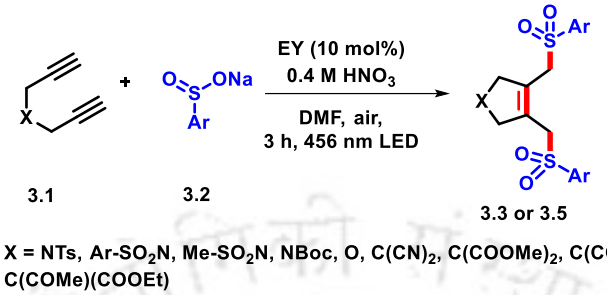

The 1,6-diynes **3.1** (0.25 mmol, 1 equiv.), sodium aryl sulfinates **3.2** (1.00 mmol, 4 equiv.) Eosin Y (10 mol%, 0.1 equiv.) was taken in an oven-dried reaction tube with a magnetic bead. After that, DMF (2 mL) was added, followed by the addition of 0.4 M HNO_3 (1 mL). The reaction mixture was allowed to stir under the 456 nm LED irradiation at room temperature in an open-air atmosphere for 3 h. The reaction was monitored by TLC, and after completion of the reaction, the reaction mixture was diluted with ethyl acetate. After that, the organic layer was washed with a saturated solution of $NaHCO_3$, followed by water. Then the organic layer was separated and dried over Na_2SO_4. The solvent was evaporated under reduced pressure to get the crude product. Further, the purification of the crude product was done by column chromatography on silica gel using petroleum ether and ethyl acetate as the eluent.

d) General Procedure for the synthesis of bi-sulfonated pyrrole:

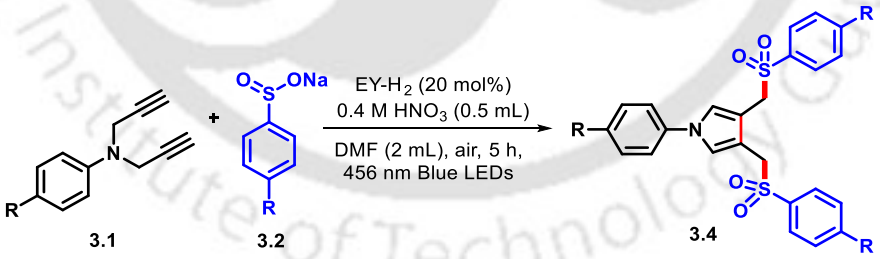

The N-aryl/alkyl 1,6-diynes **3.1** (0.25 mmol, 1 equiv.), sodium aryl sulfinates **3.2** (1.00 mmol, 4 equiv.) Eosin Y (20 mol%, 0.2 equiv.) was taken in an oven-dried reaction tube with a magnetic bead. After that, DMF (2 mL) was added, followed by the addition of 0.4 M HNO_3 (0.5 mL). The reaction mixture was allowed to stir under the 456 nm LED irradiation at room temperature in an open-air atmosphere for 5 h. The reaction was monitored by TLC, and after completion of the reaction, the reaction mixture was diluted with ethyl acetate. After that, the organic layer was washed with a saturated solution of $NaHCO_3$ followed by water. Then the organic layer was separated and dried over Na_2SO_4. The solvent was evaporated under reduced

pressure to get the crude product. Further, the purification of the crude product was done by column chromatography on silica gel using petroleum ether and ethyl acetate as the eluent.

e) Gram scale synthesis of products 3.3a, 3.3i, and 3.5a:

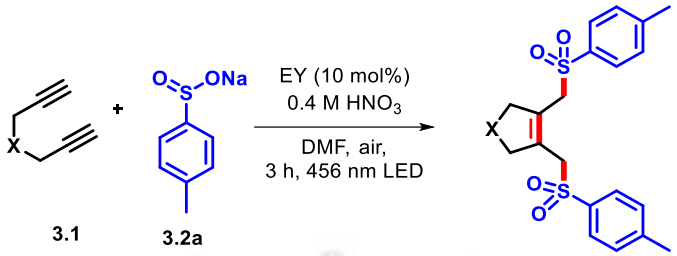

X = NTs, 1.657 g, **3.3a**, 74 %
X = NBoc, 1.173 g, **3.3i**, 58 %
X = O, 1.057 g, **3.5a**, 65 %

The 1,6-diynes **3.1** (4.0 mmol, 1 equiv.), sodium aryl sulfinates **3.2a** (16.0 mmol, 4equiv.) Eosin Y (10 mol%, 0.1 equiv.) was taken in an oven-dried reaction tube with a magnetic bead. After that, DMF (32 mL) was added, followed by the addition of 0.4 M HNO_3 (16 mL). The reaction mixture was allowed to stir under the 456 nm LED irradiation at room temperature in an open-air atmosphere for 10 h. The reaction was monitored by TLC, and after completion of the reaction, the reaction mixture was diluted with ethyl acetate. After that, the organic layer was washed with a saturated solution of $NaHCO_3$, followed by water. Then the organic layer was separated and dried over Na_2SO_4. The solvent was evaporated under reduced pressure to get the crude product. Further, the purification of the crude product was done by column chromatography on silica gel using petroleum ether and ethyl acetate as the eluent.

3.10 Analytical data:

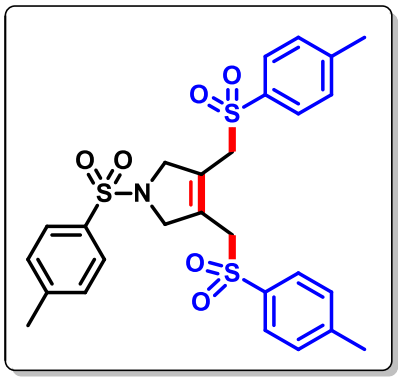

1-tosyl-3,4-bis(tosylmethyl)-2,5-dihydro-1H-pyrrole (**3.3a**): White solid (50 % ethyl acetate in petroleum ether) Yield: (119 mg) 85 %; **^{1}H NMR** (500 MHz, $CDCl_3$) δ 7.64 (d, *J* = 8.0 Hz, 2H), 7.47 (d, *J* = 8.2 Hz, 4H), 7.31 (d, *J* = 8.0 Hz, 2H), 7.22 (d, *J* = 8.0 Hz, 4H), 4.02 (s, 4H), 3.48 (s, 4H), 2.38 (s, 3H), 2.38 (s, 6H). **^{13}C NMR** (125 MHz, $CDCl_3$) δ 145.8, 144.0, 135.1, 133.5, 130.2, 130.0, 128.3, 128.1, 127.7, 57.4, 53.7, 21.7, 21.6. **HRMS** (ESI-TOF) m/z: $[M+Na]^+$ Calcd for $C_{27}H_{29}NO_6S_3Na$ 582.1055; Found 582.1069.

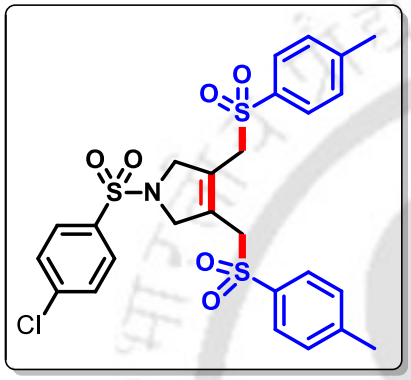

1-((4-chlorophenyl)sulfonyl)-3,4-bis(tosylmethyl)-2,5-dihydro-1H-pyrrole (**3.3b**): White solid (50 % ethyl acetate in petroleum ether) Yield: (120 mg) 83 %; **^{1}H NMR** (500 MHz, $CDCl_3$) δ 7.69 (d, *J* = 8.6 Hz, 2H), 7.51 (d, *J* = 8.2 Hz, 4H), 7.48 (d, *J* = 8.5 Hz, 2H), 7.25 (d, *J* = 8.0 Hz, 4H), 4.05 (s, 4H), 3.55 (s, 4H), 2.38 (s, 6H). **^{13}C NMR** (125 MHz, $CDCl_3$) δ 145.8, 139.7, 135.2, 135.1, 130.2, 129.7, 129.0, 128.2, 128.0, 57.5, 53.8, 21.7. **HRMS** (ESI-TOF) m/z: $[M+Na]^+$ Calcd for $C_{26}H_{26}ClNO_6S_3Na$ 602.0508; Found 602.0492.

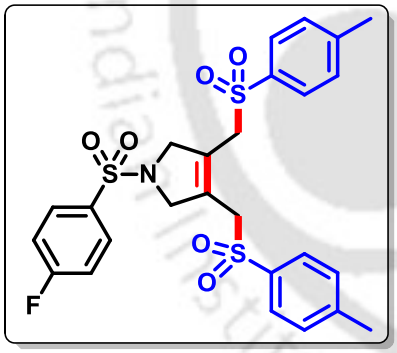

1-((4-fluorophenyl)sulfonyl)-3,4-bis(tosylmethyl)-2,5-dihydro-1H-pyrrole (**3.3c**): White solid (50 % ethyl acetate in petroleum ether) Yield: (100 mg) 71 %; **^{1}H NMR** (600 MHz, $CDCl_3$) δ 7.86 – 7.84 (m, 2H), 7.61 (d, *J* = 8.3 Hz, 4H), 7.34 (d, *J* = 8.0 Hz, 4H), 7.29 – 7.26 (m, 2H), 4.14 (s, 4H), 3.65 (s, 4H), 2.47 (s, 6H). **^{13}C NMR** (150 MHz, $CDCl_3$) δ 165.4 (d, *J* = 253.9 Hz), 145.8, 135.2, 132.7, 130.3, 130.2, 128.3, 128.0, 116.6 (d, *J* = 22.4 Hz), 57.5, 53.7, 21.8. **^{19}F NMR** (470 MHz, $CDCl_3$) δ -104.4. **HRMS** (ESI-TOF) m/z: $[M+Na]^+$ Calcd for $C_{26}H_{26}FNO_6S_3Na$ 586.0804; Found 586.0778.

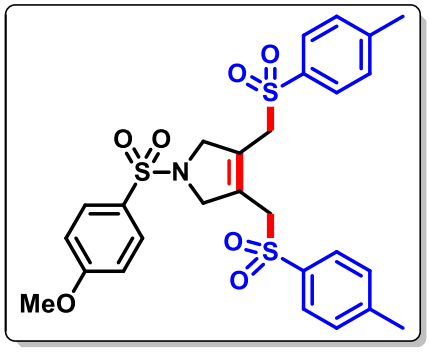

1-((4-methoxyphenyl)sulfonyl)-3,4-bis(tosylmethyl)-2,5-dihydro-1H-pyrrole (**3.3d**): White solid (50 % ethyl acetate in petroleum ether) Yield: (120 mg) 84 %; **^{1}H NMR** (600 MHz, $CDCl_3$) δ 7.77 (d, *J* = 8.9 Hz, 2H), 7.56 (d, *J* = 8.3 Hz, 4H), 7.31 (d, *J* = 7.8 Hz, 4H), 7.06 (d, *J* = 8.9 Hz, 2H), 4.10 (s, 4H), 3.89 (s, 3H), 3.56 (s, 4H), 2.45 (s, 6H). **^{13}C NMR** (150 MHz, $CDCl_3$) δ 163.3, 145.8, 135.1, 130.2, 129.8, 128.3, 128.1, 114.5, 57.4, 55.7, 53.7, 21.8. **HRMS** (ESI-TOF) m/z: $[M+Na]^+$ Calcd for $C_{27}H_{29}NO_7S_3Na$ 598.1004; Found 598.0969.

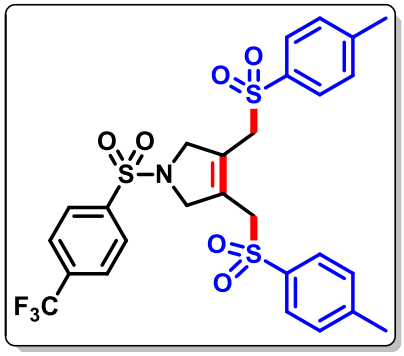

3,4-bis(tosylmethyl)-1-((4-(trifluoromethyl)phenyl)sulfonyl)-2,5-dihydro-1H-pyrrole (**3.3e**): White solid (50 % ethyl acetate in petroleum ether) Yield: (103 mg) 67 %; **^{1}H NMR** (500 MHz, $CDCl_3$) δ 7.88 (d, *J* = 8.2 Hz, 2H), 7.78 (d, *J* = 8.2 Hz, 2H), 7.52 (d, *J* = 8.3 Hz, 4H), 7.24 (d, *J* = 7.9 Hz, 4H), 4.09 (s, 4H), 3.57 (s, 4H), 2.38 (s, 6H). **^{13}C NMR** (125 MHz, $CDCl_3$) δ 146.0, 140.5, 135.4, 134.9 (q, *J* = 32.9 Hz), 130.4, 128.3, 128.12, 128.10 126.5 (q, *J* = 3.8 Hz), 123.2 (d, *J* = 271.4 Hz), 57.7, 53.9, 21.8. **^{19}F NMR** (470 MHz, $CDCl_3$) δ -63.1. **HRMS** (ESI-TOF) m/z: $[M+Na]^+$ Calcd for $C_{27}H_{26}F_3NO_6S_3Na$ 636.0772; Found 636.0724.

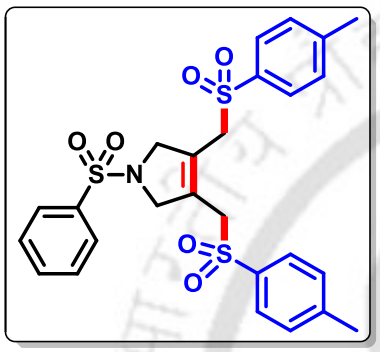

1-(phenylsulfonyl)-3,4-bis(tosylmethyl)-2,5-dihydro-1H-pyrrole (**3.3f**): White solid (50 % ethyl acetate in petroleum ether) Yield: (116 mg) 85 %; **^{1}H NMR** (500 MHz, $CDCl_3$) δ 7.76 (d, *J* = 7.6 Hz, 2H), 7.60 (t, *J* = 7.2 Hz, 1H), 7.53 (t, *J* = 7.5 Hz, 2H), 7.47 (d, *J* = 7.9 Hz, 4H), 7.22 (d, *J* = 7.9 Hz, 4H), 4.04 (s, 4H), 3.48 (s, 4H), 2.37 (s, 6H). **^{13}C NMR** (125 MHz, $CDCl_3$) δ 145.9, 136.6, 135.2, 133.2, 130.3, 129.5, 128.4, 128.2, 127.7, 57.6, 53.8, 21.9. **HRMS** (ESI-TOF) m/z: $[M+Na]^+$ Calcd for $C_{26}H_{27}NO_6S_3Na$ 568.0898; Found 568.0865.

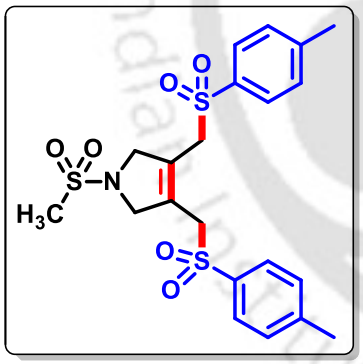

1-(methylsulfonyl)-3,4-bis(tosylmethyl)-2,5-dihydro-1H-pyrrole (**3.3g**): White solid (50 % ethyl acetate in petroleum ether) Yield: (103 mg) 85 %; **^{1}H NMR** (500 MHz, $CDCl_3$) δ 7.78 (d, *J* = 7.9 Hz, 4H), 7.41 (d, *J* = 7.8 Hz, 4H), 4.19 (s, 4H), 3.90 (s, 4H), 2.83 (s, 3H), 2.49 (s, 6H). **^{13}C NMR** (125 MHz, $CDCl_3$) δ 146.0, 135.7, 130.5, 128.7, 128.2, 57.9, 54.1, 35.1, 21.9. **HRMS** (ESI-TOF) m/z: $[M+Na]^+$ Calcd for $C_{21}H_{25}NO_6S_3Na$ 506.0742; Found 506.0715.

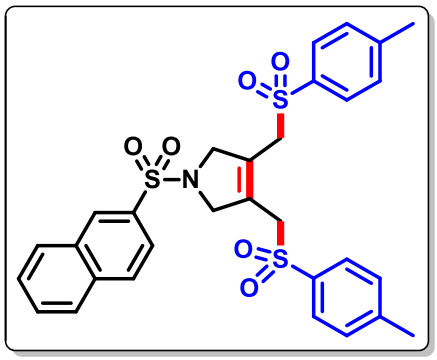

1-(naphthalen-2-ylsulfonyl)-3,4-bis(tosylmethyl)-2,5-dihydro-1H-pyrrole (**3.3h**): White solid (50 % ethyl acetate in petroleum ether) Yield: (115 mg) 77 %; **^{1}H NMR** (500 MHz, $CDCl_3$) δ 8.33 (s, 1H), 7.97 (t, *J* = 7.5 Hz, 2H), 7.88 (d, *J* = 7.7 Hz, 1H), 7.76 (d, *J* = 8.4 Hz, 1H), 7.60 (m, 2H), 7.39 (d, *J* = 8.0 Hz, 4H), 7.07 (d, *J* = 7.9 Hz, 4H), 4.10 (s, 4H), 3.44 (s, 4H), 2.30 (s, 6H). **^{13}C NMR** (125 MHz, $CDCl_3$) δ 145.8, 135.2, 135.1, 133.7, 132.4, 130.2, 129.8, 129.6, 129.2, 129.0, 128.4, 128.1, 127.9, 123.0, 57.6, 53.8, 21.8. **HRMS** (ESI-TOF) m/z: $[M+Na]^+$ Calcd for $C_{30}H_{29}NO_6S_3Na$ 618.1055; Found 618.1021.

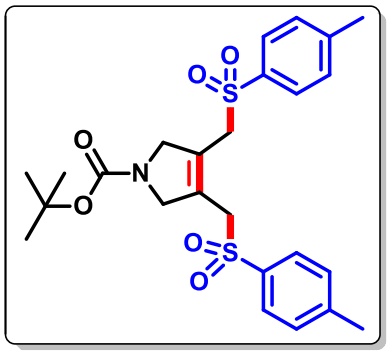

tert-butyl 3,4-bis(tosylmethyl)-2,5-dihydro-1H-pyrrole-1-carboxylate (**3.3i**): White solid (50 % ethyl acetate in petroleum ether) Yield: (77 mg) 61 %; **^{1}H NMR** (500 MHz, $CDCl_3$) δ 7.69 – 7.64 (m, 4H), 7.30 (t, *J* = 8.7 Hz, 4H), 4.10 (s, 2H), 4.00 (s, 2H), 3.78 (s, 2H), 3.65 (s, 2H), 2.38 (s, 6H), 1.38 (s, 9H). **^{13}C NMR** (125 MHz, $CDCl_3$) δ 153.6, 145.72, 145.66, 135.9, 130.29, 130.27, 128.7, 128.6, 128.3, 128.2, 80.1, 56.4, 56.1, 54.3, 54.1, 28.5, 21.83, 21.81. **HRMS** (ESI-TOF) m/z: $[M+Na]^+$ Calcd for $C_{25}H_{31}NO_6S_2Na$ 528.1490; Found 528.1509.

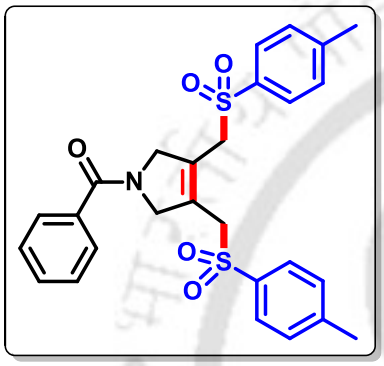

(3,4-bis(tosylmethyl)-2,5-dihydro-1H-pyrrol-1-yl)(phenyl)methanone (**3.3j**): White solid (50 % ethyl acetate in petroleum ether) Yield: (108 mg) 85 %; **^{1}H NMR** (500 MHz, $CDCl_3$) δ 7.76 (d, *J* = 7.9 Hz, 2H), 7.71 (d, *J* = 8.0 Hz, 2H), 7.45 – 7.34 (m, 9H), 4.41 (s, 2H), 4.25 (s, 2H), 3.89 (s, 2H), 3.86 (s, 2H), 2.47 (s, 3H), 2.43 (s, 3H). **^{13}C NMR** (125 MHz, $CDCl_3$) δ 169.6, 145.9, 145.8, 135.9, 135.76, 135.74, 130.5, 130.4, 130.3, 128.9, 128.6, 128.19, 128.16, 128.11, 127.0, 58.8, 56.7, 54.23, 54.19, 21.9, 21.8. **HRMS** (ESI-TOF) m/z: $[M+Na]^+$ Calcd for $C_{27}H_{27}NO_5S_2Na$ 532.1228; Found 532.1233.

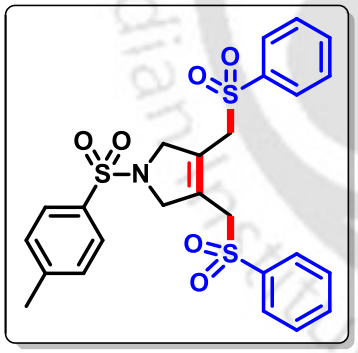

3,4-bis((phenylsulfonyl)methyl)-1-tosyl-2,5-dihydro-1H-pyrrole (**3.3k**): White solid (50 % ethyl acetate in petroleum ether) Yield: (102 mg) 77 %; **^{1}H NMR** (600 MHz, $CDCl_3$) δ 7.73 – 7.67 (m, 8H), 7.52 (t, *J* = 7.4 Hz, 4H), 7.41 (d, *J* = 8.0 Hz, 2H), 4.11 (s, 4H), 3.60 (s, 4H), 2.47 (s, 3H). **^{13}C NMR** (150 MHz, $CDCl_3$) δ 144.2, 138.1, 134.7, 133.5, 130.1, 129.7, 128.4, 128.2, 127.8, 57.5, 53.7, 21.7. **HRMS** (ESI-TOF) m/z: $[M+Na]^+$ Calcd for $C_{25}H_{25}NO_6S_3Na$ 554.0742; Found 554.0741.

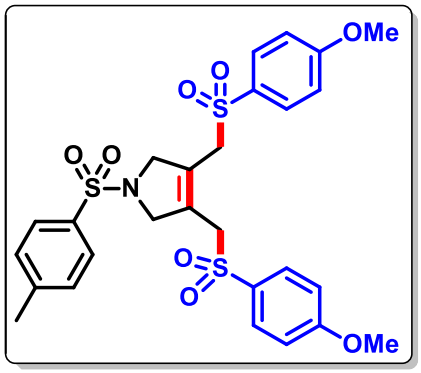

3,4-bis(((4-methoxyphenyl)sulfonyl)methyl)-1-tosyl-2,5-dihydro-1H-pyrrole (**3.3l**): White solid (50 % ethyl acetate in petroleum ether) Yield: (102 mg) 69 %; **^{1}H NMR** (600 MHz, $CDCl_3$) δ 7.72 (d, *J* = 8.3 Hz, 2H), 7.60 (d, *J* = 8.9 Hz, 4H), 7.41 (d, *J* = 8.0 Hz, 2H), 6.96 (d, *J* = 8.9 Hz, 4H), 4.09 (s, 4H), 3.91 (s, 6H), 3.60 (s, 4H), 2.48 (s, 3H). **^{13}C NMR** (150 MHz, $CDCl_3$) δ 164.4, 144.2, 133.5, 130.1, 129.5, 128.5, 127.8, 114.8, 114.4, 57.5, 56.0, 54.1, 21.7. **HRMS** (ESI-TOF) m/z: $[M+Na]^+$ Calcd for $C_{27}H_{29}NO_8S_3Na$ 614.0953 Found 614.0959.

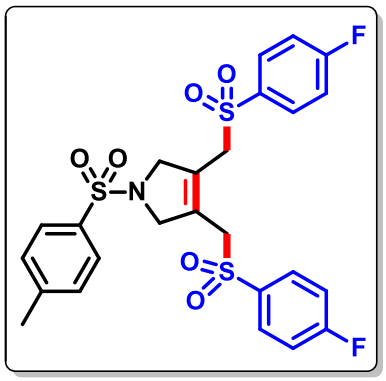

3,4-bis(((4-fluorophenyl)sulfonyl)methyl)-1-tosyl-2,5-dihydro-1H-pyrrole (**3.3m**): White solid (50 % ethyl acetate in petroleum ether) Yield: (92 mg) 65 %; **^{1}H NMR** (600 MHz, $CDCl_3$) δ 7.81 – 7.78 (m, 4H), 7.70 (d, *J* = 8.3 Hz, 2H), 7.40 (d, *J* = 8.0 Hz, 2H), 7.22 (t, *J* = 8.4 Hz, 4H), 4.11 (s, 4H), 3.80 (s, 4H), 2.49 (s, 3H). **^{13}C NMR** (150 MHz, $CDCl_3$) δ 166.3 (d, *J* = 257.1 Hz), 144.3, 134.4 (d, *J* = 3.2 Hz), 133.5, 131.2 (d, *J* = 9.8 Hz), 130.2, 128.5, 127.7, 117.2 (d, *J* = 22.4 Hz), 57.6, 54.2, 21.7. **^{19}F NMR** (565 MHz, $CDCl_3$) δ -101.1. **HRMS** (ESI-TOF) m/z: $[M+Na]^+$ Calcd for $C_{25}H_{23}F_2NO_6S_3Na$ 590.0553; Found 590.0555.

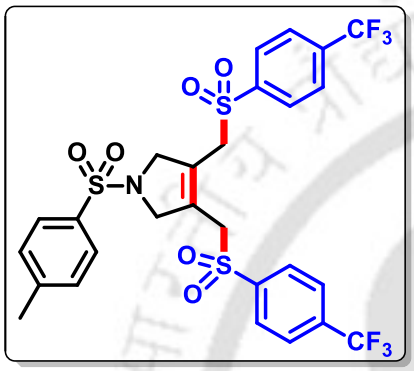

1-tosyl-3,4-bis(((4-(trifluoromethyl)phenyl)sulfonyl)methyl)-2,5-dihydro-1H-pyrrole (**3.3n**): White solid (50 % ethyl acetate in petroleum ether) Yield: (98 mg) 59 %; **^{1}H NMR** (500 MHz, $CDCl_3$) δ 7.87 (d, *J* = 8.1 Hz, 4H), 7.75 (d, *J* = 8.2 Hz, 4H), 7.62 (d, *J* = 8.0 Hz, 2H), 7.30 (d, *J* = 8.0 Hz, 2H), 4.11 (s, 4H), 3.81 (s, 4H), 2.38 (s, 3H). **^{13}C NMR** (125 MHz, $CDCl_3$) δ 143.2 (d, *J* = 285.4 Hz), 136.4 (q, *J* = 33.2 Hz), 133.7, 130.2, 128.9, 128.5, 127.7, 126.9 (q, *J* = 3.6 Hz), 126.3, 123.0 (d, *J* = 271.8 Hz), 57.7, 54.1, 21.7. **^{19}F NMR** (470 MHz, $CDCl_3$) δ -63.3. **HRMS** (ESI-TOF) m/z: $[M+Na]^+$ Calcd for $C_{27}H_{23}F_6NO_6S_3Na$ 690.0489; Found 690.0483.

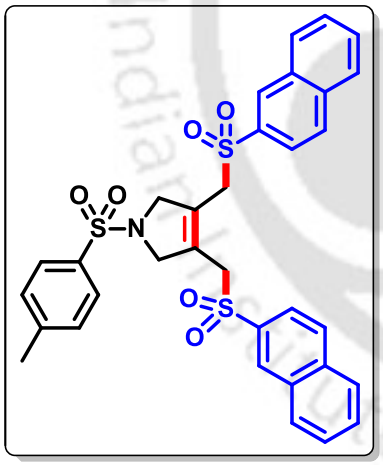

3,4-bis((naphthalen-2-ylsulfonyl)methyl)-1-tosyl-2,5-dihydro-1H-pyrrole (**3.3o**): White solid (50 % ethyl acetate in petroleum ether) Yield: (96 mg) 61 %; **^{1}H NMR** (600 MHz, $CDCl_3$) δ 8.33 (s, 2H), 7.94 (d, *J* = 8.3 Hz, 6H), 7.74 – 7.70 (m, 3H), 7.69 – 7.66 (m, 3H), 7.63 (dd, *J* = 8.6, 1.9 Hz, 2H), 7.37 (d, *J* = 8.1 Hz, 2H), 4.18 (s, 4H), 3.67 (s, 4H), 2.48 (s, 3H). **^{13}C NMR** (150 MHz, $CDCl_3$) δ 144.1, 135.5, 135.1, 133.7, 132.2, 130.2, 130.1, 130.0, 129.6, 128.5, 128.3, 128.2, 127.8, 122.8, 122.3, 57.6, 53.9, 21.8. **HRMS** (ESI-TOF) m/z: $[M+Na]^+$ Calcd for $C_{33}H_{29}NO_6S_3Na$ 654.1055; Found 654.1067.

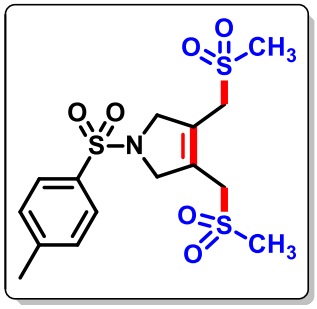

3,4-bis((methylsulfonyl)methyl)-1-tosyl-2,5-dihydro-1H-pyrrole (**3.3p**): White solid (50 % ethyl acetate in petroleum ether) Yield: (65 mg) 64 %; **^{1}H NMR** (500 MHz, DMSO-d_6) δ 6.85 (d, *J* = 7.9 Hz, 2H), 6.60 (d, *J* = 7.9 Hz, 2H), 3.40 (s, 4H), 3.35 (s, 4H), 2.06 (s, 6H), 1.56 (s, 3H). **^{13}C NMR** (125 MHz, DMSO-d_6) δ 143.8, 133.2, 130.1, 128.0, 127.3, 56.6, 51.4, 40.1, 21.0. **HRMS** (ESI-TOF) m/z: $[M+Na]^+$ Calcd for $C_{15}H_{21}NO_6S_3Na$ 430.0429; Found 430.0404.

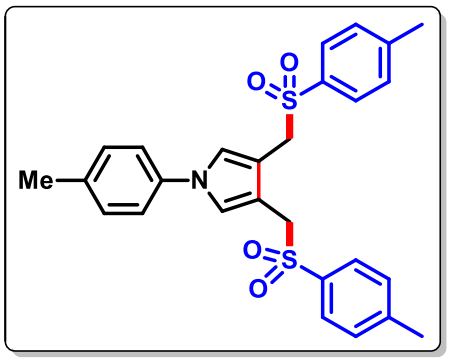

1-(p-tolyl)-3,4-bis(tosylmethyl)-1H-pyrrole (**3.4a**): White solid (50 % ethyl acetate in petroleum ether) Yield: (88 mg) 71 %; **^{1}H NMR** (500 MHz, $CDCl_3$) δ 7.64 (d, *J* = 7.9 Hz, 4H), 7.29 (d, *J* = 7.9 Hz, 4H), 7.18 (d, *J* = 8.0 Hz, 2H), 7.05 (d, *J* = 8.0 Hz, 2H), 6.78 (s, 2H), 4.26 (s, 4H), 2.43 (s, 6H), 2.36 (s, 3H). **^{13}C NMR** (125 MHz, $CDCl_3$) δ 144.8, 137.4, 136.5, 135.8, 130.3, 129.7, 128.6, 122.2, 120.5, 111.9, 54.1, 21.8, 21.0. **HRMS** (ESI-TOF) m/z: $[M+Na]^+$ Calcd for $C_{27}H_{27}NO_4S_2Na$ 516.1279; Found 516.1283.

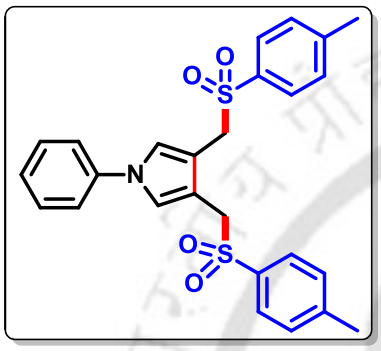

1-phenyl-3,4-bis(tosylmethyl)-1H-pyrrole (**3.4b**): White solid (50 % ethyl acetate in petroleum ether) Yield: (80 mg) 67 %; **^{1}H NMR** (500 MHz, $CDCl_3$) δ 7.57 (d, *J* = 8.2 Hz, 4H), 7.31 (t, *J* = 7.8 Hz, 2H), 7.22 (d, *J* = 8.0 Hz, 5H), 7.09 (d, *J* = 7.7 Hz, 2H), 6.74 (s, 2H), 4.19 (s, 4H), 2.35 (s, 6H). **^{13}C NMR** (125 MHz, $CDCl_3$) δ 144.8, 139.7, 135.7, 129.8, 129.7, 128.6, 126.6, 122.1, 120.6, 112.3, 54.1, 21.7. **HRMS** (ESI-TOF) m/z: $[M+Na]^+$ Calcd for $C_{26}H_{25}NO_4S_2Na$ 502.1123; Found 502.1100.

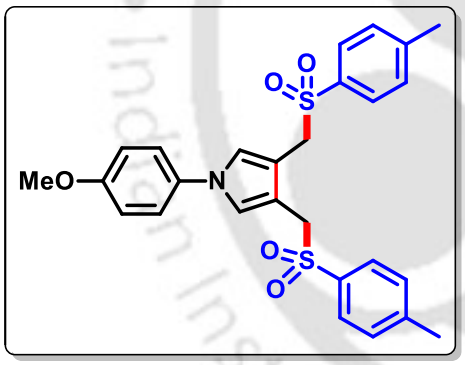

1-(4-methoxyphenyl)-3,4-bis(tosylmethyl)-1H-pyrrole (**3.4c**): White solid (50 % ethyl acetate in petroleum ether) Yield: (93 mg) 73 %; **^{1}H NMR** (500 MHz, $CDCl_3$) δ 7.57 (d, *J* = 8.0 Hz, 4H), 7.22 (d, *J* = 7.9 Hz, 4H), 7.01 (d, *J* = 8.8 Hz, 2H), 6.82 (d, *J* = 8.9 Hz, 2H), 6.65 (s, 2H), 4.19 (s, 4H), 3.75 (s, 3H), 2.35 (s, 6H). **^{13}C NMR** (125 MHz, $CDCl_3$) δ 158.4, 144.7, 135.8, 133.3, 129.7, 128.6, 122.5, 122.2, 114.8, 111.7, 55.7, 54.1, 21.7. **HRMS** (ESI-TOF) m/z: $[M+Na]^+$ Calcd for $C_{27}H_{27}NO_5S_2Na$ 532.1228; Found 532.1225.

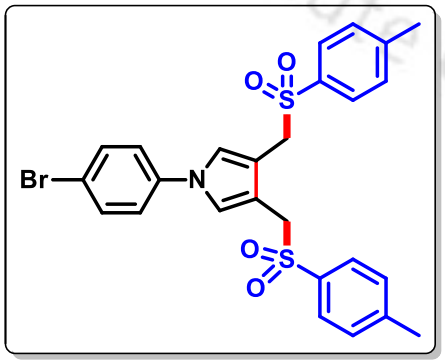

1-(4-bromophenyl)-3,4-bis(tosylmethyl)-1H-pyrrole (**3.4d**): White solid (50 % ethyl acetate in petroleum ether) Yield: (89 mg) 64 %; **^{1}H NMR** (500 MHz, $CDCl_3$) δ 7.59 (d, *J* = 7.8 Hz, 4H), 7.45 (d, *J* = 8.0 Hz, 2H), 7.23 (d, *J* = 7.6 Hz, 4H), 7.00 (d, *J* = 8.0 Hz, 2H), 6.74 (s, 2H), 4.19 (s, 4H), 2.36 (s, 6H). **^{13}C NMR** (125 MHz, $CDCl_3$) δ 144.9, 138.7, 135.8, 132.9, 129.8, 128.6, 122.0, 119.9, 112.8, 54.0, 21.8. **HRMS** (ESI-TOF) m/z: $[M+Na]^+$ Calcd for $C_{26}H_{24}BrNO_4S_2Na$ 580.0228; Found 580.0228.

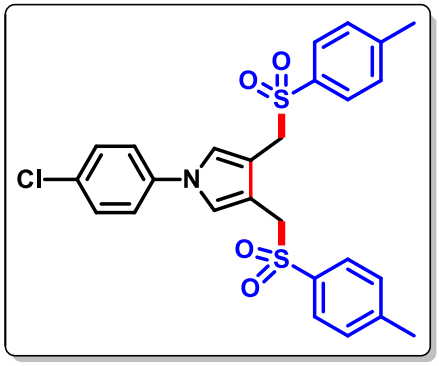

1-(4-chlorophenyl)-3,4-bis(tosylmethyl)-1H-pyrrole (**3.4e**): White solid (50 % ethyl acetate in petroleum ether) Yield: (78 mg) 61 %; **^{1}H NMR** (400 MHz, $CDCl_3$) δ 7.66 (d, *J* = 8.3 Hz, 4H), 7.37 (d, *J* = 8.8 Hz, 2H), 7.30 (d, *J* = 7.9 Hz, 4H), 7.13 (d, *J* = 8.8 Hz, 2H), 6.81 (s, 2H), 4.27 (s, 4H), 2.43 (s, 6H). **^{13}C NMR** (125 MHz, $CDCl_3$) δ 144.9, 138.2, 135.8, 132.3, 129.9, 129.8, 128.6, 122.1, 121.7, 112.7, 54.0, 21.8. **HRMS** (ESI-TOF) m/z: $[M+Na]^+$ Calcd for $C_{26}H_{24}ClNO_4S_2Na$ 536.0733; Found 536.0735.

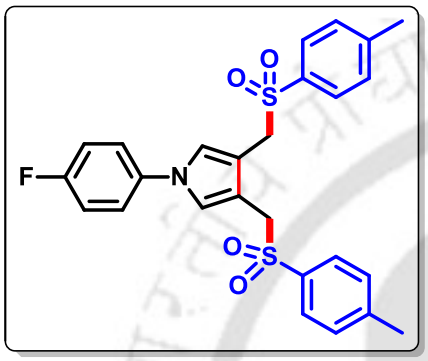

1-(4-fluorophenyl)-3,4-bis(tosylmethyl)-1H-pyrrole (**3.4f**): White solid (50 % ethyl acetate in petroleum ether) Yield: (71 mg) 57 %; **^{1}H NMR** (500 MHz, $CDCl_3$) δ 7.66 (d, *J* = 8.2 Hz, 4H), 7.31 (d, *J* = 8.0 Hz, 4H), 7.17 – 7.14 (m, 2H), 7.09 (t, *J* = 8.4 Hz, 2H), 6.78 (s, 2H), 4.26 (s, 4H), 2.43 (s, 6H). **^{13}C NMR** (125 MHz, $CDCl_3$) δ 161.2 (d, *J* = 244.9 Hz), 144.9, 136.1 (d, *J* = 3.2 Hz), 135.8, 129.8, 128.6, 122.49 (d, *J* = 5.6 Hz), 122.45, 116.6 (d, *J* = 22.8 Hz), 112.3, 54.0, 21.8. **^{19}F NMR** (470 MHz, $CDCl_3$) δ -115.4. **HRMS** (ESI-TOF) m/z: $[M+Na]^+$ Calcd for $C_{26}H_{24}FNO_4S_2Na$ 520.1028; Found 520.1029.

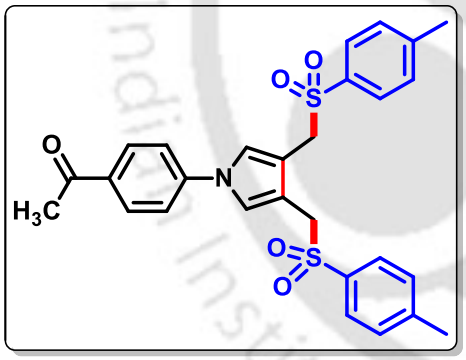

1-(4-(3,4-bis(tosylmethyl)-1H-pyrrol-1-yl)phenyl)ethanone (**3.4g**): White solid (50 % ethyl acetate in petroleum ether) Yield: (64 mg) 49 %; **^{1}H NMR** (600 MHz, $CDCl_3$) δ 8.00 (d, *J* = 8.8 Hz, 2H), 7.67 (d, *J* = 8.3 Hz, 4H), 7.32 (d, *J* = 7.8 Hz, 4H), 7.28 (d, *J* = 8.8 Hz, 2H), 6.95 (s, 2H), 4.29 (s, 4H), 2.62 (s, 3H), 2.44 (s, 6H). **^{13}C NMR** (150 MHz, $CDCl_3$) δ 196.7, 145.0, 142.8, 135.7, 135.0, 130.3, 129.8, 128.5, 121.8, 119.6, 113.4, 54.0, 26.7, 21.8. **HRMS** (ESI-TOF) m/z: $[M+Na]^+$ Calcd for $C_{28}H_{27}NO_5S_2Na$ 544.1228; Found 544.1220.

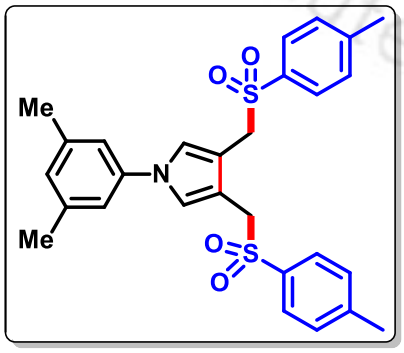

1-(3,5-dimethylphenyl)-3,4-bis(tosylmethyl)-1H-pyrrole (**3.4h**): White solid (50 % ethyl acetate in petroleum ether) Yield: (80 mg) 63 %; **^{1}H NMR** (500 MHz, $CDCl_3$) δ 7.56 (d, *J* = 7.9 Hz, 4H), 7.22 (d, *J* = 7.9 Hz, 4H), 6.83 (s, 1H), 6.69 (s, 4H), 4.17 (s, 4H), 2.36 (s, 6H), 2.25 (s, 6H). **^{13}C NMR** (125 MHz, $CDCl_3$) δ 144.7, 139.7, 139.6, 135.7, 129.7, 128.7, 128.2, 122.2, 118.5, 111.9, 54.1, 21.8, 21.4. **HRMS** (ESI-TOF) m/z: $[M+Na]^+$ Calcd for $C_{28}H_{29}NO_4S_2Na$ 530.1436; Found 530.1440.

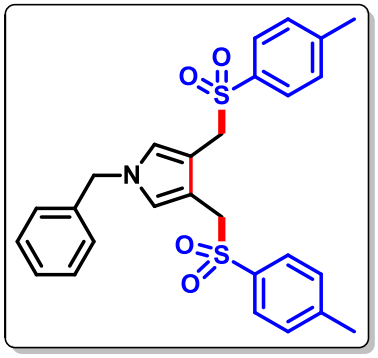

1-benzyl-3,4-bis(tosylmethyl)-1H-pyrrole (**3.4i**): White solid (50 % ethyl acetate in petroleum ether) Yield: (75 mg) 61 %; **^{1}H NMR** (500 MHz, $CDCl_3$) δ 7.49 (d, *J* = 8.2 Hz, 4H), 7.26 – 7.25 (m, 3H), 7.14 (d, *J* = 8.0 Hz, 4H), 6.94 – 6.92 (m, 2H), 6.34 (s, 2H), 4.79 (s, 2H), 4.12 (s, 4H), 2.33 (s, 6H). **^{13}C NMR** (125 MHz, $CDCl_3$) δ 144.5, 137.0, 135.6, 129.6, 128.9, 128.6, 128.1, 127.3, 123.9, 110.6, 54.0, 53.7, 21.8. **HRMS** (ESI-TOF) m/z: $[M+Na]^+$ Calcd for $C_{27}H_{27}NO_4S_2Na$ 516.1279; Found 516.1252.

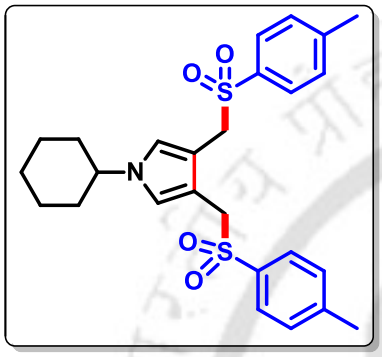

1-cyclohexyl-3,4-bis(tosylmethyl)-1H-pyrrole (**3.4j**): White solid (50 % ethyl acetate in petroleum ether) Yield: (66 mg) 54 %; **^{1}H NMR** (500 MHz, $CDCl_3$) δ 7.48 (d, *J* = 8.1 Hz, 4H), 7.18 (d, *J* = 8.0 Hz, 4H), 6.31 (s, 2H). 4.09 (s, 4H), 3.54 – 3.48 (m, 1H), 2.34 (s, 6H), 1.83 – 1.80 (m, 2H), 1.76 – 1.72 (m, 2H), 1.64 – 1.60 (m, 2H), 1.35 – 1.21 (m, 4H). **^{13}C NMR** (125 MHz, $CDCl_3$) δ 144.4, 135.7, 129.5, 128.6, 121.4, 109.3, 58.9, 54.2, 34.5, 25.5, 25.4, 21.7. **HRMS** (ESI-TOF) m/z: $[M+Na]^+$ Calcd for $C_{26}H_{31}NO_4S_2Na$ 508.1587; Found 508.1565.

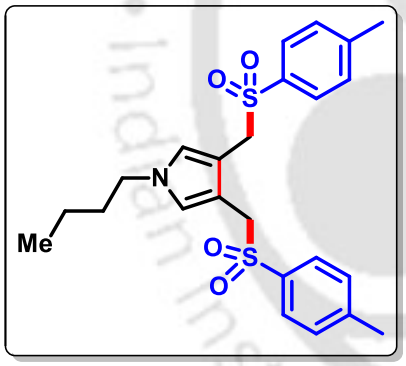

1-butyl-3,4-bis(tosylmethyl)-1H-pyrrole (**3.4k**): White solid (50 % ethyl acetate in petroleum ether) Yield: (59 mg) 51 %; **^{1}H NMR** (500 MHz, $CDCl_3$) δ 7.50 (d, *J* = 8.0 Hz, 4H), 7.18 (d, *J* = 7.9 Hz, 4H), 6.27 (s, 2H), 4.09 (s, 4H), 3.60 (t, *J* = 7.0 Hz, 2H), 2.34 (s, 6H), 1.50 – 1.44 (m, 2H), 1.13 – 1.05 (m, 2H), 0.82 (t, *J* = 7.4 Hz, 3H). **^{13}C NMR** (125 MHz, $CDCl_3$) δ 144.5, 135.6, 129.5, 128.5, 123.3, 109.7, 54.0, 49.6, 33.3, 21.7, 19.7, 13.7. **HRMS** (ESI-TOF) m/z: $[M+Na]^+$ Calcd for $C_{24}H_{29}NO_4S_2Na$ 482.1431; Found 482.1412.

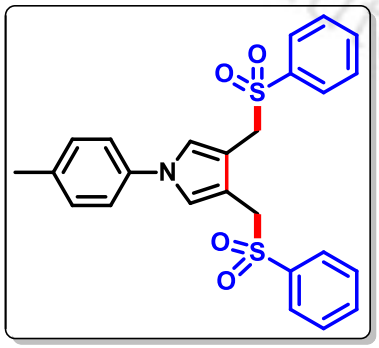

3,4-bis((phenylsulfonyl)methyl)-1-(p-tolyl)-1H-pyrrole (**3.4l**): White solid (50 % ethyl acetate in petroleum ether) Yield: (75 mg) 64 %; **^{1}H NMR** (600 MHz, $CDCl_3$) δ 7.77 (d, *J* = 7.5 Hz, 4H), 7.63 (t, *J* = 7.5 Hz, 2H), 7.51 (t, *J* = 7.6 Hz, 4H), 7.18 (d, *J* = 7.9 Hz, 2H), 7.03 (d, *J* = 8.0 Hz, 2H), 6.76 (s, 2H), 4.31 (s, 4H), 2.36 (s, 3H). **^{13}C NMR** (150 MHz, $CDCl_3$) δ 138.5, 137.3, 136.6, 133.8, 130.3, 129.1, 128.6, 122.3, 120.5, 111.7, 54.0, 21.0. **HRMS** (ESI-TOF) m/z: $[M+Na]^+$ Calcd for $C_{25}H_{23}NO_4S_2Na$ 488.0961; Found 488.0964.

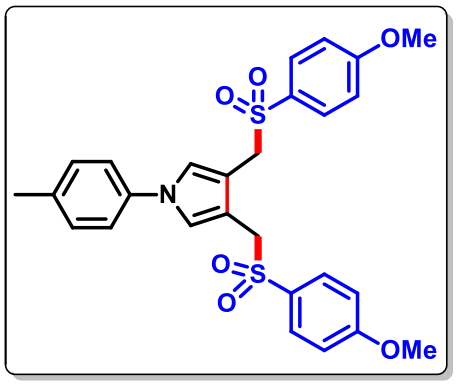

3,4-bis(((4-methoxyphenyl)sulfonyl)methyl)-1-(p-tolyl)-1H-pyrrole (**3.4m**): White solid (50 % ethyl acetate in petroleum ether) Yield: (89 mg) 68 %; **^{1}H NMR** (500 MHz, $CDCl_3$) δ 7.67 (d, *J* = 8.7 Hz, 4H), 7.19 (d, *J* = 8.0 Hz, 2H), 7.07 (d, *J* = 8.3 Hz, 2H), 6.95 (d, *J* = 8.8 Hz, 4H), 6.79 (s, 2H), 4.25 (s, 4H), 3.86 (s, 6H), 2.36 (s, 3H). **^{13}C NMR** (125 MHz, $CDCl_3$) δ 163.8, 137.4, 136.5, 130.8, 130.3, 130.1, 122.1, 120.5, 114.3, 112.2, 55.8, 54.2, 21.0. **HRMS** (ESI-TOF) m/z: $[M+Na]^+$ Calcd for $C_{27}H_{27}NO_6S_2Na$ 548.1172; Found 548.1179.

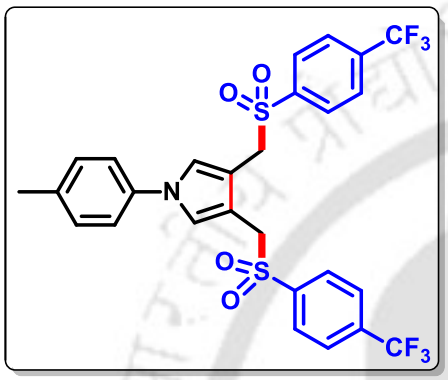

1-(p-tolyl)-3,4-bis(((4-(trifluoromethyl)phenyl)sulfonyl)methyl)-1H-pyrrole (**3.4n**): White solid (50 % ethyl acetate in petroleum ether) Yield: (77 mg) 51 %; **^{1}H NMR** (500 MHz, $CDCl_3$) δ 7.85 (d, *J* = 8.1 Hz, 4H), 7.72 (d, *J* = 8.1 Hz, 4H), 7.10 (d, *J* = 8.0 Hz, 2H), 6.86 (d, *J* = 8.0 Hz, 2H), 6.65 (s, 2H), 4.40 (s, 4H), 2.28 (s, 3H). **^{13}C NMR** (125 MHz, $CDCl_3$) δ 142.0, 137.1, 137.0, 135.6 (q, *J* = 32.9 Hz), 130.4, 129.3, 126.2 (q, *J* = 3.6 Hz), 123.2 (d, *J* = 271.4 Hz), 122.7, 120.6, 111.1, 54.2, 21.0. **^{19}F NMR** (470 MHz, $CDCl_3$) δ -63.2. **HRMS** (ESI-TOF) m/z: $[M+Na]^+$ Calcd for $C_{27}H_{21}F_6NO_4S_2Na$ 624.0709; Found 624.0701.

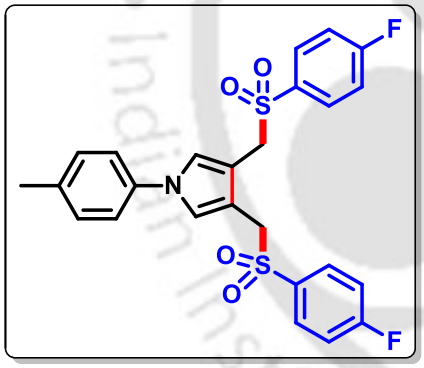

3,4-bis(((4-fluorophenyl)sulfonyl)methyl)-1-(p-tolyl)-1H-pyrrole (**3.4o**): White solid (50 % ethyl acetate in petroleum ether) Yield: (72 mg) 57 %; **^{1}H NMR** (500 MHz, $CDCl_3$) δ 7.79 – 7.77 (m, 4H), 7.20 – 7.16 (m, 6H), 7.03 (d, *J* = 8.1 Hz, 2H), 6.77 (s, 2H), 4.37 (s, 4H), 2.36 (s, 3H). **^{13}C NMR** (125 MHz, $CDCl_3$) δ 165.9 (d, *J* = 255 Hz), 137.1, 136.8, 134.5 (d, *J* = 3.2 Hz), 131.4 (d, *J* = 9.3 Hz), 130.4, 122.4, 120.5, 116.4 (d, *J* = 22.4 Hz), 111.7, 54.2, 21.0. **^{19}F NMR** (470 MHz, $CDCl_3$) δ -103.3. **HRMS** (ESI-TOF) m/z: $[M+Na]^+$ Calcd for $C_{25}H_{21}F_2NO_4S_2Na$ 524.0773; Found 524.0772.

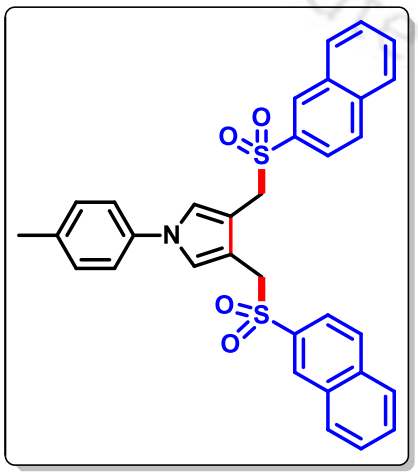

3,4-bis((naphthalen-2-ylsulfonyl)methyl)-1-(p-tolyl)-1H-pyrrole (**3.4p**): White solid (50 % ethyl acetate in petroleum ether) Yield: (83 mg) 59 %; **^{1}H NMR** (500 MHz, $CDCl_3$) δ 8.32 (s, 2H), 7.94 – 7.90 (m, 6H), 7.73 (d, *J* = 8.6 Hz, 2H), 7.67 (t, *J* = 7.5 Hz, 2H), 7.60 (t, *J* = 7.5 Hz, 2H), 7.06 (d, *J* = 7.9 Hz, 2H), 6.80 (d, *J* = 7.9 Hz, 2H), 6.69 (s, 2H), 4.39 (s, 4H), 2.31 (s, 3H). **^{13}C NMR** (126 MHz, $CDCl_3$) δ 137.2, 136.6, 135.39, 135.36, 132.1, 130.4, 130.1, 129.5, 129.4, 129.3, 128.1, 127.8, 123.3, 122.4, 120.6, 111.8, 54.1, 20.9. **HRMS** (ESI-TOF) m/z: $[M+Na]^+$ Calcd for $C_{33}H_{27}NO_4S_2Na$ 588.1274; Found 588.1269.

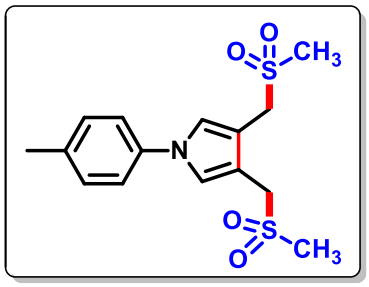

3,4-bis((methylsulfonyl)methyl)-1-(p-tolyl)-1H-pyrrole (**3.4q**): White solid (50 % ethyl acetate in petroleum ether) Yield: (46 mg) 54 %; **^{1}H NMR** (500 MHz, $CDCl_3$) δ 7.19 – 7.16 (m, 4H), 7.12 (s, 2H), 4.34 (s, 4H), 2.84 (s, 6H), 2.31 (s, 3H). **^{13}C NMR** (125 MHz, $CDCl_3$) δ 137.3, 136.9, 130.4, 122.2, 120.7, 111.6, 52.3, 39.5, 21.0. **HRMS** (ESI-TOF) m/z: $[M+Na]^+$ Calcd for $C_{15}H_{19}NO_4S_2Na$ 364.0648; Found 364.0647.

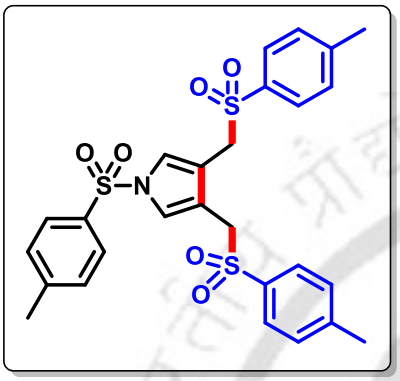

1-tosyl-3,4-bis(tosylmethyl)-1H-pyrrole (**3.4r**): White solid (50 % ethyl acetate in petroleum ether) Yield: (50 mg) 89 %; **^{1}H NMR** (600 MHz, $CDCl_3$) δ 7.66 (d, J = 8.3 Hz, 2H), 7.50 (d, J = 8.2 Hz, 4H), 7.34 (d, J = 8.1 Hz, 2H), 7.21 (d, J = 8.0 Hz, 4H), 6.84 (s, 2H), 4.20 (s, 4H), 2.46 (s, 3H), 2.43 (s, 6H). **^{13}C NMR** (150 MHz, $CDCl_3$) δ 145.9, 145.1, 135.4, 135.0, 130.3, 129.8, 128.5, 127.2, 122.7, 115.9, 53.5, 21.9, 21.8. **HRMS** (ESI-TOF) m/z: $[M+H]^+$ Calcd for $C_{27}H_{28}NO_6S_3$ 558.1074; Found 558.1056.

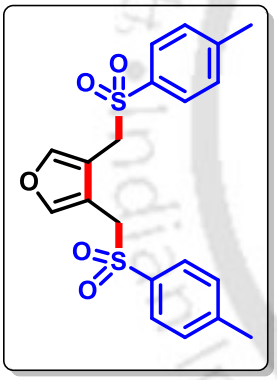

3,4-bis(tosylmethyl)furan (**3.4s**): White solid (50 % ethyl acetate in petroleum ether) Yield: (32 mg) 81 %; **^{1}H NMR** (600 MHz, $CDCl_3$) δ 7.66 (d, J = 8.0 Hz, 4H), 7.34 (d, J = 8.0 Hz, 4H), 7.20 (s, 2H), 4.29 (s, 4H), 2.46 (s, 6H). **^{13}C NMR** (150 MHz, $CDCl_3$) δ 145.2, 144.6, 135.1, 129.9, 128.5, 113.5, 51.9, 21.8. **HRMS** (ESI-TOF) m/z: $[M+H]^+$ Calcd for $C_{20}H_{21}O_5S_2$ 405.0825; Found 405.0822.

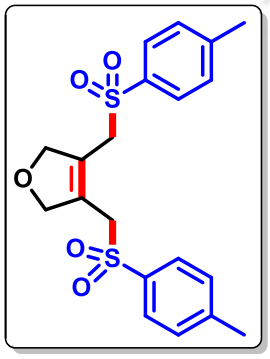

3,4-bis(tosylmethyl)-2,5-dihydrofuran (**3.5a**): White solid (50 % ethyl acetate in petroleum ether) Yield: (82 mg) 81 %; **^{1}H NMR** (400 MHz, $CDCl_3$) δ 7.66 (d, J = 8.3 Hz, 4H), 7.30 (d, J = 8.0 Hz, 4H), 4.48 (s, 4H), 3.70 (s, 4H), 2.39 (s, 6H). **^{13}C NMR** (125 MHz, $CDCl_3$) δ 145.7, 135.6, 130.3, 129.3, 128.3, 78.0, 53.2, 21.8. **HRMS** (ESI-TOF) m/z: $[M+Na]^+$ Calcd for $C_{20}H_{22}O_5S_2Na$ 429.0806; Found 429.0806.

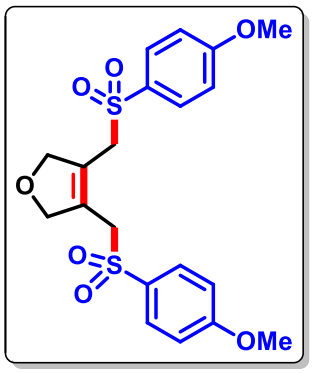

3,4-bis(((4-methoxyphenyl)sulfonyl)methyl)-2,5-dihydrofuran (**3.5b**): White solid (50 % ethyl acetate in petroleum ether) Yield: (84 mg) 77 %; **^{1}H NMR** (500 MHz, $CDCl_3$) δ 7.78 (d, *J* = 8.8 Hz, 4H), 7.02 (d, *J* = 8.8 Hz, 4H), 4.55 (s, 4H), 3.89 (s, 6H), 3.78 (s, 4H). **^{13}C NMR** (125 MHz, $CDCl_3$) δ 164.4, 130.5, 130.0, 129.4, 114.8, 78.0, 55.9, 53.4. **HRMS** (ESI-TOF) m/z: $[M+Na]^+$ Calcd for $C_{20}H_{22}O_7S_2Na$ 461.0705; Found 461.0721.

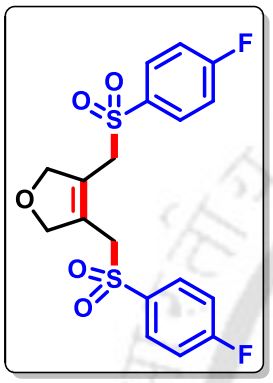

3,4-bis(((4-fluorophenyl)sulfonyl)methyl)-2,5-dihydrofuran (**3.5c**): White solid (50 % ethyl acetate in petroleum ether) Yield: (73 mg) 71 %; **^{1}H NMR** (500 MHz, $CDCl_3$) δ 7.94 – 7.91 (m, 4H), 7.28 (t, *J* = 8.3 Hz, 4H), 4.57 (s, 4H), 3.94 (s, 4H). **^{13}C NMR** (125 MHz, $CDCl_3$) δ 166.3 (d, *J* = 256.6 Hz), 134.7 (d, *J* = 3.1 Hz), 131.2 (d, *J* = 9.6 Hz), 129.4, 117.1 (d, *J* = 22.5 Hz), 78.1, 53.4. **^{19}F NMR** (470 MHz, $CDCl_3$) δ -103.9. **HRMS** (ESI-TOF) m/z: $[M+Na]^+$ Calcd for $C_{18}H_{16}F_2O_5S_2Na$: 437.0305; Found 437.0307.

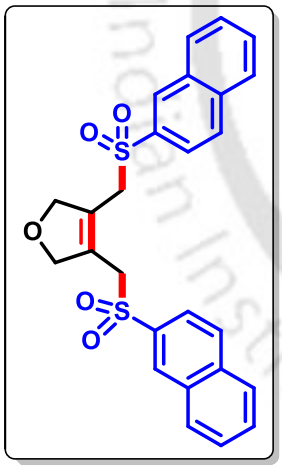

3,4-bis((naphthalen-2-ylsulfonyl)methyl)-2,5-dihydrofuran (**3.5d**): White solid (50 % ethyl acetate in petroleum ether) Yield: (78 mg) 65 %; **^{1}H NMR** (600 MHz, $CDCl_3$) δ 8.45 (s, 2H), 8.03 – 8.00 (m, 4H), 7.95 (d, *J* = 8.2 Hz, 2H), 7.81 (dd, *J* = 8.6, 1.9 Hz, 2H), 7.72 (t, *J* = 7.5 Hz, 2H), 7.67 (t, *J* = 7.8 Hz, 2H), 4.61 (s, 4H), 3.89 (s, 4H). **^{13}C NMR** (150 MHz, $CDCl_3$) δ 135.6, 135.4, 132.2, 130.3, 130.0, 129.9, 129.6, 129.4, 128.23, 128.22, 122.5, 78.1, 53.2. **HRMS** (ESI-TOF) m/z: $[M+Na]^+$ Calcd for $C_{26}H_{22}O_5S_2Na$ 501.0806; Found 501.0793.

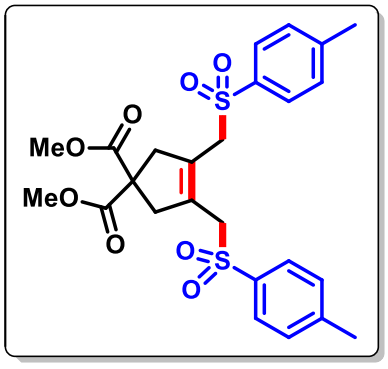

dimethyl 3,4-bis(tosylmethyl)cyclopent-3-ene-1,1-dicarboxylate (**3.5e**): White solid (50 % ethyl acetate in petroleum ether) Yield: (100 mg) 77 %; **^{1}H NMR** (500 MHz, $CDCl_3$) δ 7.58 (d, *J* = 8.2 Hz, 4H), 7.27 (d, *J* = 8.0 Hz, 4H), 3.66 (s, 6H), 3.43 (s, 4H), 2.99 (s, 4H), 2.37 (s, 6H). **^{13}C NMR** (125 MHz, $CDCl_3$) δ 171.6, 145.4, 135.6, 130.3, 130.2, 128.4, 57.1, 55.4, 53.2, 44.2, 21.8. **HRMS** (ESI-TOF) m/z: $[M+Na]^+$ Calcd for $C_{25}H_{28}O_8S_2Na$ 543.1123; Found 543.1131.

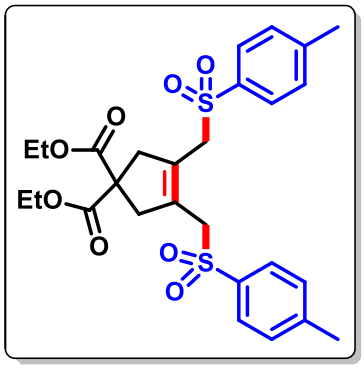

diethyl 3,4-bis(tosylmethyl)cyclopent-3-ene-1,1-dicarboxylate (**3.5f**): White solid (50 % ethyl acetate in petroleum ether) Yield: (93 mg) 68 %; **^{1}H NMR** (500 MHz, $CDCl_3$) δ 7.65 (d, *J* = 8.0 Hz, 4H), 7.34 (d, *J* = 8.0 Hz, 4H), 4.19 (q, *J* = 7.1 Hz, 4H), 3.48 (s, 4H), 3.05 (s, 4H), 2.44 (s, 6H), 1.25 (t, *J* = 7.1 Hz, 6H). **^{13}C NMR** (125 MHz, $CDCl_3$) δ 171.1, 145.4, 135.5, 130.3, 130.1, 128.4, 62.0, 57.1, 55.4, 44.1, 21.8, 14.1. **HRMS** (ESI-TOF) m/z: $[M+Na]^+$ Calcd for $C_{27}H_{32}O_8S_2Na$ 571.1436; Found 571.1449.

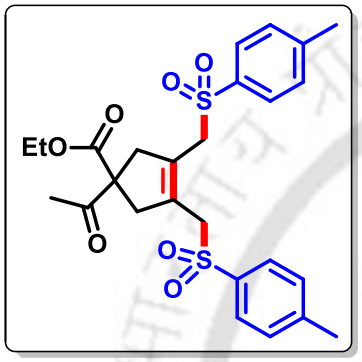

ethyl 1-acetyl-3,4-bis(tosylmethyl)cyclopent-3-enecarboxylate (**3.5g**): White solid (50 % ethyl acetate in petroleum ether) Yield: (79 mg) 61 %; **^{1}H NMR** (400 MHz, CDCl3) δ 7.63 (d, J = 8.3 Hz, 4H), 7.34 (d, J = 7.6 Hz, 4H), 4.20 (q, J = 7.1 Hz, 2H), 3.56 – 3.42 (m, 4H), 2.97 (s, 4H), 2.45 (s, 6H), 2.11 (s, 3H), 1.26 (t, J = 7.1 Hz, 3H). **^{13}C NMR** (125 MHz, $CDCl_3$) δ 201.3, 171.8, 145.4, 135.5, 130.20, 130.15, 128.4, 63.6, 62.1, 55.4, 42.5, 25.8, 21.8, 14.1. **HRMS** (ESI-TOF) m/z: $[M+Na]^+$ Calcd for $C_{26}H_{30}O_7S_2Na$ 541.1331; Found 541.1337.

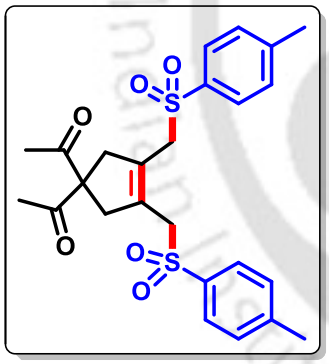

1,1'-(3,4-bis(tosylmethyl)cyclopent-3-ene-1,1-diyl)diethanone (**3.5h**): White solid (50 % ethyl acetate in petroleum ether) Yield: (77 mg) 63 %; **^{1}H NMR** (500 MHz, $CDCl_3$) δ 7.63 (d, *J* = 8.3 Hz, 4H), 7.35 (d, *J* = 8.0 Hz, 4H), 3.56 (s, 4H), 2.96 (s, 4H), 2.44 (s, 6H), 2.06 (s, 6H). **^{13}C NMR** (125 MHz, $CDCl_3$) δ 203.4, 145.5, 135.6, 130.3, 130.2, 128.3, 72.0, 55.5, 41.0, 26.3, 21.8. **HRMS** (ESI-TOF) m/z: $[M+Na]^+$ Calcd for $C_{25}H_{28}O_6S_2Na$ 511.1225; Found 511.1238.

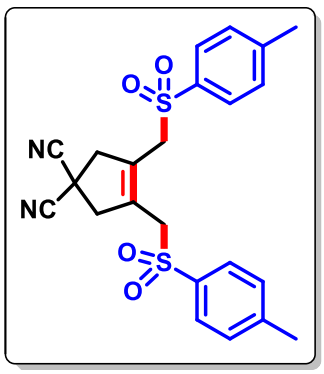

3,4-bis(tosylmethyl)cyclopent-3-ene-1,1-dicarbonitrile (**3.5i**): White solid (50 % ethyl acetate in petroleum ether) Yield: (81 mg) 71 %; **^{1}H NMR** (500 MHz, $CDCl_3$) δ 7.68 (d, *J* = 8.0 Hz, 4H), 7.33 (d, *J* = 8.0 Hz, 4H), 3.66 (s, 4H), 3.16 (s, 4H), 2.40 (s, 6H). **^{13}C NMR** (125 MHz, $CDCl_3$) δ 146.2, 135.3, 130.6, 130.2, 128.3, 115.8, 55.1, 47.9, 30.9, 21.9. **HRMS** (ESI-TOF) m/z: $[M+Na]^+$ Calcd for $C_{23}H_{22}N_2O_4S_2Na$ 477.0919; Found 477.0913.

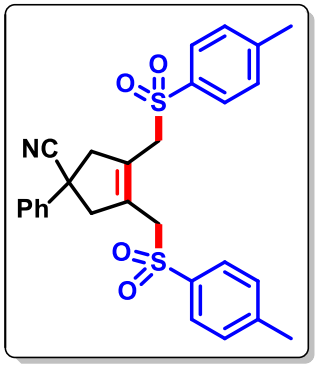

1-phenyl-3,4-bis(tosylmethyl)cyclopent-3-enecarbonitrile (**3.5j**): White solid (50 % ethyl acetate in petroleum ether) Yield: (85 mg) 67 %; **^{1}H NMR** (500 MHz, $CDCl_3$) δ 7.75 (d, *J* = 8.3 Hz, 4H), 7.39 – 7.34 (m, 9H), 3.77 (ABq, *J* = 14.2 Hz, 4H), 3.25 (d, *J* = 14.7 Hz, 2H), 3.06 (d, *J* = 14.9 Hz, 2H), 2.45 (s, 6H). **^{13}C NMR** (125 MHz, $CDCl_3$) δ 145.7, 139.5, 135.7, 130.8, 130.4, 129.2, 128.4, 128.3, 125.7, 123.9, 55.5, 51.0, 44.1, 21.8. **HRMS** (ESI-TOF) m/z: $[M+Na]^+$ Calcd for $C_{28}H_{27}NO_4S_2Na$ 528.1279; Found 528.1280.

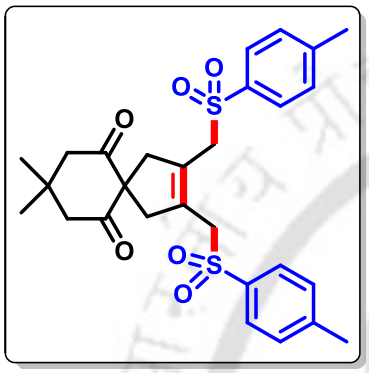

8,8-dimethyl-2,3-bis(tosylmethyl)spiro[4.5]dec-2-ene-6,10-dione (**3.5k**): White solid (50 % ethyl acetate in petroleum ether) Yield: (96 mg) 73 %; **^{1}H NMR** (600 MHz, $CDCl_3$) δ 7.57 (d, *J* = 8.3 Hz, 4H), 7.29 (d, *J* = 8.0 Hz, 4H), 3.33 (s, 4H), 2.80 (s, 4H), 2.51 (s, 4H), 2.38 (s, 6H), 0.89 (s, 6H). **^{13}C NMR** (150 MHz, $CDCl_3$) δ 205.6, 145.5, 135.1, 130.2, 129.8, 128.5, 68.0, 55.4, 51.2, 41.9, 30.5, 28.4, 21.8. **HRMS** (ESI-TOF) m/z: $[M+Na]^+$ Calcd for $C_{28}H_{32}O_6S_2Na$ 551.1538; Found 551.1525.

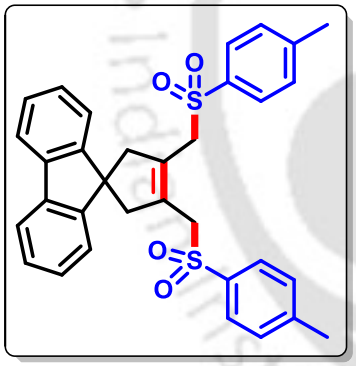

3,4-bis(tosylmethyl)spiro[cyclopent[3]ene-1,9'-fluorene] (**3.5l**): White solid (50 % ethyl acetate in petroleum ether) Yield: (93 mg) 67 %; **^{1}H NMR** (500 MHz, $CDCl_3$) δ 7.85 (d, *J* = 8.0 Hz, 4H), 7.67 (d, *J* = 7.3 Hz, 2H), 7.45 (d, *J* = 7.2 Hz, 2H), 7.39 (d, *J* = 7.9 Hz, 4H), 7.36 – 7.30 (m, 4H), 4.13 (s, 4H), 2.95 (s, 4H), 2.46 (s, 6H). **^{13}C NMR** (125 MHz, $CDCl_3$) δ 152.8, 145.3, 139.4, 136.8, 132.4, 130.2, 128.2, 127.9, 127.5, 122.8, 119.7, 56.4, 53.7, 50.2, 21.8. **HRMS** (ESI-TOF) m/z: $[M+Na]^+$ Calcd for $C_{33}H_{30}O_4S_2Na$ 577.1483; Found 577.1489.

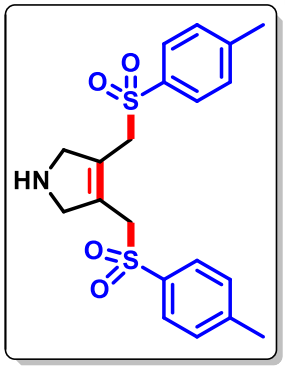

3,4-bis(tosylmethyl)-2,5-dihydro-1H-pyrrole (**3.6**): White solid (50 % ethyl acetate in petroleum ether) Yield: (86 mg) 85 %; **^{1}H NMR** (500 MHz, $CDCl_3$) δ 7.66 (d, *J* = 7.7 Hz, 4H), 7.29 (d, *J* = 7.8 Hz, 4H), 3.71 (s, 4H), 3.65 (s, 4H), 2.38 (s, 6H), 1.87 (s, 1H). **^{13}C NMR** (125 MHz, $CDCl_3$) δ 145.5, 136.0, 131.9, 130.2, 128.3, 57.8, 54.4, 21.8. **HRMS** (ESI-TOF) m/z: $[M+H]^+$ Calcd for $C_{20}H_{24}NO_4S_2$ 406.1142; Found 406.1148.

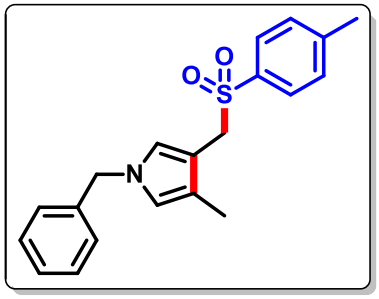

1-benzyl-3-methyl-4-(tosylmethyl)-1H-pyrrole (**3.7a**): White solid (15 % ethyl acetate in petroleum ether) Yield: (54 mg) 63 %; **^{1}H NMR** (600 MHz, $CDCl_3$) δ 7.47 (d, *J* = 8.2 Hz, 2H), 7.25 – 7.23 (m, 3H), 7.11 (d, *J* = 7.9 Hz, 2H), 7.00 (d, *J* = 7.0 Hz, 2H), 6.37 (d, *J* = 2.4 Hz, 1H), 6.27 (s, 1H), 4.82 (s, 2H), 4.07 (s, 2H), 2.32 (s, 3H), 1.66 (s, 3H). **^{13}C NMR** (150 MHz, $CDCl_3$) δ 144.3, 138.0, 135.6, 129.4, 128.9, 128.8, 127.9, 127.2, 122.6, 119.7, 119.6, 109.3, 54.5, 53.5, 21.7, 9.6. **HRMS** (ESI-TOF) m/z: $[M+Na]^+$ Calcd for $C_{20}H_{21}NO_2SNa$ 362.1186; Found 362.1176.

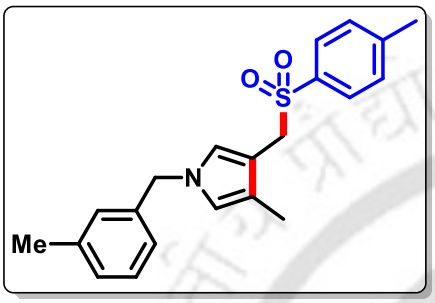

3-methyl-1-(3-methylbenzyl)-4-(tosylmethyl)-1H-pyrrole (**3.7b**): colorless liquid (15 % ethyl acetate in petroleum ether) Yield: (52 mg) 59 %; **^{1}H NMR** (500 MHz, $CDCl_3$) δ 7.55 (d, *J* = 8.2 Hz, 2H), 7.23 – 7.17 (m, 3H), 7.11 (d, *J* = 7.2 Hz, 1H), 6.93 (s, 1H), 6.87 (d, *J* = 7.3 Hz, 1H), 6.47 (d, *J* = 2.4 Hz, 1H), 6.34 (s, 1H), 4.86 (s, 2H), 4.15 (s, 2H), 2.40 (s, 3H), 2.34 (s, 3H), 1.70 (s, 3H). **^{13}C NMR** (125 MHz, $CDCl_3$) δ 144.3, 138.5, 137.9, 135.6, 129.4, 128.9, 128.7, 128.6, 128.0, 124.3, 122.6, 119.6, 119.5, 109.2, 54.5, 53.5, 21.8, 21.5, 9.6. **HRMS** (ESI-TOF) m/z: $[M+Na]^+$ Calcd for $C_{21}H_{23}NO_2SNa$ 376.1347; Found 376.1339.

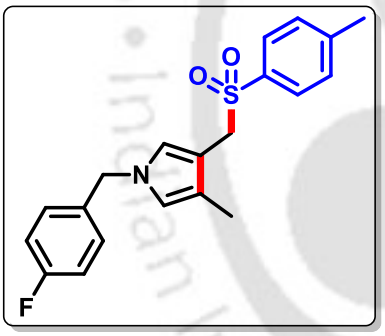

1-(4-fluorobenzyl)-3-methyl-4-(tosylmethyl)-1H-pyrrole (**3.7c**): white solid (15 % ethyl acetate in petroleum ether) Yield: (42 mg) 47 %; **^{1}H NMR** (500 MHz, $CDCl_3$) δ 7.56 (d, *J* = 7.5 Hz, 2H),7.20 (d, *J* = 7.9 Hz, 2H), 7.06 – 6.99 (m, 4H), 6.46 (d, *J* = 2.5 Hz, 1H), 6.33 (s, 1H), 4.88 (s, 2H), 4.15 (s, 2H), 2.41 (s, 3H), 1.72 (s, 3H). **^{13}C NMR** (125 MHz, $CDCl_3$) δ 162.4 (d, *J* = 244.8 Hz), 144.4, 135.7, 133.7 (d, *J* = 3.2 Hz), 129.4, 128.9 (d, *J* = 8.2 Hz), 128.83, 122.5, 119.9, 119.5, 115.7 (d, *J* = 21.4 Hz), 109.5, 54.4, 52.8, 21.8, 9.6. **^{19}F NMR** (470 MHz, $CDCl_3$) δ -114.5. **HRMS** (ESI-TOF) m/z: $[M+Na]^+$ Calcd for $C_{20}H_{20}FNO_2SNa$ 380.1096; Found 380.1084.

3.11 Crystal data:

30 mg of compound **3.3a** was dissolved in 1:1 DCM/MeOH (2 mL) and kept for 2-3 days for crystal growth. The crystal measurement was done in 'Bruker APEX-II CCD'. The ellipsoid contour probability is 50 % for the image of the structure.

SC-XRD data of compound **3.3a**:

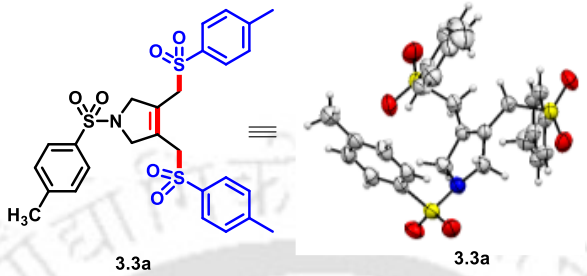

CCDC	2384281
Empirical formula	C27 H29 N O6 S3
Formula weight	559.69
Temperature, T	297(2)
Crystal system	monoclinic
Space group	P 1 21/c 1
Unit cell dimensions	a=10.3155(10) Å α=90° b=15.1561(15) Å β=96.683(3)° c= 17.3400(17)Å γ=90°
Volume, V ($Å^3$)	2692.6(5)
Z	4
Density (calculated), g cm^{-3}	1.381
Absorption coefficient, μ (mm^{-1})	0.318
F (000)	1176
Crystal size, mm^3	0.35 × 0.28 × 0.24
Theta range for data collection	1.790 to 24.735
Index ranges	-12 ≤ h ≤ 12 -17 ≤ k ≤ 17 -20 ≤ l ≤ 20
Reflections collected	4565
Independent reflections	4187
Completeness to theta	0.990
Absorption correction	none
Refinement method	'\f and \w scans'
Data / restraints / parameters	4565/0/337
Goodness-of-fit on F^2	1.064
Final R indices [I>2sigma(I)]	R1 = 0.0405, wR2 = 0.1077
R indices (all data)	R1 = 0.0433, wR2 = 0.1100
Largest diff. peak and hole	0.337 and -0.409 e·$Å^{-3}$

Bond Distances [Å]	Bond angles [°]
S001 O004 1.4342(15)	O004 S001 O007 119.45(9)
S001 O007 1.4356(15)	O004 S001 C00I 108.98(8)
S001 C00I 1.7647(19)	O004 S001 C00M 107.26(9)

S001 C00M 1.7973(18)	O007 S001 C00I 108.11(9)
S002 O005 1.4263(14)	O007 S001 C00M 107.78(9)
S002 O008 1.4241(15)	C00I S001 C00M 104.24(8)
S002 N00A 1.6295(15)	O005 S002 N00A 105.79(9)
S002 C00B 1.7640(19)	O005 S002 C00B 107.47(9)
S003 O006 1.4338(15)	O008 S002 O005 120.67(9)
S003 O009 1.4333(15)	O008 S002 N00A 106.54(8)
S003 C00N 1.757(2)	O008 S002 C00B 108.50(9)
S003 C00T 1.7975(19)	N00A S002 C00B 107.17(8)
N00A C00J 1.477(2)	O006 S003 C00N 107.91(9)
N00A C00K 1.476(2)	O006 S003 C00T 108.93(9)
C00B C00E 1.385(3)	O009 S003 O006 119.15(9)
C00B C00F 1.388(3)	O009 S003 C00N 110.02(10)
C00C C00D 1.332(2)	O009 S003 C00T 106.74(9)
C00C C00J 1.500(3)	C00N S003 C00T 102.88(8)
C00C C00M 1.497(2)	C00J N00A S002 120.73(12)
C00D C00K 1.490(2)	C00K N00A S002 117.88(12)
C00D C00T 1.491(2)	C00K N00A C00J 110.57(14)
C00E H00E 0.9300	C00E C00B S002 120.05(14)
C00E C00O 1.373(3)	C00E C00B C00F 120.12(18)
C00F H00F 0.9300	C00F C00B S002 119.78(14)
C00F C00H 1.375(3)	C00D C00C C00J 111.26(15)
C00G H00G 0.9300	C00D C00C C00M 126.85(17)
C00G C00I 1.387(3)	C00M C00C C00J 121.89(15)
C00G C00Q 1.377(3)	C00C C00D C00K 111.68(16)
C00H H00H 0.9300	C00C C00D C00T 128.19(16)
C00H C00L 1.382(3)	C00K C00D C00T 120.08(15)
C00I C00U 1.379(3)	C00B C00E H00E 120.4
C00J H00A 0.9700	C00O C00E C00B 119.18(17)
C00J H00B 0.9700	C00O C00E H00E 120.4
C00K H00C 0.9700	C00B C00F H00F 120.3
C00K H00D 0.9700	C00H C00F C00B 119.42(18)
C00L C00O 1.387(3)	C00H C00F H00F 120.3
C00L C00Y 1.516(3)	C00I C00G H00G 120.4
C00M H00I 0.9700	C00Q C00G H00G 120.4
C00M H00J 0.9700	C00Q C00G C00I 119.29(17)
C00N C00R 1.384(3)	C00F C00H H00H 119.3
C00N C00V 1.386(3)	C00F C00H C00L 121.46(17)
C00O H00O 0.9300	C00L C00H H00H 119.3
C00P C00Q 1.388(3)	C00G C00I S001 120.27(14)
C00P C00S 1.391(3)	C00U C00I S001 119.37(14)
C00P C00Z 1.497(3)	C00U C00I C00G 120.35(18)
C00Q H00Q 0.9300	N00A C00J C00C 103.06(14)
C00R H00R 0.9300	N00A C00J H00A 111.2
C00R C00W 1.377(3)	N00A C00J H00B 111.2
C00S H00S 0.9300	C00C C00J H00A 111.2
C00S C00U 1.382(3)	C00C C00J H00B 111.2
C00T H00K 0.9700	H00A C00J H00B 109.1
C00T H00L 0.9700	N00A C00K C00D 103.34(14)
C00U H00U 0.9300	N00A C00K H00C 111.1

C00V H00V 0.9300	N00A C00K H00D 111.1
C00V C00X 1.366(4)	C00D C00K H00C 111.1
C00W H00W 0.9300	C00D C00K H00D 111.1
C00W C010 1.393(3)	H00C C00K H00D 109.1
C00X H00X 0.9300	C00H C00L C00O 117.96(18)
C00X C010 1.387(4)	C00H C00L C00Y 120.46(18)
C00Y H00M 0.9600	C00O C00L C00Y 121.58(19)
C00Y H00N 0.9600	S001 C00M H00I 109.1
C00Y H00P 0.9600	S001 C00M H00J 109.1
C00Z H00T 0.9600	C00C C00M S001 112.67(12)
C00Z H00Y 0.9600	C00C C00M H00I 109.1
C00Z H 0.9600	C00C C00M H00J 109.1
C010 C011 1.507(4)	H00I C00M H00J 107.8
C011 H01A 0.9600	C00R C00N S003 119.48(15)
C011 H01B 0.9600	C00R C00N C00V 120.9(2)
C011 H01C 0.9600	C00V C00N S003 119.33(16)
	C00E C00O C00L 121.80(18)
	C00E C00O H00O 119.1
	C00L C00O H00O 119.1
	C00Q C00P C00S 117.71(18)
	C00Q C00P C00Z 121.19(19)
	C00S C00P C00Z 121.09(18)
	C00G C00Q C00P 121.74(17)
	C00G C00Q H00Q 119.1
	C00P C00Q H00Q 119.1
	C00N C00R H00R 120.3
	C00W C00R C00N 119.5(2)
	C00W C00R H00R 120.3
	C00P C00S H00S 119.3
	C00U C00S C00P 121.44(18)
	C00U C00S H00S 119.3
	S003 C00T H00K 109.3
	S003 C00T H00L 109.3
	C00D C00T S003 111.42(12)
	C00D C00T H00K 109.3
	C00D C00T H00L 109.3
	H00K C00T H00L 108.0
	C00I C00U C00S 119.47(18)
	C00I C00U H00U 120.3
	C00S C00U H00U 120.3
	C00N C00V H00V 120.6
	C00X C00V C00N 118.8(2)
	C00X C00V H00V 120.6
	C00R C00W H00W 119.8
	C00R C00W C010 120.4(2)
	C010 C00W H00W 119.8
	C00V C00X H00X 119.1
	C00V C00X C010 121.7(2)
	C010 C00X H00X 119.1
	C00L C00Y H00M 109.5

	C00L C00Y H00N 109.5 C00L C00Y H00P 109.5 H00M C00Y H00N 109.5 H00M C00Y H00P 109.5 H00N C00Y H00P 109.5 C00P C00Z H00T 109.5 C00P C00Z H00Y 109.5 C00P C00Z H 109.5 H00T C00Z H00Y 109.5 H00T C00Z H 109.5 H00Y C00Z H 109.5 C00W C010 C011 119.7(3) C00X C010 C00W 118.7(2) C00X C010 C011 121.6(3) C010 C011 H01A 109.5 C010 C011 H01B 109.5 C010 C011 H01C 109.5 H01A C011 H01B 109.5 H01A C011 H01C 109.5 H01B C011 H01C 109.5

30 mg of compound **3.4a** was dissolved in 1:1 DCM/MeOH (2 mL) and kept for 2-3 days for crystal growth. The crystal measurement was done in 'Bruker APEX-II CCD'. The ellipsoid contour probability is 50 % for the image of the structure.

SC-XRD data of compound **3.4a**:

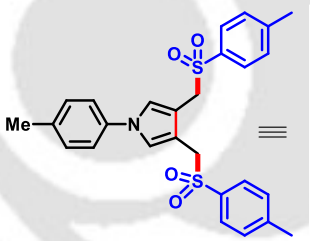

3.4a

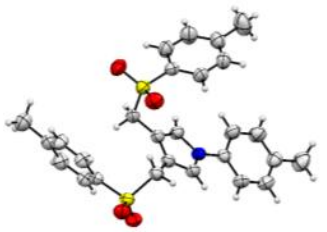

3.4a

CCDC	2384280
Empirical formula	C27 H27 N O4 S2
Formula weight	493.61
Temperature, T	300(2)
Crystal system	orthorhombic
Space group	P b c a
Unit cell dimensions	a=13.5414(6)Å α=90° b=11.9690(5)Å β=90° c=31.2008(12)Å γ=90°
Volume, V ($Å^3$)	5056.9(4)
Z	8
Density (calculated), g cm^{-3}	1.297
Absorption coefficient, μ (mm^{-1})	0.244
F (000)	2080
Crystal size, mm^3	0.35 × 0.28 × 0.24

Theta range for data collection	2.363 to 25.000
Index ranges	-16 ≤ h ≤ 16 -14 ≤ k ≤ 14 -36 ≤ l ≤ 37
Reflections collected	4425
Independent reflections	3729
Completeness to theta	0.993
Absorption correction	none
Refinement method	'\f and \w scans'
Data / restraints / parameters	4425/0/311
Goodness-of-fit on F^2	1.114
Final R indices [I>2sigma(I)]	R1 = 0.0382, wR2 = 0.0971
R indices (all data)	R1 = 0.0491, wR2 = 0.1135
Largest diff. peak and hole	0.236 and -0.303 e·Å^{-3}

Bond Distances [Å]	Bond angles [°]
S001 O004 1.4328(15)	O004 S001 O003 118.06(9)
S001 O003 1.4418(15)	O004 S001 C00C 109.44(10)
S001 C00C 1.760(2)	O003 S001 C00C 107.71(9)
S001 C00F 1.794(2)	O004 S001 C00F 109.20(10)
S002 O005 1.4363(17)	O003 S001 C00F 106.41(9)
S002 O007 1.4380(16)	C00C S001 C00F 105.24(9)
S002 C00G 1.762(2)	O005 S002 O007 118.25(11)
S002 C00D 1.793(2)	O005 S002 C00G 108.56(10)
N006 C009 1.373(2)	O007 S002 C00G 108.88(10)
N006 C00E 1.373(2)	O005 S002 C00D 108.86(10)
N006 C008 1.425(3)	O007 S002 C00D 107.82(11)
C008 C00P 1.379(3)	C00G S002 C00D 103.48(10)
C008 C00L 1.384(3)	C009 N006 C00E 107.95(17)
C009 C00B 1.359(3)	C009 N006 C008 125.71(16)
C00A C00E 1.362(3)	C00E N006 C008 126.13(16)
C00A C00B 1.432(3)	C00P C008 C00L 118.9(2)
C00A C00D 1.493(3)	C00P C008 N006 120.48(17)
C00B C00F 1.491(3)	C00L C008 N006 120.66(18)
C00C C00H 1.379(3)	C00B C009 N006 109.31(17)
C00C C00K 1.385(3)	C00E C00A C00B 106.97(17)
C00G C00I 1.373(3)	C00E C00A C00D 123.96(18)
C00G C00T 1.376(3)	C00B C00A C00D 128.80(19)
C00H C00M 1.382(3)	C009 C00B C00A 106.75(18)
C00I C00S 1.382(3)	C009 C00B C00F 123.30(18)
C00J C00M 1.380(3)	C00A C00B C00F 129.89(19)
C00J C00R 1.386(3)	C00H C00C C00K 120.26(19)
C00J C00W 1.512(3)	C00H C00C S001 120.40(16)
C00K C00R 1.375(3)	C00K C00C S001 119.31(16)
C00L C00Q 1.375(3)	C00A C00D S002 112.18(14)
C00N C00O 1.380(3)	C00A C00E N006 109.02(17)
C00N C00Q 1.385(3)	C00B C00F S001 115.57(14)
C00N C00X 1.508(3)	C00I C00G C00T 120.2(2)
C00O C00P 1.380(3)	C00I C00G S002 120.01(16)
C00S C00U 1.380(3)	C00T C00G S002 119.75(16)

C00T C00V 1.378(3) C00U C00V 1.378(3) C00U C00Y 1.511(3)	C00C C00H C00M 119.28(19) C00G C00I C00S 119.6(2) C00M C00J C00R 118.0(2) C00M C00J C00W 121.4(2) C00R C00J C00W 120.7(2) C00R C00K C00C 119.3(2) C00Q C00L C008 120.1(2) C00J C00M C00H 121.5(2) C00O C00N C00Q 116.6(2) C00O C00N C00X 120.9(2) C00Q C00N C00X 122.4(2) C00N C00O C00P 122.3(2) C008 C00P C00O 119.9(2) C00L C00Q C00N 122.1(2) C00K C00R C00J 121.6(2) C00U C00S C00I 121.1(2) C00G C00T C00V 119.4(2) C00V C00U C00S 118.1(2) C00V C00U C00Y 121.2(2) C00S C00U C00Y 120.6(2) C00U C00V C00T 121.5(2)

30 mg of compound **3.5e** was dissolved in 1:1 DCM/MeOH (2 mL) and kept for 2-3 days for crystal growth. The crystal measurement was done in 'Bruker APEX-II CCD'. The ellipsoid contour probability is 50 % for the image of the structure.

SC-XRD data of compound **3.5e**:

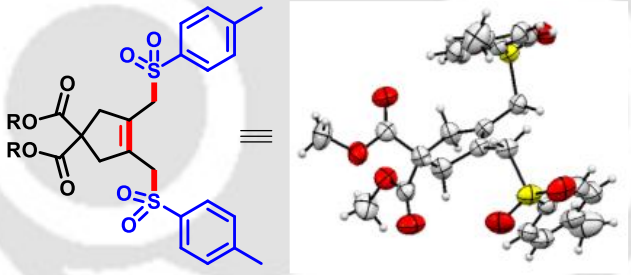

3.5e ≡ **3.5e**

CCDC	2384277
Empirical formula	C25 H28 O8 S2
Formula weight	520.59
Temperature, T	295(2)
Crystal system	triclinic
Space group	P -1
Unit cell dimensions	a=13.883(3)Å α=92.312(6)° b=14.569(3)Å β=102.411(6)° c=14.922(3)Å γ=117.750(5)°
Volume, V ($Å^3$)	2573.9(10)
Z	4
Density (calculated), g cm^{-3}	1.343
Absorption coefficient, μ (mm^{-1})	0.253
F (000)	1096
Crystal size, mm^3	0.35 × 0.28 × 0.24

Theta range for data collection	1.686 to 25.022
Index ranges	-16 ≤ h ≤ 16 -17 ≤ k ≤ 17 -17 ≤ l ≤ 17
Reflections collected	8978
Independent reflections	7277
Completeness to theta	0.993
Absorption correction	none
Refinement method	'\f and \w scans'
Data / restraints / parameters	8978/0/639
Goodness-of-fit on F^2	1.031
Final R indices [I>2sigma(I)]	R1 = 0.0444, wR2 = 0.1069
R indices (all data)	R1 = 0.0585, wR2 = 0.1225
Largest diff. peak and hole	0.442 and -0.455 e·Å^{-3}

Bond Distances [Å]	Bond angles [°]
S1 O5 1.4253(19)	O5 S1 O6 119.07(12)
S1 O6 1.4375(18)	O5 S1 C10 109.13(11)
S1 C10 1.785(2)	O5 S1 C11 108.48(11)
S1 C11 1.758(2)	O6 S1 C10 106.58(11)
O1 C6 1.187(3)	O6 S1 C11 108.27(11)
C1 C2 1.550(3)	C11 S1 C10 104.34(10)
C1 C5 1.547(3)	C5 C1 C2 104.95(17)
C1 C6 1.521(3)	C6 C1 C2 110.09(18)
C1 C8 1.517(3)	C6 C1 C5 110.86(19)
S2 O7 1.4291(17)	C8 C1 C2 109.16(18)
S2 O8 1.4413(17)	C8 C1 C5 114.68(19)
S2 C18 1.792(2)	C8 C1 C6 107.08(18)
S2 C19 1.758(2)	O7 S2 O8 119.06(11)
O2 C6 1.316(3)	O7 S2 C18 108.43(10)
O2 C7 1.455(3)	O7 S2 C19 109.08(11)
C2 H2A 0.9700	O8 S2 C18 106.77(10)
C2 H2B 0.9700	O8 S2 C19 108.62(11)
C2 C3 1.502(3)	C19 S2 C18 103.80(10)
O3 C8 1.168(3)	C6 O2 C7 116.5(2)
C3 C4 1.333(3)	C1 C2 H2A 111.0
C3 C18 1.493(3)	C1 C2 H2B 111.0
S3 O14 1.439(2)	H2A C2 H2B 109.0
S3 O13 1.440(2)	C3 C2 C1 104.02(16)
S3 C35 1.792(2)	C3 C2 H2A 111.0
S3 C36 1.756(2)	C3 C2 H2B 111.0
O4 C8 1.279(3)	C4 C3 C2 111.56(18)
O4 C9 1.456(3)	C4 C3 C18 126.80(19)
S4 O15 1.4387(17)	C18 C3 C2 121.59(17)
S4 O16 1.4319(17)	O14 S3 O13 118.94(13)
S4 C43 1.793(2)	O14 S3 C35 107.21(12)
S4 C44 1.762(2)	O14 S3 C36 108.93(13)
C4 C5 1.498(3)	O13 S3 C35 108.41(12)
C4 C10 1.493(3)	O13 S3 C36 108.72(12)
C5 H5A 0.9700	C36 S3 C35 103.56(10)

C5 H5B 0.9700	C8 O4 C9 118.5(3)
C7 H7A 0.9600	O15 S4 C43 108.62(11)
C7 H7B 0.9600	O15 S4 C44 108.66(10)
C7 H7C 0.9600	O16 S4 O15 118.41(11)
C24 H24 0.9300	O16 S4 C43 107.49(11)
C24 C23 1.381(4)	O16 S4 C44 109.01(10)
C24 C19 1.390(3)	C44 S4 C43 103.65(10)
C23 H23 0.9300	C3 C4 C5 112.40(18)
C23 C22 1.387(4)	C3 C4 C10 127.35(19)
C22 C21 1.378(4)	C10 C4 C5 120.14(18)
C22 C25 1.517(4)	C1 C5 H5A 111.0
O9 C31 1.193(3)	C1 C5 H5B 111.0
C9 H9A 0.9600	C4 C5 C1 103.98(17)
C9 H9B 0.9600	C4 C5 H5A 111.0
C9 H9C 0.9600	C4 C5 H5B 111.0
C21 H21 0.9300	H5A C5 H5B 109.0
C21 C20 1.385(3)	O1 C6 C1 125.3(2)
C20 H20 0.9300	O1 C6 O2 123.2(2)
C20 C19 1.380(3)	O2 C6 C1 111.5(2)
C18 H18A 0.9700	O2 C7 H7A 109.5
C18 H18B 0.9700	O2 C7 H7B 109.5
C10 H10A 0.9700	O2 C7 H7C 109.5
C10 H10B 0.9700	H7A C7 H7B 109.5
O10 C31 1.329(3)	H7A C7 H7C 109.5
O10 C32 1.443(3)	H7B C7 H7C 109.5
C11 C12 1.393(3)	C23 C24 H24 120.5
C11 C16 1.379(3)	C23 C24 C19 119.0(2)
O11 C33 1.195(3)	C19 C24 H24 120.5
C12 H12 0.9300	C24 C23 H23 119.4
C12 C13 1.380(4)	C24 C23 C22 121.2(2)
O12 C33 1.323(3)	C22 C23 H23 119.4
O12 C34 1.441(3)	C23 C22 C25 121.4(3)
C13 H13 0.9300	C21 C22 C23 118.6(2)
C13 C14 1.384(4)	C21 C22 C25 120.0(3)
C14 C15 1.392(4)	O3 C8 C1 122.9(2)
C14 C17 1.511(4)	O3 C8 O4 123.0(2)
C15 H15 0.9300	O4 C8 C1 113.8(2)
C15 C16 1.374(4)	O4 C9 H9A 109.5
C17 H17A 0.9600	O4 C9 H9B 109.5
C17 H17B 0.9600	O4 C9 H9C 109.5
C17 H17C 0.9600	H9A C9 H9B 109.5
C16 H16 0.9300	H9A C9 H9C 109.5
C27 H27A 0.9700	H9B C9 H9C 109.5
C27 H27B 0.9700	C22 C21 H21 119.2
C27 C28 1.552(3)	C22 C21 C20 121.5(2)
C27 C26 1.499(3)	C20 C21 H21 119.2
C28 C29 1.555(3)	C21 C20 H20 120.5
C28 C31 1.513(3)	C19 C20 C21 119.0(2)
C28 C33 1.517(3)	C19 C20 H20 120.5
C29 H29A 0.9700	S2 C18 H18A 108.9

C29 H29B 0.9700	S2 C18 H18B 108.9
C29 C30 1.502(3)	C3 C18 S2 113.28(15)
C30 C35 1.492(3)	C3 C18 H18A 108.9
C30 C26 1.336(3)	C3 C18 H18B 108.9
C32 H32A 0.9600	H18A C18 H18B 107.7
C32 H32B 0.9600	S1 C10 H10A 109.1
C32 H32C 0.9600	S1 C10 H10B 109.1
C34 H34A 0.9600	C4 C10 S1 112.31(14)
C34 H34B 0.9600	C4 C10 H10A 109.1
C34 H34C 0.9600	C4 C10 H10B 109.1
C35 H35A 0.9700	H10A C10 H10B 107.9
C35 H35B 0.9700	C31 O10 C32 118.0(2)
C36 C37 1.369(3)	C12 C11 S1 120.43(19)
C36 C41 1.385(4)	C16 C11 S1 119.25(19)
C37 H37 0.9300	C16 C11 C12 120.3(2)
C37 C38 1.382(4)	C11 C12 H12 120.4
C38 H38 0.9300	C13 C12 C11 119.2(2)
C38 C39 1.372(4)	C13 C12 H12 120.4
C39 C40 1.367(4)	C33 O12 C34 117.7(2)
C39 C42 1.518(4)	C12 C13 H13 119.3
C40 H40 0.9300	C12 C13 C14 121.3(3)
C40 C41 1.380(4)	C14 C13 H13 119.3
C41 H41 0.9300	C13 C14 C15 118.2(3)
C42 H42A 0.9600	C13 C14 C17 121.2(3)
C42 H42B 0.9600	C15 C14 C17 120.6(3)
C42 H42C 0.9600	C14 C15 H15 119.4
C43 H43A 0.9700	C16 C15 C14 121.3(3)
C43 H43B 0.9700	C16 C15 H15 119.4
C43 C26 1.493(3)	C14 C17 H17A 109.5
C44 C45 1.383(3)	C14 C17 H17B 109.5
C44 C49 1.383(3)	C14 C17 H17C 109.5
C45 H45 0.9300	H17A C17 H17B 109.5
C45 C46 1.379(3)	H17A C17 H17C 109.5
C46 H46 0.9300	H17B C17 H17C 109.5
C46 C47 1.380(3)	C24 C19 S2 119.76(17)
C47 C48 1.384(3)	C20 C19 S2 119.54(17)
C47 C50 1.516(3)	C20 C19 C24 120.7(2)
C48 H48 0.9300	C11 C16 H16 120.2
C48 C49 1.382(3)	C15 C16 C11 119.6(3)
C49 H49 0.9300	C15 C16 H16 120.2
C50 H50A 0.9600	H27A C27 H27B 108.8
C50 H50B 0.9600	C28 C27 H27A 110.8
C50 H50C 0.9600	C28 C27 H27B 110.8
C25 H25A 0.9600	C26 C27 H27A 110.8
C25 H25B 0.9600	C26 C27 H27B 110.8
C25 H25C 0.9600	C26 C27 C28 104.89(16)
	C27 C28 C29 105.23(17)
	C31 C28 C27 110.49(18)
	C31 C28 C29 112.87(19)
	C31 C28 C33 107.69(18)

	C33 C28 C27 111.58(19) C33 C28 C29 109.02(18) C28 C29 H29A 110.8 C28 C29 H29B 110.8 H29A C29 H29B 108.9 C30 C29 C28 104.70(17) C30 C29 H29A 110.8 C30 C29 H29B 110.8 C35 C30 C29 121.18(18) C26 C30 C29 112.13(18) C26 C30 C35 126.7(2) O9 C31 O10 124.2(2) O9 C31 C28 126.4(2) O10 C31 C28 109.4(2) O10 C32 H32A 109.5 O10 C32 H32B 109.5 O10 C32 H32C 109.5 H32A C32 H32B 109.5 H32A C32 H32C 109.5 H32B C32 H32C 109.5 O11 C33 O12 124.3(2) O11 C33 C28 125.4(2) O12 C33 C28 110.28(19) O12 C34 H34A 109.5 O12 C34 H34B 109.5 O12 C34 H34C 109.5 H34A C34 H34B 109.5 H34A C34 H34C 109.5 H34B C34 H34C 109.5 S3 C35 H35A 108.8 S3 C35 H35B 108.8 C30 C35 S3 113.59(16) C30 C35 H35A 108.8 C30 C35 H35B 108.8 H35A C35 H35B 107.7 C37 C36 S3 120.82(19) C37 C36 C41 120.0(2) C41 C36 S3 119.07(19) C36 C37 H37 120.3 C36 C37 C38 119.3(2) C38 C37 H37 120.3 C37 C38 H38 119.3 C39 C38 C37 121.4(3) C39 C38 H38 119.3 C38 C39 C42 121.1(3) C40 C39 C38 118.5(3) C40 C39 C42 120.4(3) C39 C40 H40 119.3 C39 C40 C41 121.3(3) C41 C40 H40 119.3

	C36 C41 H41 120.3 C40 C41 C36 119.4(2) C40 C41 H41 120.3 C39 C42 H42A 109.5 C39 C42 H42B 109.5 C39 C42 H42C 109.5 H42A C42 H42B 109.5 H42A C42 H42C 109.5 H42B C42 H42C 109.5 S4 C43 H43A 109.0 S4 C43 H43B 109.0 H43A C43 H43B 107.8 C26 C43 S4 113.07(14) C26 C43 H43A 109.0 C26 C43 H43B 109.0 C45 C44 S4 119.75(16) C49 C44 S4 119.31(16) C49 C44 C45 120.9(2) C44 C45 H45 120.5 C46 C45 C44 119.0(2) C46 C45 H45 120.5 C45 C46 H46 119.3 C45 C46 C47 121.3(2) C47 C46 H46 119.3 C46 C47 C48 118.7(2) C46 C47 C50 121.3(2) C48 C47 C50 120.1(2) C47 C48 H48 119.4 C49 C48 C47 121.2(2) C49 C48 H48 119.4 C44 C49 H49 120.5 C48 C49 C44 118.9(2) C48 C49 H49 120.5 C47 C50 H50A 109.5 C47 C50 H50B 109.5 C47 C50 H50C 109.5 H50A C50 H50B 109.5 H50A C50 H50C 109.5 H50B C50 H50C 109.5 C30 C26 C27 112.24(18) C30 C26 C43 127.32(19) C43 C26 C27 120.43(17) C22 C25 H25A 109.5 C22 C25 H25B 109.5 C22 C25 H25C 109.5 H25A C25 H25B 109.5 H25A C25 H25C 109.5 H25B C25 H25C 109.5

3.12 References:

1. (a) Fan, H.; Peng, J.; Hamann, M. T.; Hu, J.-F. Lamellarins and Related Pyrrole-Derived Alkaloids from Marine Organisms. *Chem. Rev.* **2008**, *108*, 264−287. (b) Boto, A.; Álvarez, L. Heterocy-cles inNatural Products Synthesis; Majumdar, K. C., Chattopadh-yay, S. K.,Eds.; Wiley-VCH: Weinheim, **2011**; pp 99−152. (c) Sharipov B. T.; Davydova A. N.; Valeev F. A. Synthesis of C(3)–C(8) eleutheside blocks from levoglucosenone. *Chem. Heterocycl. Compd.* **2020**, *56*, 982–989.

2. (a) Harrak, Y.; Casula, G.; Basset, J.; Rosell, G.; Plescia, S.; Raffa, D.; Cusimano, M. G.; Pouplana, R.; Pujol, M. D. Synthesis, Anti-Inflammatory Activity, and in Vitro Antitumor Effect of a Novel Class of Cyclooxygenase Inhibitors: 4-(Aryloyl)Phenyl Me-thyl Sulfones. *J. Med. Chem.* **2010**, *53*, 6560–6571. (b) Liu, K. G.; Robichaud, A. J.; Bernotas, R. C.; Yan, Y.; Lo, J. R.; Zhang, M.-Y.; Hughes, Z. A.; Huselton, C.; Zhang, G. M.; Zhang, J. Y.; Kowal, D. M.; Smith, D. L.; Schechter, L. E.; Comery, T. A. 5-Piperazinyl-3-Sulfonylindazoles as Potent and Selective 5-Hydroxytryptamine-6 Antagonists. *J. Med. Chem.* **2010**, *53*, 7639–7646. (c) Noshi, M. N.; El-awa, A.; Torres, E.; Fuchs, P. L. Conversion of Cyclic Vinyl Sul-fones to Transposed Vinyl Phosphonates. *J. Am. Chem. Soc*. **2007**, *129*, 11242–11247. (d) Aziz, J.; Messaoudi, S.; Alami, M.; Hamze, A. Sulfinate Derivatives: Dual and Versatile Partners in Organic Synthesis. *Org. Biomol. Chem.* **2014**, *12*, 9743–9759. (e) Emmett, E. J.; Willis, M. C. The Development and Application of Sulfur Dioxide Surrogates in Synthetic Organic Chemistry. *Asian J. Org. Chem.* **2015**, *4*, 602–611. (f) Frankel, B. A.; Bentley, M.; Kruger, R. G.; McCafferty, D. G. Vinyl Sulfones: Inhibitors of SrtA, a Transpeptidase Required for Cell Wall Protein Anchoring and Viru-lence in Staphylococcus Aureus. *J. Am. Chem. Soc*. **2004**, *126*, 3404–3405. (g) Chen, Y.; Guo, H.; Cai, M.; Geng, C.; Yue, C.; Teng, C. Effect of Polyether Sulfone Resin on Micromorphology, Thermal, Mechanical, and Dielectric Properties of Epoxy–Bismaleimide Composite Material, *J. Electron. Mater.* **2018**, *47*, 6021–6027.

3. (a) Emmett, E. J.; Hayter, B. R.; Willis, M. C. Palladium-Catalyzed Synthesis of Ammonium Sulfinates from Aryl Halides and a Sulfur Dioxide Surrogate: A Gas- and Reductant-Free Pro-cess. *Angew. Chem., Int. Ed.* **2014**, *53*, 10204–10208. (b) Richards-Taylor, C. S.; Blakemore, D. C.; Willis, M. C. One-Pot Three-Component Sulfone Synthesis Exploiting Palladium-Catalysed Aryl Halide Aminosulfonylation. *Chem. Sci.* **2014**, *5*, 222–228. (c) Mitchell, G.; Bartlett, D. W.; Fraser, T. E.; Hawkes, T. R.; Holt, D. C.; Townson, J. K.; Wichert, R. A. Mesotrione: A New Selective Herbicide for Use in Maize. *Pest. Manag. Sci.* **2001**, *57*, 120–128. d) Böger, P. Mode of Action for Chloroacetamides and Functionally Related Compounds. *J. Pestic. Sci.* **2003**, *28*, 324–329. e) Tfelt-Hansen, P.; De Vries, P.; Saxena, P. R. Triptans in

Migraine. *Drugs* **2000**, *60,* 1259−1287. (f) Bachi, M. D.; Korshin, E. E.; Hoos, R.; Szpilman, A. M.; Ploypradith, P.; Xie, S.; Shapiro, T. A.; Posner, G. H. A Short Synthesis and Biological Evaluation of Potent and Nontoxic Antimalarial Bridged Bicyclic β-Sulfonyl-Endoperoxides. *J. Med. Chem.* **2003**, *46*, 2516–2533.

4. (a) Organic Chemistry of Sulfur; Oae, S.,Ed.; Plenum Press: New York, **1977**. (b) Shigeru, O.; Tadashi, O.Organic Sulfur Chemistry: Bio-chemical Aspects; CRC Press: Boca Raton,FL, **1992**.

5. (a) Ueda, M.; Uchiyama, K.; Kano,T. A new synthesis of diaryl sulfones. *Synthesis* **1984**, *1984*, 323−325. (b) Graybill, B. M. Synthesis of aryl sulfones. *J. Org. Chem.* **1967**, *32*, 2931−2933.

6. (a) Chen, C.; Su, J.; Tong, X. Rhodium-Catalyzed Carbo-cyclization and Chlorosulfonylation of 1,6-Enynes with Sulfonyl Chlorides, *Chem.–Eur. J.* **2013**, *19*, 5014–5018. (b) Herrera, F.; Esteban, P.; Luna, A.;Almendros, P. Metal-Catalyzed Reactivity Reversal in the Sulfonyla-tion Reaction of α-Allenols: Controlled Synthesis of 4-(Arylsulfonyl)-2,5-Dihydrofurans. *Adv. Synth. Catal.* **2021**, *363*, 3952−3956. (c) Dong, W.; Fang, Z. Y.; Cao, T. Y.; Cao, J. H.; Zhao,Z. Q.; Zhang, L.; Li, W.; Qi, L.; Wang, L. J. Copper-CatalyzedIminosulfonylation of O-Homoallyl Benzimidates with SodiumSulfinates to Access Sulfonylated 1,3-Oxazines. *Org. Lett.* **2021**, *23*, 5809−5814. (d) Wu, W.; Yi, S.; Huang, W.; Luo, D.; Jiang, H. Ag-Catalyzed Oxidative Cyclization Reaction of 1,6-Enynes and Sodium Sulfinate: Access to Sulfonylated Benzofurans. *Org. Lett*. **2017**, *19*, 2825−2828. (e) Zhou, K.; Zhang, J.; Qiu, G.; Wu, J. Cop-per (II)-Catalyzed Reaction of 2,3-Allenoic Acids, Sulfur Dioxide, and Aryldiazonium Tetrafluoroborates: Route to 4-Sulfonylated Furan-2(5H)-ones. *Org. Lett.* **2019**, *21*, 275−278.

7. (a) Yang, Y.; Li, W.; Xia, C.; Ying, B.; Shen, C.; Zhang, P. Catalyst-Controlled Selectivity in C−S Bond Formation: Highly Efficient Synthesis of C2- and C3-Sulfonylindoles. *ChemCatChem* **2016**, *8*, 304−307. (b) Wu, Z.; Song, H.; Cui, X.; Pi, C.; Du, W.; Wu, Y. Sufonylation of Quinoline N-Oxides with Aryl Sulfonyl Chlo-rides via Copper-Catalyzed C−H Bonds Activation. *Org. Lett.* **2013**, *15*, 1270−1273. (c) Du, B.; Qian, P.; Wang, Y.; Mei, H.; Han, J.; Pan, Y. Cu-Catalyzed Deoxygenative C2-Sulfonylation Reaction of Quinoline N-Oxides with Sodium Sulfinate. *Org. Lett.* **2016**, *18*, 4144−4147. (d) Friedrich, M.; Schulz, L.; Hofman, K.; Zangl, R.; Morgner, N.; Shaaban, S.; Manolikakes, G. Direct C−H-sulfonylation of 6-membered nitrogen-heteroaromatics. *Tetrahedron Chem*. **2022**, *1*, 100003. (e) Xiao, F.; Chen, H.; Xie, H.; Chen, S.; Yang, L.; Deng, G.-J. Iodine-Catalyzed Regioselective 2-Sulfonylation of Indoles with Sodium Sulfinates. *Org. Lett*. **2014**, *16*, 50–53.

8. (a) Zhang, L.; Chen, S.; Gao, Y.; Zhang, P.; Wu, Y.; Tang, G.; Zhao, Y. tert-Butyl hydroperoxide mediated cascade synthesis of 3-arylsulfonylquinolines. *Org. Lett.* **2016**, *18*, 1286−1289. (b) Zheng, L.; Zhou, Z.-Z.; He, Y.-T.; Li, L.-H.; Ma, J.-W.; Qiu, Y.-F.; Zhou, P.-X.; Liu, X.-Y.; Xu, P.-F.; Liang, Y.-M. Iodine-Promoted radical cyclization in water: A selective reaction of 1,6-enynes with sulfonyl hydrazides. *J. Org. Chem*. **2016**, *81*, 66−76. (c) Yu, X. C.; Zheng, Y.-N.; Zhang, J. H.; Zhang, J.; Liu, F. L.; Tang, K. Q.; Li, T.; Wei, W.-T. Metal-Catalyst-Free Radical Cyclization of 1,6-Enynes for the Selective and Switchable Synthesis of Lactams in Water. *ACS Sustain. Chem. Eng.* **2022**, *10*, 6057−6062. (d) Wang, X.; You, F.; Xiong, B.; Chen, L.; Zhang, X.; Lian, Z. Metal and base-free tandem sulfonylation/cyclization of 1,5-dienes with aryldiazonium salts via the insertion of sulfur dioxide. *RSC Adv.* **2022**, *12*, 16745−16750. (e) Yang, R.; Yi, D.; Shen, K.; Fu, Q.; Wei, J.; Lu, J.; Yang, L.; Wang, L.; Wei, S.; Zhang, Z. Indole and Pyrrole Deriva-tives as Pre-photocatalysts and Substrates in the Sulfonyl Radical-Triggered Relay Cyclization Leading to Sulfonylated Heterocycles. *Org. Lett*. **2022**, *24*, 2014−2019.

9. (a) Hou, H.; Li, H.; Xu, Y.; Song, C.; Wang, C.; Shi, Y.; Han, Y.;Yan, C.; Zhu, S. Visible-Light-Mediated Chlorosulfonyla-tive Cyclizations of 1,6-Enynes. *Adv. Synth. Catal.* **2018**, *360*, 4325−4329. (b) Meng, X.-X.; Kang, Q.-Q.; Zhang, J.-Y.; Li, Q.; Wei, W. T.; He, W. M. Visible-light-initiated Regioselective Sulfonylation/Cyclization of 1,6-Enynes under Photocatalyst- and Additive-free Conditions. *Green Chem.* **2020**, *22*, 1388−1392. (c) Zhu, S.; Pathigoolla, A.; Lowe, G.; Walsh, D. A.; Cooper, M.; Lewis, W.; Lam, H. W. Sulfonylative and Azidosulfonylative Cyclizations by Visible-Light-Photosensitization of Sulfonyl Azides in THF. *Chem. Eur. J.* **2017**, *23*, 17598. (d) Chen, F.; Huang, X.; Yang, C.; Jiang, H.; Zeng, W. Photocatalyzed Coupling−Cyclization of ortho-AlkynylarylVinylethers with Arylsulfonyl Azides. *J. Org. Chem.* **2021**, *86*, 14572−14585. (e) Cheng, Q.; Zhang, F.; Chen, X.; Han, Y.; Yan, C.; Shi, Y.; Hou, H.; Zhu, S. Visible-Light-Mediated Three-Component Radical Iodosulfonylative Cyclization of Enynes. *Org. Lett.* **2022**, *24*, 2515–2519.

10. Reddy Mutra, M.; Chen, Y.; Wang, J. Photoinduced Radical Cyclization of 1,6-Diynes: Rapid Access to Highly Substituted Carbocyclic and Heterocyclic Compounds. *Adv. Synth. Catal.* **2023**, *365*, 1012–1019.

11. F. Martinelli, A. Palmieri and M. Petrini, Regioselective Synthesis of 3-Substituted Pyrroles by Nucleophilic Addition of 3-(1-Arylsulfonylalkyl) Pyrroles Activated under Basic or Acid Conditions, *Chem.–Eur. J.* **2011,** *17*, 7183-7187.

12. Muralirajan, K.; Kancherla, R.; Rueping, M. Dehydrogenative Aromatization and Sulfonylation of Pyrrolidines: Orthogonal Reactivity in Photoredox Catalysis. *Angew. Chem., Int. Ed.* **2018**, *57*, 14787−14791.

13. Muralirajan, K.; Kancherla,R.; Maity, B.; Karuthedath, S.; Laquai, F.; Cavallo, L.; Rueping, M. Mechanistic insights into excit-ed-state palladium catalysis for C–S bond formations and dehydro-genative sulfonylation of amines. *Nat. Commun.* **2023**, *14*, 6622.

14. (a) Sahoo, M. K.; Midya, S. P.; Landge, V. G.; Balaraman, E. A.Unified Strategy for Silver-, Base-, And Oxidant-Free Direct Arylation of C-H Bonds. *Green Chem.* **2017**, *19*, 2111−2117. (b) Midya, S. P.; Rana, J.; Abraham, T.; Aswin, B.; Balaraman, E.Metal-Free Radical Trifluoromethylation of β-Nitroalkenes through Visible-Light Photoredox Catalysis. *Chem. Commun.* **2017**, *53*, 6760−6763.

15. (a) Alvarez-Montoya, A.; Gillions, J. P.; Winfrey, L.; Hawker, R.R.; Singh, K.; Ortu, F.; Fu, Y.; Li, Y.; Pulis, A. P. $B(C_6F_5)_3$-Catalyzed Dehydrogenation of Pyrrolidines to Form Pyr-roles. *ACS Catal.* **2024**, *14*, 4856−4864. (b) Scalacci, N.; Black, G. W.; Mattedi, G.; Brown, N. L.; Turner, N.J.; Castagnolo, D. Unveiling the Biocatalytic Aromatizing Activity of Monoamine Oxidases MAO-N and 6-HDNO: Development of Chemoenzymatic Cascades for the Synthesis of Pyrroles. *ACS Catal.* **2017**, *7*, 1295–1300. (c) An, X.-D.; Yang, S.; Qiu, B.; Yang, T.-T.; Li,X.-J.; Xiao, J. Photore-dox-Enabled Synthesis of β-Substituted Pyrroles from Pyrrolidines. *J. Org. Chem.* **2020**, *85*, 9558-9565. (d) Tong, J.; Li, H.; Zhu, Y.; Liu, P.; Sun, P. Visible-light-induced dehydrogenative sulfonylation of tertiary amines under transition-metal and photocatalyst-free conditions. *Green Chem*. **2022**, *24*, 1995–1999.

16. Liu, N.-W.; Liang, S.; Manolikakes, G. Recent Advances in the Synthesis of Sulfones. *Synthesis* **2016**, *48*, 1939−1973.

17. (a) Wu, W.; Yi, S.; Yu, Y.; Huang, W.; Jiang, H. Synthesis of Sulfonylated Lactones via Ag-Catalyzed Cascade Sulfonylation/Cyclization of 1,6-Enynes with Sodium Sulfinates. *J. Org. Chem.* **2017**, *82*, 1224–1230. (b) Ramaiah, M. Radical Reactions in Organic Synthesis. *Tetrahedron* **1987**, *43*, 3541–3676. (c) Cad-dick, S.; Shering, C. L.; Wadman, S. N. Synthesis of P-Tolylsulfonyl-Substituted Dienes via Radical Cyclization of Diynes. *Chem. Commun.* **1997**, *2*, 171–172.

18. Xie, L. Y.; Fang, T.-G.; Tan, J. X.; Zhang, B.; Cao, Z.; Yang, L. H.; He, W. M. Visible-Light-Induced Deoxygenative C2-Sulfonylation of Quinoline N-oxides with Sulfinic Acids. *Green Chem*. **2019**, *21*, 3858−3863.

19. Vila, J.; Vinardell, R.; Solà, M.; Pla- Quintana, A.; Roglans, A. A Rh(I)-Catalyzed Cascade Cyclization of 1,5-Bisallenes and Alkynes for the Formation of cis-3,4-Arylvinyl Pyrrolidines and Cyclopentanes. *Adv. Synth. Catal.* **2022**, **364**, 206–217.

20. Mohy El Dine, T.; Jimmidi, R.; Diaconu, A.; Fransolet, M.; Michiels, C.; De Winter, J.; Gillon, E.; Imberty, A.; Coenye, T.; Vincent, S. P. Pillar[5]arene-Based Polycationic Glyco[2]rotaxanes Designed as Pseudomonas aeruginosa Antibiofilm Agents. *J. Med. Chem.* **2021**, *64*, 14728–14744.

21. Tran-Van, A.-F.; Huxol, E.; Basler, J. M.; Neuburger, M.; Adjizian, J.-J.; Ewels, C. P.; Wegner, H. A. Synthesis of substituted [8] cycloparaphenylenes by [2+ 2+ 2] cycloaddition. *Org. Lett.* **2014**, *16*, 1594–1597.

22. Shi, Y.; Gevorgyan, V. Intramolecular transannulation of alkynyl triazoles via alkyne–carbene metathesis step: access to fused pyrroles. *Org. Lett.* **2013**, *15*, 5394–5396.

23. Meyer, A. U.; Jäger, S.; Prasad Hari, D.; König, B. Visible Light-Mediated Metal-Free Synthesis of Vinyl Sulfones from Aryl Sulfinates. *Adv. Synth. Catal.* **2015**, *357*, 2050–2054.

3.13 Selected NMR spectra:

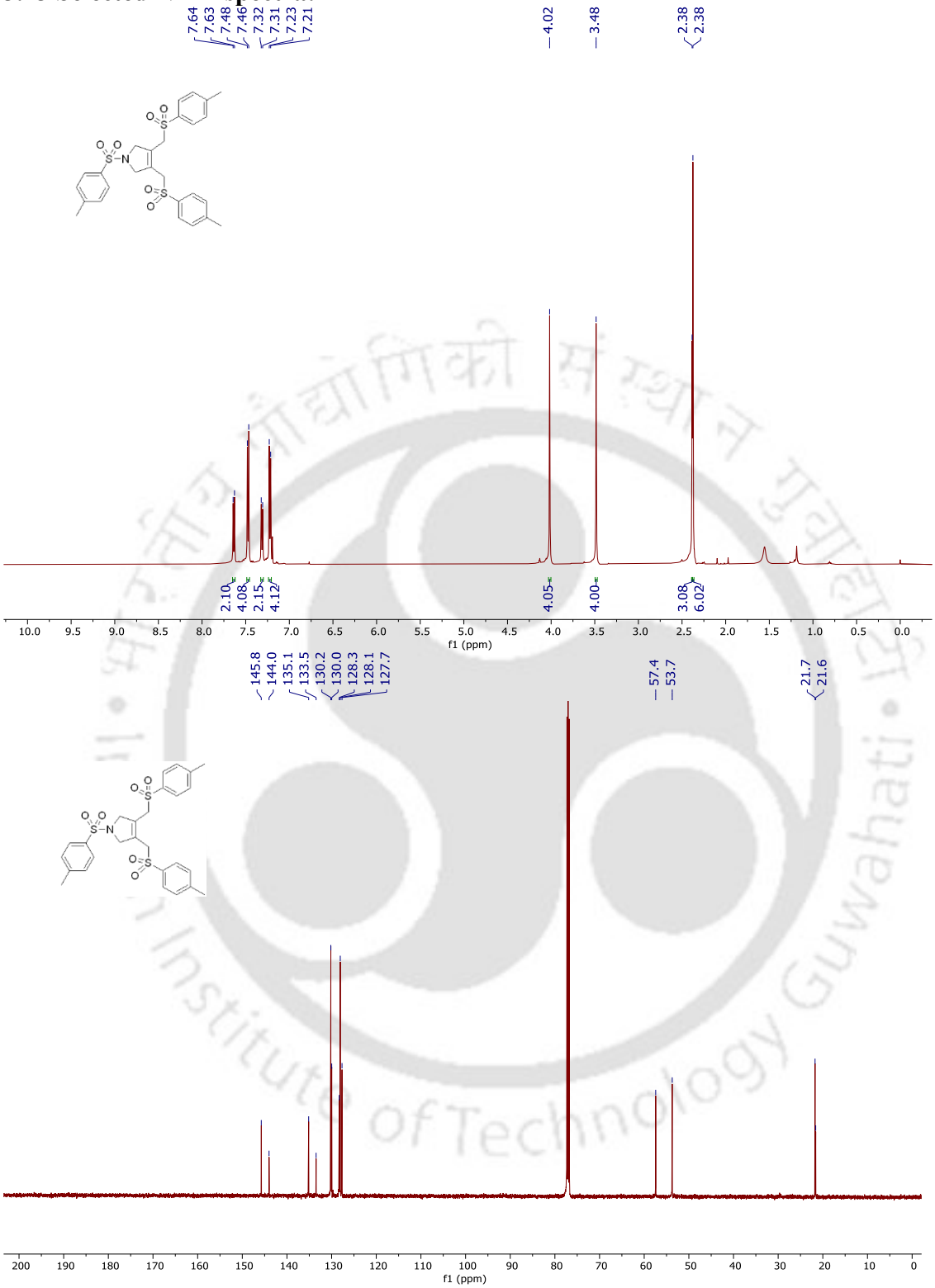

Figure 3.11: ^{1}H NMR (500 MHz) and $^{13}C\{^{1}H\}$ NMR (125 MHz) spectrum of Compound **3.3a** in $CDCl_3$

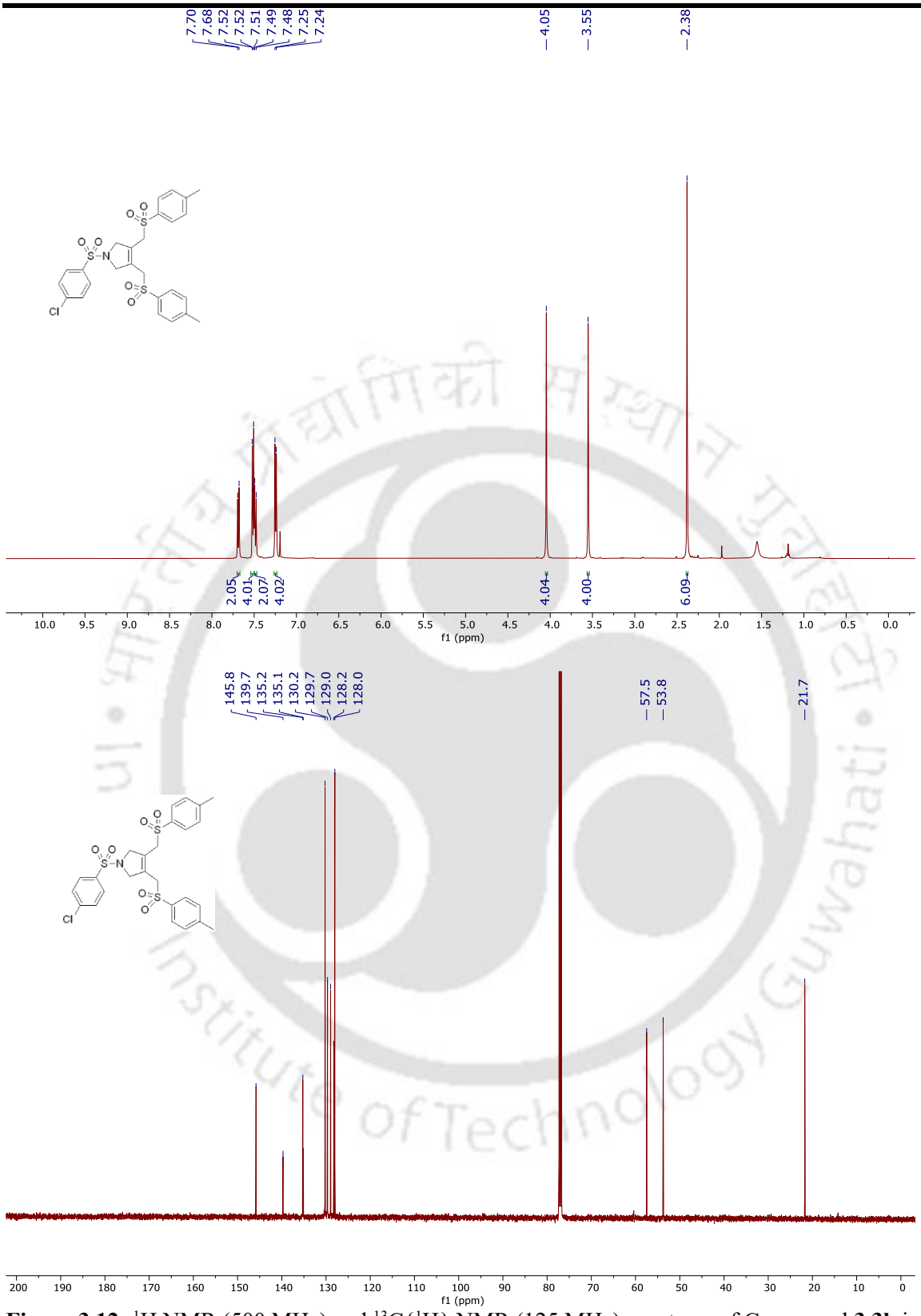

Figure 3.12: ^{1}H NMR (500 MHz) and $^{13}C\{^{1}H\}$ NMR (125 MHz) spectrum of Compound **3.3b** in $CDCl_3$

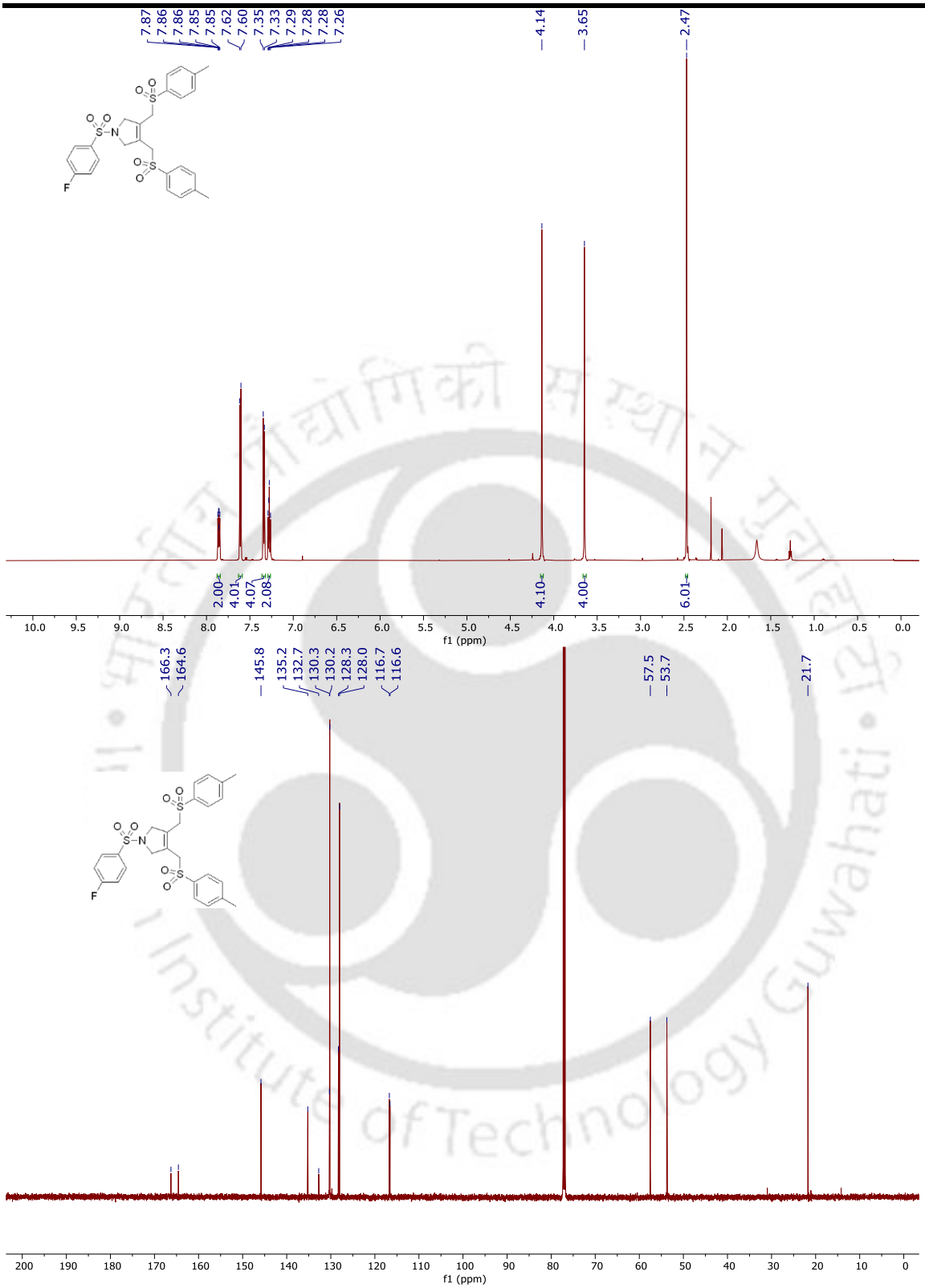

Figure 3.13: ^{1}H NMR (600 MHz) and $^{13}C\{^{1}H\}$ NMR (150 MHz) spectrum of Compound **3.3c** in $CDCl_3$

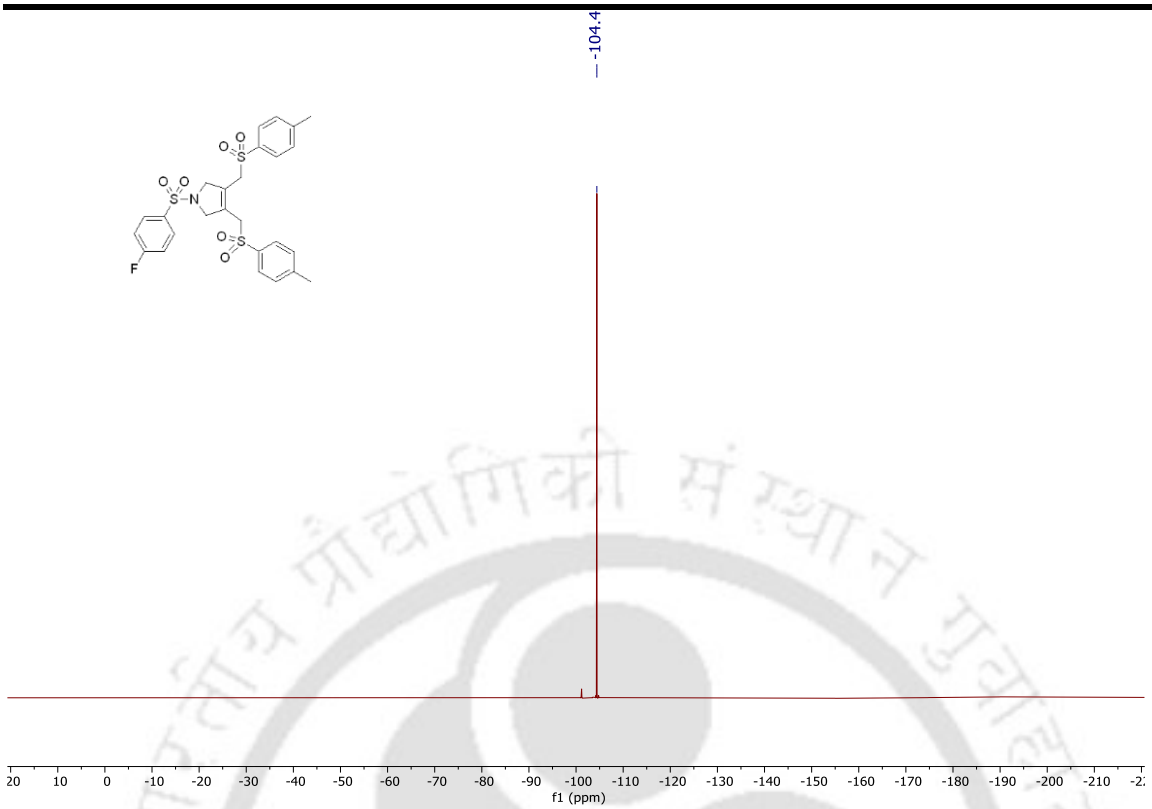

Figure 3.14: $^{19}F\{^{1}H\}$ NMR (470 MHz) spectrum of Compound **3.3c** in $CDCl_3$

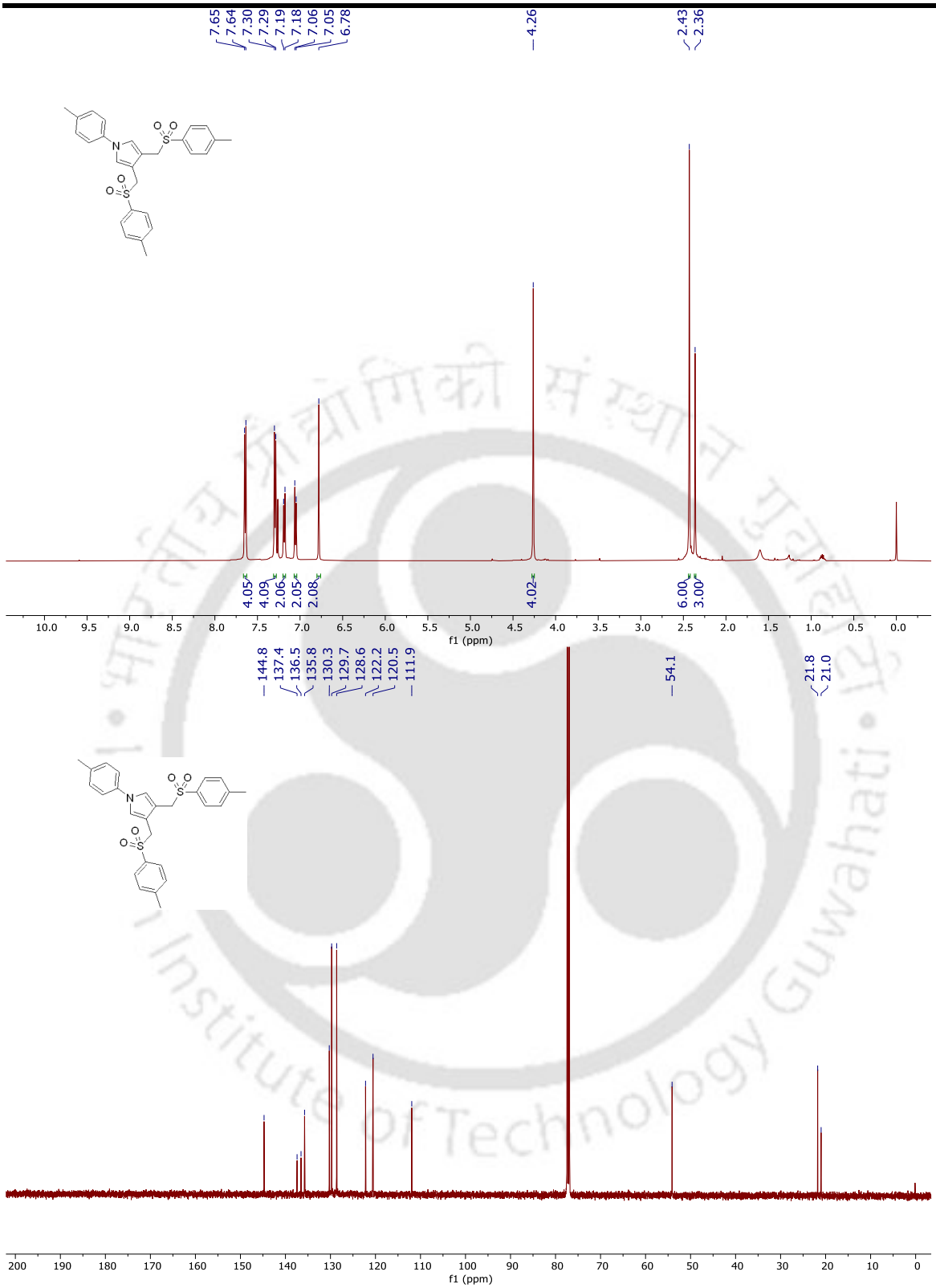

Figure 3.15: ^{1}H NMR (500 MHz) and $^{13}C\{^{1}H\}$ NMR (125 MHz) spectrum of Compound **3.4a** in $CDCl_3$

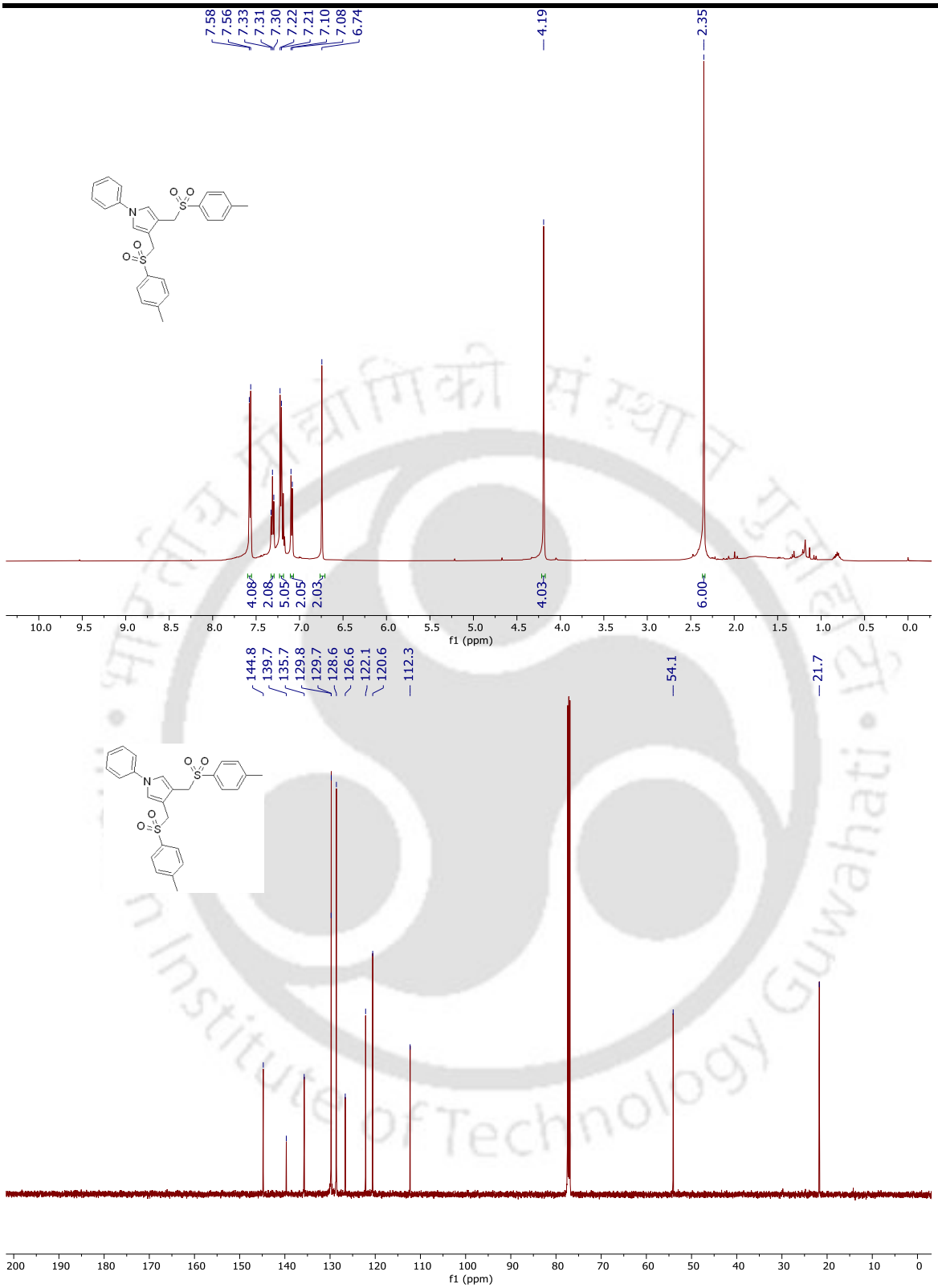

Figure 3.16: ^{1}H NMR (500 MHz) and $^{13}C\{^{1}H\}$ NMR (125 MHz) spectrum of Compound **3.4b** in $CDCl_3$

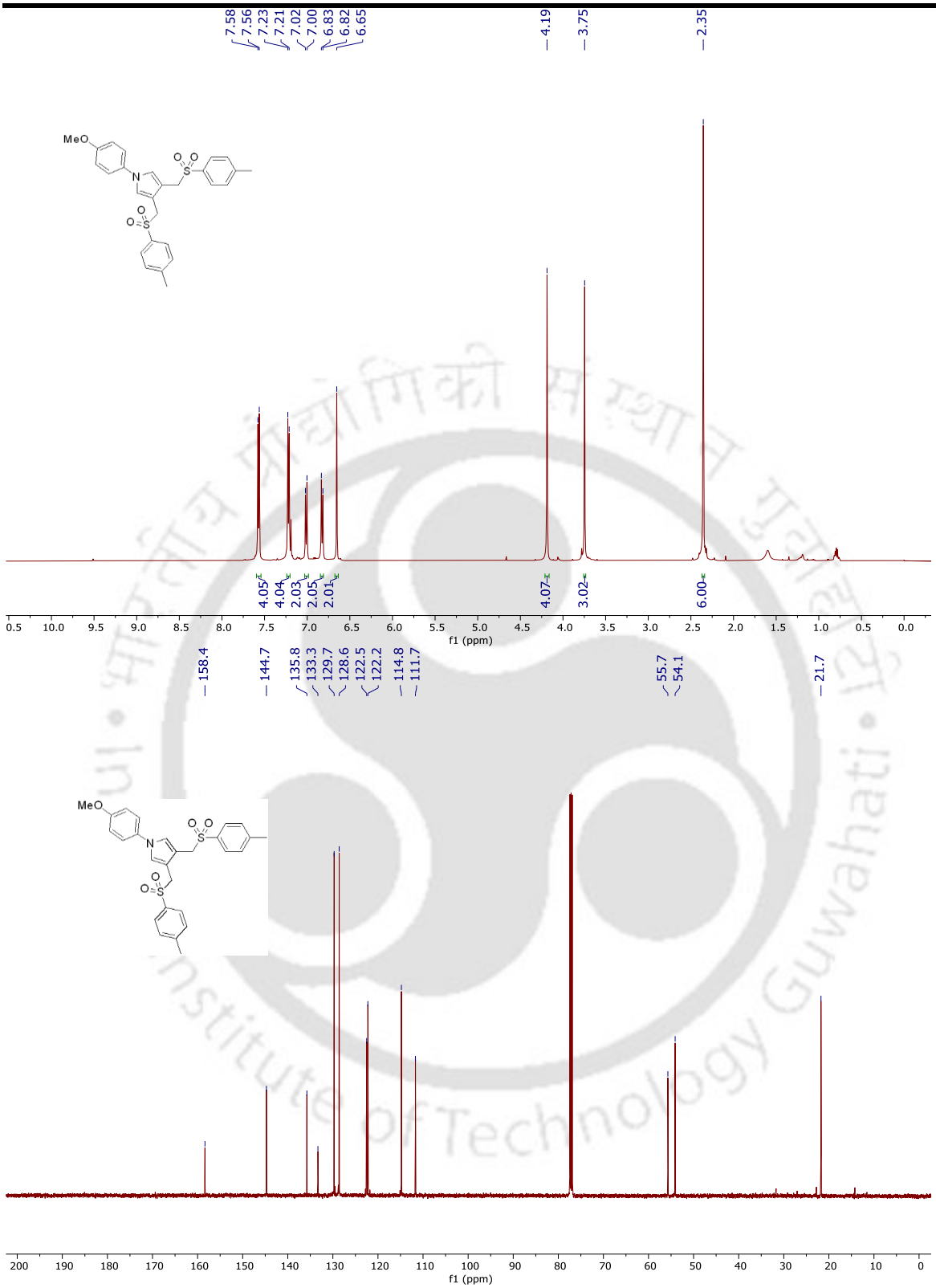

Figure 3.17: ^{1}H NMR (500 MHz) and $^{13}C\{^{1}H\}$ NMR (125 MHz) spectrum of Compound **3.4c** in $CDCl_3$

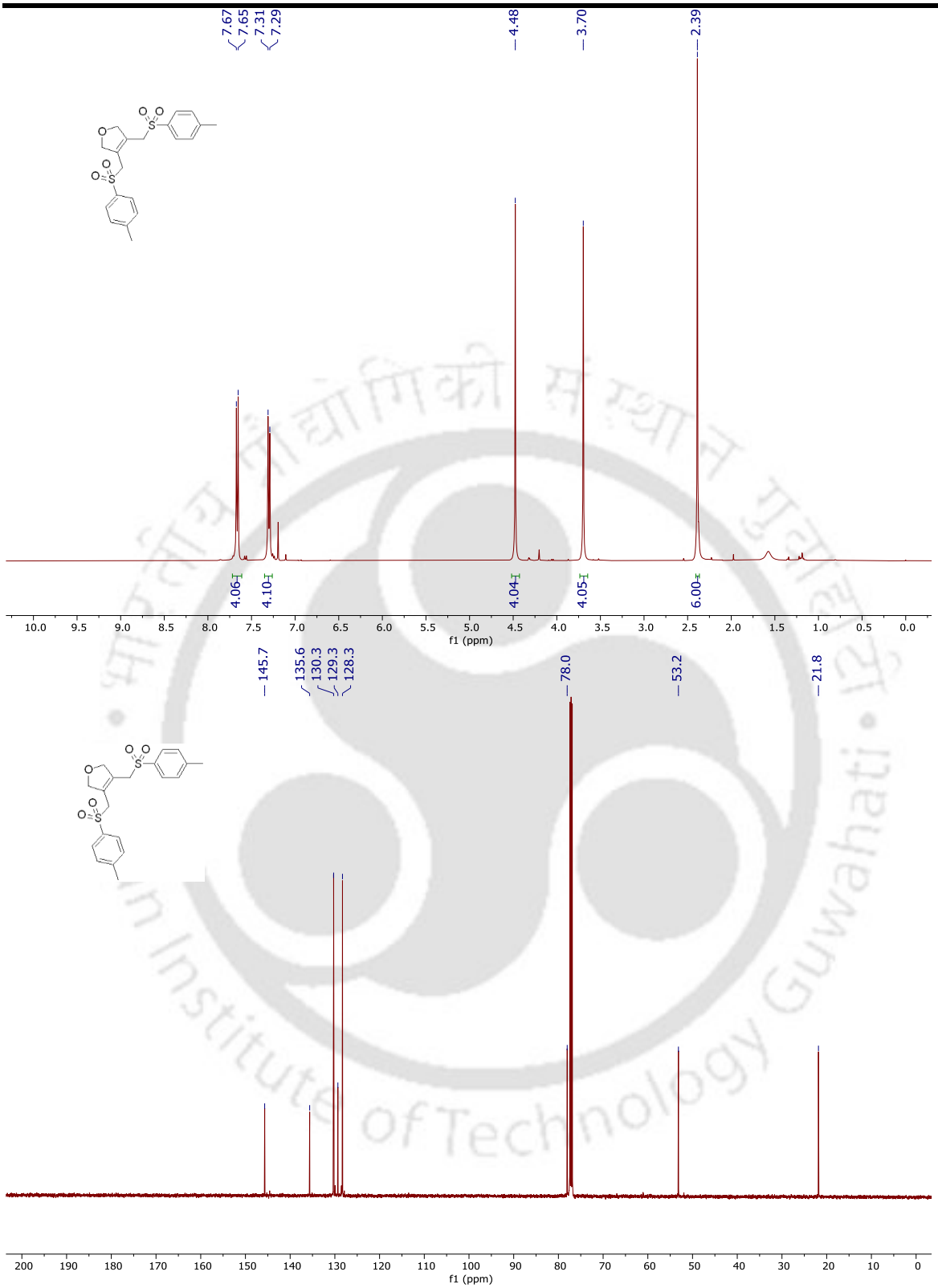

Figure 3.18: ^{1}H NMR (400 MHz) and $^{13}C\{^{1}H\}$ NMR (125 MHz) spectrum of Compound **3.5a** in $CDCl_3$

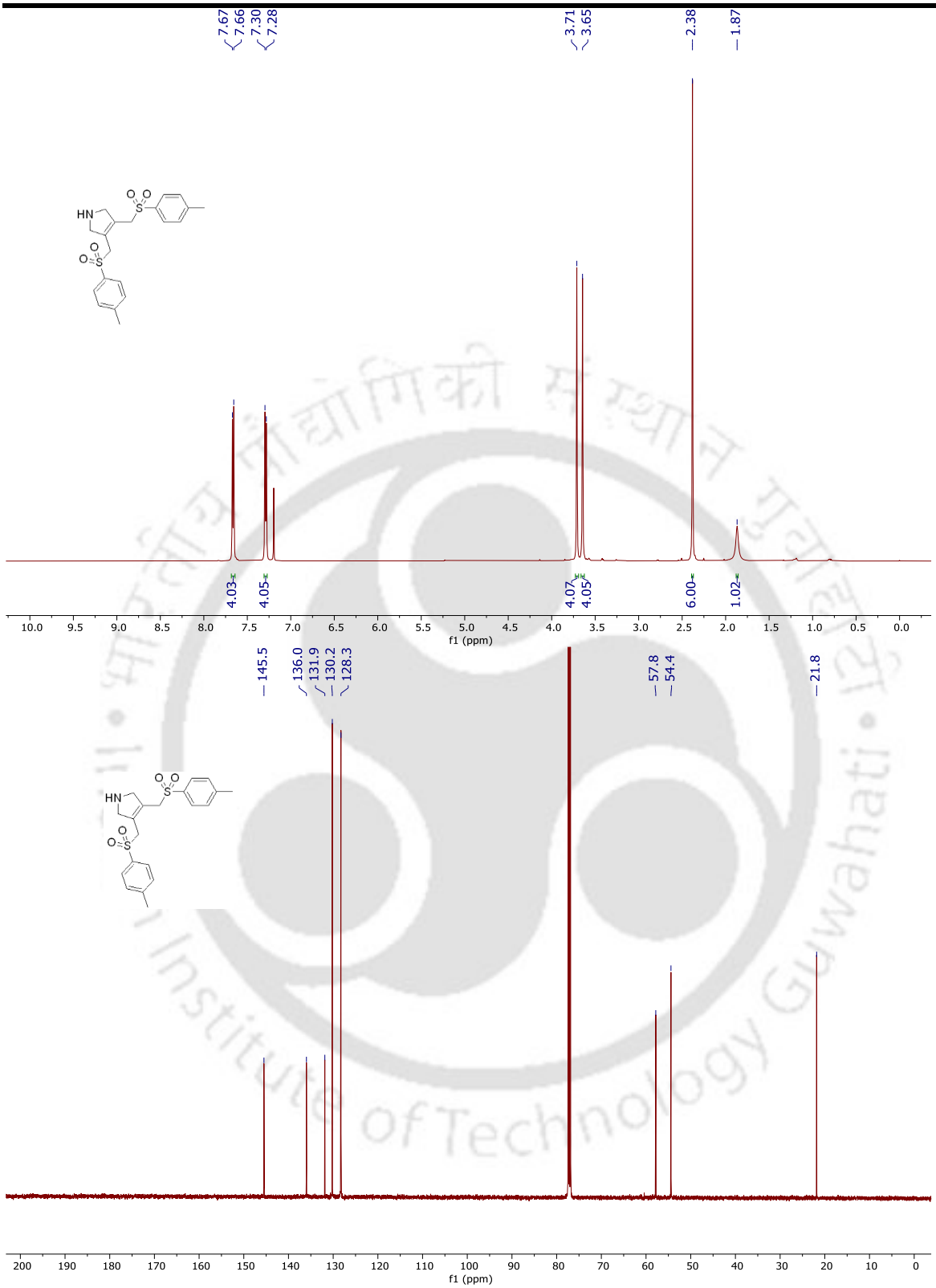

Figure 3.19: ^{1}H NMR (500 MHz) and $^{13}C\{^{1}H\}$ NMR (125 MHz) spectrum of Compound **3.6** in $CDCl_3$

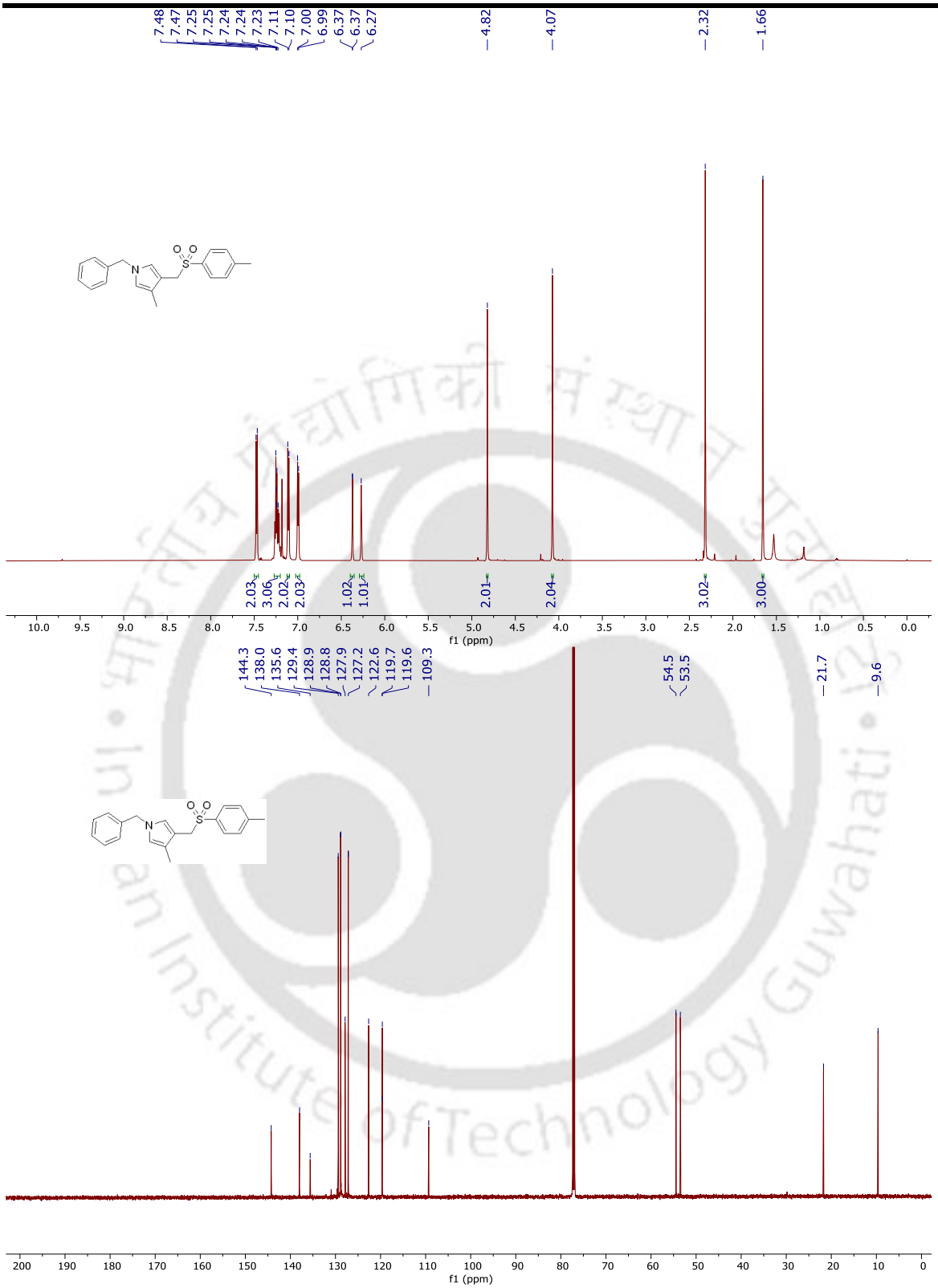

Figure 3.20: ^{1}H NMR (600 MHz) and $^{13}C\{^{1}H\}$ NMR (150 MHz) spectrum of Compound **3.7a** in $CDCl_3$

Chapter IV:

Visible-Light Mediated Divergent Synthesis of Sulfonylated Dihydropyrrole-3-Carboxaldehydes and Tricyclic Sulfones via Sulfonyl Radical Source Modulation

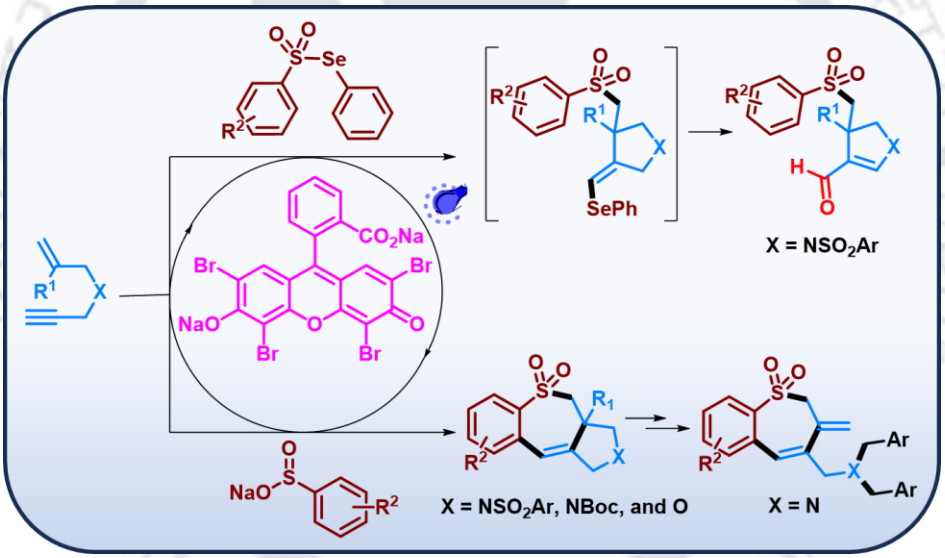

Roy, M.; Mallick, I; Siuli, S.; Bera, A.; Srimani, D. *Chem. Eur. J.* **2025**, *31*, e02052.

4.1 Introduction:

Radical chemistry has emerged as a highly versatile and creative field of synthetic organic chemistry, enabling the construction of complex molecular structures found in natural products, pharmaceuticals, and advanced materials.[1] Among the most impactful uses of radical chemistry are radical cyclization and radical cascade cyclization, which are particularly effective for constructing cyclic and polycyclic frameworks.[2] The strategy involves intramolecular addition of a carbon-centered radical to an unsaturated acceptor, such as an alkene or alkyne, leading to ring formation and enabling the synthesis of carbocyclic and heterocyclic compounds.

Sulfones are important organosulfur compounds with broad applications as solvents, polymer components, and biopharmaceutical agents.[4] Their utility as synthetic intermediates in the production of diverse chemical and biologically active molecules has established their importance in both industrial and medicinal contexts, like β-lactamase and protease inhibitors (Figure 4.1).[5] Therefore, the construction of sulfone molecules using a sulfonyl radical source under visible-light photoredox catalysis, employing 1,6-enynes as radical receptors, is important. This scaffold offers the potential to form five- or six-membered rings through radical cyclization[6] or create polycyclic compounds via radical cascade cyclization.[7]

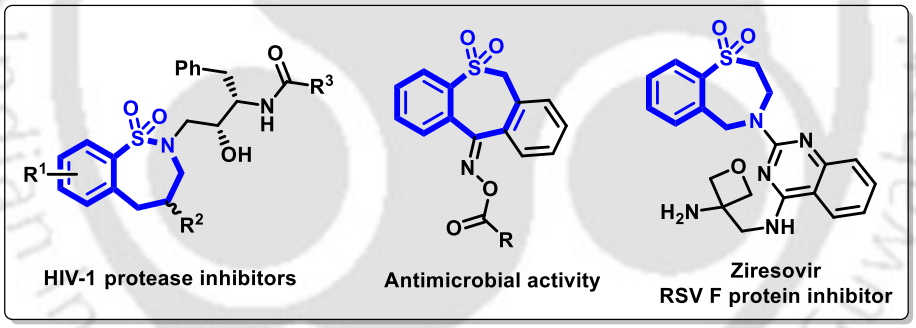

Figure 4.1: Important sulfone compounds.

4.2 Previous reports:

In 2022, Zhu and co-workers described a visible-light-driven, oxidant- and catalyst-free iodosulfonylative cyclization of 1,6-enynes, in which sodium aryl sulfinates serve as the radical source to generate a range of vinyl-iodide-containing sulfones. (Figure 4.2a).[6a] The procedure is limited to the synthesis of the five-membered ring with vinyl iodide and sulfone moieties. The Ackermann group demonstrated that two new families of sulfonamides with medium-sized rings are obtained by cyclizing 1,6-enynes using an electrooxidative radical cascade method (Figure 4.2b).[7a] Chemo-selective addition and regioselective 7- and 9-membered ring-formation are caused by differences in the activation barrier for radical addition between

alkynyl and alkenyl moieties. Under light-driven conditions, it is possible to precisely control both simple radical cyclization and more complex cascade processes of 1,6-enynes. By selecting suitable sulfonyl radical precursors, it was anticipated that either monocyclic or polycyclic sulfones could be obtained selectively. Such a strategy would not only broaden the range of accessible structures but also provide a highly adjustable method for building sulfur-containing cyclic scaffolds. Selenosulfonates are known to produce sulfonyl and selenyl radicals concomitantly under photochemical conditions.[8] Therefore, this radical precursor has the potential to be employed in the synthesis of five-membered selenosulfones via diradical addition and subsequent cyclization. Thus, devising new routes for synthesizing functionalized sulfones using visible light catalysis would be important.

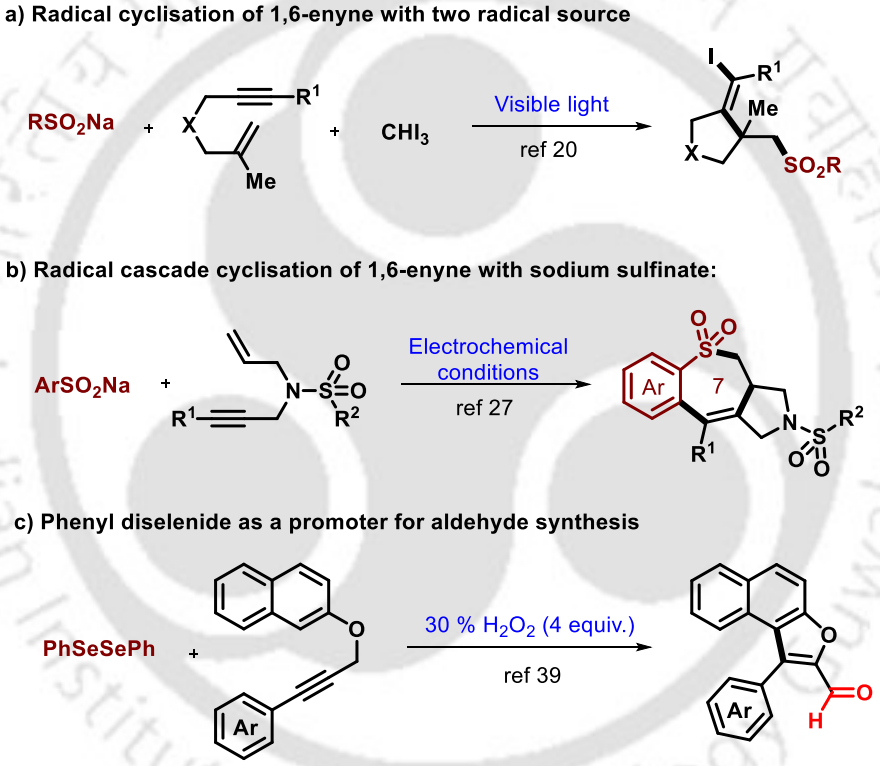

Figure 4.2: Previous literature reports.

Organoselenium compounds have recently been utilized to construct aldehyde groups using TBHP or H_2O_2 as oxidants (Figure 4.2c).[9] Therefore, it was anticipated that a sustainable route for the synthesis of sulfonylated heterocyclic carboxaldehydes could be achieved directly via visible-light-induced radical cyclization of selenosulfonates with 1,6-enynes without using a strong oxidant like TBHP or H_2O_2. Additionally, the presence of a single aryl sulfonyl radical source may trigger a radical cascade cyclization, resulting in the formation of polycyclic sulfones selectively.

4.3 Present work:

In this chapter, an efficient photocatalytic strategy for the selective synthesis of the sulfonylated heterocyclic carboxaldehyde and tricyclic benzo-fused seven-membered sulfone was developed through sulfonyl radical-triggered cyclisation of 1,6-enynes. Furthermore, the tricyclic sulfone can be transformed into a novel bicyclic seven-membered sulfone having an exocyclic double bond by rupturing of pyrrolidine ring. Here, an environmentally benign switchable synthesis of diverse heterocyclic sulfones was introduced by controlling the radical cyclization and radical cascade cyclization (Figure 4.3).

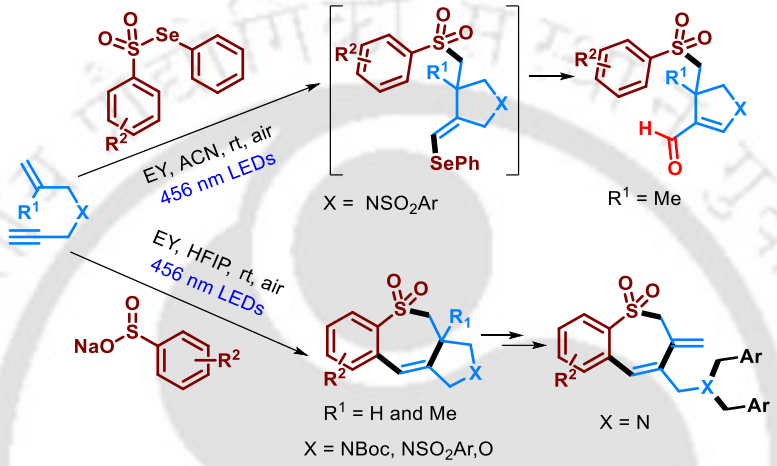

Figure 4.3: Present work for photocatalytic radical cyclisation and radical cascade cyclisation of 1,6-enyne.

4.4 Results and Discussion:

To pursue these objectives, the reactivity of selenosulfonates and sodium aryl sulfinate with 1,6-enynes was studied under visible light catalysis. The investigation was started by taking selenosulfonates (**4.1h**, 1.2 equiv.) and N-tosyl-1,6-enyne (**4.2l**, 1 equiv.) as the model substrates and performing the reaction using EY-Na_2 (10 mol %) as the photocatalyst in DMF (2 mL) under 456 nm blue light irradiation. The formation of sulfonylated pyrrolidine 3-carbaldehyde **4.3a** with a 21 % yield (Table 4.1, entry 1) was observed. A variety of additives, such as Na_2CO_3, K_2CO_3, TBHP, and $K_2S_2O_8$, were tested but failed to enhance the yield of **4.3a** (Table 4.1, entries 2-5). Screening of different solvents revealed that acetonitrile was the most effective, delivering a 79% yield of the desired compound **4.3a**. Evaluation of other photocatalysts, such as Fluorescein, Rose Bengal, and 4CzIPN, showed detrimental results (Table 4.1, entries 13-15). Trace amount of the product was detected in the absence of a photocatalyst, but no formation of product **4.3a** was observed under argon and in dark

conditions (Table 4.1, entries 16-18). This highlights the importance of light and atmospheric oxygen in the formation of product **4.3a**.

Table 4.1: Optimization of reaction parameters for carboxaldehyde formation[a]

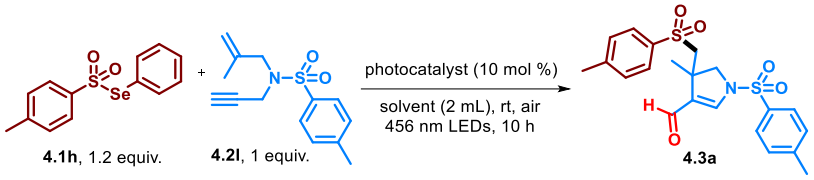

Entry	Catalyst (mol %)	Additive (equiv.)	Solvent (mL)	Yield[b] (%)
1.	EY-Na_2 (10)	-	DMF (2)	21
2.	EY-Na_2 (10)	Na_2CO_3 (2)	DMF (2)	25
3.	EY-Na_2 (10)	K_2CO_3 (2)	DMF (2)	23
4.	EY-Na_2 (10)	TBHP (2)	DMF (2)	-
5.	EY-Na_2 (10)	$K_2S_2O_8$ (2)	DMF (2)	-
6.	EY-Na_2 (10)	-	DMSO (2)	31
7.	EY-Na_2 (10)	-	Dioxane (2)	43
8.	EY-Na_2 (10)	-	ACN (2)	79
9.	EY-Na_2 (10)	-	THF (2)	35
10.	EY-Na_2 (10)	-	DCM (2)	45
11.	EY-Na_2 (10)	-	DCE (2)	57
12.	EY-Na_2 (10)	-	HFIP (2)	13
13.	Fluorescene (10)	-	ACN (2)	37
14.	Rose Bengal (10)	-	ACN (2)	49
15.	4CzIPN (10)	-	ACN (2)	43
16.	-	-	ACN (2)	trace
17[c].	EY-Na_2 (10)	-	ACN (2)	-
18[d].	EY-Na_2 (10)	-	ACN (2)	-

[a]Condition: **4.1h** (0.30 mmol), **4.2l** (0.25 mmol), photocatalyst (10 mol%), solvent (2 mL) in open air, was irradiated with 456 nm Blue LEDs for 10 h. b = isolated yield, c = in dark, d = under argon.

After finalizing the reaction conditions, the viability of the process was checked with different substrates (Scheme 4.1). Various N-tethered 1,6-enynes bearing electron-donating (-Me and -OMe) and electron-withdrawing (-F, -CF_3, -COOMe, and -NO_2) groups smoothly generate the sulfonylated 4,5-dihydropyrrole 3-carbaldehyde derivatives with a decent yield (**4.3a-4.3d**,

4.3m, and **4.3n** 51-79 %). Next, the scope of selenosulfonates was explored. Differently substituted selenosulfonates work well with this method. Electron-releasing group (-Me and -OMe) and electron-poor group (-F and -CF_3) are present at the aryl ring of the sulfonate moiety, providing the carbaldehyde product with good yield (**4.3g-4.3j**, 53-78 %). Selenosulfonates having naphthyl and cyclopropyl rings attached to the sulfone moieties were also well compatible in this method (**4.3k** and **4.3l**, 68 and 59 % respectively).

Table 4.2: Optimization of reaction parameters for tricyclic sulfone formation[a]

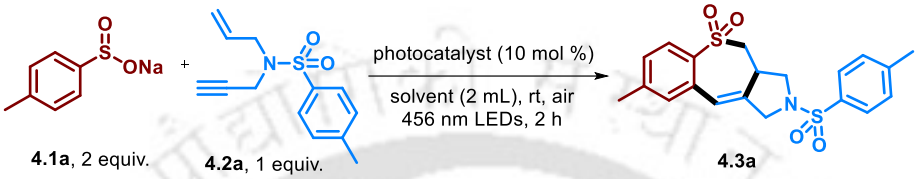

Entry	Catalyst (mol %)	Solvent (mL)	Yield[b] (%)
1.	EY-Na_2 (10)	ACN (2)	13
2.	EY-Na_2 (10)	DMF (2)	23
3.	EY-Na_2 (10)	DMSO (2)	24
4.	EY-Na_2 (10)	ACN (2)	13
5.	EY-Na_2 (10)	THF (2)	-
6.	EY-Na_2 (10)	DCM (2)	-
7.	EY-Na_2 (10)	HFIP (2)	71
8.	EY-Na_2 (10)	^{i}PrOH (2)	-
9.	Fluorescene (10)	HFIP (2)	53
10.	Rose Bengal (10)	HFIP (2)	39
11.	4CzIPN (10)	HFIP (2)	31
12.	-	HFIP (2)	-
13[c].	EY-Na_2 (10)	HFIP (2)	-
14[d].	EY-Na_2 (10)	HFIP (2)	trace

[a]Condition: **4.1a** (0.50 mmol), **4.2a** (0.25 mmol), photocatalyst (10 mol%), solvent (2 mL) in open air, was irradiated with 456 nm Blue LEDs for 2 h. b = isolated yield, c = in dark, d = under argon.

After successfully performing the radical cyclization to form 5-membered sulfonylated dihydropyrrole-3-carboxaldehydes, it was interesting to explore the possibility of sequential radical cyclizations to produce polycyclic sulfones using visible light (Scheme 4.2). Thus, when aryl sulfinates were reacted with analogous 1,6-enynes instead of selenosulfonate under the same reaction conditions, a tricyclic benzo-fused 7-membered sulfone (**4.4a**) was obtained in 13 % yield. Reaction parameters were systematically screened to maximize the yield of product **4.4a**. N-tosyl-1,6-enyne (**4.2a**, 1 equiv.), when treated with sodium p-toluenesulfinate (**4.1a**, 2 equiv.) using EY-Na_2 (10 mol%) as a photocatalyst in HFIP (1,1,1,3,3,3-Hexafluoro-

2-propanol, 2 mL) solvent under 456 nm blue LED irradiation, provides the tricyclic benzo-fused 7-membered sulfone **4.4a** with 77 % yield (Table 4.2).

With this result, the substituent effect of this method was explored. Various N-arylsulfonyl-1,6-enynes bearing electron-donating (–Me, –OMe) and electron-withdrawing (–F) substituents at the *para*-position of the aryl ring underwent the reaction smoothly, affording the desired products in good yields (**4.4a**-**4.4c**). Methyl, fluoro, and nitro substituents at the *meta* and *ortho*-positions of the N-aryl rings were well tolerated, leading to the formation of the desired products in appreciable yields (**4.4d**-**4.4f**, 63-69 %). Due to the mild nature of the protocol strained cyclopropyl ring survived and produced the corresponding tricyclic sulfone with a decent yield (**4.4g**, 58 %). N-thiophene sulfone, N-pyridine sulfone, and N-Boc protected 1,6-enyne were able to produce the requisite benzo-fused 7-membered sulfone derivatives with a respectable yield (**4.4h**-**4.4j**, 53-65 %). The methyl substituent present in the alkene part of 1,6-enynes smoothly produced the corresponding tricyclic sulfone with good yield (**4.4k**, 51 %).

Scheme 4.1: Substrate scope for sulfonylated dihydropyrrole 3-carboxaldehydes[a]

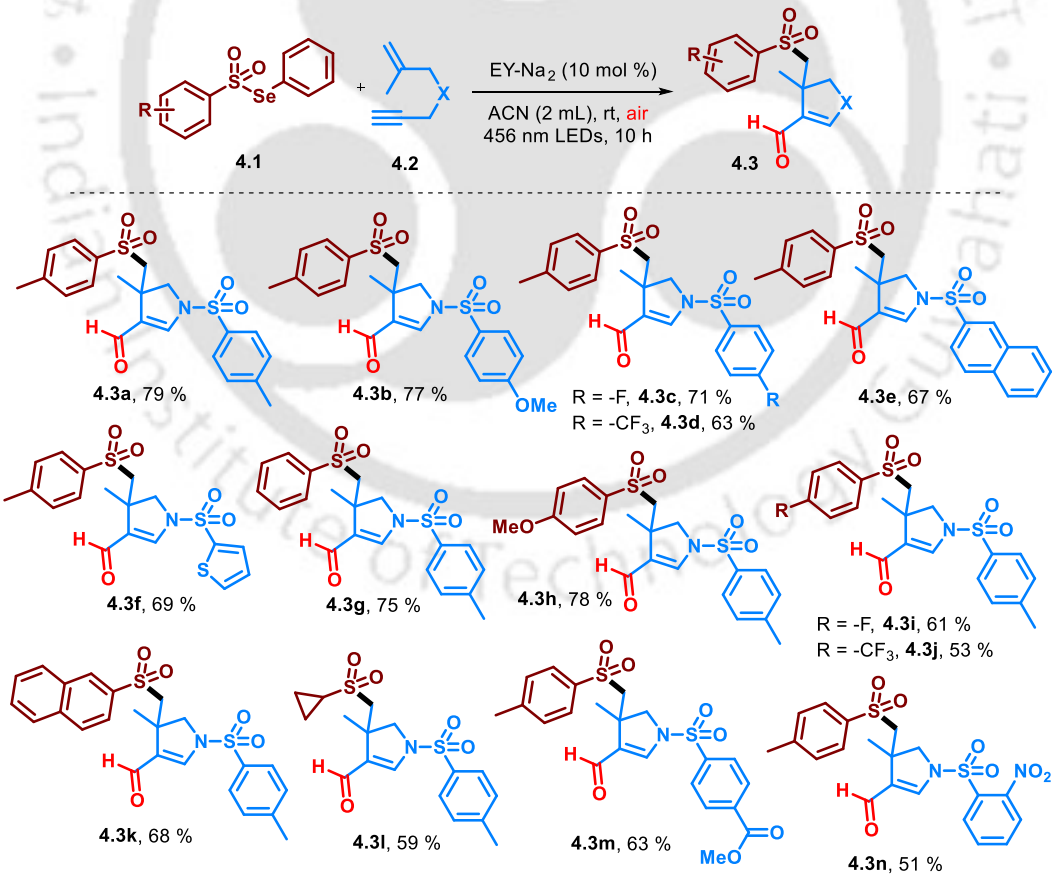

[a]Condition: **4.1** (0.30 mmol), **4.2** (0.25 mmol), EY-Na_2 (10 mol%), ACN (2 mL) in open air, was irradiated with 456 nm Blue LEDs for 10 h.

Sodium aryl sulfinates bearing both electron-donating and electron-withdrawing substituents demonstrated good reactivity under this protocol, affording the corresponding tricyclic sulfones in decent yields (**4.4l-4.4n**, 51-69 %). When sodium 3-methylphenyl sulfinate was employed, a mixture of products **4.4o** and **4.4o'** was obtained, with isolated yields of 41% and 17%, respectively. The lower yield of the **4.4o'** product may be due to the steric factor. Sodium 3-pyridine sulfinate was well-compatible with this method and generated product **4.4p** with a 63 % yield. Next, allyl-propargyl ether was employed as the 1,6-enyne to carry out the reactions with various sodium aryl sulfinates. The transformations proceeded efficiently, affording the corresponding annulated seven-membered sulfones in good yields (**4.4q-4.4v**, 51-69 %). For practical utility, the reaction between **4.1a** and **4.2j** was performed up to 10.0 mmol, scale to produce **4.4j** (1.853 g) in 53 % yield. Additionally, a single-crystal X-ray investigation confirmed the structure of molecules **4.4q** (CCDC:2463338) and **4.4v** (CCDC:2463339).

Scheme 4.2: Substrate Scope for tricyclic sulfone[a]

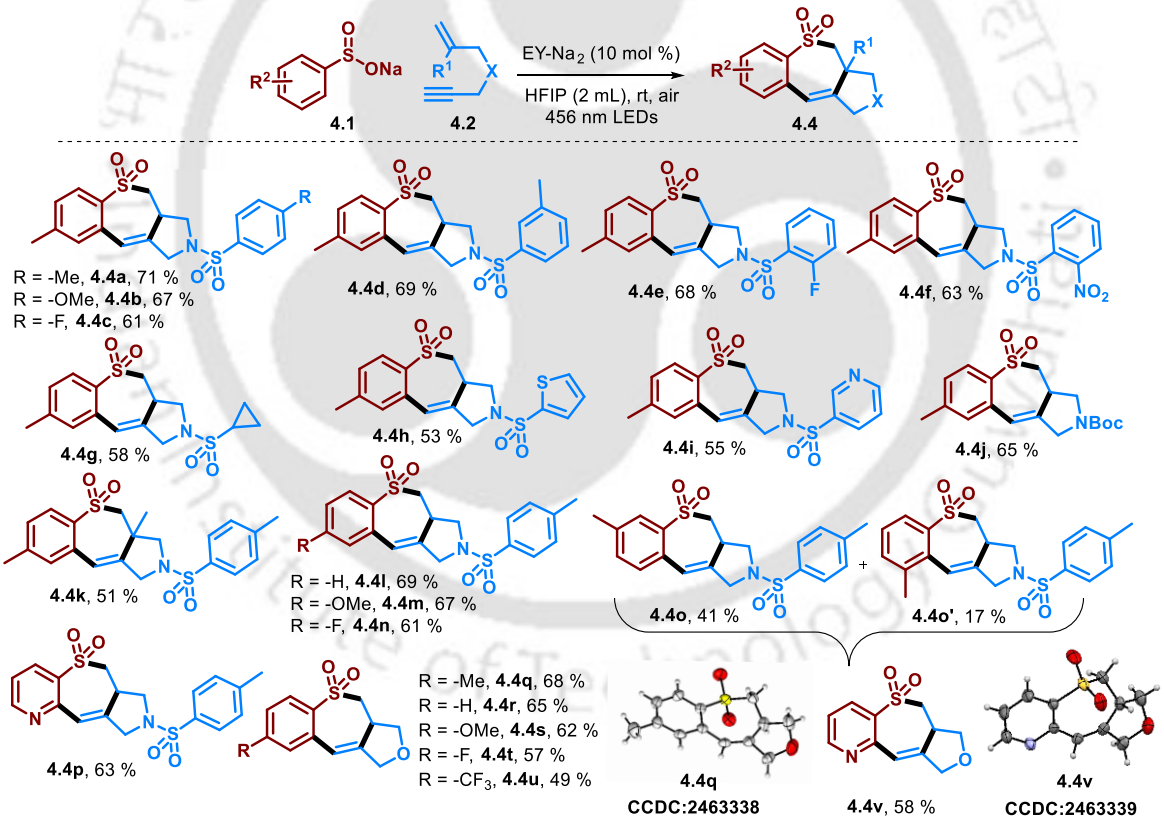

[a]Condition: **4.1** (0.50 mmol), **4.2** (0.25 mmol), EY-Na_2 (10 mol%), HFIP (2 mL) in open air, was irradiated with 456 nm Blue LEDs for 2 h.

4.5 Post-synthetic modification:

The resulting tricyclic benzo-fused 7-membered sulfones were further diversified to showcase their synthetic utility (Scheme 4.3). TFA-induced N-Boc deprotection of the **4.4j** molecule produced **4.5** in an 81% yield, which, via chemoselective N-sulfonylation with 4-(Bromomethyl)benzenesulfonyl chloride, forms **4.4w**. Compound **4.5** can be N-benzylated in the presence of K_2CO_3 (1 equiv.) and benzyl bromide (1 equiv.).

Scheme 4.3: Post-functionalization and substrate scope of bicyclic sulfone[a]

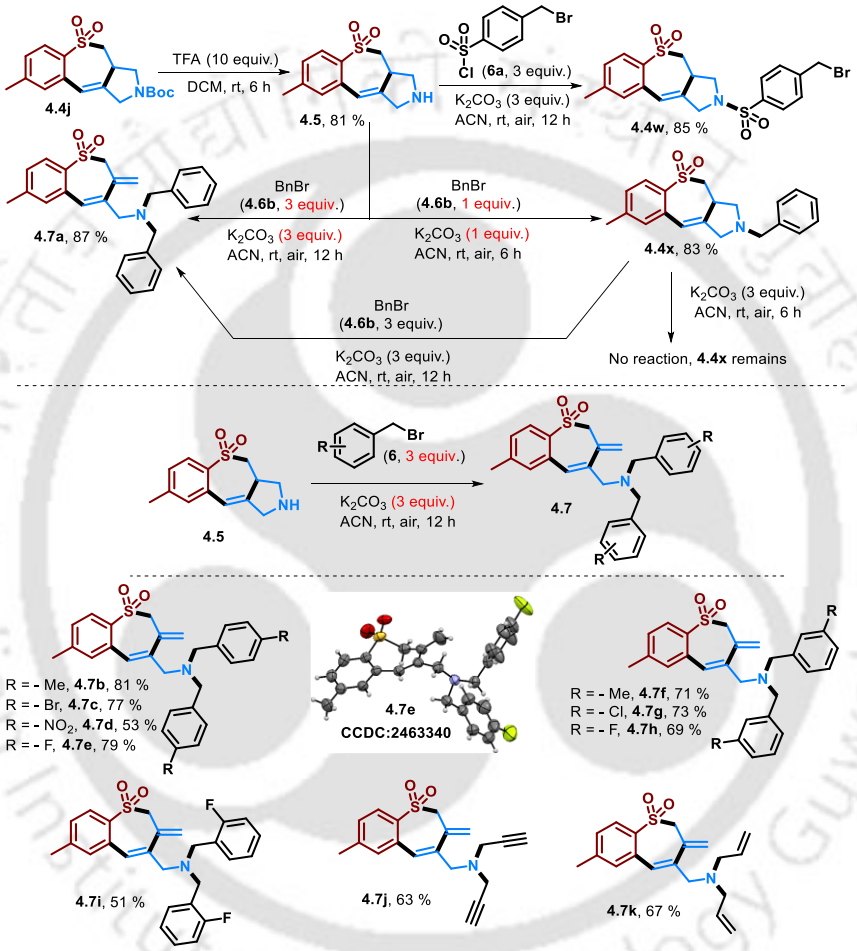

[a]Condition: **4.5** (0.20 mmol), **4.6** (0.60 mmol), K_2CO_3 (0.60 mmol), ACN (5 mL) in the open air, at room temperature, was stirred for 12 h.

Interestingly, a new bicyclic sulfone having an exocyclic double bond **4.7a** was formed in the presence of an excess amount of K_2CO_3 (3 equiv.) and benzyl bromide (3 equiv.). To gain insight into the ring-opening process, the compound **4.4x** was treated with only K_2CO_3 (3 equiv.) and observed that no changes occurred, which suggests that the base alone was not able to open the annulated dihydropyrrole ring. Then **4.4x** was also treated with K_2CO_3 and benzyl bromide, and the formation of product **4.7a** was observed, which suggested that ring opening may be via quaternary ammonium salts (QAs) formation, followed by Hoffmann-type

elimination. Encouraged by these results, the scope of this new bicyclic sulfone scaffold synthesis was investigated, which demonstrates broad substrate compatibility and delivers good yields (Scheme 4.3). The structure of the molecule was confirmed from the single-crystal X-ray data of molecule **4.7e** (CCDC:2463340).

4.6 Control experiments:

4.6.1 Procedure for radical trapping experiment with TEMPO/BHT/1,1-diphenylethylene:

In case of carboxaldehyde formation: The 1,6-enynes **4.2m** (0.25 mmol, 1 equiv.), selenosulfonates **4.1j** (0.30 mmol, 1.2 equiv.) Eosin Y (10 mol%, 0.1 equiv.), and radical scavengers (0.75 mmol, 3 equiv.) were taken in an oven-dried reaction tube with a magnetic bead. After that, dry ACN (2 mL) was added, and the reaction mixture was allowed to stir under the 456 nm LED irradiation at room temperature in an open-air atmosphere for 10 h. The reaction was monitored through TLC, and it was noticed that after the reaction time, there was no spot of our desired product, which suggested the radical pathway for the reaction.

In the case of tricyclic sulfone formation: The 1,6-enynes **4.2a** (0.25 mmol, 1 equiv.), sodium aryl sulfinates **4.1a** (0.50 mmol, 2 equiv.) Eosin Y (10 mol%, 0.1 equiv.), and TEMPO (0.75 mmol, 3 equiv.) were taken in an oven-dried reaction tube with a magnetic bead. After that, HFIP (2 mL) was added, and the reaction mixture was allowed to stir under the 456 nm LED irradiation at room temperature in an open-air atmosphere for 2 h. TLC monitored the reaction, and it was observed that after the reaction time, there was no spot of our desired product.
Similarly, the reaction was also performed with another radical scavenger such as BHT (5 equiv.) and 1,1-diphenylethylene (5 equiv.), in the case of BHT a lower yield of the product (**4.4a**, 43 %) was observed and also detected a BHT-adduct (**4.10**, Figure 4.2) in HRMS, and in case of 1,1-diphenylethylene no desired product (**4.4a**) formation was observed, but the intermediate compound **4.9** was isolated with 77 % yield. These findings suggested the involvement of a radical route.

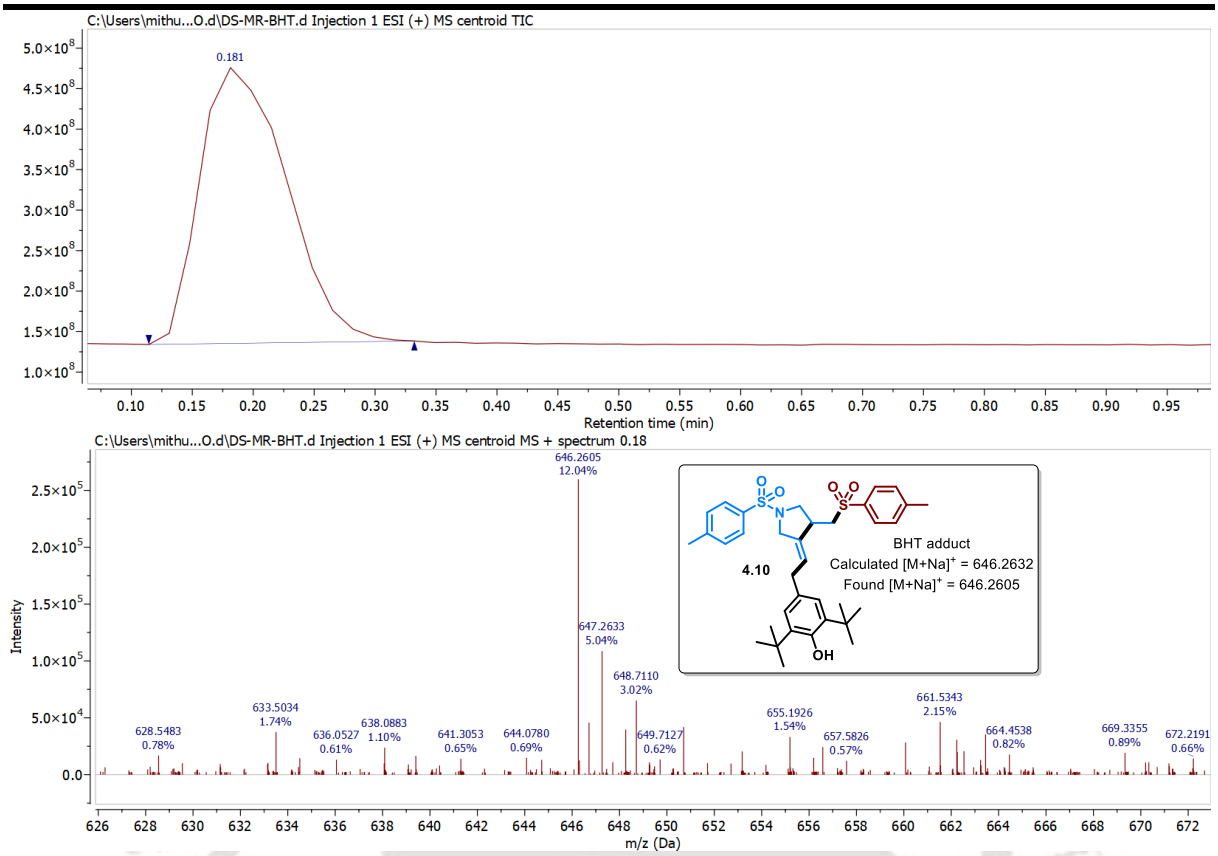

Figure 4.4: HRMS spectra of BHT adduct.

4.6.2 Role of photocatalyst and atmospheric oxygen for carboxaldehyde formation: Selenosulfonate **4.1j** (0.30 mmol, 1.2 equiv.) and 1,6-enyne **4.2m** (0.025 mmol, 1 equiv.) was taken in a round bottom flask and then dry ACN (2 mL) was added and the reaction mixture was irradiated with 456 nm blue LEDs under an argon atmosphere in the absence of photocatalyst. This resulted in the formation of a selenosulfonyl-substituted pyrrolidine **4.8** in 91% yield. This suggests that the photocatalyst is not playing any role for the cleavage of slenosulfonates only light is enough for that.

Next, selenosulfonyl-substituted pyrrolidine **4.8** (0.20 mmol, 1equiv.) was taken in a reaction tube and dissolved in 2 mL ACN and irradiated with 456 nm blue LEDs in open air conditions both in the presence of photocatalyst (10 mol%, 0.1 equiv.) and absence of photocatalyst separately. In the presence of a photocatalyst, it produces the corresponding aldehyde product **4.3b** with 77 % yield, but in the absence of a photocatalyst fails to produce the aldehyde product. These findings suggested that for the conversion of selenosulfonyl-substituted pyrrolidine to the corresponding aldehyde, both photocatalyst and air have a prominent role.

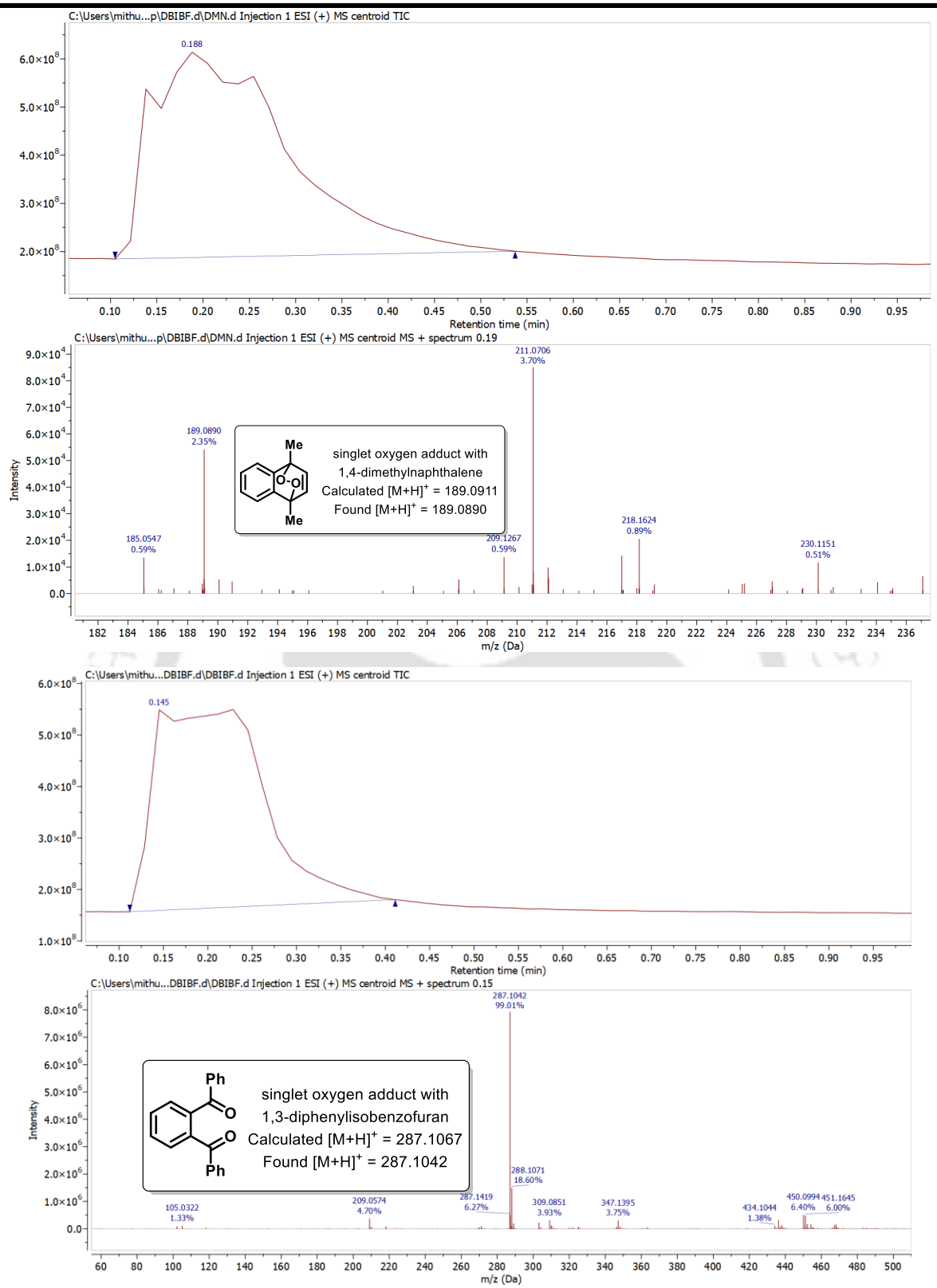

Figure 4.5: HRMS spectrum of singlet oxygen adducts with 1,4-dimethylnaphthalene and 1,3-diphenylisobenzofuran respectively.

4.6.3 Singlet oxygen quenching: To know the ($^1O_2$) singlet or ($^3O_2$) triplet nature of the molecular oxygen, a singlet oxygen quenching experiment was performed. The selenosulfonyl-substituted 4,5-dihydropyrrole **4.8** (0.1 mmol, 1.0 equiv.) was treated under the standard conditions in the presence of singlet oxygen scavenger DABCO (0.15 mmol, 1.5 equiv.) and did not produce the corresponding aldehyde product (**4.3b**), which confirms the participation of singlet oxygen in this oxygenation process. The *in situ* generated singlet oxygen was then trapped using either 1,4-dimethyl naphthalene or 1,3-diphenylisobenzofuran (0.15 mmol, 1.5 equiv.) and detected their singlet oxygen-trapped adducts in HRMS (Figure 4.3).

Several control experiments were conducted to gain insight into the reaction mechanism (Figure 4.4). The radical scavenger test indicates that the reaction likely proceeds through a radical pathway. In the absence of a photocatalyst, selenosulfonate **4.1j** and 1,6-enyne **4.2m** underwent a blue LED–promoted reaction under an argon atmosphere, resulting in the formation of a selenosulfonyl-substituted 4,5-dihydropyrrole **4.8** in 91% yield. This underpins that selenosulfonate cleavage can be efficiently driven by light alone, eliminating the need for any photocatalyst. However, for the conversion of selenosulfonyl-substituted 4,5-dihydropyrrole to the corresponding aldehyde, both photocatalyst and air play a prominent role. In the absence of either component, the reaction ceases entirely. Then it was important to clarify whether the molecular oxygen involved in the aldehyde formation processes is ($^1O_2$) singlet or ($^3O_2$) triplet in nature. The selenosulfonyl-substituted 4,5-dihydropyrrole **4.8** was treated under the standard conditions in the presence of singlet oxygen scavenger DABCO and did not produce the corresponding aldehyde product (**4.3b**), which confirms the participation of singlet oxygen in this oxygenation process. The *in situ* generated singlet oxygen was then trapped using either 1,4-dimethyl naphthalene or 1,3-diphenylisobenzofuran and detected their singlet oxygen-trapped adducts in HRMS.[41] In the synthesis of compound **4.4a**, the presence of a radical scavenger inhibited the cascade cyclization. Additionally, the formation of a tosyl radical was confirmed by the isolation of the DPE adduct **4.9** in 77% yield. Reactions with sodium methanesulfinate (**4.1i**) and 2,4,6-triisopropylbenzenesulfinate (**4.1h**) gave no products, which highlights the crucial role of an aryl ring bearing a free *ortho*-position in sulfinate salts for radical cascade cyclization. A competitive experiment revealed that sulfinates bearing electron-donating groups reacted more rapidly than those with electron-withdrawing groups, while the critical role of light was confirmed through an on/off light control experiment (Figure 4.5).

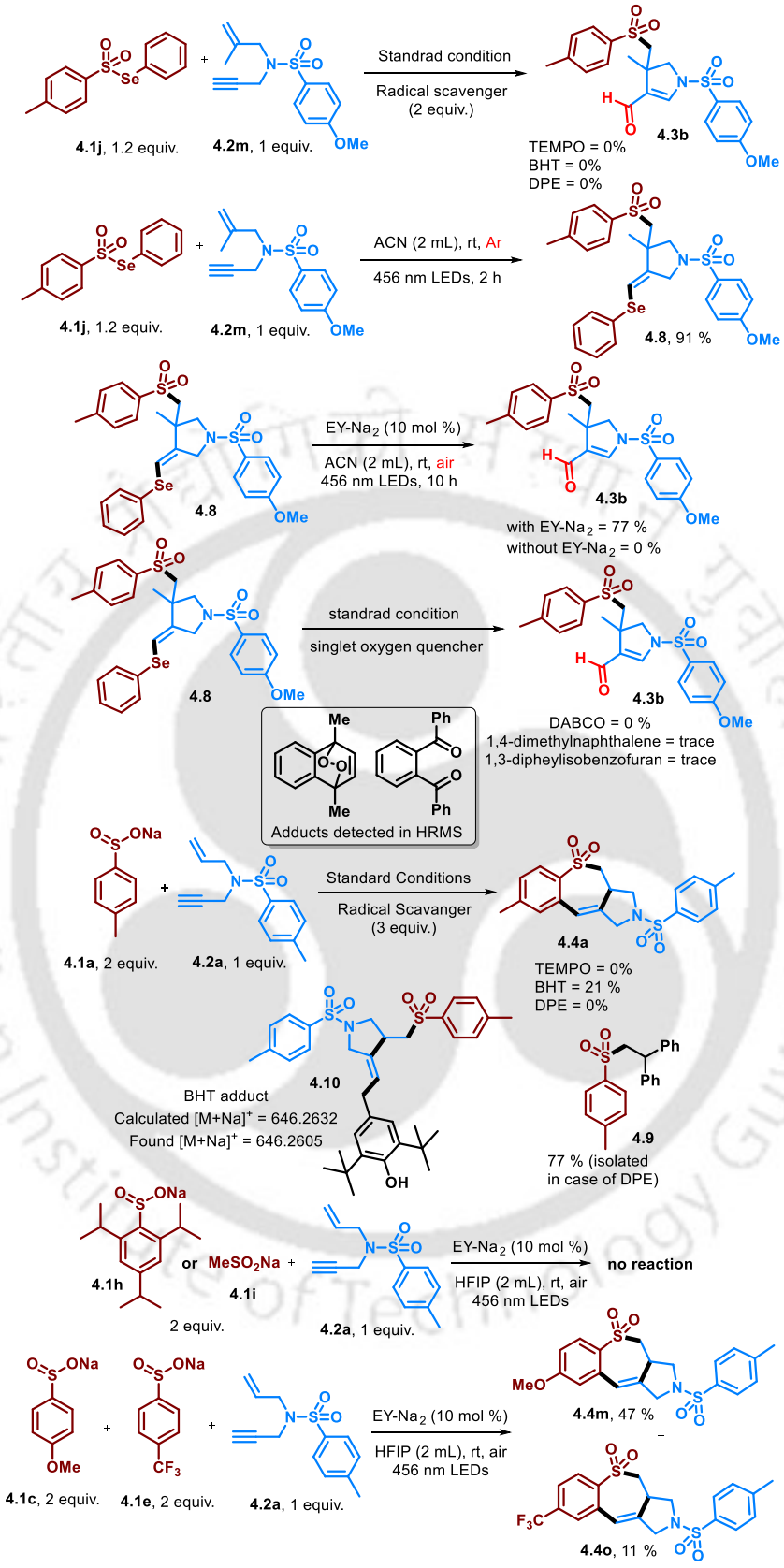

Figure 4.6: Control Experiments

4.6.4 Light On/Off experiment:

To investigate the effect of light on this reaction, an On/Off experiment was conducted. The experiment was conducted following the general procedure 4.7.a by alternating 30 minutes of exposure to light and darkness. These demonstrated that the chemical process was entirely halted in the absence of light and restarted in the presence of additional light. These findings show that light plays a crucial role in this reaction.

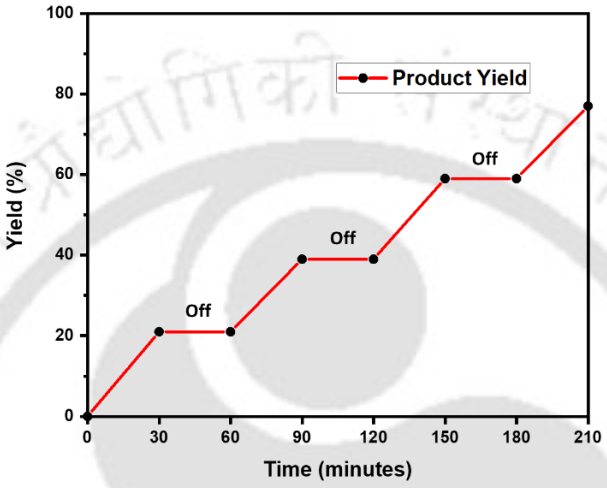

Figure 4.7: Light On/Off Experiment

4.7 Plausible reaction mechanism:

Based on literature reports[10, 7a] and control experiments, a probable reaction pathway was proposed for both the cyclization process (Figure 4.6). The synthesis of sulfonylated 4,5-dihydropyrrole-3-carboxaldehyde starts with the concurrent formation of sulfonyl and phenylselenyl radicals under blue LED irradiation. Subsequently, the sulfonyl radical undergoes chemoselective addition to the alkene, initiating a 5-exo-dig cyclization, followed by the addition of the selenium radical to vinyl radical intermediate **4.B**, producing the selenosulfonylated compound **4.C**. Then photocatalyst EY-Na_2 gets excited to its higher energy state under the blue LEDs irradiation which converts ($^3O_2$) triplet molecular oxygen to ($^1O_2$) singlet oxygen via energy transfer (EnT) and excited EY-Na_2 return to its ground state.[11] Further, ($^1O_2$) singlet oxygen undergoes ene reaction[12] with the allylic double bond of selesulfonylated compound **4.C**, leading to the formation of allylic hydroperoxide intermediate E through intermediate D. Finally, peroxide bond cleavage and elimination of phenyl selenium radical generate the desired aldehyde product **4.3**. This is further confirmed by the isolation of diphenyl diselenide in the reaction process. In the case of tricyclic sulfone formation, initially, the tosyl radical **4.G** is generated from the sodium p-toluene sulfinate **4.1a** via photocatalytic

single electron transfer (SET) with excited organo-photocatalyst EY-Na_2. Then, chemoselective addition of tosyl radical **4.G** to the C-C double bond of 1,6-enyne produces an alkyl radical **4.H**, which undergoes 5-exo-dig cyclization to afford a vinyl radical **4.I**. Radical annulation of intermediate **4.I** forms radical intermediate **4.J**, which undergoes SET with the excited photocatalyst to produce cationic intermediate **4.K**. Then, the deprotonation of intermediate **4.K** triggers aromatization, yielding the tricyclic benzo-fused seven-membered sulfone **4.4**.

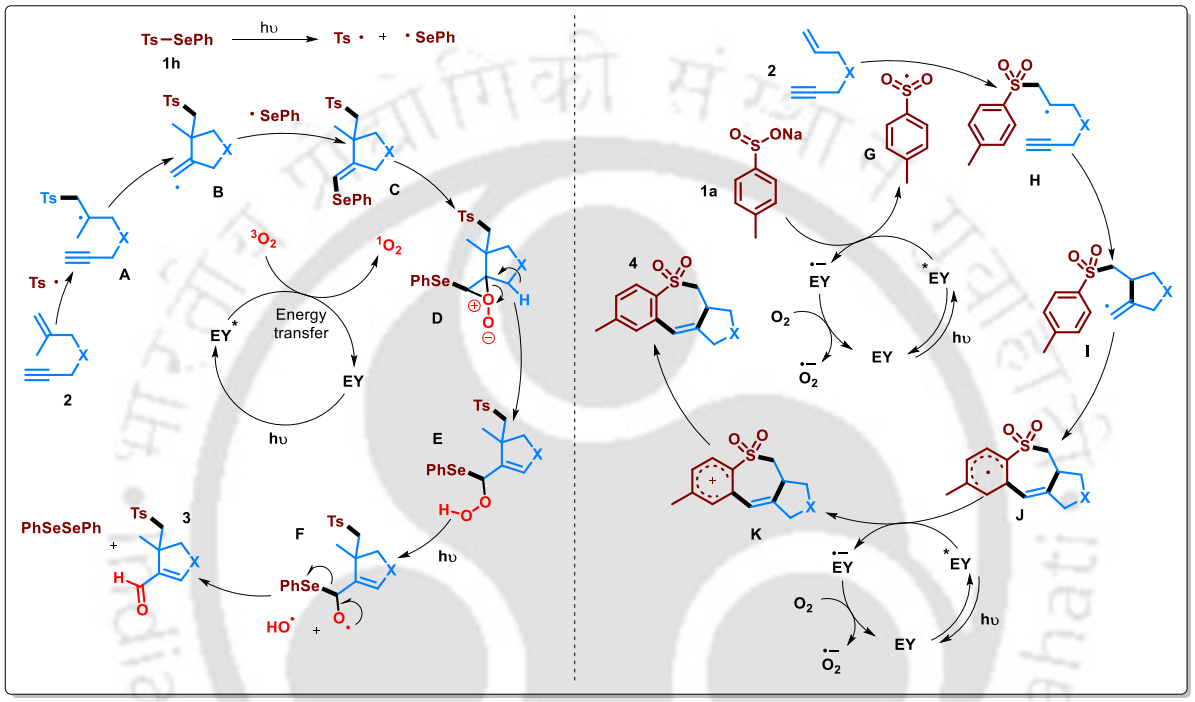

Figure 4.8a: Plausible reaction mechanism.

Selectivity of alkene over alkyne in 1,6-enyne: When the sulfonyl radical attacks the alkyne part, it will generate a vinyl radical. Vinyl radicals are sp2 hybridized, meaning the unpaired electron is in an orbital with high s-character, bringing it closer to the nucleus. This is generally less stable than an alkyl radical. But when the sulfonyl radical attacks the alkene part, it leads to the generation of a secondary or tertiary alkyl radical stabilized through hyperconjugation, which is significantly more stable than a vinyl radical. This may be the possible reason for the selectivity of the sulfonyl radical towards the double bond.

Role of HFIP: HFIP might facilitate the process by interacting with the intermediate through hydrogen bonds. The sulfonyl radical (**G**) can be produced by lowering the activation energy through the formation of a hydrogen bond, and it also prevents side reactions (such as premature quenching or dimerization). The reported redox potential value of sodium p-

toluenesulfinates (**1a**) in various solvents shows that it has a lower value in HFIP than that of the other common solvents, suggesting that **1a** was more easily oxidized to produce sulfonyl radical in HFIP.[13] The strength of the H-bond between **1a** and several popular solvents shows that HFIP has the highest hydrogen bond energy compared to other solvents. However, the HFIP may serve as a proton donor and help convert sodium p-toluenesulfinates (**1a**) to p-toluenesulfinic acid (**1a'**), which is more readily oxidized by the organophotcatalyst (EY) to produce sulfonyl radical. By stabilizing the highly reactive alkyl and vinyl radical intermediates (**H** or **I**), the hydrogen bond may prevent the H-atom abstraction process that results in the formation of the alkyl sulfone by-product.

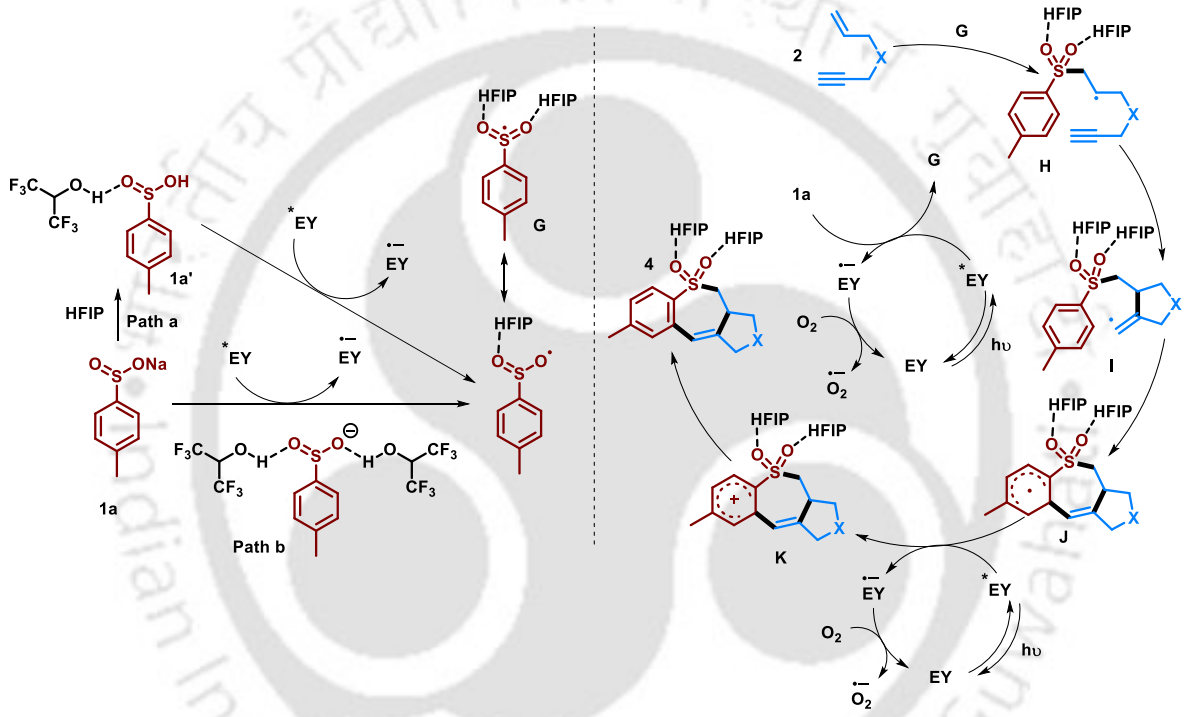

Figure 4.8b: Role of HFIP in the formation of product **4**.

4.8 Conclusion:

In summary, a photocatalytic approach for the selective synthesis of sulfonylated pyrrolidine-3-carbaldehydes and tricyclic benzo-fused sulfones was developed, directed by the choice of sulfonyl radical precursor. The tricyclic sulfone can be converted to a bicyclic benzo-fused 7-membered sulfone through dihydropyridine ring opening, driven by quaternary ammonium salt formation and Hoffmann elimination. Switchability in product formation, broad substrate tolerance, various post-synthetic applications, and scalability make this protocol practically applicable.

4.9 Experimental section:

a) General procedure for the synthesis of 1,6-enynes:

1,6-enyne derivatives were prepared by following the reported procedures.[14,15]

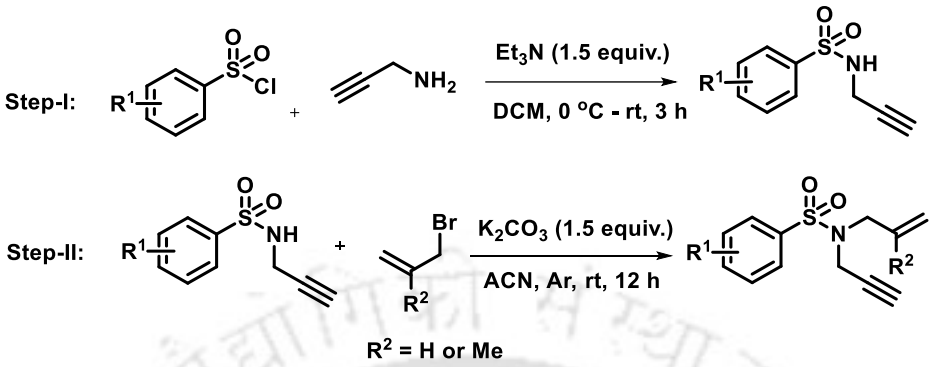

Step I: Propargylamine (5.0 mmol, 1.0 equiv.) and triethylamine (7.5 mmol, 1.5 equiv.) were taken in an oven-dried round-bottom flask then DCM (10 mL) was added and the mixture was stirred for 5 minutes. The aryl sulfonyl chloride (5.0 mmol, 1.0 equiv.) was added in portions at 0 °C, and the resulting mixture was stirred at room temperature for 12 hours. After completion of the reaction water was added to the mixture, and extracted in DCM. The combined organic phase was dried over Na_2SO_4 and concentrated under reduced pressure. The crude product is used directly in the next step without further purification.

Step II: In a round bottom flask N-(prop-2-yne-1-yl) arylsulfonamide (5.0 mmol, 1.0 equiv.) and K_2CO_3 (7.5 mmol, 1.5 equiv.) were taken in ACN (10 mL) solvent and the mixture was stirred for 5 minutes. Then allyl bromide (7.5 mmol, 1.5 equiv.) was added dropwise, and the mixture was refluxed at 80 °C for 12 h. After the reaction was completed, the solvent was evaporated under reduced pressure, and the residue was diluted with ethyl acetate and washed with water. The combined organic phase was dried over Na_2SO_4 and concentrated under reduced pressure. The residue was purified by column chromatography on silica gel with petroleum ether/ethyl acetate as the eluent.

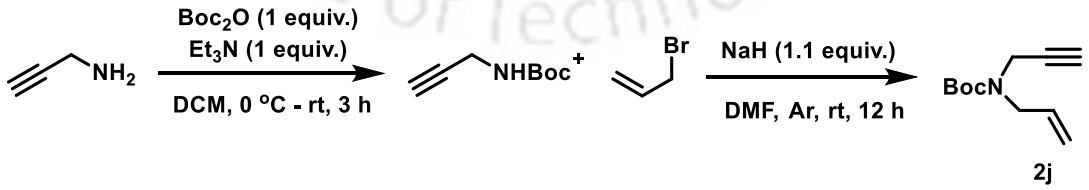

A solution of di-tert-butyl dicarbonate (5.0 mmol, 1.091 g, 1 equiv.) in dry DCM (10.0 mL) was taken in a round-bottom flask. Then propargylamine (5.0 mmol, 0.32 mL, 1 equiv.) and triethylamine (5.0 mmol, 0.70 mL, 1 equiv.) were added at 0 °C under an argon atmosphere. The reaction mixture was stirred for 5 hours. After completion of the reaction water was added, and the aqueous phase was extracted with DCM. The combined organic layer was washed with

brine solution, and dried over sodium sulphate, and the solvent was evaporated under reduced pressure to obtain the crude product. The crude product is used directly in the next step without further purification.

To a solution of tert-butyl propargylcarbamate (5.0 mmol, 0.780 g, 1.0 equiv.) in dry DMF (2.0 mL), NaH 60% in mineral oil (15.0 mmol, 0.360 g, 3.0 equiv.) was added at 0 °C under an argon atmosphere. The mixture was stirred for 15 minutes and then allyl bromide (3.39 mmol, 0.411 g, 1.5 equiv.) was added dropwise. The reaction mixture was stirred overnight and water was added to the reaction mixture and extracted with diethyl ether. The organic layer was dried over sodium sulphate and the solvent was removed under a vacuum to afford a dark brown oil. This crude product was purified by column chromatography on silica gel with petroleum ether/ethyl acetate as the eluent.[16,17]

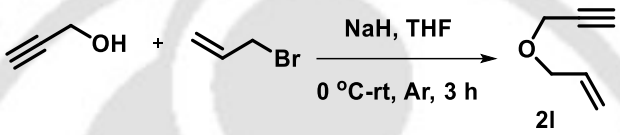

NaH 60% dispersion in mineral oil (15 mmol, 0.360 g, 3 equiv.) and THF (10 mL) were taken in a round bottom flask and the reaction mixture was cooled to 0 °C. Then propargyl alcohol (5.0 mmol, 0.288 mL, 1 equiv.) was added dropwise under an argon atmosphere and the reaction mixture was stirred for 15 minutes. Further, allyl bromide (7.5 mmol, 0.648 mL, 1.5 equiv.) was added dropwise to the reaction mixture and stirred for 5 hours at room temperature. After completing the reaction, water was added and the mixture was extracted with diethyl ether. The combined organic layers were washed with brine and dried over anhydrous Na_2SO_4. Then, the solvent was evaporated using a rotary evaporator to provide the 1,6-enyne **2l**, which was used in the next step without further purification.[18]

b) General procedure for the preparation of sodium aryl sulfinates:

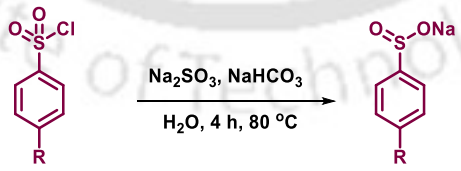

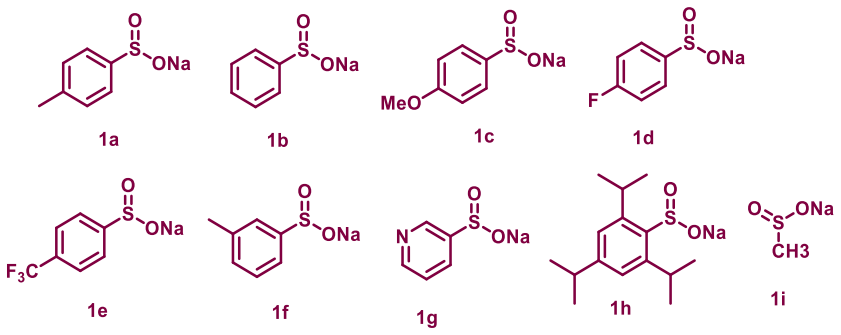

Sodium aryl sulfinates **4.1a**, **4.1b**, and **4.1i** are commercially available. **4.1c-4.1h** were synthesized by following the reported procedure.[19]

In an oven-dried round bottom flask sodium sulphite (10.0 mmol, 2.0 equiv.), sodium bicarbonate (10.0 mmol, 2.0 equiv.), and the aryl sulfonyl chloride (5.0 mmol, 1.0 equiv.) was taken and then distilled water (5 mL) was added. The reaction mixture was refluxed for 5 h and monitored by TLC. After complete consumption of the aryl sulfonyl chloride, the reaction mixture was cooled to room temperature, and water was removed by rotary evaporator. The white residue was extracted with ethanol to obtain the desired aryl sulfinate as a white solid. The product was employed in the next step without further purification.

c) General procedure for the preparation of selenosulfonates:

Selenosulfonates were synthesized by following the reported procedure.[20]

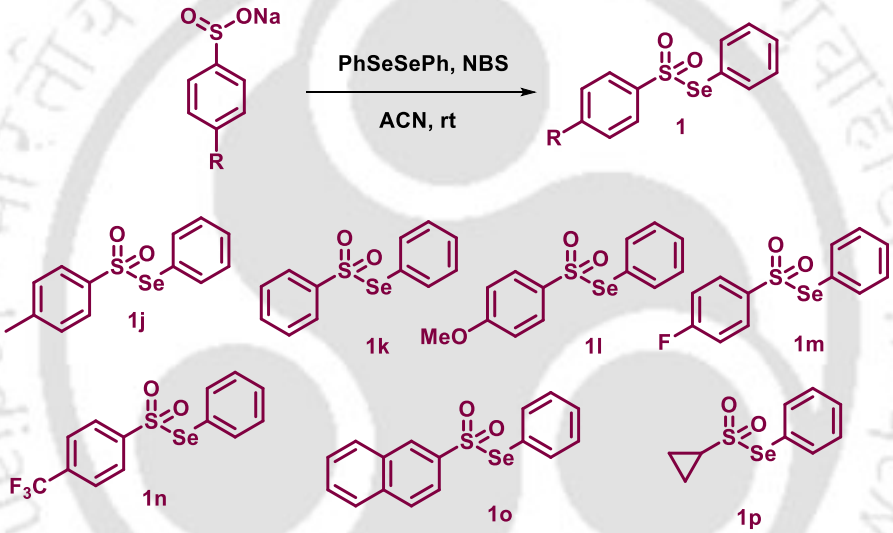

Sodium sulfinate (8 mmol, 4.0 equiv.), diphenyl diselenide (2 mmol, 1.0 equiv.), and NBS (4 mmol, 2.0 equiv.) was taken in a round bottom flask, then MeCN (10 mL) was added and the reaction mixture was stirred at room temperature for 3 hours. The reaction was monitored through TLC and after the complete consumption of diphenyl diselenide, the MeCN was evaporated, and the residue was diluted with ethyl acetate and washed with water. The organic layer was collected and dried over anhydrous Na_2SO_4. The solvent was evaporated under reduced pressure to obtain the crude product. Further, the crude product was purified by column chromatography with ethyl acetate and petroleum ether as the eluent to obtain the pure selenosulfonates **4.1**.

d) General procedure for the synthesis of sulfonylated dihydropyrrole 3-carboxaldehydes:

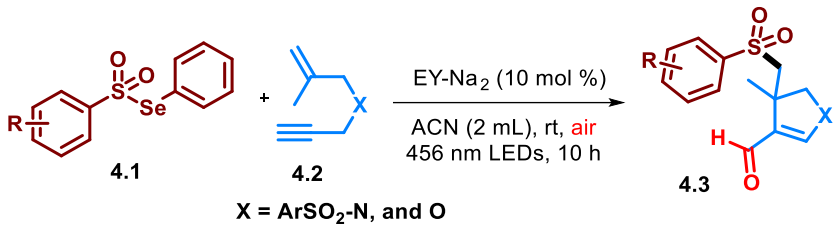

The selenosulfonates **4.1** (0.30 mmol, 1.2 equiv.), 1,6-enynes **4.2** (0.25 mmol, 1 equiv.) and Eosin Y (10 mol%, 0.1 equiv.) was taken in an oven-dried reaction tube with a magnetic bead. After that dry ACN (2 mL) was added and the reaction mixture was allowed to stir under the 456 nm LED irradiation at room temperature in an open-air atmosphere for 10 h. The reaction was monitored by TLC and after completion of the reaction the solvent was evaporated under reduced pressure to get the crude product. Further, the purification of the crude product was done by column chromatography on silica gel by using petroleum ether and ethyl acetate as the eluent.

e) General procedure for the synthesis of tricyclic sulfone:

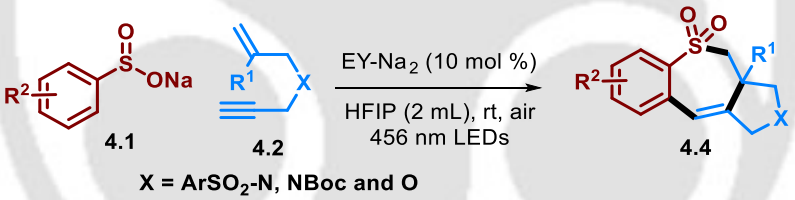

The sodium aryl sulfinates **4.1** (0.50 mmol, 2 equiv.) 1,6-enynes **4.1** (0.25 mmol, 1 equiv.), and Eosin Y (10 mol%, 0.1 equiv.) was taken in an oven-dried reaction tube with a magnetic bead. After that HFIP (2 mL) was added and the reaction mixture was allowed to stir under the 456 nm LED irradiation at room temperature in an open-air atmosphere for 2 h. The reaction was monitored by TLC and after completion of the reaction, the reaction mixture was evaporated under reduced pressure to get the crude product. Furthermore, the purification of crude product was done by column chromatography on silica gel by using petroleum ether and ethyl acetate as the eluent.

4.10 Analytical data:

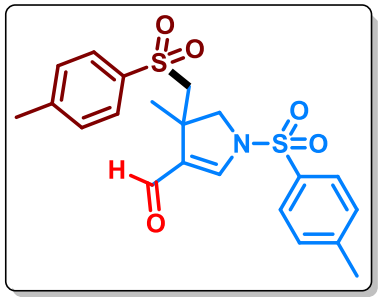

4-methyl-1-tosyl-4-(tosylmethyl)-4,5-dihydro-1H-pyrrole-3-carbaldehyde (**4.3a**): Colourless oil, (50 % ethyl acetate in petroleum ether) yield: (86 mg) 79 %; **^{1}H NMR** (500 MHz, $CDCl_3$) δ 9.30 (s, 1H), 7.77 (d, *J* = 8.3 Hz, 2H), 7.62 (d, *J* = 6.4 Hz, 2H), 7.41 (d, *J* = 8.4 Hz, 2H), 7.32 (s, 1H), 7.30 (d, *J* = 7.8 Hz, 2H), 4.39 (d, *J* = 11.0 Hz, 1H), 3.71 – 3.63 (m, 2H), 3.35 (d, *J* = 14.5 Hz, 1H), 2.46 (s, 3H), 2.42 (s, 3H), 1.38 (s, 3H). **^{13}C NMR** (125 MHz, $CDCl_3$) δ 185.2, 148.1, 145.5, 144.9, 137.6, 133.2, 130.4, 129.9, 128.9, 127.9, 127.5, 60.8, 59.7, 45.4, 25.5, 21.8, 21.7. **HRMS** (ESI-TOF) m/z: $[M+H]^+$ Calcd for $C_{21}H_{24}NO_5S_2$ 434.1091; Found 434.1103.

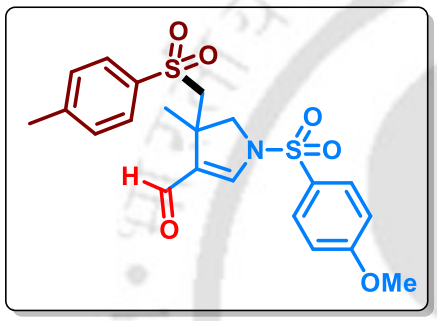

1-((4-methoxyphenyl)sulfonyl)-4-methyl-4-(tosylmethyl)-4,5-dihydro-1H-pyrrole-3-carbaldehyde (**4.3b**): Colourless oil, (50 % ethyl acetate in petroleum ether) yield: (87 mg) 77 %; **^{1}H NMR** (500 MHz, $CDCl_3$) δ 9.30 (s, 1H), 7.83 (d, *J* = 7.8 Hz, 2H), 7.63 (d, *J* = 7.2 Hz, 2H), 7.34 – 7.26 (m, 3H), 7.07 (d, *J* = 7.5 Hz, 2H), 4.39 (d, *J* = 11.2 Hz, 1H), 3.89 (s, 3H), 3.69 – 3.64 (m, 2H), 3.36 (d, *J* = 14.3 Hz, 1H), 2.42 (s, 3H), 1.40 (s, 3H). **^{13}C NMR** (125 MHz, $CDCl_3$) δ 185.2, 164.2, 148.2, 145.0, 137.8, 129.92, 129.88, 128.8, 127.9, 127.6, 115.0, 60.9, 59.7, 55.9, 45.4, 25.6, 21.7. **HRMS** (ESI-TOF) m/z: $[M+H]^+$ Calcd for $C_{21}H_{24}NO_6S_2$ 450.1040; Found 450.1048.

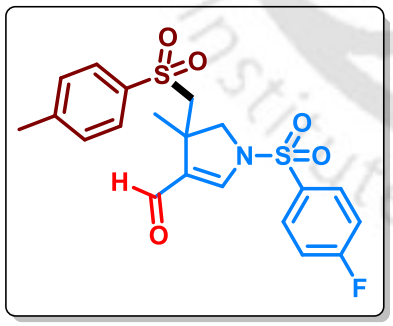

1-((4-fluorophenyl)sulfonyl)-4-methyl-4-(tosylmethyl)-4,5-dihydro-1H-pyrrole-3-carbaldehyde (**4.3c**): Colourless oil, (50 % ethyl acetate in petroleum ether) yield: (78 mg) 71 %; **^{1}H NMR** (500 MHz, $CDCl_3$) δ 9.34 (s, 1H), 7.97 – 7.90 (m, 2H), 7.65 – 7.58 (m, 2H), 7.33 – 7.28 (m, 5H), 4.43 (d, *J* = 11.0 Hz, 1H), 3.71 (d, *J* = 10.4 Hz, 1H), 3.56 (d, *J* = 14.4 Hz, 1H), 3.43 (d, *J* = 14.4 Hz, 1H), 2.43 (s, 3H), 1.41 (s, 3H). **^{13}C NMR** (125 MHz, $CDCl_3$) δ 185.2, 166.0 (d, *J* = 265.8 Hz), 147.5, 145.0, 137.6, 132.3 (d, *J* = 3.2 Hz), 130.5 (d, *J* = 9.6 Hz), 129.9, 129.0, 127.8, 117.1 (d, *J* = 22.6 Hz), 60.6, 59.5, 45.4, 25.9, 21.6. **^{19}F NMR** (471 MHz, $CDCl_3$) δ -101.95. **HRMS** (ESI-TOF) m/z: $[M+H]^+$ Calcd for $C_{20}H_{21}FNO_5S_2$ 438.0840; Found 438.0846.

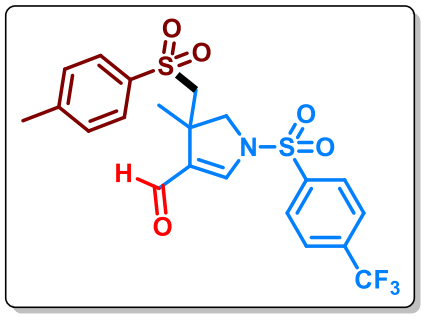

4-methyl-4-(tosylmethyl)-1-((4-(trifluoromethyl)phenyl)sulfonyl)-4,5-dihydro-1H-pyrrole-3-carbaldehyde (**4.3d**): Colourless oil, (50 % ethyl acetate in petroleum ether) yield: (77 mg) 63 %; **^{1}H NMR** (500 MHz, $CDCl_3$) δ 9.36 (s, 1H), 8.06 (d, *J* = 7.6 Hz, 2H), 7.88 (d, *J* = 6.9 Hz, 2H), 7.59 (d, *J* = 7.3 Hz, 2H), 7.37 (s, 1H), 7.29 (d, *J* = 6.9 Hz, 2H), 4.47 (d, *J* = 10.9 Hz, 1H), 3.74 (d, *J* = 10.7 Hz, 1H), 3.54 (d, *J* = 14.4 Hz, 1H), 3.43 (d, *J* = 14.3 Hz, 1H), 2.41 (s, 3H), 1.41 (s, 3H). **^{13}C NMR** (125 MHz, $CDCl_3$) δ 185.34, 147.14, 145.05, 139.83, 137.52, 135.6 (q, *J* = 33.1 Hz), 129.91, 129.41, 128.15, 127.71, 126.9 (q, *J* = 3.8 Hz), 123.0 (q, *J* = 271.5 Hz), 60.6, 59.6, 45.4, 26.0, 21.6. **^{19}F NMR** (471 MHz, $CDCl_3$) δ -63.2. **HRMS** (ESI-TOF) m/z: $[M+H]^+$ Calcd for $C_{21}H_{21}F_3NO_5S_2$ 488.0808; Found 488.0761.

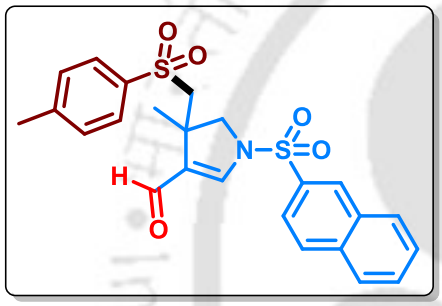

4-methyl-1-(naphthalen-2-ylsulfonyl)-4-(tosylmethyl)-4,5-dihydro-1H-pyrrole-3-carbaldehyde (**4.3e**): Colourless oil, (50 % ethyl acetate in petroleum ether) yield: (79 mg) 67 %; ^{1}H NMR (500 MHz, $CDCl_3$) δ 9.33 (s, 1H), 8.52 (s, 1H), 8.07-8.05 (m, 2H), 7.96 (d, *J* = 8.2 Hz, 1H), 7.81 (d, *J* = 8.7 Hz, 1H), 7.72 – 7.68 (m, 2H), 7.52 (d, *J* = 8.4 Hz, 2H), 7.39 (s, 1H), 7.21 (d, *J* = 8.4 Hz, 2H), 4.48 (d, *J* = 11.2 Hz, 1H), 3.75 (d, *J* = 11.2 Hz, 1H), 3.63 (d, *J* = 14.5 Hz, 1H), 3.29 (d, *J* = 14.5 Hz, 1H), 2.39 (s, 3H), 1.39 (s, 3H). **^{13}C NMR** (125 MHz, $CDCl_3$) δ 185.1, 147.9, 144.8, 137.6, 135.4, 133.1, 132.1, 130.2, 129.8, 129.7, 129.6, 129.0, 128.2, 128.1, 127.8, 121.7, 60.8, 59.8, 45.5, 25.4, 21.6. **HRMS** (ESI-TOF) m/z: $[M+H]^+$ Calcd for $C_{24}H_{24}NO_5S_2$ 470.1091; Found 470.1097.

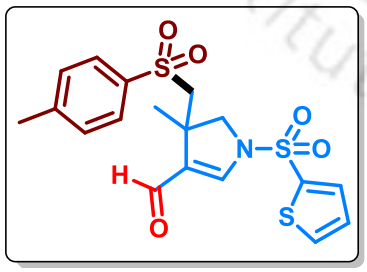

4-methyl-1-(thiophen-2-ylsulfonyl)-4-(tosylmethyl)-4,5-dihydro-1H-pyrrole-3-carbaldehyde (**4.3f**): Colourless oil, (50 % ethyl acetate in petroleum ether) yield: (73 mg) 69 %; **^{1}H NMR** (500 MHz, $CDCl_3$) δ 9.34 (s, 1H), 7.76 – 7.74 (m, 2H), 7.64 (d, *J* = 7.4 Hz, 2H), 7.32 – 7.28 (m, 3H), 7.22 – 7.19 (m, 1H), 4.49 (d, *J* = 11.1 Hz, 1H), 3.74 (d, *J* = 11.1 Hz, 1H), 3.61 (d, *J* = 14.5 Hz, 1H), 3.44 (d, *J* = 14.3 Hz, 1H), 2.42 (s, 3H), 1.40 (s, 3H). **^{13}C NMR** (125 MHz, $CDCl_3$) δ 185.3, 147.3, 145.0, 137.6, 136.1, 134.4, 134.3, 129.9, 129.7, 128.3, 127.9, 60.7, 59.6, 45.4, 25.9, 21.7. **HRMS** (ESI-TOF) m/z: $[M+H]^+$ Calcd for $C_{18}H_{20}NO_5S_3$ 426.0499; Found 426.0495.

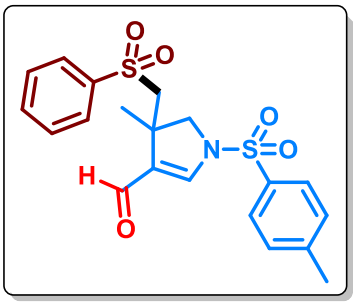

4-methyl-4-((phenylsulfonyl)methyl)-1-tosyl-4,5-dihydro-1H-pyrrole-3-carbaldehyde (**4.3g**): Colourless oil, (50 % ethyl acetate in petroleum ether) yield: (77 mg) 75 %; **^{1}H NMR** (500 MHz, $CDCl_3$) δ 9.30 (s, 1H), 7.78 – 7.74 (m, 4H), 7.64-7.61 (m 1H), 7.51 (t, *J* = 8.0 Hz, 2H), 7.41 (d, *J* = 8.1 Hz, 2H), 7.32 (s, 1H), 4.41 (d, *J* = 11.2 Hz, 1H), 3.69 – 3.66 (m, 2H), 3.39 (d, *J* = 14.3 Hz, 1H), 2.46 (s, 3H), 1.39 (s, 3H). **^{13}C NMR** (125 MHz, $CDCl_3$) δ 185.1, 148.0, 145.5, 140.5, 133.9, 133.2, 130.4, 129.3, 128.8, 127.8, 127.5, 60.7, 59.6, 45.3, 25.6, 21.7. **HRMS** (ESI-TOF) m/z: $[M+H]^+$ Calcd for $C_{20}H_{22}NO_5S_2$ 420.0934; Found 420.0944.

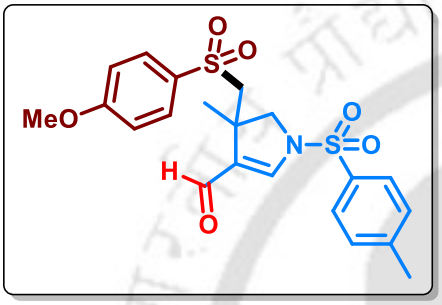

4-(((4-methoxyphenyl)sulfonyl)methyl)-4-methyl-1-tosyl-4,5-dihydro-1H-pyrrole-3-carbaldehyde (**4.3h**): Colourless oil, (50 % ethyl acetate in petroleum ether) yield: (88 mg) 78 %; **^{1}H NMR** (500 MHz, $CDCl_3$) δ 9.27 (s, 1H), 7.75 (d, *J* = 8.0 Hz, 2H), 7.63 (d, *J* = 8.9 Hz, 2H), 7.39 (d, *J* = 8.2 Hz, 2H), 7.29 (s, 1H), 6.93 (d, *J* = 8.8 Hz, 2H), 4.37 (d, *J* = 11.0 Hz, 1H), 3.84 (s, 3H), 3.65 – 3.60 (m, 2H), 3.35 (d, *J* = 14.5 Hz, 1H), 2.44 (s, 3H), 1.35 (s, 3H). **^{13}C NMR** (125 MHz, $CDCl_3$) δ 185.2, 163.8, 148.0, 145.5, 133.2, 132.1, 130.4, 130.1, 128.9, 127.5, 114.4, 61.0, 59.6, 55.8, 45.4, 25.6, 21.8. **HRMS** (ESI-TOF) m/z: $[M+H]^+$ Calcd for $C_{21}H_{24}NO_6S_2$ 450.1040; Found 450.0995.

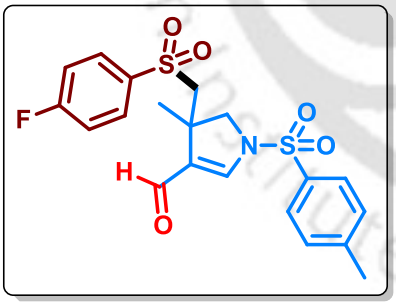

4-(((4-fluorophenyl)sulfonyl)methyl)-4-methyl-1-tosyl-4,5-dihydro-1H-pyrrole-3-carbaldehyde (**4.3i**): Colourless oil, (50 % ethyl acetate in petroleum ether) yield: (67 mg) 61 %; **^{1}H NMR** (500 MHz, $CDCl_3$) δ 9.29 (s, 1H), 7.79 – 7.69 (m, 4H), 7.39 (d, *J* = 8.2 Hz, 2H), 7.32 (s, 1H), 7.16 (t, *J* = 8.6 Hz, 2H), 4.38 (d, *J* = 11.0 Hz, 1H), 3.69 – 3.60 (m, 2H), 3.41 (d, *J* = 14.6 Hz, 1H), 2.44 (s, 3H), 1.37 (s, 3H). **^{13}C NMR** (125 MHz, $CDCl_3$) δ 185.2, 165.9 (d, *J* = 255.3 Hz), 148.2, 145.6, 136.6 (d, *J* = 3.2 Hz), 133.2, 130.8 (d, *J* = 9.6 Hz), 130.4, 128.6, 127.6, 116.6 (d, *J* = 22.5 Hz), 60.9, 59.6, 45.4, 25.7, 21.8. ^{19}F NMR (471 MHz, $CDCl_3$) δ -102.94. **HRMS** (ESI-TOF) m/z: $[M+H]^+$ Calcd for $C_{20}H_{21}FNO_5S_2$ 438.0840; Found 438.0848.

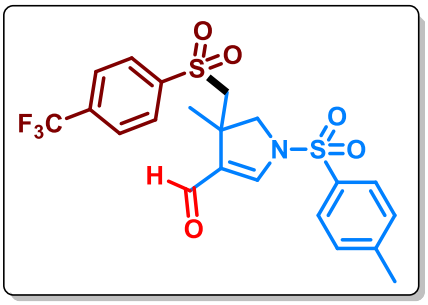

4-methyl-1-tosyl-4-(((4-(trifluoromethyl)phenyl)sulfonyl)methyl)-4,5-dihydro-1H-pyrrole-3-carbaldehyde (**4.3j**): Colourless oil, (50 % ethyl acetate in petroleum ether) yield: (65 mg) 53 %; **^{1}H NMR** (500 MHz, $CDCl_3$) δ 9.31 (s, 1H), 7.90 (d, *J* = 8.4 Hz, 2H), 7.85 – 7.74 (m, 4H), 7.40 (d, *J* = 8.3 Hz, 2H), 7.35 (s, 1H), 4.38 (d, *J* = 11.2 Hz, 1H), 3.69 (d, *J* = 11.6 Hz, 2H), 3.43 (d, *J* = 14.5 Hz, 1H), 2.45 (s, 3H), 1.39 (s, 3H). **^{13}C NMR** (125 MHz, $CDCl_3$) δ 185.28, 148.22, 145.70, 143.94, 135.6 (q, *J* = 33.0 Hz), 133.17, 130.47, 128.57, 128.51, 127.60, 126.5 (q, *J* = 3.7 Hz), 123.1 (q, *J* = 271.4 Hz), 60.68, 59.69, 45.45, 25.72, 21.81. ^{19}F NMR (471 MHz, $CDCl_3$) δ -63.19. **HRMS** (ESI-TOF) m/z: $[M+H]^+$ Calcd for $C_{21}H_{21}F_3NO_5S_2$ 488.0808; Found 488.0812.

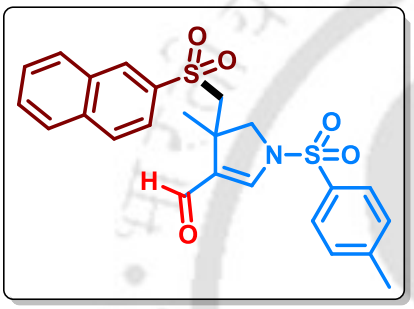

4-methyl-4-((naphthalen-2-ylsulfonyl)methyl)-1-tosyl-4,5-dihydro-1H-pyrrole-3-carbaldehyde (**4.3k**): Colourless oil, (50 % ethyl acetate in petroleum ether) yield: (65 mg) 68 %; **^{1}H NMR** (500 MHz, $CDCl_3$) δ 9.27 (s, 1H), 8.35 (s, 1H), 7.96 – 7.93 (m, 2H), 7.90 (d, *J* = 8.1 Hz, 1H), 7.77 (d, *J* = 8.0 Hz, 2H), 7.71 (d, *J* = 8.7 Hz, 1H), 7.68 – 7.61 (m, 2H), 7.39 (d, *J* = 8.0 Hz, 2H), 7.31 (s, 1H), 4.43 (d, *J* = 11.0 Hz, 1H), 3.76 (d, *J* = 14.5 Hz, 1H), 3.71 (d, *J* = 10.9 Hz, 1H), 3.43 (d, *J* = 14.5 Hz, 1H), 2.44 (s, 3H), 1.41 (s, 3H). **^{13}C NMR** (125 MHz, $CDCl_3$) δ 185.2, 148.1, 145.6, 137.4, 135.3, 133.2, 132.1, 130.4, 129.7, 129.67, 129.53 129.51, 129.0, 128.1, 127.9, 127.6, 122.5, 60.9, 59.8, 45.5, 25.6, 21.8. **HRMS** (ESI-TOF) m/z: $[M+H]^+$ Calcd for $C_{24}H_{24}NO_5S_2$ 470.1091; Found 470.1077.

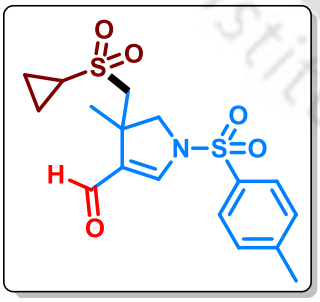

4-((cyclopropylsulfonyl)methyl)-4-methyl-1-tosyl-4,5-dihydro-1H-pyrrole-3-carbaldehyde (**4.3l**): Colourless oil, (50 % ethyl acetate in petroleum ether) yield: (57 mg) 59 %; **^{1}H NMR** (500 MHz, $CDCl_3$) δ 9.48 (s, 1H), 7.74 (d, *J* = 8.3 Hz, 2H), 7.43 – 7.34 (m, 3H), 4.23 (d, *J* = 14.2 Hz, 1H), 3.73 – 3.64 (m, 2H), 3.34 (d, *J* = 11.3 Hz, 1H), 2.46 (s, 3H), 2.35 – 2.30 (m, 1H), 1.45 (s, 3H), 1.24 – 1.16 (m, 1H), 1.12 – 1.06 (m, 1H), 1.05 – 0.93 (m, 2H). **^{13}C NMR** (125 MHz, $CDCl_3$) δ 185.5, 148.2, 145.5, 133.1, 130.4, 129.2, 127.5, 60.0, 58.7, 45.1, 32.0, 25.4, 21.8, 5.29, 5.27. **HRMS** (ESI-TOF) m/z: $[M+H]^+$ Calcd for $C_{17}H_{22}NO_5S_2$ 384.0934; Found 384.0929.

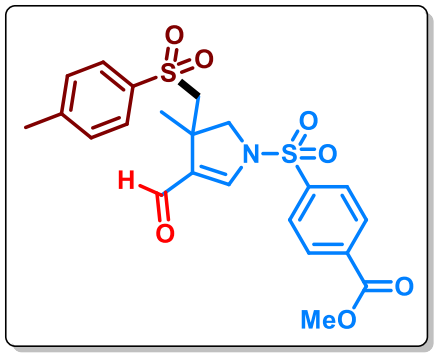

methyl 4-((4-formyl-3-methyl-3-(tosylmethyl)-2,3-dihydro-1H-pyrrol-1-yl)sulfonyl)benzoate (**4.3m**): Colourless oil, (50 % ethyl acetate in petroleum ether) yield: (75 mg) 63 %; **^{1}H NMR** (500 MHz, $CDCl_3$) δ 9.34 (s, 1H), 8.27 (d, J = 7.8 Hz, 2H), 7.98 (d, J = 7.6 Hz, 2H), 7.60 (d, J = 7.1 Hz, 2H), 7.32 (s, 1H), 7.30 (d, J = 6.7 Hz, 2H), 4.45 (d, J = 10.9 Hz, 1H), 3.97 (s, 3H), 3.73 (d, J = 11.1 Hz, 1H), 3.56 (d, J = 13.9 Hz, 1H), 3.40 (d, J = 14.4 Hz, 1H), 2.42 (s, 3H), 1.40 (s, 3H). **^{13}C NMR** (125 MHz, $CDCl_3$) δ 179.2, 159.3, 141.2, 139.1, 134.1, 131.7, 129.3, 124.9, 124.0, 123.4, 121.9, 121.6, 54.8, 53.7, 46.9, 39.5, 20.0, 15.7. **HRMS** (ESI-TOF) m/z: $[M+H]^+$ Calcd for $C_{22}H_{24}NO_7S_2$ 478.0989; Found 478.0952.

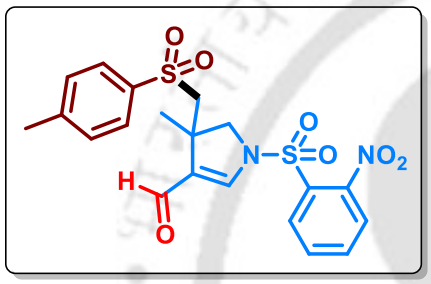

4-methyl-1-((2-nitrophenyl)sulfonyl)-4-(tosylmethyl)-4,5-dihydro-1H-pyrrole-3-carbaldehyde (**4.3n**): Colourless oil, (50 % ethyl acetate in petroleum ether) yield: (59 mg) 51 %; **^{1}H NMR** (500 MHz, $CDCl_3$) δ 9.31 (s, 1H), 8.20 (d, J = 6.4 Hz, 1H), 7.86 – 7.78 (m, 3H), 7.64 (d, J = 7.0 Hz, 2H), 7.39 (s, 1H), 7.30 (d, J = 7.3 Hz, 2H), 4.57 (d, J = 10.6 Hz, 1H), 3.81 (d, J = 10.6 Hz, 1H), 3.67 – 3.49 (m, 2H), 2.42 (s, 3H), 1.47 (s, 3H). **^{13}C NMR** (125 MHz, $CDCl_3$) δ 185.3, 148.3, 148.2, 145.1, 137.5, 135.4, 132.8, 132.3, 130.0, 129.9, 128.1, 127.8, 125.3, 61.1, 59.9, 45.5, 26.1, 21.8. **HRMS** (ESI-TOF) m/z: $[M+H]^+$ Calcd for $C_{20}H_{21}N_2O_7S_2$ 465.0785; Found 465.0758.

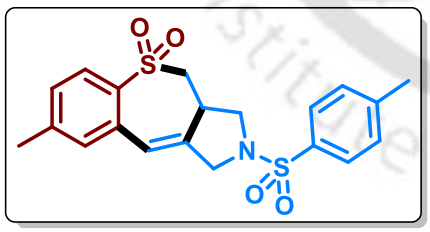

8-methyl-2-tosyl-2,3,3a,4-tetrahydro-1H-benzo[6,7]thiepino[3,4-c]pyrrole 5,5-dioxide[9] (**4.4a**): White solid, (50 % ethyl acetate in petroleum ether) yield: (72 mg) 71 %; **^{1}H NMR** (500 MHz, $CDCl_3$) δ 7.98 (d, *J* = 8.0 Hz, 1H), 7.73 (d, *J* = 8.3 Hz, 2H), 7.36 (d, *J* = 8.2 Hz, 2H), 7.20 (d, *J* = 8.2 Hz, 1H), 7.07 (s, 1H), 6.42 (s, 1H), 4.18 (d, *J* = 14.6 Hz, 1H), 4.03 (d, *J* = 14.5 Hz, 1H), 3.71 (dd, *J* = 9.5, 7.4 Hz, 1H), 3.52 (dd, *J* = 13.2, 4.1 Hz, 1H), 3.42 – 3.28 (m, 2H), 3.05 (t, *J* = 9.1 Hz, 1H), 2.44 (s, 3H), 2.38 (s, 3H). **^{13}C NMR** (125 MHz, $CDCl_3$) δ 144.1, 143.9, 141.7, 136.1, 133.0, 132.3, 132.0, 129.6, 127.9, 127.4, 127.0, 122.6, 55.3, 53.7, 51.9, 38.3, 21.2, 20.9.

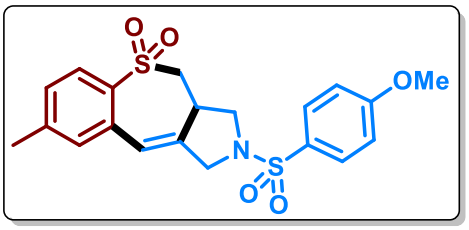

2-((4-methoxyphenyl)sulfonyl)-8-methyl-2,3,3a,4-tetrahydro-1H-benzo[6,7]thiepino[3,4-c]pyrrole 5,5-dioxide[9] (**4.4b**): White solid, (50 % ethyl acetate in petroleum ether) yield: (70 mg) 67 %; **^{1}H NMR** (500 MHz, $CDCl_3$) δ 7.97 (d, *J* = 8.0 Hz, 1H), 7.77 (d, *J* = 8.9 Hz, 2H), 7.19 (d, *J* = 8.0 Hz, 1H), 7.07 (s, 1H), 7.01 (d, *J* = 8.9 Hz, 2H), 6.41 (s, 1H), 4.16 (d, *J* = 14.5 Hz, 1H), 4.01 (d, *J* = 14.6 Hz, 1H), 3.87 (s, 3H), 3.68 (dd, *J* = 9.5, 7.4 Hz, 1H), 3.53 (dd, *J* = 13.1, 4.0 Hz, 1H), 3.45 – 3.29 (m, 2H), 3.04 (t, *J* = 9.1 Hz, 1H), 2.38 (s, 3H). **^{13}C NMR** (125 MHz, $CDCl_3$) δ 163.5, 144.6, 142.3, 136.6, 133.4, 132.6, 123.0, 128.4, 127.4, 127.2, 123.1, 114.7, 56.0, 55.8, 54.1, 52.3, 38.8, 21.4.

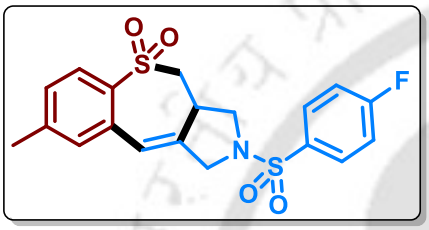

2-((4-fluorophenyl)sulfonyl)-8-methyl-2,3,3a,4-tetrahydro-1H-benzo[6,7]thiepino[3,4-c]pyrrole[9] 5,5-dioxide (**4.4c**): White solid, (50 % ethyl acetate in petroleum ether) yield: (62 mg) 61 %; **^{1}H NMR** (500 MHz, $CDCl_3$) δ 8.00 (d, *J* = 8.2 Hz, 1H), 7.94 – 7.83 (m, 2H), 7.31 – 7.18 (m, 3H), 7.09 (s, 1H), 6.43 (s, 1H), 4.21 (d, *J* = 14.5 Hz, 1H), 4.05 (d, *J* = 14.5 Hz, 1H), 3.76 – 3.69 (m, 1H), 3.54 (dd, *J* = 13.7, 4.6 Hz, 1H), 3.50 – 3.39 (m, 1H), 3.39 – 3.32 (m, 1H), 3.08 (t, *J* = 9.2 Hz, 1H), 2.39 (s, 3H). **^{13}C NMR** (125 MHz, $CDCl_3$) δ 166.5 (d, J = 254.5 Hz), 144.6, 141.7, 136.6, 133.4, 132.3, 132.0 (d, J = 3.2 Hz), 130.4 (d, J = 9.3 Hz), 128.4, 127.4, 123.2, 116.7 (d, J = 22.4 Hz), 55.5, 54.0, 52.2, 38.8, 21.3. **^{19}F NMR** (471 MHz, $CDCl_3$) δ -104.0.

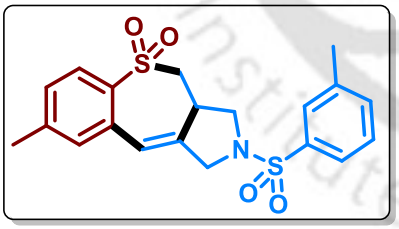

8-methyl-2-(m-tolylsulfonyl)-2,3,3a,4-tetrahydro-1H-benzo[6,7]thiepino[3,4-c]pyrrole 5,5-dioxide[9] (**4.4d**): White solid, (50 % ethyl acetate in petroleum ether) yield: (70 mg) 69 %; **^{1}H NMR** (500 MHz, $CDCl_3$) δ 7.99 (d, *J* = 8.1 Hz, 1H), 7.67 – 7.61 (m, 2H), 7.48 – 7.36 (m, 2H), 7.20 (d, *J* = 8.1 Hz, 1H), 7.08 (s, 1H), 6.42 (s, 1H), 4.20 (d, *J* = 14.5 Hz, 1H), 4.05 (d, *J* = 14.5 Hz, 1H), 3.72 (t, *J* = 8.5 Hz, 1H), 3.53 (dd, *J* = 13.6, 4.6 Hz, 1H), 3.45 – 3.37 (m, 1H), 3.36 – 3.28 (m, 1H), 3.07 (t, *J* = 9.2 Hz, 1H), 2.45 (s, 3H), 2.38 (s, 3H). **^{13}C NMR** (125 MHz, $CDCl_3$) δ 144.5, 142.1, 139.7, 136.5, 135.6, 134.2, 133.4, 132.4, 129.2, 128.3, 128.0, 127.4, 124.8, 123.0, 55.7, 54.0, 52.2, 38.7, 21.4, 21.3. **HRMS** (ESI-TOF) m/z: $[M+H]^+$ Calcd for $C_{20}H_{22}NO_4S_2$ 404.0985; Found 404.0988.

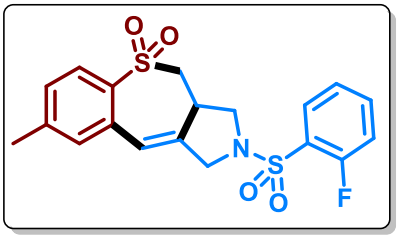

2-((2-fluorophenyl)sulfonyl)-8-methyl-2,3,3a,4-tetrahydro-1H-benzo[6,7]thiepino[3,4-c]pyrrole 5,5-dioxide (**4.4e**): White solid, (50 % ethyl acetate in petroleum ether) yield: (69 mg) 68 %; **^{1}H NMR** (500 MHz, $CDCl_3$) δ 8.01 (d, *J* = 8.2 Hz, 1H), 7.92 (t, *J* = 7.4 Hz, 1H), 7.61 (q, *J* = 6.5 Hz, 1H), 7.32 (t, *J* = 7.7 Hz, 1H), 7.24 (dd, *J* = 17.3, 7.4 Hz, 2H), 7.12 (s, 1H), 6.45 (s, 1H), 4.33 (d, *J* = 14.3 Hz, 1H), 4.19 (d, *J* = 14.5 Hz, 1H), 3.93 (t, *J* = 8.7 Hz, 1H), 3.54 (d, *J* = 9.1 Hz, 2H), 3.36 (t, *J* = 14.7 Hz, 1H), 3.26 (t, *J* = 9.5 Hz, 1H), 2.40 (s, 3H). ^{13}C NMR (126 MHz, $CDCl_3$) δ 159.1 (d, J = 253.7 Hz), 144.7, 142.1, 136.8, 135.6 (d, J = 8.4 Hz), 133.8, 132.2, 131.5, 128.5, 127.5, 125.7 (d, J = 14.7 Hz), 124.8 (d, J = 3.7 Hz), 123.2, 117.6 (d, J = 21.9 Hz), 54.8, 53.9 (d, J = 2.7 Hz), 52.0 (d, J = 2.9 Hz), 39.3, 21.5. ^{19}F NMR (471 MHz, $CDCl_3$) δ -107.4. **HRMS** (ESI-TOF) m/z: $[M+H]^+$ Calcd for $C_{19}H_{19}FNO_4S_2$ 408.0735; Found 408.0732.

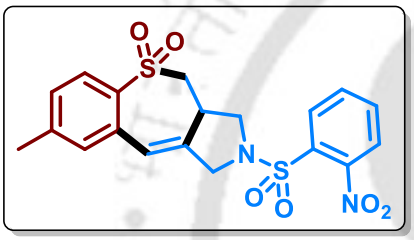

8-methyl-2-((2-nitrophenyl)sulfonyl)-2,3,3a,4-tetrahydro-1H-benzo[6,7]thiepino[3,4-c]pyrrole 5,5-dioxide (**4.4f**): White solid, (50 % ethyl acetate in petroleum ether) yield: (68 mg) 63 %; **^{1}H NMR** (500 MHz, DMSO) δ 8.08 (d, *J* = 7.8 Hz, 1H), 8.03 (d, *J* = 7.8 Hz, 1H), 7.93 (t, *J* = 7.7 Hz, 2H), 7.89 (t, *J* = 7.5 Hz, 1H), 7.32 (d, *J* = 8.4 Hz, 2H), 6.64 (s, 1H), 4.39 (d, *J* = 14.5 Hz, 1H), 4.18 (d, *J* = 15.4 Hz, 1H), 3.92 (t, *J* = 8.7 Hz, 1H), 3.81 (dd, *J* = 14.6, 6.4 Hz, 1H), 3.70 – 3.60 (m, 1H), 3.48 – 3.40 (m, 1H), 3.25 (t, *J* = 9.9 Hz, 1H), 2.37 (s, 3H).**^{13}C NMR** (125 MHz, DMSO) δ 147.9, 144.0, 142.1, 137.1, 135.0, 133.8, 132.6, 131.6, 130.2, 129.3, 128.1, 126.1, 124.4, 122.3, 53.9, 51.9, 51.7, 20.7. **HRMS** (ESI-TOF) m/z: $[M+H]^+$ Calcd for $C_{19}H_{19}N_2O_6S_2$ 435.0680; Found 435.0671.

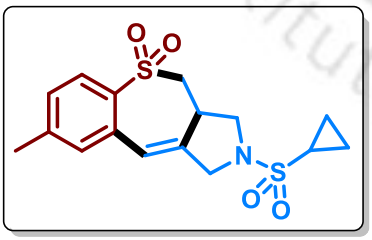

2-(cyclopropylsulfonyl)-8-methyl-2,3,3a,4-tetrahydro-1H-benzo[6,7]thiepino[3,4-c]pyrrole 5,5-dioxide[9] (**4.4g**): White solid, (50 % ethyl acetate in petroleum ether) yield: (52 mg) 58 %; **^{1}H NMR** (500 MHz, $CDCl_3$) δ 8.02 (d, *J* = 8.0 Hz, 1H), 7.23 (d, *J* = 8.2 Hz, 1H), 7.15 (s, 1H), 6.51 (s, 1H), 4.37 (d, *J* = 14.6 Hz, 2H), 4.23 (d, *J* = 14.7 Hz, 1H), 3.84 (t, *J* = 8.5 Hz, 1H), 3.66 – 3.58 (m, 2H), 3.49 – 3.40 (m, 1H), 3.29 (t, *J* = 9.3 Hz, 1H), 2.41 (s, 3H), 1.31 – 1.15 (m, 2H), 1.04 (d, *J* = 7.8 Hz, 2H), 0.89 – 0.85 (m, 1H). **^{13}C NMR** (125 MHz, $CDCl_3$) δ 144.7, 142.6, 136.7, 133.6, 132.5, 128.4, 127.5, 123.1, 55.4, 54.2, 52.3, 39.3, 26.9, 21.5, 4.93, 4.87.

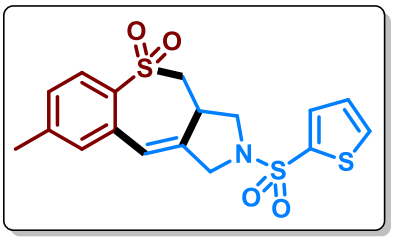

8-methyl-2-(thiophen-2-ylsulfonyl)-2,3,3a,4-tetrahydro-1H-benzo[6,7]thiepino[3,4-c]pyrrole 5,5-dioxide[9] (**4.4h**): White solid, (50 % ethyl acetate in petroleum ether) yield: (52 mg) 53 %; **^{1}H NMR** (500 MHz, $CDCl_3$) δ 8.00 (d, *J* = 8.0 Hz, 1H), 7.65 (d, *J* = 9.6 Hz, 2H), 7.22 (d, *J* = 8.0 Hz, 1H), 7.19 (s, 1H), 7.11 (s, 1H), 6.45 (s, 1H), 4.27 (d, *J* = 14.5 Hz, 1H), 4.12 (d, *J* = 14.6 Hz, 1H), 3.78 (t, *J* = 8.7 Hz, 1H), 3.54-3.51 (m, 1H), 3.47 – 3.39 (m, 1H), 3.36-3.31 (m, 1H), 3.14 (t, *J* = 10.4 Hz, 1H), 2.40 (s, 3H). **^{13}C NMR** (125 MHz, $CDCl_3$) δ 144.6, 141.7, 136.6, 135.7, 133.5, 133.0, 132.7, 132.2, 128.4, 127.9, 127.4, 123.2, 55.2, 54.4, 52.4, 38.8, 21.3.

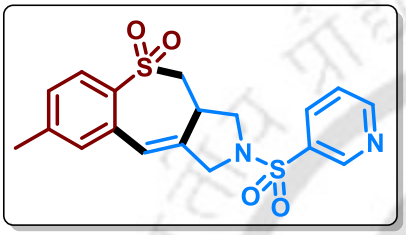

8-methyl-2-(pyridin-3-ylsulfonyl)-2,3,3a,4-tetrahydro-1H-benzo[6,7]thiepino[3,4-c]pyrrole 5,5-dioxide (**4.4i**): White solid, (50 % ethyl acetate in petroleum ether) yield: (54 mg) 55 %; ^{1}H NMR (500 MHz, $CDCl_3$) δ 9.07 (s, 1H), 8.85 (d, *J* = 3.5 Hz, 1H), 8.13 (d, *J* = 7.7 Hz, 1H), 7.98 (d, *J* = 8.0 Hz, 1H), 7.55 – 7.49 (m, 1H), 7.21 (d, *J* = 8.4 Hz, 1H), 7.09 (s, 1H), 6.43 (s, 1H), 4.25 (d, *J* = 14.5 Hz, 1H), 4.08 (d, *J* = 14.5 Hz, 1H), 3.77 (t, *J* = 8.6 Hz, 1H), 3.54 (dd, *J* = 13.8, 4.9 Hz, 1H), 3.46 (t, *J* = 12.2 Hz, 1H), 3.38 – 3.29 (m, 1H), 3.12 (t, *J* = 9.3 Hz, 1H), 2.38 (s, 3H). **^{13}C NMR** (125 MHz, $CDCl_3$) δ 154.0, 148.4, 144.7, 141.3, 136.7, 135.3, 133.7, 133.0, 132.1, 128.6, 127.5, 124.1, 123.5, 55.1, 54.1, 52.2, 39.0, 21.4. **HRMS** (ESI-TOF) m/z: $[M+H]^+$ Calcd for $C_{18}H_{19}N_2O_4S_2$ 391.0781; Found 391.0773.

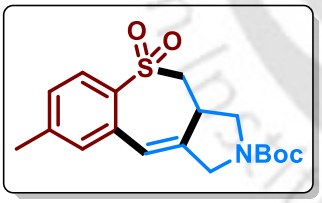

tert-butyl 8-methyl-3a,4-dihydro-1H-benzo[6,7]thiepino[3,4-c]pyrrole-2(3H)-carboxylate 5,5-dioxide (**4.4j**): White solid, (50 % ethyl acetate in petroleum ether) yield: (57 mg) 65 %; **^{1}H NMR** (500 MHz, $CDCl_3$) δ 8.03 (d, *J* = 8.1 Hz, 1H), 7.21 (d, *J* = 8.2 Hz, 1H), 7.16-7.18 (m, 1H), 6.47 (s, 1H), 4.40 – 4.28 (m, 1H), 4.14 (d, *J* = 15.4 Hz, 1H), 3.94-3.87 (m, 1H), 3.66 – 3.46 (m, 2H), 3.42-3.33 (m, 1H), 3.20 (t, *J* = 10.0 Hz, 1H), 2.40 (s, 3H), 1.48 (s, 9H).**^{13}C NMR** (125 MHz, $CDCl_3$) δ 154.1, 144.5, 144.3, 143.4, 136.8, 134.0, 133.7, 132.6, 132.2, 128.2, 127.4, 127.2, 122.5, 122.3, 80.3, 55.0, 53.8, 53.3, 50.7, 50.1, 39.3, 38.7, 28.6, 21.5. **HRMS** (ESI-TOF) m/z: $[M+Na]^+$ Calcd for $C_{18}H_{23}NNaO_4S$ 372.1240; Found 372.1236.

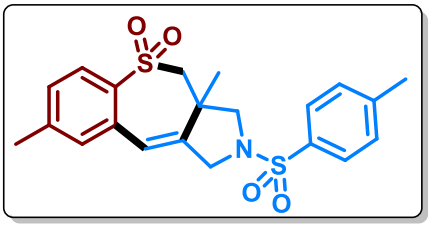

3a,8-dimethyl-2-tosyl-2,3,3a,4-tetrahydro-1H-benzo[6,7]thiepino[3,4-c]pyrrole 5,5-dioxide (**4.4k**): White solid, (50 % ethyl acetate in petroleum ether) yield: (53 mg) 51 %; **^{1}H NMR** (600 MHz, $CDCl_3$) δ 7.89 (d, *J* = 8.1 Hz, 1H), 7.72 (d, *J* = 8.2 Hz, 2H), 7.36 (d, *J* = 8.2 Hz,

2H), 7.17 (d, *J* = 8.3 Hz, 1H), 7.04 (s, 1H), 6.36 (s, 1H), 4.23 (d, *J* = 14.1 Hz, 1H), 3.92 (d, *J* = 14.1 Hz, 1H), 3.62 (q, *J* = 15.1 Hz, 2H), 3.30 (s, 2H), 2.44 (s, 3H), 2.39 (s, 3H), 1.22 (s, 3H). **^{13}C NMR** (150 MHz, $CDCl_3$) δ 147.1, 144.9, 144.4, 136.3, 134.3, 132.5, 131.4, 130.1, 128.2, 127.9, 127.8, 121.2, 67.8, 61.0, 53.9, 42.9, 26.6, 21.7, 21.5. **HRMS** (ESI-TOF) m/z: $[M+H]^+$ Calcd for $C_{21}H_{24}NO_4S_2$ 418.1142; Found 418.1148.

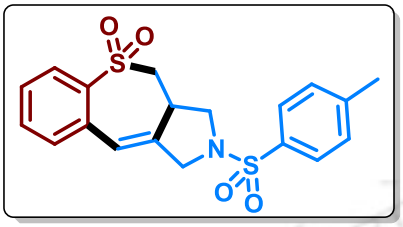

2-tosyl-2,3,3a,4-tetrahydro-1H-benzo[6,7]thiepino[3,4-c]pyrrole 5,5-dioxide (**4.4l**): White solid, (50 % ethyl acetate in petroleum ether) yield: (67 mg) 69 %; **^{1}H NMR** (500 MHz, $CDCl_3$) δ 8.12 (d, *J* = 7.9 Hz, 1H), 7.74 (d, *J* = 8.3 Hz, 2H), 7.56 (t, *J* = 7.6 Hz, 1H), 7.41 (s, 1H), 7.36 (d, *J* = 6.1 Hz, 2H), 7.28 (d, *J* = 11.7 Hz, 1H), 6.47 (s, 1H), 4.20 (d, *J* = 14.6 Hz, 1H), 4.05 (d, *J* = 14.6 Hz, 1H), 3.78 – 3.63 (m, 1H), 3.56-3.54 (m, 1H), 3.50 – 3.29 (m, 2H), 3.07 (t, *J* = 8.0 Hz, 1H), 2.44 (s, 3H). **^{13}C NMR** (125 MHz, $CDCl_3$) δ 144.5, 142.6, 139.4, 133.8, 132.8, 132.7, 130.1, 123.0, 127.9, 127.8, 127.3, 123.0, 55.8, 54.2, 52.3, 38.8, 21.7. **HRMS** (ESI-TOF) m/z: $[M+H]^+$ Calcd for $C_{19}H_{20}NO_4S_2$ 390.0829; Found 390.0830.

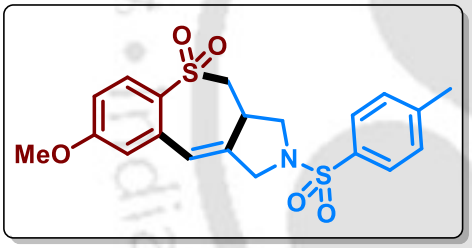

8-methoxy-2-tosyl-2,3,3a,4-tetrahydro-1H-benzo[6,7]thiepino[3,4-c]pyrrole 5,5-dioxide[9] (**4.4m**): White solid, (50 % ethyl acetate in petroleum ether) yield: (70 mg) 67 %; **^{1}H NMR** (500 MHz, $CDCl_3$) δ 8.04 (d, *J* = 8.8 Hz, 1H), 7.73 (d, *J* = 8.3 Hz, 2H), 7.36 (d, *J* = 8.0 Hz, 2H), 6.86 (d, *J* = 8.8 Hz, 1H), 6.74 (s, 1H), 6.41 (s, 1H), 4.16 (d, *J* = 14.5 Hz, 1H), 4.05 (d, *J* = 14.6 Hz, 1H), 3.85 (s, 3H), 3.68-3.66 (m, 1H), 3.56-3.54 (m, 1H), 3.37-3.33 (m, 2H), 3.07 (t, *J* = 8.8 Hz, 1H), 2.44 (s, 3H). **^{13}C NMR** (125 MHz, $CDCl_3$) δ 163.5, 144.5, 142.8, 135.0, 132.8, 131.3, 130.1, 129.9, 127.9, 123.0, 118.3, 112.2, 57.0, 55.8, 54.0, 52.4, 38.7, 21.7. **HRMS** (ESI-TOF) m/z: $[M+H]^+$ Calcd for $C_{20}H_{22}NO_5S_2$ 420.0934; Found 420.0932.

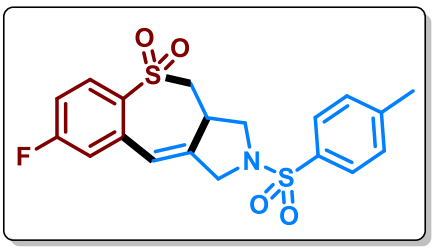

8-fluoro-2-tosyl-2,3,3a,4-tetrahydro-1H-benzo[6,7]thiepino[3,4-c]pyrrole 5,5-dioxide (**4.4n**): White solid, (50 % ethyl acetate in petroleum ether) yield: (62 mg) 61 %; **^{1}H NMR** (500 MHz, $CDCl_3$) δ 8.16 – 8.10 (m, 1H), 7.73 (d, *J* = 8.2 Hz, 2H), 7.36 (d, *J* = 8.2 Hz, 2H), 7.09 (t, *J* = 7.0 Hz, 1H), 6.97 (d, *J* = 6.7 Hz, 1H), 6.42 (s, 1H), 4.18 (d, *J* = 14.7 Hz, 1H), 4.06 (d, *J* = 14.7 Hz, 1H), 3.73 – 3.63 (m, 1H), 3.59-3.55 (m, 1H), 3.42-3.35 (m, 2H), 3.09 (t, *J* = 8.9 Hz, 1H), 2.44 (s, 3H). **^{13}C NMR** (125 MHz, $CDCl_3$) δ 165.5 (d, *J* = 254.3 Hz), 144.6, 144.3,

136.0 (d, J = 8.9 Hz), 135.5 (d, J = 3.2 Hz), 132.7, 130.5 (d, J = 9.6 Hz), 130.2, 127.9, 122.1, 119.3 (d, J = 23.1 Hz), 114.8 (d, J = 21.9 Hz), 56.6, 54.0, 52.3, 38.8, 21.7. ^{19}F NMR (471 MHz, $CDCl_3$) δ -104.4. **HRMS** (ESI-TOF) m/z: $[M+H]^+$ Calcd for $C_{19}H_{19}FNO_4S_2$ 408.0735; Found 408.0732.

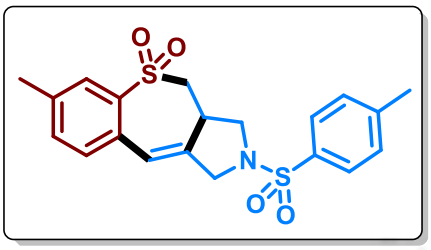

7-methyl-2-tosyl-2,3,3a,4-tetrahydro-1H-benzo[6,7]thiepino[3,4-c]pyrrole 5,5-dioxide (**4.4o**): White solid, (50 % ethyl acetate in petroleum ether) yield: (41 mg) 41 %; **^{1}H NMR** (500 MHz, $CDCl_3$) δ 7.92 (s, 1H), 7.73 (d, J = 8.2 Hz, 2H), 7.36 (d, J = 8.3 Hz, 3H), 7.16 (d, J = 7.9 Hz, 1H), 6.41 (s, 1H), 4.20 (d, J = 14.5 Hz, 1H), 4.02 (d, J = 14.5 Hz, 1H), 3.74 (t, J = 8.6 Hz, 1H), 3.50 (dd, J = 13.7, 4.5 Hz, 1H), 3.45 – 3.48 (m, 1H), 3.33 (t, J = 13.4 Hz, 1H), 3.05 (t, J = 9.3 Hz, 1H), 2.44 (s, 3H), 2.40 (s, 3H). **^{13}C NMR** (125 MHz, $CDCl_3$) δ 144.4, 141.3, 139.2, 138.5, 134.4, 133.1, 132.9, 130.1, 129.6, 127.9, 127.6, 122.9, 55.0, 54.3, 52.4, 38.9, 21.7, 21.2. **HRMS** (ESI-TOF) m/z: $[M+H]^+$ Calcd for $C_{20}H_{22}NO_4S_2$ 404.0985; Found 404.0995.

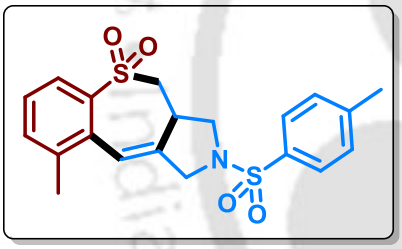

9-methyl-2-tosyl-2,3,3a,4-tetrahydro-1H-benzo[6,7]thiepino[3,4-c]pyrrole 5,5-dioxide (**4.4o'**): White solid, (50 % ethyl acetate in petroleum ether) yield: (17 mg) 17 %; **^{1}H NMR** (500 MHz, $CDCl_3$) δ 7.94 (d, J = 8.2 Hz, 1H), 7.73 (d, J = 8.2 Hz, 2H), 7.42 (d, J = 7.8 Hz, 1H), 7.37 (d, J = 8.2 Hz, 2H), 7.30 (t, J = 7.7 Hz, 1H), 6.61 (s, 1H), 4.27 (d, J = 14.5 Hz, 1H), 3.92 (d, J = 14.5 Hz, 1H), 3.86 (dd, J = 13.8, 6.7 Hz, 1H), 3.69 (t, J = 12.6 Hz, 1H), 3.31 (t, J = 9.5 Hz, 1H), 3.18 (d, J = 7.5 Hz, 2H), 2.46 (s, 3H), 2.28 (s, 3H). **^{13}C NMR** (125 MHz, $CDCl_3$) δ 144.5, 142.4, 138.9, 138.4, 135.7, 134.9, 132.2, 130.1, 128.1, 127.5, 126.3, 121.3, 67.1, 52.5, 52.4, 36.9, 21.8, 20.0. **HRMS** (ESI-TOF) m/z: $[M+H]^+$ Calcd for $C_{20}H_{22}NO_4S_2$ 404.0985; Found 404.0995.

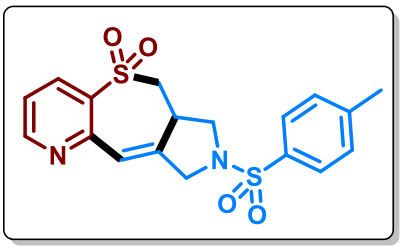

8-tosyl-6a,7,8,9-tetrahydro-6H-pyrrolo[3',4':5,6]thiepino[3,2-b]pyridine 5,5-dioxide (**4.4p**): White solid, (50 % ethyl acetate in petroleum ether) yield: (61 mg) 63 %; **^{1}H NMR** (500 MHz, $CDCl_3$) δ 8.74 (d, J = 6.6 Hz, 1H), 8.37 (d, J = 7.9 Hz, 1H), 7.73 (d, J = 8.3 Hz, 2H), 7.37 – 7.33 (m, 3H), 6.76 (s, 1H), 4.29 (d, J = 15.3 Hz, 1H), 4.07 (d, J = 15.3 Hz, 1H), 3.79 (t, J = 8.6 Hz, 1H), 3.59 – 3.44 (m, 2H), 3.34 (t, J = 12.9 Hz, 1H), 3.07 (t, J = 9.5 Hz, 1H), 2.44 (s, 3H). **^{13}C NMR** (125 MHz, $CDCl_3$) δ 153.5, 150.5, 146.1, 144.6, 136.7, 135.0, 132.6,

130.2, 127.9, 125.6, 121.9, 54.3, 54.1, 52.3, 39.3, 21.7. **HRMS** (ESI-TOF) m/z: $[M+H]^+$ Calcd for $C_{18}H_{19}N_2O_4S_2$ 391.0781; Found 391.0783.

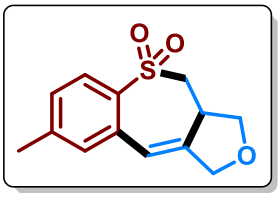

8-methyl-3a,4-dihydro-1H,3H-benzo[6,7]thiepino[3,4-c]furan 5,5-dioxide (**4.4q**): White solid, (50 % ethyl acetate in petroleum ether) yield: (43 mg) 68 %; **^{1}H NMR** (500 MHz, $CDCl_3$) δ 8.03 (d, *J* = 8.2 Hz, 1H), 7.19 (d, *J* = 7.9 Hz, 1H), 7.11 (s, 1H), 6.44 (s, 1H), 4.59 (ABq, *J*=13.8 Hz, 2H), 4.17 (t, *J* = 7.6 Hz, 1H), 3.68 – 3.59 (m, 2H), 3.51 – 3.41 (m, 2H), 2.40 (s, 3H). **^{13}C NMR** (125 MHz, $CDCl_3$) δ 146.9, 144.4, 136.8, 133.8, 133.0, 128.0, 127.5, 120.3, 73.1, 72.6, 56.9, 39.6, 21.4. **HRMS** (ESI-TOF) m/z: $[M+H]^+$ Calcd for $C_{13}H_{15}O_3S$ 251.0737; Found 251.0719.

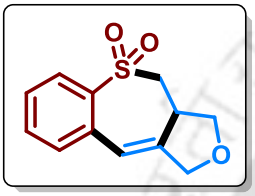

3a,4-dihydro-1H,3H-benzo[6,7]thiepino[3,4-c]furan 5,5-dioxide (**4.4r**): White solid, (50 % ethyl acetate in petroleum ether) yield: (39 mg) 65 %; **^{1}H NMR** (500 MHz, $CDCl_3$) δ 8.16 (d, *J* = 8.0 Hz, 1H), 7.57 (t, *J* = 7.6 Hz, 1H), 7.40 (t, *J* = 7.6 Hz, 1H), 7.32 (d, *J* = 7.6 Hz, 1H), 6.49 (s, 1H), 4.61(ABq, *J*=13.8 Hz, 2H), 4.18 (t, *J* = 7.5 Hz, 1H), 3.70 – 3.60 (m, 2H), 3.57 – 3.44 (m, 2H). **^{13}C NMR** (125 MHz, $CDCl_3$) δ 147.1, 139.6, 133.9, 133.6, 132.4, 127.4, 127.3, 120.2, 73.2, 72.6, 56.7, 39.6. **HRMS** (ESI-TOF) m/z: $[M+Na]^+$ Calcd for $C_{12}H_{12}NaO_3S$ 259.0400; Found 259.0387.

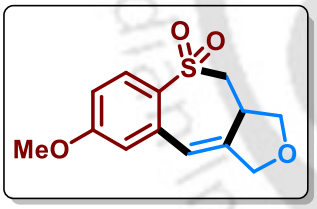

8-methoxy-3a,4-dihydro-1H,3H-benzo[6,7]thiepino[3,4-c]furan 5,5-dioxide (**4.4s**): White solid, (50 % ethyl acetate in petroleum ether) yield: (41 mg) 62 %; **^{1}H NMR** (500 MHz, $CDCl_3$) δ 8.09 (d, *J* = 8.8 Hz, 1H), 6.87 (d, *J* = 8.8 Hz, 1H), 6.79 (s, 1H), 6.46 (s, 1H), 4.63-4.57 (m, 2H), 4.15 (t, *J* = 7.6 Hz, 1H), 3.87 (s, 3H), 3.71 – 3.62 (m, 2H), 3.53 – 3.48 (m, 2H).**^{13}C NMR** (125 MHz, $CDCl_3$) δ 163.5, 147.4, 136.4, 131.5, 130.0, 120.3, 117.7, 111.9, 73.0, 72.7, 58.2, 55.8, 39.7. **HRMS** (ESI-TOF) m/z: $[M+H]^+$ Calcd for $C_{13}H_{15}O_4S$ 267.0686; Found 267.0672.

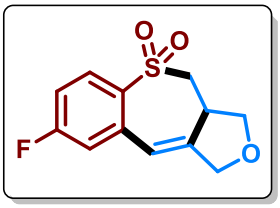

8-fluoro-3a,4-dihydro-1H,3H-benzo[6,7]thiepino[3,4-c]furan 5,5-dioxide (**4.4t**): White solid, (50 % ethyl acetate in petroleum ether) yield: (36 mg) 57 %; **^{1}H NMR** (500 MHz, $CDCl_3$) δ 8.21 – 8.14 (m, 1H), 7.09 (t, *J* = 8.2 Hz, 1H), 7.01 (d, *J* = 9.3 Hz, 1H), 6.46 (s, 1H), 4.62 (s, 2H), 4.17 (t, *J* = 7.4 Hz, 1H), 3.70 – 3.66 (m, 2H), 3.54 – 3.50 (m, 2H). **^{13}C NMR** (125 MHz, $CDCl_3$) δ 166.5 (d, *J* = 254.0 Hz), 148.85, 137.4 (d, *J* = 8.8 Hz), 135.6 (d, *J* = 3.2 Hz), 130.6 (d, *J* = 9.6 Hz), 119.41, 118.8 (d, J = 22.9 Hz), 114.3 (d, *J* = 22.0 Hz), 73.02, 72.60,

57.67, 39.70. **^{19}F NMR** (471 MHz, $CDCl_3$) δ -104.9. **HRMS** (ESI-TOF) m/z: $[M+H]^+$ Calcd for $C_{12}H_{12}FO_3S$ 255.0486; Found 255.0477.

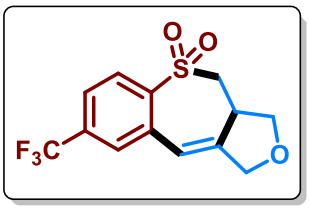

8-(trifluoromethyl)-3a,4-dihydro-1H,3H-benzo[6,7]thiepino[3,4-c]furan 5,5-dioxide (**4.4u**): White solid, (50 % ethyl acetate in petroleum ether) yield: (37 mg) 49 %; ^{1}H NMR (500 MHz, $CDCl_3$) δ 8.30 (d, *J* = 8.3 Hz, 1H), 7.66 (d, *J* = 8.2 Hz, 1H), 7.58 (s, 1H), 6.55 (s, 1H), 4.63 (q, *J* = 14.2 Hz, 2H), 4.24 – 4.16 (m, 1H), 3.76 – 3.65 (m, 2H), 3.59 – 3.46 (m, 2H). ^{13}C NMR (126 MHz, $CDCl_3$) δ 149.5, 142.7, 135.5 (q, *J* = 33.0 Hz), 135.0, 129.1 (q, *J* = 3.7 Hz), 128.4, 124.0 (q, *J* = 3.7 Hz), 123.1 (q, *J* = 271.4 Hz), 119.3, 73.1, 72.5, 56.7, 39.7. ^{19}F NMR (471 MHz, $CDCl_3$) δ -63.4. **HRMS** (ESI-TOF) m/z: $[M+H]^+$ Calcd for $C_{13}H_{12}F_3O_3S$ 305.0454; Found 305.0439.

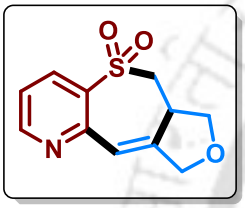

6a,7-dihydro-6H,9H-furo[3',4':5,6]thiepino[3,2-b]pyridine 5,5-dioxide (**4.4v**): White solid, (50 % ethyl acetate in petroleum ether) yield: (34 mg) 58 %; **^{1}H NMR** (500 MHz, $CDCl_3$) δ 8.76 (s, 1H), 8.43 (d, *J* = 5.5 Hz, 1H), 7.38 – 7.31 (m, 1H), 6.80 (s, 1H), 4.72 (d, *J* = 14.6 Hz, 1H), 4.62 (d, *J* = 14.2Hz, 1H), 4.28 – 4.21 (m, 1H), 3.71 – 3.56 (m, 3H), 3.49-3.43 (m, 1H). **^{13}C NMR** (125 MHz, $CDCl_3$) δ 153.4, 151.5, 150.7, 136.8, 135.2, 122.9, 121.6, 73.5, 72.6, 54.9, 40.0. **HRMS** (ESI-TOF) m/z: $[M+H]^+$ Calcd for $C_{11}H_{12}NO_3S$ 238.0533; Found 238.0533.

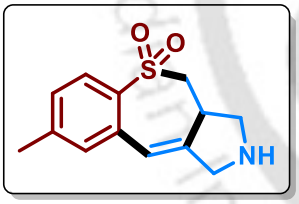

8-methyl-2,3,3a,4-tetrahydro-1H-benzo[6,7]thiepino[3,4-c]pyrrole 5,5-dioxide (**4.5**): White solid, (5 % methanol in dichloromethane) yield: (34 mg) 81 %; ^{1}H NMR (500 MHz, $CDCl_3$) δ 8.02 (d, *J* = 8.2 Hz, 1H), 7.17 (d, *J* = 8.2 Hz, 1H), 7.09 (s, 1H), 6.46 (s, 1H), 3.87 (d, *J* = 16.0 Hz, 1H), 3.78 (d, *J* = 16.1Hz, 1H), 3.65 (dd, *J* = 14.0, 4.8 Hz, 1H), 3.44 – 3.32 (m, 2H), 3.31 – 3.25 (m, 1H), 2.80 – 2.76 (m, 1H), 2.38 (s, 3H), 2.08 (s, 1H). ^{13}C NMR (126 MHz, $CDCl_3$) δ 149.8, 144.2, 136.6, 134.3, 132.7, 127.6, 127.4, 120.8, 57.8, 54.3, 53.3, 40.7, 21.5. **HRMS** (ESI-TOF) m/z: $[M+H]^+$ Calcd for $C_{13}H_{16}NO_2S$ 250.0897; Found 250.0898.

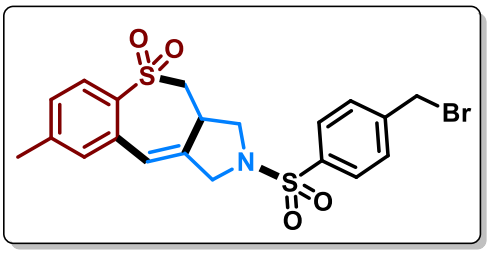

2-((4-(bromomethyl)phenyl)sulfonyl)-8-methyl-2,3,3a,4-tetrahydro-1H-benzo[6,7]thiepino[3,4-c]pyrrole 5,5-dioxide (**4.4w**): White solid, (50 % ethyl acetate in petroleum ether) yield: (102 mg) 85 %; ^{1}H NMR (500 MHz, $CDCl_3$) δ 7.99 (d, *J* = 8.0 Hz, 1H), 7.82 (d, *J* = 8.4 Hz, 2H), 7.58 (d, *J* = 8.4 Hz, 2H), 7.21 (d, *J* = 8.2 Hz, 1H), 7.09 (s, 1H), 6.43 (s, 1H), 4.50 (s, 2H), 4.22 (d, *J* = 14.5 Hz, 1H), 4.06 (d, *J* = 14.5 Hz, 1H), 3.73 (t, *J* = 8.5 Hz, 1H), 3.53 (dd, *J* = 13.5, 4.6 Hz, 1H), 3.48 – 3.41 (m, 1H), 3.35 (t, *J* = 9.1 Hz, 1H), 3.09 (t, *J* =

9.3 Hz, 1H), 2.39 (s, 3H). ^{13}C NMR (126 MHz, $CDCl_3$) δ 144.7, 143.4, 141.8, 136.6, 135.8, 133.6, 132.4, 130.1, 128.5, 128.3, 127.5, 123.3, 55.6, 54.1, 52.3, 38.9, 31.5, 21.5. **HRMS** (ESI-TOF) m/z: $[M+H]^+$ Calcd for $C_{20}H_{21}{}^{79}BrNO_4S_2$ 482.0095; Found 482.0071 (11.48 %). $[M+H]^+$ Calcd for $C_{20}H_{21}{}^{81}BrNO_4S_2$ 484.0075; Found 484.0051 (11.73 %).

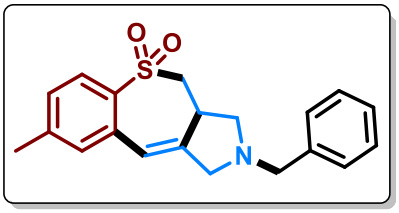

2-benzyl-8-methyl-2,3,3a,4-tetrahydro-1H-benzo[6,7]thiepino[3,4-c]pyrrole 5,5-dioxide (**4.4x**): White solid, (20 % ethyl acetate in petroleum ether) yield: (34 mg) 83 %; ^{1}H NMR (500 MHz, $CDCl_3$) δ 8.00 (d, J = 8.2 Hz, 1H), 7.38 – 7.30 (m, 4H), 7.28 (t, J = 4.3 Hz, 1H), 7.16 (d, J = 8.0 Hz, 1H), 7.05 (s, 1H), 6.44 (s, 1H), 3.75 – 3.62 (m, 4H), 3.48 (q, J = 14.5 Hz, 2H), 3.39 – 3.29 (m, 1H), 2.92 (t, J = 7.9 Hz, 1H), 2.47 (t, J = 7.4 Hz, 1H), 2.39 (s, 3H). ^{13}C NMR (126 MHz, $CDCl_3$) δ 147.7, 144.2, 138.3, 136.4, 135.3, 132.0, 128.7, 128.6, 127.7, 127.5, 127.4, 121.4, 62.3, 60.01, 59.98, 58.9, 38.2, 21.5. **HRMS** (ESI-TOF) m/z: $[M+H]^+$ Calcd for $C_{20}H_{22}NO_2S$ 340.1366; Found 340.1352.

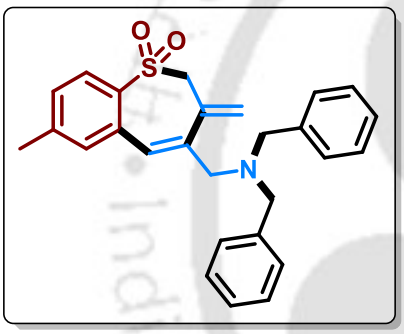

4-((dibenzylamino)methyl)-7-methyl-3-methylene-2,3-dihydrobenzo[b]thiepine 1,1-dioxide (**4.7a**): White solid (15 % ethyl acetate in petroleum ether) Yield: (93 mg) 87 %; **^{1}H NMR** (500 MHz, $CDCl_3$) δ 7.97 (d, J = 7.6 Hz, 1H), 7.37 – 7.24 (m, 8H), 7.25-7.19 (m, 4H), 6.86 (s, 1H), 5.61 (s, 1H), 5.36 (s, 1H), 3.97 (s, 2H), 3.60 (s, 4H), 3.45 (s, 2H), 2.42 (s, 3H). **^{13}C NMR** (125 MHz, CDCl3) δ 143.9, 139.2, 138.0, 137.3, 135.3, 134.5, 132.3, 129.2, 129.2, 128.4, 128.4, 127.3, 126.4, 125.5, 61.8, 61.3, 58.8, 21.5. **HRMS** (ESI-TOF) m/z: $[M+H]^+$ Calcd for $C_{27}H_{28}NO_2S$ 430.1836; Found 430.1811.

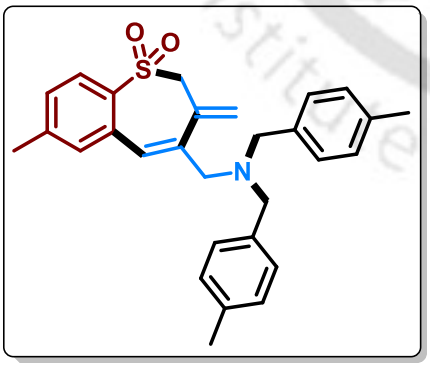

4-((bis(4-methylbenzyl)amino)methyl)-7-methyl-3-methylene-2,3-dihydrobenzo[b]thiepine 1,1-dioxide (**4.7b**): White solid (15 % ethyl acetate in petroleum ether) Yield: (99 mg) 81 %; **^{1}H NMR** (500 MHz, $CDCl_3$) δ 7.97 (d, J = 5.7 Hz, 1H), 7.22 (d, J = 7.1 Hz, 6H), 7.11 (s, 4H), 6.86 (s, 1H), 5.62 (s, 1H), 5.35 (s, 1H), 3.97 (s, 2H), 3.54 (s, 4H), 3.42 (s, 2H), 2.41 (s, 3H), 2.32 (s, 6H). **^{13}C NMR** (125 MHz, $CDCl_3$) δ 143.8, 138.1, 137.2, 136.7, 136.0, 135.3, 134.4, 132.3, 129.1, 129.1, 128.9, 128.2, 126.3, 125.5, 61.8, 60.9, 58.3, 21.5, 21.2. **HRMS** (ESI-TOF) m/z: $[M+H]^+$ Calcd for $C_{29}H_{32}NO_2S$ 458.2149; Found 458.2129.

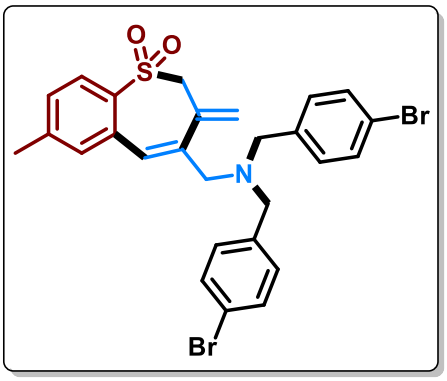

4-((bis(4-bromobenzyl)amino)methyl)-7-methyl-3-methylene-2,3-dihydrobenzo[b]thiepine 1,1-dioxide (**4.7c**): White solid (15 % ethyl acetate in petroleum ether) Yield: (113 mg) 77 %; **^{1}H NMR** (500 MHz, $CDCl_3$) δ 7.98 (d, *J* = 7.7 Hz, 1H), 7.46 – 7.41 (m, 4H), 7.27 – 7.16 (m, 6H), 6.79 (s, 1H), 5.60 (s, 1H), 5.37 (s, 1H), 4.02 (s, 2H), 3.51 (s, 4H), 3.41 (s, 2H), 2.42 (s, 3H). **^{13}C NMR** (126 MHz, $CDCl_3$) δ 144.0, 137.9, 137.6, 137.3, 135.2, 134.6, 132.2, 131.6, 130.8, 129.7, 128.6, 126.5, 125.3, 121.2, 62.0, 61.3, 57.9, 21.5. **HRMS** (ESI-TOF) m/z: $[M+H]^+$ Calcd for $C_{27}H_{26}{}^{79}Br_2NO_2S$ 586.0051; Found 586.0048 (54.48 %). $[M+H]^+$ Calcd for $C_{27}H_{26}{}^{79}Br^{81}BrNO_2S$ 588.0031; Found 588.0037 (100.0 %). $[M+H]^+$ Calcd for $C_{27}H_{26}{}^{81}Br_2NO_2S$ 590.0010; Found 590.0014 (58.12 %).

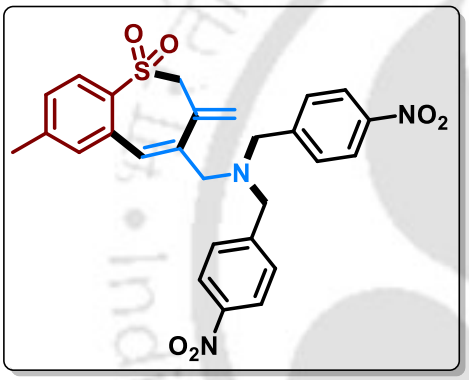

4-((bis(4-nitrobenzyl)amino)methyl)-7-methyl-3-methylene-2,3-dihydrobenzo[b]thiepine 1,1-dioxide (**4.7d**): White solid (15 % ethyl acetate in petroleum ether) Yield: (69 mg) 53 %; **^{1}H NMR** (500 MHz, $CDCl_3$) δ 8.25 (d, *J* = 7.0 Hz, 4H), 8.03 (d, *J* = 6.7 Hz, 1H), 7.61 – 7.52 (m, 4H), 7.31-7.26 (m, 2H), 6.85 (s, 1H), 5.64 (s, 1H), 5.45 (s, 1H), 4.13 (s, 2H), 3.76 (s, 4H), 3.52 (s, 2H), 2.48 (s, 3H). **^{13}C NMR** (125 MHz, $CDCl_3$) δ 147.6, 146.2, 144.2, 137.4, 136.9, 134.9, 134.9, 132.1, 130.4, 129.8, 128.9, 126.6, 124.8, 123.9, 62.5, 61.8, 58.1, 21.5. **HRMS** (ESI-TOF) m/z: $[M+H]^+$ Calcd for $C_{27}H_{26}N_3O_6S$ 520.1537; Found 520.1532.

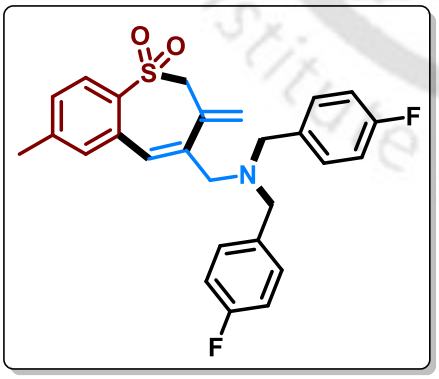

4-((bis(4-fluorobenzyl)amino)methyl)-7-methyl-3-methylene-2,3-dihydrobenzo[b]thiepine 1,1-dioxide (**4.7e**): White solid (15 % ethyl acetate in petroleum ether) Yield: (92 mg) 79 %; **^{1}H NMR** (500 MHz, $CDCl_3$) δ 7.98 (d, *J* = 7.6 Hz, 1H), 7.28-7.20 (m, 6H), 7.00 (t, *J* = 8.8 Hz, 4H), 6.80 (s, 1H), 5.59 (s, 1H), 5.36 (s, 1H), 4.02 (s, 2H), 3.53 (s, 4H), 3.42 (s, 2H), 2.42 (s, 3H). ^{13}C NMR (125 MHz, $CDCl_3$) δ 162.2 (d, *J* = 243.8 Hz), 144.0, 137.8, 137.3, 135.2, 134.6 (d, *J* = 3.2 Hz), 134.5, 132.2, 130.6 (d, *J* = 7.9 Hz), 129.6, 128.5, 126.4, 125.4, 115.3 (d, *J* = 21.2 Hz), 62.0, 61.3, 57.8, 21.5. **^{19}F NMR** (471 MHz, $CDCl_3$) δ -115.5. **HRMS** (ESI-TOF) m/z: $[M+H]^+$ Calcd for $C_{27}H_{26}F_2NO_2S$ 466.1647; Found 466.1618.

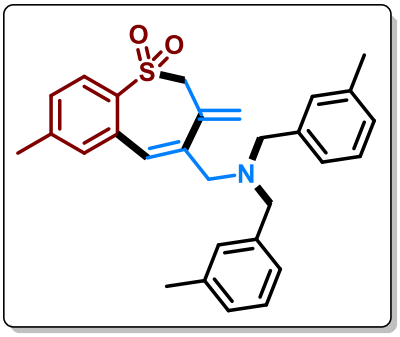

4-((bis(3-4-((bis(3-methylbenzyl)amino)methyl)-7-methyl-3-methylene-2,3-dihydrobenzo[b]thiepine 1,1-dioxide **(4.7f)** : White solid (15 % ethyl acetate in petroleum ether) Yield: (81 mg) 71 %; **^{1}H NMR** (500 MHz, $CDCl_3$) δ 7.97 (d, *J* = 7.8 Hz, 1H), 7.25-7.13(m, 8H), 7.04 (d, *J* = 7.0 Hz, 2H), 6.86 (s, 1H), 5.62 (s, 1H), 5.36 (s, 1H), 3.94 (s, 2H), 3.56 (s, 4H), 3.43 (s, 2H), 2.42 (s, 3H), 2.32 (s, 6H).**^{13}C NMR** (125 MHz, $CDCl_3$) δ 143.8, 139.1, 138.1, 137.8, 137.2, 135.3, 134.5, 132.3, 130.0, 129.1, 128.3, 127.9, 126.4, 126.2, 125.3, 61.7, 61.3, 59.0, 21.6, 21.5. **HRMS** (ESI-TOF) m/z: $[M+H]^+$ Calcd for $C_{29}H_{32}NO_2S$ 458.2149; Found 458.2127.

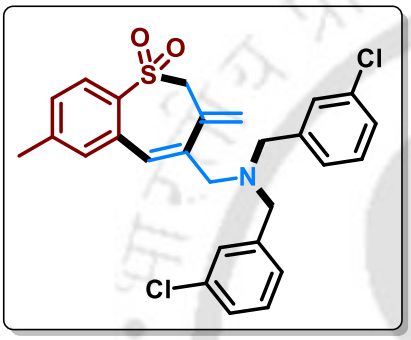

4-((bis(3-chlorobenzyl)amino)methyl)-7-methyl-3-methylene-2,3-dihydrobenzo[b]thiepine 1,1-dioxide **(4.7g)**: White solid (15 % ethyl acetate in petroleum ether) Yield: (91 mg) 73 %; **^{1}H NMR** (500 MHz, $CDCl_3$) δ 7.97 (d, *J* = 7.7 Hz, 1H), 7.32 (s, 2H), 7.22 (d, *J* = 8.2 Hz, 8H), 6.80 (s, 1H), 5.60 (s, 1H), 5.40 (s, 1H), 3.99 (s, 2H), 3.57 (s, 4H), 3.44 (s, 2H), 2.43 (s, 3H). **^{13}C NMR** (125 MHz, $CDCl_3$) δ 144.0, 141.0, 137.5, 137.3, 135.3, 134.4, 132.1, 129.8, 129.7, 129.2, 128.6, 127.6, 127.2, 126.4, 125.2, 61.9, 61.5, 58.4, 21.5. **HRMS** (ESI-TOF) m/z: $[M+H]^+$ Calcd for $C_{27}H_{26}Cl_2NO_2S$ 498.1056; Found 498.1064.

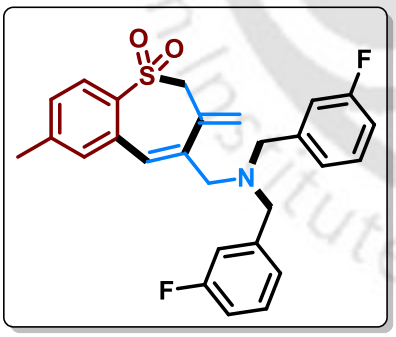

4-((bis(3-fluorobenzyl)amino)methyl)-7-methyl-3-methylene-2,3-dihydrobenzo[b]thiepine 1,1-dioxide **(4.7h)**: White solid (15 % ethyl acetate in petroleum ether) Yield: (80 mg) 69 %; **^{1}H NMR** (500 MHz, $CDCl_3$) δ 7.97 (d, *J* = 7.7 Hz, 1H), 7.31 – 7.21 (m, 4H), 7.10 (d, *J* = 7.7 Hz, 2H),7.05(d, *J* = 10.0 Hz, 2H), 6.94 (t, *J* = 7.9 Hz, 2H), 6.82 (s, 1H), 5.62 (s, 1H), 5.40 (s, 1H), 4.01 (s, 2H), 3.58 (s, 4H), 3.45 (s, 2H), 2.42 (s, 3H). **^{13}C NMR** (125 MHz, $CDCl_3$) δ 162.1 (d, *J* = 244.5 Hz), 144.0, 141.6 (d, J = 7.0 Hz), 137.5, 137.3, 135.2, 134.6, 132.1, 130.0 (d, *J* = 8.2 Hz), 129.6, 128.5, 126.4, 125.2, 124.7 (d, *J* = 2.8 Hz), 115.8 (d, *J* = 21.1 Hz), 114.3 (d, *J* = 21.0 Hz), 62.0, 61.4, 58.3, 21.5. **^{19}F NMR** (565 MHz, $CDCl_3$) δ -113.3. **HRMS** (ESI-TOF) m/z: $[M+H]^+$ Calcd for $C_{27}H_{26}F_2NO_2S$ 466.1647; Found 466.1642.

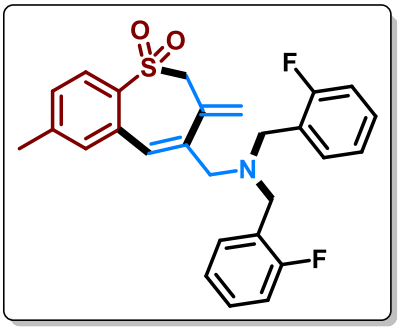

4-((bis(2-fluorobenzyl)amino)methyl)-7-methyl-3-methylene-2,3-dihydrobenzo[b]thiepine 1,1-dioxide **(4.7i)**: White solid (15 % ethyl acetate in petroleum ether) Yield: (51 mg) 51 %; **^{1}H NMR** (500 MHz, $CDCl_3$) δ 7.96 (d, *J* = 7.3 Hz, 1H), 7.39 (t, *J* = 7.1 Hz, 2H), 7.27 – 7.16 (m, 4H), 7.09 (d, *J* = 7.1 Hz, 2H), 6.98 (t, *J* = 9.0 Hz, 2H), 6.86 (s, 1H), 5.55 (s, 1H), 5.32 (s, 1H), 3.90 (s, 2H), 3.70 (s, 4H), 3.50 (s, 2H), 2.41 (s, 3H). **^{13}C NMR** (125 MHz, $CDCl_3$) δ 161.5 (d, *J* = 244.8 Hz), 143.8, 137.5, 137.2, 135.4, 134.5, 132.1, 131.6 (d, *J* = 4.5 Hz), 129.1, 128.9 (d, J = 8.2 Hz), 128.4, 126.3, 125.7 (d, *J* = 14.1 Hz), 125.1, 124.1 (d, *J* = 3.7 Hz), 115.4 (d, *J* = 22.0 Hz), 61.6, 61.4, 51.7, 21.5. **^{19}F NMR** (471 MHz, $CDCl_3$) δ -117.7. **HRMS** (ESI-TOF) m/z: $[M+H]^+$ Calcd for $C_{27}H_{26}F_2NO_2S$ 466.1647; Found 466.1624.

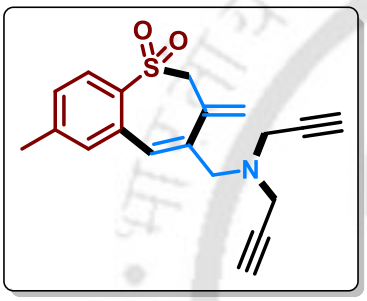

4-((di(prop-2-yn-1-yl)amino)methyl)-7-methyl-3-methylene-2,3-dihydrobenzo[b]thiepine 1,1-dioxide **(4.7j)**: White solid (15 % ethyl acetate in petroleum ether) Yield: (51 mg) 63 %; **^{1}H NMR** (500 MHz, $CDCl_3$) δ 8.00 (d, *J* = 8.0 Hz, 1H), 7.26 – 7.23 (m, 2H), 6.78 (s, 1H), 6.04 (s, 1H), 5.47 (s, 1H), 4.10 (s, 2H), 3.62 (s, 2H), 3.46 (s, 4H), 2.42 (s, 3H), 2.31 (s, 2H). **^{13}C NMR** (125 MHz, $CDCl_3$) δ 144.0, 137.4, 136.37, 135.41, 134.21, 132.06, 130.14, 128.59, 126.34, 125.84, 78.7, 73.7, 62.0, 59.4, 42.3, 21.4. **HRMS** (ESI-TOF) m/z: $[M+H]^+$ Calcd for $C_{19}H_{20}NO_2S$ 326.1210; Found 326.1226.

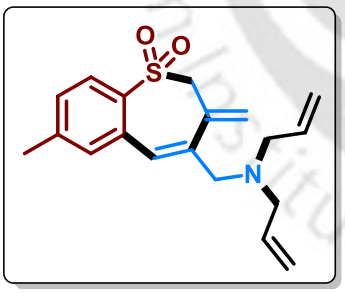

4-((diallylamino)methyl)-7-methyl-3-methylene-2,3-dihydrobenzo[b]thiepine 1,1-dioxide **(4.7k)**: White solid (15 % ethyl acetate in petroleum ether) Yield: (55 mg) 67 %; **^{1}H NMR** (500 MHz, $CDCl_3$) δ 8.00 (d, *J* = 8.1 Hz, 1H), 7.29 – 7.19 (m, 2H), 6.84 (s, 1H), 5.95 – 5.83 (m, 2H), 5.81 (s, 1H), 5.41 (s, 1H), 5.23– 5.16 (m, 4H), 4.09 (s, 2H), 3.44 (s, 2H), 3.14 (d, *J* = 6.1 Hz, 4H), 2.42 (s, 3H). **^{13}C NMR** (126 MHz, $CDCl_3$) δ 143.9, 137.8, 137.2, 135.5, 135.3, 134.9, 132.4, 128.6, 128.2, 126.3, 124.4, 117.9, 62.0, 59.7, 57.0, 21.5. **HRMS** (ESI-TOF) m/z: $[M+H]^+$ Calcd for $C_{19}H_{24}NO_2S$ 330.1523; Found 330.1545.

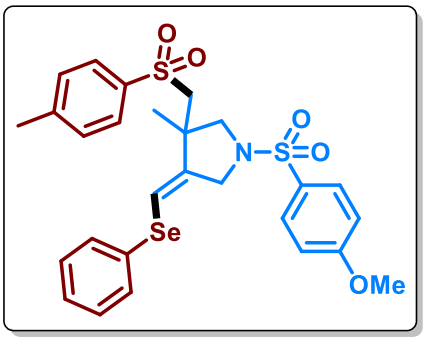

(Z)-1-((4-methoxyphenyl)sulfonyl)-3-methyl-4-((phenylselanyl)methylene)-3-(tosylmethyl)pyrrolidine (**4.8**): White solid (15 % ethyl acetate in petroleum ether) Yield: (135 mg) 91 %; **^{1}H NMR** (500 MHz, $CDCl_3$) δ 7.77 (d, *J* = 6.6 Hz, 2H), 7.73 (d, *J* = 5.2 Hz, 2H), 7.38 (s, 2H), 7.34 (d, *J* = 7.2 Hz, 2H), 7.28 – 7.26 (m, 3H), 7.02 (d, *J* = 5.8 Hz, 2H), 6.35 (s, 1H), 3.88 (s, 3H), 3.76 (d, *J* = 10.1 Hz, 1H), 3.69 (s, 2H), 3.23 (s, 2H), 3.02 (d, *J* = 9.5 Hz, 1H), 2.45 (s, 3H), 1.47 (s, 3H). **^{13}C NMR** (125 MHz, $CDCl_3$) δ 163.4, 144.9, 144.8, 138.1, 132.3, 130.13, 130.1, 129.9, 129.6, 127.84, 127.79, 127.0, 115.0, 114.5, 62.7, 58.5, 55.8, 51.4, 46.4, 23.0, 21.8. **HRMS** (ESI-TOF) m/z: $[M+H]^+$ Calcd for $C_{27}H_{30}NO_5S_2Se$ 592.0726; Found 592.0703.

4.11 Crystal data:

SC-XRD data of compound 4.4q: 50 mg of compound **4.4q** was dissolved in 1:1 $CHCl_3$/MeOH (3 mL) and kept for 2-3 days for crystal growth. The crystal measurement was done in 'Bruker APEX-II CCD'. The ellipsoid contour probability is 50 % for the image of the structure.

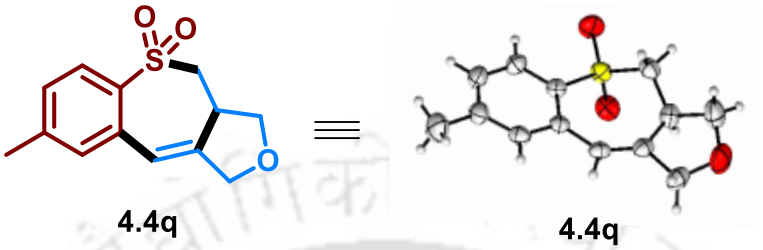

CCDC	2463338	
Empirical formula	C13 H14 O3 S	
Formula weight	250.30	
Temperature, T	295(2)	
Crystal system	monoclinic	
Space group	P 21/c	
Unit cell dimensions	a= 9.1311(7) Å b=13.5298(10) Å c= 9.8753(7) Å	α=90° β=99.931(2)° γ=90°
Volume, V ($Å^3$)	1201.73(15)	
Z	4	
Density (calculated), g cm^{-3}	1.383	
Absorption coefficient, μ (mm^{-1})	0.262	
F (000)	528	
Crystal size, mm^3	0.33 × 0.26 × 0.22	
Theta range for data collection	3.19 to 25.01	
Index ranges	-10 ≤ h ≤ 10 -16 ≤ k ≤ 16 -11 ≤ l ≤ 11	
Reflections collected	2094	
Independent reflections	1944	
Completeness to theta	0.988	
Absorption correction	none	

Refinement method	'\f and \w scans'
Data / restraints / parameters	2094/0/155
Goodness-of-fit on F^2	0.747
Final R indices [I>2sigma(I)]	R1 = 0.0332, wR2 = 0.1045
R indices (all data)	R1 = 0.0360, wR2 = 0.1121
Largest diff. peak and hole	0.273 and -0.287 e·Å^{-3}

Bond Distances [Å]	Bond angles [°]
S001 O003 1.4357(14)	O003 S001 O002 117.16(9)
S001 O002 1.4405(13)	O003 S001 C006 108.17(8)
S001 C006 1.7660(16)	O002 S001 C006 108.31(8)
S001 C00A 1.7681(17)	O003 S001 C00A 107.91(9)
O004 C00G 1.418(3)	O002 S001 C00A 108.71(8)
O004 C00F 1.421(3)	C006 S001 C00A 106.04(8)
C005 C008 1.401(2)	C00G O004 C00F 108.90(14)
C005 C006 1.409(2)	C008 C005 C006 115.86(14)
C005 C007 1.469(2)	C008 C005 C007 115.47(14)
C006 C00B 1.391(2)	C006 C005 C007 128.63(14)
C007 C009 1.328(2)	C00B C006 C005 121.18(14)
C008 C00D 1.386(2)	C00B C006 S001 115.22(12)
C009 C00C 1.495(3)	C005 C006 S001 123.49(12)
C009 C00F 1.510(2)	C009 C007 C005 134.04(15)
C00A C00C 1.514(2)	C00D C008 C005 123.68(16)
C00B C00E 1.381(3)	C007 C009 C00C 132.58(15)
C00C C00G 1.527(3)	C007 C009 C00F 121.75(16)
C00D C00E 1.383(3)	C00C C009 C00F 105.59(15)
C00D C00H 1.506(3)	C00C C00A S001 111.22(12)
	C00E C00B C006 120.39(16)
	C009 C00C C00A 116.45(14)
	C009 C00C C00G 101.19(15)
	C00A C00C C00G 113.05(16)
	C00E C00D C008 118.34(16)
	C00E C00D C00H 120.93(18)

	C008 C00D C00H 120.72(18) C00B C00E C00D 120.49(16) O004 C00F C009 106.91(16) O004 C00G C00C 105.53(17)

SC-XRD data of compound 4.4v: 50 mg of compound **4.4v** was dissolved in 1:1 $CHCl_3$/MeOH (3 mL) and kept for 2-3 days for crystal growth. The crystal measurement was done in 'Bruker APEX-II CCD'. The ellipsoid contour probability is 50 % for the image of the structure.

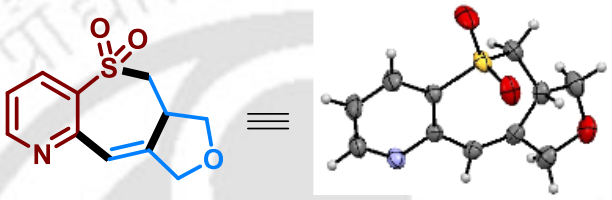

4.4v ≡ **4.4v**

CCDC	2463339	
Empirical formula	C11 H11 N O3 S	
Formula weight	237.27	
Temperature, T	295(2)	
Crystal system	orthorhombic	
Space group	P b c a	
Unit cell dimensions	a= 11.5410(13) Å b= 9.9946(12) Å c= 18.340(2) Å	α=90° β=90° γ=90°
Volume, V ($Å^3$)	2115.4(4)	
Z	8	
Density (calculated), g cm^{-3}	1.490	
Absorption coefficient, μ (mm^{-1})	0.296	
F (000)	992	
Crystal size, mm^3	0.37 × 0.29 × 0.23	
Theta range for data collection	2.32 to 25.04	
Index ranges	-13 ≤ h ≤ 13 -11 ≤ k ≤ 11 -21 ≤ l ≤ 21	

Reflections collected	1828
Independent reflections	1710
Completeness to theta	0.987
Absorption correction	none
Refinement method	'\f and \w scans'
Data / restraints / parameters	1828/0/145
Goodness-of-fit on F^2	1.114
Final R indices [I>2sigma(I)]	R1 = 0.0321, wR2 = 0.1116
R indices (all data)	R1 = 0.0346, wR2 = 0.1198
Largest diff. peak and hole	0.287 and -0.302e·$Å^{-3}$

Bond Distances [Å]	Bond angles [°]
S001 O004 1.4347(14)	O004 S001 O002 117.81(9)
S001 O002 1.4414(14)	O004 S001 C008 108.01(8)
S001 C008 1.7671(14)	O002 S001 C008 107.56(7)
S001 C00A 1.7689(16)	O004 S001 C00A 108.48(9)
O003 C00E 1.422(2)	O002 S001 C00A 108.80(8)
O003 C00G 1.423(2)	C008 S001 C00A 105.51(7)
N005 C00D 1.331(2)	C00E O003 C00G 106.72(13)
N005 C007 1.349(2)	C00D N005 C007 119.46(13)
C006 C009 1.339(2)	C009 C006 C007 133.30(14)
C006 C007 1.468(2)	N005 C007 C008 119.27(14)
C007 C008 1.405(2)	N005 C007 C006 111.73(13)
C008 C00C 1.386(2)	C008 C007 C006 128.95(14)
C009 C00B 1.502(2)	C00C C008 C007 120.16(14)
C009 C00E 1.515(2)	C00C C008 S001 115.12(12)
C00A C00B 1.511(2)	C007 C008 S001 124.58(12)
C00B C00G 1.523(2)	C006 C009 C00B 131.87(14)
C00C C00F 1.372(2)	C006 C009 C00E 122.21(15)
C00D C00F 1.380(3)	C00B C009 C00E 105.89(13)
	C00B C00A S001 111.07(11)
	C009 C00B C00A 116.88(12)
	C009 C00B C00G 100.81(13)

	C00A C00B C00G 114.15(14) C00F C00C C008 119.36(15) N005 C00D C00F 123.94(15) O003 C00E C009 106.23(14) C00C C00F C00D 117.61(15) O003 C00G C00B 104.14(14)

SC-XRD data of compound 4.7e: 30 mg of compound **4.7e** was dissolved in 1:1 DCM/MeOH (3 mL) and kept for 2-3 days for crystal growth. The crystal measurement was done in 'Bruker APEX-II CCD'. The ellipsoid contour probability is 50 % for the image of the structure.

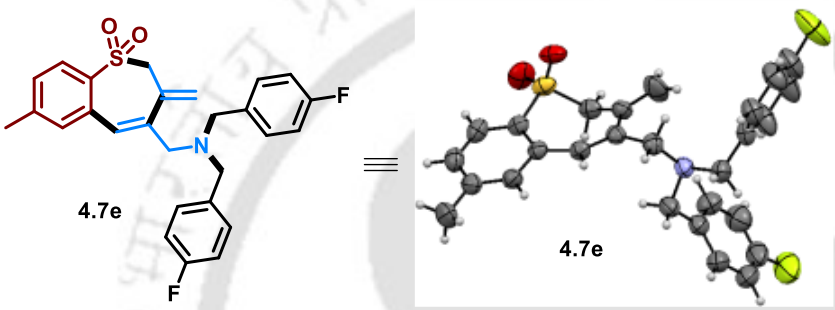

CCDC	2463340	
Empirical formula	C27 H25 F2 N O2 S	
Formula weight	465.54	
Temperature, T	295(2)	
Crystal system	monoclinic	
Space group	P 21/c	
Unit cell dimensions	a= 16.831(5) Å b= 7.961(2) Å c= 18.149(5) Å	α=90° β=93.977(8)° γ=90°
Volume, V ($Å^3$)	2426.0(12)	
Z	4	
Density (calculated), g cm^{-3}	1.275	
Absorption coefficient, μ (mm^{-1})	0.172	
F (000)	976	
Crystal size, mm^3	0.31 × 0.23 × 0.21	
Theta range for data collection	2.25 to 24.90	
Index ranges	$-19 \leq h \leq 19$	

	$-9 \leq k \leq 9$ $-21 \leq l \leq 21$
Reflections collected	4229
Independent reflections	3571
Completeness to theta	0.991
Absorption correction	none
Refinement method	'\f and \w scans'
Data / restraints / parameters	4229/0/299
Goodness-of-fit on F^2	1.497
Final R indices [I>2sigma(I)]	R1 = 0.0460, wR2 = 0.1667
R indices (all data)	R1 = 0.0563, wR2 = 0.1859
Largest diff. peak and hole	0.442 and -0.455 $e \cdot Å^{-3}$

Bond Distances [Å]	Bond angles [°]
S001 O002 1.4346(16)	O002 S001 O004 118.04(10)
S001 O004 1.4389(16)	O002 S001 C00C 109.57(8)
S001 C00C 1.7614(19)	O004 S001 C00C 107.53(9)
S001 C00B 1.7675(19)	O002 S001 C00B 109.19(10)
N003 C00J 1.465(2)	O004 S001 C00B 108.19(10)
N003 C00I 1.466(2)	C00C S001 C00B 103.30(9)
N003 C00H 1.467(2)	C00J N003 C00I 111.41(16)
F1 C00R 1.370(3)	C00J N003 C00H 110.72(16)
C006 C009 1.401(2)	C00I N003 C00H 112.69(14)
C006 C00C 1.416(2)	C009 C006 C00C 115.63(16)
C006 C00A 1.463(2)	C009 C006 C00A 115.16(16)
F2 C00W 1.368(3)	C00C C006 C00A 129.21(16)
C008 C00A 1.362(2)	C00A C008 C00D 127.01(17)
C008 C00D 1.466(3)	C00A C008 C00H 115.96(17)
C008 C00H 1.515(3)	C00D C008 C00H 117.02(16)
C009 C00L 1.385(3)	C00L C009 C006 124.07(18)
C00B C00D 1.503(3)	C008 C00A C006 136.67(17)
C00C C00G 1.388(3)	C00D C00B S001 113.35(14)
C00D C1 1.331(3)	C00G C00C C006 121.25(17)

C00E C00K 1.367(3)	C00G C00C S001 117.01(14)
C00E C00T 1.385(3)	C006 C00C S001 121.72(14)
C00E C00J 1.503(3)	C1 C00D C008 122.5(2)
C00F C00O 1.380(3)	C1 C00D C00B 117.44(19)
C00F C00N 1.384(3)	C008 C00D C00B 119.97(15)
C00F C00I 1.505(3)	C00K C00E C00T 117.8(2)
C00G C00M 1.378(3)	C00K C00E C00J 122.18(19)
C00K C00S 1.389(3)	C00T C00E C00J 120.1(2)
C00L C00M 1.393(3)	C00O C00F C00N 118.1(2)
C00L C00P 1.505(3)	C00O C00F C00I 119.99(19)
C00N C00Q 1.387(3)	C00N C00F C00I 121.8(2)
C00O C00V 1.385(4)	C00M C00G C00C 120.48(19)
C00Q C00R 1.342(4)	N003 C00H C008 113.45(15)
C00R C00V 1.358(4)	N003 C00I C00F 110.08(16)
C00S C00W 1.336(4)	N003 C00J C00E 112.32(16)
C00T C00X 1.377(4)	C00E C00K C00S 121.8(2)
C00W C00X 1.373(4)	C009 C00L C00M 117.86(18)
	C009 C00L C00P 120.8(2)
	C00M C00L C00P 121.34(19)
	C00G C00M C00L 120.65(18)
	C00F C00N C00Q 120.9(2)
	C00F C00O C00V 121.1(2)
	C00R C00Q C00N 118.7(2)
	C00Q C00R C00V 123.0(2)
	C00Q C00R F1 119.0(3)
	C00V C00R F1 118.1(3)
	C00W C00S C00K 118.3(2)
	C00X C00T C00E 121.4(2)
	C00R C00V C00O 118.3(3)
	C00S C00W F2 118.2(3)
	C00S C00W C00X 122.9(2)
	F2 C00W C00X 118.9(3)
	C00W C00X C00T 117.9(2)

4.12 References:

1. (a) Togo, H. Advanced Free Radical Reactions for Organic Synthesis; Elsevier: Amsterdam, **2004**. (b) Motherwell, W. B.; Crich, D. Free Radical Chain Reactions in Organic Synthesis; Katritzky, A. R., Meth-Cohn, O., Rees, C.S., Eds.; Academic Press Limited: London, **1992**. (c) Albert, M.; Fensterbank, L.; Lacô te, E.; Malacria, *M. Top. Curr. Chem.* **2006**, *264*, 1−62. (d) Walton, J. C. *Top. Curr. Chem.* **2006**, *264*, 163−200. (e) Encyclopedia of Radicals in Chemistry, Biology, and Materials; Chatgilialoglu, C., Studer, A., Eds.; John Wiley & Sons, **2012**. (f) Yan, M.; Lo, J. C.; Edwards, J. T.; Baran, P. S. Radicals: Reactive Intermediates with Translational Potential. *J. Am. Chem. Soc.* **2016**, *138*, 12692−12714. (g) Romero, K. J.; Galliher, M. S.; Pratt, D. A.; Stephenson, C. R. J. Radicals in Natural Product Synthesis. *Chem. Soc. Rev.* **2018**, *47*, 7851−7866. (h) Li, Y.; Bao, H. Radical transformations for allene synthesis. *Chem. Sci.* **2022**, *13*, 8491−8506.

2. Xuan, J.; Studer, A. Radical Cascade Cyclization of 1, n-Enynes and Diynes for the Synthesis of Carbocycles and Hetero-cycles. *Chem. Soc. Rev.* **2017**, *46*, 4329−4346.

3. (a) Prier, C. K.; Rankic, D. A.; MacMillan, D. W. C. Visible Light Photoredox Catalysis with Transition Metal Complexes: Applications in Organic Synthesis. *Chem. Rev.* **2013**, *113*, 5322−5363 (b) Romero, N. A.; Nicewicz, D. A. Organic Photoredox Catalysis. *Chem. Rev.* **2016**, *116*, 10075−10166. (c) Jamatia, R.; Mondal, A.; Srimani, D. Visible-Light-Induced Manganese-Catalyzed Reactions: Present Approach and Future Prospects. *Adv. Synth. Catal.* **2021**, *363*, 2969−2995. (d) Roy, M.; Sardar, B.; Mallick, I.; Srimani, D. Generation of alkyl and acyl radicals by visible-light photoredox catalysis: direct activation of C−O bonds in organic transformations. *Beilstein J. Org. Chem.* **2024**, *20*, 1348−1375.

4. (a) *Organic Chemistry of Sulfur*; Oae, S., Ed.; Plenum Press: New York, 1977. (b) Shigeru, O.; Tadashi, O. *Organic Sulfur Chemistry*: Biochemical Aspects; CRC Press: Boca Raton, FL, 1992. (c) Simpkins, N. S. *Sulphones in Organic Synthesis*; Pergamon Press: Oxford, 1993. (d) Manolikakes, G.; Liu, N. W.; Liang, S. Recent advances in the synthesis of sulfones. *Synthesis* **2016**, *48*, 1939−1973. (e) Alam, M. A.; Shimada, K.; Jahan, A.; Khan, M. W.; Bhuiyan, M.M. H.; Alam, M. S.; Matin, M. M. Synthesis, reactions and medicinal importance of cyclic sulfone derivatives: A review. *Nat. Prod. Chem. Res.* **2018**, *6*, 1000350−1000357. (f) Leonard, J.; Hague, A. B.; Jones, M. F. A One-Pot Tandem Pictet-Spengler-Diels-Alder Synthesis of Apoyohimbines from 3-Carbomethoxy-2-(formylmethyl)-3-sulfolene *Tetrahedron Lett.* **1997**, *38*, 3071-3074. (g) MaGee, D. I.; Beck, E. J. Use of the Ramberg−Bäcklund Rearrangement for the Synthesis of Medium and Large Heterocyclic Alkenes: Stereoselective Olefin Formation. *J. Org. Chem.* **2000**, *65*, 8367−8371. (h) McAllister, G.D.; Taylor, R. J. K. The

synthesis of polyoxygenated, enantiopure cyclopentene derivatives using the Ramberg−Bäcklund rearrangement. *Tetrahedron Lett*. **2001**, *42*, 1197-1200.

5. (a) Ghosh, A. K.; Thompson, W. J.; Munson, P. M.; Liu, W.; Huff, J. R. cyclic sulfone-3-carboxamides as novel P2-ligands for Ro 31-8959 based HIV-1 protease inhibitors Bioorg. *Med. Chem. Lett.* **1995**, *5*, 83-88. (b) Richter, H. G. F.; Angehrn, P.; Hub-schwerlen, C.; Kania, M.; Page, M. G. P.; Specklin, J.-L.; Winkler,F. K. Design, Synthesis, and Evaluation of 2â-Alkenyl Penam Sulfone Acids as Inhibitors of â-Lactamases *J. Med. Chem.* **1996**, *39*, 3712-3722. (c) Kim, C. U.; McGee, L. R.; Krawczyk, S. H.; Harwood, E.; Harada, Y.; Swaminathan, S.; Bischofberger, N.; Chen, M. S.; Cher-rington, J. M.; Xiong, S. F.; Griffin, L.; Cundy, K. C.; Lee, A.; Yu, B.; Gulnik, S.; Erickson, J. W. New Series of Potent, Orally Bioavaila-ble, Non-Peptidic Cyclic Sulfones as HIV-1 Protease Inhibitors. *J. Med. Chem.* **1996**, *39*, 3431−3434. (d) Buynak, J. D.; Vogeti, L.; Chen, H. Coupling Reactions of Cephalosporin Sulfones: A Stable 3-Stannylated Cephem *Org. Lett.* **2001**, *3*, 2953-2956.

6. (a) Cheng, Q.; Zhang, F.; Chen, X.; Han, Y.; Yan, C.; Shi, Y.; Hou, H.; Zhu, S. Visible-Light-Mediated Three-Component Radical Iodosulfonylative Cyclization of Enynes. *Org. Lett.* **2022**, *24*, 2515−2519. (b) Hou, H.; Li, H.; Xu, Y.; Song, C.; Wang, C.; Shi, Y.; Han, Y.; Yan, C.; Zhu, S. Visible-Light-Mediated Chlorosulfonylative Cyclizations of 1,6-Enynes. *Adv. Synth. Catal.* **2018**, *360*, 4325−4329. (c) Meng, X.-X.; Kang, Q.-Q.; Zhang, J.-Y.; Li, Q.; Wei, W. T.; He, W.M. Visible-light-initiated Regioselective Sulfonylation/Cyclization of1,6-Enynes under Photocatalyst- and Additive-free Conditions. *Green Chem.* **2020**, *22*, 1388−1392. (d) Zhu, S.; Pathigoolla, A.; Lowe, G.; Walsh, D. A.; Cooper, M.; Lewis, W.; Lam, H. W. Sulfonylative and Azidosulfonylative Cyclizations by Visible-Light-Photosensitization of Sulfonyl Azides in THF. *Chem.-Eur. J.* **2017**, *23*, 17598. (e) Wu, W.; Yi, S.; Huang, W.; Luo, D.; Jiang, H. Ag-Catalyzed Oxidative Cyclization Reaction of 1,6-Enynes and Sodium Sulfinate: Access to Sulfonylated Benzofurans. *Org. Lett.* **2017**, *19*, 2825−2828.

7. (a) Zhang, Y.; Cai, Z.; Zhao, C.; Zheng, H.; Ackermann, L. Electrosynthesis of Bridged or Fused Sulfonamides through Complex Radical Cascade Reactions: Divergence in Medium-Sized Ring Formation. *Chem. Sci.* **2023**, *14*, 3541−3547. (b) Chen, F.; Huang, X.; Yang, C.; Jiang, H.; Zeng, W. Photocatalyzed Coupling-Cyclization of ortho-AlkynylarylVinylethers with Aryl-sulfonyl Azides. *J. Org. Chem.* **2021**, *86*, 14572−14585. (c) Zuo, H.-D.; Chen, X.; Zhang, Y.; Liu, J.-W.; Yan, S.-H.; Li, G.; Wang, J.-Y. Photocatalytic Thio/Selenosulfonylation-Bicyclization of Indole-Tethered 1,6-Enynes Leading to Substituted Benzo[c]pyrrolo[1,2,3-lm]carbazoles. *Org. Lett.* **2024**, *26*, 3828−3833. (d) Cai, Z.; Trienes, S.;

Liu, K.; Ackermann, L.; Zhang, Y. Radical cascade cyclization of 1, n-enynes under photo/electrochemical conditions. *Org. Chem. Front.* **2023**, *10*, 5735−5745.

8. Mutra, M. R.; Kudale, V. S.; Li, J.; Tsai, W.-H.; Wang, J.-J. Alkene Versus Alkyne Reactivity in Unactivated 1,6-Enynes: Re-gio-and Chemoselective Radical Cyclization with Chalcogens under Metal- and Oxidant-Free Conditions. *Green Chem*. **2020**, *22*, 2288−2300.

9. (a) Fang, J.-D.; Yan, X.-B.; Lin, W.-J.; Zhao, Y.-C.; Liu, X.-Y. Diphenyl-Diselenide-Mediated Domino Claisen-Type Rearrangement/Cyclization of Propargylic Aryl Ethers: Synthesis of Naphthofuran-2-carboxaldehyde Derivatives. *Org. Lett*. **2019**, *21*, 7635−7638. (b) Wu, Q.; Zhang, X.; Yang, Q.; Song, Z.; Ding, Q.; Peng, Y. Synthesis of Selenium-Containing N-Quinazolinyl Acro-leins via a 3,3-Radical Rearrangement Cascade Reaction. *Org. Lett. 2024*, *26*, 530−535.

10. (a) Chen, F.; Yang, C.; Hu, X.; Zhang, X.; Xie, H.; Jiang, H.; Jiang, F.; Zeng, W. Photocatalyzed Formal Carbooxygenation of Terminal Alkynes. *Org. Chem. Front.* **2020**, *7*, 1600−1605. (b) Inoa, J.; Patel, M.; Dominici, G.; Eldabagh, R.; Patel, A.; Lee, J.; Xing, Y. Benzylic Hydroperoxidation via Visible-Light-Induced Csp3−H Activation. *J.Org. Chem.* **2020**, *85*, 6181−6187.

11. (a) Zhang, J.; Wang, L.; Liu, Q.; Yang, Z.; Huang, Y. Synthesis of α,β-Unsaturated Carbonyl Compounds via a Visible-Light-Promoted Organocatalytic Aerobic Oxidation. *Chem. Commun.* **2013**, *49*, 11662-11664. (b) Zhang, Y.; Ye, C.; Li, S.; Ding, A.; Gu, G.; Guo, H. Eosin YCatalyzed Photooxidation of Triarylphosphines under Visible Light Irradiation and Aerobic Conditions. *RSC Adv.* **2017**, *7*, 13240−13243.

12. (a) Stephenson, L. M.; Grdina, M. B.; Orfanopoulos, M. Mechanism of the Ene Reaction Between Singlet Oxygen and Olefins. Acc. Chem. Res. 1980, 13, 419−425. (b) Alberti, M. N.; Orfanopoulos, M. Unraveling the Mechanism of the Singlet Oxygen Ene Reaction: Recent Computational and Experimental Approaches. *Chem. - Eur. J.* **2010**, *16*, 9414−9421.

13. Chen, X.; Lu, S.; Zheng, Y.; Wang, J.; Yang, L.; Sun, P.Synthesis of β-Keto Sulfones by Oxy-Sulfonylation of Alkynes in HFIP. *Adv. Synth. Catal.* **2022**, *364*, 1305−1312.

14. Hou, F.; Ning, Y. T.; Song, L. L.; Tan, Z. Q.; Yang, J. W.; Liu, Z. G.; Chen, F. E. Rhodium-Catalyzed Asymmetric Hydroboration/Cyclization of 1,6-Enynes Enabled by Spirosiladiphosphine Ligands: Constructing Chiral Five-Membered Rings with a Boron Handle. *Org. Lett.* **2023**, *25*, 7810−7815.

15. Tan, Y.-X.; Li, S.; Song, L.; Zhang, X.; Wu, Y.-D.; Sun, J. RutheniumCatalyzed Geminal Hydrative Cyclization of Enynes. *Angew. Chem., Int. Ed.* **2022**, *61*, No. e202204319.

16. Mohy El Dine, T.; Jimmidi, R.; Diaconu, A.; Fransolet, M.; Michiels, C.; De Winter, J.; Gillon, E.; Imberty, A.; Coenye, T.; Vincent, S. P. Pillar [5] Arene-Based Polycationic Glyco [2] Rotaxanes Designed as Pseudomonas Aeruginosa Antibiofilm Agents. *J. Med. Chem.* **2021**, *64*, 14728−14744.

17. Lemoine, R. C.; Petersen, A. C.; Setti, L.; Baldinger, T.; Wanner, J.; Jekle, A.; Heilek, G.; deRosier, A.; Ji, C.; Rotstein, D. M. Evaluation of a 3-amino-8-azabicyclo[3.2.1]octane replacement in the CCR5 antagonist maraviroc. *Bioorg. Med. Chem. Lett.* **2010**, *20*, 1674−1676.

18. Abbasi Kejani, A.; Khosravi, H.; Rominger, F.; Balalaie, S.; Breit, B. Metal-free domino oligocyclization reactions of enynals and enynones with molecular oxygen. *Org. Lett.* **2021**, *23*, 1291−1295.

19. Meyer, A. U.; Jaeger, S.; Prasad Hari, D.; Koenig, B. Visible Light-Mediated Metal-Free Synthesis of Vinyl Sulfones from Aryl Sulfinates. Adv. Synth. Catal. 2015, 357, 2050-2054.

20. Li, S.; Ling, J.; Zhou, L. Visible-LightPromoted Radical gem-Selenosulfonylation or -Iodosulfonylation of 2,2,2-Trifluorodiazoethane under Photosensitizer-Free Conditions. *Org. Lett.* **2024**, *26*, 5220−5225.

4.13 Selected NMR spectra:

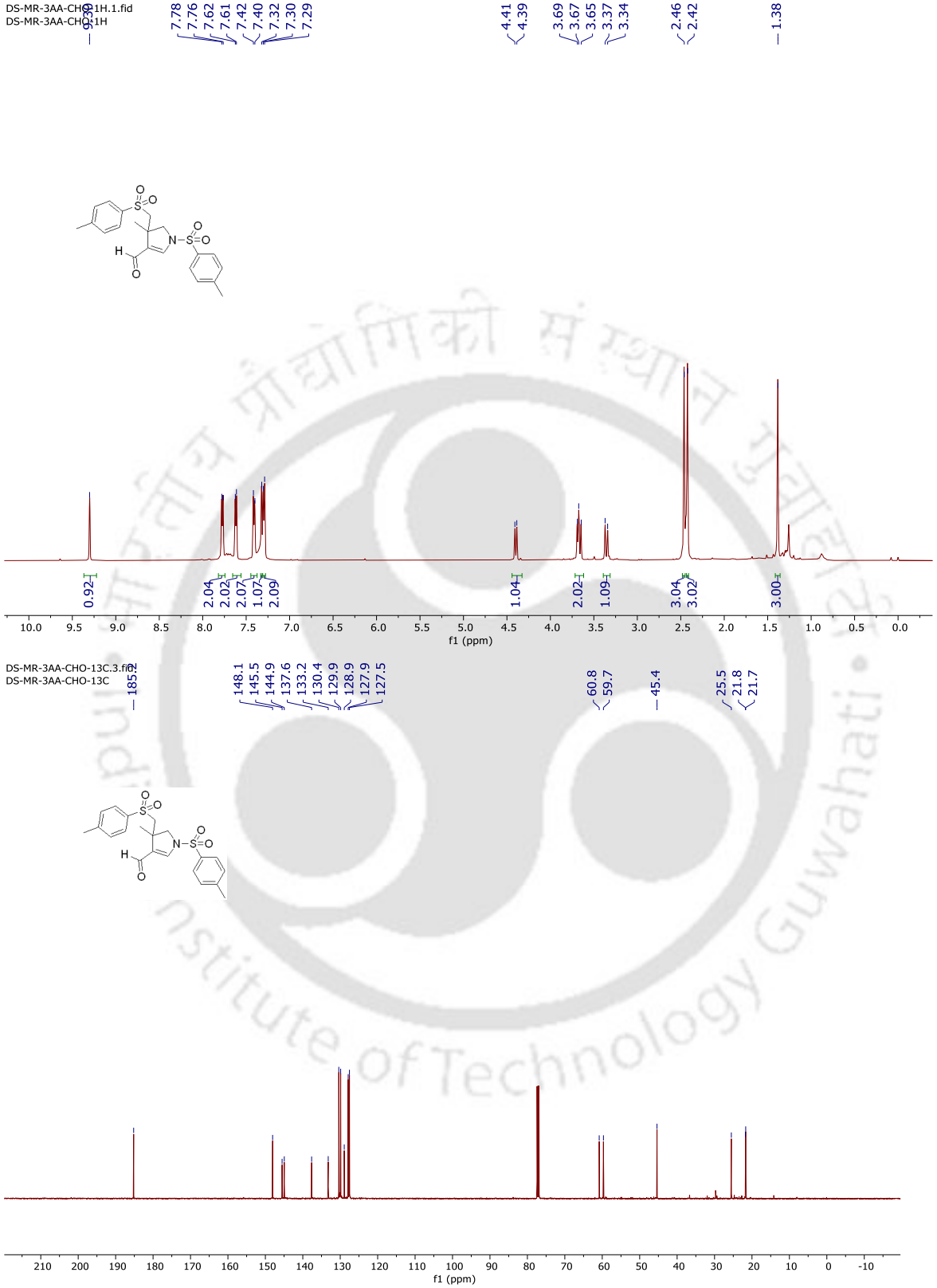

Figure 4.9: ^{1}H NMR (500 MHz) and $^{13}C\{^{1}H\}$ NMR (125 MHz) spectrum of Compound **4.3a** in $CDCl_3$.

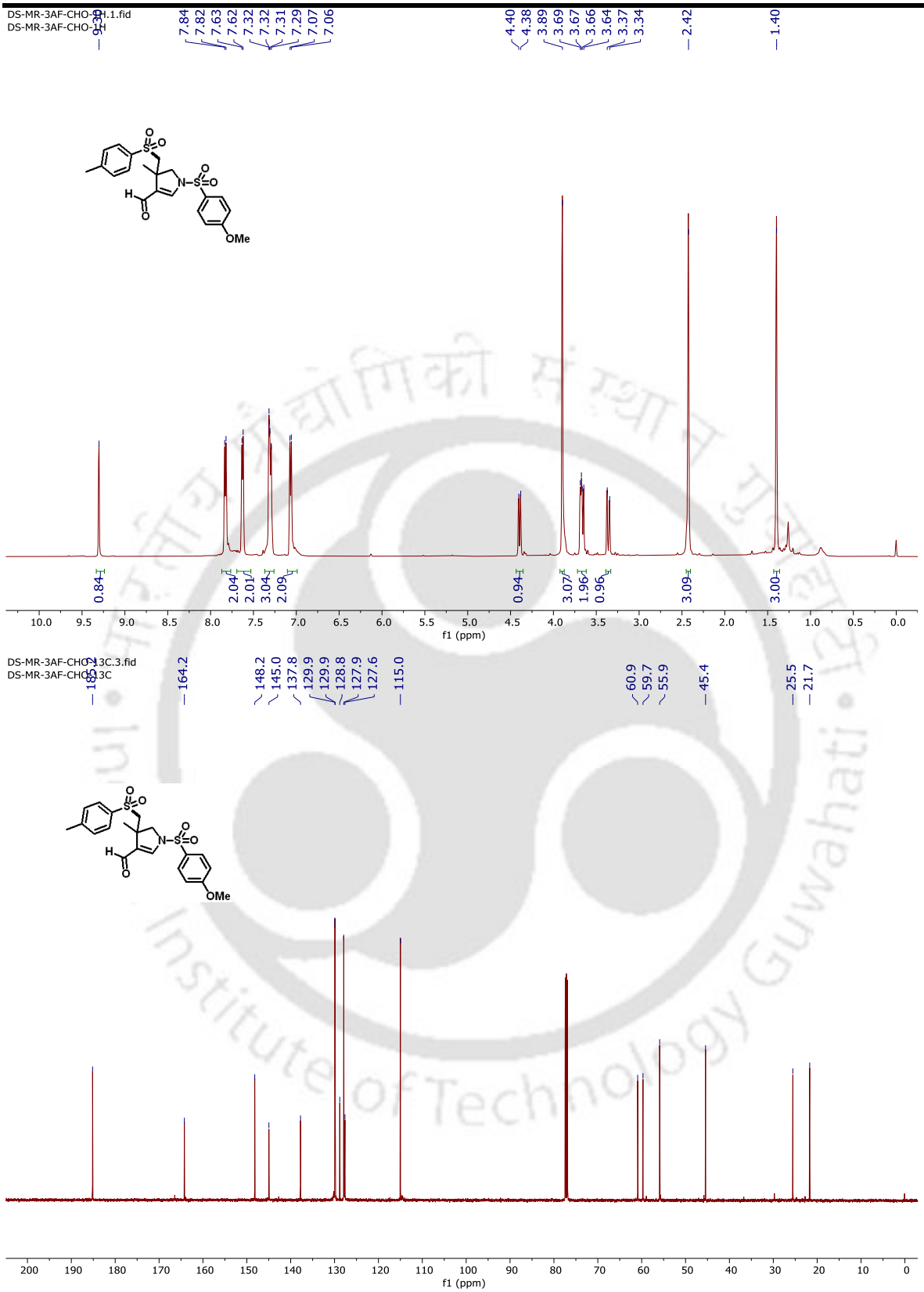

Figure 4.10: ^{1}H NMR (500 MHz) and $^{13}C\{^{1}H\}$ NMR (125 MHz) spectrum of Compound **4.3b** in $CDCl_3$.

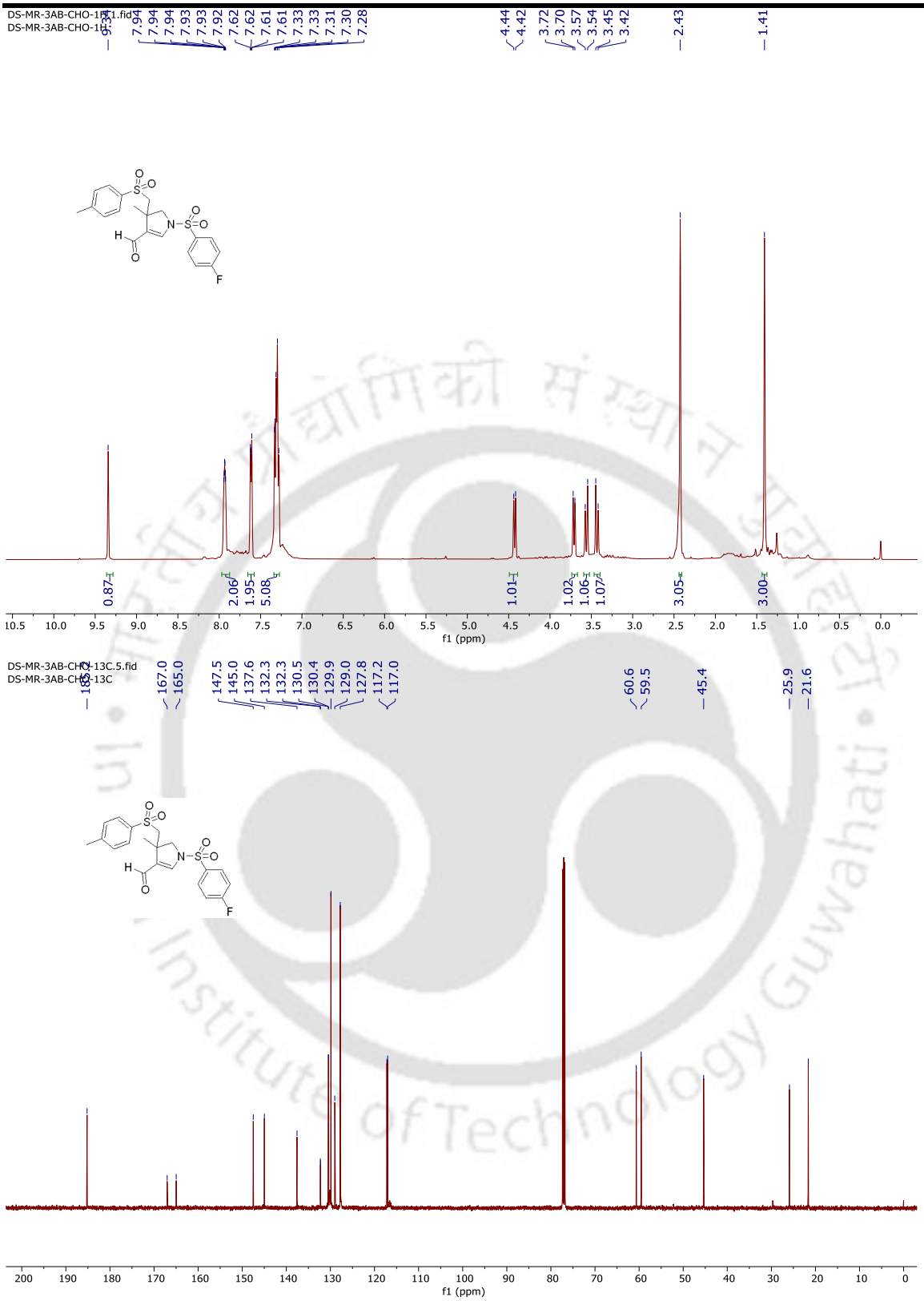

Figure 4.11: ^{1}H NMR (500 MHz) and $^{13}C\{^{1}H\}$ NMR (125 MHz) spectrum of Compound **4.3c** in $CDCl_3$.

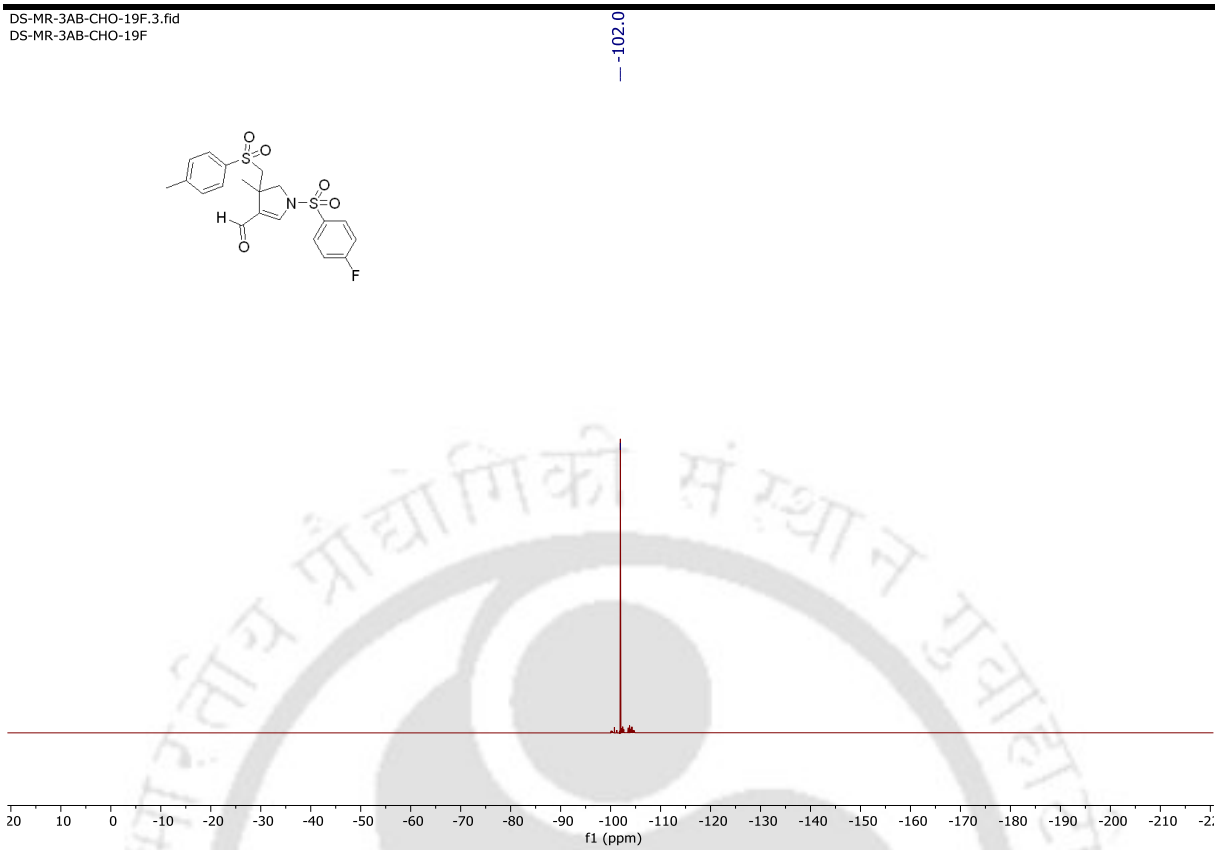

Figure 4.12: $^{19}F\{^{1}H\}$ NMR (470 MHz) spectrum of Compound **4.3c** in $CDCl_3$.

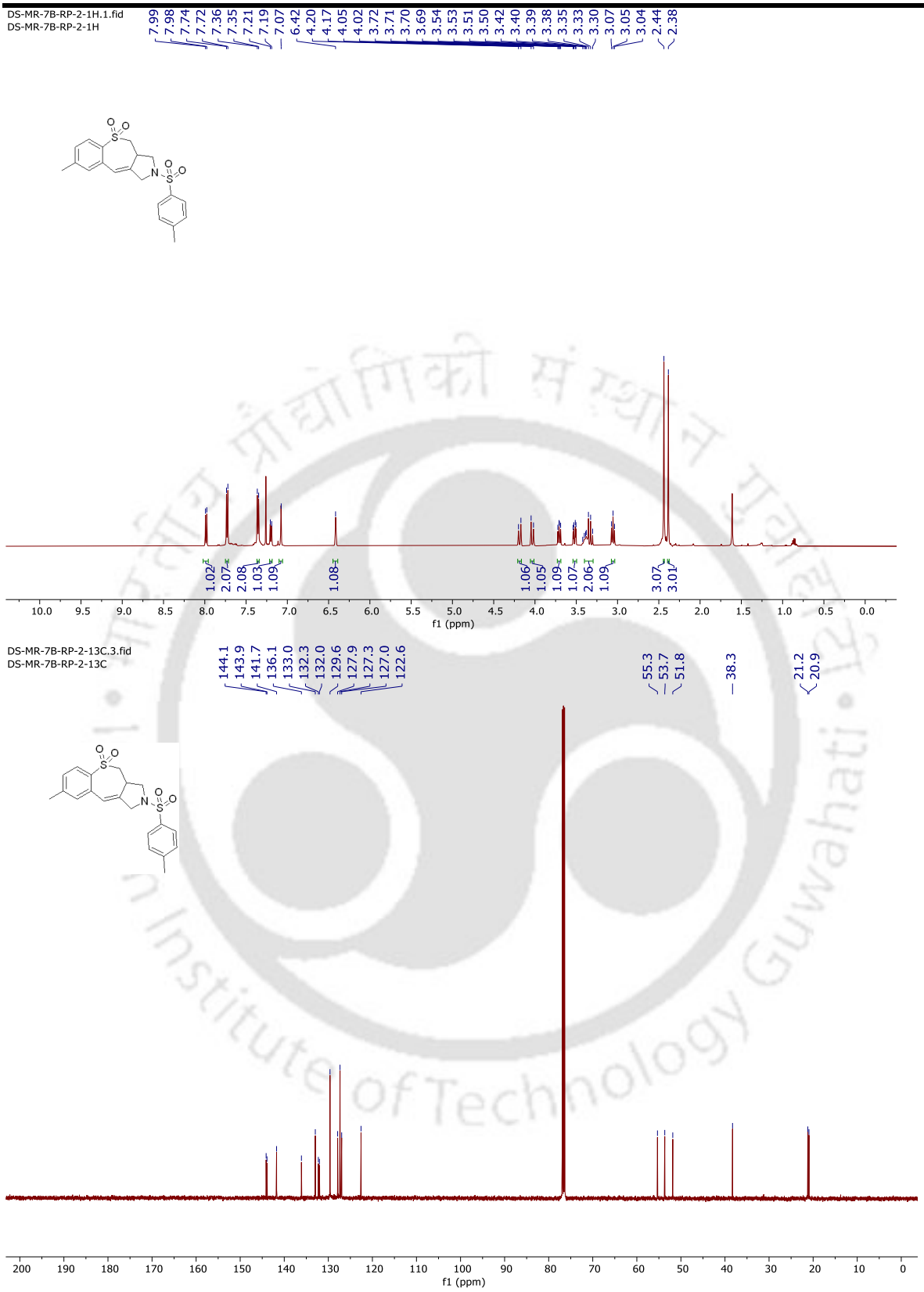

Figure 4.13: ^{1}H NMR (500 MHz) and $^{13}C\{^{1}H\}$ NMR (125 MHz) spectrum of Compound **4.4a** in $CDCl_3$.

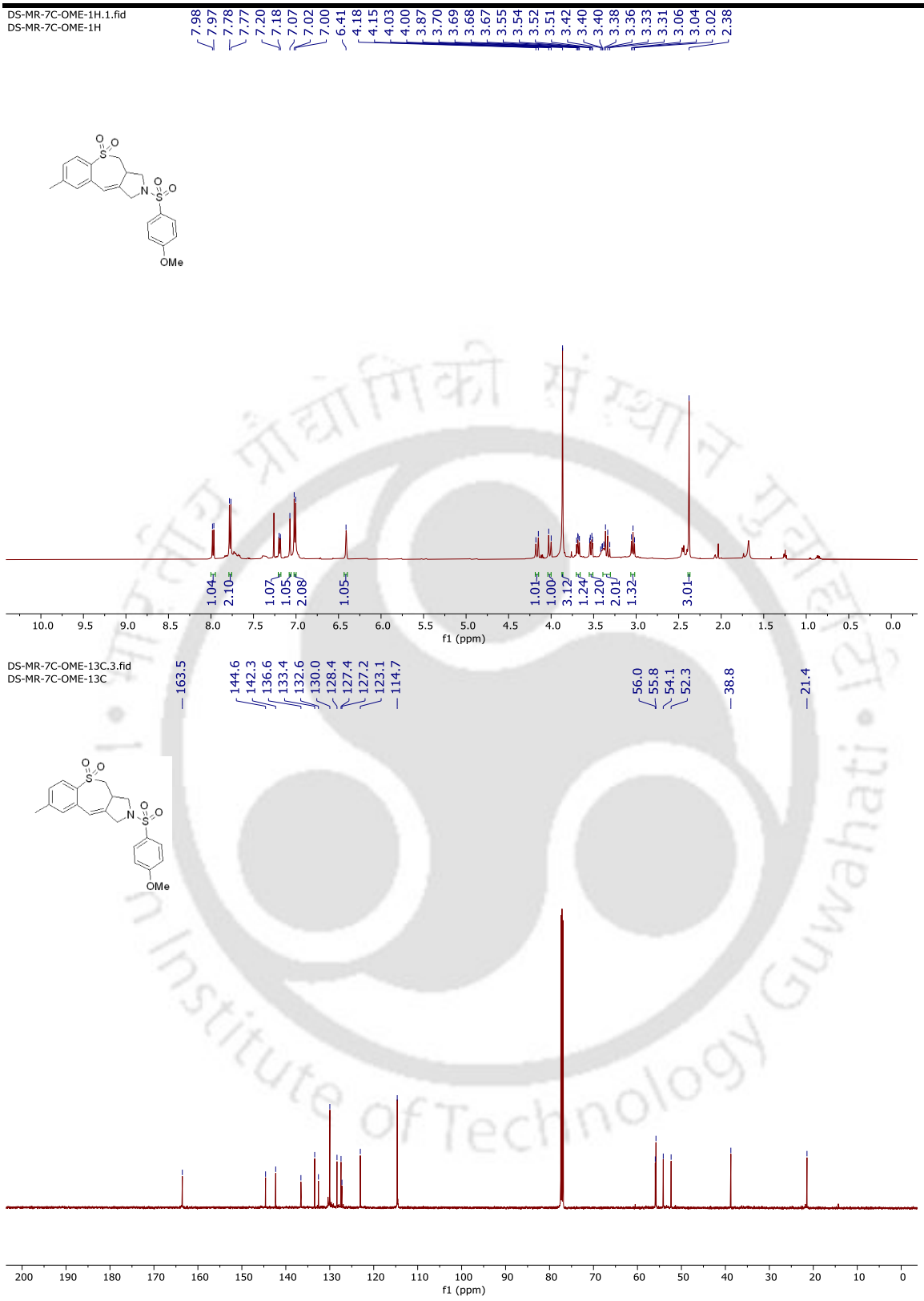

Figure 4.14: ^{1}H NMR (500 MHz) and $^{13}C\{^{1}H\}$ NMR (125 MHz) spectrum of Compound **4.4b** in $CDCl_3$.

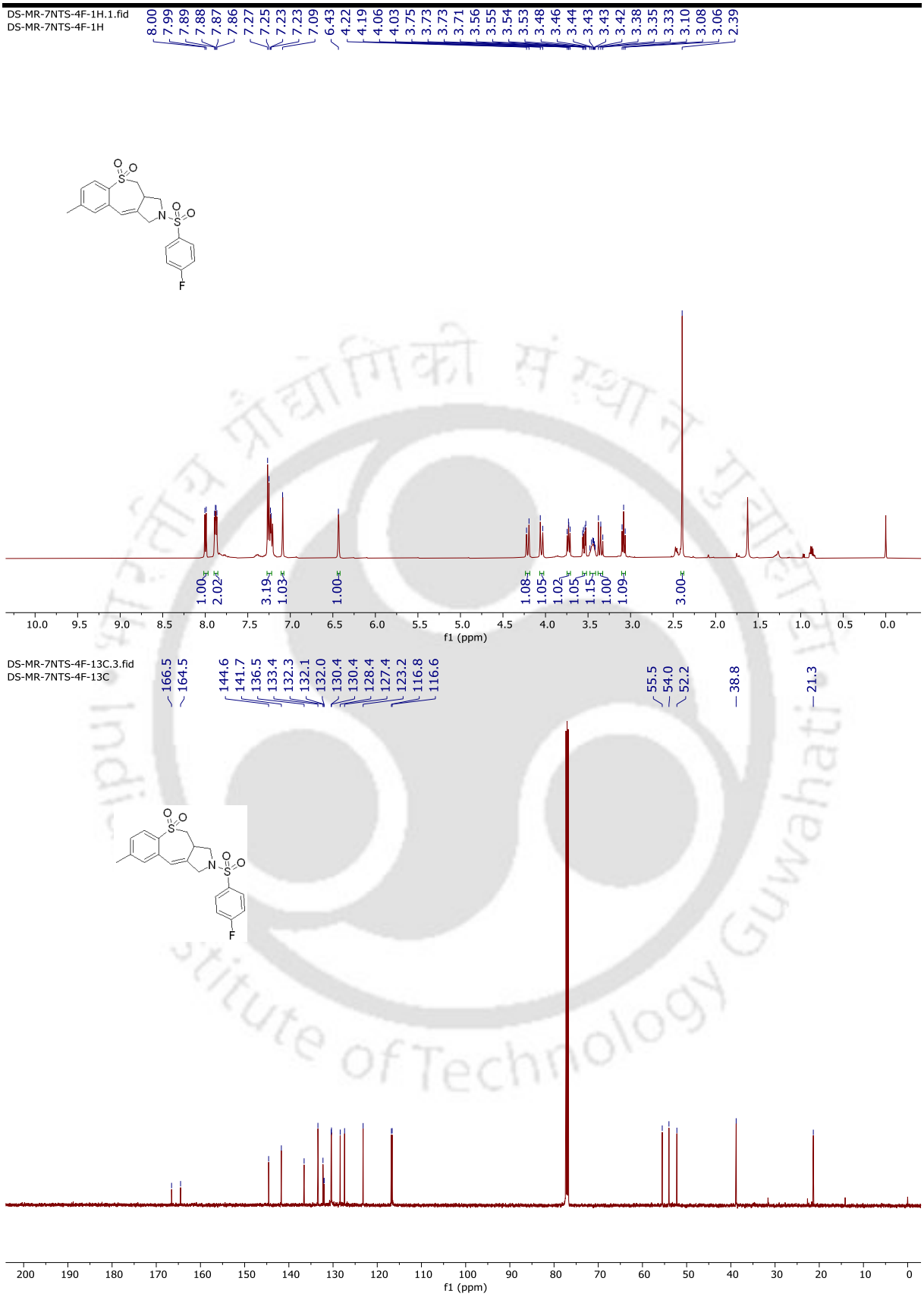

Figure 4.15: ^{1}H NMR (500 MHz) and $^{13}C\{^{1}H\}$ NMR (125 MHz) spectrum of Compound **4.4c** in $CDCl_3$.

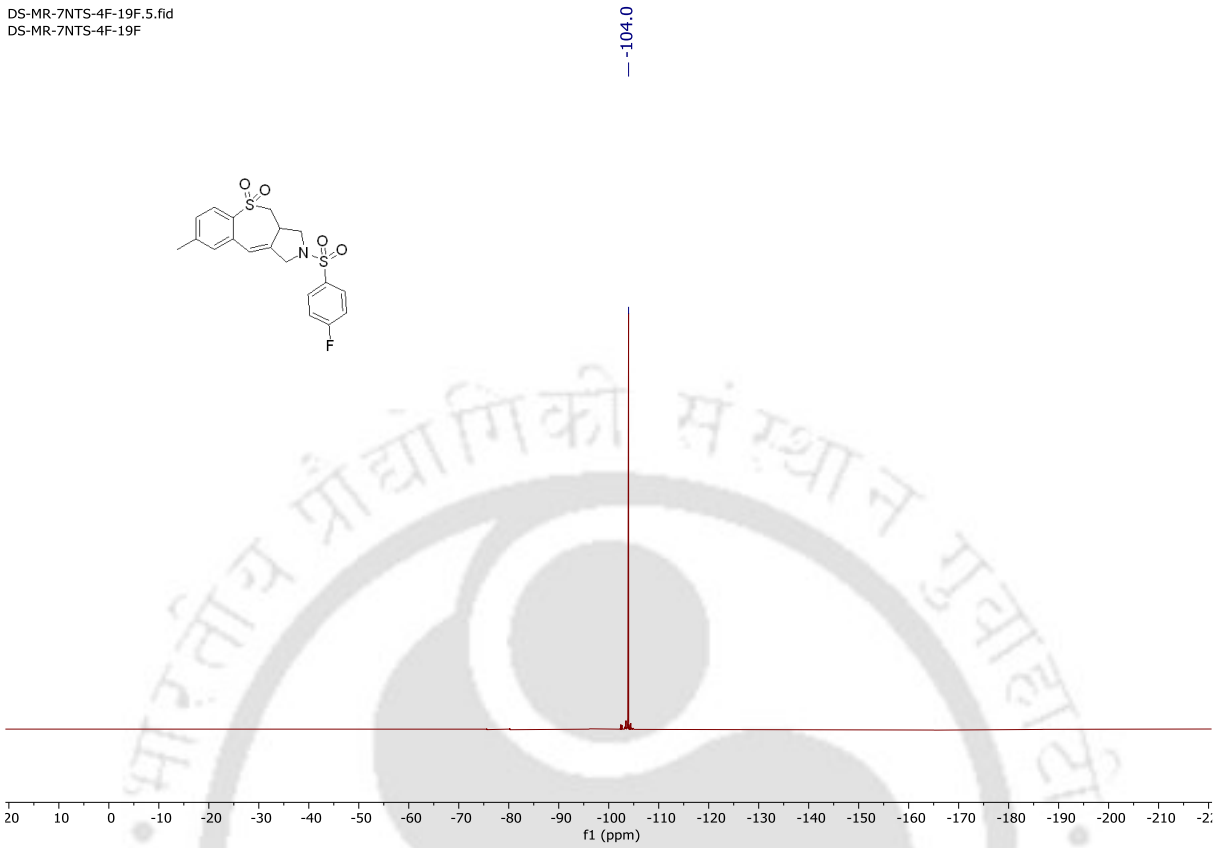

Figure 4.16: $^{19}F\{^{1}H\}$ NMR (470 MHz) spectrum of Compound **4.4c** in $CDCl_3$.

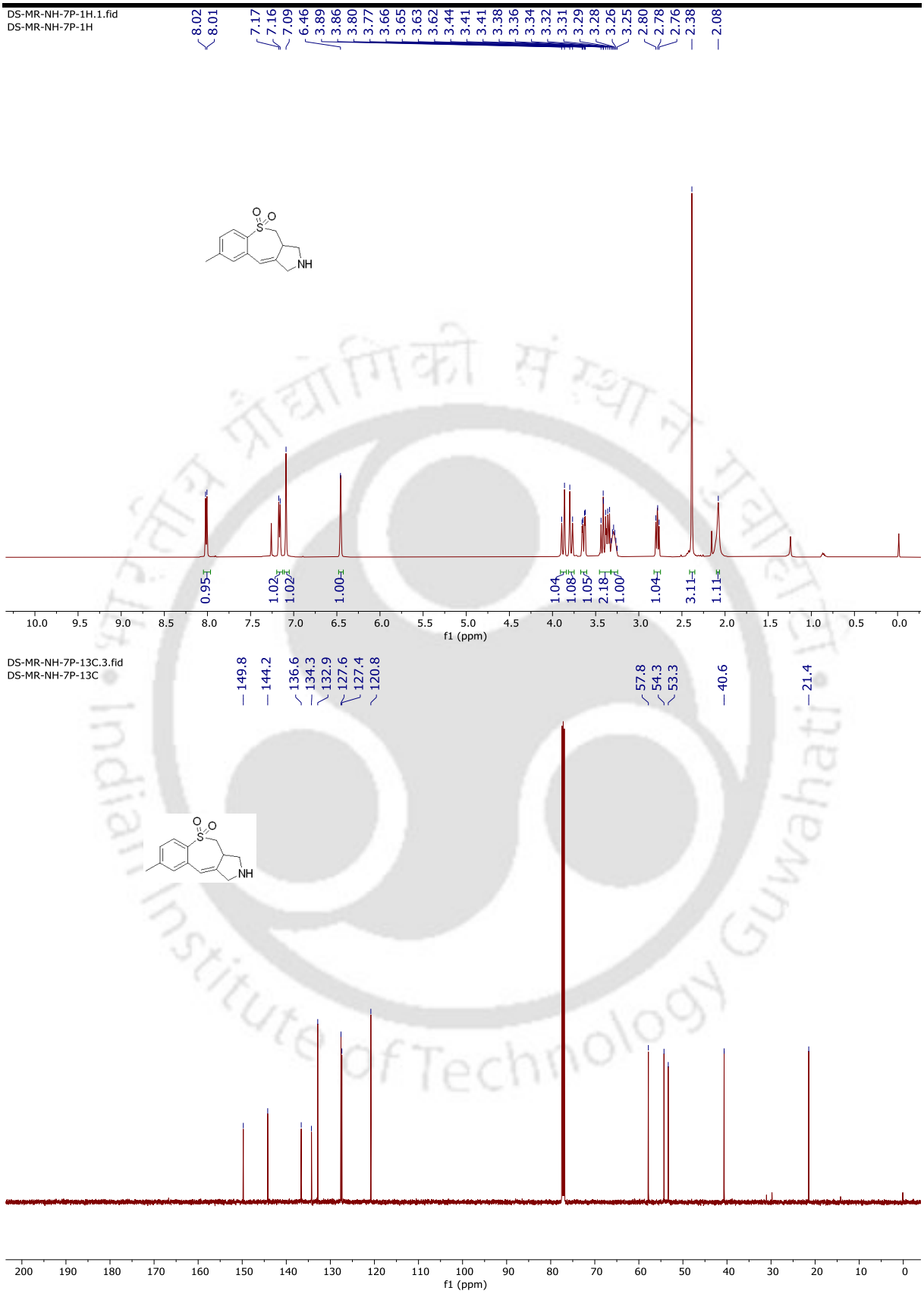

Figure 4.17: ^{1}H NMR (500 MHz) and $^{13}C\{^{1}H\}$ NMR (125 MHz) spectrum of Compound **4.5** in $CDCl_3$.

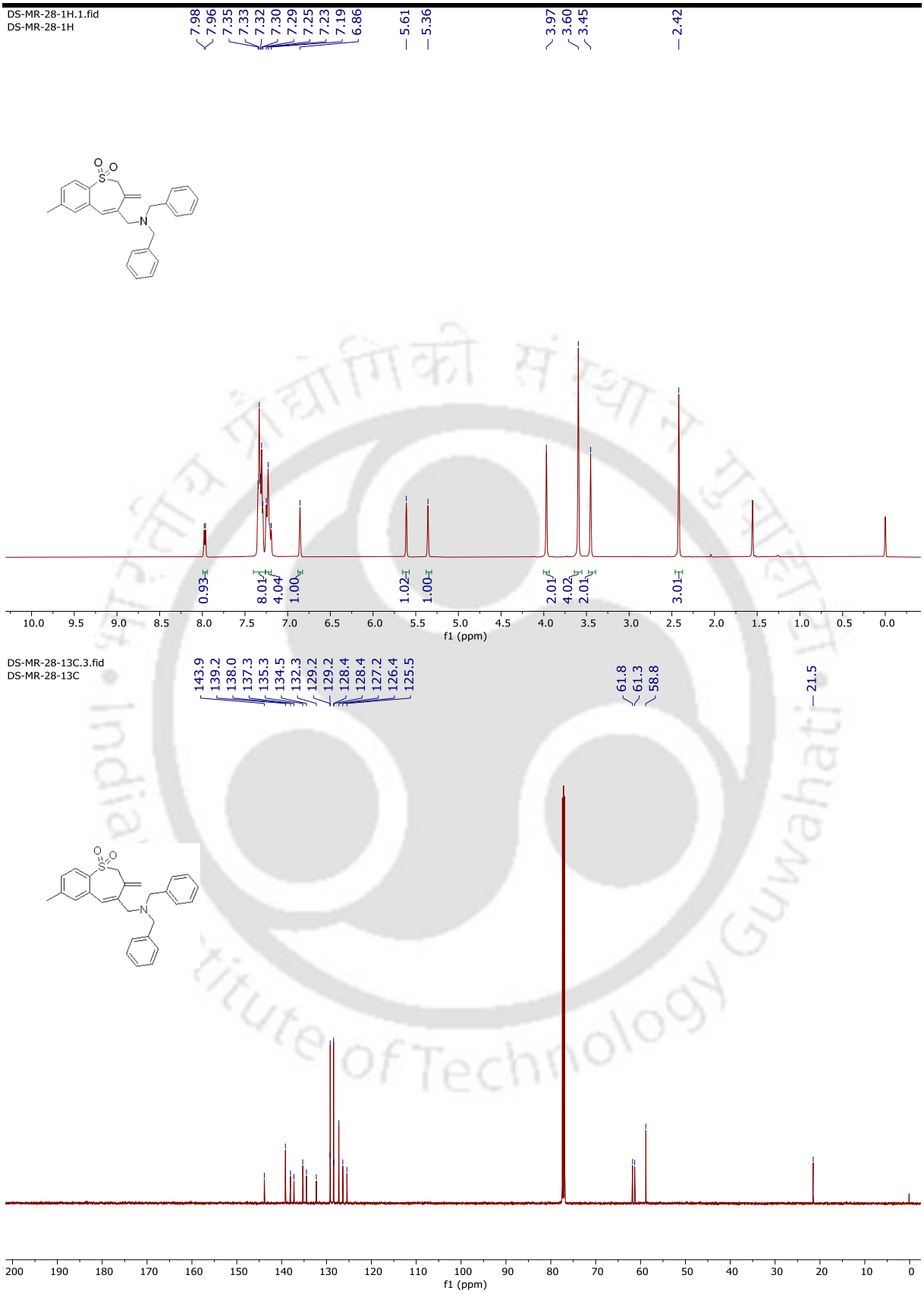

Figure 4.18: ^{1}H NMR (500 MHz) and $^{13}C\{^{1}H\}$ NMR (125 MHz) spectrum of Compound **4.7a** in $CDCl_3$.

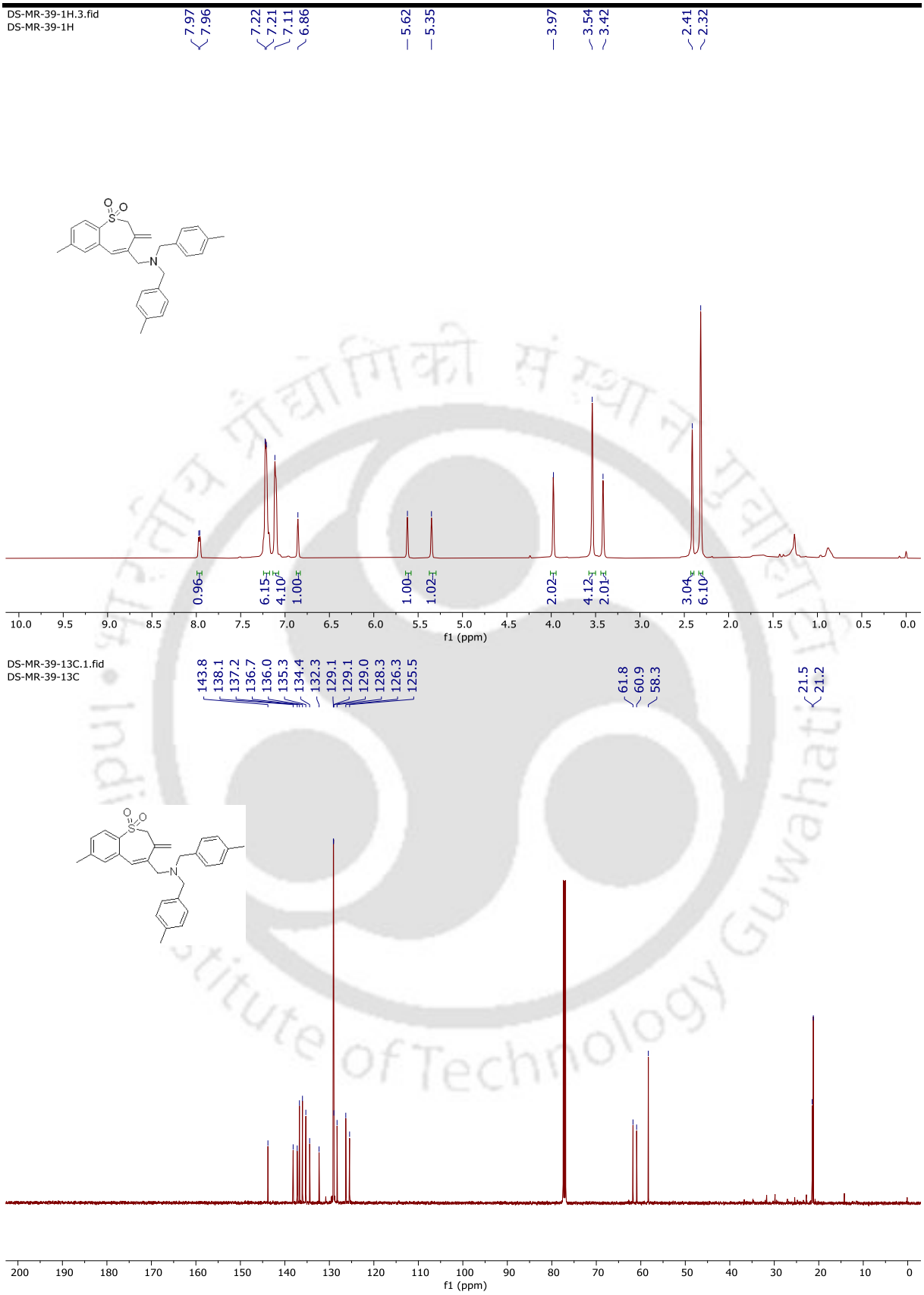

Figure 4.19: ^{1}H NMR (500 MHz) and $^{13}C\{^{1}H\}$ NMR (125 MHz) spectrum of Compound **4.7b** in $CDCl_3$.

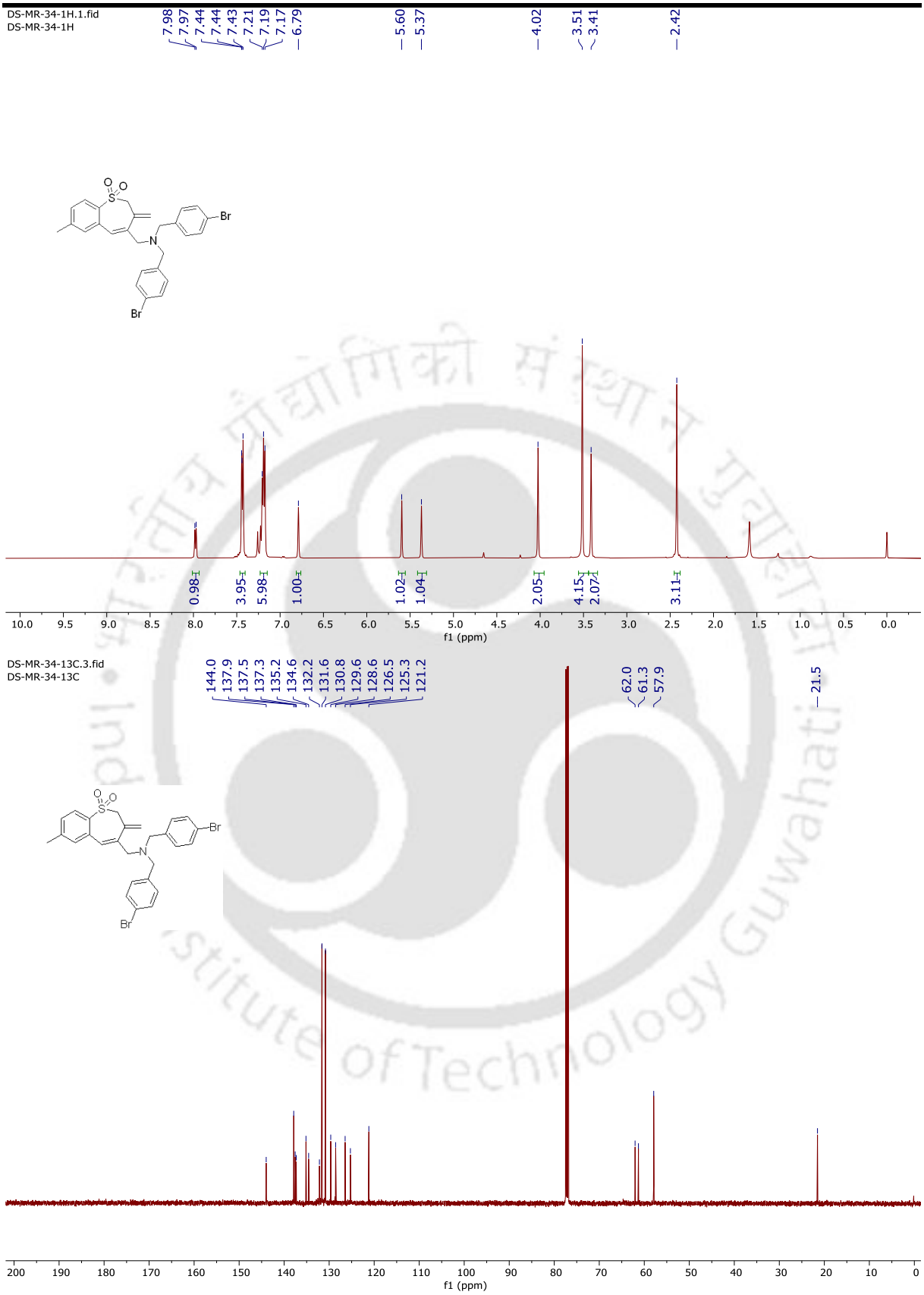

Figure 4.20: ^{1}H NMR (500 MHz) and $^{13}C\{^{1}H\}$ NMR (125 MHz) spectrum of Compound **4.7c** in $CDCl_3$.

Chapter V:

Visible-light-enabled sulfonyl radical-triggered radical cyclization strategy for the efficient synthesis of benzosultams

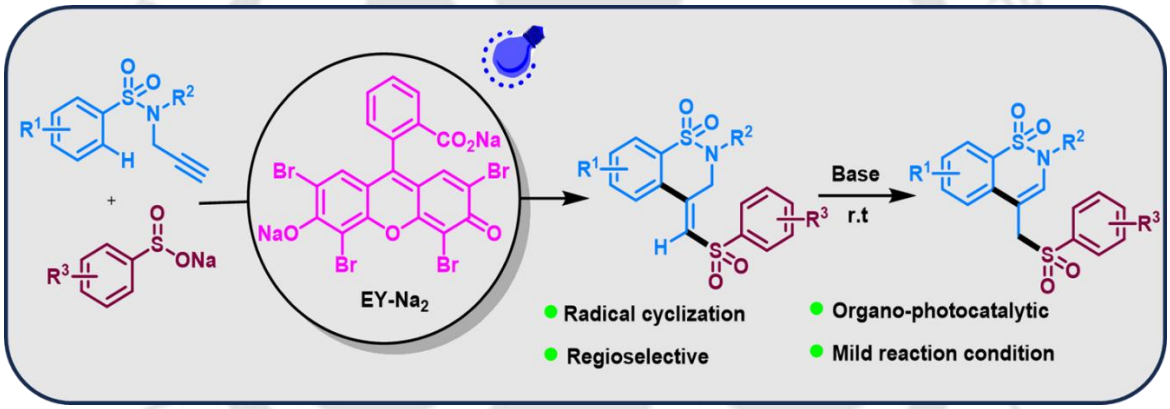

Manuscript under preparation.

5.1 Introduction:

Sultams are the cyclic equivalents of sulfonamide molecules and a significant class of heterocycles due to their extensive applications in various domains, including agricultural, pharmaceutical, and synthetic organic chemistry.[1] Particularly, benzosultams are present in a wide range of medicines, agricultural agents, and physiologically active substances. Numerous interesting bioactivities, including antibacterial, antidiabetic, and anticancer properties, are exhibited by them.[2] Commercially available drug molecules like the oxicam class of nonsteroidal anti-inflammatory drugs (NSAIDs) and some inhibitor molecules are made up of six-membered benzosultam derivatives (Figure 5.1).[3] Benzosultams are also found to be used in organic optoelectronics.[4] Additionally, in asymmetric synthesis, benzosultams can be used as chiral auxiliaries for stereoselective reactions.[5] They are frequently employed in synthetic organic chemistry as essential substrates for the creation of a wide range of heterocyclic systems and different functionalized benzosultam derivatives. Owing to their significant and diverse biological activities, benzosultams have attracted extensive synthetic interest. Consequently, various synthetic methods, ranging from classical cyclization to modern catalytic and photocatalytic approaches, have been developed to produce diverse benzosultam structures.

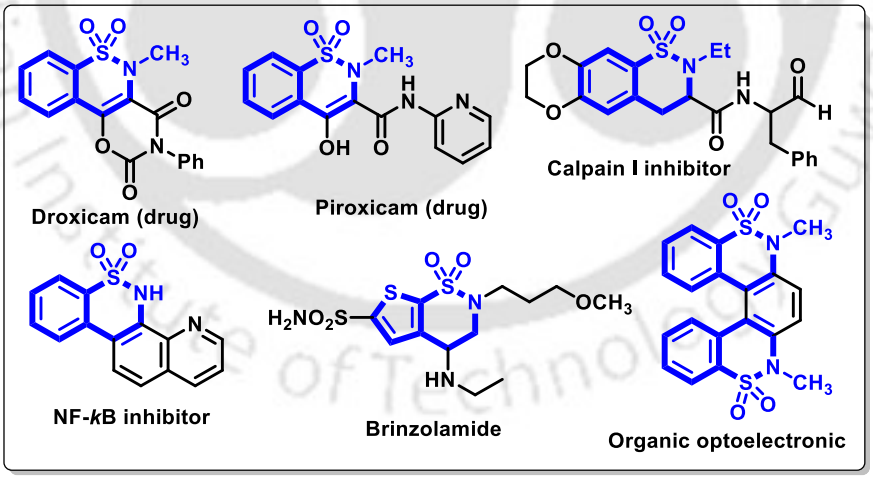

Figure 5.1: Biologically active benzosultam derivatives.

5.2 Previous reports:

Mondal and his group reported a palladium-catalyzed hydrocarbonation of propargyl tethered bromosulfonamides for the synthesis of benzosultams (Figure 5.2a).[6] Swamy and coworkers documented another approach for benzosultams synthesis via palladium-catalyzed cyclization of propargyl tethered iodosulfonamides with boronic acids (Figure 5.2b).[7] Hashmi and his

group reported a gold-catalyzed difunctionalization of o-alkynylbenzenesulfonamide with aryl diazonium salts. They have synthesized benzosultam derivatives under blue LEDs irradiation via gold-catalysed aminoarylation and subsequent release of the nitrogen gas (Figure 5.2c).[8] Suga and coworkers reported an electrochemical approach for the synthesis of a variety of benzosultams via the proton-coupled electron transfer (PCET) process. They have shown that a sulfonamide and Bu_4NOAc form a 1:1 hydrogen bonding complex, which gets oxidized under the electrochemical condition to afford a sulfonamidyl radical and initiate the radical cascade reaction (Figure 5.2d).[9] Recently, Li and his group demonstrated another method for the synthesis of benzosultams by reacting N-aryl N-propargyl arylsulfonamide with p-toluene sulfonyl hydrazide using an iron catalyst (Figure 5.2e).[10]

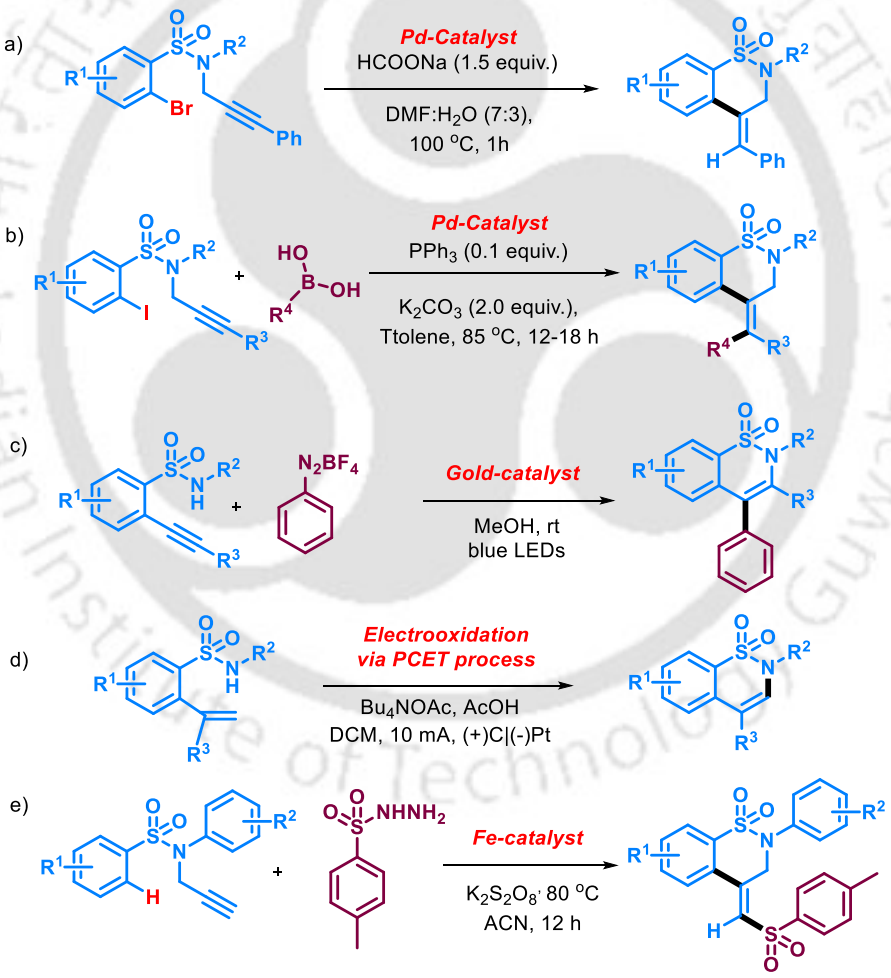

Figure 5.2: Previous literature reports for the benzosultam synthesis

All these methodologies rely on harsh reaction conditions, like the use of low-abundant novel or transition metal catalysts, high reaction temperature, and a stoichiometric amount of electrolyte. Therefore, it was envisioned that adopting a transition-metal-free

organophotocatalytic method operating under ambient conditions would offer substantial advantages, both in terms of sustainability and operational simplicity. So, the development of a visible light-induced, efficient, and sustainable method for the synthesis of benzosultams is of high importance. So here, a sustainable organophotocatalytic strategy for constructing benzosultams was developed.

5.3 Present work:

In this chapter, a sustainable organophotocatalytic approach for the synthesis of benzosultams was developed by reacting N-alkyl N-propargyl aryl-sulfonamide with sodium p-toluenesulfinate using eosin Y as the photocatalyst at room temperature under blue LEDs irradiation (Figure 5.3). Furthermore, the benzosultams with exocyclic double bonds can easily isomerize to the benzosultams with endocyclic double bonds through simple room-temperature base treatment. The technique also exhibits good yields and a broad substrate scope, and the procedure is gentle, metal-free, non-toxic, and environmentally benign.

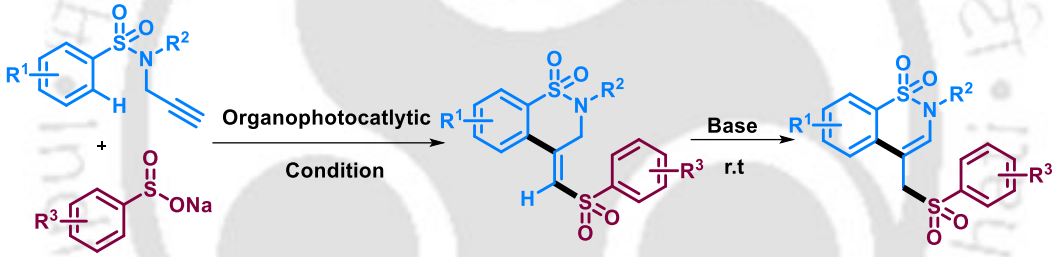

Figure 5.3: Present work for the benzosultam synthesis

5.4 Results and discussion:

Under visible light exposure, the experiment was initiated by selecting N-methyl N-propargyl p-toluenesulfonamide **5.1a** and sodium p-toluenesulfinate **5.2a** as model substrates. First **5.1a** and **5.2a** were reacted in the presence of photocatalyst EY-Na_2 (10 mol%), additive $K_2S_2O_8$ (2 equiv.), and 2.5 mL of DMF:H_2O (1:1) as the solvent system under the irradiation of 456 nm LEDs for 2 hours, producing the benzosultam derivative **5.3a** with 11 % isolated yield (Table 5.1, entry 1). After that, the reaction was tried in only DMF as the solvent, but it was not able to produce the product **5.3a** (Table 5.1, entry 2). Then DMSO:H_2O (1:1) and ACN:H_2O (1:1) were tried as the solvent system, and it was observed that the ACN:H_2O (4:1) solvent system provided the 49 % yield of **5.3a** (Table 5.1, entries 4-8). Next, using $(NH_4)_2S_2O_8$ as the additive, the highest yield, 73% of the benzosultams **5.3a**, was observed (Table 5.1, entry 9). Later, various additives, including TBHP, DTBP, and BPO, were screened, yielding inferior results

(Table 5.1, entries 10-12). Various photocatalysts were also checked, and the formation of product **5.3a** was observed with a lower yield (Table 5.1, entries 13-16).

Table 5.1: Optimization of reaction parameters for benzosultam formation[a]

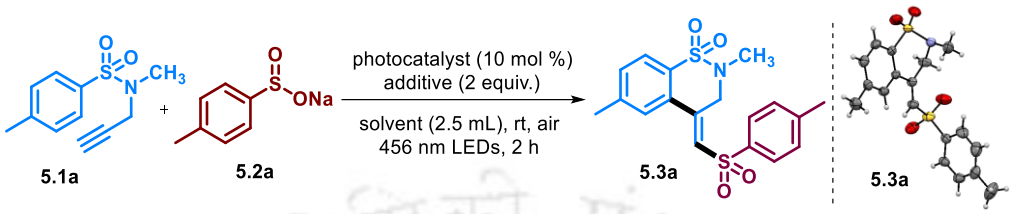

Entry	Catalyst (mol %)	Additive (equiv.)	Solvent (2.5 mL)	Yield[b] (%)
1.	EY-Na_2 (10)	$K_2S_2O_8$ (2)	DMF:H_2O (1:1)	11
2.	EY-Na_2 (10)	$K_2S_2O_8$ (2)	DMF (2.5)	-
3.	EY-Na_2 (10)	$K_2S_2O_8$ (2)	DMSO:H_2O (1:1)	21
4.	EY-Na_2 (10)	$K_2S_2O_8$ (2)	ACN:H_2O (1:1)	29
5.	EY-Na_2 (10)	$K_2S_2O_8$ (2)	ACN:H_2O (2:1)	35
6.	EY-Na_2 (10)	$K_2S_2O_8$ (2)	ACN:H_2O (3:1)	41
7.	EY-Na_2 (10)	$K_2S_2O_8$ (2)	ACN:H_2O (4:1)	49
8.	EY-Na_2 (10)	$K_2S_2O_8$ (2)	ACN:H_2O (5:1)	48
9.	EY-Na_2 (10)	$(NH_4)_2S_2O_8$ (2)	ACN:H_2O (4:1)	73
10.	EY-Na_2 (10)	TBHP (2)	ACN:H_2O (4:1)	31
11.	EY-Na_2 (10)	DTBP (2)	ACN:H_2O (4:1)	25
12.	EY-Na_2 (10)	BPO (2)	ACN:H_2O (4:1)	17
13.	EY-H_2 (10)	$(NH_4)_2S_2O_8$ (2)	ACN:H_2O (4:1)	59
14.	Fluorescein (10)	$(NH_4)_2S_2O_8$ (2)	ACN:H_2O (4:1)	47
15.	Rose Bengal (10)	$(NH_4)_2S_2O_8$ (2)	ACN:H_2O (4:1)	41
16.	4CzIPN (10)	$(NH_4)_2S_2O_8$ (2)	ACN:H_2O (4:1)	53
17.	-	$(NH_4)_2S_2O_8$ (2)	ACN:H_2O (4:1)	-
18[c].	EY-Na_2 (10)	$(NH_4)_2S_2O_8$ (2)	ACN:H_2O (4:1)	-
19.	EY-Na_2 (10)	-	ACN:H_2O (4:1)	trace
20[d].	EY-Na_2 (10)	$(NH_4)_2S_2O_8$ (2)	ACN:H_2O (4:1)	71

[a]**Conditions: 5.1a** (0.25 mmol), **5.2a** (0.75 mmol), additive (0.5 mmol), solvent (2 mL: 0.5 mL), 2h, 456 nm blue LED irradiation. b = isolated yields, c = in the dark, d = in argon atmosphere.

In the absence of a photocatalyst and under dark conditions reaction did not produce the **5.3a** product, and in the absence of an additive, it generated a trace amount of **5.3a** product (Table 5.1, entries 17-19). Further, under an argon atmosphere, the reaction provided an almost similar yield of the **5.3a** product, showing that atmospheric oxygen is not hampering the reaction (Table 5.1, Entry 20). From all these findings it was observed that when **5.1a** (1 equiv.) reacted with **5.2a** (3 equiv.) in the presence of photocatalyst EY-Na_2 (10 mol%), additive $(NH_4)_2S_2O_8$ (2 equiv.), and 2.5 mL of ACN:H_2O (4:1) solvent under the irradiation of 456 nm LEDs for 2 hour is the optimized reaction conditions (table 5.1, entry 5, 73 %).

Scheme 5.1: Substrate scope for the variation of N-alkyl N-propargyl arylsulfonamides[a]

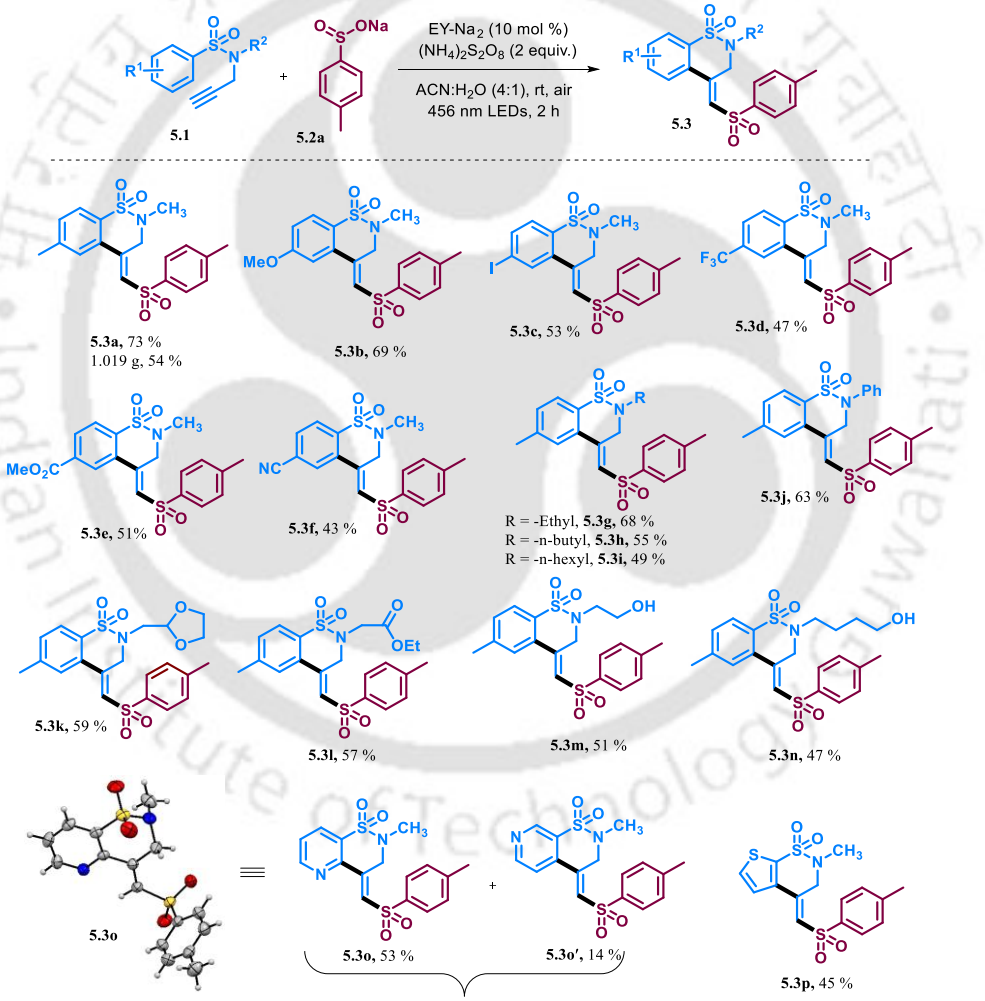

[a]Conditions: **5.1** (0.25 mmol), **5.2a** (0.75 mmol), $(NH_4)_2S_2O_8$ (0.50 mmol), ACN:H_2O (2 ml:0.5 mL), 2 h, 456 nm blue LED irradiation.

After getting the best conditions for benzosultam synthesis, the versatility of the process for various substrates was studied. First, N-alkyl N-propargyl arylsulfonamide **5.1**, was varied, and it was noticed that a diverse range of N-alkyl N-propargyl arylsulfonamides **5.1**, undergo this

process very smoothly (Scheme 5.1). Electron-releasing group (-Me, -OMe) present at the *para*-position of the aryl ring of **5.1**, generated the corresponding benzosultam product with good yield (**5.3a** and **5.3b**, 73 and 69 %), but the electron-withdrawing functional group (-CF_3, -CO_2Me and -CN) provided a little lower yield of the product (**5.3d-5.3f**, 43-51 %). Then various N-substituted N-propargyl arylsulfonamides **5.1**, like N-ethyl, N-n-butyl, N-nHexyl, N-phenyl, and also N-atom bearing cyclic acetal moiety, ester moiety, and free alcoholic group, participated in this reaction very well and produced the product with good yield (**5.3g-5.3n**, 47-68 %). N-methyl N-propargyl pyridinesulfonamide **5.1**, and N-methyl N-propargyl thiophenesulfonamide **5.1**, were well compatible in this method (**5.3o** and **5.3p**, 53 and 45 %).

Scheme 5.2. Substrate scope for the variation of sodium aryl sulfinates[a]

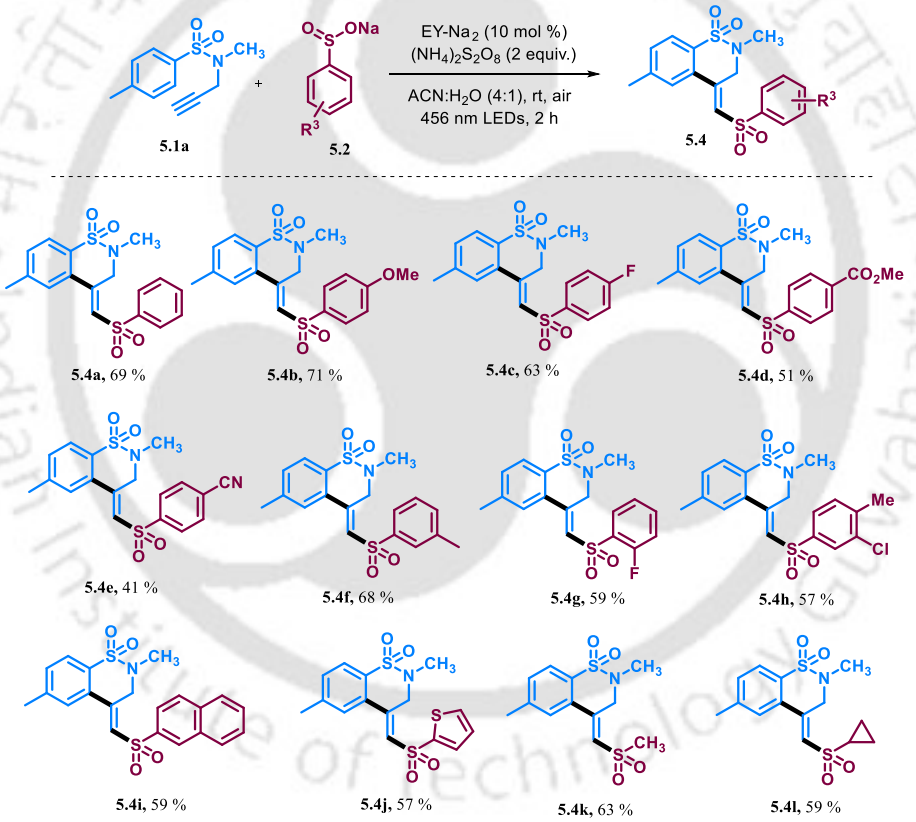

[a]Conditions: **5.1a** (0.25 mmol), **5.2** (0.75 mmol), $(NH_4)_2S_2O_8$ (0.50 mmol), ACN:H_2O (2 ml:0.5 mL), 2 h, 456 nm blue LED irradiation.

Later, differently substituted sodium arylsulfinates **5.2**, were also varied, and it was observed that these generate the corresponding product without any hindrance (Scheme 5.2). Electron-pushing group (-OMe) situated at the *para*-position of sodium arylsulfinates **5.2**, producing the desired product with good yield (**5.4b**, 71 %), but the electron-pulling functional group (-F, -CO_2Me, and -CN) provides a slightly lower yield of the product (**5.4c-5.4e**, 41-51 %). Sodium

naphthyl sulfinates and sodium thiophene sulfinates are also working well in this method and generating the corresponding product with decent yield (**5.4i** and **5.4j**, 59 and 57 %). Even aliphatic sodium methyl sulfinates and sodium cyclopropyl sulfinates are also well compatible in this process and furnish the corresponding benzoslutam product with significant yield (**5.4k** and **5.4l**, 63 and 59 %). The structure of the molecules was also supported by single-crystal X-ray data of compounds **5.3a** (CCDC:2507153) and **5.3o** (CCDC:2507209). A 5 mmol scale reaction between **5.1a** and **5.2a** was performed to demonstrate the scalability of the protocol (Figure 5.4).

5.5 Post-functionalization:

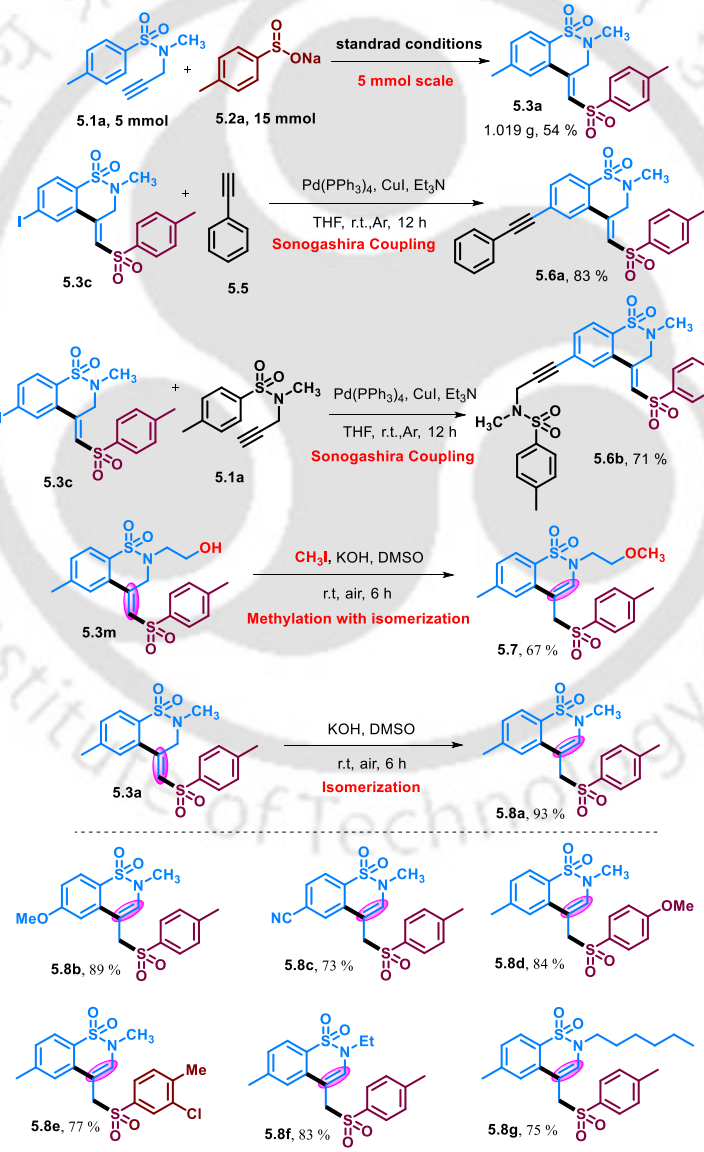

Figure 5.4: Post-functionalization.

For the post-synthetic functionalization, a Sonogashira coupling of compounds **5.3c** with phenyl acetylene (**5.5**) and alkyne **5.1a** was also performed. The methylation of compound **5.3m**, along with the isomerization of exocyclic double bonds to endocyclic double bonds, was achieved by treating it with KOH in DMSO at room temperature (Figure 5.4, **5.7**, 67 %). Later, this isomerization was performed for various other derivatives and observed that in spite of the substituent present on the benzosultams, they isomerize to the endo cyclic double-bonded partner very smoothly (Figure 5.4, **5.8a**-**5.8g**, 73-93 %).

5.6 Control experiments:

Various control experiments were conducted to elucidate the reaction mechanism. Under the standard conditions, 4.0 equiv. of 2,2,6,6-tetramethylpiperidine N-oxide (TEMPO), 2,6-di-tert-butyl-4-methylphenol (BHT), and 1,1-diphenylethylene were introduced to the model reactions as radical scavengers. The desired product **5.3a** was not observed at all. This finding suggested the involvement of a radical route.

a) Procedure for radical trapping experiment with TEMPO/BHT/1,1-diphenylethylene:

The N-methyl N-propargyl *p*-toluenesulfonamide **5.1a** (0.25 mmol, 1 equiv.), sodium p-toluene sulfinates **5.2a** (0.75 mmol, 3 equiv.), $(NH_4)_2S_2O_8$ (0.50 mmol, 2 equiv.), Eosin Y (10 mol%), and TEMPO (1.00 mmol, 4 equiv.) were taken in an oven-dried reaction tube with a magnetic bead. After that, ACN:H_2O (2.5 mL, 4:1) was added, and the reaction mixture was allowed to stir under the 456 nm LED irradiation at room temperature in an open-air atmosphere for 2 h. The reaction was monitored through TLC, and it was noticed that after the reaction time, there was no spot of the desired product.

Similarly, the reaction with another radical scavenger such as BHT (1.00 mmol, 4 equiv.) and 1,1-diphenylethylene (1.00 mmol, 4 equiv.) was also performed. In the case of BHT a lower yield of the product (**5.3a**, 15 %) was observed, and in the case of 1,1-diphenylethylene the desired product (**5.3a**) was not obtained.

Later, two competitive experiments were done, and it was found that an electron-donating group present at the *para*-position of the aryl ring of N-methyl N-propargyl arylsulfonamide and sodium aryl sulfinates exhibits higher reactivity over the electron-withdrawing group (Figure 5.5).

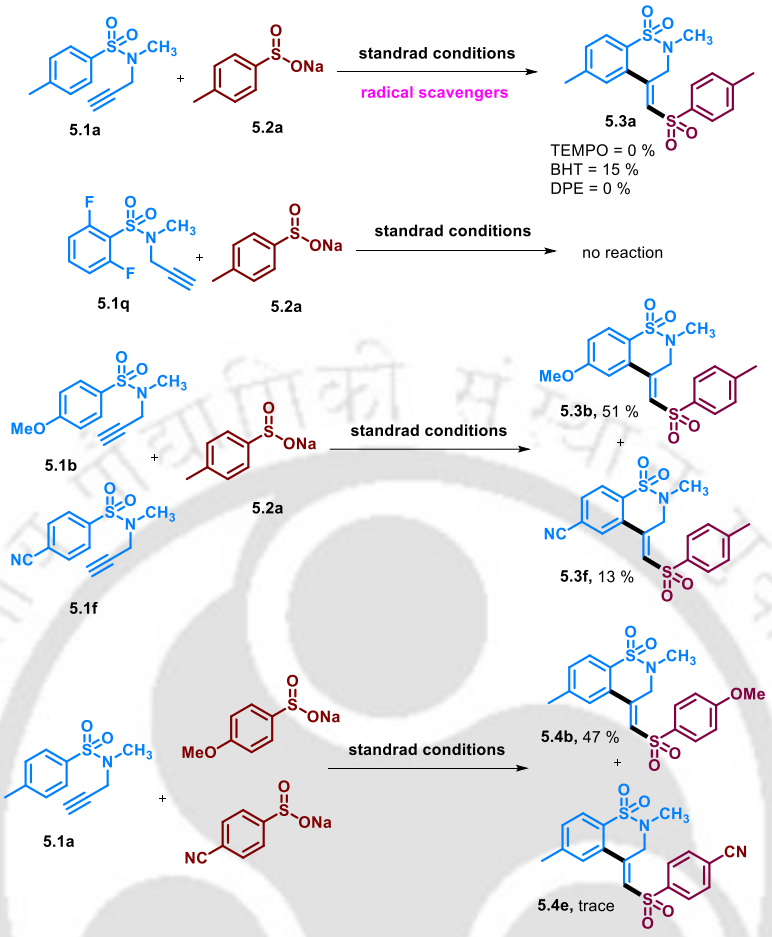

Figure 5.5: Control experiments.

b) Fluorescence quenching experiments:

Firstly, the fluorescence quenching of photocatalyst eosin Y (3 mL, 20 μM) was tried by exciting with the wavelength 470 nm and recording the emission spectra at 539 nm with reactant **5.1a** (N-methyl N-propargyl *p*-toluenesulfonamide, 30 mM), no changes in the fluorescence spectrum of the photocatalyst was observed. Then quenching was tried with reactant **5.2a** (sodium p-toluene-sulfinate, 30 mM), in this case also no quenching of the fluorescence spectrum of the photocatalyst was noticed. Neither the N-methyl N-propargyl *p*-toluenesulfonamide **5.1a** nor the sodium aryl sulfinate **5.2a** was able to quench the excited state of eosin Y (Figure 5.6a and 5.6b). These results suggest that there is no direct energy or electron transfer between reactants **5.1a** or **5.2a** and the excited photocatalyst. Next, the fluorescence quenching experiments was performed with $(NH_4)_2S_2O_8$ (APS) and observed that the fluorescence spectrum of the excited photocatalyst was quenched and exhibited a linear quenching in the Stern-Volmer plot (Figures 5.6c and 5.6d). These findings suggested the direct interaction of $(NH_4)_2S_2O_8$ (APS) with the excited photocatalyst.

c) Light On/Off Experiment:

An On/Off experiment was performed to check the impact of light on this reaction by following the general procedure 7 with alternating exposure (30 minutes) of light and darkness. These showed that the reaction process was completely stopped in the absence of light and resumed with further illumination. These results demonstrate that light is an essential component for this reaction (Figure 5.6e).

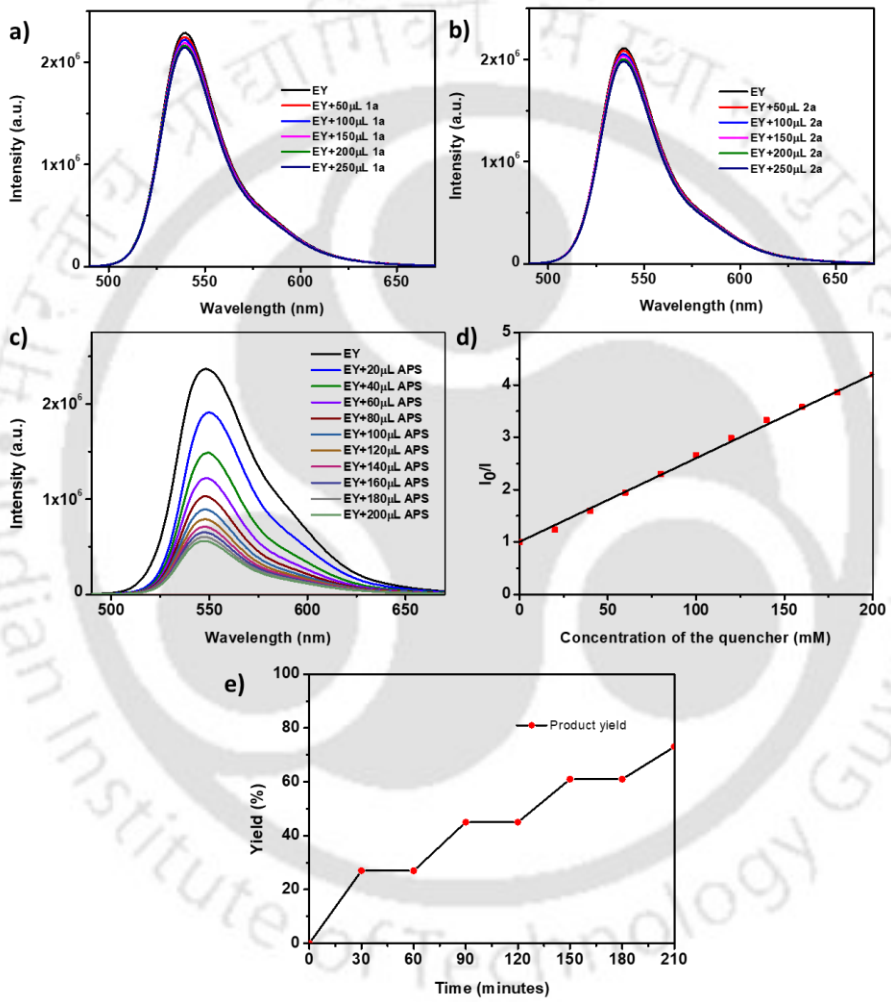

Figure 5.6: a) Fluorescence quenching with **5.1a**, a) Fluorescence quenching with **5.2a**, c) Fluorescence quenching with ammonium persulfate (APS), d) Stern-Volmer plot, e) Light on/off experiment

5.7. Plausible mechanism:

Based on earlier studies,[11,13] and validated by our control experiments, and DFT calculations, we have outlined a plausible mechanism for benzosultam formation. (Figure 5.7). Under blue LED irradiation first organophotocatalyst EY gets excited to its higher energy state, and then

undergoes single electron transfer (SET) with $(NH_4)_2S_2O_8$, generating SO_4^{2-} and $SO_4^{\bullet-}$ ion (E^{ox}= + 1.86 V vs SCE),[14] and the catalyst itself goes to its oxidised form $EY^{\bullet+}$ [E^{ox}(EY* to $EY^{\bullet+}$)= + 1.11 V vs SCE].[15] Then this oxidised form of the catalyst takes one electron [E^{red}($EY^{\bullet+}$ to EY)= + 0.78 V vs SCE][15] from sodium p-toluenesulfinates (E^{ox}= -0.37 V vs SCE, see SI),[15] to produce the sulfonyl radical, and the catalyst goes back to its ground state.

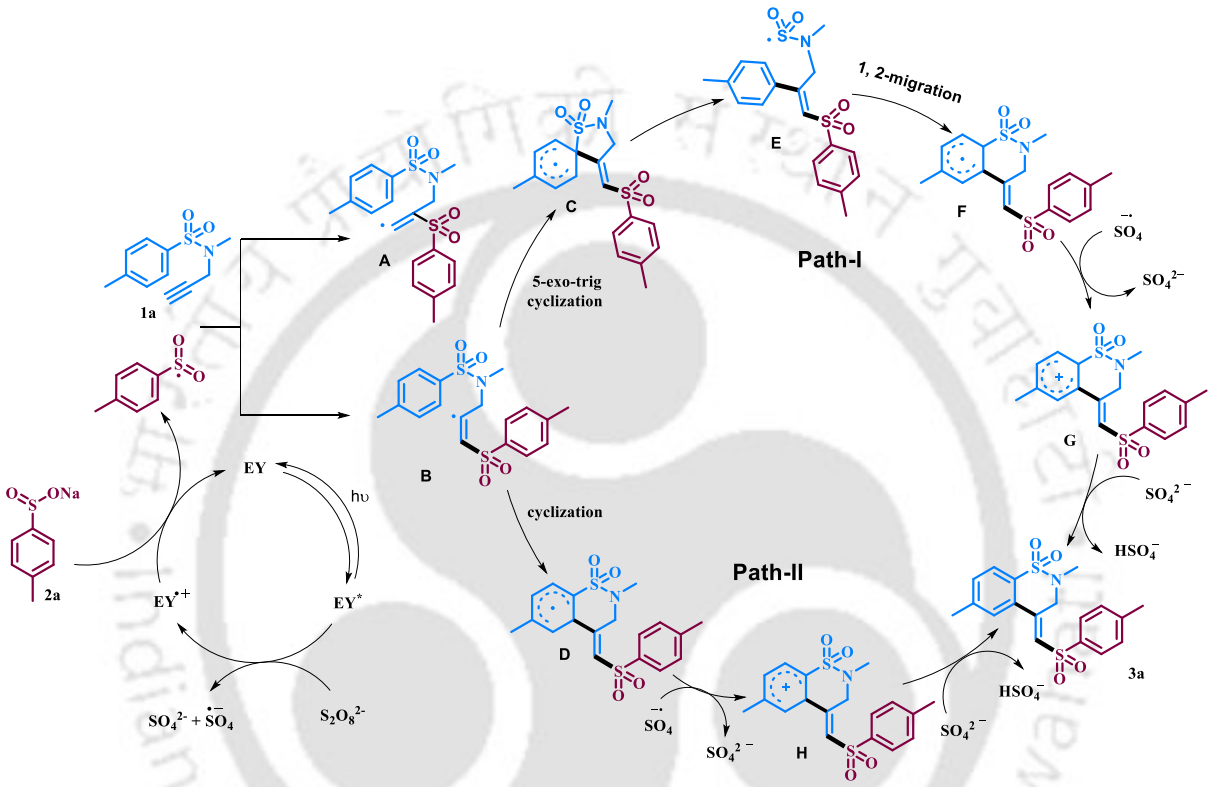

Figure 5.7: Plausible reaction mechanism and DFT calculation.

After that, the sulfonyl radical attacks the terminal position of the alkynes and generates the vinyl radical intermediate **B**, which can follow two different pathways to produce the desired product **3a**. Path-I, follows a 5-exo-trig cyclization, 1,2-migration, single-electron trans-fer (SET) with $SO4^{\bullet-}$ or $EY^{\bullet+}$, and aromatization to provide the benzosultam product **3a**. In Path-II, radical intermediate **B** undergoes a cyclisation followed by single-electron transfer (SET) with $SO4^{\bullet-}$ or $EY^{\bullet+}$, and aromatization leads to the formation of benzosultam product **3a**. To identify the suitable mechanistic pathway, a DFT calculation was done, and it was observed that Path-I is energetically more favorable than Path-II.

5.8 Conclusion:

In conclusion, a sustainable and effective organophotocatalytic synthesis of benzosultams was developed. Here, N-alkyl N-propargyl arylsulfonamide undergoes sulfonyl radical-triggered 6-exo-dig cyclization to provide the benzosultam derivative. Exocyclic double bonds of the benzosultams very smoothly isomerize to the corresponding endocyclic double bonds by simple KOH treatment in DMSO at room temperature. The mild and simple nature of this protocol makes the process better and a suitable alternative to previously reported methods.

5.9 Experimental sections:

a) General procedure for the synthesis of N-alkyl N-propargyl arylsulfonamides:

N-alkyl N-propargyl arylsulfonamide derivatives were prepared by following the reported procedures.[12]

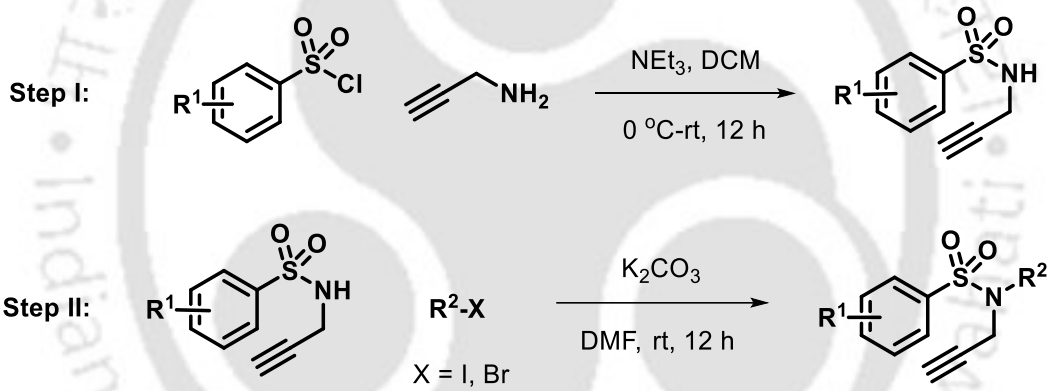

Step I: Propargylamine (5.0 mmol, 1.0 equiv.) and triethylamine (7.5 mmol, 1.5 equiv.) were taken in a round-bottom flask, and then DCM (10 mL) was added, and the mixture was stirred for 5 minutes. After that, aryl sulfonyl chloride (5.0 mmol, 1.0 equiv.) was added portion-wise at an ice bath. This mixture was stirred by a magnetic stirrer for 12 h and the reaction was monitored through TLC. After the reaction was completed, the mixture was washed with water and extracted with DCM. The combined organic phase was dried over Na_2SO_4 and concentrated under reduced pressure. Crude product is used directly in the next step without further purification.

Step II: N-(prop-2-yn-1-yl) arylsulfonamide (3.0 mmol, 1.0 equiv.) and K_2CO_3 (4.5 mmol, 1.5 equiv.) were taken in a round-bottom flask in DMF (10 mL) and stirred for 5 minutes. Then methyl iodide (4.5 mmol, 1.5 equiv.) was added dropwise, and the mixture was stirred at room temperature for 12 h. After completion of the reaction, the mixture was diluted with ethyl acetate and washed with water. The combined organic phase was dried over Na_2SO_4 and

concentrated under reduced pressure. The crude product was purified by column chromatography on silica gel eluting with petroleum ether/ethyl acetate.

b) General procedure for the preparation of sodium aryl sulfinates

Sodium aryl sulfinates **5.2a**, **5.2b**, and **5.2n** are commercially available. **5.2c-5.2m** and **5.2o** were synthesized by following the reported procedure.[13]

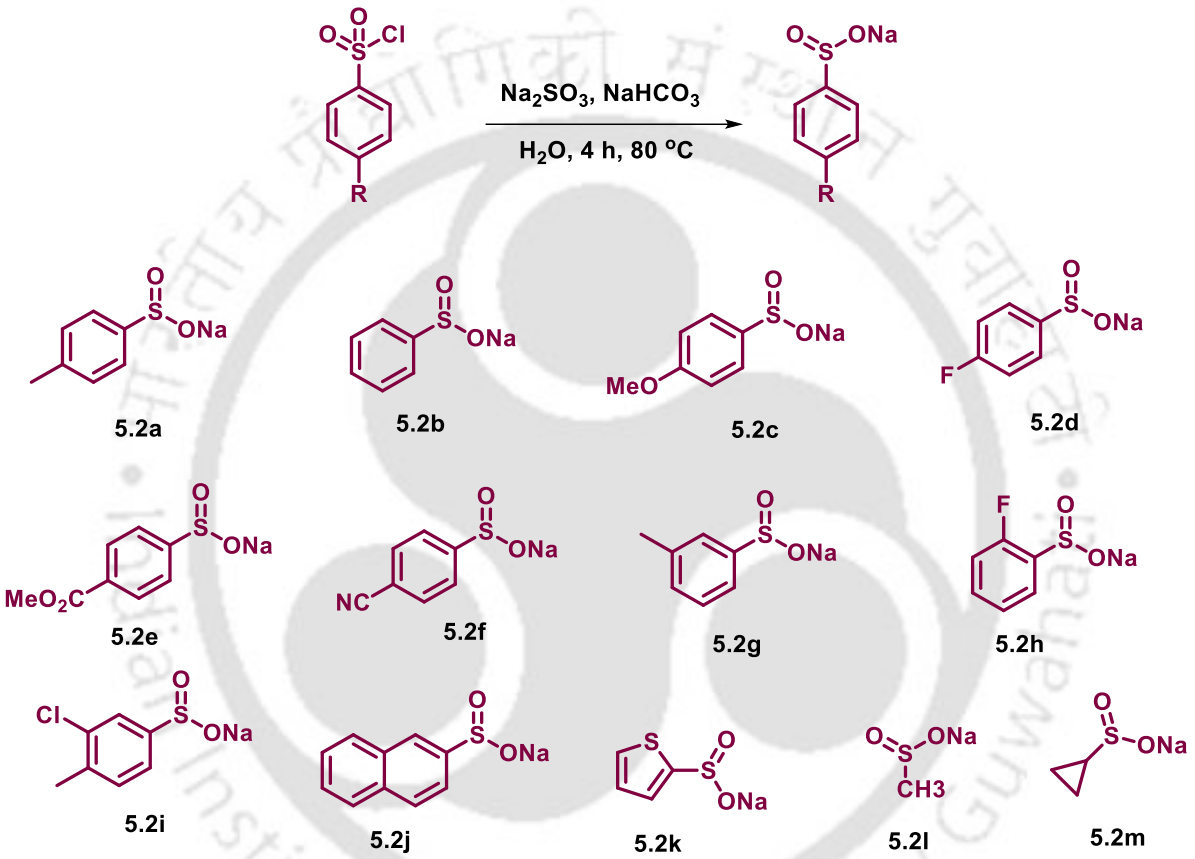

Sodium sulphite (20.0 mmol, 2.0 equiv.), sodium bicarbonate (20.0 mmol, 2.0 equiv.) and the corresponding aryl sulfonyl chloride (10.0 mmol, 1.0 equiv.) were dissolved in distilled water (10 mL). The reaction mixture was stirred for 4 h at 80 °C. After cooling to room temperature, water was removed by lyophilization overnight. The white residue was extracted with ethanol (25 mL) to obtain the desired aryl sulfinate as a white crystalline powder. The product was used for the next step without further purification.

c) General Procedure for the synthesis of benzosultams:

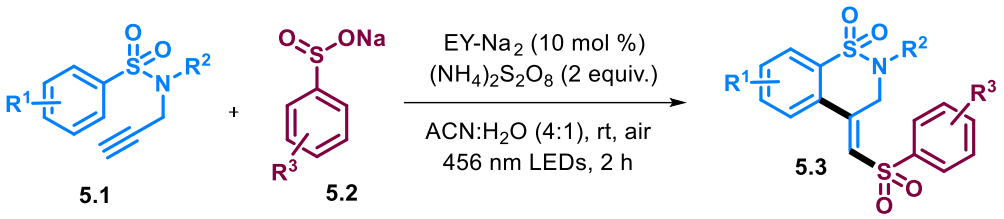

The N-alkyl N-propargyl arylsulfonamide **5.1** (0.25 mmol, 1 equiv.), sodium aryl sulfinates **5.2** (0.75 mmol, 3 equiv.), $(NH_4)_2S_2O_8$ (0.50 mmol, 2 equiv.) and organophotocatalyst Eosin Y (10 mol%, 0.1 equiv.) were taken in an oven-dried reaction tube with a magnetic bead. After that ACN:H_2O (2.5 mL, 4:1) was added, and the reaction mixture was allowed to stir under the 456 nm LED irradiation at room temperature in an open-air atmosphere for 2 h. The reaction was monitored by TLC, and after completion of the reaction, the reaction mixture was diluted with ethyl acetate. After that, the organic layer was washed with water. Then the combined organic layer was separated and dried over Na_2SO_4. The solvent was evaporated under reduced pressure to get the crude product. Furthermore, the purification of the crude product was achieved through column chromatography on silica gel, using a mixture of petroleum ether and ethyl acetate as the eluent.

5.10 Analytical data:

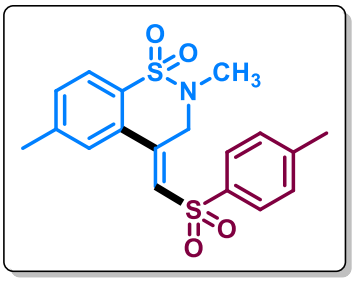

(Z)-2,6-dimethyl-4-(tosylmethylene)-3,4-dihydro-2H-benzo[e][1,2]thiazine 1,1-dioxide (**3a**): White solid, (30 % ethyl acetate in petroleum ether) yield: (69 mg) 73 %; **^{1}H NMR** (500 MHz, $CDCl_3$) δ 7.84 (d, J = 8.4 Hz, 2H), 7.76 (d, J = 7.9 Hz, 1H), 7.44 – 7.35 (m, 4H), 6.95 (t, J = 2.0 Hz, 1H), 5.00 (d, J = 2.0 Hz, 2H), 2.71 (s, 3H), 2.45 (s, 3H), 2.42 (s, 3H). **^{13}C NMR** (125 MHz, $CDCl_3$) δ 145.5, 143.8, 140.1, 137.8, 132.7, 132.2, 130.9, 130.4, 129.4, 127.6, 126.2, 126.0, 50.8, 37.4, 21.8. **HRMS** (ESI-TOF) m/z: $[M+H]^+$ Calcd for $C_{18}H_{20}NO_4S_2$ 378.0829; Found 378.0810.

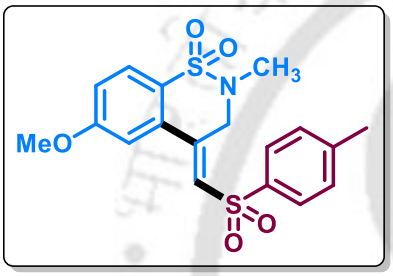

(Z)-6-methoxy-2-methyl-4-(tosylmethylene)-3,4-dihydro-2H-benzo[e][1,2]thiazine 1,1-dioxide (**3b**): White solid, (30 % ethyl acetate in petroleum ether) yield: (68 mg) 69 %; **^{1}H NMR** (500 MHz, $CDCl_3$) δ 7.84 (d, J = 8.0 Hz, 2H), 7.81 (d, J = 8.5 Hz, 1H), 7.38 (d, J = 8.0 Hz, 2H), 7.09 (d, J = 8.7 Hz, 1H), 7.05 (s, 1H), 6.92 (s, 1H), 4.99 (s, 2H), 3.87 (s, 3H), 2.70 (s, 3H), 2.45 (s, 3H). **^{13}C NMR** (125 MHz, $CDCl_3$) δ 162.8, 145.6, 140.2, 137.7, 132.9, 130.5, 129.7, 128.1, 127.6, 127.3, 117.1, 111.2, 56.0, 51.0, 37.4, 21.8. **HRMS** (ESI-TOF) m/z: $[M+H]^+$ Calcd for $C_{18}H_{20}NO_5S_2$ 394.0778; Found 394.0761.

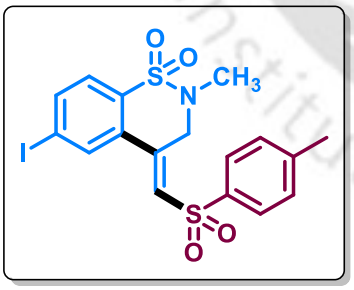

(Z)-6-iodo-2-methyl-4-(tosylmethylene)-3,4-dihydro-2H-benzo[e][1,2]thiazine 1,1-dioxide (**3c**): White solid, (30 % ethyl acetate in petroleum ether) yield: (65 mg) 53 %; **^{1}H NMR** (500 MHz, $CDCl_3$) δ 7.93 (d, J = 9.2 Hz, 2H), 7.84 (d, J = 8.1 Hz, 2H), 7.57 (d, J = 8.0 Hz, 1H), 7.40 (d, J = 8.0 Hz, 2H), 6.91 (s, 1H), 5.01 (d, J = 2.0 Hz, 2H), 2.73 (s, 3H), 2.46 (s, 3H). **^{13}C NMR** (125 MHz, $CDCl_3$) δ 145.8, 140.7, 138.3, 137.5, 134.7, 134.5, 132.6, 130.6, 130.5, 127.7, 127.2, 99.6, 50.7, 37.4, 21.9. **HRMS** (ESI-TOF) m/z: $[M+H]^+$ Calcd for $C_{17}H_{17}INO_4S_2$ 489.9639; Found 489.9609.

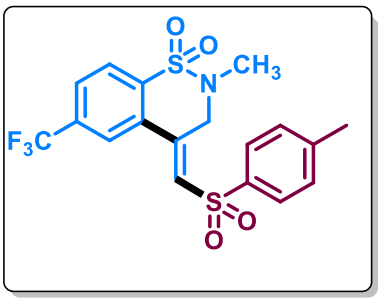

(Z)-2-methyl-4-(tosylmethylene)-6-(trifluoromethyl)-3,4-dihydro-2H-benzo[e][1,2]thiazine 1,1-dioxide (**3d**): White solid (50 % ethyl acetate in petroleum ether) Yield: (51 mg) 47 %; **^{1}H NMR** (500 MHz, $CDCl_3$) δ 8.01 (d, *J* = 8.0 Hz, 1H), 7.87 – 7.84 (m, 4H), 7.41 (d, *J* = 8.0 Hz, 2H), 7.01 (t, *J* = 2.0 Hz, 1H), 5.07 (d, *J* = 2.1 Hz, 2H), 2.76 (s, 3H), 2.46 (s, 3H). **^{13}C NMR** (125 MHz, $CDCl_3$) δ 138.30, 138.27, 137.29, 134.9 (q, J= 33.3 Hz), 132.20, 131.30, 130.56, 130.53, 128.3 (q, J= 28.1 Hz), 127.77, 126.90, 123.1 (q, J= 3.7 Hz), 122.8 (q, J= 272.1 Hz), 50.7, 37.3, 21.8. **^{19}F NMR** (470 MHz, $CDCl_3$) δ -63.2. **HRMS** (ESI-TOF) m/z: $[M+H]^+$ Calcd for $C_{18}H_{17}F_3NO_4S_2$ 432.0546; Found 432.0522.

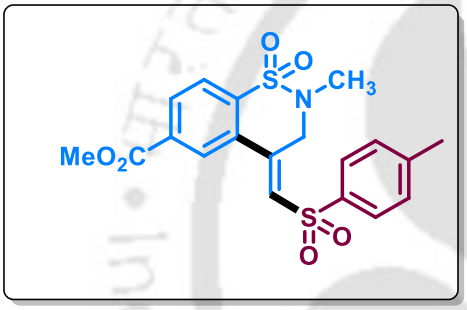

(Z)-2-methyl-1,1-dioxido-4-(tosylmethylene)-3,4-dihydro-2H-benzo[e][1,2]thiazin-6-yl acetate (**3e**): White solid (50 % ethyl acetate in petroleum ether) Yield: (54 mg) 51 %; **^{1}H NMR** (500 MHz, $CDCl_3$) δ 8.28 (s, 1H), 8.20 (d, *J* = 7.8 Hz, 1H), 7.94 (d, *J* = 8.1 Hz, 1H), 7.84 (d, *J* = 7.6 Hz, 2H), 7.39 (d, *J* = 7.5 Hz, 2H), 7.07 (s, 1H), 5.06 (s, 2H), 3.96 (s, 3H), 2.74 (s, 3H), 2.45 (s, 30H). **^{13}C NMR** (125 MHz, $CDCl_3$) δ 164.1, 145.8, 138.7, 138.5, 137.5, 134.3, 132.3, 131.5, 130.7, 130.5, 127.7, 127.2, 126.3, 53.1, 50.6, 37.2, 21.8. **HRMS** (ESI-TOF) m/z: $[M+H]^+$ Calcd for $C_{19}H_{20}NO_6S_2$ 422.0727; Found 422.0734.

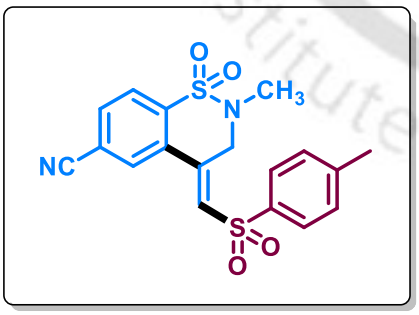

(Z)-2-methyl-4-(tosylmethylene)-3,4-dihydro-2H-benzo[e][1,2]thiazine-6-carbonitrile 1,1-dioxide (**3f**): White solid (30 % ethyl acetate in petroleum ether) Yield: (42 mg) 43 %; **^{1}H NMR** (500 MHz, $CDCl_3$) δ 7.99 (d, *J* = 8.0 Hz, 1H), 7.91 (s, 1H), 7.85 (dd, *J* = 8.4, 1.9 Hz, 3H), 7.41 (d, *J* = 8.1 Hz, 2H), 7.00 (t, *J* = 2.0 Hz, 1H), 5.07 (d, *J* = 2.0 Hz, 2H), 2.77 (s, 3H), 2.46 (s, 3H). **^{13}C NMR** (125 MHz, $CDCl_3$) δ 146.0, 138.8, 137.2, 137.1, 134.4, 132.6, 131.8, 130.6, 129.8, 127.8, 126.9, 117.1, 116.6, 50.5, 37.2, 21.8. **HRMS** (ESI-TOF) m/z: $[M+H]^+$ Calcd for $C_{18}H_{17}N_2O_4S_2$ 389.0625; Found 389.0620.

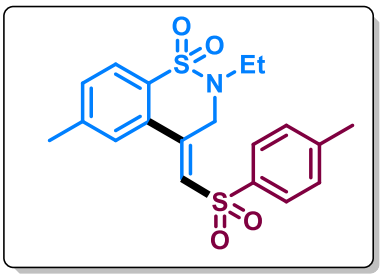

(Z)-2-ethyl-6-methyl-4-(tosylmethylene)-3,4-dihydro-2H-benzo[e][1,2]thiazine 1,1-dioxide (**3g**): White solid (30 % ethyl acetate in petroleum ether) Yield: (67 mg) 68 %; **^{1}H NMR** (600 MHz, $CDCl_3$) δ 7.76 (d, *J* = 8.1 Hz, 1H), 7.67 (d, *J* = 8.3 Hz, 2H), 7.22 (dd, *J* = 8.4, 3.1 Hz, 3H), 7.00 (s, 1H), 6.33 (s, 1H), 4.25 (s, 2H), 3.71 (q, *J* = 7.2 Hz, 2H), 2.34 (s, 3H), 2.33 (s, 3H), 1.25 (t, *J* = 7.2 Hz, 3H). **^{13}C NMR** (151 MHz, $CDCl_3$) δ 145.0, 142.5, 134.7, 134.4, 131.7, 129.8, 129.3, 128.6, 128.5, 123.9, 122.1, 105.9, 57.7, 43.4, 21.9, 21.6, 15.9. **HRMS** (ESI-TOF) m/z: $[M+H]^+$ Calcd for $C_{19}H_{22}NO_4S_2$ 392.0985; Found 392.0956.

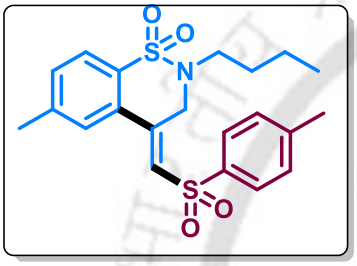

(Z)-2-butyl-6-methyl-4-(tosylmethylene)-3,4-dihydro-2H-benzo[e][1,2]thiazine 1,1-dioxide (**3h**): White solid (30 % ethyl acetate in petroleum ether) Yield: (58 mg) 55 %; **^{1}H NMR** (500 MHz, $CDCl_3$) δ 7.77 (d, *J* = 8.1 Hz, 1H), 7.67 (d, *J* = 8.0 Hz, 2H), 7.22 (dd, *J* = 8.8, 3.3 Hz, 3H), 7.00 (s, 1H), 6.32 (s, 1H), 4.25 (s, 2H), 3.63 (t, *J* = 7.4 Hz, 1H), 2.35 (s, 3H), 2.33 (s, 3H), 1.62 – 1.56 (m, 2H), 1.27 (q, *J* = 7.4 Hz, 2H), 0.90 (t, *J* = 7.4 Hz, 3H). **^{13}C NMR** (125 MHz, $CDCl_3$) δ 145.0, 142.5, 135.0, 134.4, 131.7, 129.8, 129.3, 128.6, 128.5, 123.9, 122.1, 105.8, 57.7, 48.1, 32.4, 21.9, 21.6, 19.7, 13.7. **HRMS** (ESI-TOF) m/z: $[M+H]^+$ Calcd for $C_{21}H_{26}NO_4S_2$ 420.1298; Found 420.1267.

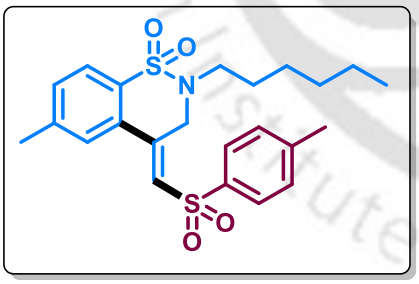

Z)-2-hexyl-6-methyl-4-(tosylmethylene)-3,4-dihydro-2H-benzo[e][1,2]thiazine 1,1-dioxide (**3i**): White solid (30 % ethyl acetate in petroleum ether) Yield: (55 mg) 49 %; **^{1}H NMR** (500 MHz, $CDCl_3$) δ 7.83 (d, *J* = 8.2 Hz, 2H), 7.72 (d, *J* = 7.9 Hz, 1H), 7.42 (s, 1H), 7.37 – 7.35 (m, 3H), 6.95 (s, 1H), 5.01 (s, 2H), 2.88 (t, *J* = 7.3 Hz, 2H), 2.43 (s, 3H), 2.39 (s, 3H), 1.56 (dd, *J* = 10.1, 4.5 Hz, 2H), 1.26 (td, *J* = 9.6, 9.0, 5.5 Hz, 6H), 0.86 (t, *J* = 6.6 Hz, 3H). **^{13}C NMR** (125 MHz, $CDCl_3$) δ 145.4, 143.5, 140.6, 137.9, 133.7, 132.4, 131.1, 130.3, 128.8, 127.5, 126.3, 125.4, 49.7, 47.9, 31.3, 297., 26.2, 22.6, 21.7, 21.7, 14.0. **HRMS** (ESI-TOF) m/z: $[M+H]^+$ Calcd for $C_{23}H_{30}NO_4S_2$ 448.1611; Found 448.1582.

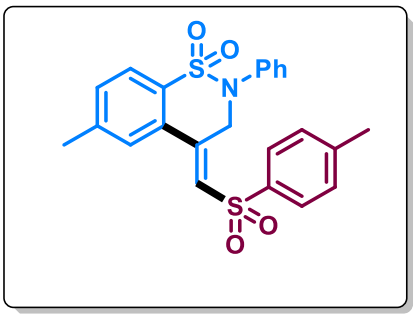

(Z)-6-methyl-2-phenyl-4-(tosylmethylene)-3,4-dihydro-2H-benzo[e][1,2]thiazine 1,1-dioxide (**3j**): White solid (30 % ethyl acetate in petroleum ether) Yield: (70 mg) 63 %; **^{1}H NMR** (500 MHz, $CDCl_3$) δ 7.81 (d, *J* = 7.9 Hz, 2H), 7.66 (d, *J* = 7.9 Hz, 1H), 7.51 (s, 1H), 7.34 (dd, *J* = 14.0, 8.0 Hz, 3H), 7.26 – 7.20 (m, 3H), 7.04 (d, *J* = 7.3 Hz, 2H), 6.93 (s, 1H), 5.49 (s, 2H), 2.45 (s, 3H), 2.44 (s, 3H). ^{13}C NMR (125 MHz, $CDCl_3$) δ 145.5, 144.0, 141.6, 140.7, 137.7, 134.3, 132.3, 131.9, 130.4, 129.2, 127.7, 127.6, 127.5, 126.7, 125.6, 125.4, 52.4, 21.9, 21.8. **HRMS** (ESI-TOF) m/z: $[M+H]^+$ Calcd for $C_{23}H_{22}NO_4S_2$ 440.0985; Found 440.0964.

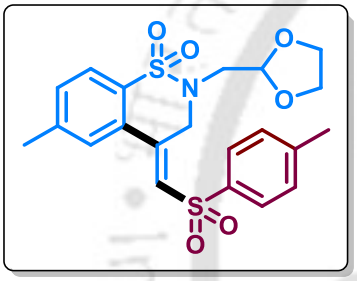

(Z)-2-((1,3-dioxolan-2-yl)methyl)-6-methyl-4-(tosylmethylene)-3,4-dihydro-2H-benzo[e][1,2]thiazine 1,1-dioxide (**3k**): White solid (30 % ethyl acetate in petroleum ether) Yield: (66 mg) 59 %; **^{1}H NMR** (500 MHz, $CDCl_3$) δ 7.86 (d, *J* = 6.8 Hz, 2H), 7.74 (d, *J* = 7.8 Hz, 1H), 7.40 – 7.36(m, 4H), 6.87 (s, 1H), 5.21 (s, 2H), 5.03 (t, *J* = 3.9 Hz, 1H), 3.95 – 3.87 (m, 4H), 3.12 (d, *J* = 4.1 Hz, 2H), 2.44 (s, 3H), 2.41 (s, 3H). **^{13}C NMR** (125 MHz, $CDCl_3$) δ 145.4, 143.6, 140.1, 137.1, 134.4, 132.2, 131.6, 130.3, 128.5, 127.7, 126.6, 125.1, 102.7, 65.3, 51.6, 50.1, 21.8, 21.8. **HRMS** (ESI-TOF) m/z: $[M+H]^+$ Calcd for $C_{21}H_{24}NO_6S_2$ 450.1040; Found 450.1016.

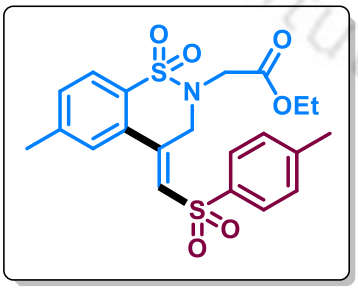

ethyl (Z)-2-(6-methyl-1,1-dioxido-4-(tosylmethylene)-3,4-dihydro-2H-benzo[e][1,2]thiazin-2-yl)acetate (**3l**): White solid (30 % ethyl acetate in petroleum ether) Yield: (64 mg) 57 %; **^{1}H NMR** (500 MHz, $CDCl_3$) δ 7.83 (d, *J* = 8.0 Hz, 2H), 7.72 (d, *J* = 8.0 Hz, 1H), 7.40 – 7.36 (m, 4H), 6.90 (s, 1H), 5.12 (s, 2H), 4.16 (q, *J* = 7.2 Hz, 2H), 3.89 (s, 3H), 2.44 (s, 3H), 2.41 (s, 3H), 1.24 (t, *J* = 7.1 Hz, 3H). **^{13}C NMR** (125 MHz, $CDCl_3$) δ 167.9, 145.4, 143.7, 140.4, 137.8, 134.6, 132.2, 131.5, 130.4, 128.9, 127.6, 126.5, 124.7, 61.8, 50.3, 48.9, 21., 821.7, 14.1. **HRMS** (ESI-TOF) m/z: $[M+H]^+$ Calcd for $C_{21}H_{24}NO_6S_2$ 450.1040; Found 450.1014.

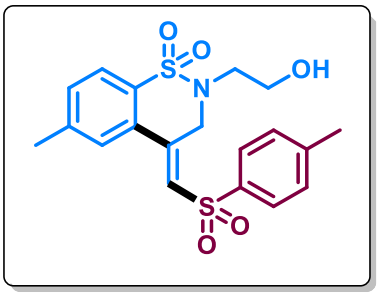

(Z)-2-(2-hydroxyethyl)-6-methyl-4-(tosylmethylene)-3,4-dihydro-2H-benzo[e][1,2]thiazine 1,1-dioxide compound with methane (1:1) (**3m**): White solid (30 % ethyl acetate in petroleum ether) Yield: (54 mg) 51 %; **^{1}H NMR** (500 MHz, $CDCl_3$) δ 7.84 (d, *J* = 8.3 Hz, 2H), 7.74 (d, *J* = 7.9 Hz, 1H), 7.42 (s, 1H), 7.37 (d, *J* = 8.1 Hz, 3H), 6.95 (s, 1H), 5.12 (d, *J* = 2.0 Hz, 2H), 3.76 (t, *J* = 5.3 Hz, 2H), 3.10 (t, *J* = 5.3 Hz, 2H), 2.43 (s, 3H), 2.40 (s, 3H). **^{13}C NMR** (125 MHz, $CDCl_3$) δ 145.5, 143.8, 140.3, 137.7, 133.7, 132.4, 131.2, 130.4, 129.0, 127.6, 126.5, 125.4, 60.7, 51.9, 49.4, 21.8, 21.7. **HRMS** (ESI-TOF) m/z: $[M+H]^+$ Calcd for $C_{19}H_{22}NO_5S_2$ 408.0934; Found 408.0947.

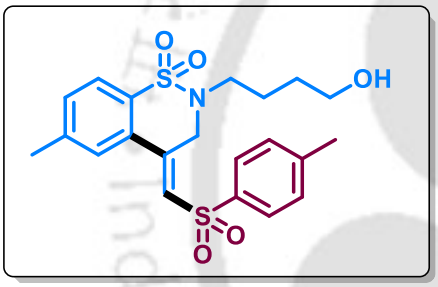

(Z)-2-(4-hydroxybutyl)-6-methyl-4-(tosylmethylene)-3,4-dihydro-2H-benzo[e][1,2]thiazine 1,1-dioxide (**3n**): White solid (30 % ethyl acetate in petroleum ether) Yield: (51 mg) 47 %; **^{1}H NMR** (500 MHz, $CDCl_3$) δ 7.83 (d, *J* = 8.2 Hz, 2H), 7.73 (d, *J* = 7.9 Hz, 1H), 7.41 (s, 1H), 7.37 (d, *J* = 8.0 Hz, 2H), 6.94 (d, *J* = 2.0 Hz, 1H), 5.02 (d, *J* = 2.0 Hz, 2H), 3.65 (t, *J* = 6.3 Hz, 2H), 2.95 (t, *J* = 7.0 Hz, 2H), 2.44 (s, 3H), 2.40 (s, 3H), 1.86 (s, 1H), 1.70 – 1.67 (m, 2H), 1.60 (dt, *J* = 8.8, 6.3 Hz, 2H). **^{13}C NMR** (125 MHz, $CDCl_3$) δ 145.6, 143.7, 140.5, 137.8, 133.7, 132.6, 131.1, 130.5, 129.0, 127.6, 126.4, 125.6, 62.2, 49.4, 48.0, 29.6, 24.5, 21.9, 21.8. **HRMS** (ESI-TOF) m/z: $[M+H]^+$ Calcd for $C_{21}H_{26}NO_5S_2$ 436.1247; Found 436.1257.

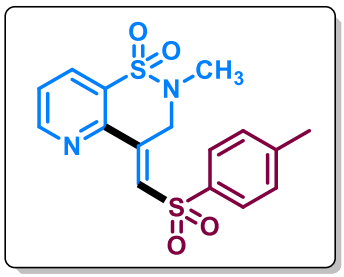

(E)-2-methyl-4-(tosylmethylene)-3,4-dihydro-2H-pyrido[2,3-e][1,2]thiazine 1,1-dioxide compound with methane (1:1) (**3o**): White solid (30 % ethyl acetate in petroleum ether) Yield: (48 mg) 53 %; **^{1}H NMR** (500 MHz, $CDCl_3$) δ 8.72 (dd, *J* = 4.6, 1.7 Hz, 1H), 8.15 (dd, *J* = 7.9, 1.7 Hz, 1H), 7.95 (t, *J* = 1.9 Hz, 1H), 7.85 (d, *J* = 8.1 Hz, 2H), 7.50 (dd, *J* = 8.0, 4.7 Hz, 1H), 7.39 (d, *J* = 8.0 Hz, 2H), 5.15 (d, *J* = 1.9 Hz, 2H), 2.82 (s, 3H), 2.45 (s, 3H). **^{13}C NMR** (125 MHz, $CDCl_3$) δ 152.0, 146.8, 145.7,

137.8, 137.2, 134.1, 134.0, 132.2, 130.5, 127.9, 126.1, 49.0, 37.1, 21.9. **HRMS** (ESI-TOF) m/z: $[M+H]^+$ Calcd for $C_{16}H_{17}N_2O_4S_2$ 365.0625; Found 365.0615.

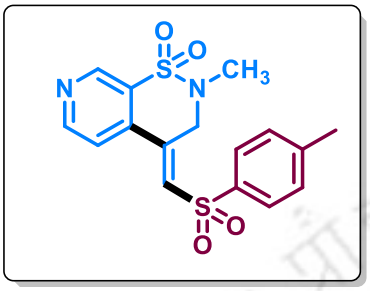

(Z)-2-methyl-4-(tosylmethylene)-3,4-dihydro-2H-pyrido[4,3-e][1,2]thiazine 1,1-dioxide (**3o**): White solid (30 % ethyl acetate in petroleum ether) Yield: (13 mg) 14 %; **^{1}H NMR** (500 MHz, $CDCl_3$) δ 9.08 (s, 1H), 8.81 (d, *J* = 5.4 Hz, 1H), 7.84 (d, *J* = 7.9 Hz, 2H), 7.45 (d, *J* = 5.4 Hz, 1H), 7.41 (d, *J* = 8.1 Hz, 2H), 7.11 (s, 1H), 5.08 (d, *J* = 2.1 Hz, 2H), 2.77 (s, 3H), 2.46 (s, 3H). **^{13}C NMR** (125 MHz, $CDCl_3$) δ 153.7, 147.4, 146.2, 138.6, 137.0, 136.0, 133.1, 130.6, 130.3, 127.8, 118.4, 50.4, 37.2, 21.9. **HRMS** (ESI-TOF) m/z: $[M+H]^+$ Calcd for $C_{16}H_{17}N_2O_4S_2$ 365.0625; Found 365.0616.

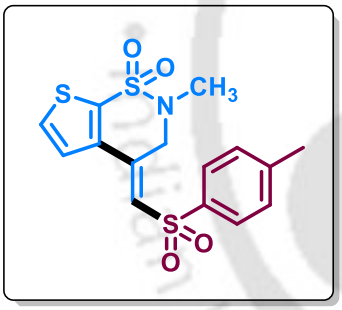

(Z)-2-methyl-4-(tosylmethylene)-3,4-dihydro-2H-thieno[3,2-e][1,2]thiazine 1,1-dioxide (**3p**): White solid (30 % ethyl acetate in petroleum ether) Yield: (42 mg) 45 %; **^{1}H NMR** (500 MHz, $CDCl_3$) δ 7.82 (d, *J* = 8.2 Hz, 2H), 7.55 (d, *J* = 5.3 Hz, 1H), 7.38 (d, *J* = 8.1 Hz, 2H), 7.19 (d, *J* = 5.3 Hz, 1H), 6.94 (t, *J* = 1.8 Hz, 1H), 5.03 (d, *J* = 1.8 Hz, 2H), 2.76 (s, 3H), 2.45 (s, 3H). **^{13}C NMR** (125 MHz, $CDCl_3$) δ 145.6, 137.9, 136.9, 136.5, 136.1, 130.5, 130.2, 130.1, 127.6, 123.4, 50.3, 37.3, 21.8. **HRMS** (ESI-TOF) m/z: $[M+H]^+$ Calcd for $C_{15}H_{16}N_2O_4S_3$ 370.0236; Found 370.0250.

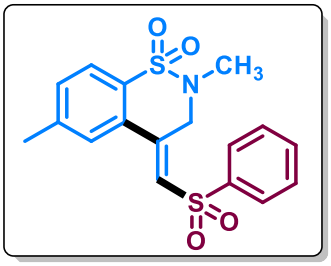

(Z)-2,6-dimethyl-4-((phenylsulfonyl)methylene)-3,4-dihydro-2H-benzo[e][1,2]thiazine 1,1-dioxide (**4a**): White solid (30 % ethyl acetate in petroleum ether) Yield: (63 mg) 69 %; **^{1}H NMR** (500 MHz, $CDCl_3$) δ 7.97 (d, *J* = 7.6 Hz, 2H), 7.77 (d, *J* = 7.8 Hz, 1H), 7.68 (t, *J* = 7.4 Hz, 1H), 7.60 (t, *J* = 7.8 Hz, 2H), 7.42 (d, *J* = 9.9 Hz, 2H), 6.95 (s, 1H), 5.02 (s, 2H), 2.71 (s, 3H), 2.43 (s, 3H). **^{13}C NMR** (125 MHz, $CDCl_3$) δ 143.8, 140.8, 140.7, 134.3, 132.8, 132.3, 130.9, 129.8, 128.0, 127.6, 126.3, 126.0, 50.9, 37.4, 21.8. **HRMS** (ESI-TOF) m/z: $[M+H]^+$ Calcd for $C_{17}H_{18}NO_4S_2$ 364.0672; Found 364.0662.

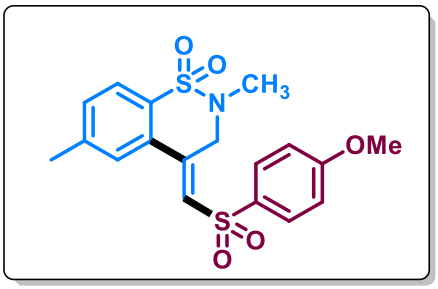

(Z)-4-(((4-methoxyphenyl)sulfonyl)methylene)-2,6-dimethyl-3,4-dihydro-2H-benzo[e][1,2]thiazine 1,1-dioxide (**4b**): White solid (30 % ethyl acetate in petroleum ether) Yield: (70 mg) 71 %; **^{1}H NMR** (500 MHz, $CDCl_3$) δ 7.84 (d, *J* = 8.0 Hz, 2H), 7.81 (d, *J* = 8.8 Hz, 1H), 7.38 (d, *J* = 8.0 Hz, 2H), 7.09 (d, *J* = 8.7 Hz, 1H), 7.05 (s, 1H), 6.92 (s, 1H), 4.99 (s, 2H), 3.87 (s, 3H), 2.70 (s, 3H), 2.45 (s, 3H). **^{13}C NMR** (125 MHz, $CDCl_3$) δ 163.0, 145.9, 140.4, 137.0, 133.1, 130.7, 129.0, 128.3, 127.9, 127.5, 117.3, 111.4, 56.3, 51.2, 37.9, 22.1. **HRMS** (ESI-TOF) m/z: $[M+Na]^+$ Calcd for $C_{18}H_{19}NNaO_5S_2$ 416.0597; Found 416.0578.

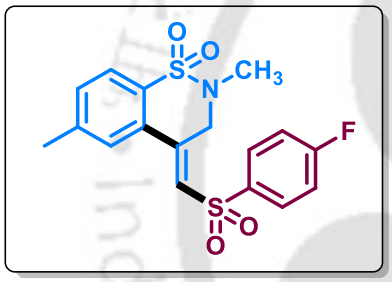

(Z)-4-(((4-fluorophenyl)sulfonyl)methylene)-2,6-dimethyl-3,4-dihydro-2H-benzo[e][1,2]thiazine 1,1-dioxide (**4c**): White solid (30 % ethyl acetate in petroleum ether) Yield: (60 mg) 63 %; **^{1}H NMR** (500 MHz, $CDCl_3$) δ 7.97 – 7.94 (m, 2H), 7.74 (d, *J* = 7.9 Hz, 1H), 7.40 (d, *J* = 8.1 Hz, 2H), 7.24 (d, *J* = 8.2 Hz, 2H), 6.87 (s, 1H), 4.98 (s, 2H), 2.69 (s, 3H), 2.41 (s, 3H). **^{13}C NMR** (125 MHz, $CDCl_3$) δ 166.4 (d, J= 255.1 Hz), 144.2, 141.2, 137.1, 133.1, 132.6, 131.1, 130.7 (d, J= 9.7 Hz), 128.8, 126.6, 126.3, 117.4 (d, J= 22.6 Hz), 51.3, 37.8, 22.1. **^{19}F NMR** (470 MHz, $CDCl_3$) δ -102.1. **HRMS** (ESI-TOF) m/z: $[M+H]^+$ Calcd for $C_{17}H_{17}FNO_4S_2$ 382.0578; Found 382.0562.

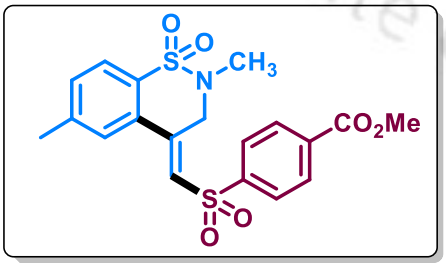

Methyl (Z)-4-(((2,6-dimethyl-1,1-dioxido-2,3-dihydro-4H-benzo[e][1,2]thiazin-4-ylidene)methyl)sulfonyl)benzoate (**4d**): White solid (30 % ethyl acetate in petroleum ether) Yield: (54 mg) 51 %; **1H NMR** (500 MHz, CDCl3) δ 8.25 (d, *J* = 8.5 Hz, 2H), 8.04 (d, *J* = 8.3 Hz, 2H), 7.78 (d, *J* = 7.7 Hz, 1H), 7.43 (d, *J* = 8.3 Hz, 2H), 6.93 (s, 1H), 5.02 (s, 2H), 3.97 (s, 3H), 2.72 (s, 3H), 2.44 (s, 3H). **^{13}C NMR** (125 MHz, $CDCl_3$) δ 165.7, 144.7, 144.2, 142.3, 135.6, 133.2, 132.7, 131.2, 131.0, 128.3, 127.9, 126.6, 126.3, 53.2, 51.4, 37.7, 22.0. **HRMS** (ESI-TOF) m/z: $[M+H]^+$ Calcd for $C_{19}H_{20}NO_6S_2$ 422.0727; Found 422.0727.

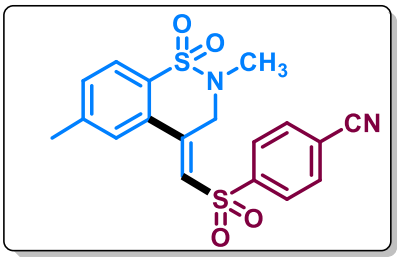

(Z)-4-(((2,6-dimethyl-1,1-dioxido-2,3-dihydro-4H-benzo[e][1,2]thiazin-4-ylidene)methyl)sulfonyl)benzonitrile (**4e**): White solid (30 % ethyl acetate in petroleum ether) Yield: (40 mg) 41 %; **^{1}H NMR** (500 MHz, $CDCl_3$) δ 8.09 (d, *J* = 8.1 Hz, 2H), 7.89 (d, *J* = 8.1 Hz, 2H), 7.77 (d, *J* = 7.9 Hz, 1H), 7.45 (d, *J* = 7.9 Hz, 1H), 7.42 (s, 1H), 6.86 (s, 1H), 5.00 (s, 2H), 2.72 (s, 3H), 2.44 (s, 3H). **^{13}C NMR** (125 MHz, $CDCl_3$) δ 144.0, 144.3, 143.4, 133.8, 133.4, 132.7, 130.0, 128.4, 127.3, 126.8, 126.3, 118.2, 117.3, 51.6, 37.9, 22.0. **HRMS** (ESI-TOF) m/z: $[M+H]^+$ Calcd for $C_{18}H_{17}N_2O_4S_2$ 389.0625; Found 389.0638.

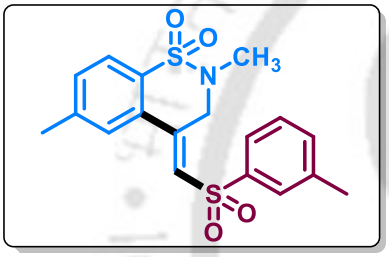

(Z)-2,6-dimethyl-4-((m-tolylsulfonyl)methylene)-3,4-dihydro-2H-benzo[e][1,2]thiazine 1,1-dioxide (**4f**): White solid (30 % ethyl acetate in petroleum ether) Yield: (64 mg) 68 %; ^{1}H NMR (500 MHz, $CDCl_3$) δ 7.77 (d, *J* = 6.9 Hz, 3H), 7.48 – 7.47 (m, 2H), 7.43-7.40 (m, 2H), 5.02 (s, 2H), 2.72 (s, H), 2.46 (s, 3H), 2.43 (s, 3H). **^{13}C NMR** (125 MHz, $CDCl_3$) δ 143.8, 1403.6, 140.4, 140.2, 135.1, 132.7, 132.3, 129.7, 129.1, 127.8, 126.3, 126.0, 124.7, 50.9, 37.4, 21.8, 21.5. **HRMS** (ESI-TOF) m/z: $[M+H]^+$ Calcd for $C_{18}H_{20}NO_4S_2$ 378.0829; Found 378.0803.

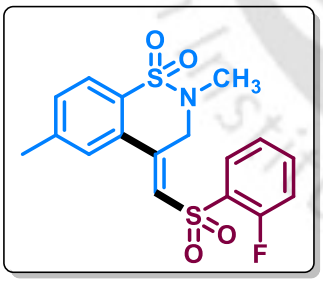

(Z)-4-(((2-fluorophenyl)sulfonyl)methylene)-2,6-dimethyl-3,4-dihydro-2H-benzo[e][1,2]thiazine 1,1-dioxide (**4g**): White solid (30 % ethyl acetate in petroleum ether) Yield: (57 mg) 59 %; **^{1}H NMR** (500 MHz, $CDCl_3$) δ 8.06 (t, *J* = 7.5 Hz, 1H), 7.81 (d, *J* = 7.9 Hz, 1H), 7.73 – 7.69 (m, 1H), 7.51 (s, 1H), 7.47 (d, *J* = 8.0 Hz, 1H), 7.42 (t, *J* = 7.8 Hz, 1H), 7.29 (d, *J* = 9.2 Hz, 1H), 7.11 (s, 1H), 5.04 (s, 2H), 2.73 (s, 3H), 2.48 (s, 3H). **^{13}C NMR** (125 MHz, $CDCl_3$) δ 159.78 (d, J= 254.75 Hz), 143.9, 142.3, 136.7 (d, J= 8.55 Hz), 133.0, 132.4, 130.7, 129.6, 128.8 (d, J= 13.9 Hz), 127.8, 126.3, 126.1, 125.1 (d, J= 3.72 Hz), 117.6 (d, J= 20.7 Hz), 50.8, 37.3, 21.8. **HRMS** (ESI-TOF) m/z: $[M+H]^+$ Calcd for $C_{17}H_{17}FNO_4S_2$ 382.0578; Found 382.0553.

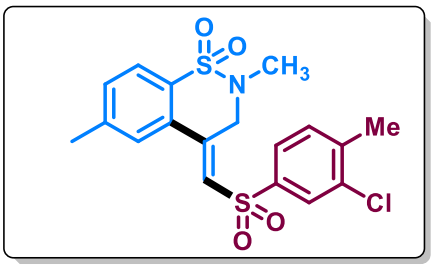

(Z)-4-(((3-chloro-4-methylphenyl)sulfonyl)methylene)-2,6-dimethyl-3,4-dihydro-2H-benzo[e][1,2]thiazine 1,1-dioxide (**4h**): White solid (30 % ethyl acetate in petroleum ether) Yield: (59 mg) 57 %; **^{1}H NMR** (500 MHz, $CDCl_3$) δ 8.27 (s, 1H), 8.11 – 8.07 (m, 2H), 7.79 (d, *J* = 8.0 Hz, 1H), 7.76 (d, *J* = 6.5 Hz, 3H), 7.26 (t, *J* = 2.0 Hz, 1H), 5.35 (s, 2H), 3.07 (s, 3H), 2.81 (s, 3H), 2.77 (s, 3H). **^{13}C NMR** (125 MHz, $CDCl_3$) δ 143.9, 143.6, 141.0, 139.6, 135.0, 132.9, 132.3, 132.2, 130.8, 128.5, 128.1, 126.3, 126.0, 125.6, 50.9, 37.4, 21.8, 20.6. **HRMS** (ESI-TOF) m/z: $[M+H]^+$ Calcd for $C_{18}H_{19}ClNO_4S_2$ 412.0439; Found 412.0409.

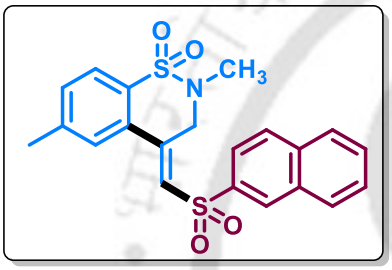

(Z)-2,6-dimethyl-4-((naphthalen-2-ylsulfonyl)methylene)-3,4-dihydro-2H-benzo[e][1,2]thiazine 1,1-dioxide (**4i**): White solid (30 % ethyl acetate in petroleum ether) Yield: (61 mg) 59 %; **^{1}H NMR** (500 MHz, $CDCl_3$) δ 8.56 (s, 1H), 8.03 (d, *J* = 9.2 Hz, 2H), 7.92 (dd, *J* = 19.0, 9.3 Hz, 1H), 7.76 (d, *J* = 7.9 Hz, 1H), 7.68 (dt, *J* = 20.4, 7.2 Hz, 1H), 7.42 – 7.39 (m, 2H), 7.02 (s, 1H), 5.08 (s, 2H), 2.73 (s, 3H), 2.41 (s, 3H). **^{13}C NMR** (125 MHz, $CDCl_3$) δ 144.1, 140.9, 137.8, 135.8, 133.0, 132.6, 132.6, 131.1, 130.5, 130.0, 129.9, 129.6, 129.3, 128.5, 128.4, 126.5, 126.3, 122.4, 51.1, 37.6, 22.0. **HRMS** (ESI-TOF) m/z: $[M+H]^+$ Calcd for $C_{21}H_{20}NO_4S_2$ 414.0829; Found 414.0810.

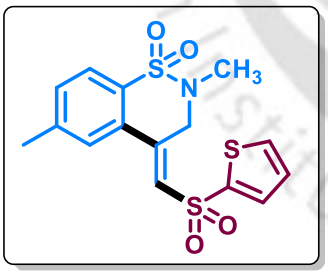

(Z)-2,6-dimethyl-4-((thiophen-2-ylsulfonyl)methylene)-3,4-dihydro-2H-benzo[e][1,2]thiazine 1,1-dioxide (**4j**): White solid (30 % ethyl acetate in petroleum ether) Yield: (53 mg) 57 %; **^{1}H NMR** (500 MHz, $CDCl_3$) δ 7.78 – 7.75 (m, 3H), 7.45 – 7.42 (m, 2H), 7.19 (s, 1H), 7.02 (s, 1H), 5.04 (s, 2H), 2.73 (s, 3H), 2.44 (s, 3H). **^{13}C NMR** (125 MHz, $CDCl_3$) δ 144.2, 142.3, 140.9, 135.2, 134.3, 133.1, 132.6, 131.1, 129.5, 128.8, 126.6, 126.3, 51.1, 37.7, 22.1. **HRMS** (ESI-TOF) m/z: $[M+H]^+$ Calcd for $C_{15}H_{16}NO_4S_3$ 370.0236; Found 370.0216.

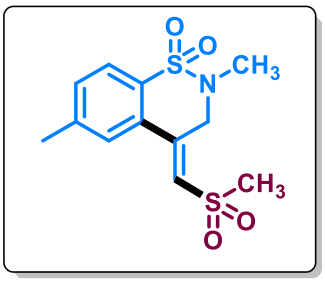

(Z)-2,6-dimethyl-4-((methylsulfonyl)methylene)-3,4-dihydro-2H-benzo[e][1,2]thiazine 1,1-dioxide (**4k**): White solid (30 % ethyl acetate in petroleum ether) Yield: (48 mg) 63 %; **^{1}H NMR** (500 MHz, $CDCl_3$) δ 7.80 (d, *J* = 7.8 Hz, 1H), 7.46 (d, *J* = 8.9 Hz, 2H), 6.90 (s, 1H), 4.99 (s, 2H), 3.10 (s, 3H), 2.73 (s, 3H), 2.47 (s,

3H). **^{13}C NMR** (125 MHz, $CDCl_3$) δ 144.3, 142.5, 133.1, 132.7, 131.1, 127.7, 126.6, 126.3, 51.3, 44.3, 37.8, 22.1. **HRMS** (ESI-TOF) m/z: $[M+H]^+$ Calcd for $C_{12}H_{16}NO_4S_2$ 302.0516; Found 302.0495.

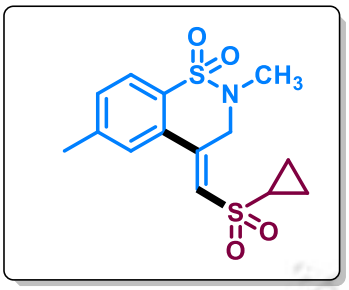

(Z)-4-((cyclopropylsulfonyl)methylene)-2,6-dimethyl-3,4-dihydro-2H-benzo[e][1,2]thiazine 1,1-dioxide (**4l**): White solid (30 % ethyl acetate in petroleum ether) Yield: (48 mg) 59 %; **1H NMR** (500 MHz, CDCl3) δ 7.78 (d, *J* = 7.9 Hz, 1H), 7.48 (s, 1H), 7.44 (d, *J* = 8.0 Hz, 1H), 6.93 (t, *J* = 2.0 Hz, 1H), 4.98 (d, *J* = 2.0 Hz, 2H), 2.73 (s, 3H), 2.46 (s, 3H), 1.34-1.32 (m, 2H), 1.13 – 1.11 (m, 2Hz)**.** **^{13}C NMR** (125 MHz, $CDCl_3$) δ 144.1, 141.1, 132.9, 132.5, 131.3, 127.6, 126.5, 126.2, 51.2, 37.6, 32.6, 22.1, 5.7. **HRMS** (ESI-TOF) m/z: $[M+H]^+$ Calcd for $C_{14}H_{18}NO_4S_2$ 328.0672; Found 328.0685.

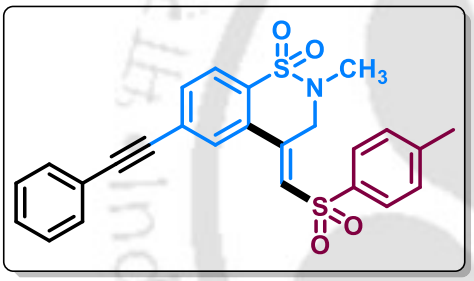

(Z)-2-methyl-6-(phenylethynyl)-4-(tosylmethylene)-3,4-dihydro-2H-benzo[e][1,2]thiazine 1,1-dioxide (**6a**): White solid (30 % ethyl acetate in petroleum ether) Yield: (77 mg) 83 %; **^{1}H NMR** (500 MHz, $CDCl_3$) δ 7.83 (d, *J* = 8.2 Hz, 1H), 7.68 (d, *J* = 8.0 Hz, 2H), 7.57 – 7.55 (m, 2H), 7.49 (d, *J* = 8.2 Hz, 1H), 7.42 – 7.39 (m, 3H), 7.19 (d, *J* = 8.0 Hz, 2H), 7.14 (s, 1H), 6.49 (s, 1H), 4.25 (s, 2H), 3.36 (s, 3H), 2.31 (s, 3H). **^{13}C NMR** (125 MHz, $CDCl_3$) δ 145.5, 136.9, 134.4, 132.0, 131.9, 130.2, 129.9, 129.26, 129.25, 128.7, 127.5, 126.3, 122.4, 122.3, 105.5, 92.7, 87.6, 57.5, 34.5, 21.7. **HRMS** (ESI-TOF) m/z: $[M+H]^+$ Calcd for $C_{25}H_{21}NaNO_4S_2$ 486.0805; Found 486.0781.

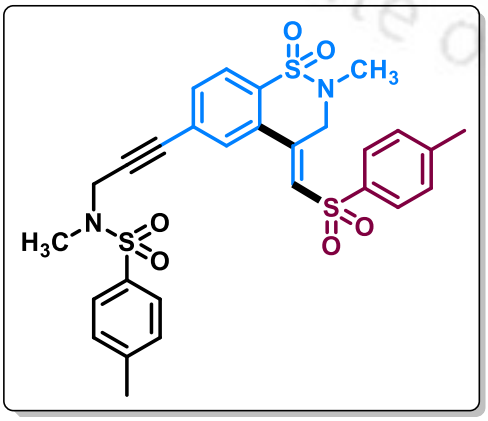

(Z)-N,4-dimethyl-N-(3-(2-methyl-1,1-dioxido-4-(tosylmethylene)-3,4-dihydro-2H-benzo[e][1,2]thiazin-6-yl)prop-2-yn-1-yl)benzenesulfonamide (**6b**): White solid (30 % ethyl acetate in petroleum ether) Yield: (83 mg) 71 %; **^{1}H NMR** (500 MHz, $CDCl_3$) δ 7.85 (d, *J* = 8.2 Hz, 2H), 7.76 (d, *J* = 8.0 Hz, 1H), 7.73 (d, *J* = 8.1 Hz, 2H), 7.41 (d, *J* = 7.8 Hz, 3H), 7.28 (d, *J* = 8.9 Hz, 4H), 6.89 (s, 1H), 5.02 (d, *J* = 2.0 Hz, 2H), 4.24 (s, 2H), 2.89 (s, 3H), 2.73 (s, 3H), 2.46 (s, 3H), 2.35 (s, 3H).

^{13}C NMR (125 MHz, $CDCl_3$) δ 145.8, 144.0, 138.8, 137.5, 134.5, 134.4, 134.3, 131.4, 130.5, 130.4, 129.7, 128.6, 128.1, 127.7, 127.4, 125.9, 86.6, 83.5, 50.7, 40.7, 37.3, 35.0, 21.9, 21.6. **HRMS** (ESI-TOF) m/z: $[M+H]^+$ Calcd for $C_{28}H_{29}N_2O_6S_3$ 585.1183; Found 585.1152.

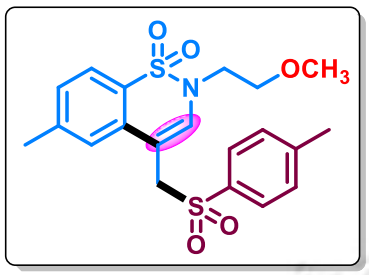

2-(2-methoxyethyl)-6-methyl-4-(tosylmethyl)-2H-benzo[e][1,2]thiazine 1,1-dioxide (**7**): White solid (30 % ethyl acetate in petroleum ether) Yield: (56 mg) 67 %; **^{1}H NMR** (500 MHz, $CDCl_3$) δ 7.82 (d, *J* = 8.3 Hz, 2H), 7.71 (d, *J* = 7.9 Hz, 1H), 7.38 – 7.33 (m, 3H), 7.29 (d, *J* = 7.8 Hz, 1H), 5.85 (s, 1H), 5.63 (s, 1H), 5.61 (s, 1H), 3.97 – 3.93 (m, 1H), 3.90 – 3.85 (m, 1H), 3.64 – 3.60 (m, 1H), 3.28 – 3.23 (m, 1H), 3.02 (s, 3H), 2.44 (s, 3H), 2.44 (s, 3H). **^{13}C NMR** (125 MHz, $CDCl_3$) δ 144.8, 144.2, 137.8, 136.5, 134.9, 132.3, 130.1, 129.6, 128.4, 127.5, 124.5, 121.9, 93.7, 66.1, 49.0, 44.7, 21.8, 21.7. **HRMS** (ESI-TOF) m/z: $[M+H]^+$ Calcd for $C_{20}H_{24}NO_5S_2$ 422.1091; Found 422.1072.

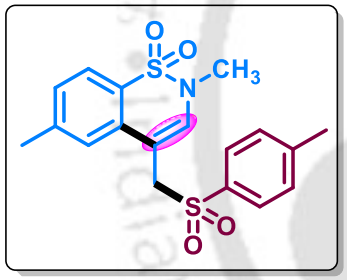

2,6-dimethyl-4-(tosylmethyl)-2H-benzo[e][1,2]thiazine 1,1-dioxide (**8a**): White solid (30 % ethyl acetate in petroleum ether) Yield: (70 mg) 93 %; **^{1}H NMR** (500 MHz, $CDCl_3$) δ 7.76 (d, *J* = 8.1 Hz, 1H), 7.67 (d, *J* = 8.1 Hz, 2H), 7.21 – 7.19 (m, 3H), 6.92 (s, 1H), 6.35 (s, 1H), 4.22 (s, 2H), 3.31 (s, 3H), 2.34 (s, 3H), 2.31 (s, 3H). **^{13}C NMR** (125 MHz, $CDCl_3$) δ 145.1, 142.6, 136.3, 134.5, 131.8, 129.7, 129.3, 128.6, 128.0, 123.8, 122.3, 105.6, 57.6, 34.3, 21.8, 21.61. **HRMS** (ESI-TOF) m/z: $[M+H]^+$ Calcd for $C_{18}H_{19}NNaO_4S_2$ 400.0648; Found 400.0629.

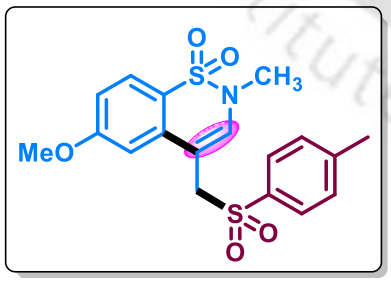

6-methoxy-2-methyl-4-(tosylmethyl)-2H-benzo[e][1,2]thiazine 1,1-dioxide (**8b**): White solid (30 % ethyl acetate in petroleum ether) Yield: (70 mg) 89 %; **^{1}H NMR** (500 MHz, $CDCl_3$) δ 7.80 (d, *J* = 8.8 Hz, 1H), 7.68 (d, *J* = 8.0 Hz, 2H), 7.22 (d, *J* = 7.9 Hz, 2H), 6.93 (dd, *J* = 8.8, 2.3 Hz, 1H), 6.70 (d, *J* = 2.3 Hz, 1H), 6.31 (s, 1H), 4.20 (s, 2H), 3.81 (s, 3H), 3.28 (s, 3H), 2.35 (s, 3H). **^{13}C NMR** (125 MHz, $CDCl_3$) δ 161.3, 144.2, 136.0, 133.5, 133.0, 128.8, 128.2, 123.4, 122.2, 113.3, 107.0, 104.2, 56.8, 54.7, 33.2, 20.7. **HRMS** (ESI-TOF) m/z: $[M+H]^+$ Calcd for $C_{18}H_{19}NNaO_5S_2$ 416.0597; Found 416.0577.

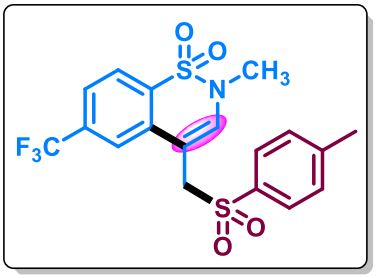

2-methyl-4-(tosylmethyl)-6-(trifluoromethyl)-2H-benzo[e][1,2]thiazine 1,1-dioxide (**8c**): White solid (30 % ethyl acetate in petroleum ether) Yield: (63 mg) 73 %; **^{1}H NMR** (500 MHz, $CDCl_3$) δ 7.98 (d, *J* = 8.3 Hz, 1H), 7.64 (d, *J* = 7.9 Hz, 2H), 7.60 (d, *J* = 8.4 Hz, 1H), 7.25 (s, 1H), 7.15 (d, *J* = 7.9 Hz, 2H), 6.66 (s, 1H), 4.28 (s, 2H), 3.41 (s, 3H), 2.29 (s, 3H). **^{13}C NMR** (125 MHz, $CDCl_3$) δ 145.6, 137.7, 134.3, 133.7 (q, *J* = 32.9), 132.58, 132.56, 130.0, 129.1, 124.1 (q, *J* = 3.5), 123.3, 120.4 (q, *J* = 4.1), 105.7, 57.3, 34.8, 21.5. **^{19}F NMR** (471 MHz, $CDCl_3$) δ -63.21. **HRMS** (ESI-TOF) m/z: $[M+H]^+$ Calcd for $C_{18}H_{17}F_3NO_4S_2$ 432.0546; Found 432.0513.

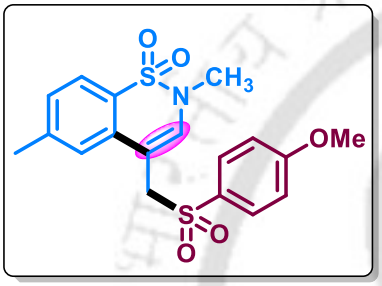

4-(((4-methoxyphenyl)sulfonyl)methyl)-2,6-dimethyl-2H-benzo[e][1,2]thiazine 1,1-dioxide (**8d**): White solid (30 % ethyl acetate in petroleum ether) Yield: (66 mg) 84 %; **^{1}H NMR** (500 MHz, $CDCl_3$) δ 7.76 (d, *J* = 8.1 Hz, 1H), 7.70 (d, *J* = 8.9 Hz, 2H), 7.21 (d, *J* = 8.0 Hz, 1H), 6.91 (s, 1H), 6.84 (d, *J* = 8.9 Hz, 2H), 6.36 (s, 1H), 4.22 (s, 2H), 3.78 (s, 3H), 3.32 (s, 3H), 2.32 (s, 3H). **^{13}C NMR** (125 MHz, $CDCl_3$) δ 164.1, 142.7, 136.3, 131.9, 131.5, 128.9, 128.7, 128.1, 123.8, 122.3, 114.3, 105.9, 57.8, 55.8, 34.4, 21.9. **HRMS** (ESI-TOF) m/z: $[M+H]^+$ Calcd for $C_{18}H_{19}NNaO_5S_2$ 416.0597; Found 416.0581.

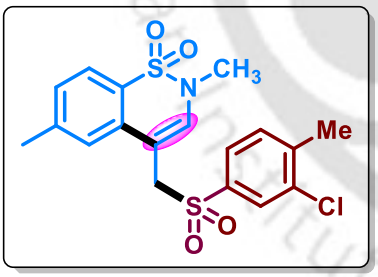

4-(((3-chloro-4-methylphenyl)sulfonyl)methyl)-2,6-dimethyl-2H-benzo[e][1,2]thiazine 1,1-dioxide (**8e**): White solid (30 % ethyl acetate in petroleum ether) Yield: (63 mg) 77 %; **^{1}H NMR** (500 MHz, $CDCl_3$) δ 7.82 (s, 1H), 7.76 (d, *J* = 8.0 Hz, 1H), 7.52 (d, *J* = 7.7 Hz, 1H), 7.21 (t, *J* = 6.7 Hz, 2H), 6.90 (s, 1H), 6.43 (s, 1H), 4.25 (s, 2H), 3.34 (s, 3H), 2.34 (s, 3H), 2.32 (s, 3H). ^{13}C NMR (125 MHz, $CDCl_3$) δ 143.2, 142.7, 136.5, 136.4, 135.5, 131.6, 131.5, 129.3, 128.7, 128.2, 127.9, 123.5, 122.4, 105.3, 57.7, 34.4, 21.9, 20.4. **HRMS** (ESI-TOF) m/z: $[M+H]^+$ Calcd for $C_{18}H_{19}ClNO_4S_2$ 412.0439; Found 412.0413.

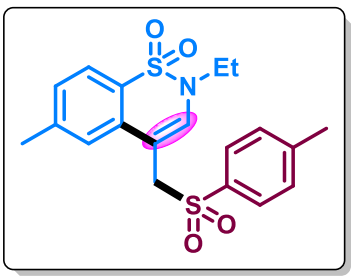

2-ethyl-6-methyl-4-(tosylmethyl)-2H-benzo[e][1,2]thiazine 1,1-dioxide (**8f**): White solid (30 % ethyl acetate in petroleum ether) Yield: (65 mg) 83 %; **^{1}H NMR** (500 MHz, $CDCl_3$) δ 7.76 (d, *J* = 8.1 Hz, 1H), 7.67 (d, *J* = 7.9 Hz, 2H), 7.21 (d, *J* = 7.5 Hz, 3H), 7.00 (s, 1H), 6.33 (s, 1H), 4.25 (s, 2H), 3.71 (q, *J* = 7.2 Hz, 2H),

2.34 (s, 3H), 2.33 (s, 3H), 1.25 (t, J = 7.2 Hz, 3H). **^{13}C NMR** (125 MHz, $CDCl_3$) δ 145.1, 142.5, 134.7, 134.4, 131.8, 129.8, 129.3, 128.6, 128.6, 123.9, 122.1, 106.0, 57.7, 43.4, 21.9, 21.6, 15.9. **HRMS** (ESI-TOF) m/z: $[M+H]^+$ Calcd for $C_{19}H_{22}NO_4S_2$ 392.0985; Found 392.0957.

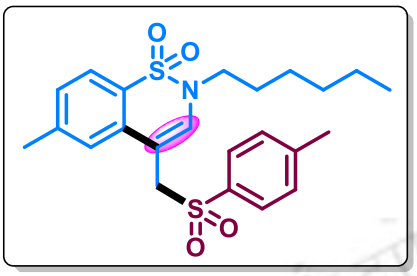

2-hexyl-6-methyl-4-(tosylmethyl)-2H-benzo[e][1,2]thiazine 1,1-dioxide (**8g**): White solid (30 % ethyl acetate in petroleum ether) Yield: (67 mg) 75 %; **^{1}H NMR** (500 MHz, $CDCl_3$) δ 7.76 (d, J = 8.1 Hz, 1H), 7.67 (d, J = 8.3 Hz, 2H), 7.24 – 7.18 (m, 3H), 6.99 (s, 1H), 6.35 (s, 1H), 4.26 (s, 2H), 3.62 (t, J = 7.5 Hz, 2H), 2.34 (s, 3H), 2.32 (s, 3H), 1.60 (p, J = 7.1 Hz, 2H), 1.32 – 1.22 (m, 6H), 0.86 – 0.83 (m, 3H). ^{13}C NMR (126 MHz, $CDCl_3$) δ 145.0, 142.4, 135.0, 134.4, 131.7, 129.7, 129.3, 128.6, 128.4, 123.8, 122.1, 105.8, 57.7, 48.3, 31.3, 30.3, 26.1, 22.5, 21.8, 21.6, 14.0. **HRMS** (ESI-TOF) m/z: $[M+H]^+$ Calcd for $C_{23}H_{30}NO_4S_2$ 448.1611; Found 448.1580.

5.11 Crystal data:

20 mg of compound **5.3a** was dissolved in $CHCl_3$ (2 mL) and kept for 2-3 days for crystal growth. The crystal measurement was done in 'Bruker APEX-II CCD'. The ellipsoid contour probability is 50 % for the image of the structure.

SC-XRD data of compound **5.3a**:

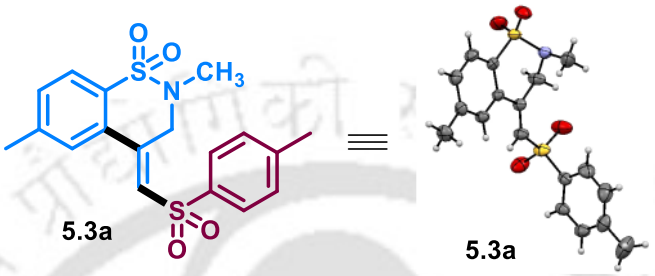

CCDC	2507153
Empirical formula	C18 H19 N O4 S2
Formula weight	377.46
Temperature, T	295(2)
Crystal system	monoclinic
Space group	P 21/c
Unit cell dimensions	a=10.863(4) Å α=90° b=7.823(3) Å β=99.655(9)° c= 20.905(7) Å γ=90°
Volume, V ($Å^3$)	1751.4(10)
Z	4
Density (calculated), g cm^{-3}	1.431
Absorption coefficient, μ (mm^{-1})	0.327
F (000)	792
Crystal size, mm^3	0.30 × 0.26 × 0.23
Theta range for data collection	2.503 to 24.985
Index ranges	-12 ≤ h ≤ 12 -9 ≤ k ≤ 9 -24 ≤ l ≤ 24
Reflections collected	3065
Independent reflections	2764

Completeness to theta	0.995
Absorption correction	none
Refinement method	'\f and \w scans'
Data / restraints / parameters	3065/0/229
Goodness-of-fit on F^2	1.517
Final R indices [I>2sigma(I)]	R1 = 0.0435, wR2 = 0.1711
R indices (all data)	R1 = 0.0387, wR2 = 0.1556
Largest diff. peak and hole	0.360 and -0.382 e·Å^{-3}

Bond Distances [Å]	Bond angles [°]
S001 O003 1.4223(14)	O003 S001 O004 118.22(10)
S001 O004 1.4284(15)	O003 S001 N007 108.88(9)
S001 N007 1.6224(17)	O004 S001 N007 107.87(10)
S001 C00A 1.7596(19)	O003 S001 C00A 108.73(9)
S002 O005 1.4358(16)	O004 S001 C00A 109.47(9)
S002 O006 1.4417(16)	N007 S001 C00A 102.53(8)
S002 C00B 1.759(2)	O005 S002 O006 117.51(10)
S002 C00G 1.7620(19)	O005 S002 C00B 108.74(9)
N007 C00N 1.466(3)	O006 S002 C00B 107.80(10)
N007 C00J 1.470(3)	O005 S002 C00G 106.85(10)
C008 C00G 1.330(2)	O006 S002 C00G 110.90(9)
C008 C009 1.508(2)	C00B S002 C00G 104.22(9)
C008 C00J 1.520(2)	C00N N007 C00J 114.72(16)
C009 C00E 1.390(2)	C00N N007 S001 116.32(16)
C009 C00A 1.405(2)	C00J N007 S001 111.28(14)
C00A C00C 1.392(3)	C00G C008 C009 120.15(16)
C00B C00D 1.387(2)	C00G C008 C00J 122.73(16)
C00B C00L 1.388(3)	C009 C008 C00J 116.94(15)
C00C C00H 1.375(3)	C00E C009 C00A 117.05(15)
C00D C00I 1.374(3)	C00E C009 C008 121.53(15)

C00E C00F 1.388(3)	C00A C009 C008 121.41(15)
C00F C00H 1.386(3)	C00C C00A C009 120.95(16)
C00F C00K 1.507(3)	C00C C00A S001 117.73(13)
C00I C00M 1.390(3)	C009 C00A S001 121.20(13)
C00L C00O 1.366(4)	C00D C00B C00L 119.92(19)
C00M C00O 1.385(3)	C00D C00B S002 119.47(15)
C00M C00P 1.519(4)	C00L C00B S002 120.52(15)
	C00H C00C C00A 120.04(17)
	C00I C00D C00B 119.16(18)
	C00F C00E C009 122.55(17)
	C00H C00F C00E 118.77(16)
	C00H C00F C00K 121.17(17)
	C00E C00F C00K 120.05(17)
	C008 C00G S002 128.49(15)
	C00C C00H C00F 120.59(16)
	C00D C00I C00M 121.71(19)
	N007 C00J C008 113.94(15)
	C00O C00L C00B 119.8(2)
	C00O C00M C00I 117.8(2)
	C00O C00M C00P 121.1(2)
	C00I C00M C00P 121.1(2)
	C00L C00O C00M 121.5(2)

25 mg of compound **5.3o** was dissolved in $CHCl_3$ (2 mL) and kept for 2-3 days for crystal growth. The crystal measurement was done in 'Bruker APEX-II CCD'. The ellipsoid contour probability is 50 % for the image of the structure.

SC-XRD data of compound **5.3o**:

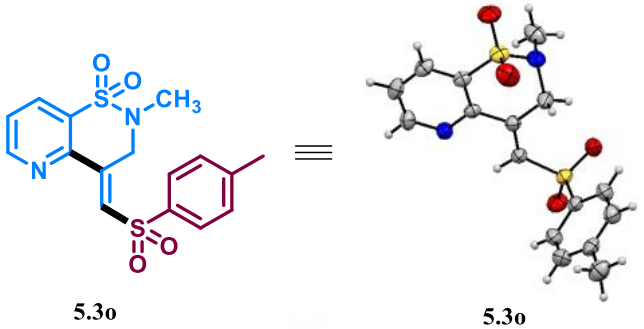

5.3o 5.3o

CCDC	2507209
Empirical formula	C16 H16 N2O4 S2
Formula weight	364.43
Temperature, T	298(2)
Crystal system	monoclinic
Space group	P 1 21/n 1
Unit cell dimensions	a=7.3763(12) Å α=90° b=8.7528(14) Å β=94.092(4)° c=24.970(4) Å γ=90°
Volume, V ($Å^3$)	1608.1(4)
Z	4
Density (calculated), g cm^{-3}	1.505
Absorption coefficient, μ (mm^{-1})	0.355
F (000)	760
Crystal size, mm^3	0.31 × 0.27 × 0.22
Theta range for data collection	2.466 to 25.000
Index ranges	-8 ≤ h ≤ 8 -10 ≤ k ≤ 10 -29 ≤ l ≤ 29
Reflections collected	2812
Independent reflections	2554
Completeness to theta	0.989
Absorption correction	none
Refinement method	'\f and \w scans'
Data / restraints / parameters	2812/0/219

Goodness-of-fit on F^2	1.093
Final R indices [I>2sigma(I)]	R1 = 0.0312, wR2 = 0.0829
R indices (all data)	R1 = 0.0355, wR2 = 0.0885
Largest diff. peak and hole	0.261 and -0.265 e·Å^{-3}

Bond Distances [Å]	Bond angles [°]
S001 O003 1.4379(14)	O003 S001 C009 108.56(8)
S001 O004 1.4366(14)	O003 S001 C00A 110.47(8)
S001 C009 1.7600(19)	O004 S001 O003 118.65(9)
S001 C00A 1.7622(17)	O004 S001 C009 108.46(8)
S002 O005 1.4261(15)	O004 S001 C00A 106.23(8)
S002 O006 1.4266(15)	C009 S001 C00A 103.39(8)
S002 N1 1.6266(17)	O005 S002 O006 118.38(9)
S002 C00D 1.7607(18)	O005 S002 N1 109.12(9)
N007 C00B 1.341(2)	O005 S002 C00D 109.64(9)
N007 C00F 1.333(2)	O006 S002 N1 107.98(10)
N1 C00M 1.473(2)	O006 S002 C00D 108.21(9)
N1 C00N 1.474(3)	N1 S002 C00D 102.30(8)
C009 C00E 1.386(3)	C00F N007 C00B 118.03(15)
C009 C00G 1.390(3)	C00M N1 S002 111.52(14)
C00A H00A 0.9300	C00N N1 S002 115.25(14)
C00A C00C 1.334(2)	C00N N1 C00M 115.41(16)
C00B C00C 1.491(2)	C00E C009 S001 120.63(14)
C00B C00D 1.407(2)	C00E C009 C00G 120.28(17)
C00C C00M 1.523(2)	C00G C009 S001 119.09(14)
C00D C00K 1.386(3)	S001 C00A H00A 116.5
C00E H00E 0.9300	C00C C00A S001 127.02(14)
C00E C00L 1.382(3)	C00C C00A H00A 116.5
C00F H00F 0.9300	N007 C00B C00C 116.68(14)
C00F C00H 1.378(3)	N007 C00B C00D 120.74(15)

C00G H00G 0.9300	C00D C00B C00C 122.58(15)
C00G C00I 1.378(3)	C00A C00C C00B 118.10(15)
C00H H00H 0.9300	C00A C00C C00M 123.45(16)
C00H C00K 1.376(3)	C00B C00C C00M 118.38(15)
C00I H00I 0.9300	C00B C00D S002 119.32(13)
C00I C00J 1.392(3)	C00K C00D S002 120.56(14)
C00J C00L 1.388(3)	C00K C00D C00B 120.11(16)
C00J C00O 1.503(3)	C009 C00E H00E 120.3
C00K H00K 0.9300	C00L C00E C009 119.32(18)
C00L H00L 0.9300	C00L C00E H00E 120.3
C00M H00B 0.9700	N007 C00F H00F 117.8
C00M H00C 0.9700	N007 C00F C00H 124.40(17)
C00N H00D 0.9600	C00H C00F H00F 117.8
C00N H00J 0.9600	C009 C00G H00G 120.3
C00N H00M 0.9600	C00I C00G C009 119.34(17)
C00O H00N 0.9600	C00I C00G H00G 120.3
C00O H00O 0.9600	C00F C00H H00H 120.8
C00O H00P 0.9600	C00K C00H C00F 118.45(17)
	C00K C00H H00H 120.8
	C00G C00I H00I 119.2
	C00G C00I C00J 121.50(18)
	C00J C00I H00I 119.2
	C00I C00J C00O 120.14(19)
	C00L C00J C00I 117.97(18)
	C00L C00J C00O 121.89(19)
	C00D C00K H00K 120.9
	C00H C00K C00D 118.20(17)
	C00H C00K H00K 120.9
	C00E C00L C00J 121.57(18)
	C00E C00L H00L 119.2
	C00J C00L H00L 119.2
	N1 C00M C00C 114.98(15)

	N1 C00M H00B 108.5 N1 C00M H00C 108.5 C00C C00M H00B 108.5 C00C C00M H00C 108.5 H00B C00M H00C 107.5 N1 C00N H00D 109.5 N1 C00N H00J 109.5 N1 C00N H00M 109.5 H00D C00N H00J 109.5 H00D C00N H00M 109.5 H00J C00N H00M 109.5 C00J C00O H00N 109.5 C00J C00O H00O 109.5 C00J C00O H00P 109.5 H00N C00O H00O 109.5 H00N C00O H00P 109.5 H00O C00O H00P 109.5

5.12 References:

1. (a) Azevedo, C. M.; Watterson, K. R.; Wargent, E. T.; Hansen, S. V.; Hudson, B. D.; Kepczynska, M. A.; Dunlop, J.; Shim-pukade, B.; Christiansen, E.; Milligan, G.; Stocker, C. J.; Ulven, T. Non-Acidic Free Fatty Acid Receptor 4 Agonists with Antidiabetic Activity. *J. Med. Chem.* **2016**, *59*, 8868−8878. (b) Valente, C.; Guedes, R. C.; Moreira, R.; Iley, J.; Gut, J.; Rosenthal, P. J. Dipep-tide vinyl sultams: Synthesis via the Wittig–Horner reaction and activity against papain, falcipain-2 and Plasmodium falciparum *Bioorg. Med. Chem. Lett.* **2006**, *16*, 4115-4119. (c) Silvestri, R.; Marfe, G.; Artico, M.; La Regina, G.; Lavecchia, A.; Novellino, E.; Morgante, M.; Di Stefano, C.; Catalano, G.; Filomeni, G.; Abruzz-ese, E.; Ciriolo, M. R.; Russo, M. A.; Amadori, S.; Cirilli, R.; LaTor-re, F.; Sinibaldi Salimei, P. Pyrrolo[1,2-b][1,2,5]benzothiadiazepines (PBTDs): A New Class of Agents with High Apoptotic Activity in Chronic Myelogenous Leukemia K562 Cells and in Cells from Patients at Onset and Who Were Imatinib-Resistant *J. Med. Chem*. **2006**, *49*, 5840-5844. (d) Lebegue, N.; Gallet, S.; Flouquet, N.; Carato, P.; Pfeiffer, B.; Renard, P.; Leonce, S.; Pierre, A.; Chavatte, P.; Berthelot, P. Novel Benzopyridothiadi-azepines as Potential Active Antitumor Agents. *J. Med. Chem*. **2005**, *48*, 7363-7373.

2. (a) Brzozowski, Z.; Saczewski, F.; Neamati, N. Synthesis and anti-HIV-1 activity of a novel series of 1,4,2-benzodithiazine-dioxides *Bioorg. Med. Chem. Lett.* **2006**, *16*, 5298-5302. (b) Patel, C.; Bassin, J. P.; Scott, M.; Flye, J.; Hunter, A. P.; Martin, L.; Goyal, M. Synthesis and Antimicrobial Activity of 1,2-Benzothiazine De-rivatives. *Molecules* **2016**, *21*, 861. (c) Ahmad, N.; Ziaur-Rehman, M.; Siddiqui, H. L.; Ullah, M. F.; Parvez, M. Microwave-assisted synthesis and structure activity relationship of 4-hydroxy-N-[1-phenylethylidene]-2H/2methyl-1,2-benzothiazine-3-carbohydrazide 1,1-dioxides as antimicrobial agents. *Eur. J. Med. Chem.* **2011**, *46*, 2368−2377. (d) Lei, K.; Hua, X. W.; Tao, Y. Y.; Liu, Y.; Liu, N.; Ma, Y.; Li, Y. H.; Xu, X. H.; Kong, C. H. Discovery of (2-benzoylethen-1-ol)-containing 1,2-benzothiazine derivatives as novel 4-hydroxyphenylpyruvate dioxygenase (HPPD) inhibiting-based herbicide lead compounds. *Bioorg. Med. Chem.* **2016**, *24*, 92−103. (e) Mondal, S.; Mukherjee, S.; Malakar, S.; Debnath, S.; Roy, P.; Sinha Babu, S.P. Studying the Biological Activities and Molecular Docking of Some Novel Benzosultams and Benzosul-tones. *Curr. Bioact. Comp.* **2017**, *13*, 347–355.

3. (a) Ivanova, D.; Deneva, V.; Nedeltcheva, D.; Kamounah, F. S.; Gergov, G.; Hansen, P. E.; Kawauchi, S.; Antonov, L. Tauto-meric Transformations of Piroxicam in Solution: a

Combined Ex-perimental and Theoretical Study. *RSC Adv.* **2015**, *5*, 31852−31860. (b) Wells, G. J.; Tao, M.; Josef, K.A.; Bihovsky, R. 1,2-Benzothiazine 1,1-Dioxide P2-P3 Peptide Mimetic Aldehyde Cal-pain I Inhibitors. *J. Med. Chem.* **2001**, *44*, 3488–3503. (c) Xie, Y.; Gong, G.; Liu, Y.; Deng, S.; Rinderspacher, A.; Branden, L.; Landry, D. W. Convenient Preparation of N-8-quinolinyl Benzenesultams as Novel NF-kB Inhibitors. *Tetrahedron Lett.* **2008**, *49*, 2320-2323. d) Silver, L. H. Clinical efficacy and safety of brinzolamide (Azopt), a new topical carbonic anhydrase inhibitor for primary open-angle glaucoma and ocular hypertension. Brinzolamide primary therapy study group. *Am. J. Ophthalmol.* **1998**, *126*, 400−408. e) Conrow, R. E.; Dean, W. D.; Zinke, P. W.; Deason, M. E.; Sproull, S. J.; Danta-narayana, A. P.; DuPriest, M. T. Enantioselective synthesis of brinzolamide (AL-4862), a new topical carbonic anhydrase inhibi-tor. The "DCAT route" to thiophenesulfonamides. *Org. Process Res. Dev.* **1999**, *3*, 114−120. (f) Huang, Q.; Rui, E. Y.; Cobbs, M.; Dinh, D. M.; Gukasyan, H. J.; Lafontaine, J. A.; Mehta, S.; Patterson, B. D.; Rewolinski, D. A.; Richardson, P. F.; Edwards, M. P. Design, synthesis, and evaluation of NO-donor containing carbonic anhy-drase inhibitors to lower intraocular pressure. *J. Med. Chem*. **2015**, *58*, 2821−2833.

4. Virk, T. S.; Ilawe, N. V.; Zhang, G.; Yu, C. P.; Wong, B. M.; Chan, J. M. W. Sultam-Based Hetero[5]helicene: Synthesis, Structure, and Crystallization-Induced Emission Enhancement. *ACS Omega* **2016**, *1*, 1336−1342.

5. (a) Kumaraswamy, G.; Padmaja, M.; Markondaiah, B.; Jena, N.; Sridhar, B.; Kiran, M. U. Oppolzer Sultam Directed Aldol as a Key Step for the Stereoselective Syntheses of Antitumor Anti-biotic Belactosin C and Its Synthetic Congeners *J. Org. Chem.* **2006**, *71*, 337-340. (b) Ahn, K. H.; Kim, S.; Ham, C. The Evaluation of Chiral Benzosultams as Auxiliaries in Asymmetric Azidation Reaction. *Tetrahedron Lett*. **1998**, *39*, 6321. (c) Ahn, K. H.; Baek, H.-H.; Lee, S. J.; Cho, C.-W. Synthesis of Chiral Benzosultams: 3-Functionalized 1,2-Benzisothiazoline 1,1-Dioxides *J. Org. Chem.* **2000**, *65*, 7690-7696.

6. Debnath, S.; Mondal, S. Regio- and Stereoselective Syn-thesis of Benzo–sultams by Palladium-Catalyzed Hydrocarbonation of Alkynes. *Synthesis* **2016**, *48*, 710−722.

7. Sandeep, K.; Siva Reddy, A.; Kumara Swamy, K. C. Pal-ladium-catalyzed cyclisation of ynamides and propargyl tethered iodosulfonamides with boronic acids leading to benzosultams. *Org. Biomol. Chem.* **2021**, *19*, 6871−6882.

8. Li, J.; Shi, H.; Zhang, S.; Rudolph, M.; Rominger, F.; Hashmi, A. S. K. Switchable Divergent Synthesis in Gold-Catalyzed Difunctionalizations of o-Alkynylbenzenesulfonamides with Aryldiazonium Salts. *Org. Lett.* **2021**, *23*, 7713−7717.

9. Okumura, Y.; Sato, E.; Mitsudo, K.; Suga, S. Electrochem-ical Generation of Sulfonamidyl Radicals via Anodic Oxidation of Hydrogen-Bonding Complexes: Applications to Electrosynthesis of Benzosultams. *JACS Au* **2025**, *5*, 3974−3981.

10. Zhang, M.; Yu, X.; Zhu, W. J.; Liu, Y.; Zhang, Z. H.; Zhao, J. B.; Xia, C. C.; Li, K. Iron-Catalyzed Synthesis of Benzosultams from NPhenyl-N-(prop-2-yn-1-yl)benzenesulfonamide and Ben-zenesulfonyl Hydrazine. *Org. Lett.* **2023**, *25*, 603−607.

11. (a) Hafeez, S.; Saeed, A. Photo-redox catalyzed dehydrazinative acylation of N-heterocycles via Minisci reaction. *RSC Adv.* **2021**, *11*, 38683–38689. (b) Bai, X.; Shi, J.; Zhang, Z.; Hu, M.; Chai, J.; Xu, L.; Jin, X.; Shi, X.; Jin, P. Efficient persulfate activation by photo-excited organic dyes: Mechanism and application for actual dyeing wastewater self-purification. *J. Clean. Prod.* **2023**, *421*, 138375-138389.

12. Campolo, D.; Arif, T.; Borie, C.; Mouysset, D.; Vanthuyne, N.; Naubron, J. V.; Bertrand, M. P.; Nechab, M. Double transfer of chirality in organocopper-mediated bis (alkylating) cycloisomerization of enediynes. *Angew. Chem., Int. Ed.* **2014**, *53*, 3227−3231.

13. Meyer, A. U.; Jäger, S.; Prasad Hari, D.; König, B. Visible Light-Mediated Metal-Free Synthesis of Vinyl Sulfones from Aryl Sulfinates. *Adv. Synth. Catal.* **2015**, *357*, 2050–2054.

5.13 Selected NMR spectra:

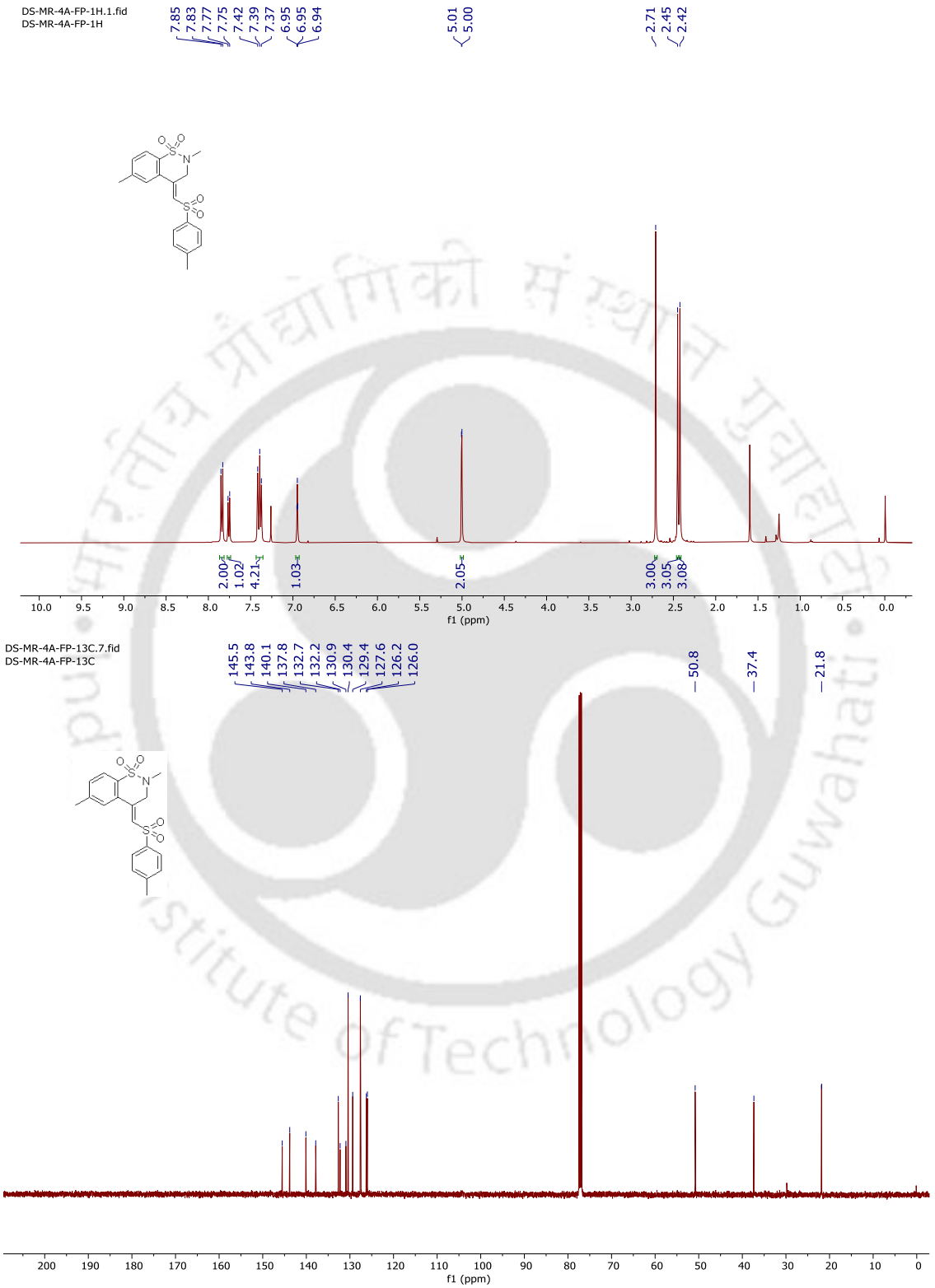

Figure 5.8: ^{1}H NMR (500 MHz) and $^{13}C\{^{1}H\}$ NMR (125 MHz) spectrum of Compound **5.3a** in $CDCl_3$.

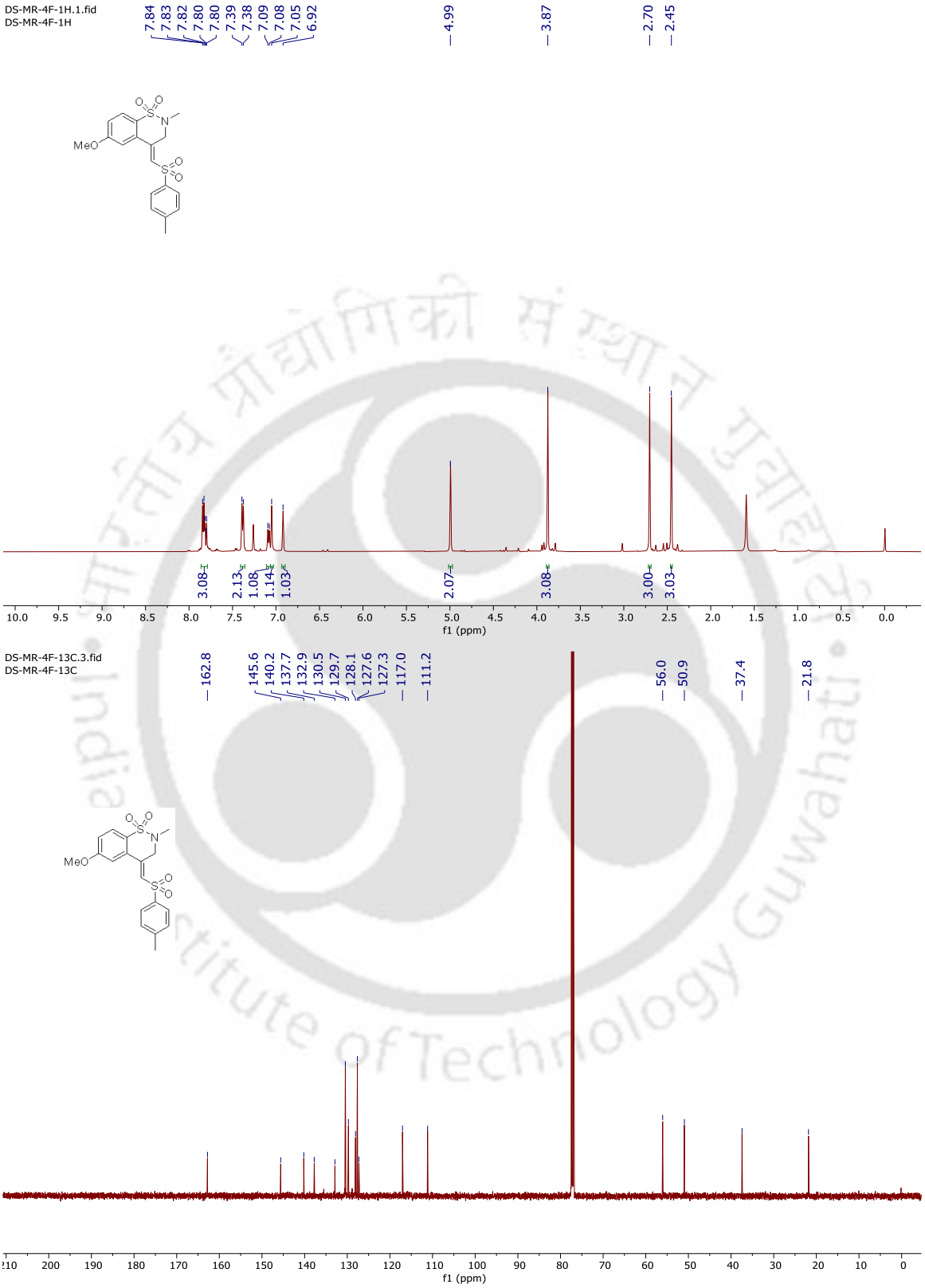

Figure 5.9: ^{1}H NMR (500 MHz) and $^{13}C\{^{1}H\}$ NMR (125 MHz) spectrum of Compound **5.3b** in $CDCl_3$.

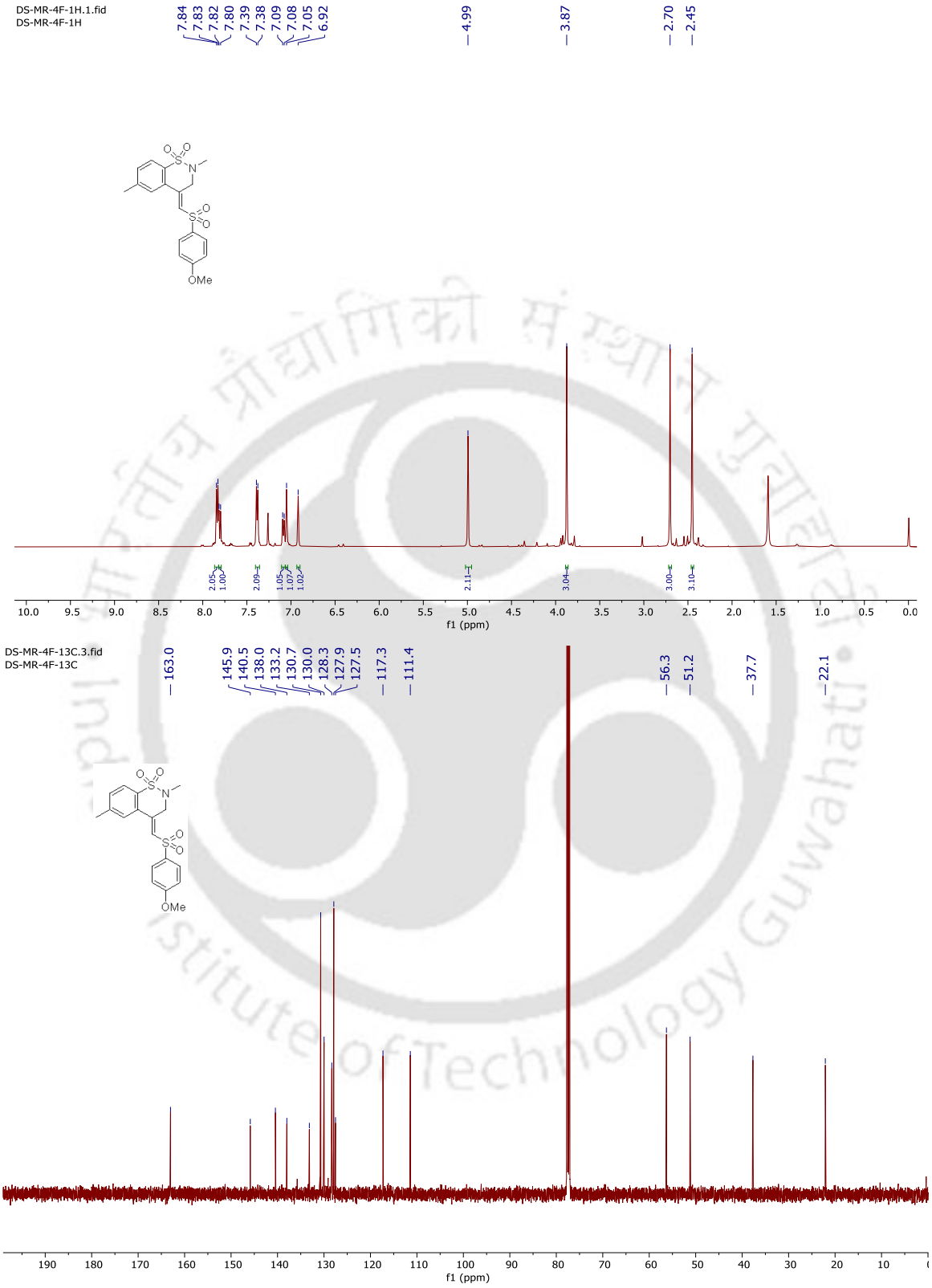

Figure 5.10: ^{1}H NMR (500 MHz) and $^{13}C\{^{1}H\}$ NMR (125 MHz) spectrum of Compound **5.4b** in $CDCl_3$.

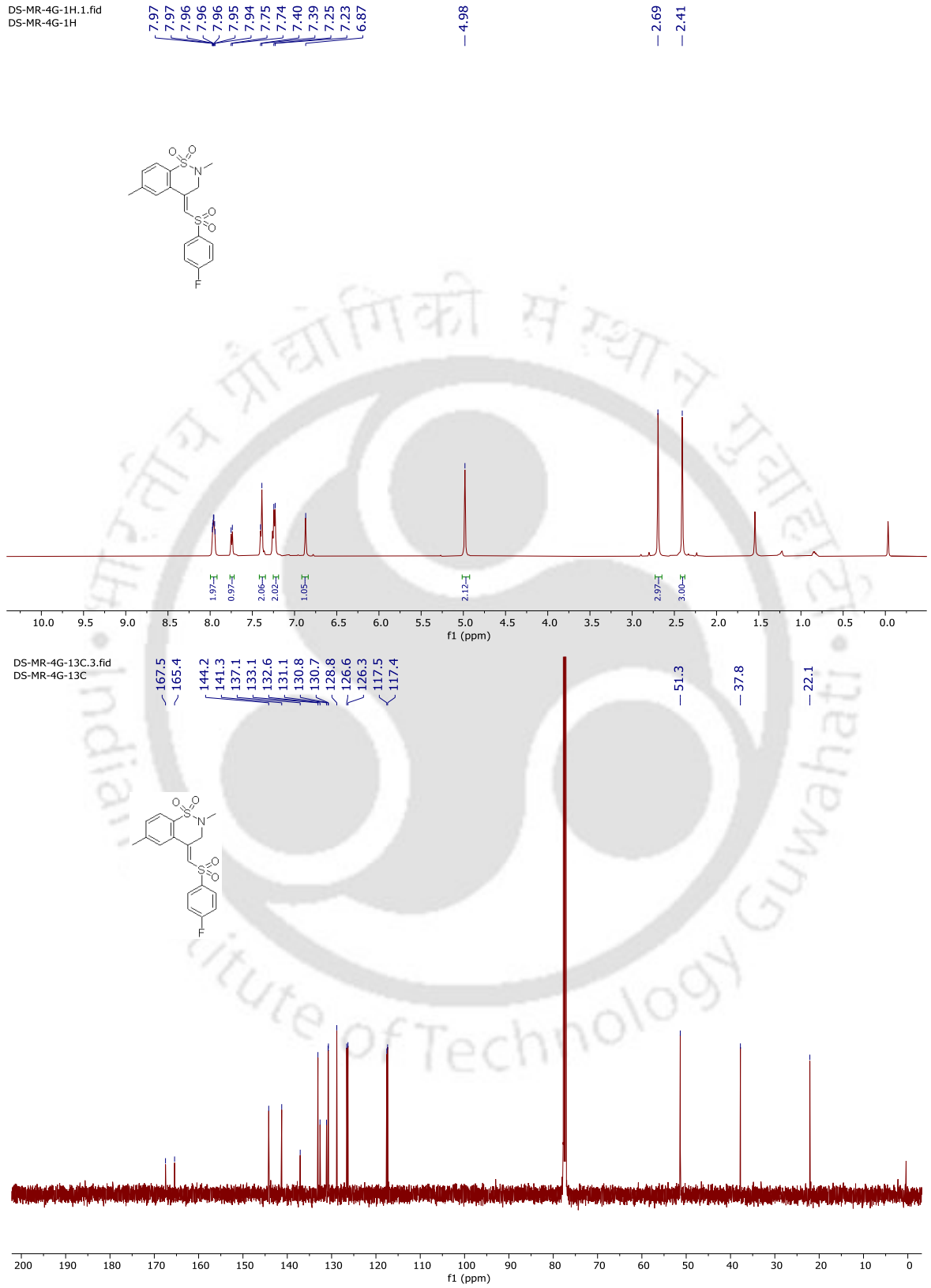

Figure 5.11: ^{1}H NMR (500 MHz) and $^{13}C\{^{1}H\}$ NMR (125 MHz) spectrum of Compound **5.4c** in $CDCl_3$.

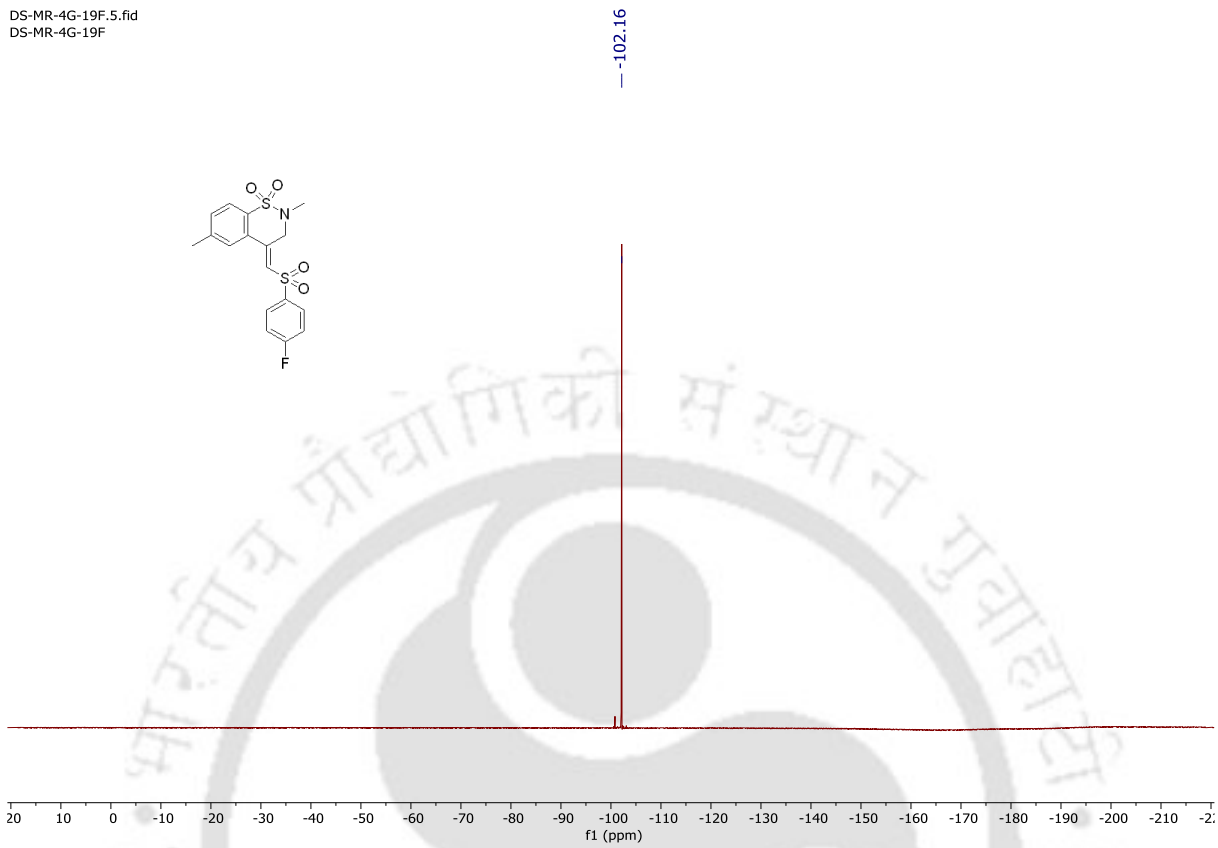

Figure 5.12: $^{19}F\{^{1}H\}$ NMR (470 MHz) spectrum of Compound **5.4c** in $CDCl_3$.

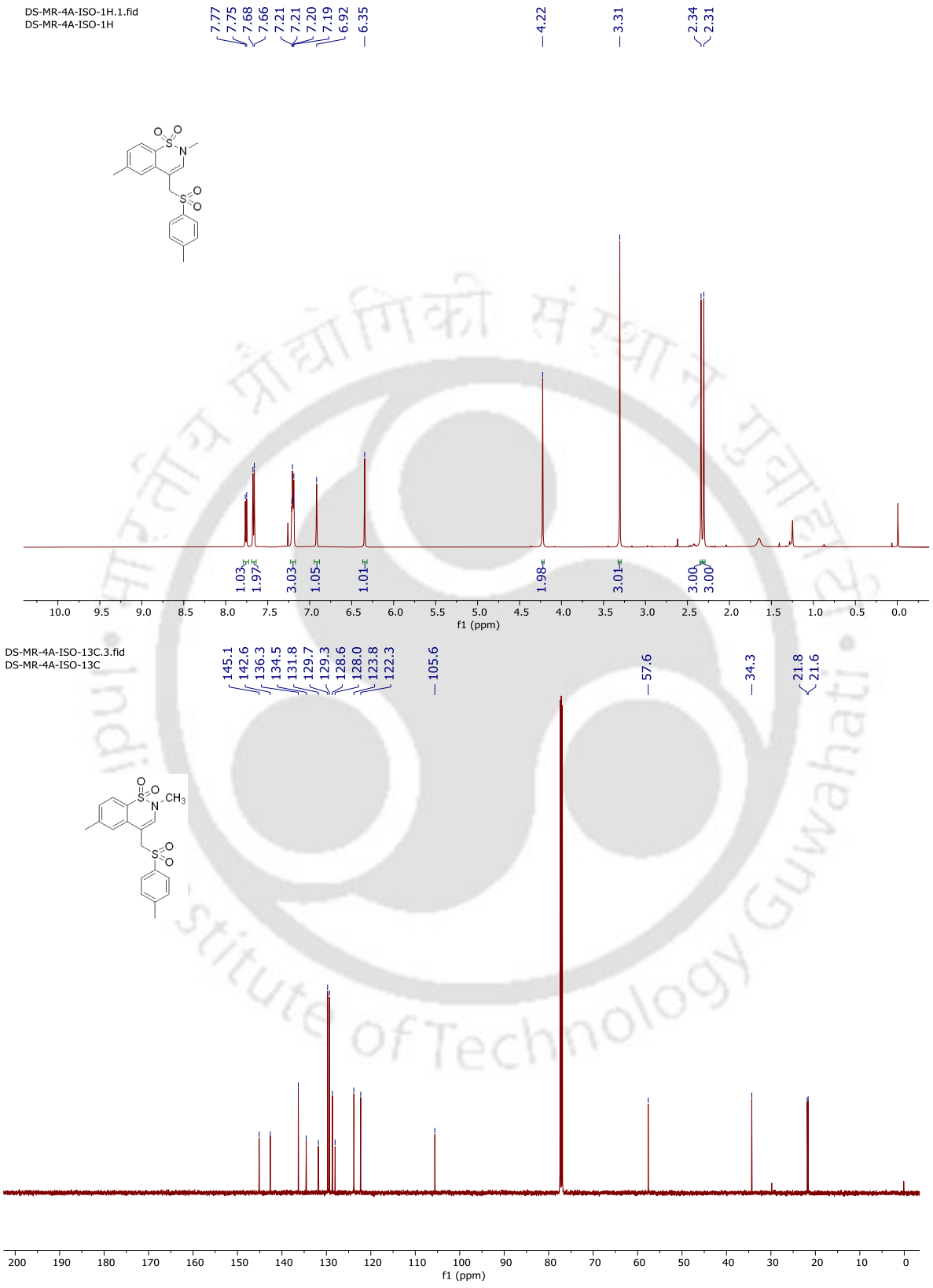

Figure 5.14: ^{1}H NMR (500 MHz) and $^{13}C\{^{1}H\}$ NMR (125 MHz) spectrum of Compound **5.8a** in $CDCl_3$.

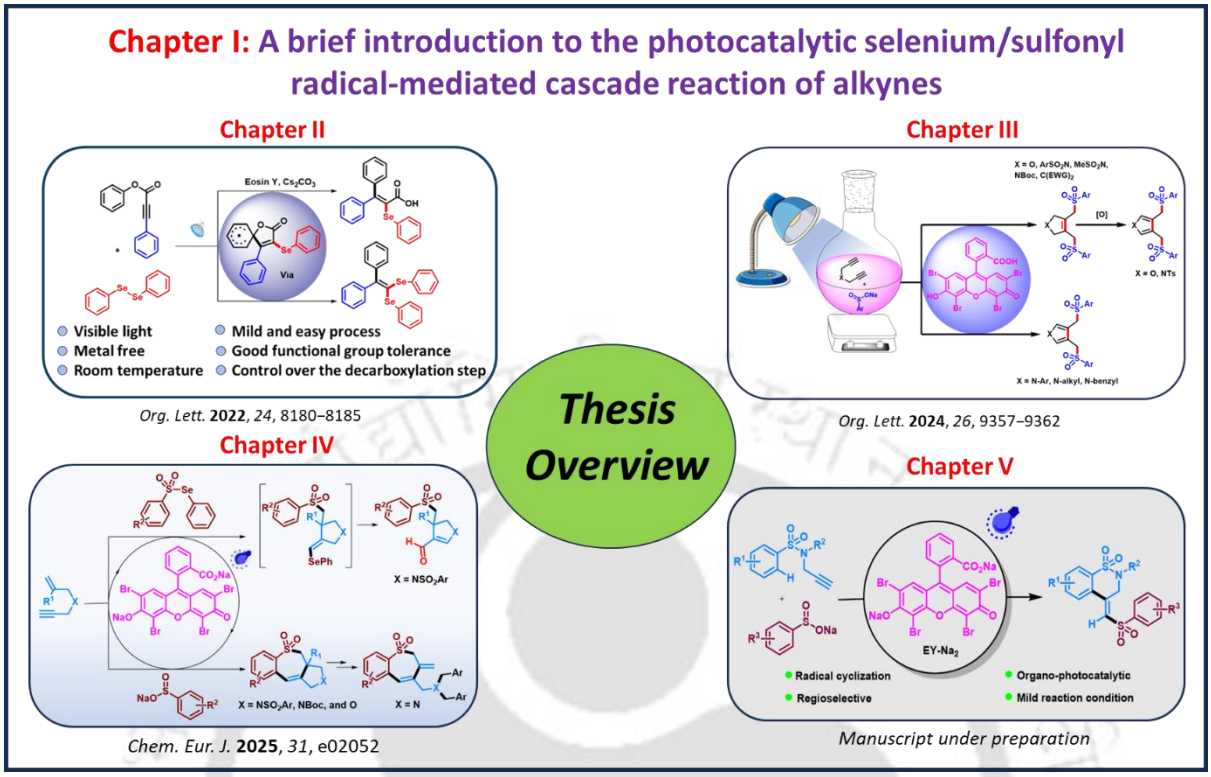

List of publications

Thesis works:

1. **Roy, M**.; Jamatia, R.; Samanta, A.; Mohar, K.; Srimani, D. Change in the Product Selectivity in the Visible Light-Induced Selenium Radical-Mediated 1,4-Aryl Migration Process. *Org. Lett.* **2022**, *24*, 8180–8185.

2. **Roy, M**.; Mallick, I.; Mahapatra, M.; Srimani, D. Substituent-Dependent, Switchable Synthesis of Nonaromatic and Aromatic Heterocyclic Sulfones Using Visible Light. *Org. Lett.* **2024**, *26*, 9357−9362.

3. **Roy, M.**; Mallick, I.; Siuli, S.; Bera, A.; Srimani, D. Visible-Light Mediated Divergent Synthesis of Sulfonylated Dihydropyrrole-3-Carboxaldehydes and Tricyclic Sulfones via Sulfonyl Radical Source Modulation. *Chem. Eur. J.* **2025**, *31*, e02052.

4. **Roy, M.**; Bera, A.; Kar, S.; Siuli, S.; Srimani, D. Visible-light-enabled sulfonyl radical-triggered cyclization strategy for the efficient synthesis of benzosultams. *Org. Lett.* (accepted)

Non-Thesis works:

5. **Roy, M**.; Sardar, B.; Mallick, I.; Srimani, D. Generation of alkyl and acyl radicals by visible-light photoredox catalysis: direct activation of C–O bonds in organic transformations. *Beilstein J. Org. Chem.* **2024**, *20*, 1348–13753.

6. Sharma, R.; Samanta, A.; Sardar, B.; **Roy, M**.; Srimani, D. Progressive Study on Ruthenium Catalysis for de(Hydrogenative) Alkylation and Alkenylation Using Alcohols as a Sustainable Source. *Org. Biomol. Chem.* **2022**, *20*, 7998–8030.

7. Mondal, A.; Phukan, H. J.; Pal, D.; Kumar, S.; **Roy, M**.; Srimani, D. Well-defined Mn(II)-complex Catalyzed Switchable De(hydrogenative) Csp3-H Functionalization of Methyl Heteroarenes: A Sustainable Approach for Diversification of Heterocyclic Motifs. *Chem. Eur. J.* **2023**, *30*, e202303315.

8. Mondal, A.; Pal, D.; Phukan, H. J.; **Roy, M**.; Kumar, S.; Purkayastha, S.; Guha, A. K.; Srimani, D. Manganese Complex Catalyzed Sequential Multi-component Reaction: Enroute to a Quinoline-Derived Azafluorenes. *ChemSusChem* **2024**, *17*, e202301138.

9. Dey, M., **Roy, M**., Borah, P. P., Roy, S., Gogoi, A. J., Bhattacharyya, K., Raidongia, K. Effect of physicochemical congestion on the catalytic conversion of arylboronic acids to phenols. Mater. Horiz. 2025.

Conferences and workshops

1. International Conference on Frontiers in Chemical Sciences (**FICS-2022**) from 2-4th December, 2022 at IIT Guwahati. (Poster Presented)

2. International Conference on Emerging Trends in Chemistry (**ICETC-2023**) from 16-17th March, 2023 at Assam Don Bosco University. (Poster Presented)

3. National Organic Symposium Trust (**J-NOST-2023**) from 10-12th October, 2023 at IISER Pune. (Poster Presented) (**Best poster award**)

4. 7th International Symposium on C-H Activation (**ISCHA7-2024**) from 6-9th December, 2024 at IIT Bombay. (Poster Presented)

Copyright permission

1. **Roy, M**.; Jamatia, R.; Samanta, A.; Mohar, K.; Srimani, D. Change in the Product Selectivity in the Visible Light-Induced Selenium Radical-Mediated 1,4-Aryl Migration Process. *Org. Lett.* **2022**, *24*, 8180–8185.

AMERICAN CHEMICAL SOCIETY LICENSE
TERMS AND CONDITIONS
Nov 28, 2025

This Agreement between Mithu Roy, IIT Guwahati ("You") and American Chemical Society ("American Chemical Society") consists of your license details and the terms and conditions provided by American Chemical Society and Copyright Clearance Center.

License Number	6155900740375
License date	Nov 25, 2025
Licensed Content Publisher	American Chemical Society
Licensed Content Publication	Organic Letters
Licensed Content Title	Change in the Product Selectivity in the Visible Light-Induced Selenium Radical-Mediated 1,4-Aryl Migration Process
Licensed Content Author	Mithu Roy, Ramen Jamatia, Arup Samanta, et al
Licensed Content Date	Nov 1, 2022
Licensed Content Volume	24
Licensed Content Issue	44
Volume number	24
Issue number	44
Type of Use	Thesis/Dissertation
Requestor type	Author (original work)
Format	Print and Electronic
Portion	Full article

Copyright permission

Title of new work	Phd thesis
Institution name	IIT Guwahati
Expected presentation date	Jul 2026
The Requesting Person / Organization to Appear on the License	Mithu Roy, IIT Guwahati
Requestor Location	Lohit Hostel, Room No.-D154 IIT Guwahati, Assam Guwahati, 781039 India
Payment Type	Invoice
Email Address	rmithu@iitg.ac.in
Billing Address	IIT Guwahati CHEL-203 Guwahati, India 781039
Total	0.00 USD

Terms and Conditions

American Chemical Society's Policy on Thesis and Dissertations

If your university requires you to obtain permission, you must use the RightsLink permission system.

See RightsLink instructions at http://pubs.acs.org/page/copyright/permissions.html.

This is regarding request for permission to include **your** paper(s) or portions of text from **your** paper(s) in your thesis.

Permission is now automatically granted; please pay special attention to the **implications** paragraph below. The Copyright Subcommittee of the Joint Board/Council Committees on Publications approved the following:

Copyright permission

Copyright permission for published and submitted material from thesis and dissertations

ACS extends blanket permission to students to include in their thesis and dissertations their own articles, or portions thereof, that have been published in ACS journals or submitted to ACS journals for publication, provided that the ACS copyright credit line is noted on the appropriate page(s).

Publishing implications of electronic publication of thesis and dissertation material

Students and their mentors should be aware that posting of thesis and dissertation material on the Web prior to submission of material from that thesis or dissertation to an ACS journal may affect publication in that journal. Whether Web posting is considered prior publication may be evaluated on a case-by-case basis by the journal's editor. If an ACS journal editor considers Web posting to be "prior publication", the paper will not be accepted for publication in that journal. If you intend to submit your unpublished paper to ACS for publication, check with the appropriate editor prior to posting your manuscript electronically.

2. **Roy, M**.; Mallick, I.; Mahapatra, M.; Srimani, D. Substituent-Dependent, Switchable Synthesis of Nonaromatic and Aromatic Heterocyclic Sulfones Using Visible Light. *Org. Lett.* **2024**, *26*, 9357−9362.

AMERICAN CHEMICAL SOCIETY LICENSE
TERMS AND CONDITIONS
Nov 28, 2025

This Agreement between Mithu Roy, IIT Guwahati ("You") and American Chemical Society ("American Chemical Society") consists of your license details and the terms and conditions provided by American Chemical Society and Copyright Clearance Center.

License Number	6155900991177
License date	Nov 25, 2025
Licensed Content Publisher	American Chemical Society
Licensed Content Publication	Organic Letters
Licensed Content Title	Substituent-Dependent, Switchable Synthesis of Nonaromatic and Aromatic Heterocyclic Sulfones Using Visible Light

Copyright permission

Licensed Content Author	Mithu Roy, Itu Mallick, Manami Mahapatra, et al
Licensed Content Date	Nov 1, 2024
Licensed Content Volume	26
Licensed Content Issue	43
Volume number	26
Issue number	43
Type of Use	Thesis/Dissertation
Requestor type	Author (original work)
Format	Print and Electronic
Portion	Full article
Title of new work	Phd thesis
Institution name	IIT Guwahati
Expected presentation date	Jul 2026
The Requesting Person / Organization to Appear on the License	Mithu Roy, IIT Guwahati
Requestor Location	Mr. Mithu Roy Lohit Hostel, Room No.-D154 IIT Guwahati, Assam Guwahati, 781039 India
Payment Type	Invoice
Email Address	mithu.roy.blk@gmail.com
Billing Address	IIT Guwahati Lohit Hostel, Room No.-D154 IIT Guwahati, Assam Guwahati, India 781039
Total	0.00 USD

Terms and Conditions

American Chemical Society's Policy on Thesis and Dissertations

If your university requires you to obtain permission, you must use the RightsLink permission system.

See RightsLink instructions at http://pubs.acs.org/page/copyright/permissions.html.

This is regarding request for permission to include **your** paper(s) or portions of text from **your** paper(s) in your thesis.

Permission is now automatically granted; please pay special attention to the **implications** paragraph below. The Copyright Subcommittee of the Joint Board/Council Committees on Publications approved the following:

> Copyright permission for published and submitted material from thesis and dissertations
> ACS extends blanket permission to students to include in their thesis and dissertations their own articles, or portions thereof, that have been published in ACS journals or submitted to ACS journals for publication, provided that the ACS copyright credit line is noted on the appropriate page(s).
> Publishing implications of electronic publication of thesis and dissertation material
> Students and their mentors should be aware that posting of thesis and dissertation material on the Web prior to submission of material from that thesis or dissertation to an ACS journal may affect publication in that journal. Whether Web posting is considered prior publication may be evaluated on a case-by-case basis by the journal's editor. If an ACS journal editor considers Web posting to be "prior publication", the paper will not be accepted for publication in that journal. If you intend to submit your unpublished paper to ACS for publication, check with the appropriate editor prior to posting your manuscript electronically.

3. Roy, M.; Mallick, I.; Siuli, S.; Bera, A.; Srimani, D. Visible-Light Mediated Divergent Synthesis of Sulfonylated Dihydropyrrole-3-Carboxaldehydes and Tricyclic Sulfones via Sulfonyl Radical Source Modulation. *Chem. Eur. J.* **2025**, *31*, e02052.

JOHN WILEY AND SONS LICENSE
TERMS AND CONDITIONS
Nov 28, 2025

This Agreement between Mithu Roy, IIT Guwahati ("You") and John Wiley and Sons ("John Wiley and Sons") consists of your license details and the terms and conditions provided by John Wiley and Sons and Copyright Clearance Center.

License Number	6155901260536
License date	Nov 25, 2025

Copyright permission

Licensed Content Publisher	John Wiley and Sons
Licensed Content Publication	Chemistry - A European Journal
Licensed Content Title	Visible-Light Mediated Divergent Synthesis of Sulfonylated Dihydropyrrole-3-Carboxaldehydes and Tricyclic Sulfones via Sulfonyl Radical Source Modulation
Licensed Content Author	Mithu Roy, Itu Mallick, Sudipta Siuli, et al
Licensed Content Date	Jul 25, 2025
Licensed Content Volume	31
Licensed Content Issue	46
Licensed Content Pages	8
Type of use	Dissertation/Thesis
Requestor type	Author of this Wiley article
Format	Print and electronic
Portion	Full article
Will you be translating?	No
Title of new work	Phd thesis
Institution name	IIT Guwahati
Expected presentation date	Jul 2026
The Requesting Person / Organization to Appear on the License	Mithu Roy, IIT Guwahati
Requestor Location	Mr. Mithu Roy Lohit Hostel, Room No.-D154 IIT Guwahati, Assam Guwahati, 781039 India
Publisher Tax ID	EU826007151
Total	0.00 USD
Terms and Conditions	

Copyright permission

TERMS AND CONDITIONS

This copyrighted material is owned by or exclusively licensed to John Wiley & Sons, Inc. or one of its group companies (each a"Wiley Company") or handled on behalf of a society with which a Wiley Company has exclusive publishing rights in relation to a particular work (collectively "WILEY"). By clicking "accept" in connection with completing this licensing transaction, you agree that the following terms and conditions apply to this transaction (along with the billing and payment terms and conditions established by the Copyright Clearance Center Inc., ("CCC's Billing and Payment terms and conditions"), at the time that you opened your RightsLink account (these are available at any time at http://myaccount.copyright.com).